NEUROBIOLOGY

An International Multidisciplinary Journal in Neurosciences

VOLUME 1, NUMBER 1, 1993

Including the former Acta Biochimica et Biophysica Hungarica

AKADÉMIAI KIADÓ, BUDAPEST

HU ISSN 1216-8063

NEUROBIOLOGY

An International Multidisciplinary Journal in Neurosciences

(Including the former Acta Biochimica et Biophysica Hungarica)

Neurobiology is a multidisciplinary international journal publishing contributions from all traditionally important and newly emerging subdisciplines of the neurosciences including neuroanatomy, morphology, biochemistry, physiology, pharmacology, molecular neurobiology, developmental neuroscience, etc.

Neurobiology is published by
AKADÉMIAI KIADÓ
Publishing House of the Hungarian Academy of Sciences
H-1117 Budapest, Prielle K. u. 19–35, Hungary

Manuscripts and editorial correspondence should be addressed to

Norbert Halász
Institute of Biophysics
Biological Research Centre
Hungarian Academy of Sciences
H-6701 Szeged, P.O. Box 521, Hungary

Subscription price for Volume 1 (1993) in 4 issues US$ 78.00, including normal postage; airmail delivery US$ 20.00

Orders should be addressed to

AKADÉMIAI KIADÓ
H-1519 Budapest, P.O. Box 245, Hungary

NEUROBIOLOGY

An International Multidisciplinary Journal in Neurosciences

Akadémiai Kiadó, Budapest

Editorial

You are keeping in your hand the first issue of a new international journal, ***Neurobiology****, and you may wonder why it was necessary to add one more forum to the great number of already existing ones. The main reason is that there was an increasing interest in studying the nervous system during the last century, since the famous silver impregnation technique was employed in the eternal work of Ramón y Cajal, capable of characterizing the neuron, as a unit and, also the primary principles of organization of the peripheral and central nervous system were discovered. With the widening range of approaches and methods, the existing scientific disciplines regularly incorporated studies of neurons by techniques relevant to their own field. An increasing number of data on neurons and the perception of the general significance of the nervous system in animal and human life led to the fact that neuroscience has become a strong discipline in the last few decades, accompanied by the publishing of many distinctive "Neuro-journals". In addition, the last decade of the century was even named the "Decade of the Brain" stressing further, for people of our age, the importance of studies on the central nervous system. In recognition of these trends, Akadémiai Kiadó has decided to change the principal discipline of one of its former journals (*Acta Biochimica et Biophysica Hungarica*) into an international, multidisciplinary neuroscience journal by launching* ***Neurobiology****.*

This new journal wishes to attract contributions from all related areas. ***Neurobiology*** *will cover all traditionally known and newly emerging subdisciplines of neuroscience, like morphology, histochemistry, physiology, biochemistry, pharmacology, behaviour, molecular neurobiology, modelling of neuronal function, glial system, sensory systems, etc. To promote studies and publications in neuroscience, discounted reprint order is offered to young authors and those without prior publications within this discipline.* ***Neurobiology*** *wishes to support rapid scientific communication of scientists from all over the world and, at the same time, wants to be the primary forum for publications from the recently formed, independent Hungarian Neuroscience Association. The Journal would like to be a mouthpiece of researchers to express their views on different matters.*

Through organization of its large, international Editorial/Advisory Board and temporary contribution by other experts, ***Neurobiology*** *will be able to advise authors to find appropriate and high quality formats for presenting their results. Readers, potential and recent authors, in turn, are expected to support by their comments and papers the initial, wide scope of the Journal, or to put an emphasis on several subdisciplines, which may suggest us to create a more specific aspect during the coming months and years, to better serve the needs of scientific communication in this field. This is our present goal supported also by the future efforts of the Board and the Publisher.*

The Editors

Neurobiology 1 (1), pp. 3–10, 1993

MINIREVIEW: REGULATION BY SECOND MESSENGERS OF PERMEABILITY IN THE CEREBRAL MICROVESSELS

F. Joó

Laboratory of Molecular Neurobiology, Institute of Biophysics,
Biological Research Centre of the Hungarian Academy of Sciences,
H–6701 Szeged, P.O. Box 521, Hungary

Summary: The view that the cerebral endothelial cells represent the cellular analogue of the blood-brain barrier has been generally accepted. The regulation of transport processes operating in the cerebral endothelial cells is of great current interest. Different elements of the intracellular signaling messenger systems have been detected in the course of our studies in the cerebral endothelial cells. Our knowledge of these regulatory mechanisms is briefly reviewed here with special emphasis on the importance of second messenger molecules and phosphorylation of certain proteins of microvascular origin.

Key words: blood-brain barrier, second messengers, permeability

INTRODUCTION

It is now generally believed that, apart from a few exceptions where the structural basis of restricted movement of certain substances is due to an impermeable glial sheath (Abbott, 1972; Abbott et al., 1981), the endothelial cells comprise the "blood-brain barrier" (BBB). This term was first used by Stern and Peyrot (1927) to summarize a number of different regulatory mechanisms that control the exchange of materials between blood and brain and cerebrospinal fluid. It is worthy of mention that, from a phylogenetic point of view, the endothelial blood-brain barrier can be regarded as an old structure: a living vertebrate *Lamperta fluviatilis*, that branched off from the general evolutionary

"tree" more than 500 million years ago, has cerebral microvessels with structural characteristics similar to those of vertebrates with a much shorter evolutionary history (Bundgaard and Cserr, 1981; Bundgaard, 1982). It was demonstrated in electron microscopic studies (Brigthman and Reese, 1969) that the barrier, which prevented the passing of proteins from blood to brain, consisted of tight junctions between cerebral endothelial cells. Another equally important feature of the cerebral endothelial cells, in contrast to those of most other tissues, is the relative lack of pinocytotic vesicles. From a physiological point of view, the cerebral endothelial cells represent a very tight cellular barrier with high (1900 ohm/cm^2) membrane resistance (Crone and Olesen, 1982; Butt et al., 1990; Butt and Jones, 1992). This potent restraint delays the penetration of solutes to the brain at the capillary endothelium. On the other hand, a number of polar metabolic substrates cross the plasma membranes of cerebral endothelium via highly specific, self-saturable and inhibitable transport systems (Oldendorf, 1977; Bradbury, 1985; Pardridge, 1988). These particular structural and functional characteristics of cerebral capillaries are determined by the surrounding central nervous tissue, especially by the influence deriving from astrocytes (Stewart and Wiley, 1981; Arthur et al., 1987; Stewart and Hayakawa, 1987; Tao-Cheng et al., 1987). It became evident, mainly from studies carried out on isolated brain microvessels, that the cerebral endothelial cells are endowed with many different receptors (for review see Joó, 1985; 1986; 1992). It remained to be seen, however, which cellular transduction system(s), if any, operate in the cerebral endothelial cells mediating possibly the effect of vasoactive substances.

RESULTS AND DISCUSSION

The effects of cyclic nucleotides on the permeability of cerebral endothelial cells

The first results indicating that the lipid soluble derivative of *cyclic AMP*, the dibutyryl (dibu-) cyclic AMP, can increase the albumin penetration in mature brain microvessels were published in 1972 (Joó). Likewise, the non-hydrolysable *cGMP* analogue, dibu- cGMP, opened also the blood-brain barrier for albumin (Joó et al.,1983) after infusions into the common carotid artery. Later, the synthesizing and degrading enzymes of both cAMP and cGMP were detected in the cerebral endothelial cells (for

review see Joó, 1985; 1992) indicating that these second messenger molecules are produced and metabolized locally. Recently, a correlation was found (Ádám et al., 1987) between the activation of adenylate cyclase in cerebral endothelial cells and the induction of transcapillary albumin transport, suggesting that elevated cAMP may trigger macromolecule permeation through the microvessels. Specific histamine H_2-receptor blockers were seen (Dux et al., 1987) to prevent the activation of this transport possibly by binding to receptors linked to the adenylate cyclase in the brain microvessels (Karnushina et al., 1980). In agreement with our findings, the data of Sen and Campochiaro (1991) also suggest that stimulation of intracellular cAMP accumulation may be a common feature of mediators that cause breakdown of the blood-retinal barrier.

In contrast to these results, Kempski et al. (1987) found no increase of permeability to trypan blue-albumin complex in a new model of cultured cerebromicrovascular endothelial cells when the endothelial synthesis of cAMP was stimulated directly by forskolin. Recent results of Stelzner et al. (1989) also showed that increase in cAMP content was in fact associated with a 3–10-fold reduction in albumin transfer across monolayers from bovine pulmonary arterial endothelial cells. By working also with endothelial cells of peripheral origin, Carson et al. (1989) reported on similar results showing that agents, which increase cAMP in endothelial cells prevent the increase in microvascular permeability to albumin that follows histamine exposure. The results of Rotrosen and Galline (1986) have, however, elucidated that the permeability enhancing effect of histamine appeared to be dependent on histamine H_1-receptor occupancy in endothelial cells of peripheral origin, causing increases in intracellular calcium. Recently, evidence has been provided (Revest et al., 1991) for a rise in intracellular calcium on the effect of vasoactive agents in the cerebral endothelial cells, as well. The important differences between endothelial cells from brain tissue and peripheral vessels should, however, be kept in mind during the interpretation of these seemingly contradictory result. As we learnt it by now, cultured cells are often unable to express fully the properties of mature cerebral endothelium with blood-brain barrier characteristics due to the absence of astrocytic influences, *in vitro*. For example, various enzymes (e.g. γ-glutamyl transpeptidase, DeBault and Cancilla, 1979; DeBault, 1981) and receptors (e.g. acetylcholine-, serotonin- and histamine H_2-receptors, Karnushina et al., 1982) are missing as a rule from the cultured cerebrovascular endothelial cells, making these cells more similar, at least in this respect, to peripheral vessels.

Fluid-phase endocytosis within primary cultures of brain microvessel endothelial cell monolayers, an in vitro blood-brain barrier model, has been shown recently (Guillot and Audus, 1990) to be significantly stimulated by nanomonal concentrations of phorbol myristate acetate. This effect of phorbol esters was not mediated by prostaglandins. Since the *protein kinase C* (PK C) is a prime target for actions of the phorbol esters (Nishizuka, 1984), the involvement of PK C in the activation of blood-brain barrier opening seems to be established.

The presence and translocation of protein kinase C (PK C), a key regulatory enzyme involved in both signal transduction and cellular proliferation, were observed (Markovac and Goldstein, 1988) to phorbol esters as well as to transforming growth factor beta, a widely distributed regulatory peptide that promotes endothelial cell differentiation, in microvessels isolated from rat brain. Similarly, stimulation of PK C translocation was found by Catalán et al. (1989b) in isolated brain microvessels on the effect of Substance P. The finding suggested that Substance P may be involved in the regulation of processes underlying protein phosphorylation in the BBB.

The presence in the cerebral endothelial cells of *calmodulin-dependent kinases* was revealed by studying protein phosphorylation (Oláh et al., 1988). Calmodulin stimulated the phosphorylation of 58 (57)-, 55-, and 50 kDa proteins over that in the control, and the phosphorylation peaked at approx. 4 min. Sometimes a short lag period could be observed during the rising phase. Dephosphorylation, carrier out by phosphoprotein phosphatases, followed relatively rapid kinetics, in contrast to the phosphorylation induced by cyclic nucleotides. The most prominent substrates of calmodulin-dependent phosphorylation were the 50- and 55 kDa polypeptides, which are most likely identical to the β- and α-subunits of the calmodulin-dependent protein kinase II (Mackie et al., 1986). These subunits are known to be phosphorylated usually by asymmetric kinetics. The very similar substrates, evaluated together with proteins of relative molecular mass of 58 (57) kDa, probably correspond to the α- and β-subunits of tubulin (Mackie et al., 1986).

Modulation of protein phosphorylation by second messengers at the cerebral endothelium

The fact that protein phosphorylation occurs in brain microvessels was first shown by Pardridge et al. (1985). Later, the isolation and partial characterization of a 56,000-

dalton phosphoprotein from the BBB was published by Weber et al. (1987). A detailed study on the kinetics of protein phosphorylation and its modulation by second messengers revealed (Oláh et al., 1988) the presence in the cerebral endothelium of Ca^{2+}-calmodulin, Ca^{2+}/phospholipid (PK C)-, cyclic GMP-, and cyclic AMP-dependent protein kinases. Since protein phosphorylation is thought to be a common effector process in the action of many second messengers, it was proposed that these protein substrates may participate in the coupling of signal transduction to endothelial metabolism.

Recently, evidence has been provided (Catalán et al., 1989a) on the regulatory action of vanadate on protein phosphorylation in brain microvessels. The authors proposed that vanadate activated the phosphorylation of cAMP-dependent protein kinase and thereby may modulate transport processes across the BBB.

Although dibu-cAMP has long been known to increase pinocytosis and macromolecular transport through the brain capillaries (Joó, 1972), it remained to be seen which proteins, if any, are the substrates of phosphorylation resulting from elevated intraendothelial accumulation of cAMP. With the use of sodium dodecyl sulfate-polyacrylamide gel electrophoresis, the efficiency of cAMP in activating phosphorylation processes in brain microvessels was found to be low.

A very fast and pronounced phosphorylation was seen after cGMP activation, which was much stronger than that obtained with cAMP. The α-and β-subunits of tubulin as well as Ca^{2+}/calmodulin-dependent protein kinase II (in the presence of 2 mM EGTA) were also phosphorylated by the cyclic nucleotide-dependent protein kinases (Oláh et al., 1988). The cGMP-dependent protein kinase had some substrates in common with the cAMP-dependent one, but in addition, some phosphoproteins specific for cGMP with relative molecular masses of 33 and 30 kDa were also revealed.

For identification of the protein substrate for PK C, exogenous enzyme (the 45-kDa fragment of PK C) was added to the incubation medium (Oláh et al., 1988). The relative molecular mass of this polypeptide was shown clearly to be lower than that of the α-subunit of CAM-dependent protein kinase. The occurrence of this activated fragment of PK C in the brain microvessel preparation was also evident, as demonstrated on the control gel. The exogenous PK C could recognize its major substrate in this fraction, and the reversibility of phosphorylation of the 40 kDA protein was impressive. A similar, but kinetically somewhat different, phosphorylation pattern was observed in the case of autophosphorylated form of the 45 KDa fragment of the PK C. The phosphorylation of

this polypeptide took place faster, whereas its dephosphorylation was slower than that of its 40 kDa substrate.

In order to elucidate the molecular interactions between different second messenger systems further studies are warranted.

ACKNOWLEDGEMENTS

The valuable work of all co-workers and collaborators, who have helped the accomplishment of research is greatly acknowledged. The research was supported by Grants from the Hungarian Research Fund (OTKA) and the Ministry of Public Welfare.

REFERENCES

Abbott, N.J. (1972) Access of ferritin to the interstitial space of *carcinus* brain from intracerebral blood vessels. Tissue and Cell 4, 99–104.

Abbott, N.J., Bundgaard, M. and Cserr, H. (1981) Fine-structural evidence for a glial blood-brain barrier to protein in the cuttlefish, *Sepia officinalis*. J. Physiol. 316, 52P–53P.

Arthur, F.E., Shivers, R.R. and Bowman, P.D. (1987) Astrocyte mediated induction of tight junctions in brain capillary endothelium: An efficient in vitro model. Dev. Brain Res. 36, 155–159.

Ádám, G., Joó, F., Temesvári, P., Dux, E., Szerdahelyi, P. (1987) Effects of acute hypoxia on the adenylate cyclase and Evans blue transport of brain microvessels. Neurochem. Int. 10, 529–532.

Bradbury, M.W.B. (1985) The blood-brain barrier in vitro. Neurochem. Int. 7, 27–28.

Brightman, M.W. and Reese, T.J. (1969) Junctions between intimately apposed cell membranes in the vertebrate brain. J. Cell Biol. 40, 648–677.

Bundgaard, M. (1982) Ultrastructure of frog cerebral and pial microvessels and their impermeability to lanthanum ions. Brain Res. 241, 57–65.

Bundgaard, M. and Cserr, H. (1981) A glial blood-brain barrier in Elasmobranchs. Brain Res. 226, 61–73.

Butt, A.M. and Jones, H.C. (1992) Effect of histamine and antagonists on electrical resistance across the blood-brain barrier in rat brain-surface microvessels. Brain Res. 569, 100–105.

Butt, A.M., Jones, H.C. and Abbott, N.J. (1990) Electrical resistance across the blood-brain barrier in anaesthetized rats: A developmental study. J. Physiol. 429, 47–62.

Carson, M.R., Shasby, S.S. and Shasby, D.M. (1989) Histamine and inositolphosphate accumulation in endothelium: cAMP and a G protein. Am. J. Physiol. 257, L259–L264.

Catalán, R.E., Martínez, A.M., Aragonés, M.D. and Díaz, G. (1989a) Evidence for a regulatory action of vanadate on protein phosphorylation in brain microvessels. Biochem. Biophys. Res. Comm. 163, 771–779.

Catalán, R.E., Martínez, A.M., Aragonés, M.D. and Fernández, I. (1989b) Substance P stimulates translocation of protein kinase C in brain microvessels. Biochem. Biophys. Res. Comm. 164, 595–600.

Crone, C. and Olesen, S.P. (1982) Electrical resistance of brain microvascular endothelium. Brain Res. 241, 49–55.

DeBault, L.E. (1981) γ-Glutamyl transpeptidase induction mediated by glial foot processes-to endothelium contact in co-culture. Brain Res. 220, 432–435.

DeBault, L.E. and Cancilla, P.A. (1979) γ-glutamyl transpeptidase in isolated brain endothelial cells: Induction by glial cells in vitro. Science 207, 653–655.

Dux, E., Temesvári, P., Szerdahelyi, P., Nagy, Á., Kovács, J. and Joó, F. (1987) Protective effect of antihistamines on cerebral oedema induced by experimental pneumothorax in newborn piglets. Neuroscience 22, 317–321.

Guillot, F.L. and Audus, K.L. (1990) Angiotensin peptide regulation of fluid-phase endocytosis in brain microvessel endothelial cell monolayer. J. Cerebr. Blood Flow Met. 10, 827–834.

Joó, F. (1972) Effect of N^6, O^6-dibutyril cyclic 3', 5'-adenosine monophosphate on the pinocytosis of brain capillaries in mice. Experientia 28, 1470–1471.

Joó F. (1985) The blood-brain barrier in vitro: Ten years of research on microvessels isolated from the brain. Neurochem. Int. 7, 1–25.

Joó F. (1986) New aspects to the function of cerebral endothelium. Nature 321, 197–198.

Joó F. (1992) The cerebral microvessels in tissue culture, an update. J. Neurochem. 58, 1–17.

Joó F., Temesvári, P. and Dux, E. (1983) Regulation of the macromolecular transport in the brain microvessels: The role of cyclic GMP. Brain Res. 278, 165–174.

Karnushina, I., Spatz, M. and Bembry, J. (1982) Cerebral endothelial cell culture. I. The presence of β_2 and α_2-adrenergic receptors linked to adenylate cyclase activity. Life Sci. 30, 849–858.

Karnushina, I.L., Palacios, J.M., Barbin, G., Dux, E., Joó, F. and Schwartz, J.C. (1980) Studies on a capillary-rich fraction isolated from brain: Histaminic components and characterization of the histamine receptors linked to adenylate cyclase. J. Neurochem. 34, 1201–1208.

Kempski, O., Villacara, A., Spatz, M., Dodson, R.F., Corn, C., Merkel, N. and Bembry, J. (1987) Cerebromicrovascular endothelial permeability. In vitro studies. Acta Neuropathol. 74, 329–334.

Mackie, K., Lai, Y., Nairn, A.C., Greengard, P., Pitt, B.R. and Lazo, J.S. (1986) Protein phosphorylation in cultured endothelial cells. J. Cell Physiol. 128, 367–374.

Markovac, J. and Goldstein, G.W. (1988) Transforming growth factor beta activates protein kinase C in microvessels isolated from immature rat brain. Biochem. Biophys. Res. Comm. 150, 575–582.

Nishizuka, Y. (1984) Studies and perspectives of protein kinase C. Science 233, 305–312.

Oláh, Z., Novák, R., Lengyel, I., Dux, E. and Joó, F. (1988) Kinetics of protein phosphorylation in microvessels isolated from rat brain: Modulation by second messengers. J. Neurochem. 51, 49–56.

Oldendorf, W.H. (1977) The blood-brain barrier. Exp. Eye Res. 25 Suppl. 177–190.

Pardridge, W.M. (1988) Recent advances in blood-brain barrier transport. Ann. Rev. Pharmacol. Toxicol. 28, 25–39.

Pardridge, W.M., Yang, J. and Eisenberg, J. (1985) Blood-brain barrier protein phosphorylation and dephosphorylation. J. Neurochem. 45, 1141–1147.

Revest, P.A., Abbott, N.J. and Gillespie, J.I. (1991) Receptor mediated changes in intracellular Ca^{2+} in cultured rat brain capillary endothelial cells. Brain Res. 549, 159–161.

Rotrosen, D. and Galline, J.I. (1986) Histamine type I receptor occupancy increases endothelial cytosolic calcium, reduces F-actin, and promotes albumin diffusion across cultured endothelial monolayers. J. Cell Biol. 103, 2379–2387.

Sen, H.A. and Campochiaro, P.A. (1991) Stimulation of cyclic adenosine monophosphate accumulation causes breakdown of the blood-retinal barrier. Invest. Ophth. and Visual Sci. 32, 2006–2010.

Stelzner, T.J., Weil, J.V. and O'Brien, R.F. (1989) Role of cyclic adenosine monophosphate in the induction of endothelial barrier properties. J. Cell Physiol. 139, 157–166.

Stern, L. and Peyrot, R. (1927) Le fonctionnement de la barrière hématoencéphalique aux divers stades de développement chez diverses espèces animales. C. r. séance. Soc. Biol. 96, 1124–1126.

Stewart, P.A. and Hayakawa, E.M. (1987) Interendothelial junctional changes underlie the developmental "tightening" of the blood-brain barrier. Dev. Brain Res. 32, 271–281.

Stewart, P.A. and Wiley, M. (1981) Developing nervous tissue induces formation of blood-brain barrier characteristics in invading endothelial cells: A study using quail-chick transplantation chimeras. Dev. Biol. 84, 183–192.

Tao-Cheng, J.H., Nagy, Z. and Brightman, M.W. (1987) Tight junctions of brain endothelium in vitro are enhanced by astroglia. J. Neurosci. 7, 3293–3299.

Weber, M., Mehler, M. and Wollny, E. (1987) Isolation and partial characterization of a 56,000-dalton phosphoprotein phosphatase from the blood-brain barrier. J. Neurochem. 49, 1050–1056.

Neurobiology 1 (1), pp. 11–31, 1993

FINE STRUCTURAL CHARACTERIZATION OF THE OLFACTORY EPITHELIUM AND ITS RESPONSE TO DIVALENT CATIONS Cd^{2+} IN THE FISH ALBURNUS ALBURNUS (TELEOSTEI, CYPRINIDAE): A SCANNING AND TRANSMISSION ELECTRON MICROSCOPIC STUDY

L. Hernádi

Balaton Limnological Research Institute of the Hungarian Academy of Sciences,
H–8237 Tihany, Váralja u. 18, Hungary

Summary: The olfactory organ of the fish *Alburnus alburnus* consists of 22 lamellae arranged into rosette like structure and are built up by supporting, gland, basal, ciliated and unspecialized epithelial cells, as well as receptor cells with microvillous, ciliated or rod shape dendritic endings. The spatial distribution of the supporting and gland cells can be considered homogeneous while the ciliated epithelial cells are dominant on the latero-marginal areas of the lamellae with a 10±3/1000 μm^2 average density. The occurrence frequency of the ciliated receptor cells is the highest in the medial area with a 30±6/1000 μm^2 average density while the microvillous receptor cells have the highest occurrence frequency in the dorso-marginal area of the olfactory lamellae with a 25±15/1000 μm^2 average density. Rod shape sensory dendrites were detected with a negligible density. The presence of divalent cations Cd^{2+} in the environment significantly increased the density of rod shape sensory dendrite 19.8±7.7/1000 μm^2. These results demonstrate that the appearance and composition of the population of sensory dendrites on the olfactory lamellae are affected by environmental factors.

INTRODUCTION

The structure and organization of the olfactory organs of fishes show different appearances that is an adaptation to the available space in the olfactory cavity during the

phylogenesis (Zeiske, 1973; 1974; Breucker et al., 1979). The Cyprinidae fishes have numerous olfactory lamellae that are organized into rosette like structure in the olfactory cavity contrary to the Cyprinidontiformes that have no lamellae in the olfactory cavity. The increase of the number of the olfactory lamellae enlarges the sensory area and the efficacy of the olfaction (Zeiske, 1973; 1974; Zeiske et al., 1976; 1979). During the lifetime of the fishes the olfaction plays the most important role in the general survey of the environment in the food searching as well as in the homing behavior (Oshima et al., 1969). In the olfactory epithelium a huge number of primary sensory neurons can be found appearing as ciliated, microvillous and rod shape sensory cells. According to the electrophysiological studies on the olfactory epithelium of different fish species, the sensory neurons show high sensitivity to different chemical compounds as amino acids and bile acids (Hara, 1976; Caprio, 1978; Thommesen, 1978; Doving et al., 1980; Thommesen, 1983; Getchell, 1986). Earlier it was suggested that the different sensory cells can be considered as different functional and structural entities with different sensitivity to an external stimuli (Bronshtein and Minor, 1977; Thommesen, 1982; Yamamoto, 1982), while Yamamoto (1982) suggested that the environmental factors are able to change the appearance and composition of the sensory dendrite population of the olfactory epithelium. This study was undertaken to describe the scanning and transmission electron microscopical appearance and the spatial distribution of the different cell types constituting the olfactory lamellae of cyprinid *Alburnus alburnus*. Furthermore, this study investigate the response of different receptor dendrites to the presence of a new environmental factor the divalent cation Cd^{2+}.

MATERIALS AND METHODS

For the experiments the adult specimens of the *Alburnus alburnus* with 70–90 mm length and 6–7 g body weight were used. The fish were kept in aquarium in normal lake water. A group of fish was kept in aquarium containing 1μM $CdCl_2$. From the Cd treated animals samples were taken after two weeks and 1 month. From the control animals samples were taken randomly and also simultaneously with the sampling of Cd treated animals. After decapitation of the animals the olfactory organs were removed from the olfactory cavity in cold fixative containing 2.5% glutaraldehyde buffered with 0.1 M sodium cacodilate (pH 7.4) and cut for lamellae. Thereafter the small samples were fixed in fresh fixative for three hours at 4 °C. After short washing the samples were postfixed in 1.5% OsO_4 buffered with 0.1 M

s-collidine (pH 7.4) for two hours at 4 °C. After fixation the samples were separated into three groups.

For scanning electron microscopy the first group of samples were dehydrated in increasing ethanol series (50, 70, 90, 96, 100%) and through isoamylacetate were dried in Balzers critical point drier. The dried samples were covered with gold and investigated in TESLA BS 300 scanning electron microscope.

For transmission electron microscopy the second group of samples were dehydrated in increasing ethanol series (50, 70, 90, 96, 100%) and were contrasted in blocks in 70% ethanol saturated with uranyl acetate. The samples were embedded into Spurr medium through propyleneoxide.

After washing in buffer the third group of samples was contrasted in 1% tannic acid buffered with 0.05 M sodium cacodilate (pH 7.4) for one hour at room temperature. Thereafter, the samples were washed in the same buffer (3x30 min) and dehydrated in ethanol and embedded into Spurr medium. The embedded samples were cut and the thin sections were contrasted with lead citrate and investigated with TESLA BS 500 electron microscope.

RESULTS

According to the scanning electron microscopical study the olfactory organ appears as paired structure situated in the bottom of the olfactory cavity rostral to the eyes. The olfactory organ consists of 22 lamellae radially arranged along a raphe forming a rosette-like structure (Fig. 1). On the dorso-marginal areas of the lamellae undifferentiated epithelial cells possessing a microridge system on their surfaces form a fingerprint like structure (Fig. 2). On the latero-marginal area of the lamellae among the undifferentiated epithelial cells ciliated epithelial cells and gland cell openings can be observed. The inner zones of the lamellae surrounded by marginal areas are occupied by supporting cells and ciliated epithelial cells as well as by sensory dendrites (Figs. 2, 3, 4).

Characterization of the different cell types building up the olfactory lamellae

Supporting cells give the basic structure of the lamellae having a microridge system on their surfaces usually covered by mucous material (Fig. 4). In some cases supporting cells having microvilli on their surfaces can also be observed (Fig. 3).

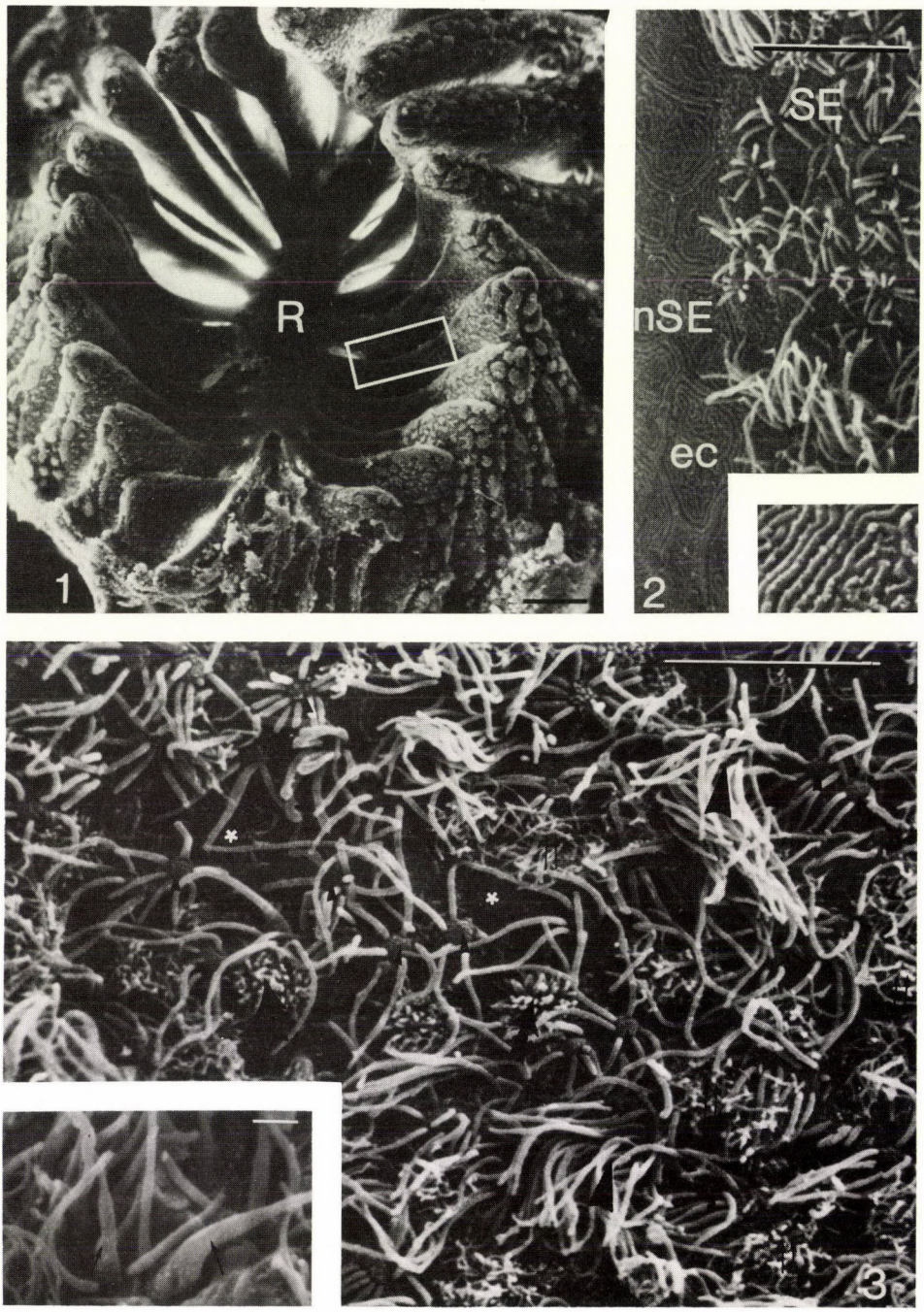
R
1
SE
nSE
ec
2
3

Ciliated epithelial cells are arranged sometimes in regular rows sometimes in random arrangement. Their density increases toward the latero-marginal direction (10±3/1000 μm^2) comparing to the medial areas (7±14/1000 μm^2). The 18–25 μm long cilia are arranged into regular rows on their surfaces (Figs. 3, 4).

The sensory dendrites of the primary sensory neurons run to the surface of the lamellae between the supporting cells and end in ciliated, microvilliated knob or rod-like endings (Figs. 3, 4). The ciliated sensory dendrites are the most frequently observed dendritic type on the surface of the olfactory lamellae. The cilia originate from a knob region emerged out from the supporting cell level and are observed in a radial arrangement on the knobs (Figs. 3, 4). The number and length of the cilia are different on the knobs. Usually if the number of cilia is lower on the knobs the lengths of cilia are shorter than on that knobs having higher number of cilia (Fig. 4). Most frequently the knobs having 5–6 cilia with 15-20 μm lengths can be observed. The spatial distribution of the ciliated sensory dendrites on the surface of the olfactory lamellae can be considered homogeneous with a 30±6/1000 μm^2 average density but sometimes extremely high density can be observed reaching the 120±17/1000 μm^2. On the surface of the lamellae small separated areas can frequently be observed where small knobs with 3–4 short outgrowing cilia can be seen (Fig. 5).

Figs. 1–5: The scanning electronmicroscopical view of the olfactory organ and olfactory lamellae.
Fig. 1: The olfactory lamellae are radially arranged around a central raphe (R) and they built up a rosette like structure in the olfactory cavity. Calibration bar represents 100 μm.
Fig. 2: The nonsensory epithelium (nSE) on the dorso-marginal area of the lamellae (enframed on Fig. 1) is built up by unspecialized epithelial cells (ec) that limit the sensory epithelium (SE) with a sharp boundary. Calibration bar represents 10 μm. **Insert**: The high magnification of the fingerprint structure demonstrates the fine ridges on the surface of the unspecialized epithelial cells. Calibration bar represents 1 μm.
Fig. 3: The ciliated (small arrowheads) and microvillous (double arrows) receptor dendrites as well as the ciliated epithelial cells (large arrowheads) and the microvillar supporting cells (large arrows) are located among the nonmicrovillar supporting cells (asteriscs) that give the basal structure of the sensory epithelium. Calibration bar represents 10 μm. **Insert**: Rarely rod-like receptor dendrite (arrow) can be detected among the ciliated dendrites. Calibration bar represents 1 μm.

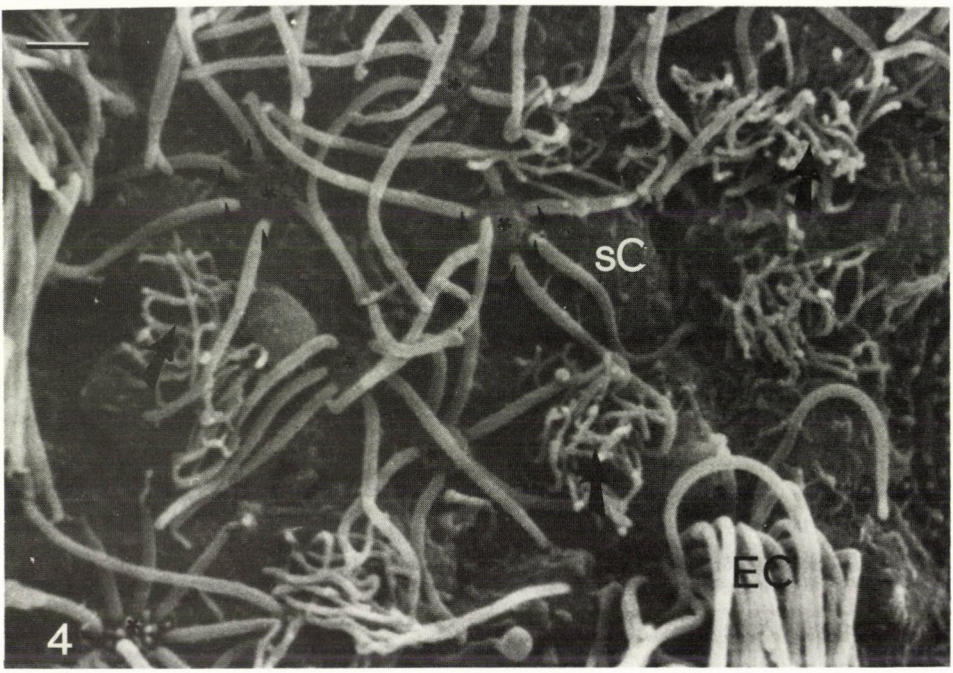
sC
EC
4

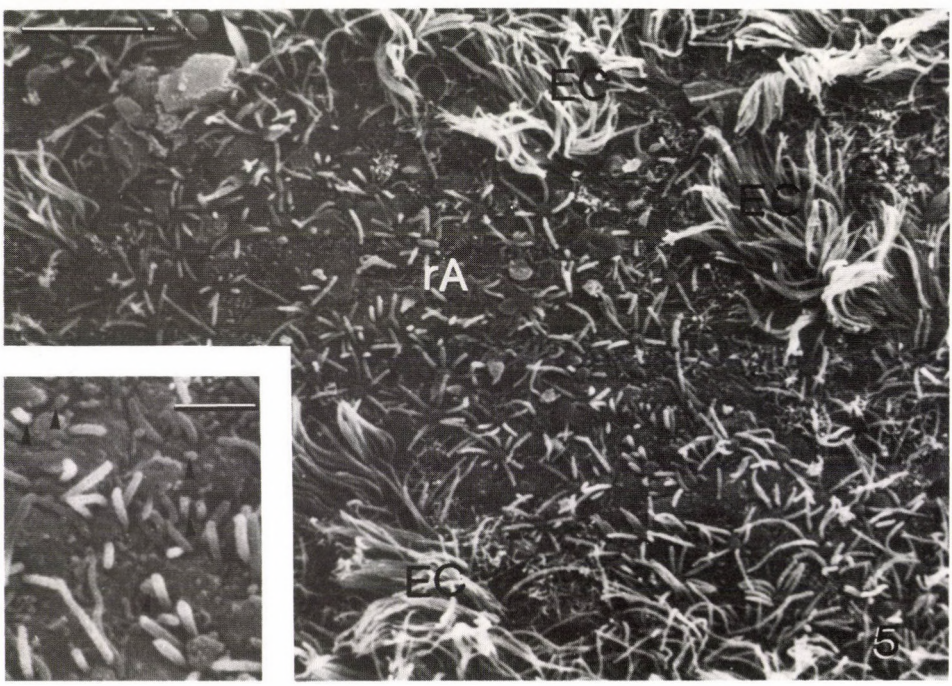
EC
EC
rA
EC
5

Microvillar sensory dendrites end in a slightly concave endings under the surface level of the supporting cells and possess numerous microvilli in a random arrangement on their surface (Figs. 3, 4). The spatial distribution of the microvillar sensory dendrites is inhomogeneous on the lamellar surface. Usually grouped in spots (Fig. 3) that are frequently observed in the dorso-marginal part of the lamellae. They can be observed with a 25±15/1000 μm^2 average density in the spots. In the medial area of the lamellae their average density is approximately 12±8/1000 μm^2. The observed density of the microvillar sensory dendrites is higher on the olfactory lamellae of the spawning fish than that observed on fishes taken during nonspawning seasons. The highest density counted during the spawning season reached the 45±20/1000 μm^2 in the spots on the dorso-marginal area of lamellae.

Rod-like sensory dendrites can be observed only randomly between the ciliated sensory dendrites mostly in the medial area of the olfactory lamellae (Fig. 3). To give an estimation on their occurrence frequency is difficult because of the high density of the ciliated sensory dendrites around them. Their approximate density is 300–500/mm^2.

According to the transmission electron microscopical observation the olfactory lamellae are constituted by supporting cells, undifferentiated and ciliated epithelial cells, gland cells, basal cells, as well as sensory cells situated on the basal lamina (Fig. 6).

Fig. 4: The high magnification scanning micrograph shows that the receptor dendrites arise from the level of the supporting cells (sC) that are covered with mucus. The radially arranged sensory cilia (arrowheads) originate from the knob regions (asteriscs), while the cilia on the epithelial cells (EC) are arranged in regular rows. The microvillous receptor dendrites have their microvilli (arrows) in a random arrangement. Calibration bar represents 1 μm.
Fig. 5: An area on the sensory epithelium is undergoing cell renewal (rA), while the neighbouring areas show normal appearance. In the regrowing area ciliated epithelial cells (EC) can not be observed. Calibration bar represents 10 μm. **Insert**: At higher magnification the short outgrowing cilia (arrowheads) on the sensory knobs are well visible. Calibration bar represents 5 μm.

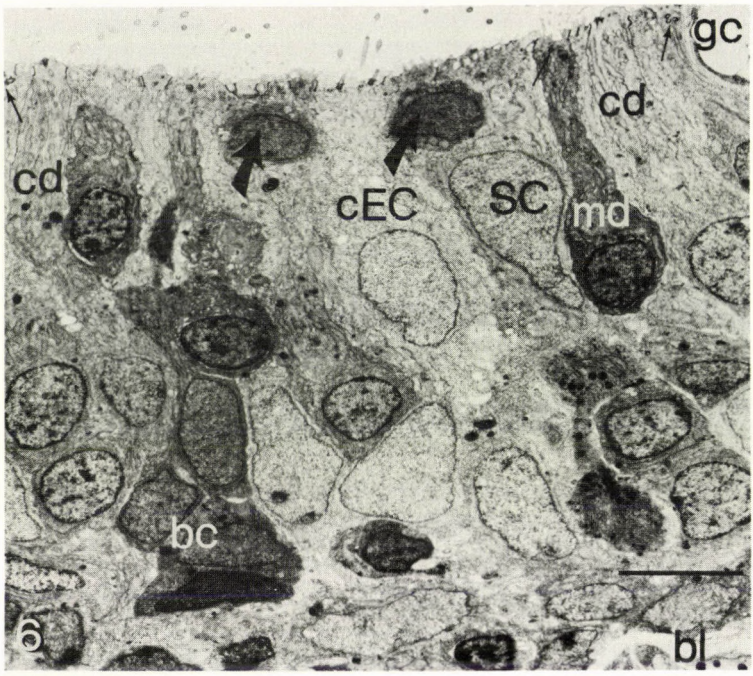

6

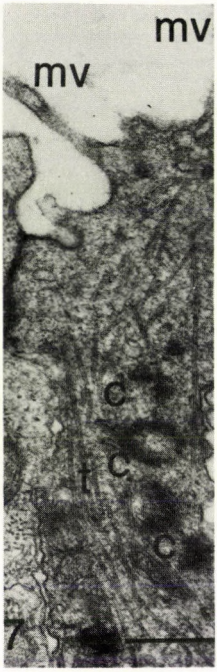

7

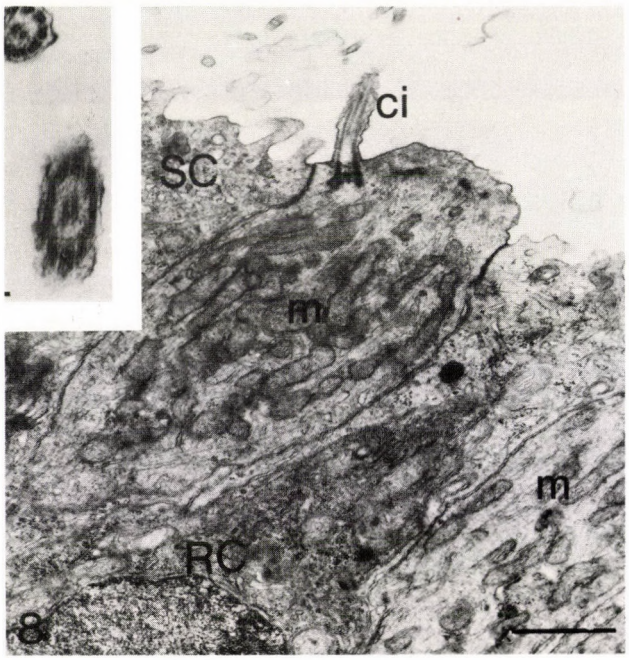

8

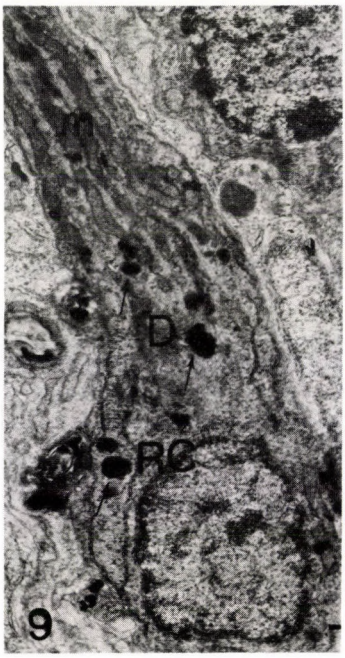

9

Supporting cells are the dominant cell type of the olfactory lamellae having two type of appearance. The supporting cells having a microridge system on their apical surfaces are the dominant type (Figs. 8, 14) while the cells having microvilli on their apical surface can be observed only scarcely (Fig. 16). In the apical part of the supporting cells numerous vacuoles enclosing fibrous material as well as numerous mitochondria can be observed (Figs. 8, 14). The supporting cells are joined to the neighbouring cells with characteristic junctional structures (septate desmosomes, zonula adherens) which is typical for all the cell types constituting the lamellae.

Ciliated epithelial cells have numerous cilia located in regular rows running parallel with each other on their apical surfaces (Figs. 6, 15). The cilia originate from basal bodies possessing long root with a characteristic angle to each other. The cilia have a 9+2 tubular system at their proximal portion while distally they may loss tubule. In the cytoplasm numerous mitochondria can be seen in the apical part grouped near the basal bodies (Fig. 15).

Figs. 6–9: Normal transmission electronmicroscopical appearance of the olfactory epithelium.
Fig. 6: In the epithelium ciliated epithelial cells (cEC), supporting cells (SC), gland cells (gc), receptor cells with ciliated (cd) or microvilliar (md) receptor dendrites, as well as basal cells (bc) can be identified located on the basal lamina (bl). Small arrows show the centrioles in the apex of the microvilliar dendrites. Large arrows show degenerated receptor cells. Calibration bar represents 5 μm.
Fig. 7: The microvillous receptor dendrites have numerous microvilli (mv), centrioles (c) and microtubules (arrowheads) in their apical parts. Calibration bar represents 0.5 μm.
Fig. 8: The ciliated receptor dendrites have numerous cilia (ci) and in their apical segments numerous mitochondria (m) can be observed. RC: receptor cell, SC: supporting cell. Calibration bar represents 1 μm. **Insert**: The 9+2 tubular structure of the sensory cilia is well demonstrated. Calibration bar represents 0.1 μm.
Fig. 9: The dendritic process (D) of the mature receptor cells (RC) originates with a broad proximal segment containing numerous mitochondria (m) and small dense cytosomes (arrows). Calibration bar represents 1 μm.

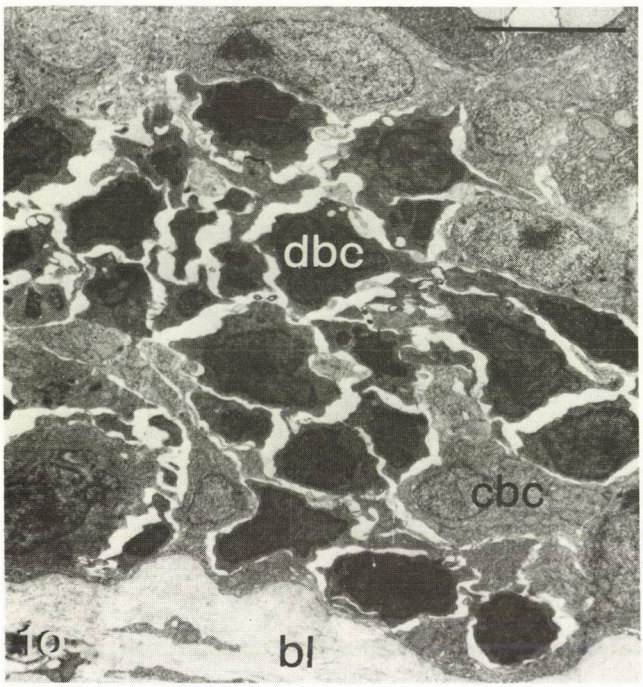

10

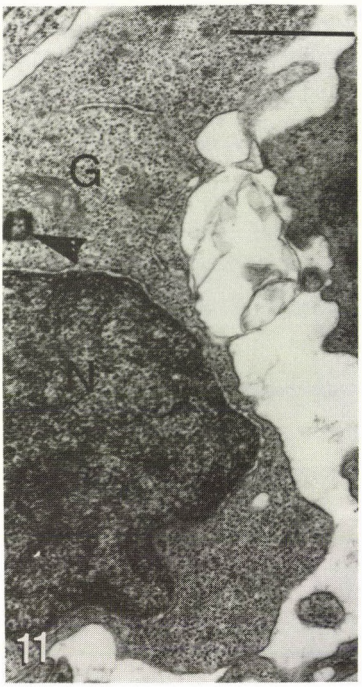

11

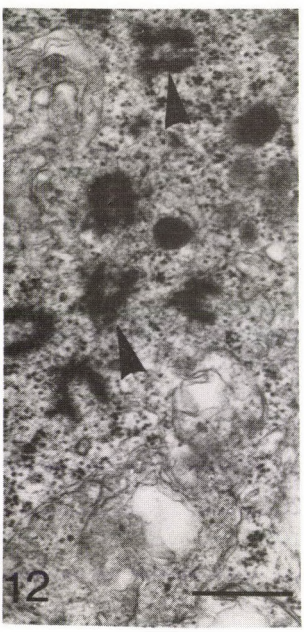

12

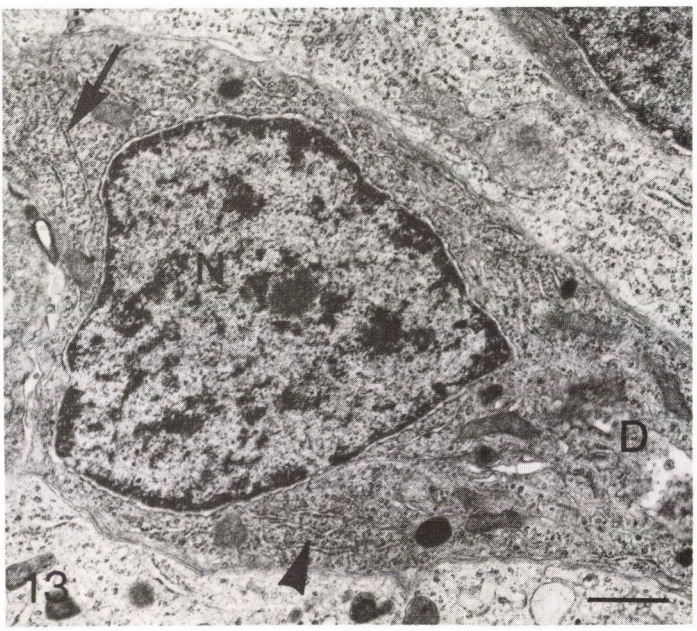

13

The somata of the primary olfactory sensory neurons can be observed in different depth of the olfactory lamellae appearing with different cytoplasmic density (Fig. 6). The bipolar sensory neurons send axons to the fila olfactoria and their sensory dendrites end in knobs at the surface of the lamellae. The knobs may have cilia or microvilli on their surfaces (Fig. 6). The sensory cilia are arranged on the knobs in a radial arrangement and have 9+2 tubular system at their proximal segments (Fig. 8). The sensory microvilli originate from the apical membrane of the knob in a random arrangement (Fig. 7). In their distal dendrite segments single or grouped centrioles are frequently observed (Figs. 6, 7). In the dendrites usually numerous neurotubules and mitochondria can be observed. The number of SER elements and multivesicular bodies are different in each sensory dendrites. The sensory cell somata usually show dense cytoplasm with numerous dense cytosomes (Figs. 9, 13). Only a few somata with a low density cytoplasm can be detected. The RER elements in the sensory neurons have a characteristic arrangement both in their perikaryon and proximal dendrite segments (Figs. 9, 13).

Figs. 10–13: The ultrastructural appearance of the different developmental stages of the receptor cells.
Fig. 10: Over the basal lamina (Bl) numerous dark (dBC) and clear (cBC) basal cells can be seen with numerous cytoplasmic protrusions. Calibration bar represents 5 μm.
Fig. 11: The cytoplasm of the basal cell is poor in cell organelles but has a high number of homogeneously distributed ribosomes. Rarely centrioles (arrowhead) can be observed in the perikaryon. G: Golgi apparatus, N: nucleus. Calibration bar represents 1 μm.
Fig. 12: In the maturing receptor cells the ribosomes are clumped together and sometimes have numerous centrioles (arrowheads). Calibration bar represents 0.5 μm.
Fig. 13: The mature receptor cell bodies have well developed rough endoplasmic reticular system in both their perikaryon (arrowhead) and their axonal origin (arrow). D: proximal dendrite segment. Calibration bar represents 1 μm.

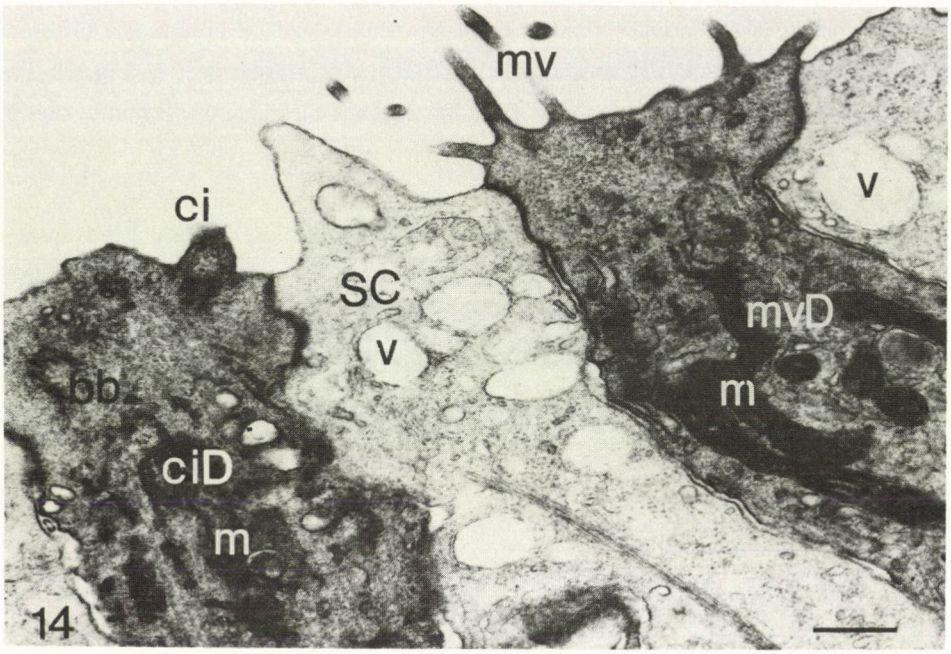
mv
ci
SC
v
v
mvD
m
bb
ciD
m
14

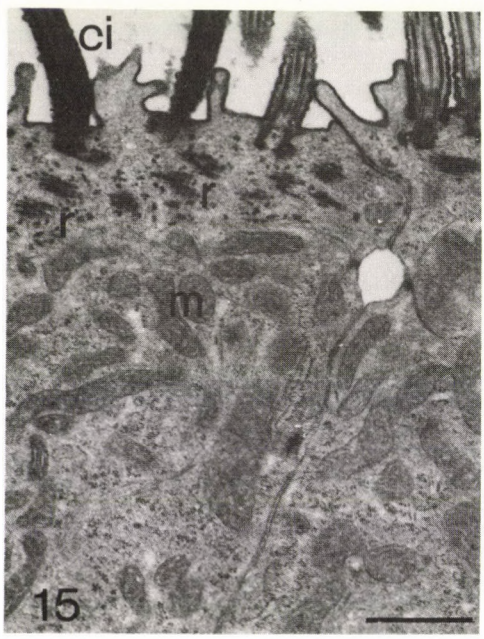
ci
r
r
m
15

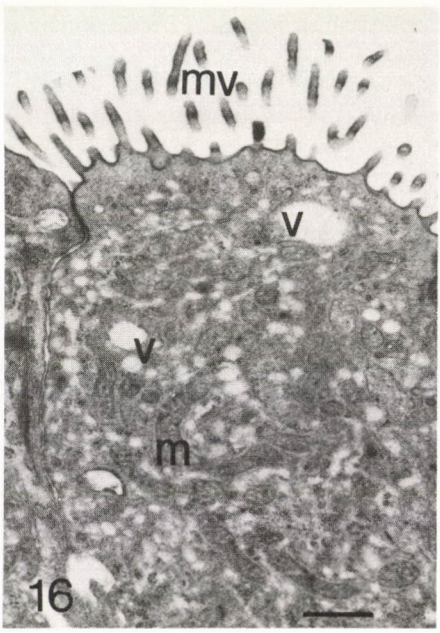
mv
v
v
m
16

The basal cells are situated on the basal lamina randomly (Fig. 6) but sometimes they can be found in groups (Figs. 10, 11). Their most characteristic ultrastructural features are the extremely high number of ribosomes giving a dense character of the narrow cytoplasm. Frequently they have numerous cytoplasmic protrusions (Figs. 10, 11). In the perikaryon of the few dark cells clumped ribosomes and few cell organelles can be observed (Fig. 12). In this area, in cases, cells undergoing mitosis can be observed.

According to the tannic acid fixation the different cell membranes behave differently to the tannic acid treatment. The dendritic membranes can be penetrated by tannic acid and therefore they show dense appearances treatment (Fig. 14). The supporting cell membranes can not be penetrated only bind tannic acid on their outer membrane surface (Fig. 14). The microvillous supporting cells can be penetrated by tannic acid and show dense appearance (Fig. 16). The ciliated epithelial cells show different appearances after tannic acid treatment. Most of them can be penetrated mainly through their cilia (Fig. 15) while others bind tannic acid only on their outer membrane surface.

Figs. 14–16: The sensitivity of apical membranes of the different cell types to tannic acid treatment.
Fig. 14: Both the ciliated (ciD) and the microvillous (mvD) dendrite membranes are permeable to, while the supporting cell membrane (SC) is not permeable to tannic acid. Calibration bar represents 1 μm.
Fig. 15: The cilia (ci) of the ciliated epithelial cell are the most sensitive part of the cells. Calibration bar represents 1 μm.
Fig. 16: The microvilli (mv) of the microvillous epithelial cell are also permeable to tannic acid. bb: basal body, m: mitochondrium, v: vacoulae. Calibration bar represents 1 μm.

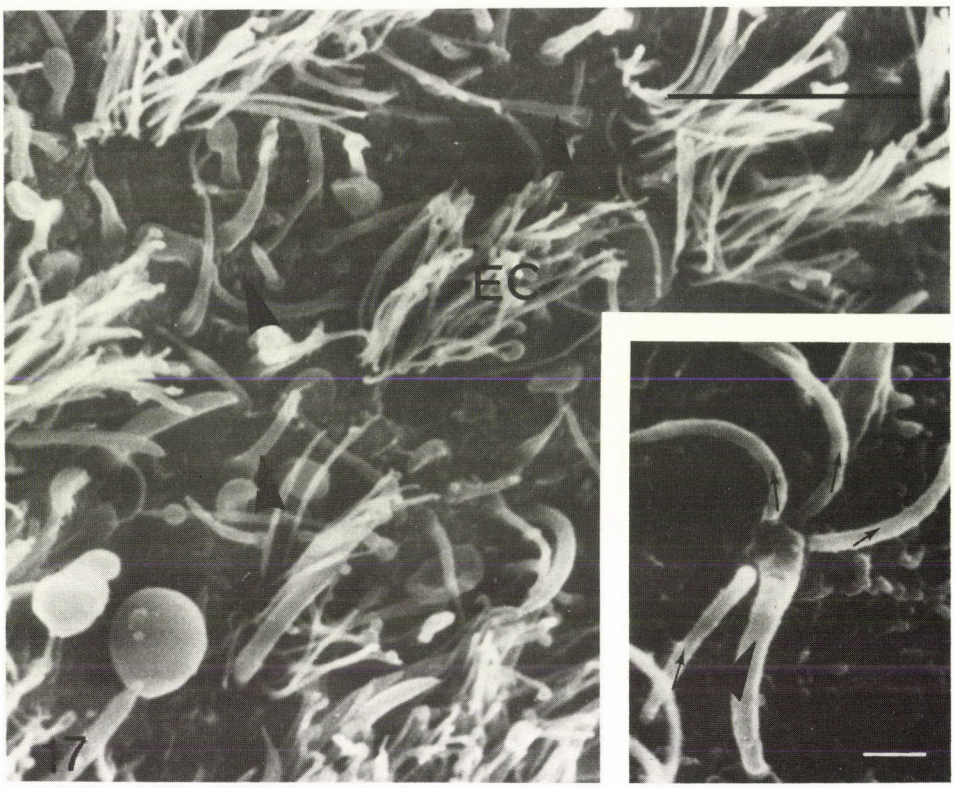
EC
7

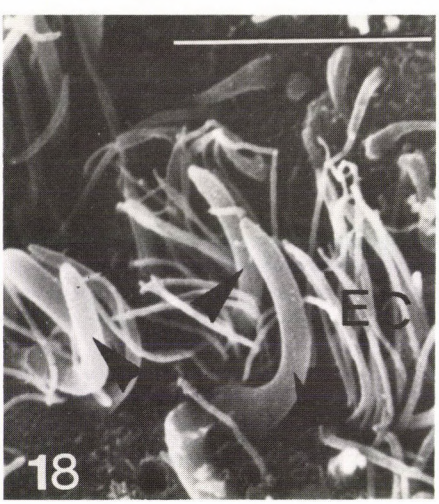
EC
18

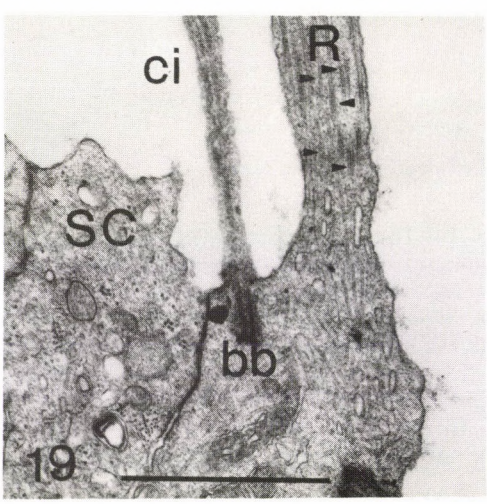
ci
R
SC
bb
19

Cadmium induced changes in the appearance and composition of the different types of sensory dendrites

After two weeks of Cd^{2+} exposition the most outstanding changes can be detected in the appearance of sensory dendrites (Figs. 17, 19). The number of rod shape dendrites has increased (19.8±7.7/1000 μm^2) and became dominant to both the ciliated (13.6±4.6/1000 μm^2) and the microvillous dendrites (4.5±3.8/1000 μm^2) (Fig. 17). Frequently the ciliated epithelial cells also show rod like appearance (Fig. 18). In the presence of Cd^{2+} the ciliated receptor dendrites are transformed into rod shape dendrites that can be observed in both scanning (Fig. 17) and transmission electron microscopic micrographs (Fig. 19).

DISCUSSION

The number and shape of the olfactory lamellae are related to the space available in the olfactory cavity of the fish and therefore represent adaptation which maximize the sensory area under the given restriction (Zeiske, 1973; 1974). The olfactory epithelia of the bleak consisting 22 lamellae arranged into rosette like structure adapted maximal to the space available and is similar to other cyprinid olfactory epithelia that belongs to the type VI

Figs. 17–19: Cadmium induced changes in the appearance of the olfactory epithelium.
Fig. 17: The presence of Cd^{2+} increases the occurrence frequency of the rod shape sensory dendrites (arrowheads). EC: ciliated epithelial cell. Calibration bar represents 10 μm. **Insert**: Some of the receptor dendrites show transitional form between the normal ciliated and the rod shape dendrite. They have a rod (arrowhead) and additionally free cilia (arrows). Calibration bar represents 1 μm.
Fig. 18: The ciliated epithelial cells can also be observed in rod shape appearance (arrowheads). EC: normal ciliated epithelial cell. Calibration bar represents 10 μm.
Fig. 19: In the rod (R) of the dendrite the cilia are fused and therefore, the rod has numerous tubular structures (arrowheads). bb: basal body, ci: normal cilium. Calibration bar represents 1 μm.

typified by Yamamoto and Ueda (1979a, b; Delfino et al., 1981). The distribution of the undifferentiated and sensory epithelia on the surface of the lamellae show large variety in the different fish species (Yamamoto and Ueda, 1979a, b; Yamamoto 1982). The olfactory epithelia of the bleak belongs to that type of olfactory epithelia where the undifferentiated epithelia is restricted to the marginal areas of the lamellae (Yamamoto and Ueda, 1979a, b). In the olfactory epithelium of the fishes, similarly to other vertebrate species (Halász, 1990), three types of sensory dendrites have been described as ciliated, microvillous as well as rod shape sensory dendrites. Usually the ciliated and microvillous sensory dendrites are dominant while the rod shape dendrites can rarely be observed. In teleost fishes both ciliated and microvillous sensory dendrites occur together but in different proportion in the different species. However, there are species possessing purely microvillar sensory dendrites as in Elasmobranchiate species (Reese and Brightman, 1970; Theisen, 1972) or purely ciliated sensory dendrites as in the lamprey (Thornhill, 1967). Our results demonstrate that on the bleak olfactory epithelia the ciliated sensory cells are the dominant to the microvillous sensory dendrites while the rod shape sensory dendrites occur only randomly in a very low number. According to the observation on the olfactory epithelia of *Scualus acanthias* Bakhtin supposed that the microvillar sensory dendrites can be considered as progenitors of the ciliated sensory dendrites (Bakhtin, 1977) but transient stages have been found neither in Acipenserid fishes as in sturgeon (Pyatkina, 1976), in rainbow fish (Breucker et al., 1979), nor in rainbow trout (Evans et al., 1982). Since in the apical parts of the microvillous sensory dendrites centrioles can frequently be observed it was supposed that the microvillous sensory dendrites originate from the ciliated sensory dendrites (Delfino et al., 1981) where the cilia-formation of centrioles are blocked as it was also observed in reptiles and mammals (Kolnberg and Altner, 1971). According to other ideas the ciliated and microvillous sensory cells originate from a stem cell. If centrioles are prevented to develop cilia the cells appear as microvillous sensory cells, therefore the two types of sensory cells represent different functional and structural entities (Pyatkina, 1976; Bronshtein and Minor, 1977; Thommesen, 1982). This hypothesis seems to be supported by the findings that the sensory cells undergo a renewal and maturation process in the fish olfactory epithelia (Evans et al., 1982) that was described first in mammals (Graziadei and Monti-Graziadei, 1979; Monti-Grazidaei and

Graziadei, 1979) and later in gastropods (Hernádi and Benedeczky, 1983; Chase and Rieling, 1986; Hernádi and Benedeczky, 1989). The maturation process can be followed well on ciliated sensory dendrites since they have in their early maturation stages short motile cilia and in their maturated stages they have long nonmotile cilia (Mair et al., 1982). In the present study the different stages of the developing ciliated dendrites were also observed on the bleak olfactory lamellae. The maturation process of the olfactory receptor neurons was also reflected in the distribution of density of intramembrane particles (IMPs) in the different parts of ciliated dendrites—cilia, knob region, lateral membrane—applying freeze-fracturing technique (Hernádi and Röhlich, 1988). The spatial distribution of the ciliated and microvillous sensory dendrites showed differences on the olfactory lamellae in catfish (Cancalon, 1982; Erickson and Caprio, 1984) in char and trout (Thommesen, 1983). The density of the microvillous sensory dendrites were the highest in the medial part of the lamellae while the density of the ciliated sensory dendrites was the highest in the lateral areas of the lamellae (Cancalon, 1982; Erickson and Caprio, 1984). On the bleak olfactory lamellae the ciliated sensory dendrites showed the highest density in the medial part of the lamellae while the microvillous sensory dendrites showed the highest density in the dorso-medial areas occurring in spots. The density of the microvillous sensory dendrites reached the highest value during spawning period. It is in good agreement with the observation on the trout olfactory lamellae that the occurrence frequency of the rod shape sensory dendrites increased when the salmon fish were in a new physiological condition (Yamamoto and Ueda, 1979). This observation suggest that the appearance of sensory dendrites as microvillous, ciliated or rod shape dendrites are affected by external or internal micro-environmental factors. In a new environment all the new stimulus molecules similarly to the specific odorant molecules are bound to the receptor molecules located dominantly in the sensory cilia and knob regions of the dendrites (Rhein and Cagan, 1981; Getchell, 1986; Lancet, 1986; Lancet and Pace, 1987; Novoselov et al., 1988; Snyder et al., 1989). They are present in the membrane of cilia and knob as intramembranous particles (Menco et al., 1976; Menco, 1980; Hernádi and Röhlich, 1988). The interaction of stimulus molecules including Cd^{2+} with IMP can induce changes in membrane permeability and channel function that can alter the appearance of olfactory receptor dendrites. This is supported by the present findings that the receptor cilia on the

knobs are fused in the presence of Cd^{2+} and the ciliated receptor dendrites appear as rod shape dendrites. The present findings that Cd^{2+} as a new environmental factor highly increased the number of the rod shape dendrites and induced unusual forms of ciliated sensory dendrites are in good accordance with the observation of Yamamoto (1982) that the number of rod shape sensory dendrites increased if salmon fish were in new environmental conditions.

REFERENCES

Altner, H. and Kolnberg, I. (1974) Freeze-fracture and tracer experiments on the permeability of the zonulae occludentes on the olfactory mucosa of vertebrates. Cell Tiss. Res. 154, 51–59.

Bakhtin, E.K. (1977) Peculiarities of the fine structure of the olfactory organ of *Scualus acanthias*. Cytologia 19, 725–731.

Breipohl, W., Bijvank, G.J. and Zippel, H.P. (1973) Scanning electron microscopy of olfactory receptors in *Carassius auratus*. Z. Zellforsch. 138, 439–454.

Breucker, H. and Zeiske, E. (1977) Eiechepithel von Fischen am Beispiel des Zahnkarpfens *Xiphophorus helleri*. Verh. Anat. Ges. 71, 1193–1196.

Breucker, H., Zeiske, H. and Melinkat, E. (1979) Development of the olfactory organ in the rainbow fish *Nematocentris maccullochi* (Atheriniformes, Melanotaeniidae). Cell Tiss. Res. 200, 53–68.

Bronshtein, A. and Minor, A.V. (1977) The regeneration of olfactory flagella and restoration of electroolfactogram after the treatment of the olfactory mucosa with triton X-100. Cytologia 19, 33–39.

Cancalon, P. (1982) Degeneration and regeneration of olfactory cells induced by $ZnSO_4$ and other chemicals. Tiss. Cell 14, 717–733.

Caprio, J. (1978) Olfaction and taste in the channel catfish: An electrophysiological study of the response to amino acids and derivatives. J. Comp. Physiol. 123, 357–371.

Caprio, J. (1984) Olfaction and taste in fish. In: Comparative Physiology of Sensory System /Bolis, L., Keyness, R.D. and Madrell, S.H.P.; eds./ pp. 257–283, Cambridge Univ. Press.

Chase, R. and Rieling, J. (1986) Autoradiographic evidence for receptor cell renewal in the olfactory epithelium of a snail. Brain Res. 384, 232–239.

Delfino, G., Bianchi, S. and Ercolini, A. (1981) On the olfactory epithelium of cyprinids: A comparison between hypogean and epigean species. Monitore Zool. Ital. Suppl. 14, 153–180.

Doving, K.B., Selset, R.E. and Thommesen, G. (1980) Olfactory sensitivity to bile acids in salmonid fishes. Acta Physiol. Scand. 108, 191–194.

Erickson, J.R. and Caprio, J. (1984) The spatial distribution of ciliated and microvillous olfactory receptor neurons in the channel catfish is not matched by differential specificity to amino acid and bile salt stimuli. Chem. Senses 9, 127–141.

Evans, R.E., Zielinski, B., Hara, T.J. (1982) Development and regeneration of the olfactory organ in rainbow trout. In: Chemoreception in Fishes. /Hara, T.J.; ed./ pp. 15–37, Elsevier, Amsterdam.

Gemme, G. and Doving, K.B. (1969) Ultrastructural properties of primary olfactory neurons in fish *Lota lota* L. Am. J. Anat. 126, 457–476.

Getchell, V.T. (1986) Functional properties of vertebrate olfactory receptor neurons. Physiol. Rev. 66, 772–818.

Graziadei, P.P.C. and Monti-Graziadei, G.A. (1979) Neurogenesis and Neuron regeneration in the olfactory system of mammals. I. Morphological aspects of differentiation and structural organization of the olfactory sensory neurons. J. Neurocytol. 8, 1–18.

Halász, N. (1990) The Vertebrate Olfactory System. Akadémiai Kiadó, Budapest.

Hara, T.J. (1976) Structure-activity relationships of amino acids in fish olfaction. Comp. Biochem. Physiol. 54A, 31–36.

Hernádi, L. and Röhlich, P. (1988) Freeze-fracture study of the receptor membranes in the olfactory organ of *Alburnus alburnus* (Teleostei). Zoomorph. 108, 41–46.

Hernádi, L. and Benedeczky, I. (1983) A comparative ultrastructural analysis on the occurrence of cilia in the tentacles and lip of *Helix pomatia*, applying serial ultrathin sectioning. Acta Biol. Hung. 34, 55–62.

Hernádi, L. and Benedeczky, I. (1989) Receptor cell renewal in the sensory epithelia of the lip of the snail *Helix pomatia* L. Acta Biol. Szeged 35, 115–120.

Ichikawa, M. and Ueda, K. (1977) Fine structure of the olfactory epithelium in the goldfish, *Carrassius auratus*. A study of retrograde degeneration. Cell Tiss. Res. 183, 445–455.

Kolnberg, I. and Altner, H. (1971) Ciliary-structure precursor bodies as stable constituents in the sensory cells of the vomero-nasal organ of reptiles and mammals. Z. Zellforsch. 118, 254–262.

Lancet, D. (1986) Vertebrate olfactory reception. Ann. Rev. Neurosci. 7, 35–38.

Lancet, D. and Pace, V. (1987) The molecular basis of odor recognition. Trends Biochem. Sci. 12, 63–66.

Mair, R.G., Gesteland, R.C. and Blank, D.L. (1982) Changes in morphology and physiology of olfactory receptor cilia during development. Neuroscience 7, 3091–3103.

Menco, B. Ph. (1980) Qualitative and quantitative freeze-fracture studies on olfactory and nasal respiratory epithelial surfaces of frog, ox, rat, and dog. IV. Ciliogenesis and ciliary necklaces. Cell Tiss. Res. 212, 1–16.

Menco, B.Ph., Dodd, G.H., Davey, M. and Bannister, L.H. (1976) Presence of membrane particles in freeze-etched bovine olfactory cilia. Nature 263, 597–599.

Monti-Graziadei, G.A. and Graziadei, P.P.C. (1979) Neurogenesis and neuron regeneration in the olfactory system of mammals. II. Degeneration and reconstruction of the olfactory sensory neurons after axotomy. J. Neurocytol. 8, 197–213.

Novoselov, V.I., Krapivinskaya, L.D. and Fesenko, E.E. (1988) Amino acid binding glycoproteins from the olfactory epithelium of skate (*Dasyatis pastinaca*). Chem. Senses 13, 267–278.

Oshima, K., Gorbman, A. and Shimada, H. (1969) Memory blocking agents: Effect on olfactory discrimination in homing salmon. Science 165, 86–88.

Pyatkina, G.A. (1976) Receptor cells of various types and their proportional interrelation in the olfactory organ of larvae and adults of Acipenserid fishes. Cytologia 18, 1444–1449.

Reese, T.S. and Brightman, M.W. (1970) Olfactory surface and central connections in some vertebrate. In: Taste and Smell in Vertebrates. /Wolstenholme, G.E.W. and Knight, J.; eds./ pp. 115–149, Ciba Foundation Symposium Churchill, London.

Rhein, L.D. and Cagan, R.H. (1981) Role of cilia in olfactory recognition. In: Biochemistry of Taste and Olfaction (Cagan, R.H. and Kare, M.R.; eds.), pp 47–68, Academic Press, New York.

Schulte, E. (1972) Studies of the regio olfactoria in the eel *Anguilla anguilla*. Z. Zellforsch. 125, 210–228.

Snyder, S.H., Sklar, P.B., Hwang, P.M. and Pevsner, J. (1989) Molecular mechanism of olfaction. Trends Neurosci. 12, 35–38.

Theisen, B. (1972) Ultrastructure of the olfactory epithelium in the Australian lungfish *Neoceratodus forsteri*. Acta Zool. (Stockh.) 53, 205–218.

Theisen, B., Breucker, H. Zeiske, E. and Melinkat, R. (1980) Structure and development of the olfactory organ in the garfish *Belone belone* L. (Teleostei, Atheriniformes). Acta Zool. (Stockh.) 61, 161–170.

Thommesen, G. (1978) The spatial distribution of odour induced potentials in the olfactory bulb of char and trout (Salmonidae). Acta Physiol. Scand. 102, 205–217.

Thommesen, G. (1982) Specificity and distribution of receptor cells in the olfactory mucosa of the char *Salmo alpinus*. Acta Physiol. Scand. 115, 47–56.

Thommesen, G. (1983) Morphology, distribution and specificity of olfactory receptor cells in salmonid fishes. Acta Physiol. Scand. 117, 241–249.

Thornhill, R.A. (1967) The ultrastructure of the olfactory epithelium of the lamprey *Lampetra fluviatilis*. J. Cell Sci. 2, 291–302.

Yamamoto, M. (1982) Comparative morphology of the peripheral olfactory organ in teleosts. In: Chemoreception in Fishes. /Hara, T.J.; ed./ pp. 39–59, Elsevier, Amsterdam.

Yamamoto, M. and Ueda, K. (1979a) Comparative morphology of fish olfactory epithelium. X. Perciformes, Bericiformes, Scorpaeniformes and Pleirorectiformes. J. Fac. Sci. Univ. Tokyo 14, 273–279.

Yamamoto, M. and Ueda, K. (1979b) Comparative morphology of fish olfactory epithelium. VII. Gadiformes, Lophiiformes and Gobiesociformes. J. Fac. Sci. Univ. Tokyo 14, 115–125.

Zeiske, E. (1973) Morphologische Untersuchungen am Geruchsorgan von Zahnkarpfen (Pisces, Ciprinodontoidea). Z. Morph. Tiere 74, 1–16.

Zeiske, E. (1974) Morphologische und morphometrische Untersuchungen am Geruchsorgan oviparer Zahnkarpfen (Pisces). Z. Morph. Tiere 77, 19–50.

Zeiske, E., Breucker, H. and Melinkat, R. (1979) Gross morphology and fine structure of the olfactory organ of rainbow fish (Atheriniformes, Melanotaeniidae). Acta Zool. (Stockh.) 60, 173–186.

Zeiske, E., Melinkat, R., Breucker, H. and Kux, J. (1976) Ultrastructural studies on the epithelia of the olfactory organ of cyprinodonts (Teleostei, Cyprinodontoidea). Cell Tiss. Res. 172, 245–267.

Zelson, Ph.R. and Cagan, R.H. (1979) Biochemical studies of taste sensation. VIII. Partial characterization of alanine binding taste receptor sites of catfish *Ictalurus punctatus* using mercurials, sulfhydril reagents, trypsin and phospholipase C. Comp. Biochem. Physiol. 64B 141–147.

Neurobiology 1 (1), pp. 33–45, 1993

SPATIAL SELECTIVITY IN THE ANTERIOR ECTOSYLVIAN VISUAL AREA OF THE CAT

Gy. Kovács, L. Fischer-Szatmári and Gy. Benedek

Department of Physiology, Albert Szent-Györgyi Medical University,
H–6720 Szeged, Dóm tér 10, Hungary

Summary: Pattern reversal visually evoked potentials (PR-VEPs) were recorded in the anterior ectosylvian visual area (AEV) of the cat, and the dependence of the PR-VEPs on the spatial frequency (SF) and the mean luminance of the stimulation was studied. Six SFs between 0.025 and 1 cycles per degree (c/d) and four light density levels between $2x10^{-2}$ and 117 cd/m^2 (candela per square meter) were tested. The latency of the first positive component (P1) and the amplitude measured between P1 and the first negative (N1) component were analyzed. The dependence of the PR-VEP latencies on the SF displayed a significant relationship, with a minimum at around 0.05 c/d. This relationship was consistent at all luminance levels tested. The dependence of the amplitudes on the SF gave a "low-pass" tuning curve at every luminance level. The higher the luminance level, the steeper was the curve. The cut-off SF of these curves was at around 1 c/d under photopic conditions and around 0.6 c/d under scotopic conditions. The contrast dependence of the PR-VEP amplitudes exhibited saturation at 0.5, which was much higher than that of either the striate cortex or other extrastriate visual cortical areas, but similar to that of the superior colliculus. These results provide further evidence in support of the notion of a tecto-extrageniculo-extrastriate visual pathway functioning separately from the geniculo-striate mechanisms.

Key words: vision, spatial selectivity, anterior ectosylvian visual area, visual evoked potential

Correspondence should be addressed to:
Prof. Dr. György Benedek
Department of Physiology
Albert Szent-Györgyi Medical University
H-6720 Szeged, Dóm tér 10.

Akadémiai Kiadó, Budapest

INTRODUCTION

The anterior ectosylvian visual area (AEV) was recently described in the feline visual system. It occupies the ventral bank of the anterior ectosylvian sulcus and has connections with the superior colliculus (SC) and with extrageniculate thalamic and extrastriatal cortical areas (Mucke et al., 1982; Norita and Katoh, 1986; Olson and Graybiel, 1987). It seems to be a unique visual cortical area in that it has no direct connections either from the lateral geniculate complex or to the striate cortical area. Accordingly, this area has been proved to function even after the removal of area 17 (A17). Hence, it seems to be an excellent object for studies of extrastriate visual information processing. Responses of the cells in the AEV to moving light stimuli have been investigated extensively (Mucke et al., 1982; Benedek et al., 1986; Olson and Graybiel, 1987; Benedek et al., 1988; Hicks et al., 1988). Little is known, however, on the spatial frequency (SF) spectrum of neurons in the AEV. Further, since the AEV seems to have all the attributes necessary for "ambient vision" in Trevarthen's concept (Trevarthen, 1968) we have studied the dependence of the visual functions of the AEV on the luminance and contrast properties of the stimulation.

MATERIALS AND METHODS

Pattern reversal visually evoked potentials (PR-VEPs) were recorded in seven adult cats. Animals were initially anesthetized with an intramuscular injection of ketamine hydrochloride (30 mg/kg) and immobilized with gallamine (20 mg/kg). The anesthesia was maintained with a supplementary dose of Nembutal (pentobarbital, 2.0–3.0 mg/kg/hour). This supplementation was introduced 2 hours after the ketamine application and was given every 2 hours on average. The anesthesia was repeatedly and carefully controlled by monitoring the cortical electrical activity. The end-tidal CO_2 level and the rectal temperature were kept constant at 3.5–4.5% and 37–38 °C, respectively. The corneas were covered with unpowered contact lenses after the administration of phenylephrine and atropine eye-drops. The cortex around the anterior ectosylvian sulcus was exposed on the right side by removing the bone and the dura mater. Warm agar-agar protected the surface. The fundus of the contralateral (left) eye was projected onto a screen placed at a distance of 57 cm in front of the cat's eye. The position of the area centralis was drawn on the screen by reflection. The screen was then replaced by a TV set centered on zero azimuth. The ipsilateral eye was covered during the experiments. PR-VEPs were recorded with stainless-steel fiber-filled glass semi-micropipettes penetrating the cortex along the anterior ectosylvian sulcus. All cortical entrance points of the penetrations are presented in Fig. 1. Reference electrode was put on the nuchal muscles. The impedances of the

microelectrodes ranged between 100 and 500 kΩ. Visual activity was assessed by producing a moving light stimulus in front of the cat's eye and recording of the evoked potentials was performed in the area found most sensitive to visual stimuli (see shaded area in Fig. 1C. The VEPs were elicited by the reversal of a vertical black-and-white grating pattern generated on the screen of the TV set under computer control. The pattern subtended an angle of 45 degrees of the visual field. The contrast (C) (if this was not the subject of change) was 75% ($C=(L_{max}-L_{min})/(L_{max}+L_{min})$, where L_{max} is the luminance of the light stripes, while L_{min} is that of the dark stripes). The retinal illumination was varied between light density levels of 117 and $2x10^{-2}$ cd/m^2 in four steps by introducing neutral density filters. There was at least a 10-minute interval between the display of two different luminance levels in order to allow adaptation. The SF of the stimuli was varied

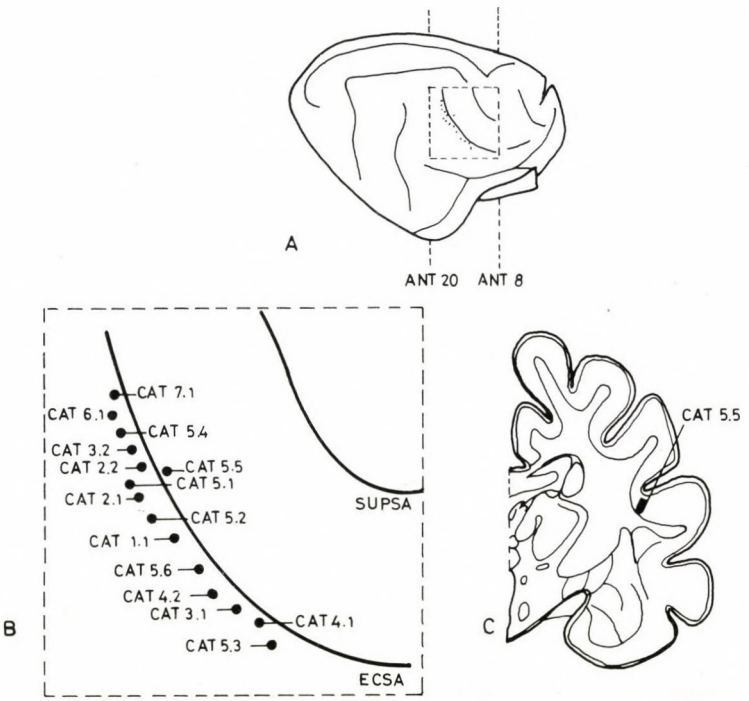

Fig. 1: The position of the penetrations along the anterior ectosylvian sulcus. The area explored is shown in insert **A** as well as in **B** in higher magnification. Serial number of the cats and that of the penetrations is indicated at every penetration points (**B**). The angle and the debth of the penetrations is presented in a vertical sections (**C**). Abbreviations: SUPSA—superior suprasylvian sulcus, ECSA—anterior ectosylvian sulcus.

between 0.025 and 3.5 cycles per degree (c/d) of visual angle in a pseudo-random mode. The reversal rate of the black and white stripes was 1.2 Hz. One-hundred responses were averaged; 500 msec long epoches were analyzed. Latencies of the PR-VEPs were measured at the peak of the first positive component (P1), and the amplitude at the P1-N1 interpeak amplitudes (the difference in voltage between P1 and the first negative component (N1)). Statistical analysis was performed by using one-way analysis of variance (ANOVA). A probability (p) of less than 0.05 was considered significant. The Statistical Graphics System "Statgrafics" software package was used to perform ANOVA.

RESULTS

A representative series of PR-VEPs recorded at five SFs and four mean luminance levels over the AEV exhibited a consistently appearing large positive-negative deflection (Fig. 2). This was occasionally preceded by an early negative wave. This configuration is largely similar to that recorded over the striate cortex by Creutzfeldt and Kuhnt (1973); merely the secondary oscillations after the primary waves seemed more pronounced in the AEV. It was not possible to record reproducible PR-VEPs with high SFs (0.2 and 0.6 c/d) at a luminance level of 0.02 cd/m^2. The interindividual variability of the amplitudes of these transient evoked potentials was higher than that of the latency values. This coincides with data obtained on human experimental subjects (Oken et al., 1987; Spafford and Lu, 1989; Joost and Bach, 1990; McCulloch and Skarf, 1991).

The PR-VEP amplitudes

Figure 3 shows the relationship between the PR-VEP amplitudes and the logarithm of the SF. These curves display a "low- pass" character at every luminance level: in other words, the amplitude is rather high at low SFs and decreases monotonously at higher SFs. The lower the luminance level, the less steep was this curve. The SF resolution of the evoked potentials seems to be best at a luminance level of 13 cd/m^2 and is weaker at 117 cd/m^2. The cut-off SF that may correspond to the "acuity" (just discriminable grating) of AEV is at around 1 c/d at photopic luminance levels and at around 0.6 c/d at a scotopic (0.02 cd/m^2) luminance level.

The PR-VEP amplitudes increase linearly with the logarithm of the luminance level at lower SFs (below 0.2 c/d), while at higher SFs, as described above, a luminance-tuning can be seen. No significant differences were found between the luminance dependence

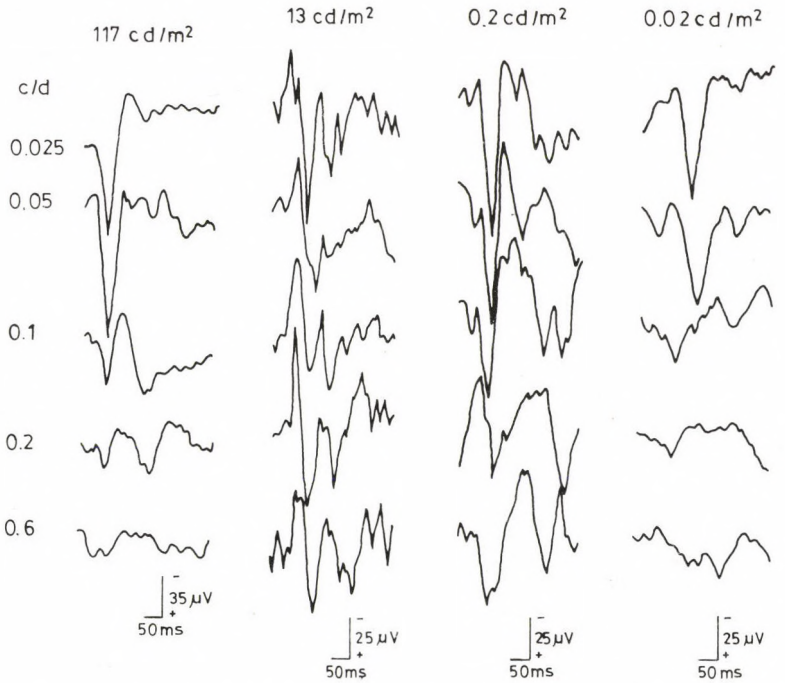

Fig. 2: Representative PR-VEP tracings recorded at five different spatial frequencies (SFs) and at four different light densities. The curves are the averages of 200 repetition from one animal.

functions at 0.025 and 0.05 c/d stimulation (Fig. 4). At high SF (1 c/d) and low luminance level (0.02 cd/m^2) PR-VEPs were not recorded.

The PR-VEP latencies

There was a significant relationship between the PR-VEP latencies and the logarithm of SF (Fig. 5). The relationship of the latency values to the SF seems to exhibit linearity, and the curves therefore run fairly parallel. The minimal latencies were found

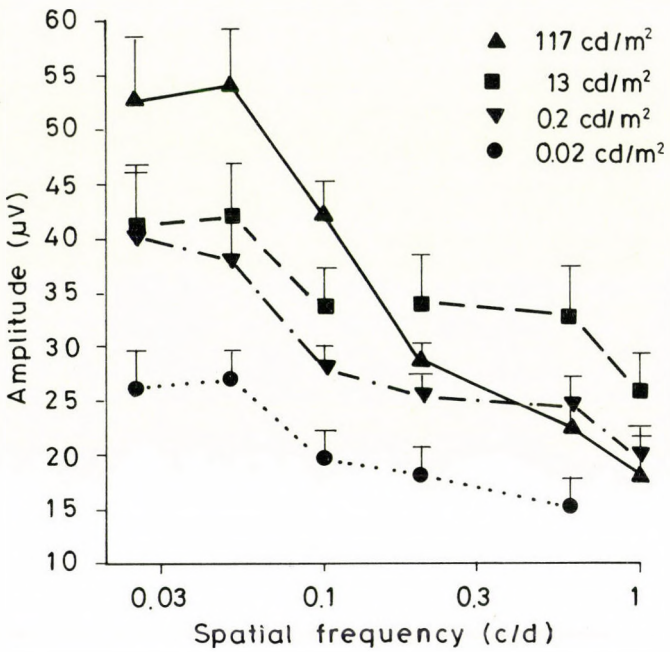

Fig. 3: Spatial frequency dependence of the P1-N1 interpeak amplitude at four different light density levels. The curves represents the mean and standard error (SE) of seven animals. Abbreviations: c/d—cyclus/degree, cd/m^2—candela/square meter.

at around 0.05 c/d SF at every luminance level. On increase of the SF over this value, the latencies increased monotonously. There was no significant difference between the latencies recorded at 117 and 13 cd/m^2 luminance levels.

However, there was a significant relationship between the logarithm of the luminance level and the latencies at each SF (Fig. 6). As described for humans (Mansfield, 1973; Froehlich and Kaufman, 1991), the lower the luminance level, the longer the latencies. The luminance dependence of the latencies was similar, independently of the SFs. At a luminance level above 13 cd/m^2, the curves displayed a saturation phenomenon. At high SF (1 c/d) and low luminance level (0.02 cd/m^2) PR-VEPs were not recorded.

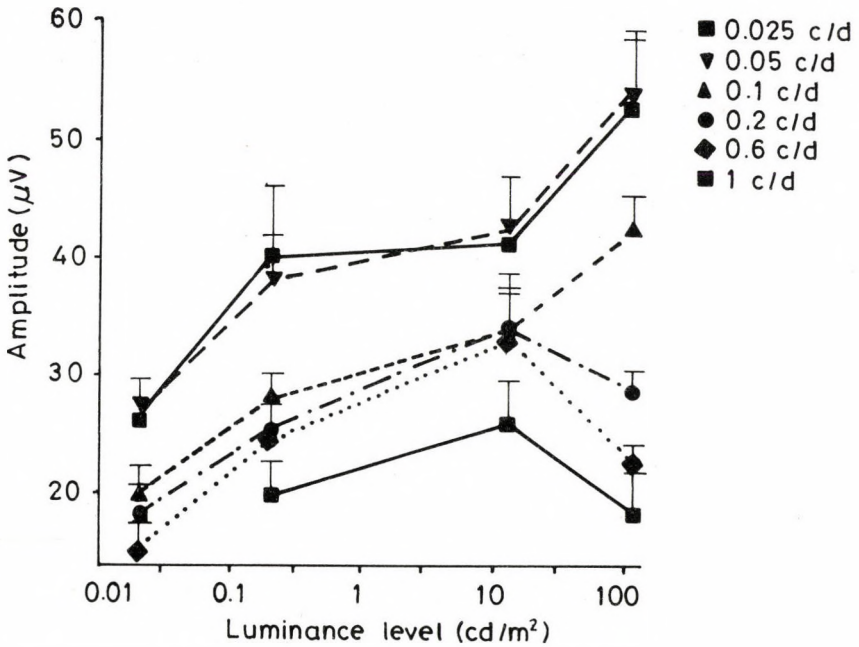

Fig. 4: The luminance dependence of the P1-N1 interpeak amplitude at six different SFs (mean of seven animal + SE). Abbreviations: c/d—cyclus/degree, cd/m^2—candela/square meter.

Contrast dependence

A significant relationship was obtained when the PR-VEP amplitudes were studied versus the contrast of the stimuli (Fig. 7). The AEV displayed a contrast threshold of around 0.3, i.e. we were not able to record reproducible PR-VEPs by delivering stimuli under this contrast level. Between contrast levels of 0.4 and 0.5, the amplitude of the response showed a steep increase. Above a contrast level of 0.5, however, saturation was found in the curve. No significant relationship was obtained between the contrast level and the PR-VEP latency values.

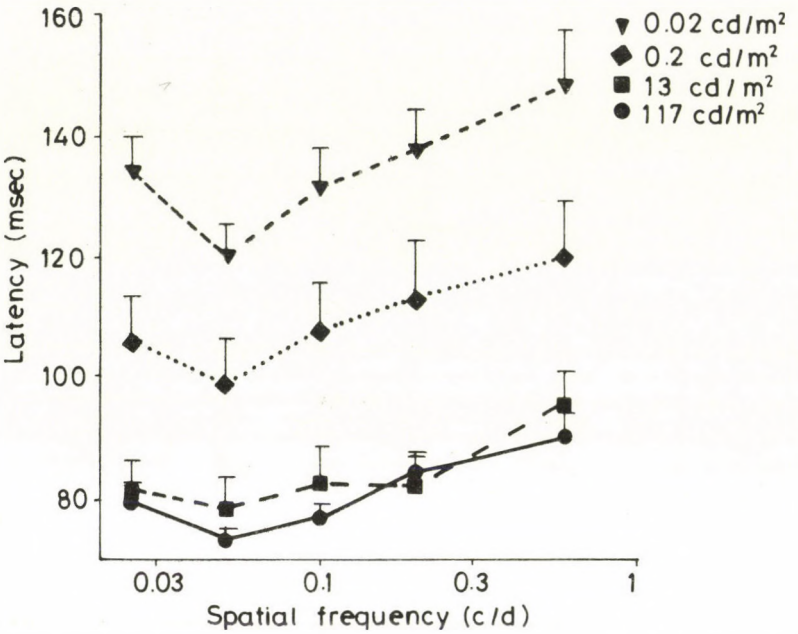

Fig. 5: The latency of the P1 as a function of log SF at different luminance levels (mean of 7 animals + SE). Abbreviations: c/d—cyclus/degree, cd/m^2—candela/square meter.

DISCUSSION

Visual information processing can be regarded as a transformation of the retinal picture into spatial and temporal frequency bands (Burr et al., 1986). Accordingly, the visual system may function as a Fourier transformer which has separate channels, tuned for different spatial and temporal frequency bands (Campbell and Robson, 1968; Campbell and Maffei, 1970; Maffei and Fiorentini, 1973; DeValois et al., 1979; Berkley, 1990). These considerations provide a reason for comparison of the SF dependences of different cortical areas. Indeed, several reports have appeared on the SF characteristics of A17 and several extrastriate visual areas (Dean, 1981; Pinter and Harris, 1981; Tolhurst and Thompson, 1981; Morrone et al., 1986; Frishman et al., 1987; Zumbroich and Blakemore, 1987; Zumbroich et al., 1988; Guido et al., 1989; Gizzi et al., 1990; Hammond and

Pomfrett, 1990). These studies demonstrated the presence of various "band-pass", "low-pass" and "high-pass" SF tuning curves from the different cortical areas. A17 was found to have a "band-pass" type tuning of the SFs, with a preference for a narrow band of SFs, attenuation at low frequencies and a cut-off frequency in the high-frequency range. This type of frequency tuning was also found to be characteristic for the majority of cells in the lateral suprasylvian visual area (LS) (mainly in the posteromedial lateral suprasylvian visual area (PMLS)) (Morrone et al., 1986; Gizzi et al., 1990).

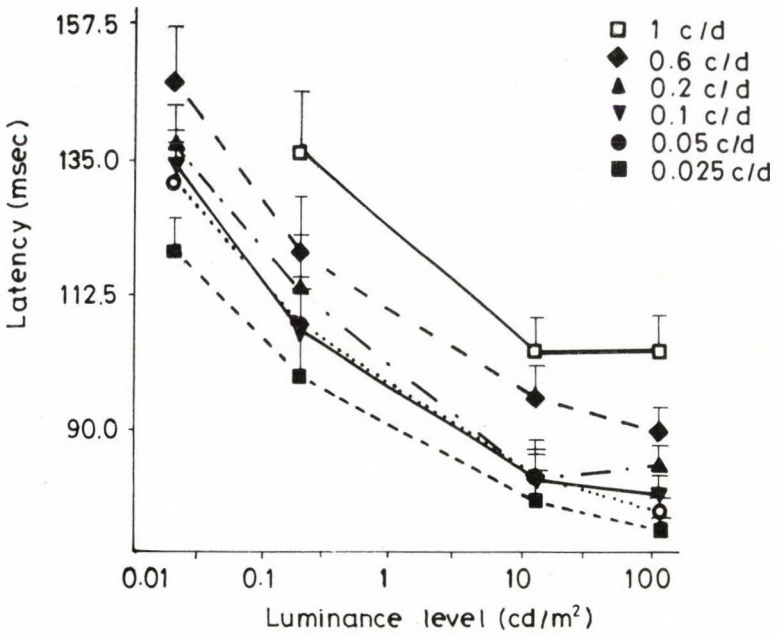

Fig. 6: Effect of increased luminance level on the latency of the P1 wave (mean of 7 animals + SE). Abbreviations: c/d—cyclus/degree, cd/m^2—candela/square meter.

The SF dependence of the AEV differs from that of both A17 and the extrastriate areas (Morrone et al., 1986; Zumbroich and Blakemore, 1987; Gizzi et al., 1990; Hammond and Pomfrett, 1990). The SF tuning curve of the AEV shows "low-pass" characteristics. This means that the AEV is rather sensitive to the very low (below 0.1 c/d) SFs, and the cut-off frequency is also rather low. The optimal SF in the AEV is at around 0.05 c/d, where PR-VEPs with the largest amplitude and the shortest latency values were found. These findings are in line with previous single-unit studies with drifting grating stimulation in this area (Hicks et al., 1988). This optimal SF is much lower than that of A17 (0.77 c/d) (Zumbroich and Blakemore, 1987) or the LS (between 0.1 and 1 c/d) (Morrone et al., 1986; Zumbroich and Blakemore, 1987). The SF tuning curves of the AEV, however, are in the same range of SF as that found for the SC (0.05-0.1 c/d) (Zumbroich and Blakemore, 1987). This is in line with the anatomical data of Mucke et al., 1982; Norita and Katoh, 1986; that the SC is one of the two main inputs of visual information towards AEV.

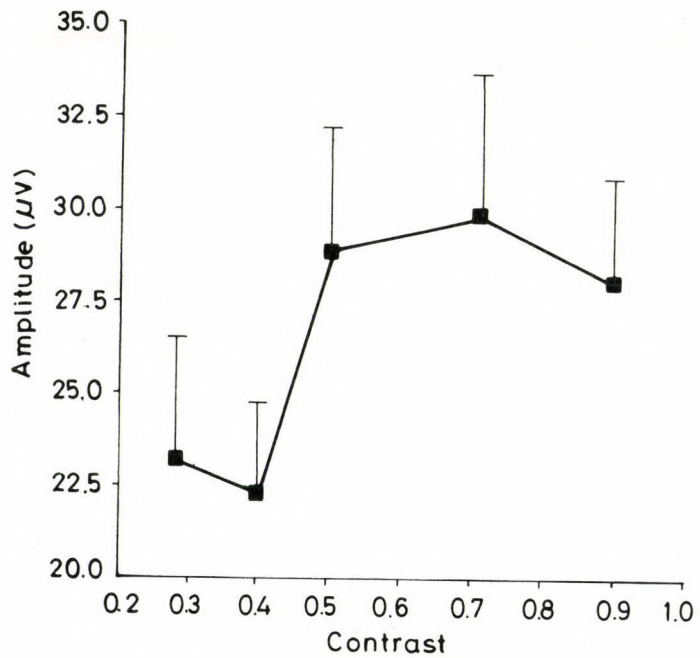

Fig. 7: The contrast dependency of the P1-N1 interpeak PR-VEP amplitude (mean of 7 animals + SE).

The upper cut-off frequency of the AEV was found by us at around 1 c/d under photopic circumstances. Under scotopic conditions, this upper cut-off frequency was at around 0.6 c/d. These values are far lower than those observed in the case of A17 (around 3.5 c/d), the LS (2.1 c/d) or even the SC (around 2.2 c/d) (Zumbroich and Blakemore, 1987).

The finding that the AEV tends to prefer a very low SF range seems to provide an interesting contrast to early physiological observations on a preference in this area for small stimuli moving in a huge receptive field (Mucke et al., 1982; Benedek et al., 1986). Later, cells with a preference for large moving stimuli were also described (Benedek et al., 1988; Hicks et al., 1988). These latter observations, however, were obtained not with stationary stimuli, but with fast moving ones.

The AEV seems to respond more intensively to stimuli with higher contrast than to low-contrast stimuli. The minimal contrast (0.3), i.e. the threshold for a PR-VEP to be evoked from the AEV, is much higher than that for either the LS or A17 (Morrone et al., 1986). The SC, which is one of the structures providing the major input towards the AEV via a Y-pathway, has a lower contrast threshold, of around 0.1 (Morrone et al., 1986). No data have appeared about the contrast dependence of the extrageniculate thalamus, which provides the other main visual input of the AEV. The saturation level of the AEV is around a contrast value of 0.5, which is higher than that of A17 and the LS, but again falls in the range of saturation of the SC (0.4) (Morrone et al., 1986).

It seems a general phenomenon that the lower the stimulating luminance level, the longer the latencies and the smaller the amplitudes observed over the visual areas of the cat. This is in line with the data obtained in experiments with healthy humans. The latency of the visual evoked potentials in the AEV seems to consistently exceed that recorded in A17, irrespectively of the stimulating SF. This yields parallel latency functions for the SF tuning of the two areas in question. The longer latencies of AEV as compared to those of A17 may suggest that the AEV has a more complex, connectional pattern than A17.

To summarize, the AEV seems to reveal response properties that are unique in the feline cortical visual system. It displays characteristics different from either the striate cortex or the earlier-described extrastriate ones, but the properties found by us largely resemble the characteristics of the SC. This phenomenon can be treated as further evidence in favour of a separate, tecto-extrageniculo-extrastriate visual pathway, operating

fairly independently of the geniculo-striate one. The physiological properties described, the low-pass filter properties of the spatial frequency tuning, the sensitivity to high contrasts and the luminance dependence add data to Trevarthen's concept (Trevarthen, 1968) on the "ambient vision" of primates and man.

ACKNOWLEDGEMENTS

The authors wish to thank to Péter Liszli and György Rubicsek, Ph.D. for preparing the software and hardware, to Gabriella Dósai-Molnár for the excellent technical assistance and to Mr. David Durham for correcting the manuscript.

REFERENCES

Benedek, G., Jang, E.K. and Hicks, T.P. (1986) Physiological properties of visually responsive neurones in the insular cortex of the cat. Neurosci. Lett. 64, 269–274.

Benedek, G., Mucke, L., Norita, M., Albowitz, B. and Creutzfeldt, O.D. (1988) Anterior ectosylvian visual area (AEV) of the cat: Physiological properties. Prog. Brain Res. 75, 245–255.

Berkley, M.A. (1990) Behavioral determination of the spatial selectivity of contrast adaptation in cats: Some evidence for a common plan in the mammalian visual system. Visual Neurosci. 4, 413–426.

Burr, D.C., Ross, J. and Morrone, M.C. (1986) Seeing objects in motion. Proc. R. Soc. Lond. 227, 249–265.

Campbell, F.W. and Maffei, L. (1970) Electrophysiological evidence for the existence of orientation and size detectors in the human visual system. J. Physiol. 207, 635–652.

Campbell, F.W. and Robson, J.G. (1968) Application of fourier analysis to the visibility of gratings. J. Physiol. 197, 223–235.

Creutzfeldt, O.D. and Kuhnt, U. (1973) Electrophysiology and topographical distribution of visual evoked potential in animals. In: Handbook of Sensory Physiology, Vol. 7/3B, pp. 595–646. Springer Verlag, Berlin (Heidelberg, New York).

Dean, A.F. (1981) The relationship between amplitude and contrast for cat striate cortical neurones. J. Physiol. 318, 413–427.

DeValois, K., DeValois, R.L. and Yund, E.W. (1979) Responses of striate cortex cells to grating and checkerboard patterns. J. Physiol. 291, 483–505.

Frishman, L.J., Freeman, A.W., Troy, J.B., Schweitzer-Tong, D.E. and Enroth-Cugell, C. (1987) Spatiotemporal frequency responses of cat retinal ganglion cells. J. Gen. Physiol. 89, 599–628.

Froehlich, I. and Kaufman, D.I. (1991) Effect of decreased retinal illumination on simultaneously recorded pattern electroretinogramms and visual-evoked potentials. Invest. Ophth. Visual. 32, 310–318.

Gizzi, M.S., Katz, E. and Movshon, A. (1990) Spatial and temporal analysis by neurons in the representation of the central visual field in the cat's lateral suprasylvian visual cortex. Visual Neurosci. 5, 463–468.

Guido, W., Tumosa, N. and Spear, P.D. (1989) Binocular interactions in the cat's dorsal lateral geniculate nucleus.I spatial frequency analysis of responses of x, y and w cells to nondominant-eye stimulation. J. Neurophysiol. 62, 526–543.

Hammond, P. and Pomfrett, C.J.D. (1990) Influence of spatial frequency on tuning and bias for orientation and direction in the cat's striate cortex. Vision Res. 30, 359–369.

Hicks, T.P., Benedek, G. and Thurlow, G.A. (1988) Organization and properties of neurons in a visual area within the insular cortex of the cat. J. Neurophysiol. 60, 397–421.

Joost, W. and Bach, M. (1990) Variability of the steady-state visually evoked potential: Interindividual variance and interindividual reproductibility of spatial frequency tuning. Doc. Ophthalmol. 75, 59–66.

Maffei, L. and Fiorentini, A. (1973) The visual cortex as a spatial frequency analyzer. Vision Res. 13, 1255–1267.

Mansfield, R.I.W. (1973) Latency function in human vision. Vision Res. 13, 2219–2234.

McCulloch, D.L. and Skarf, B. (1991) Development of the human visual system: Monocular and binocular pattern VEP latency. Invest. Ophth. Visual 32, 2372–2381.

Morrone, M.C., DiStefano, M. and Burr, D.C. (1986) Spatial and temporal properties of neurons of the lateral suprasylvian cortex of the cat. J. Neurophysiol. 56, 969–986.

Mucke, L., Norita, M., Benedek, G. and Creutzfeldt, O. (1982) Physiologic and anatomic investigation of a visual cortical area situated in the ventral bank of the anterior ectosylvian sulcus of the cat. Exp. Brain Res. 46, 1–11.

Norita, M. and Katoh, Y. (1986) Cortical and tectal afferent terminals in the suprageniculate nucleus of the cat. Neurosci. Lett. 65, 104–108.

Oken, B.S., Chiappa, K.H. and Gill, E. (1987) Normal temporal variability of the P100. Electroen. Clin. Neuro. 68, 153–156.

Olson, C.R. and Graybiel, A.N. (1987) Ectosylvian visual area of the cat: Location, retinotopic organization, and connections. J. Comp. Neurol. 261, 277–294.

Pinter, R.B. and Harris, L.R. (1981) Temporal and spatial response characteristics of the cat superior colliculus. Brain Res. 207, 73–94.

Spafford, M.M. and Lu, S.L. (1989) Retinal adaptation effects on the patterned VEP and ERG. Optometry and Vision Sci. 66, 507–514.

Tolhurst, B.J. and Thompson, I.D. (1981) On the variety of spatial frequency selectivities shown by neurons in area 17 of the cat. Proc. R. Soc. Lond. 213, 183–199.

Trevarthen, C.B. (1968) Two mechanisms of vision in primates. Psychologische Forschung. 31, 299–337.

Zumbroich, T.J. and Blakemore, C. (1987) Spatial and temporal selectivity in the suprasylvian visual cortex of the cat. J. Neurosci. 7, 482–500.

Zumbroich, T.J., Price, D.J. and Blakemore, C. (1988) Development of spatial and temporal selectivity in the suprasylvian visual cortex of the cat. J. Neurosci. 8, 2713–2728.

Neurobiology 1 (1), pp. 47–54, 1993

VIMENTIN PERSISTS IN THE MATURE GLIA OF FISH BRAIN

M. Kálmán

1st Department of Anatomy, Semmelweis University of Medicine,
H–1450 Budapest, Tűzoltó u. 58, Hungary

Summary: Adult carp brains were processed for immunohistochemical staining against vimentin and glial fibrillary acidic protein. The shape, density and distribution of immunopositive structures were found to be very similar with both types of antibody. Thus, it appears that vimentin, the cytoskeletal protein typical for immature glia in the early phase of ontogenesis in mammals can also be demonstrated in the adult glia of the phylogenetically older fish brain.

Key words: vimentin, glial fibrillary acidic protein (GFAP), glial development, fish brain

INTRODUCTION

Vimentin, which was described originally in fibroblasts, is a characteristic cytoskeletal protein during a definite stage of development of mammalian glia (Dahl et al., 1981). Later, vimentin gradually decreases, while glial fibrillary acidic protein (GFAP) accumulates. These phenomena progress in parallel with the transformation of radial glia into stellate-shaped cells (Dahl, 1981; Pixley and de Vellis, 1984; McDermott and Lantos, 1989). A similar but incomplete process takes place in the reptilian and avian neurohistogenesis: numerous long and straight glial fibers persist as remnants of radial glia, and vimentin persists in more areas (Tapscott et al., 1981; Onteniente et al., 1983; Pixley and de Vellis, 1984; Roeling and Feirabend, 1988; Monzon-Mayor et al., 1990; Yanes et al., 1990).

Akadémiai Kiadó, Budapest

In lower vertebrates (fishes and amphibia) the glial system is represented by long and straight fibers resembling the early embryonic glia of higher vertebrates (King, 1966; Stensaans and Stensaans, 1968; Korte and Rosenbluth, 1981; Onteniente et al., 1983; Miller and Liuzzi, 1986; Naujoks-Manteuffel and Roth, 1989). The GFAP has similar immunological characteristics in the different groups of vertebrates: cartilaginous and bony fishes, reptiles, birds and mammals (Dahl and Bignami, 1973; Onteniente et al., 1983; Dahl et al., 1985).

These facts raise the question, whether the piscine adult glia which resembles in appearance the embryonic type of mammalian glia, contains persistently vimentin.

MATERIALS AND METHODS

Adult carps (*Cyprinus carpio* L.), five of either sexes, were decapitated after cooling, the brains were removed from the skull and fixed in 4% paraformaldehyde dissolved in phosphate buffer (0.05 M, pH 7.4). After a 48-h fixation and a 24-h washing in phosphate buffer the brains were embedded in agar and sectioned by a Vibroslice vibrating microtome (70 μm thickness). Parallel series os sections were processed for either vimentin or GFAP immunostaining or cresylviolet staining according to Nissl. Anti-vimentin monoclonal mouse antibodies were prepared by Viklicky and co-workers, Prague (Lukaš et al., 1989). Anti-GFAP monoclonal mouse antibodies were purchased from Boehringer (Mannheim). Sections were preincubated for 5 min in 3% H_2O_2 and for 1.5 h in 20% normal goat serum to suppress nonspecific reactions. Three rinses in phosphate buffer followed every step. Primary antisera, anti-vimentin and anti-GFAP were diluted 1:1000 and 1:100, respectively, in phosphate buffer containing 0.5% Triton-X 100 and were applied for 40 h at 4 °C. Then the sections were incubated with biotinylated anti-mouse immunoglobulin and with streptavidin-horseradish peroxidase complex (Amersham), each in 1:100 dilution, for 1.5 hours at room temperature. The immunocomplex was visualized by diamminobenzidine reaction. No diaminobenzidine reaction product was observed if the primary antibodies were omitted from the incubation medium.

In the terminology of the description of fish brain we followed Äriens Kappers and co-workers (1960).

RESULTS

A strong immunostaining against both vimentin and GFAP was observed throughout the fish brain. Generally, the GFAP-immunopositive structures proved also to be positive to vimentin and *vice versa* as demonstrated in the following representative brain regions. A detailed mapping of immunopositivity is the topic of a forthcoming paper.

In the brain stem, the most spectacular immunostaining was seen in the vagal lobes (*lobi vagi*) with characteristic straight, thick fibers toward the ventricular surface (Figs. 1, 2). The glial fibers formed strong sheaths and septa, immunopositive for both vimentin and GFAP, around and between the nerve tracts of brain stem (not shown in figure). In the cerebellum the glial fibers of molecular layer resembled the Bergmann-glia of higher Vertebrates although their arrangement was far less regular (Figs. 3, 4). Immediately below this layer, the fibers were tangled, forming a dense network, quasi an equivalent of the strong GFAP-immunopositive glia of the granular layer of avian and mammalian cerebellum. The density of vimentin-immunostained fibers usually seemed to be less than that of GFAP-positive ones. In the facial lobe (*tuberculum impar n. facialis*) we found

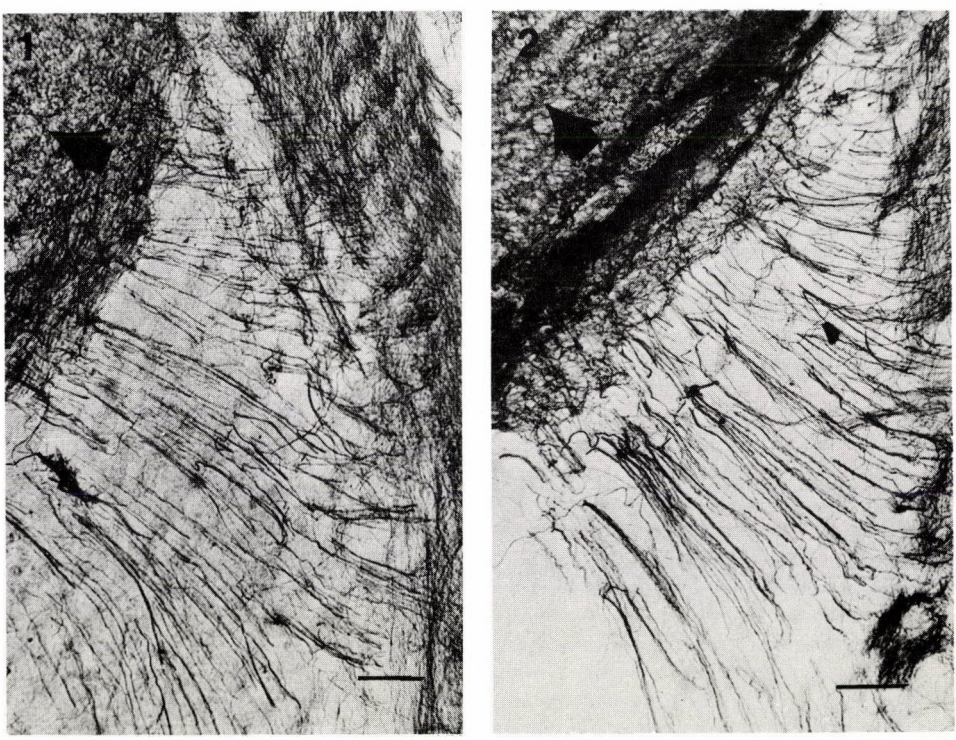

Figs. 1, 2: Similar areas of the vagal lobe immunostained against vimentin (**Fig. 1**) or GFAP (**Fig. 2**). Arrows are oriented to the ventricular surface. Bars represent 100 μm.

the best specimens of perivascular glia: straight fibers following the blood vessels (Fig. 5). These fibers proved to be immunopositive for either vimentin or GFAP. Vimentin- and GFAP-positive radial fibers directed from the brain surface towards deeper zones were frequently seen, for example around the 3rd ventricle (Figs. 6, 7), in the optic tectum and in the lateral lobes.

A similar arrangement of glial fibers could be observed in the telencephalon (Fig. 8) so that their pattern resembled that observed in the mammalian telencephalon in the early phase of development.

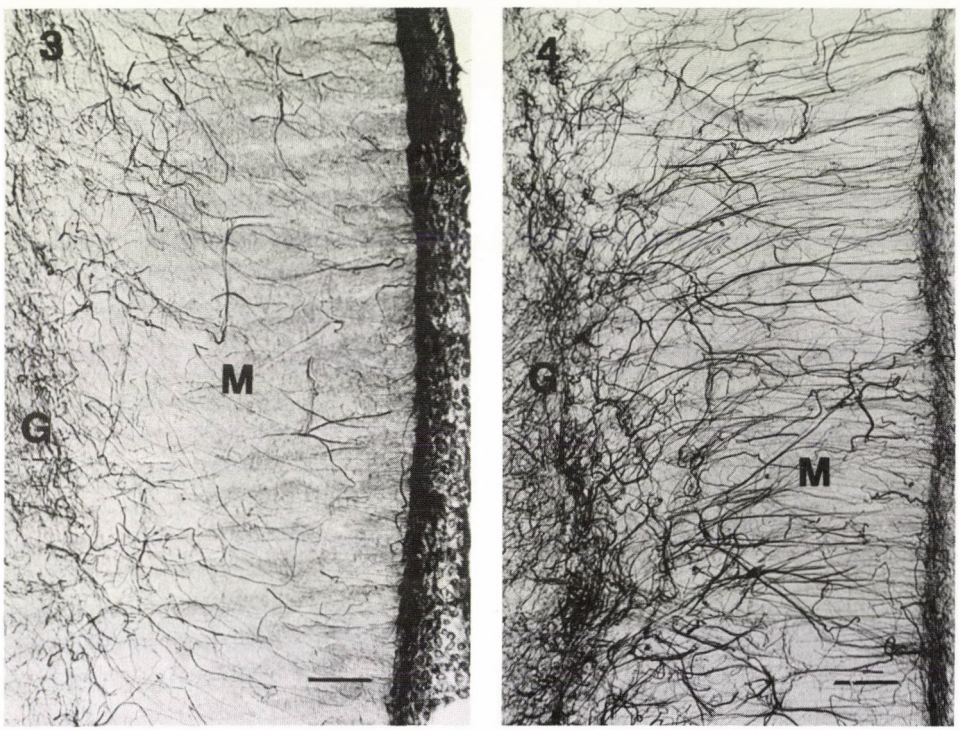

Figs. 3, 4: Similar areas of the carp cerebellum immunostained against vimentin (**Fig. 3**) or GFAP (**Fig. 4**). M, G—molecular and granular layers, respectively. Bars represent 100 μm.

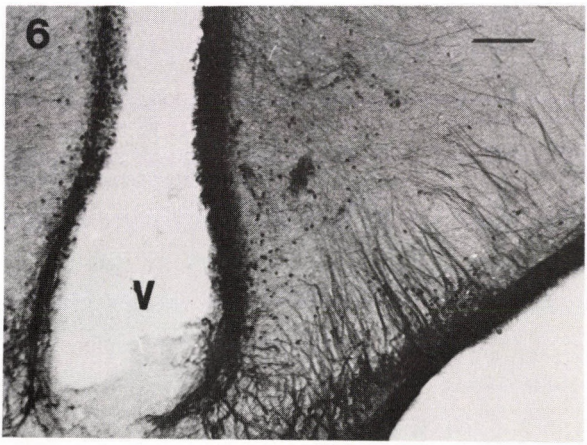

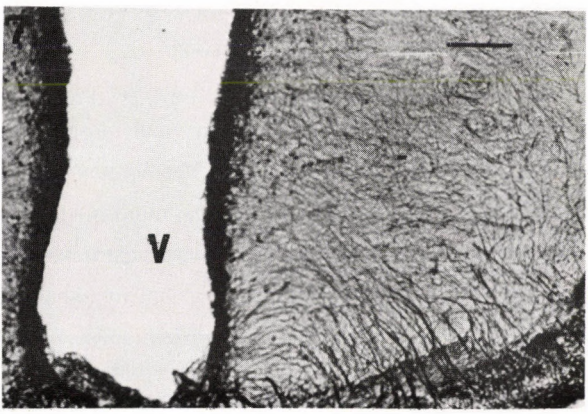

Fig. 5: A detail of the facial lobe immunostained against vimentin. Arrowheads show glial fibers along the blood vessels. Bar: 50 μm.
Figs. 6, 7: The bottom of the 3rd ventricle immunostained against vimentin (**Fig. 6**) or GFAP (**Fig. 7**). Note the fibers curving from the surface toward the ventricle (V). Bars represent 200 μm.

DISCUSSION

In conclusion, we found that vimentin, the cytoskeletal protein of the immature glia of developing brain in mammals and birds (Dahl, 1981; Dahl et al., 1981; Tapscott et al., 1981; Pixley and de Vellis, 1984; McDermott and Lantos, 1989) can also be demonstrated in the adult glia of the phylogenetically older brains of Teleostei, even in the adulthood.

Vimentin immunopositivity was found in goldfish (*Carassius auratus*), in the optic nerve (Jones et al., 1986) and also in the optic tectum (Cardone and Roots, 1990). Recently, Rubio et al., (1992) have reported the occurrence of vimentin immunopositivity in the posterior rhombencephalon or the iberian barb (*Barbus comiza*). Our studies indicate that vimentin is expressed regularly throughout the carp brain. The vimentin and GFAP immunopositivities have nearly identical distributions. A similar finding has been published by Zamora and Mutin (1988) who investigated the spinal cord of an Urodele (*Pleurodeles waltli*). The system of the radially oriented glial fibers of carp brain resembled some embryonic glial patterns of the equivalent regions of higher Vertebrates (Levitt and Rakič, 1980; Hajós and Bascó, 1984; Pixley and de Vellis, 1984). The similar patterns of vimentin and GFAP immunopositivities suggest a coexistence of these proteins in the carp brain. Some differences indicate, however, for example in the cerebellum, that the coexistence is not a general obligation.

The persistence of vimentin in the piscine glia may be associated with the preservation of regenerative capacity and morphological plasticity of fish brain which features are restricted in higher Vertebrates (Maggs and Scholes, 1986). In adult mammalian brain there are also several regions where morphological plasticity takes place under physiological conditions and where astrocytes were shown to contain vimentin, for example the supraoptic nucleus of rodent hypothalamus (Bonfanti et al., 1993).

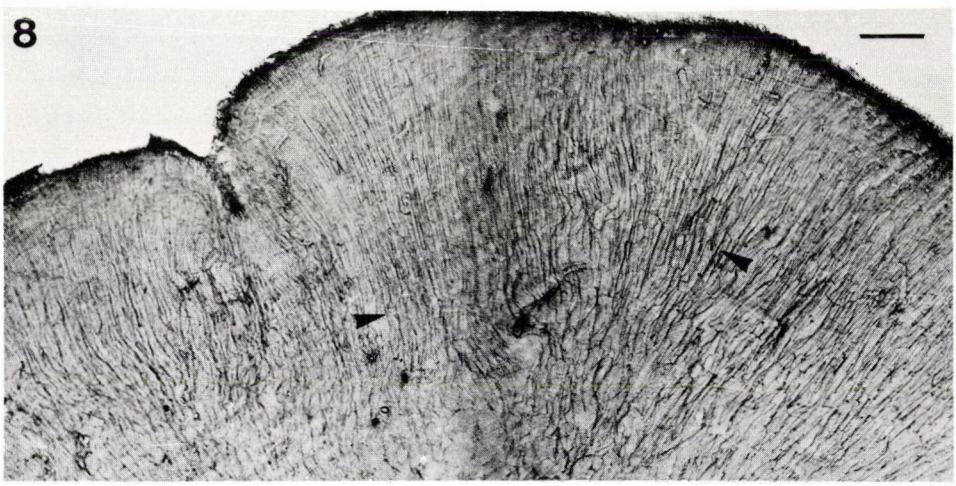

Fig. 8: A detail of telencephalon immunostained against vimentin. Note the dense pattern of straight fibers (arrowheads). Bar: 200 μm.

REFERENCES

Äriens Kappers, C.U., Huber, C.G. and Crosby, E.C. (1960) The Comparative Anatomy of the Nervous System of Vertebrates, Including Man. Hafner Publishing Co., New York.

Bonfanti, L., Poulain, D.A. and Theodosis, D.T. (1993) Radial glia-like cells in the supraoptic nucleus of the adult rat. J. Neuroendocrinol. In press.

Cardone, B. and Roots, B.I. (1990) Comparative immunohistochemical study of glial filament proteins (glial fibrillary acidic protein and vimentin) in goldfish, octopus and snail. Glia 3, 180–192.

Dahl, D. (1981) The vimentin-GFA transition in rat neuroglia cytoskeleton occurs at the time of myelination. J. Neurosci. Res. 6, 741–748.

Dahl, D. and Bignami, A. (1973) Immunohistochemical and immunofluorescence studies of the glial fibrillary acidic protein in Vertebrates. Brain Res. 61, 279–293.

Dahl, D., Crosby, C.J., Sethi, A. and Bignami, A. (1985) Glial fibrillary acidic protein in Vertebrates: Immunofluorescence and immunoblotting study with monoclonal and polyclonal antibodies. J. Comp. Neurol. 239, 75–88.

Dahl, D., Rueger, D.C. and Bignami, A. (1981) Vimentin, the 57,000 molecula weight protein in fibroblast filaments is the major cytoskeletal protein in immature glia. Eur. J. Cell Biol. 24, 191–196.

Hajós, F. and Bascó, E. (1984) The surface-contact glia. Adv. Anat. Embryol. Cell Biol. 84, 1–81.

Jones, P.S., Tesser, P., Keyser, K.I., Quitschke, W., Samadi, R., Karten, H.J. and Schechter, N. (1986) Immunohistochemical localization of intermediate filament proteins of neuronal and nonneuronal origin in goldfish optic nerve: Specific molecular markers for optic nerve structures. J. Neurochem. 47, 1226–1234.

King, J.S. (1966) A comparative investigation of neuroglia in representative Vertebrates: A silver carbonate study. J. Morphol. 119, 435–466.

Korte, G.E. and Rosenbluth, J. (1981) Ependymal astrocytes in frog cerebellum. Anat. Rec. 199, 267–279.

Levitt, P. and Rakič, P. (1980) Immunoperoxidase localization of glial fibrillary acidic protein in radial glial cells and astrocytes of the developing Rhesus monkey brain. J. Comp. Neurol. 193, 815–840.

Lukaš, L., Draber, P., Bucek, J., Dráberková, E., Viklicky, V. and Straskova, Z. (1989) Expression of vimentin and glial fibrillary acidic protein in human developing spinal cord. Histochem. J. 21, 693–702.

Maggs, A. and Scholes, J. (1986) Glial domains and nerve fiber patterns in the fish retinotectal pathway. J. Neurosci. 6, 424–438.

McDermott, K.W. and Lantos, P.L. (1989) The distribution of glial fibrillary acidic protein and vimentin in postnatal marmoset (*Callithrix jacculus*) brain. Dev. Brain Res. 45, 169–177.

Miller, R.H. and Liuzzi, F.J. (1986) Regional specialization of the radial glial cells of the adult frog spinal cord. J. Neurocyt. 15, 187–196.

Monzon-Mayor, M., Yanes, C., Ghandour, M.S., de Barry, J. and Gombos, G. (1990) GFAP and vimentin immunohistochemistry in the adult and developing midbrain of the lizard *Gallotia galloti*. J. Comp. Neurol. 295, 569–579.

Naujoks-Manteuffel, C. and Roth, G. (1989) Astroglial cells in a salamander brain (*Salamadra salamandra*) as compared to mammals: A glial fibrillary acidic protein immunohistochemistry study. Brain Res. 487, 397–401.

Onteniente, B., Kimura, H. and Maeda, T. (1983) Comparative study of the glial fibrillary acidic protein in Vertebrates by PAP immunohistochemistry. J. Comp. Neurol. 215, 427–436.

Pixley, S.R. and de Vellis, J. (1984) Transition between immature radial glia and the mature astrocytes studied with monoclonal antibody to vimentin. Dev. Brain Res. 15, 201–209.

Roeling, T.A.P. and Feirabend, H.K.P. (1988) Glial fiber pattern in the developing chicken cerebellum: Vimentin and glial fibrillary acidic protein (GFAP) immunostaining. Glia 1, 398–402.

Rubio, M., Suarez, I., Bodego, G. and Fernandez, B. (1992) Glial fibrillary acidic protein and vimentin immunohistochemistry in the posterior rhombencephalon of the iberian barb (*Barbus comiza*). Neurosci. Lett. 134, 203–207.

Stensaans, L.J. and Stensaans, S.S. (1968) Astrocytic neuroglial cells, oligodendrocytes and microgliocytes in the spinal cord of the toad: I. Light microscopy. Z. Zellforsch. 84, 473–489.

Tapscott, S.J., Bennett, G.S., Toyama, J., Kleinbart, F. and Holtzer, H. (1981) Intermediate filament proteins in the developing chick spinal cord. Dev. Biol. 86, 40–50.

Zamora, A.J. and Mutin, M. (1988) Vimentin and glial fibrillary acidic protein filaments in radial glia of the adult Urodele spinal cord. Neuroscience 27, 279–288.

Yanes, C., Monzon-Mayer, M., Ghandour, M.S., de Barry, J. and Gombos, G. (1990) Radial glia and astrocytes in the adult and developing telencephalon of the lizard *Gallotia galloti* as revealed by immunohistochemistry with anti-GFAP and anti-vimentin antibodies. J. Comp. Neurol. 295, 559–568.

Neurobiology 1 (1), pp. 55–63, 1993

A COMPUTER MODEL OF THE CONVULSIVE MEMBRANE

O. Fehér and F. Simigla

Department of Comparative Physiology, Attila József University,
H–6701 Szeged, P.O. Box 533, Hungary

Summary: A computer model of the convulsive membrane was built up by combining the H-H equations of normal ionic currents with a pathological current flowing through calcium channels and carrying sodium ions. Thus any form of paroxysmal depolarization shift could be simulated, by varying two rate constants and potassium conductance. The simulated PDSs are initiated by a minimal conductance pulse and terminate spontaneously according to the inherent rules of the model system. The program is written in Turbo-Pascal language and can be run on any PC.

Key words: computer simulation, ionic currents, paroxysmal depolarization shift

INTRODUCTION

Since the basic discovery of Matsumoto and Ajmone-Marsan (1969), according to which the central phenomenon of the epileptic electrogram is the so called paroxysmal depolarization shift (PDS), the investigation has centered around the nature of the membrane defect, which leads unavoidably to this long-lasting depolarization, disorganizing the fine coordination of the central neural activity. It seemed obvious from the beginning, that the

Akadémiai Kiadó, Budapest

abnormal electrical activity relies upon abnormal ionic permeabilities, present in the membrane. On the basis of fundamental studies of Connor and Stevens (1971a, b); Williamson and Crill (1976a, b); Ducreux and Gola (1975); it turned out, that the elementary conditions of the convulsive state consist in i) decrease of the potassium conductance and ii) appearance of a slowly inactivating inward current, transmitted by voltage dependent cationic channels having slow kinetics.

Valuable support has gained this theory from observations on Molluscan neurons. As it was reported by Smith et al. (1975), bursting pacemaker activity in the snail is substantiated by a slow inward current, carried mainly by sodium ions. Heinemann et al. (1977), were the first to emphasize the importance of calcium ions in the chemically induced paroxysmal phenomena. Swandulla and Lux (1985) suppose, that such a current can be activated by elevating the intracellular calcium concentration. On invertebrate and vertebrate neurons Walden et al. (1986, 1988a, 1988b) have provided ample evidence, that calcium channel blockers (inorganic and organic ones) effectively reduce paroxysmal discharges. Our own experiments (Fehér et al., 1982, 1988; Papp et al., 1990, 1991) on Helix metacerebral ganglion cells have shown, that pentylenetetrazol (PTZ), this well known convulsant, depresses potassium conductances (I_A and I_K, to different extent), induces the appearance of a slow inward current, carried mainly by sodium ions and blockable by calcium channel blockers. It was supposed by us, that PTZ exerts its convulsive action by impairing calcium channels, which loose their specifity to calcium ions, begin to transmit sodium, but retain their slow kinetics. The same is not excluded in case of potassium channels, too. Thus, a new kind of current begins to flow in maybe a restricted area of the neuronal membrane, but being able to disturb the normal relations between different parts of the neuron. This acts on the output of the convulsive cell and destroys the genetically and physiologically determined pathways of inhibition and excitation.

Besides the extensive physiological work, directed to clear up the origin of the PDS, a good number of mathematical and computer models were constructed (Connor and Stevens, 1971; Ducreux and Gola, 1975; Traub, 1979; Fehér et al., 1982) to help the experimental work or in order to integrate our knowledge about this process.

Our computer model is an attempt to describe the convulsive state at two levels: in

the neuronal membrane and in the whole neuron, consisting of many interactive compartments. In this paper the membrane model will be dealt with in detail.

METHODS

The basis of the model relies upon the kinetics constructed by Hodgkin and Huxley (1952) for the squid axon and modified by Traub (1979) for neocortical pyramidal cells. The rate constants, equilibrium potentials, ion-channel densities of the normal membrane were taken over from his paper, with minimal modifications. As inward currents sodium and calcium currents were built in and additionally a slow and slowly inactivating non-specific current, constructed by us, for the convulsive membrane. Active outward currents were lumped into a potassium current, having the well known kinetics. A voltage independent leakage current has a –5 mV equilibrium potential as related to the resting membrane potential. The numerical integration was performed by making use of the Runge-Kutta method.

The equations and functional parameters used in simulation of the normal membrane were as follows:

$$I_M=I_C+I_I \qquad I_I=I_{Na}+I_{Ca}+I_K+I_L$$
$$I_{Na}=g_{Na}m^3h(E_M-E_{Na}) \qquad I_{Ca}=g_{Ca}c^4s(E_M-E_{Ca})$$
$$I_K=g_Kn^4(E_M-E_K) \qquad I_L=g_L(E_M-E_L)$$

H-H rate constants were the following:

$$\alpha_m=0.6\ (13-V)/(\exp\ ((13-V)/5)-1) \qquad \beta_n=0.5\ (V-45)/(\exp\ ((V-45)/5)-1)$$
$$\beta_m=0.35\ (\exp\ ((7.5-V)/20) \qquad \alpha_c=5/(\exp\ ((37.5-V)/10)+1)$$
$$\alpha_h=0.098\ (30-V)/((\exp\ (30-V)/6)-1) \qquad \beta_c=0.14\ \exp\ ((5-V)/80)$$
$$\beta_h=0.05\ (45-V)/(\exp\ ((45-v)/10)-1) \qquad \alpha_s=0.01\ (V-15)/(\exp\ ((V-15)/10)-1)$$
$$\alpha_n=0.014\ (\exp\ ((-25-V)/20) \qquad \beta_s=0.2/(\exp\ ((45-V)/10)+1)$$

Ion-channel densities (i.e. conductances calculated for unit membrane area) were as follows: g_{Na}: 300 mmho/cm^2, g_{Ca}: 40 mmho/cm^2, g_K: 60 mmho/cm^2, for the normal membrane, g_L: 1.5 mmho/cm^2. The equilibrium potentials of the ion species were: E_{Na}: 125 mV, E_{Ca}: 140 mV, E_K: –10 mV, E_L: –5 mV. The convulsant drug was supposed to depress potassium conductances to the half. A brief (0.2 ms) conductance pulse served as stimulus.

RESULTS AND DISCUSSION

Simulation of the convulsive membrane

As it was mentioned earlier, the convulsive state has two prerequisites: i) depression of potassium conductances, and ii) a slow and slowly inactivating inward current, lacking ionic specificity. Since the overwhelming majority of the experimental models of epilepsy relies upon application of chemical convulsants, the binding and dissociation of drugs to and from the ionic channels has been included into the model. If g_{NK} is the density of ionic channels attacked by the convulsant, a monomolecular reaction between the channel protein and receptor can be described by the equation:

$$dg_{NK}/dt=kg_{NK} \tag{1}$$

at a given concentration of the drug where k is the association constant of the drug, g_{NK} represents the density of calcium channels attacked by the convulsant at zero time expressed in terms of conductance. Its rate of change in time can be described by this monomolecular reaction.

In view of the dissociation of the convulsant, the data of Ulbricht and Wagner (1976) were taken into account. They report, that the dissociation of 4-aminopyridin from potassium channels of the frog Ranvier node is dependent of the time integral of depolarization. For our model this was formulated in the equation:

$$pg_{NK}V(t)=-dg_{NK}/dt \tag{2}$$

where p is the dissociation constant, and V(t) is the absolute value of depolarization as related to the resting membrane potential.

The kinetics of the slow inward current was borrowed from the calcium channels. It was complemented with the kinetics of the drug association and dissociation. The electrochemical potential of the sodium was used as electromotive force, because, according to our results (Papp et al., 1990, 1991) this current is carried mainly by sodium ions. The equation of the slow inward current in its final form is thus:

$$I_{NK}=g_{NK}c^4s\ [\ \exp\ (kt-p\int V(t)dt)]\ (E_M-E_{Na}) \tag{3}$$

where g_{NK} is the number of channels per square μm bound by the convulsant at zero time of computation. The H-H equations of the normal membrane has to be complemented with I_{NK} in order to reach simulation of the convulsive membrane.

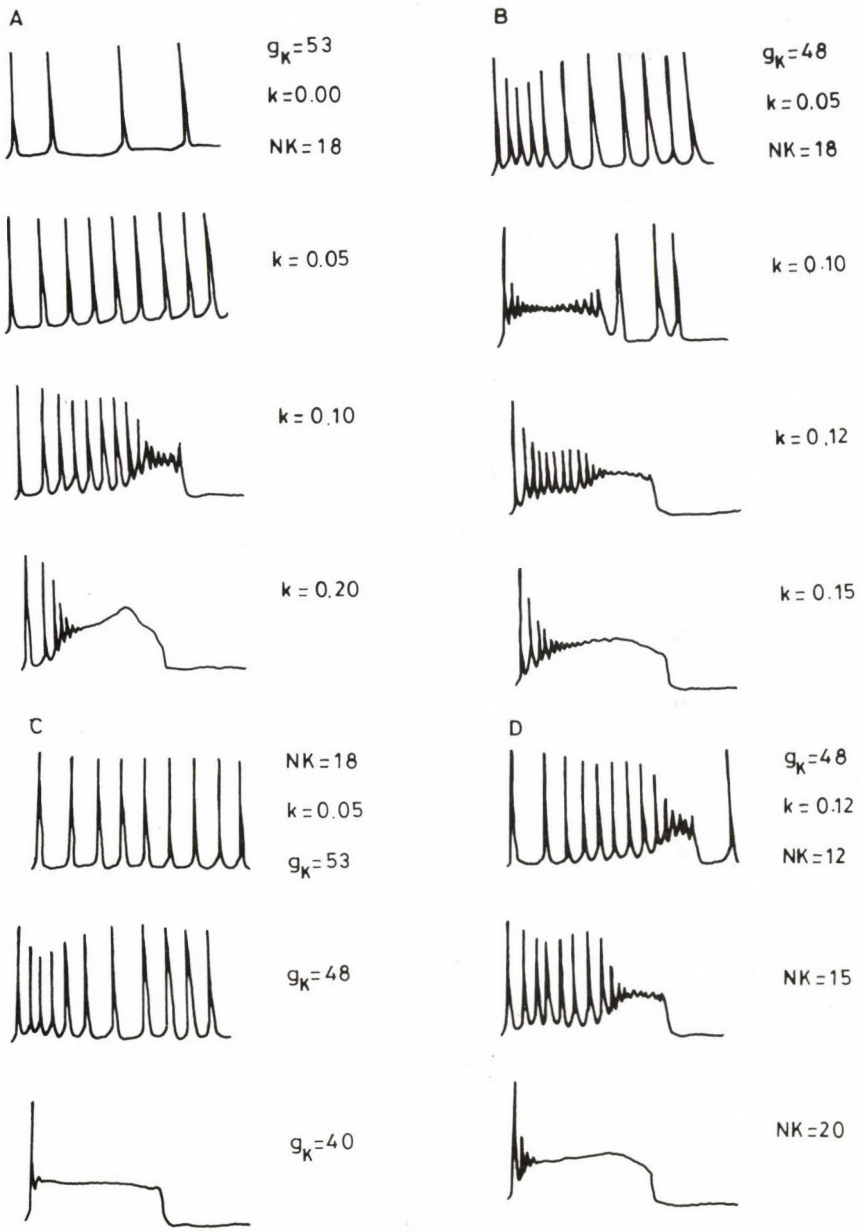

Fig. 1: Simulation of different types of paroxysmal depolarization shifts as determined by the association constant (k), potassium conductance (g_K) and initially occupied calcium channels (NK). The amplitude of full blown spike potentials is 100 mV, the duration of PDSs is 4 ms.

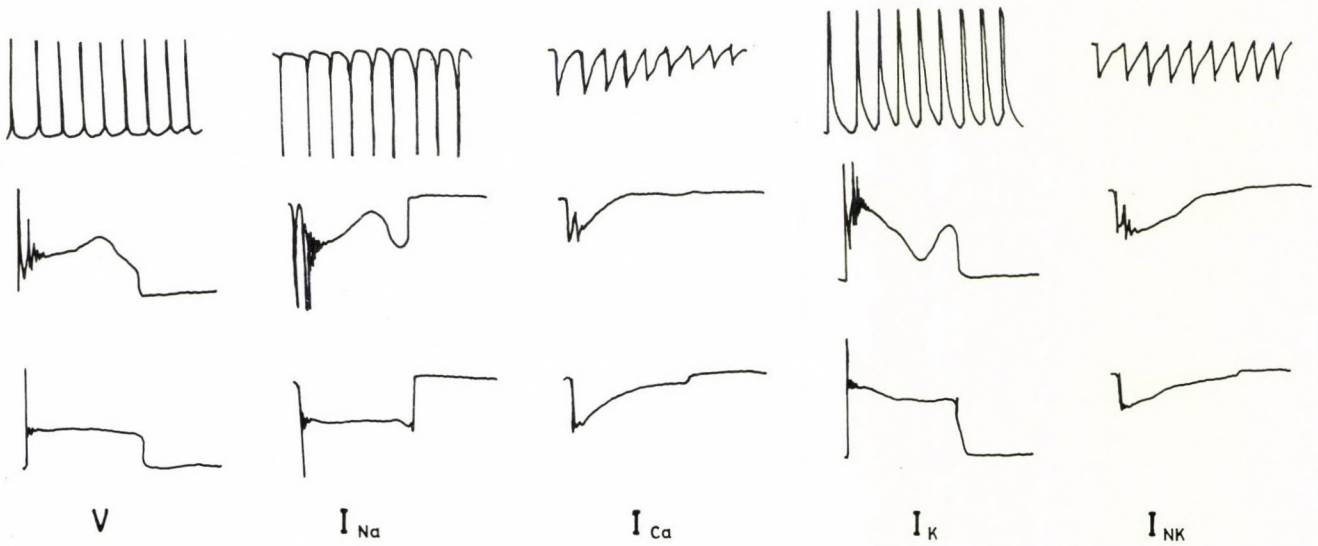

Fig. 2: Membrane potential changes and ionic currents flowing during three different types of paroxysmal depolarizations. **V**: membrane potential, I_{Na}: sodium current, I_{Ca}: calcium current, I_K: potassium current, I_{NK}: non-specific inward current.

During PDS, the number (density) of calcium channels, occupied by the convulsant increases on the expenses of the previously normal ones, with a kinetics determined by the association constant. Simultaneously it decreases with a rate regulated by the dissociation constant, so that by the end of PDS the number of impaired calcium channels returns to its initial value. The interplay of association and dissociation of convulsant determines the strength of the non-specific inward current and consequently the time course and duration of PDS.

If the set of equations of normal ionic currents is complemented with I_{NK}, by suitable choice of its variables, any form of PDS can be simulated.

In Figure 1A to D simulations of the convulsive membrane are presented at different values of the association constant (k), potassium conductance (g_K), and number of initially occupied calcium channels (NK). With appropriate choice of these variables any form of PDS, observable in intracellular records can be simulated, beginning with a somewhat elevated firing up to the PDS with smooth plateau and total sodium spike inactivation. In these simulations the full blown spike potentials have 100 mV amplitude and every record lasts for 4 ms. In Figure 1A the association constant is varied from zero to 0.20, at almost normal potassium conductance (g_K=53) and at 18 initially occupied calcium channels/μm^2. In Figure 1B the same is done but at lower potassium conductance. This leads already at k=0.12 association constant to fast sodium inactivation. In Figure 1C the effect of lowering of potassium conductance is exemplified. At normal (60 mmho/μm^2) potassium conductance PDS can not be provoked. At 53 mmho/μm^2 relatively low association constants provoke high frequency discharge of normal spikes; further diminution of potassium conductance leads rapidly to smooth PDS. In Figure 1D the initial decrease of calcium channels caused by the drug (NK) is varied from 12 to 20 at middle size of association constant and potassium conductance. This leads also to rapid sodium inactivation. The dissociation constant was held throughout at constant value. Its variation influences only the length of PDS without acting on the discharge pattern.

The model gives opportunity to visualize and analyze all the currents underlying to PDS, in correlation with membrane voltage and changes in occupancy of calcium channels or in potassium conductance. In Figure 2 the component ionic currents and the consecutive membrane potential changes are presented during three different types of paroxysmal depolarization.

Sodium, calcium, potassium currents and non-specific inward current (NK) are plotted. Their highly synchronized time courses show,that paroxysmal depolarization is governed by voltage dependent ionic channels, therefore its onset, duration and termination is determined by the inherent rules of a pathological *circulus vitiosus*.

REFERENCES

Connor, J.A. and Stevens, C.F. (1971) Inward and delayed outward membrane currents in isolated neuronal somata under voltage clamp. J. Physiol. (London) 213, 1–19.

Connor, J.A. and Stevens, C.F. (1971) Voltage clamp studies of transient outward currents in gastropod neuron somata. J. Physiol. (London) 213, 21–30.

Ducreux, C. and Gola, M. (1975) Ondes paroxysmales induites par le metrazol (PTZ) sur les neurones d'Helix p: Modele fonctionnel. Pflüger's Archiv. 361, 43–53.

Fehér, O., Baranyi, A. and Gyimóthy, T. (1982) A model for the ionic mechanism of the paroxysmal depolarization shift. In: Physiology and Pharmacology of Epileptogenic Phenomena. (eds. M. Klee et al.), pp. 343–351. Raven Press, New York.

Fehér, O., Erdélyi, L. and Papp, A. (1988) The effect of pentylenetetrazol on the metacerebral neuron of Helix pomatia. Gen. Physiol. Biophys. 7, 505–516.

Heinemann, U., Lux, H.D. and Gutnick, M.J. (1977) Extracellular free calcium and potassium during paroxysmal activity in the cerebral cortex of the cat. Exp. Brain Res. 27, 237–243.

Hodgkin, A.L. and Huxley, A.F. (1952) Currents carried by sodium and potassium ions through the membrane of the giant axon of Loligo. J. Physiol. (London) 116, 449–472.

Matsumoto, H. and Ajmone-Marsan, C. (1969) Cortical cellular phenomena in experimental epilepsy: Interictal manifestations. Exp. Neurol. 9, 286–304.

Papp, A., Fehér,O. and Erdélyi, L. (1990) Properties of the slow inward current induced by pentylenetetrazol in Helix neurons. Epilepsy Res. 6, 119–125.

Papp, A. and Fehér, O. (1991) Analysis of the slow inward current induced by pentyleletetrazol. Exp. Brain Res. Series 20, pp. 31–34.

Smith, T.G., Barker, J.L. and Gainer, H. (1975) Requirements for bursting pacemaker potential activity in molluscan neurones. Nature 253, 450–452.

Swandulla, D. and Lux, H.D. (1985) Activation of a non-specific cation conductance by intracellular Ca^{2+} activation in bursting pacemaker neurons. J. Neurophysiol. 56, 1430–1453.

Traub, R.D. (1979) Neocortical pyramidal cells: A model with dendritic calcium conductance reproduces repetitive firing and epileptic behavior. Brain Res. 173, 243–257.

Ulbricht, W. and Wagner, H.H. (1976) Block of potassium channels of the nodal membrane by 4-aminopyridine and its partial removal on depolarization. Pflüger's Arch. 367, 77–87.

Walden, J., Pockberger, H., Witte, O.W., Speckmann, E.-J. and Petsche, H. (1986) Effects of organic calcium antagonists and agonists on invertebrate neurons. In: Epilepsy and Calcium (eds. E.-J. Speckmann, H. Schulze, J. Walden) pp. 275–276. Urban und Schwarzenberg, Munich.

Walden, J., Speckmann, E.-J. and Witte, O.W. (1988a) Membrane currents induced by pentylenetetrazol in identified neurons of Helix pomatia. Brain Res. 473, 294–305.

Walden, J. and Speckmann, E.-J. (1988b) Suppression of recurrent generalized tonic–clonic seizure discharges by intraventricular perfusion of a calcium antagonist. EEG Clin. Neurophysiol. 69, 353–362.

Williamson, T.L. and Crill, W.E. (1976a) The effects of pentylenetetrazol on molluscan neurons I, Intracellular recording and stimulation. Brain Res. 116, 217–229.
Williamson, T.L. and Crill, W.E. (1976b) The effects of pentylenetetrazol on molluscan neurons II, Voltage clamp studies. Brain Res. 116, 231–279.

Neurobiology 1 (1), pp. 65–82, 1993

THE ASTROCYTIC LOCALIZATION OF PROTEIN KINASE C IN THE NEOCORTEX, HIPPOCAMPUS AND IN VITRO HIPPOCAMPAL SLICES OF THE GUINEA PIG

A. Mihály[1], U. Kuhnt[2] and T. Krenács[3]

[1]Department of Anatomy, Albert Szent-Györgyi Medical University, H–6701 Szeged, P.O. Box 512, Hungary, [2]Department of Neurobiology, Max Planck Institute for Biophysical Chemistry, D–3400 Göttingen, Germany and [3]Department of Pathology, Albert Szent-Györgyi Medical University, H–6701 Szeged, Hungary

Summary: Immunohistochemical studies prove that most of the neurons of the central nervous system express one or more protein kinase C isoenzymes. However, there are only a few descriptions of the glial localization. In the present study, we detected protein kinase C immunohistochemically in guinea pig sensory neocortex, hippocampus and hippocampal slices following *in vitro* maintenance. Monoclonal antibodies against types II and III of protein kinase C were used. Consecutive sections were stained with polyclonal anti-glial-fibrillary-acidic protein serum. Scattered astrocytes contained protein kinase C in layers I and VI of the cerebral cortex, in the subcortical white matter, the subiculum, alveus and molecular layer of Ammon's horn, in the hilus and molecular layer of the dentate fascia. Ultrastructurally, immunostaining of glial processes in the neuropil and around blood vessels was observed. Strong staining of the endoplasmic reticulum and nuclear envelope was noted in glial cell bodies. The ultrastructural localization of protein kinase C suggests its participation in receptor-mediated processes, which may influence the shape and function of astrocytes.

Key words: immunohistochemistry, protein kinases, glia, guinea pig

Correspondence should be addressed to:
András Mihály, M.D., Ph.D.
Albert Szent-Györgyi Medical University
Department of Anatomy
P.O. Box 512
H–6701 Szeged, Hungary

Akadémiai Kiadó, Budapest

INTRODUCTION

Protein kinase C (PKC) plays an important role in receptor-mediated biochemical pathways. It can be activated by 1,2-sn-diacylglycerol (DAG) and arachidonic acid, which are generated by the receptor-mediated hydrolysis of phosphatidylinositol 4,5 biphosphate (PIP2) (Kishimoto et al., 1989). Whilst the biochemical machinery of PKC activation is similar in a variety of cells (Shearman et al., 1989), different outputs of the regulation are achieved by the differential localization patterns of the isoenzymes of PKC. The specific activity of the four subspecies or isoenzymes (alpha, βI, II, gamma) showed obvious regional differences in the rat brain (Ase et al., 1988). Immunohistochemical localization of the isoenzymes proved that neocortical neurons expressed the four subspecies variously: the most numerous being those which were stained with the anti-βII-PKC serum (Tsujino et al., 1990).

However, there are only a few descriptions dealing with the localization of PKC in glial cells. The PKC-like immunoreactivity (PKC-IR) of oligodendroglia cells was described at the level of the light microscope (Girard et al., 1985). With the help of monoclonal antibodies, PKC immunostaining was localized not only in neurons but also in astrocytes (Mochly-Rosen et al., 1987). Recently, it turned out that monoclonal antibodies against type III PKC (which corresponds to the subspecies alpha—(Kishimoto et al., 1989) stained exclusively astroglial cells in the human brain (Todo et al., 1990) and rat optic nerve (Komoly et al., 1991). On the other hand, the same antibody did not stain glial cells in mouse central nervous system (CNS) (Todo et al., 1990). In the present experiments, we localized PKC isoenzymes in the neocortex and allocortex of the adult guinea pig. Furthermore, we performed *in vitro* experiments when slices of the hippocampus were maintained in oxygenated incubation medium. Since this *in vitro* model is an important object of neurophysiological and pharmacological experiments, we intended to describe the astrocytic PKC-staining in detail.

MATERIALS AND METHODS

Two adult male guinea pigs were anesthetized with Nembutal (50 mg/kg) given intraperitoneally, then perfused through the heart with 4% paraformaldehyde, 0.1% glutaraldehyde in 0.1 M phosphate buffer (pH 7.4). The brain was removed, postfixed for 6 hours and 40≤μm thin coronal sections were cut with vibratome, between the approximate stereotaxic coordinates anterior 7.8 mm and 5.8 mm (Luparello, 1967). The sections were washed in phosphate-buffered saline (PBS, pH 7.4) overnight, treated with 0.5% sodium borohydride in PBS (Willingham, 1983) and processed for immunohistochemistry.

We used monoclonal antibodies (MC5, RPN 536, Amersham) directed against bovine brain-PKC. This antibody recognizes the α and β species of PKC which correspond to types III and II in hydroxy-apatite chromatographic subfractions (Kishimoto et al., 1989). The antibody was diluted in PBS, containing 10% normal horse serum. Free-floating sections were incubated with the antibodies (1:50 dilution) for 40 hours at 4 °C with constant agitation. The reaction was visualized with avidin-biotin-peroxidase detection system (Hsu et al., 1981) using diaminobenzidine-HCl as chromogen. Endogenous peroxidase activity was not inhibited. The biotinylated antibody was diluted to 1:200 in PBS, containing 0.1% bovine serum albumin. The sections were incubated for 2 hours at 4 °C with constant agitation. For light microscopy, the sections were mounted on gelatinized slides, dehydrated and coverslipped. Control sections were incubated in mouse IgG, diluted to 1:50, or in normal horse serum diluted to 1:10. The biotinylated antibody, the ABC reagent and the normal horse serum were manufactured by Vector (Burlingame, Calif. U.S.A.)

Consecutive vibratome sections were incubated with polyclonal anti-glial-fibrillary-acidic-protein (anti-GFAP) antibodies (DAKO) diluted to 1:300, visualized with the avidin-biotin-peroxidase method using 3-amino-9-ethylcarbazole (AEC) as a substrate. The PKC- and GFAP-containing cells were plotted at a 100x magnification with the help of an *xy* plotter. No counting procedures were applied. No ultrastructural studies were performed.

Four adult male guinea pigs (400–600 g) were killed by a blow to the neck, the brain was quickly dissected, both hippocampuses were removed and kept in ice-cold incubation solution during sectioning. 400≤μm thick transverse slices were cut with vibratome and placed in the oxygenated incubation medium (in mM: 124 NaCl; 5 KCl; 2 $CaCl_2$; 2 $MgSO_4$; 1.25 NaH_2PO_4; 26 $NaHCO_3$; 10 glucose; 95% O_2; 5% CO_2; pH 7.3–7.4). This method of slice preparation and maintenance has been regularly used in our laboratory (see *e.g.* Kuhnt et al., 1988).

The slices were kept at 24 °C for 1 hour, then fixed in 4% paraformaldehyde, 0.1% glutaraldehyde in 0.1 M phosphate buffer (pH 7.4) for 4–6 h. Vibratome sections (40≤μm thick) were cut parallel with the plane of the slice, washed in several changes of PBS for 6–8 h, and treated with 0.5% sodium borohydride (Willingham, 1983) in PBS. Regularly the first two sections were discarded, because the superficial layer of the slice contains damaged cells. This is the consequence of the preparation procedure (Tseng et al., 1987). Free-floating sections were incubated with the anti-PKC antibodies as

described above. No GFAP detection was performed. Altogether 16 slices (4 from each animal) were processed for immunohistochemistry.

For electron microscopy, the sections were treated with 1% OsO_4, dehydrated and flat embedded in Durcupan. Following light microscopic photography, the sections were reembedded in gelatin capsules, the appropriate areas trimmed and ultrathin sections were cut parallel with the surface of the block. These sections were mounted on formvar-coated single slot grids, some of them were stained with lead citrate, and observed in a Zeiss EM100 electron microscope.

RESULTS

Scattered glial cells contained PKC-IR in layers I and VI of the neocortex (Figs. 1a and 3a). Fine, thread-like (0.5–1≤μm thick) processes containing PKC-IR were observed in layer I (Figs. 1a and 3a) and in the alveus of the hippocampus (Fig. 3a). Several immunostained glia-like cells were present in the subcortical white matter (Figs. 1b and 3a), where they were more numerous than those containing GFAP immunoreactivity (Figs. 1a and d). On the contrary, the grey matter of the neocortex contained more GFAP-positive than PKC-containing cell bodies (Fig. 1c).

In the hippocampus glial PKC-IR was encountered in the alveus, fimbria and in the molecular layer of Ammon's horn (CA) and dentate fascia (FD) (Figs. 2a, b and 3a). Although we did not count the cells, the number of GFAP-stained glial cells was larger than the number of cells containing PKC-IR. GFAP immunostaining was distributed more or less evenly in every part of the hippocampal formation (Fig. 3b). The fusiform glial cells of the dentate granular layer (Cajal, 1911), which stained well with GFAP antibodies (Fig. 2c) did not show PKC-like immunostaining.

In slices, maintained *in vitro* PKC-IR was found mainly in glial cells and their fiber-like processes (Figs. 4a, e). These glial cells were located in the white matter of the subiculum, alveus of the Ammon's horn, fimbria, subgranular layer of the dentate gyrus and in the molecular layer of all parts of the hippocampal formation, close to the hippocampal fissure. In these areas not only glial cell bodies, but also numerous fiber-like processes exhibited strong PKC-IR (Fig. 4a). Some of these were attached to blood vessels (Fig. 4a). No immunoreactive glial cell bodies were seen in strata oriens, radiatum

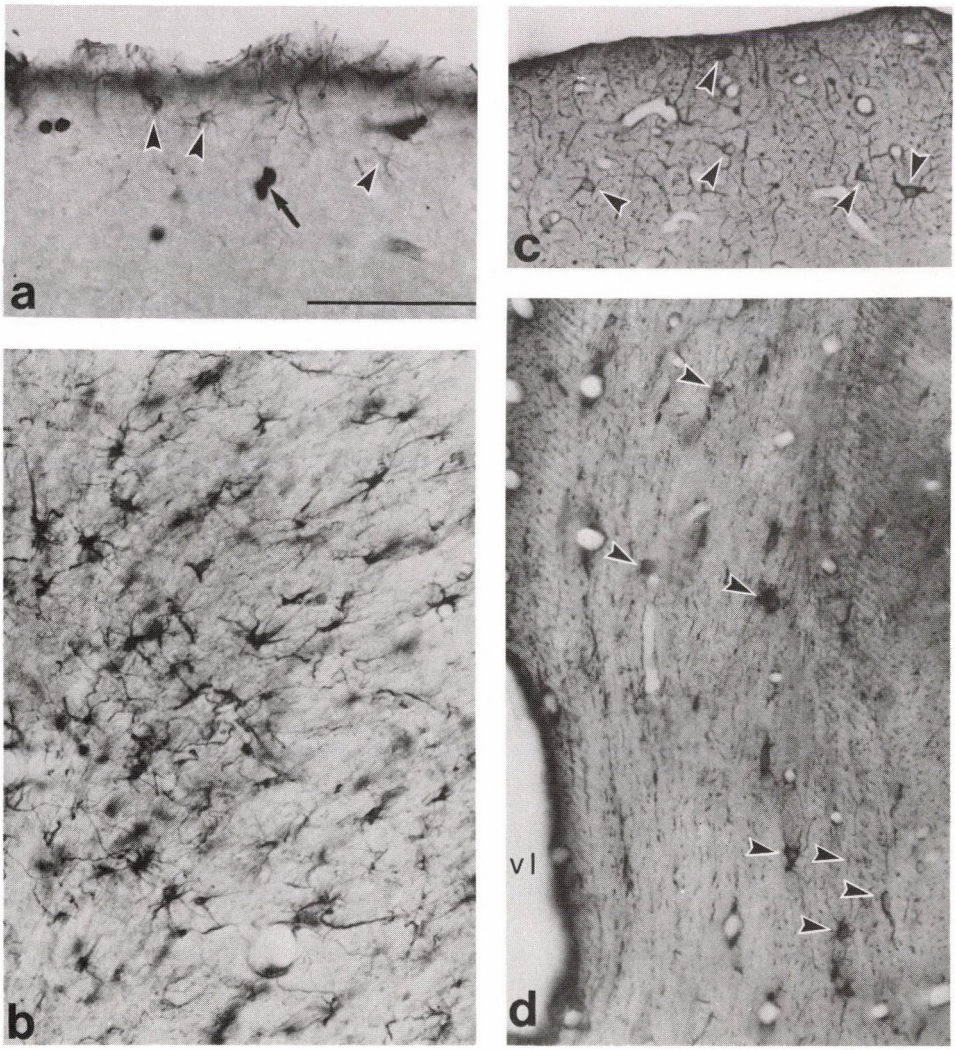

Fig. 1: Light microscopic localization of PKC-IR (**a**, **b**) and GFAP (**c**, **d**) in the neocortex of the adult guinea pig. Arrowheads point to immunoreactive glia-like cells, arrow to red blood cells. Bar: 100≤μm. Figs. **1a** and **c** show the immunoreactivity in layer I, Figs. **1b** and **d** the subcortical white matter. Note the abundance of PKC-containing cells (vl: lateral ventricle).

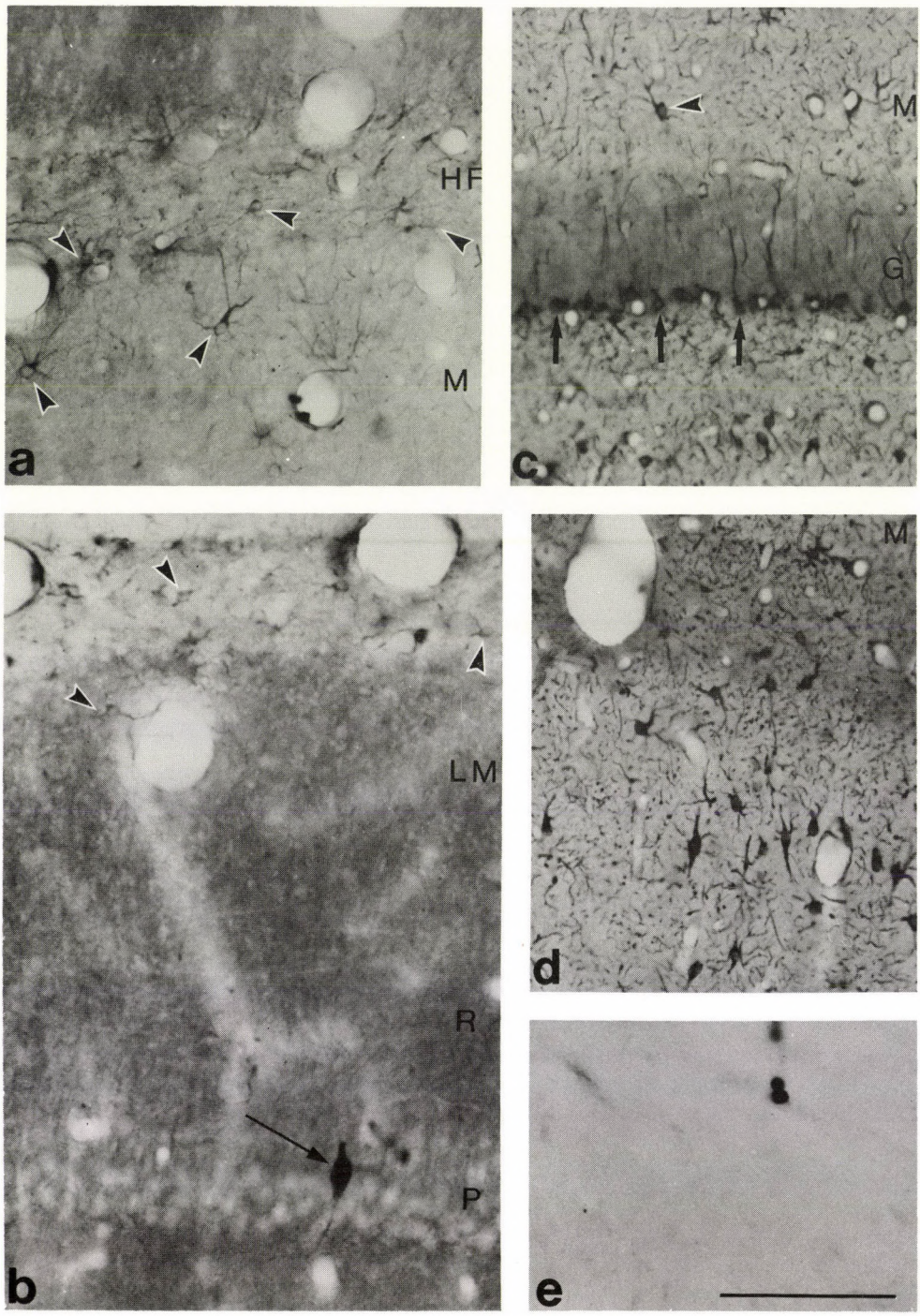
HF
M
a
M
G
c
LM
R
P
b
M
d
e

and in the inner segments of the dentate molecular layer. Although we did not count the immunoreactive cell bodies, their distribution was similar *in vivo* and *in vitro*.

Ultrastructurally, swelling of glial cell bodies and glial processes were observed (Figs. 5, 6,). Sometimes, glial filaments could be observed in the cytoplasm. The glial cells exhibiting PKC-IR seemed to be astrocytes (Fig. 5a). PKC-IR was present in the cell body, and in the processes (Fig. 5). PKC-IR could be localized on the inner surface of the cell membrane, on the surface of the rough surface endoplasmic reticulum (rER) and perinuclear cistern (Fig. 5a). The glial processes were similarly stained, i.e. the reaction product was attached to the inner surface of the cell membrane and found scattered in the cytoplasm (Fig. 6). The perivascular endfeet were stained, too (Figs. 5, 6). However, no PKC-IR was detected in the endothelium and in the basement membrane (Fig. 6a). Pericytes contained diffuse cytoplasmic staining (Fig. 6a). We observed flattened segments of glial membranes, which were closely attached to each other and only tiny gaps (2-4 nm, as judged on the electron micrographs) were observed between them (Figs. 5, 6). At these plaques strong PKC-IR was localized at the inner surfaces of both cell membranes. These gap junction-like structures could be seen mainly between the perivascular astrocytic processes (Fig. 6b), but rarely in the neuropil, too (Fig. 5).

PKC-IR was detected in few neurons in any part of the neocortex and hippocampal formation. Most of these hippocampal neurons were found in the strata oriens, radiatum and in the hilus of the dentate fascia. Occasionally, non-pyramidal cells containing PKC-IR were seen in the pyramidal cell layer of CA1 and CA2 (Figs. 2b and 4b, d). Rarely, varicose fibers containing immunoreactivity were seen (Fig. 4c).

Fig. 2: Light microscopic localization of PKC-IR (**a**, **b**) and GFAP (**c**, **d**) in the hippocampus of the adult guinea pig. Arrowheads point to immunoreactive glial cells. **a**: Molecular layer of the FD and CA1 (M). HF: Hippocampal fissure. **b**: Single neuron in CA1 (arrow) displaying PKC-IR (P: stratum pyramidale; R: stratum radiatum; LM: stratum lacunosum-moleculare). **c**: Fusiform glial cells (arrows) contain GFAP in the dentate granular layer (G). M: molecular layer. **d**: GFAP-containing astrocytes along the hippocampal fissure (M: molecular layer of FD). **e**: Control section incubated in diluted mouse IgG (bar: 100≤μm).

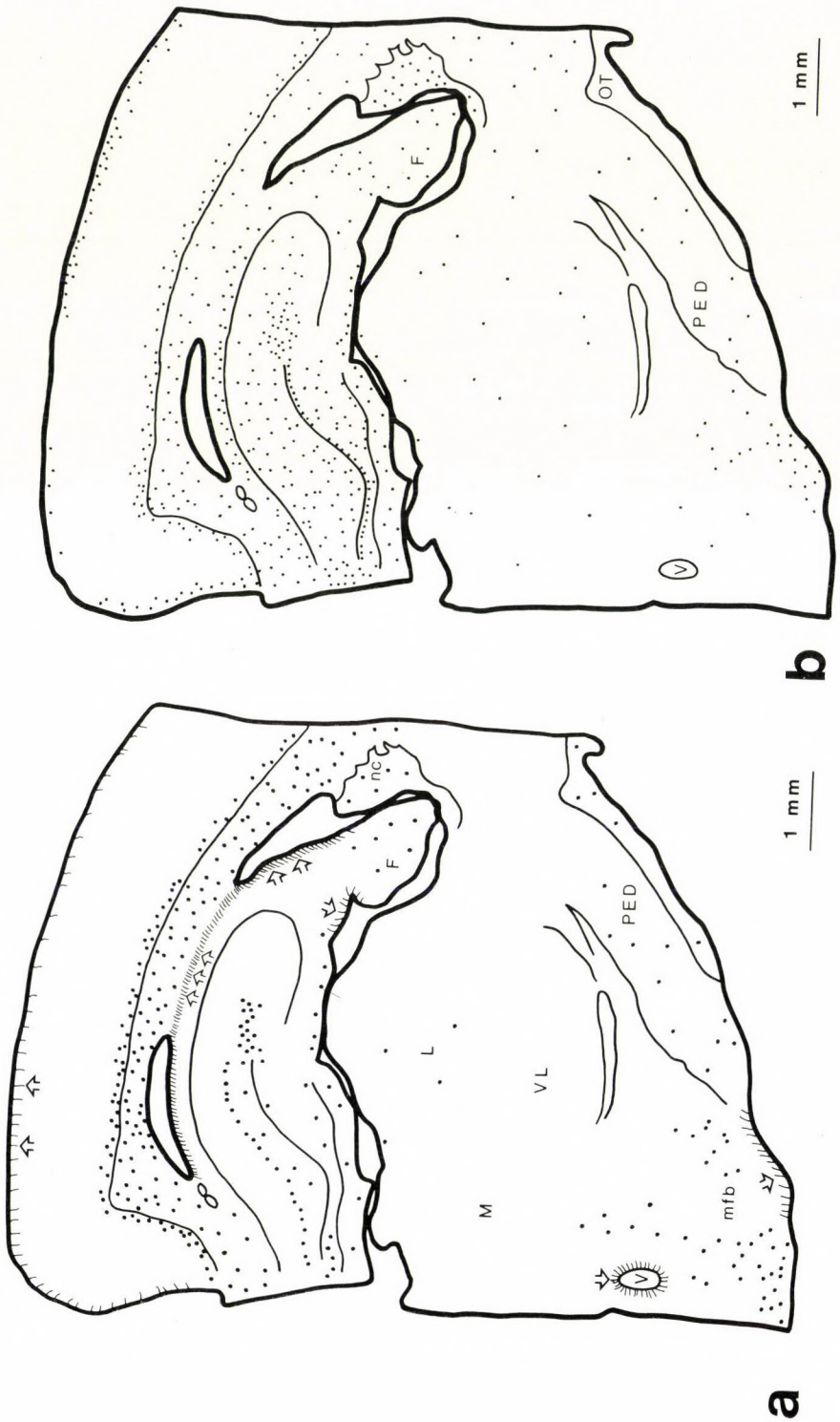
a
b
1 mm
1 mm
nc
F
L
VL
M
PED
mfb
OT
V

Sections incubated with mouse IgG or in diluted normal horse serum did not show immunostaining (Fig. 2e).

DISCUSSION

PKC is more abundant in the brain than in any other tissues (Kishimoto et al., 1989). Up to now three distinct fractions, types I, II and III have been separated with the help of hydroxyapatite column chromatography. The structure of each fraction has been determined by comparison with the enzymes that were separately expressed in cell cultures after transfection with the respective cDNA-containing plasmids (Kikkawa et al., 1987). Type I corresponds to the subspecies encoded by the gamma sequence, type II is a mixture of the βI and βII subspecies, and type III has the alpha sequence. These types exhibit different modes of activation and kinetic properties, slightly different pattern of phosphorylation and calcium sensitivity (Kishimoto et al., 1989). Their immunohistochemical localizations are different, too. Namely, types I and II are mainly neuronal, and there are abundant data about the light- and electron microscopic localization of the βI and βII subspecies in different structures of the CNS (Girard et al., 1985; Wood et al., 1986; Mochly-Rosen et al., 1987; Stichel and Singer, 1988; Kose et al., 1988; Tsujino et al., 1990).

Our results are strongly indicating the presence of PKC in astrocytes. Although the perfused brains were not investigated under electron microscope, the similarities of size, shape and distribution of GFAP- and PKC-containing structures suggested that

Fig. 3: Distribution of immunoreactive glial cells on sections stained with anti-PKC serum (**a**) and anti-GFAP serum (**b**). Each dot represents 3–5 cells. Empty arrows point to those parts of the section where PKC staining was observed in thread-like structures. (M, L, VL: medial, lateral and ventrolateral thalamic areas; PED: cerebral peduncle; OT: optic tract; mfb: medial forebrain bundle; V: third ventricle; F: fimbria; nc: caudate nucleus—after Luparello, 1967).

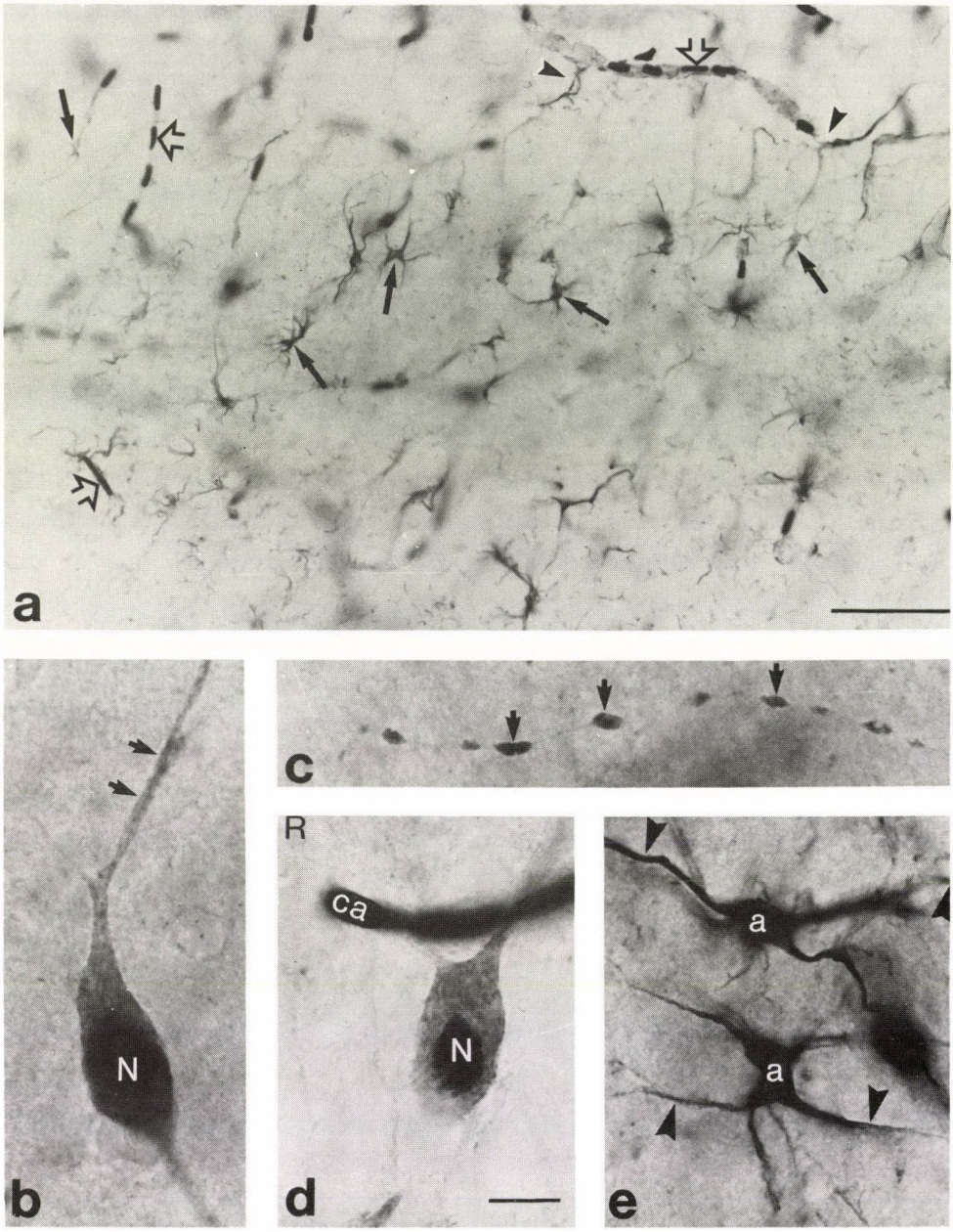
a
b
N
c
R
ca
N
d
a
a
e

they were astrocytes. Literature data are supporting our observations, proving the presence of PKC in glial cells both in cell cultures and in perfusion-fixed brains (Girard et al., 1986; Mobley et al., 1986; Mochly-Rosen et al., 1987; Hidaka et al., 1988; Murphy et al., 1988; Todo et al., 1990; Yong et al., 1991). Moreover, the observations of Todo et al. (1990) suggest that type III (alpha subspecies) of PKC is present in astrocytes. Our results are supporting the observations of Todo et al. (1990), since the monoclonal antibodies from clone MC5 can be blocked by pre-incubation with a synthetic peptide corresponding to the residues 296-309 of bovine PKC-alpha (Young et al., 1988). The neuronal staining obtained with this antibody is due to cross reaction with the β-type PKC, since the 296-309 region is largely conserved in the β forms as well (Ohno et al., 1987). This could be the explanation of the neuronal staining in the neocortex and hippocampus of the rat (Stichel and Singer, 1988). The fact, that the authors (Stichel and Singer, 1988) did not observe glial staining could be explained with a different tissue expression pattern in the rat. It has to be noted that monoclonal antibodies against type III brain PKC did not stain glial cells in the rat brain (Todo et al., 1990). In these experiments only astrocytes from the human brain were stained (Todo et al., 1990). The fact that we detected type III PKC in the astrocytes of the guinea pig indicated further diversities in the level of PKC expression between the rodent species. However, our results are strongly supported by the observations of Komoly et al. (1991),

Fig. 4: Light microscopic localization of PKC-IR in hippocampal slices. Bars: 100≤μm (1a) and 10≤μm (1b-e). **a**: Astrocytes containing PKC-IR (arrows) in the white matter of the subiculum. Empty arrows point to blood vessels containing red blood cells (RBCs). Arrowheads point to glial processes attached to vessels. **b**: Neuronal PKC-IR in stratum radiatum of CA1 (arrows: dendrite). **c**: Varicose fiber (arrows) of unknown origin with PKC-IR in stratum moleculare of CA3. **d**: Neuronal PKC-IR in stratum pyramidale of CA1(R: stratum radiatum; ca: capillary containing RBCs; N: cell nucleus). **e**: Astrocytes containing PKC-IR in the white matter of the subiculum (A: cell bodies; arrowheads: processes).

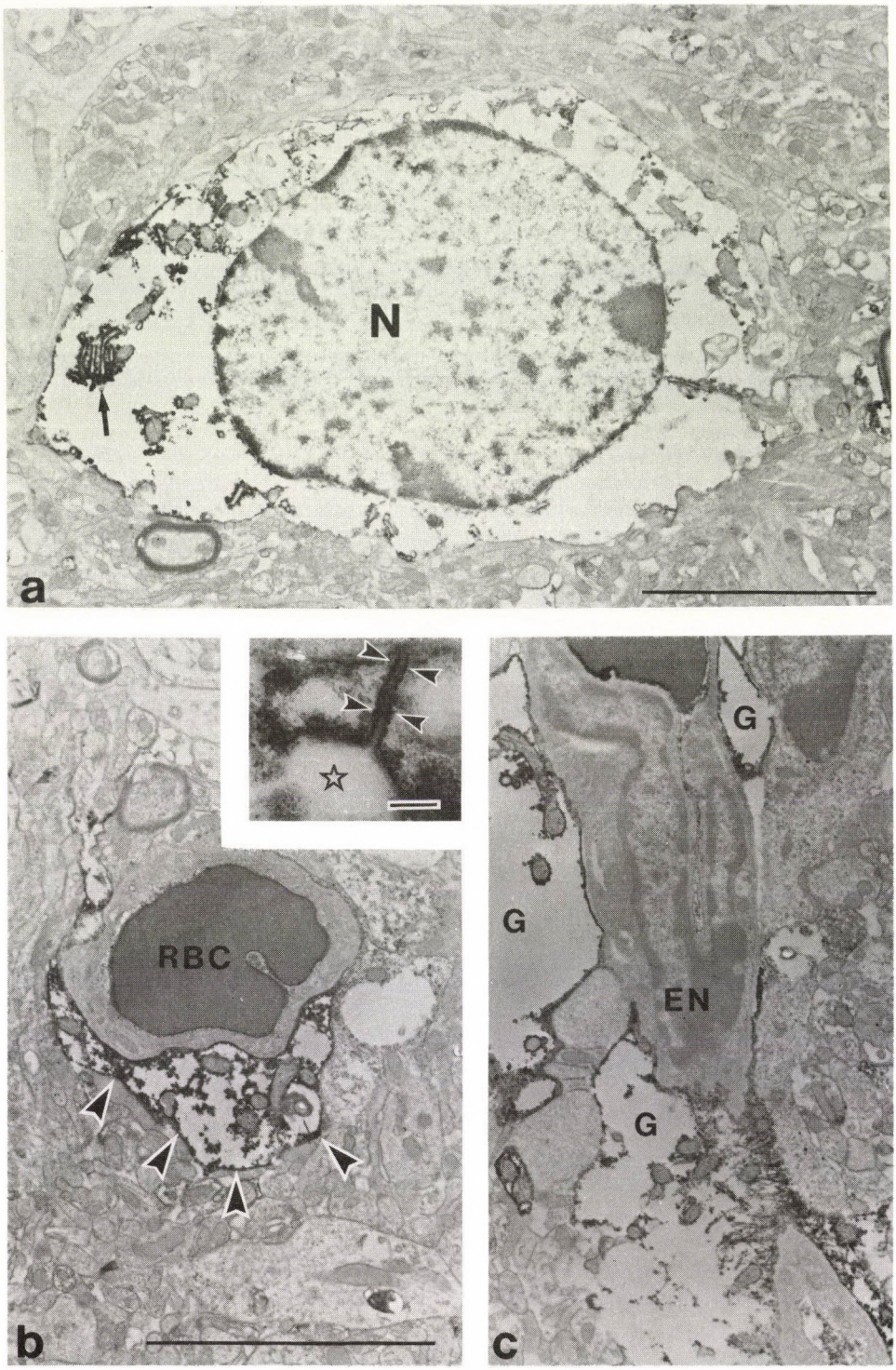
N
a
RBC
b
G
G
EN
G
c

who described astrocytic immunoreactivity in rat optic nerve. The ultrastructural studies demonstrated PKC-IR in glial endfeet around blood vessels (Komoly et al., 1991). Endothelial cells—similarly to our observations—did not contain type III PKC (Komoly et al., 1991). The fact that they did not observe PKC-IR in pericytes (Komoly et al., 1991) indicates that there might be differences between rats and guinea pigs as to their PKC expression pattern. The inter-species differences in the localization and distribution of PKC isoenzymes are well-known from previous experiments (for review see Nishizuka, 1988). As to the sweeling of astrocytic cell bodies and their processes in vitro, this is a reaction coupled to alterations of the microenvironment. Astrocytic swelling and slight dilatation of the extracellular space are common features of in vitro slice preparations (Tseng et al., 1987; Kuhnt et al., 1988). In the same time, neuronal processes are relatively well preserved (see also Tseng et al., 1987; Kuhnt et al., 1988).

Our observations proved that not every astrocytes expressed PKC-IR. Although not counted, the plots showed conspicuous differences between the density and distribution of PKC- and GFAP-containing cells, the latter being more numerous. Furthermore, it was shown that not every astrocyte contained GFAP immunoreactivity in normal adult brains (Faddis and Vijayan, 1988). It seems therefore, that only a subpopulation of astrocytes contain detectable amount of PKC. If it is reflecting some functional differences between astrocytes, remains to be elucidated.

Fig. 5: Ultrastructural localization of PKC-IR in astrocytes in the molecular layer of CA2 (**a**) and dentate fascia (**b**, **c**). **a**: Tipically swollen cell body of an astrocyte (N: nucleus; arrow points to rER cistern). No synaptic contacts were observed on the surface of the cell body with high magnification. Bar: 5≤μm. **b**: Pericapillary astrocytic process (arrowheads) containing PKC-IR. There is an erythrocyte (RBC) in the lumen of the capillary. Bar for 2b and 2c: 5≤μm. **Inset**: Gap-junction-like attachment of glial membranes. Arrowheads point to PKC-IR attached to the inner surface of the membranes (star indicates extracellular space). Bar: 0.1≤m. **c**: Swollen glial processes (G) containing PKC-IR around a blood vessel. Endothelial cell (EN) does not display PKC-IR.

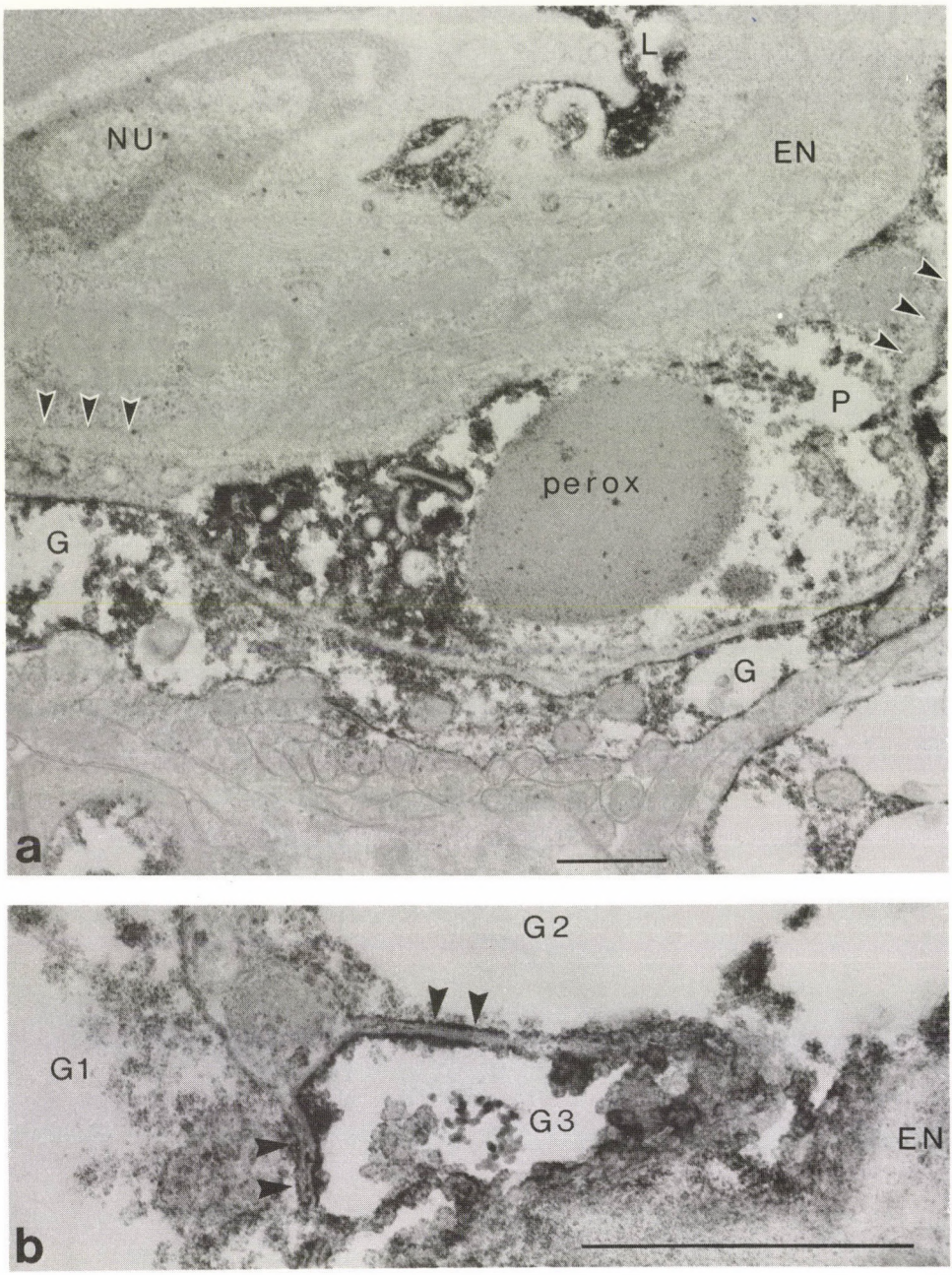
L
NU
EN
P
perox
G
G
a
G2
G1
G3
EN
b

Several studies, performed on cell cultures discussed the possible functions of PKC in glial cells. Activators of PKC induced the growth of astrocytic processes (Mobley et al., 1986), and stimulated the glial DNA synthesis (Bhat, 1989). It seems therefore, that PKC activity is an important step in the regulation of glial proliferation.

The translocation of PKC from the cytosol to the cell membrane (Mobley et al., 1986; Bhat, 1989; Mudd and Raizada, 1990) indicated that some of the membrane proteins could be the targets of the phosphorylating action of PKC. The activation of astrocytic PKC by phorbol esters induced oscillations of membrane conductance (MacVicar et al., 1987), indicating that PKC may regulate the function of glial ion channels (Shearman et al., 1989). From this point, our observations regarding the localization of PKC-IR at gap-junction-like membrane appositions are very interesting and raise the possibility of the control of gap-junction permeability by PKC. It is important to note, that elevation of intracellular Ca^{++} level (which is also activating PKC) decreases the permeability of gap junctions (Rose et al., 1977). The presence of gap junctions between glial cells has been proven by means of the freeze-fracturing technique (Brightman et al., 1978) and electrophysiological methods (Kettenmann and Ransom, 1988). Whether the membrane appositions observed in our preparations were true gap junctions or preparation-artifacts has to be elucidated in further experiments. More sophisticated immunohistochemical techniques (postembedding immunogold staining, or staining of ultrathin frozen sections) are needed to verify this very interesting possibility.

The subcortical white matter and corpus callosum contain only a few astrocytes which are stainable with anti-GFAP serum (Faddis and Vijayan, 1988). The total number

Fig. 6: Ultrastructural localization of PKC-IR in perivascular structures. Bars: 1≤μm. **a**: Diffuse cytoplasmic PKC-IR in the process of a pericyte (P). The cytoplasm contains peroxisome (perox). The pericyte is surrounded by glial endfeet (G) displaying PKC-IR (arrowheads: basement membrane). The cytoplasm and nucleus (NU) of the endothelial cell (EN) are devoid of immunostaining. The luminal surface (L) of the endothelial cell shows immunoreactivity. **b**: Perivascular glia-like processes (G1, G2, G3) with gap-junction-like membrane appositions (arrowheads). The inner surface of the membranes (mainly in G3) is heavily decorated with PKC-IR. EN: endothelial cell.

of astrocytes is always larger than after GFAP-staining (Faddis and Vijayan, 1988). Our observations with GFAP staining support these literature data. The fact that the number of PKC-positive cells was larger raised the possibility that at least some cells could be oligodendroglia cells. However, we have to confirm this suggestion with double staining methods.

The fact, that we did not encounter oligodendroglia cells containing PKC-IR in the hippocampal slice under the electron microscope, did not mean that the oligodendroglia is free from PKC. Immunocytochemical observations prove the existence of PKC-IR in oligodendroglia cells of rat brain (Girard et al, 1985). On the other hand, stimulation of PKC by tumour promoters *in vitro*, brought about morphological changes in oligodendroglia cells indicating the operation of the enzyme (Althaus et al, 1991). Different expression pattern of the different isoenzymes may explain our findings. Further experiments or different experimental conditions are needed to clarify this controversy.

ACKNOWLEDGEMENT

This work was supported by OTKA, Hungary (grant No. 912). Part of this work has been done during the time of a fellowship (A. M.) granted by the Alexander von Humboldt Foundation. The authors thank Miss I. Bódi (Dept. Anatomy, Szeged) for the excellent secretarial assistance.

REFERENCES

Althaus, H.H., Schröter, J., Spoerri, P., Schwartz, P., Klöppner, S., Rohmann, A. and Neuhoff, V. (1991) Protein kinase C stimulation enhances the process formation of adult oligodendrocytes and induces proliferation. J. Neurosci. Res. 29, 481–489.

Ase, K., Saito, N., Shearman, M.S., Kikkawa, U., Ono, Y., Igarashi, K., Tanaka, C. and Nishizuka, Y. (1988) Distinct cellular expression of βI- and βII-subspecies of protein kinase C in rat cerebellum. J. Neurosci. 8, 3850–3856.

Bhat, N.R. (1989) Role of protein kinase C in glial cell proliferation. J. Neurosci. Res. 22, 20–27.

Brightman, M.W., Anders, J.J., Schmechel, D. and Rosenstein, J.M. (1978) The lability of the shape and content of glial cells. In: Dynamic properties of glia cells. (ed. Schoffeniels, E., Franck, G., Hertz, L., Tower, B.D.) pp. 21–44. Pergamon Press, Oxford.

Cajal, S.Ry. (1911) Histologie du systeme nerveux. Part 2. Paris: Maloine.

Faddis, B.T. and Vijayan, V.K. (1988) Application of glial fibrillary acidic protein immunohistochemistry in the quantification of astrocytes in the rat brain. Am. J. Anat. 183, 316–322.

Girard, P.R., Mazzei, G.J., Wood, J.G. and Kuo, J.F. (1985) Polyclonal antibodies to phospholipid/Ca^{2+}-dependent protein kinase and immunocytochemical localization of the enzyme in rat brain. Proc. Natl. Acad. Sci. USA 82, 3030–3034.

Hidaka, H., Tanaka, T., Onoda, K., Hagiwara, M., Watanabe, M., Ohta, H., Ito, Y., Tsurudome, M. and Yoshida, T. (1988) Cell type-specific expression of protein kinase C isoenzymes in the rabbit cerebellum. J. Biol. Chem. 263, 4523–4526.

Hsu, S.M., Raine, L. and Fanger, H.J. (1981) Use of avidin-biotin-peroxidase complex (ABC) in immunoperoxidase techniques: A comparison between ABC and unlabelled antibody (PAP) procedure. J. Histochem. Cytochem. 29, 577–580.

Kettenmann, H. and Ransom, B.R. (1988) Electrical coupling between astrocytes and between oligodendrocytes in mammalian cell cultures. Glia 1, 64–73.

Kikkawa, U., Ono, Y., Ogita, K., Fujii, T., Asaoka, Y., Sekiguchi, A., Kosaka, Y., Igarashi, K. and Nishizuka, Y. (1987) Identification of the structures of multiple subspecies of protein kinase C expressed in rat brain. FEBS Lett. 217, 227–231.

Kishimoto, A., Kikkawa, U., Ogita, K., Shearman, M.S. and Nishizuka, Y. (1989) The protein kinase C family in the brain: Heterogeneity and its implications. Ann. N. Y. Acad. Sci. 568, 181–186.

Komoly, S., Liu, Y., Webster, H. deF. and Chan, K.-F.J. (1991) Distribution of protein kinase C isozymes in rat optic nerves. J. Neurosci. Res. 29, 379–389.

Kose, A., Saito, N., Ito, H., Kikkawa, U., Nishizuka, Y. and Tanaka, C. (1988) Electron microscopic localization of type I protein kinase C in rat Purkinje cells. J. Neurosci. 8, 4262–4266.

Kuhnt, U., Mihály, A., Siklós, L. and Joó, F. (1988) Increased retention of calcium in the dendrites of long-term potentiated CA1 neurons of the hippocampal slice. A combined electrophysiological and electron histochemical study. Histochemistry 90, 185–193.

Luparello, T.J. (1967) Stereotaxic atlas of the forebrain of the guinea pig. Karger, Basel.

MacVicar, B.A., Crichton, S.A., Burnard, D.M. and Tse, F.W.Y. (1987) Membrane conductance oscillations in astrocytes induced by phorbol ester. Nature 329, 242–243.

Mobley, P.L., Scott, S.L. and Cruz, E.G. (1986) Protein kinase C in astrocytes: A determinant of cell morphology. Brain Res. 398, 366–369.

Mochly-Rosen, D., Basbaum, A.I. and Koshland Jr., D.E. (1987) Distinct cellular and regional localization of immunoreactive protein kinase C in rat brain. Proc. Natl. Acad. Sci. USA 84, 4660–4664.

Mudd, L.M. and Raizada, M.K. (1990) Effects of phorbol ester on immunoreactive protein kinase C, insulin binding, and glucose uptake in astrocytic glial and neuronal cells from the brain. Neurochem. Res. 15, 273–278.

Murphy, J.A., Chapman, J.A., Suckling, A.J. and Rumsby, M.G. (1988) Protein kinase C activity in soluble fractions from glial cells in primary culture and subcultures. Neurosci. Lett. 85, 255–260.

Nishizuka, Y. (1988) The molecular heterogeneity of protein kinase C and its implications for cellular regulation. Nature 334, 661–665.

Ohno, S., Kawasaki, H., Imajoh, S., Suzuki, K., Inagaki, M., Yokokura, H., Satoh, T. and Hidaka, H. (1987) Tissue-specific expression of three distinct types of rabbit protein kinase C. Nature 325, 161–166.

Rose, B., Simpson, I. and Loewenstein, W.R. (1977) Calcium ion produces graded changes in permeability of membrane channels in cell junctions. Nature 267, 625–627.

Shearman, M.S., Sekiguchi, K. and Nishizuka, Y. (1989) Modulation of ion channel activity: A key function of the protein kinase C enzyme family. Pharmacol. Rev. 41, 211–237.

Stichel, C.C. and Singer, W. (1988) Localization of isoenzymes II/III of protein kinase C in the rat visual cortex (area 17), hippocampus and dentate gyrus. Exp. Brain Res. 72, 443–449.

Todo, T., Shitara, N., Nakamura, H., Takakura, K., Tomonaga, M. and Ikeda, K. (1990) Astrocytic localization of the immunoreactivity for protein kinase C isoenzyme (type III) in human brain. Brain Res. 517, 351–353.

Tseng, M.T., McClure, G.D., Jackson, C.B. and Schurr, A. (1987) Functional morphology of the hippocampal CA1 subfield. In: Brain slices: Fundamentals, applications and implications (eds. Schurr, A., Teyler, T.J. and Tseng, M.T.) pp. 22–38. Karger, Basel.

Tsujino, T., Kose, A., Saito, N. and Tanaka, C. (1990) Light and electron microscopic localization of βI-, II-, and gamma-subspecies of protein kinase C in rat cerebral neocortex. J. Neurosci. 10, 870–884.

Yong, V.W., Cheung, J.C.B., Uhm, J.H. and Kim, S.U. (1991) Age-dependent decrease of process formation by cultured oligodendrocytes is augmented by protein kinase C stimulation. J. Neurosci. Res. 29, 87–99.

Young, S., Rothbard, J. and Parker, P.J. (1988) A monoclonal antibody recognizing the site of limited proteolysis of protein kinase C. Inhibition of down-regulation in vivo. Eur. J. Biochem. 173, 247–252.

Willingham, M.C. (1983) An alternative fixation-processing method for preembedding ultrastructural immunocytochemistry of cytoplasmic antigens: The GBS (glutaraldehyde-borohydride-saponin) procedure. J. Histochem. Cytochem. 31, 791–798.

Wood, J.G., Girard, P.R., Mazzei, G.J. and Kuo, J.F. (1986) Immunocytochemical localization of protein kinase C in identified neuronal compartments of rat brain. J. Neurosci. 6, 2571–2577.

Neurobiology 1 (1), pp. 83–90, 1993

THE EFFECTS OF IN VIVO SELENIUM SUPPLEMENTATION ON THE AMPLITUDE OF THE SPONTANEOUS CONTRACTIONS AND THE RESPONSES TO ACETYLCHOLINE IN ISOLATED RABBIT ILEUM

N. Dalay[1], B. Turan[2], E. Koç[3], L. Afrasyap[1], E. Delilbaşi[4]

[1]Oncology Institute, Istanbul University, Istanbul, Turkey; [2]Department of Biophysics, Faculty of Medicine, Ankara University, Ankara, Turkey; [3]Department of Physiology, Faculty of Medicine, Ankara University, Ankara, Turkey and [4]Department of Surgery, Faculty of Dentistry, Gazi University, Ankara, Turkey

Summary: This study was carried out to investigate the effect of selenium supplementation at a therapeutic level on the isolated ileum contractions and the acetylcholine responses in New Zealand rabbits. While no difference with respect to the controls was found in the spontaneous ileum contraction frequencies a significant increase in the contraction amplitude was noted after 15 days of supplementation. Increasing concentrations of acetylcholine in the perfusion solution resulted in a significant increase of the contraction amplitudes in the supplemented animals as compared to controls. The tissue selenium levels and the gluthathione peroxidase activities were also found significantly higher than the controls. No difference was observed between the contraction numbers in the two groups. These findings indicate that selenium supplementation does not influence the smooth muscle resting potential.

Key words: selenium, contraction amplitudes, acetylcholine

Correspondence should be addressed to:
Prof. Dr. Nejat Dalay
I.U. Oncology Institute
34390 Çapa
Istanbul, Turkey

Akadémiai Kiadó, Budapest

INTRODUCTION

Selenium occupies a unique position among the metals and nonmetals while also sharing similarities with sulphur. It plays an important part in the synthesis of organic chemicals which occurs by a series of redox reactions. While until 1957 only the toxic effects of selenium were known, different studies have revealed the importance of selenium in the gluthathione peroxidase (GSH-Px) activity thereafter (Schwartz and Foltz, 1957; Flohe et al., 1973; Rotruck et al., 1973). GSH-Px is an antioxidative enzyme which participates in the removal of toxic hydrogen peroxides from the cell thus acting as an intracellular defense element in the hydrogen peroxide catabolism (Tappel, 1984; Parnham and Graf, 1987; Stadtman, 1990). GSH-Px and similar antioxidative enzymes require essential elements as cofactors for their catalitic activities. GSH-Px utilizes selenium while superoxide dismutase can use copper, zinc and manganese.

The activities of these enzymes in the mammalian cell is a function of the complex mutual interactions between the mineral cofactor and the regulation of the enzyme synthesis rate. Deficiencies of Cu, Zn, Mn and Se lead to a decrease in the activity of the enzyme which requires this element.

However, the correlation between the deficiency of these elements and the decline in the antioxidative enzyme activity is still controversial (Wendel and Reiter, 1985). Studies have shown that selenium deficiency may cause certain diseases due to the increased concentrations of peroxidation products and decreased GSH-Px activity (Chen et al., 1980; Bhene and Walters, 1983; Combs and Clark, 1985; Kiremidjian-Schumacher and Stotzky, 1987; Salonen et al., 1989). Surveys conducted in Turkey have revealed that the mean blood selenium levels are lower in the Turkish population when compared to the developed countries (Delilbasi et al., 1991). This study was undertaken to investigate the effect of selenium supplementation at a therapeutic dose level on the smooth muscle contraction parameters and the responses to acetylcholine in the rabbit ileum.

MATERIALS AND METHODS

Twenty male New Zealand white rabbits with a mean weight of 2600 g were taken into the study. The rabbits were fed under standard conditions on a standard diet for 10 days. After this period sodium selenite was added to the diet of 10 animals at a dose of

50 μg selenium per kg while the other group was kept as control. At the completion of 15 days the organs were removed under light anesthesia after blood samples were taken. All tissue samples were immediately frozen in liquid nitrogen and kept at -70 °C until enzyme determinations.

In order to isolate the ileum samples 1-1.5 cm pieces were taken from the terminal ileum and washed with Tirot solution (NaCl, 137 mM; KCl, 2.7 mM; $MgSO_4$, 1.4 mM; CaCl, 1.8 mM; NaH_2PO_4, 12 mM; Glucose, 5.5 mM). The pH (7.3-7.4) and the organ temperatures were kept constant at 36.5-37.5 °C and the perfusion solution was aerated with 95% oxygen and 5% carbon dioxyde. The samples were equilibrated for 30-60 minutes in the organ bath containing the perfusion solution and isotonic records were taken. The peak to peak contraction amplitudes were measured and the number of the spontaneous contractions per minute were determined from the records.

The tissue samples were homogenized in 0.1 M phosphate buffer, pH 7.1. Ileum GSH-Px levels were measured by an improved coupled test procedure (Günzler et al., 1974). Tissue selenium levels were determined using a graphic furnace atomic absorption spectrometer (Varian Spectra AA-30-40). In order to achieve maximum sensitivity deviations which might arise from the metallic states in graphite were eliminated by use of a palladium-ascorbic acid chemical modifier (Knowles and Brodie, 1988). The significance levels of the results which espect to the controls were calculated by the Student-*t* Test.

RESULTS

The number of the spontaneous contractions and the amplitude values in the control and study groups after 15 days of selenium supplementation are given in Table I as means and standard deviations. The data shows that the number of the contractions remains practically unchanged in the study group.

However, an increase of almost 100% was noted in the contraction amplitudes of the supplemented animals. The acetylcholine concentrations in the perfusion solution are shown in the first column. The contraction amplitudes in the control and supplemented groups are depicted in the second and third columns, respectively.

The effect of increasing acetylcholine concentrations on the concentration amplitudes are summerized in Table II as percentile changes. It can be observed that the rate of the increase in the concentration amplitudes are similar for both groups.

The ileum tissue selenium and GSH-Px levels in the groups and the significances of the intergroup differences are given in Table III. The data reveals a significant increase in both the tissue selenium levels and the GSH-Px activities in the supplemented group.

Table I

The contraction parameters, significance levels and changing rate of experimental and control groups. Results are expressed as the mean ±SD

Parameters	Control group	Experimental group	Changing rate and significance levels
Contraction number (min^{-1})	7.33±0.75	7.89±1.79	7.5% P>0.05
Contraction amplitude (mm)	18.17±3.48	36.56±9.28	101% P<0.05
Contraction amplitude (mm) in $3.3x10^{-5}$M ACh	21.80±3.43	42.22±17.28	94% P<0.05
Contraction amplitude (mm) in $6.7x10^{-5}$M ACh	28.40±7.39	61.78±25.37	110% P<0.05
Contraction amplitude (mm) in $1.3x10^{-4}$M ACh	29.20±6.74	67.56±26.05	110% P<0.05
Contraction amplitude (mm) in $2.6x10^{-4}$M ACh	34.80±13.75	69.44±16.78	99.5% P<0.05

Table II

Percentile rate of change in the contraction amplitudes with respect to the increasing acetylcholine concentrations

Acetylcholine concentration	Control group	Experimental group
$3.3x10^{-5}$M	20%	16%
$6.7x10^{-5}$M	56%	64%
$1.3x10^{-4}$M	61%	84%
$2.6x10^{-4}$M	92%	90%

Table III

The selenium concentrations and GSH-Px activities measured in the control and experimental groups and significance levels of differences. Results are measured as the mean ±SD

Parameters	Control group	Experimental group	Significance levels
Selenium (μg/g wet tissue)	0.21±0.01	0.28±0.03	P<0.05
GSH-Px (U/g wet tissue)	0.212±0.042	0.392±0.137	P<0.05

DISCUSSION

Our results show that selenium supplementation leads to an increase in the ileum tissue selenium levels and the GSH-Px activities when compared to the levels in the control group. An increase in the selenium content and the GSH-Px activity in different tissue types in response to selenium supplementation has been reported by several authors (Spears, 1984; Korpela et al., 1989; Smyth et al., 1990; Spallholz et al., 1990). It has been suggested that addition of acetylcholine to the perfusion solution may lead to calcium intake by modulating the calcium channels in isolated hamster ileum (Rosenberger et al., 1979). Data on immobilization of calcium from intracellular sources by acetylcholine are also available (Hurwitz et al., 1967).

In our study we observed higher spontaneous contraction amplitudes in the selenium supplemented animals. This can be ascribed to the higher selenium absorption in the ileum due to the increased selenium intake. Accordingly, Table III shows that the tissue selenium content is increased as compared to the control group. The selenite and selenate transport and absorption in the ileum is achieved by a carrier-mediated mechanism (Wolfram et al., 1985; Turner et al., 1990) where the sodium gradient and the Na/K-ATPase are involved in the active selenium transport in the ileum (Ardüser et al., 1985).

While high doses of selenium may exert a growth-inhibitory effect, various biological functions are stimulated by lower doses at therapeutic levels. Selenium supplementation at low, non-toxic doses protects the cell membranes by increasing the antioxidative capacity of GSH-Px. This effect is achieved by different mechanisms depending on the type of tissue, applied dose and the way of administration (Kiremidjian-Schumacher and Stotzky, 1987).

The presence of independent mechanisms linked to the selenium uptake and release kinetics in the cells are known already. Before being metabolized selenium binds to the cell membrane (Grünwedel, 1984). The timing and degree of selenium uptake, retention and release may vary according to the type of the cell (Medina et al., 1985) depending on the specific surface properties, the composition of the medium and the amount of selenium available and hence can be controlled by these factors. Thus, we can conclude that the interaction of selenium with the cell membrane modulates the surface properties leading to changes in the ion transport and retention at the same time changing the capacity of the cell to respond to external stimuli. This assumption is supported by the finding that added selenium modulates the active calcium channels in the endothelial cell membranes (Neve, 1989). Furthermore, multivalent ions like selenium have been shown to compete for stimulating and inhibiting the effect of calcium on calmoduline (Manalan and Klee, 1984). Accordingly, the highest activity after selenium supplementation is observed in the mitochondrial fraction (Clausen, 1991). On the other hand, GSH-Px is mainly found in the cytosol and to a lesser extent in mitochondria. The membrane phase accounts only for 20% of the activity of this enzyme (Clausen, 1991). These data indicates that selenium supplementation has resulted in increases in the uptake and retention of selenium from the ileum. This may have induced changes in the cell membranes opening voltage-gated calcium channels leading to the enhanced calcium uptake possibly stimulating the release of calcium from mitochondria as well. The same effect could also have prompted calmoduline in inducing the increase in the intracellular calcium concentration. The elevated calcium content then might have led to the observed increase in the contraction amplitudes.

Introduction of acetylcholine to the perfusion solution does not seem to lead to different effects in the contraction amplitudes and the frequencies in both groups. However, the contraction amplitudes are elevated due to the increased calcium levels when compared to the normal while the spontaneous contraction frequency remains the same

for both groups. Thus, selenium does not appear to affect the acetylcholine mechanism in smooth muscle. Since variations in the contraction frequency can only be induced by the change of the membrane permeability to sodium and potassioum ions these results imply that selenium supplementation does not affect the smooth muscle membrane resting potential.

REFERENCES

Ardüser, F., Wolfram, S. and Scharrer, E. (1985) Active absorption of selenate by rat ileum. J. Nutr. 195, 1203–1208.

Bhene, D. and Walters, W. (1983) Distribution of selenium and gluthathione peroxidase inthe rat. J. Nutr. 113, 456–459.

Chen, X.,Yang, G., Chen, J., Wen, Z. and Ge, K. (1980) Studies on the relations of selenium and Keeshan desease. Biol. Trace Elem. Res. 2, 91–107.

Clausen, J. (1991) Uptake and distribution in rat brain of organic and inorganic selenium. Biol. Trace Elem. Res. 28(1), 57–68.

Combs Jr., G.F. and Clark, L.C. (1985) Can dietary selenium modify cancer risk? Nutr. Rev. 43, 325–331.

Delilbasi, E., Turan, B., Yücel, E., Sasmaz, K., Isimer, A. and Sayal, A. (1991) Selenium and Bechet's disease. Biol. Trace Elem. Res. 28(1), 21–25.

Flohe, L., Günzler, W.A. and Shock, H.H. (1973) Gluthathione peroxidase is a selenoenzyme. FEBS Lett. 32,132.

Grünwedel, D.W. (1984) Differential effects of sodium selenite and methylmercury(II) on membrane permeability and DNA replication in HeLa S3 carcinoma cells: A preliminary report regarding the modification of organomercurial toxicity by selenium compounds. Adv. Exp. Med. Biol. 177, 229–240.

Günzler, W.A., Kremers, H. and Flohe, L. (1974) An improved coupled test procedure for gluthathione peroxidase (EC 1.11.1.9) in blood. Z. Klin. Biochem. 12, 444–448.

Hurwitz, I., Joiner, P.D. and Van Hagen, S. (1967) Calcium pools utilized for contraction in smooth muscle. Am. J. Physiol. 213, 1299–1304.

Kiremidjian-Schumacher, L. and Stotzky, G. (1987) Selenium and immune responses. Environ. Res. 42, 277–303.

Knowles, M.B. and Brodie, K.G. (1988) Determinationof selenium in blood by Zeeman graphite furnace atomic absorption spectrometry using a palladium-ascorbic acid chemical modifier. J. Anal. Atom. Spectrom. 3, 511–516.

Korpela, H., Kumpulainen, J., Jussila, E., Kemila, S., Kaariainen, M., Kaariainen, T. and Sotainemi, E.A. (1989) Effect of selenium supplementation after acute myocordial infarction. Res. Commun. Chem. Path. 65(2), 249–252.

Manalan, A.S. and Klee, B.C. (1984) Calmoduline. Adv. Cyclic Nucl. Res. 18, 227–278.

Medina, D., Morrison, D. and Oborn, C.J. (1985) Selenium retention and inhibition of cell growth in mouse mammary epithelial cell lines in vitro. Biol. Trace Elem. Res. 8, 19–35.

Neve, J. (1989) Selenium and cardiovascular diseases. Pathol. Biol. 37(10), 1102–1106.

Parnham, M.J. and Graf,E. (1987) Selenoorganic compounds and the therapy of hydroxiperoxide-linked pathological conditions. Biochem. Pharmacol. 36(19), 3095–4001.

Rosenberger, C.B., Ticlev, M.K. and Triggle, D.S. (1979) The effects of Ca antagonist on mechanical responses and Ca movements in guinea pig ileal-longitudinal smooth muscle. Can. J. Physiol. Pharmacol. 54(4), 334–347.

Rotruck, J.T., Pope, A.L., Ganther, H.E., Swansen, A.B., Hafeman, D.G. and Hoekstra, W.G. (1973) Selenium; biochemical role of a component of gluthathione peroxidase. Science 179, 588–590.

Salonen, J.T., Alftan, G., Huttunen, J.K. and Puska, P. (1989) Association between serum selenium and the risk of cancer. Am. J. Epidemiol. 120, 342–349.

Schwartz, K. and Foltz, C.M. (1957) Selenium as an integral part of factor 3 against dietary necrotic liver degeneration. J. Am. Chem. Soc. 79, 3292.

Smyth, J.B.A., Wang, J.A., Barlow, R.M., Humphreys, D.J., Robins, M. and Stodulski, J.B.J. (1990) Experimental acute selenium intoxication in lambs. J. Comp. Path. 102, 197–209.

Spallholz, J.E. (1990) Selenium and gluthathione peroxidase: Essential nutrient and antioxidant component of the immune system. Adv. Exp. Med. Biol. 262, 145–158.

Spears, J.M. (1984) Nickel as a "newer trace element"in the nutrition of domestic animals. J. Anim. Sci. 59, 823–835.

Stadtman, T.C. (1990) Selenium biochemistry. Ann. Rev. Biochem. 59, 111–125.

Tappel, A.L. (1984) Selenium-gluthathione peroxidase; properties and synthesis. Curr. Top. Cell. Reg. 24, 87–92.

Turner, J.C., Osborn, P.J. and McVeagh, S.M. (1990) Studies on selenate and selenite absorption by sheep ileum using an everted sac method and an isolated vascularly perfused system. Comp. Biochem. Physiol. 95 A(2), 297–301.

Wendel, A. and Reiter, R. (1985) In: Trace elements in man and animals. (eds. Mills, C.F., Brenner, I., Chester, J.K.) pp. 93–101. Commonwealth Agricultural Bureaux, Slough, UK.

Wolfram, S., Ardüser, F. and Scharrer, E. (1985) In vivo intestinal absorption of selenate and selenite by rats. J. Nutr. 115, 454–459.

Neurobiology 1 (1), pp. 91–100, 1993

APPEARANCE OF DIAMINOBENZIDINE-STAINING GLIAL CELLS IN THE RAT CNS: AN ONTOGENETIC HISTOCHEMICAL STUDY

A. Ambrus and G. Jancsó

Department of Physiology, Albert Szent-Györgyi Medical University, Dóm tér 10, H–6720 Szeged, Hungary

Summary: The postnatal appearance of diaminobenzidine (DAB)-staining glial cells was studied in certain regions of the rat central nervous system. DAB-positive cells appeared in the hypothalamus, the nucleus of the solitary tract and the most superficial laminae of the spinal dorsal horn on the 7th, 8th and 14th postnatal day, respectively. The number and staining intensity of these DAB-positive cells progressively increased and reached the adult levels at the end of the third postnatal week. Glial staining is likely to result from a non-enzymatic oxidation of DAB, since it was resistant to heat pretreatment, but was abolished if hydrogen peroxide was omitted from the incubation medium. The present results reveal that a particular population of glial cells exhibit a characteristic developmental change which can be detected by means of peroxidase histochemistry. The close topographical relationship is suggestive of a functional association between capsaicin-sensitive primary afferents and DAB-positive glial cells.

Key words: neuroglia, peroxidase, capsaicin, solitary tract nucleus, spinal cord, arcuate nucleus

INTRODUCTION

In the rat central nervous system a population of glial cells exhibit a strong reaction with diaminobenzidine (DAB) after staining with a histochemical procedure for peroxidase

(Keefer and Christ, 1976). More recent studies, using double labelling immunohistochemical techniques, have revealed that DAB-positive cells in the rat hypothalamic arcuate nucleus express glial fibrillary acidic protein. Accordingly, these cells have been identified as astrocytes (Schipper et al., 1990; Schipper and Mateescu-Cantuniari, 1991). Further investigations into the possible functional significance of these cells have demonstrated that they specifically bind oestrogen (Keefe et al., 1991) and respond to oestrogen with an increase in the number of DAB-positive cytoplasmic granules (Schipper et al., 1990). It has been concluded that these particular astrocytes display marked changes with respect to the oestrus cycle and may participate in synaptic remodelling within the arcuate nucleus (Schipper et al., 1990; Keefe et al., 1991).

The DAB staining of glial cytoplasmic granules has been suggested to result from the activity of endogenous peroxidase or catalase (Keefer and Christ, 1976). Further studies, however, have indicated that glial DAB staining is unlikely to result from enzymatic action, for staining can invariably be demonstrated at various pH-s and cannot be abolished by prior heat treatment of the specimens. Histochemical studies on the possible mechanism of this pseudoperoxidase reaction have indicated that it may be attributed to a non-enzymatic reduction of DAB by haeme compounds (Schipper et al., 1990; Schipper and Mateescu-Cantuniari, 1991).

There is a close resemblance between the topographical distribution of DAB-staining glial cells and the termination areas of capsaicin-sensitive primary afferent fibres in the medulla and the spinal cord (Jancsó and Király, 1980; Ritter and Dinh, 1988). Since DAB-positive glial cells have been implicated in processes related to the transmitter metabolism and the formation of synaptic connections (Schipper et al., 1990), it seemed to be of interest to study their histochemical features during a period of postnatal development involving changes in the chemistry and formation of synaptic connections of capsaicin-sensitive primary afferents (Jancsó et al., 1977; Coimbra et al., 1986; Pignatelli et al., 1989). Therefore, the aim of the present study was to examine, in the course of early postnatal development, the appearance of DAB-positive glial cells in certain medullary and spinal regions known to be the termination areas of capsaicin-sensitive primary afferents. The development of DAB-positive glial cells was also studied in the hypothalamic arcuate nucleus,

the only brain region in which DAB-positive astrocytes have been suggested to possess a special function (Schipper et al., 1990; Keefe et al., 1991).

MATERIALS AND METHODS

Wistar rats of either sex, aged 1–60 days, were used in these experiments. The animals were anaesthetized with ether and perfused transcardially with a fixative containing 1% paraformaldehyde and 1.25% glutaraldehyde in 0.1 M phosphate buffer, pH 7.4. The brain and the spinal cord were removed and postfixed in the same solution for 4 h at 4 °C and then immersed in a 10% sucrose solution in 0.1 M phosphate buffer overnight. Sections 25–60 μm in thickness were cut either on a vibratome or on a freezing microtome and incubated for the demonstration of peroxidase activity according to the technique of Graham and Karnovsky (1966) as modified by Adams (1981). Frozen sections were dehydrated, mounted in Entellan and coverslipped. Vibratome sections were embedded in Araldite and 1–2 μm thick sections were cut on a Reichert ultrotome and stained with toluidine blue. In some cases the reaction was performed after the omission of H_2O_2 from the incubation medium or after prior exposure of the sections to a temperature of 95 °C for 1 h. In some experiments peroxidase activity was demonstrated by Mesulam's method (1978), with tetramethylbenzidine (TMB) as substrate.

RESULTS

DAB-positive structures were characterized by clusters of reactive granules distributed in the vicinity of small round or oval nuclei. This was especially clearly seen in semithin sections (Fig. 1B), in which the majority of these cells could be identified as astrocytes, although some cells resembled microglia on the basis of the cytological criteria established by Ling et al. (1973). Staining with DAB in the peroxidase reaction was not abolished by prior exposure of the sections to 95 °C for 1 h. However, glial staining could not be demonstrated after the omission of H_2O_2 from the incubation medium. This is in agreement with previous findings by Keefe et al. (1991), who concluded that DAB staining of glial cells is a result of a pseudoperoxidase reaction mediated by haeme-containing compounds present in these cells (cf. Schipper et al., 1990).

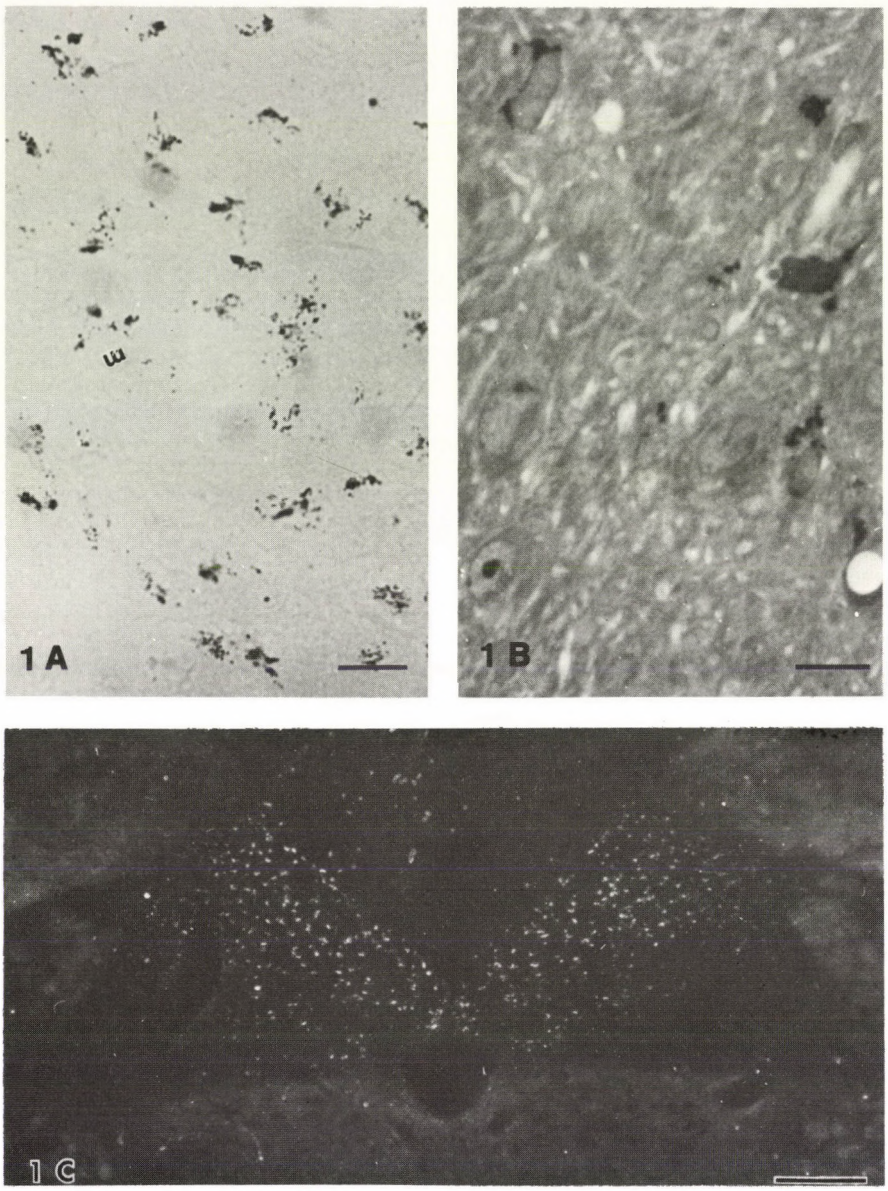

Fig. 1: DAB-positive glial cells in the nucleus of the solitary tract. **A**: Many cells show intense staining on the 16th postnatal day. **B**: Toluidine blue-stained semithin section obtained from an adult rat. DAB-positive granules are associated with cells exhibiting characteristics of astrocytes or microglial cells. **C**: Dark-field photomicrograph of a transverse section of the medulla at the level of the area postrema (AP) of an adult rat. DAB-positive cells are confined to the nucleus of the solitary tract. Scale bar represents 25 μm (A, B) or 200 μm (C).

DAB-staining granules were not observed in any of the brain regions studied during the first 6 days of postnatal life. DAB-reactive glial cells appeared on the 8th postnatal day in the nucleus of the solitary tract. Their number was low and their staining intensity weak. Both the staining intensity and the number of DAB-positive cells gradually increased during the second and third postnatal weeks (Fig. 1A). From the end of the second postnatal week on, their distribution was similar to that seen in adult animals (Fig. 1C).

DAB-reactive structures were not observed in the spinal cord until the 14th or 15th postnatal day, when a few faintly stained clusters of DAB-positive granules were noted in the superficial dorsal horn (Fig. 2A). The number and intensity of these granular structures rapidly increased during the next few days. On day 20, DAB-positive cells with moderate staining intensity were numerous; reactive cells were confined to the marginal zone and the substantia gelatinosa (Fig. 2B). In adult animals, intensely stained DAB-positive cells clearly outlined these laminae (Fig. 2C). The distribution of DAB-positive cells was similar at all segmental levels. Various numbers of reactive glial cells were also encountered in the spinal white matter, and in particular in the lateral spinal nucleus.

In the hypothalamus, small clusters of DAB-positive granules appeared first within the median eminence on the 7th postnatal day and persisted throughout early postnatal development (Fig. 3A). DAB-stained cells appeared in the arcuate nucleus on the 8th day. Their number and staining intensity increased progressively towards adulthood (Fig. 3B–D). In contrast, the number of reactive cells within the median eminence subsequently gradually decreased with age, and DAB-staining cells could not be detected in this region of adult animals (Fig. 3D).

A similar topographical distribution of peroxidase-positive glial cells was observed if TMB was used instead of DAB for the demonstration of peroxidase activity. There was no apparent difference in the histochemical maturation of these glial cells with respect to sex in any of the brain regions investigated.

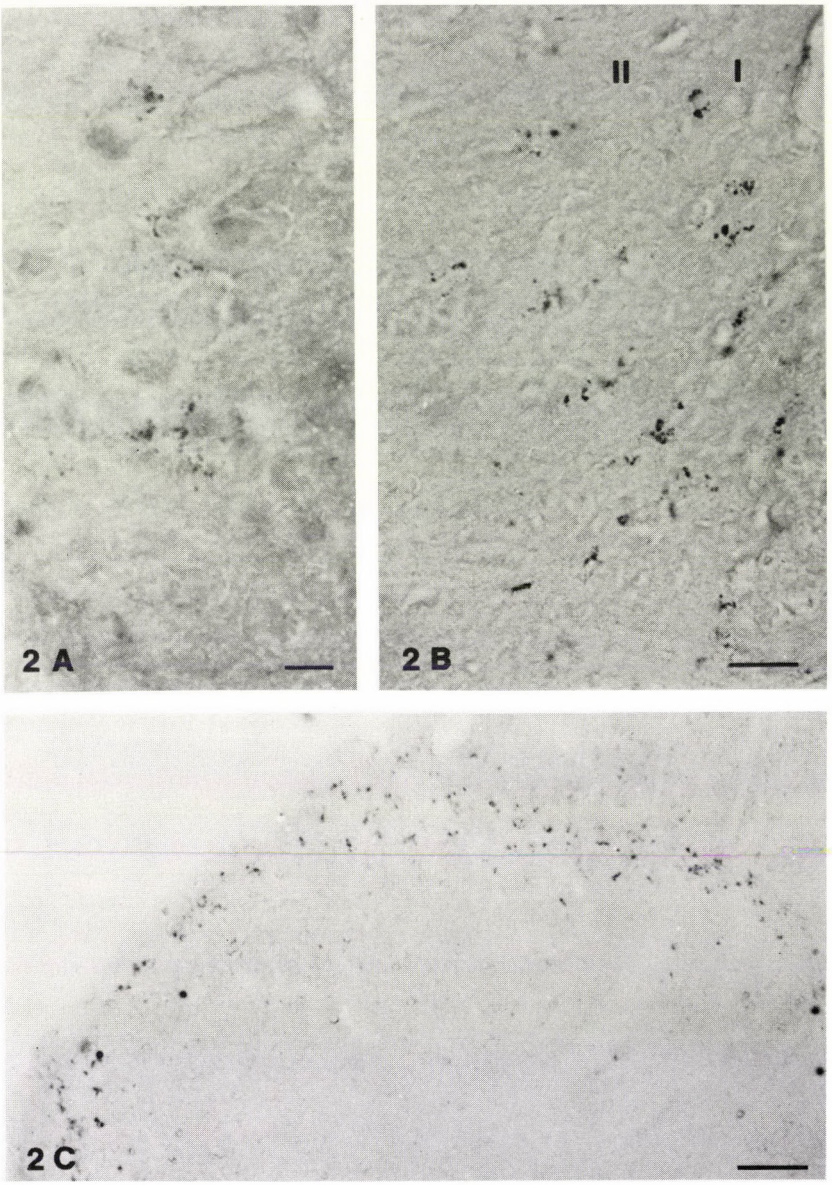

Fig. 2: DAB-positive glial cells in the dorsal horn of the lumbar spinal cord. **A**: Few reactive cells can be observed in the substantia gelatinosa on the 16th postnatal day. **B**: Numerous DAB-positive cells can be demonstrated in the most superficial laminae I and II of the spinal dorsal horn on the 20th postnatal day (dorsal is on the right, medial is on the top). **C**: This low-power photomicrograph shows the confinement of DAB-staining cells to the marginal zone and the substantia gelatinosa in an adult rat. Scale bar represents 10, 25 and 100 μm in A, B and C, respectively.

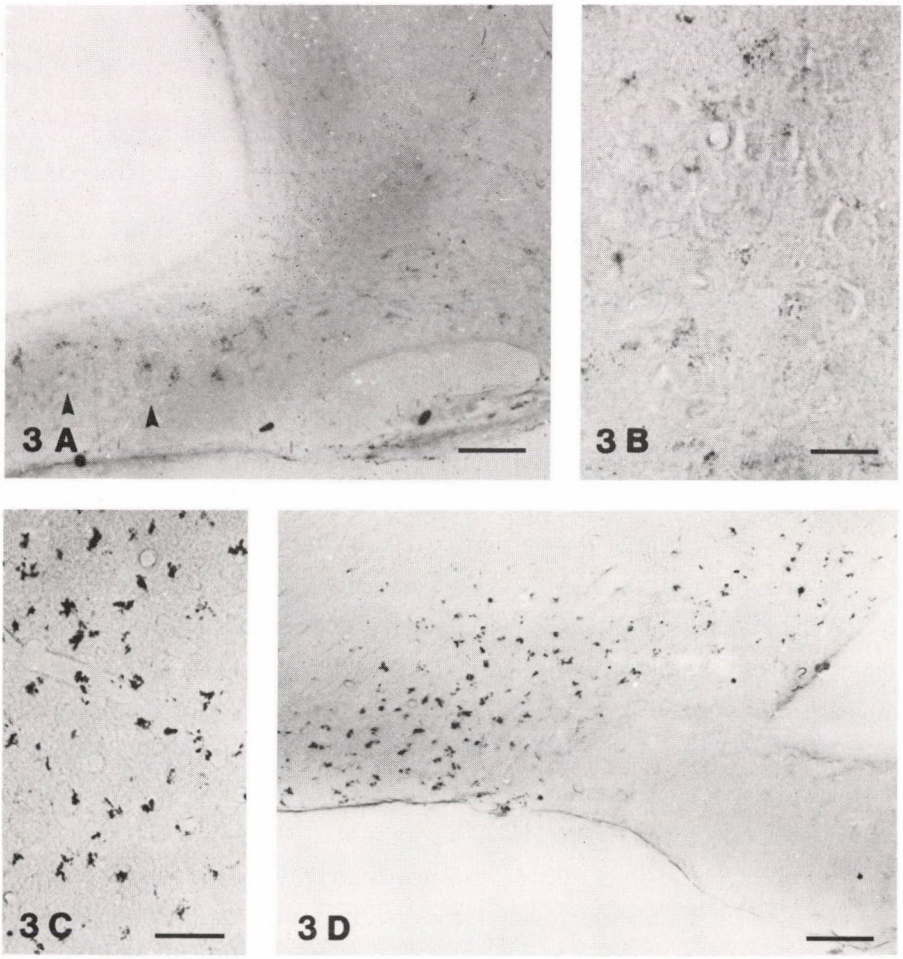

Fig. 3: DAB-positive glial cells in the median eminence and arcuate nucleus of the hypothalamus. **A**: This photomicrograph shows the appearance of DAB-positive cells (arrowheads) in the median eminence on the 10th postnatal day. **B**: Reactive glial cells in the arcuate nucleus of a 14-day-old rat. **C**: The appearance of DAB-staining glial cells in the arcuate nucleus of an adult rat. **D**: Low-power photomicrograph showing the distribution of reactive cells within the arcuate nucleus of an adult rat. Note the absence of DAB-positive structures in the median eminence at this age. Scale bar represents 50 μm in **A** and **C**, 25 μm in **B** and 100 μm in **D**.

DISCUSSION

The present results confirm previous reports on the occurrence of a special population of DAB-staining glial cells in certain hypothalamic, medullary and spinal regions (Keefer and Christ, 1976). DAB-positive glial cells appear only a week after birth, and their number and staining intensity progressively increase and reach adult levels by the end of the third postnatal week. This indicates that the expression of pseudoperoxidase activity may reflect a maturation process of these particular glial cells. However, some glial cells may express pseudoperoxidase activity only transiently; indeed, DAB-staining could be demonstrated in the median eminence of young, but not of adult animals. DAB-positive glial cells have been shown to bind oestrogen and to express glial fibrillary acidic protein in the arcuate nucleus of adult rats. Further studies are needed to clarify whether the development of DAB positivity is correlated with the appearance of the oestrogen sensitivity of these particular cells and, in turn, with the development of the hormonal regulatory functions of the arcuate nucleus.

DAB-positive glial cells are generally believed to be astrocytes (Keefer and Christ, 1976; Schipper et al., 1990; Keefe et al., 1991). However, the present results and our preliminary electron microscopic findings indicate that a population of these cells may be microglia. In the solitary tract nucleus of adult rats both astrocytes and microglial cells contained DAB reaction product. It is noteworthy that the microglial cells also contain haeme compounds (Goldfischer et al., 1966), which have been suggested to be responsible for the pseudoperoxidase reaction of astrocytes (Schipper et al., 1990).

The topographical distribution of DAB-reactive cells within the nucleus of the solitary tract and the spinal dorsal horn closely resembled that of the capsaicin-sensitive primary sensory afferents (cf. Jancsó and Király, 1980; Ritter and Dinh, 1988). This may suggest a possible functional association between primary afferent nerve terminals and these particular glial cells. Astrocytes related to glutamatergic synapses have been shown to participate in neurotransmitter degradation (Derouiche and Frotscher, 1991). It is tempting to suggest that DAB-staining glial cells may be involved in the degradation of transmitter substances released from primary afferent nerve terminals.

Studies on the development of spinal glial systems have revealed a transition in the

expression of vimentin to glial fibrillary acidic protein in the dorsal horn during the second and third postnatal weeks (Oudega and Marani, 1991). This has been suggested to represent a change in the functional state of the astrocytes (Dahl, 1981). The present results support this assumption by showing a progressive increase in the number of DAB-positive glial cells in the spinal dorsal horn, which might reflect the functional maturation of these particular cells in the course of the third postnatal week. The findings also suggest that DAB staining is a characteristic of a population of mature astrocytes and, in turn, stainability with DAB may be taken as an index of the level of maturation of this particular population of glial cells.

Further studies are needed to clarify the functional significance of these glial cells in both the developing and the adult central nervous system.

ACKNOWLEDGEMENTS

This work was supported in part by a grant (2710) from OTKA. The authors thank K. Mohácsi for skillful technical assistance.

REFERENCES

Adams, J. C. (1981) Heavy metal intensification of DAB-based HRP reaction product. J. Histochem. Cytochem. 29, 775.

Coimbra, A., Ribeiro-da-Silva, A. and Pignatelli, D. (1986) Rexed's laminae and acid phosphatase (FRAP)-band in the superficial dorsal horn of the neonatal rat spinal cord. Neurosci. Lett. 71, 131–136.

Dahl, D. (1981) The vimentin-GFA protein transition in rat neuroglia cytoskeleton occurs at the time of myelination. J. Neurosci. Res. 6, 741–748.

Derouiche, A. and Frotscher, M. (1991) Astroglial processes around identified glutamatergic synapses contain glutamine synthetase: Evidence for transmitter degradation. Brain Res. 552, 346–350.

Goldfischer, S., Villaverde, H. and Forschirm, R. (1966) The demonstration of acid hydrolase, thermostable reduced diphosphopiridine nucleotide tetrazolium reductase and peroxidase activities in human lipofuscin pigment granules. J. Histochem. Cytochem. 14, 641–652.

Graham, R.C. and Karnovsky, M.J. (1966) The early stages of absorption of injected horseradish peroxidase in the proximal tubule of mouse kidney: Ultrastructural cytochemistry by a new technique. J. Histochem. Cytochem. 14, 291–302.

Jancsó, G. and Király, E. (1980) The distribution of chemosensitive primary sensory afferents in the central nervous system of the rat. J. Comp. Neurol. 191, 781–792.

Jancsó, G., Király, E. and Jancsó-Gábor, A. (1977) Pharmacologically induced selective degeneration of chemosensitive primary sensory neurones. Nature 270, 741–743.

Keefe, L.D., Michelson, S.D., Lee, H.S. and Naftolin, F. (1991) Astrocytes within the hypothalamic arcuate nucleus contain estrogen-sensitive peroxidase, bind fluorescein-conjugated estradiol, and may mediate synaptic plasticity in the rat. Am. J. Obstet. Gynecol. 164, 959–966.

Keefer, A.D. and Christ, F.J. (1976) Distribution of endogenous diaminobenzidine-staining cells in the normal rat brain. Brain Res. 116, 312–316.

Ling, E.A., Paterson, J.A., Privat, A., Mori, S. and Leblond, C.P. (1973) Investigation of glial cells in semithin sections. I. Identification of glial cells in the brain of young rats. J. Comp. Neurol. 149, 43–72.

Mesulam, M.-M. (1978) Tetramethyl benzidine for horseradish peroxidase neurochemistry: A non-carcinogenic blue reaction product with superior sensitivity for visualizing neural afferents and efferents. J. Histochem. Cytochem. 26, 106–117.

Oudega, M. and Marani, E. (1991) Expression of vimentin and glial fibrillary acidic protein in the developing rat spinal cord: An immunocytochemical study of the spinal cord glial system. J. Anat. 179, 97–114.

Pignatelli, D., Ribeiro-da-Silva, A. and Coimbra, A. (1989) Postnatal maturation of primary afferent terminations in the substantia gelatinosa of the rat spinal cord. An electron microscopic study. Brain Res. 491, 33–44.

Ritter, S. and Dinh, T.T. (1988) Capsaicin-induced neuronal degeneration: Silver impregnation of cell bodies, axons and terminals in the central nervous system of the rat. J. Comp. Neurol. 271, 79–90.

Schipper, M.H., Lechan, M.R. and Reichlin, S. (1990) Glial peroxidase activity in the hypothalamic arcuate nucleus: Effect of estradiol valerate-induced persistent estrus. Brain Res. 507, 200–207.

Schipper, M.H. and Mateescu-Cantuniari, A. (1991) Identification of peroxidase-positive astrocytes by combined histochemical and immunolabeling techniques in situ and in cell culture. J. Histochem. Cytochem. 39, 1009–1016.

PRINTED IN HUNGARY

Akadémiai Kiadó és Nyomda Vállalat, Budapest

INSTRUCTIONS TO AUTHORS

Aims and Scope. *Neurobiology* is a multidisciplinary international journal, which publishes contributions from all traditionally important and newly emerging subdisciplines of the neurosciences including neuroanatomy, morphology, histochemistry, physiology, pharmacology, molecular neurobiology, developmental neuroscience, etc. Referees from a large international Editorial/Advisory Board will review submissions critically.

Submission. The journal publishes original, unpublished papers and reviews (conference abstracts, book reviews, announcements, advertisements, etc. may also appear from time to time) in English. The text should not exceed 15 typewritten pages (total length with illustrations, tables, etc., 20 pages).
Manuscripts should be submitted in triplicate to the Editorial Office:

Norbert Halász
Institute of Biophysics
Biological Research Centre
Hungarian Academy of Sciences
H-6701 Szeged, P.O. Box 521, Hungary
Telefax: 36 (62) 433 133
Phone: 36 (62) 432 232
E-mail: H3186HAL@ELLA.HU

Accepted manuscripts will not be returned to the authors.

To accelerate publication the papers will be reproduced directly from the authors' manuscripts, so those must be suitable for photographic reproduction. Authors should use electric typewriters with black (carbon) ribbon or high quality printers. Manuscripts not conforming to the specified instructions will be returned for reorganizing and retyping. Authors are encouraged to submit their papers also on floppy discs, using preferably WordPerfect, or Word as processors on IBM compatible computers.

Manuscripts should be typed on A4 (210x297 mm) papers. All margins should be 2.5 cm except upper margins on front (6 cm) and other pages (4 cm). Page numbering should be done only by soft pencil.

Regular papers should be organized into sections in the following order: Summary, Key words, Introduction, Materials and Methods, Results, Discussion (followed by Conclusions and Acknowledgements, if relevant), References. Illustrations, tables and their explanations should be inserted into the appropriate sections; all these should be centred.

The Introduction, Results and Discussion should be typed by a one and a half line spacing, while the rest of the sections should be typed by single space. The title, authors, and their affiliation should be centred.

Title. Use bold, block capital letters, enlarged if possible.

Authors and their Affiliation. Type by single space. Leave two and one line spaces above and below the authors' names, respectively.

Summary. Keep three line spaces above and one below the summary (not exceeding 150 words). The summary should be indented by five spaces on both sides.

Key words. A maximum of six key words or short phrases should be given and be indented similar to the summary.

At the rest of the text, *headlines* of the sections should be centred and typed in bold, capital letters. Use two line spaces above and one below headlines. *Subheadings* (if present) should be typed to the left side of the margin in italics (or should be underlined); line spacing: one above and below.

References. The lists should be arranged in alphabetical order. Their second and following lines should be indented by five spaces. Use abbreviated journal names. They should be arranged as the following examples show for journal and book references:

Butt, A.M., Jones, H.C. and Abbott, N.J. (1990) Electrical resistance across the blood-brain barrier in anaesthetized rats: A developmental study. J. Physiol. 429, 47-62.

Shepherd, G.M. (1988) Neurobiology. 2nd edition. Oxford Univ. Press, New York and Oxford.

Balázs, R. and Richter, D. (1973) Effects of hormones on the biochemical maturation of the brain. In: Biochemistry of the Developing Brain (ed. Himwich, W.) Vol. 1, pp. 254-304. M. Dekker, New York.

These should be cited in the text by the names of the authors and the year of publication, e.g. [Balázs and Richter, 1973; Shepherd, 1988; Butt et al., 1990].

Tables. These should be typed into the appropriate part of the text, together with their numbers, titles (above) and explanations (which should appear below the tables). Leave at least one line space between the Arabic table numbering and title, its explanation (single spaced) and the table itself, respectively. Separate the table from the text by one line space at least. Please, try to find the best fit between the width of the tables and their explanations. Data should not be duplicated in tables and figures.

Figures (line drawings, diagrams, photographs). These should be numbered consecutively by Arabic numerals. One original copy and two additional copies should be sent. Please, indicate numbers and the name of the first author and the top of the figure on the back. For *Legends* (single spaced) use the full length of text lines. Figure numbering should be followed by its legend in the same line. Do not glue Figures into the text. Please, type, however, their legends onto proper place. Legends should appear below figures, separated by one line space above (and below if the text continues on that page). Maximal (printed) size of Figures should not exceed 120x180 mm and should preferably leave enough space for the explanation on the same page. Leave at least one line space above figures.

Line drawings and diagrams. Please, prepare those in black ink by expecting a possible reduction (by 30-50%) and select lettering and symbols ensuring their recognizable final size (min. 2 mm). Please, leave enough space for them in the text plus at least one line space above and below. Reduction of line illustrations, if needed, will be done by the Publisher. *Formulae* if complex (and not typed into the text) should be prepared similarly.

Photographs. High quality half tones (please prefer higher contrast) should be prepared on glossy paper (and labelled clearly by Letraset) at their expected final size. Micrographs should also be completed by a scale bar representing the magnification and serial numbers in corners of the front of pictures. A limited number of colour photographs will also be accepted (if absolutely necessary) at no extra charge.

Abbreviations and symbols. These should be used according to the latest internationally accepted rules. They should be explained at their first appearance (and may also be listed in an alphabetical order, when desired). The SI System should be used.

Running title and address. The running title (not exceeding 50 characters and spaces) should be submitted on a separate page together with the full address, phone and fax numbers (E-mail if avaible) of the corresponding author.

Reprints. Fifty free reprints are provided to the authors. Additional reprints can be ordered from the Publisher at the time of acceptance. Fifty percent discount will be offered to young investigators and newcomers, without prior publications in this discipline.

CONTENTS

NEUROBIOLOGY

An International Multidisciplinary Journal in Neurosciences

VOLUME 1, NUMBER 2, 1993

Including the former Acta Biochimica et Biophysica Hungarica

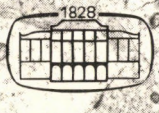

AKADÉMIAI KIADÓ, BUDAPEST

HU ISSN 1216–8063

NEUROBIOLOGY

An International Multidisciplinary Journal in Neurosciences

Includin the Former Acta Biochimica et Biophysica Hungarica

Neurobiology is a multidisciplinary international journal publishing contributions from all traditionally important and newly emerging subdisciplines of the neurosciences including neuroanatomy, morphology, biochemistry, physiology, pharmacology, molecular neurobiology, developmental neuroscience, etc.

Neurobiology is published by
AKADÉMIAI KIADÓ
Publishing House of the Hungarian Academy of Sciences
H-1117 Budapest, Prielle K. u. 19–35, Hungary

Manuscripts and editorial correspondence should be addressed to

Norbert Halász
Institute of Biohysics
Biological Research Centre
Hungarian Academy of Sciences
H-6701 Szeged, P.O. Box 521, Hungary

Subscription price for Volume 1 (1993) in 4 issues US $78.00, including normal postage; airmail delivery US $20.00

Orders should be addressed to

AKADÉMIAI KIADÓ
H-1519 Budapest, P.O. Box 245, Hungary

NEUROBIOLOGY

An International Multidisciplinary Journal in Neurosciences

Akadémiai Kiadó, Budapest

PRINTED IN HUNGARY
Akadémiai Kiadó és Nyomda Vállalat, Budapest

Neurobiology 1 (2), pp. 101-122, 1993

ANIMAL MODELS OF ALZHEIMER'S, PARKINSON'S AND HUNTINGTON'S DISEASE. A MINIREVIEW

A. Antal[1,2] and I. Bodis-Wollner[2]

[1]Department of Comparative Physiology, József Attila University of Sciences, Szeged, Hungary and [2]Department of Internal Medicine, Division of Neurology, University of Nebraska at Omaha, Omaha, U.S.A.

Summary: Animal studies have contributed significantly to deeper understanding of several neurodegenerative disorders but fully developed models are lacking. The best models to study motor, sensory and cognitive changes and the effects of therapeutic attempts are rodents and non-human primates. This review describes neuropharmacologic, neuroanatomic and behavioral features of animal models of Alzheimer's, Parkinson's and Huntington's disease.

Key words: Neurodegenerative Disorders, Animal models, Alzheimer's disease, Parkinson's disease, Huntington's disease

INTRODUCTION

During recent decades seminal experiments were performed to test or prove hypotheses concerning mechanisms of progressive neuronal cell death. Since many of these experiments, using anatomical, physiological and pharmacological techniques, cannot be performed in humans, great interest has been generated in developing animal models of neurodegenerative diseases. Their purpose is to provide better understanding of the neurophysiopathology and behavioral aspects of these disorders and to develop new therapeutic avenues. The most extensively used models are surgically or pharmacologically lesioned or normally

aging animals. In particular selective neurotoxins have been applied with success to create models relevant to therapeutic considerations.

Neurodegenerative disorders are characterized by progressive loss of nerve cell populations resulting in a spectrum of behavioral changes. Only some of the presently available models successfully mirror both the cellular and behavioral aspects of these diseases. The ideal model should provide both homology (the same biological origin) and analogy (similar functional effect). Given the close phylogenetic relationship and the similarities of brain anatomy, physiology, electrophysiology, and behavior between monkey and man (Creel et al., 1973; Premack, 1983), the monkey seems to be the most appropriate subject for these studies. Indeed, the non-human primate model does provide a reasonable tool for neuroscientists since demonstrable similarities exist between several dementing disorders and their non-human primate models. Nevertheless, in many laboratories more common and less expensive species, rodents (mice, rats) or carnivores (cats) are also used, in particular for studying specific details of neurodegeneration. In this review we summarize monkey, cat and rodent models of Alzheimer's, Parkinson's and Huntington's disease.

Alzheimer's disease

Alzheimer's disease (AD) is diagnosed on the basis of clinical signs of dementia and the postmortem presence of senile plaques and neurofibrillary tangles mainly in the hippocampus and the frontotemporal cortex (Rathman and Conner, 1984). AD is accompanied by a noteworthy deficiency of cholinergic neurotransmission. The clinical manifestations of this disease include psychotic behavior, loss of recent memory, confusion related to loss of memory, diminished verbal expression, deficits in attention and orientation (Coyle et al., 1987; Rubin et al., 1990).

Since AD is primarily a disease of old age, it has been proposed that the closest behavioral approximation to a

homologous animal model of AD is the aged animal, especially the monkey. A short term behavioral model can be produced in monkeys by administering cholinergic antagonists such as scopolamine. More selective models are induced by lesioning the nucleus basalis of Meynert (NBM. A rodent equivalent of the NBM is the nucleus basalis magnocellularis [nbm].). Nbm lesioning can be produced surgically or by administration of selective cholinergic neurotoxins such as kainic and ibotenic acids or ethylcholine mustard aziridinium ion (AF64A). Kainic and ibotenic acids are glutamate analogues and destroy cell bodies and dendrites.(Coyle et al., 1983). AF64A is a toxin that destroys cholinergic nerve terminals and produces presynaptic cholinergic dysfunction. It is structurally similar to choline and has a specific effect on the cholinergic system (Fisher et., al 1986). AF64A administration produces reductions in choline-acetyl-transferase, acetylcholine and in choline uptake in cell bodies and terminals (Walsch et al., 1984).

A. Rodent models. Rodents are typically used in spatial learning tasks to assess AD-like memory and learning changes. There are two principal types of tasks which are well suited for rodents: maze learning and avoidance learning tasks. In the maze learning task animals are required to learn, remember and recall the location of food or a platform upon which they can escape from the water. In a radial arm maze animals are allowed to explore all arms (usually eight), each of which contains food. If the animal repeatedly returns to previously explored arms, a deficit of learning or memory is indicated. In active avoidance tasks the animal must respond in order to avoid an electrical shock. In a passive avoidance task the animal must remember not to enter a test box where it had previously experienced a shock.

1. Acute models. Scopolamine is a muscarinic cholinergic antagonist. Its effects on learning and memory have been demonstrated in humans and in monkeys (Bartus and Johnson, 1976, Bartus et al., 1978; Drachman and Leawitt, 1974; Drachman, 1977) but the use of scopolamine in rodents has given the most valuable information among mammals. In a radial arm maze paradigm working

memory was impaired after scopolamine administration in rats (Buresova et al., 1986). In the Morris water maze memory acquisition deteriorated if scopolamine was administered twenty minutes prior to training although a higher dose was needed to disrupt retention if the response was overtrained (Buresova et al., 1986).

2. Chronic models. Studies involving training in the radial-arm maze prior to nbm lesioning suggest that their permanent lesion may affect working memory. Rats with nbm lesions produced by electrocoagulation and by ibotenic acid administration made more errors and required more trials to reach criterion than controls (Dubois et al., 1985). This result suggests a difficulty in using previously acquired information to organize the response. Ibotenic acid nbm lesioned rats were more impaired in recalling information than were rats lesioned by electrocoagulation.

Ibotenic acid nbm lesioned rats also showed impairments in active and passive avoidance tasks (Flicker et al., 1983).

In a Morris water maze rats had to swim in a tank of opaque water to an underwater platform to escape from the water. Learning and memory were indicated by the length of time they needed to reach the platform. In this maze the nbm lesioned rats using AF64A showed a deficit in acquisition and retrieval (Spencer et al., 1984). In the same study nbm lesioned rats were significantly slower to learn an active avoidance task.

AF64A injection to the lateral ventricles of rats produced motoric hyperactivity and an inability to adopt a spatial performance strategy in a radial-arm maze (Walsch et al., 1984). Performance in the Morris water maze also deteriorated as a result of AF64A administration (Brandeis et al., 1986).

3. "Spontaneous" models. New Zealand Black mice (NZB) have elevated brain-reactive antibody levels during young adult life and they show reduced learning and memory capabilities (Nandy et al., 1983). It is thought that there may be a correlation between the immunological abnormality and deficits in learning and memory of mice and human AD. The reason is because the amyloid in the

senile plaques and vascular walls of brain of AD also contains proteins identical to or very similar in structure to components or fragments of human immunoglobulins (Ishii and Haga, 1976). The problem is that neurofibrillary tangles and senile plaques are not found in the NZB mice model.

B. Monkey models. Operant tasks provide one of the best methods to measure the cognitive abilities of animals. In this task animals have to depress or release one or more levers in order to obtain reward or avoid punishment. Monkeys are superior for this task because rats do not easily learn these tasks.

1. Aged monkeys. They are used to study short-term memory impairment associated with aging and dementia. Bartus and his colleagues (1978) studied this model in detail. In an automated delayed-response procedure aged rhesus monkeys were trained to pay attention to nine stimulus-response panels. A light flash as a stimulus appeared four times in one of the nine panels and afterwards a retention interval was initiated. When the retention interval expired the monkey could respond to a stimulus by pushing one of the nine panels. In the case of a correct response the light flash was repeated on the correct panel and was reinforced with a piece of food. It was demonstrated that aged rhesus monkeys suffer from a profound specific impairment of short-term memory. They performed normally when the delay interval was short and showed impairment with increasing retention interval (Bartus et al., 1978).

2. Acute models. A match-to-sample task was used to study cognitive functions in primates treated with scopolamine. In this paradigm a sample stimulus was presented, followed by two or three alternatives from which the monkey had to select the same stimulus (match) just presented. Right answers were reinforced. Delays between the stimuli were used to manipulate task difficulty. Scopolamine had a significant effect on short-term memory in this task in rhesus monkeys (Bartus and Johnson, 1976).

In a nonmatching-to-sample task forty sample stimuli first were given to rhesus monkeys. After a series of stimuli were presented, these same stimuli were given in the reverse order,

each paired with a novel stimulus. The animal was rewarded when choosing the novel stimulus in each pair. The performance was impaired if scopolamine was administered before but not after the first series of stimuli (Aigner et al., 1991).

In addition to the behavioral tests event-related potentials (ERPs) also have been utilized to measure cognitive decline both in humans or in non-human primates. Recording from the scalp, using computer extraction techniques, time-locked field potentials could be recorded in association with sensory, motor and cognitive events. Short latency ERP components vary with the physical properties of the stimulus and the functional integrity of the sensory pathways and so they are often termed "exogenous". In contrast, the so called "endogenous" ERPs are of longer latency and vary in amplitude, latency and distribution as a function of psychological variables and task-specific processes triggered by the stimulus (Donchin et al., 1978). The most intensively studied "endogenous" potential is the P300 or P3. P300 is a positive ERP component that typically peaks at about 300 msec or more after the presentation of the informative auditory stimulus. In the visual modality its latency is longer. It is well established that this component of ERPs is associated with cognitive processing (Kutas et al., 1977; Donchin et al., 1978, Donchin, 1979) and it may give some insight into the neuronal bases of cognitive activity. P300 is usually elicited by an unexpected stimulus as well as by an unexpected absence of a stimulus. It is most commonly recorded during a randomly ordered sequence of stimuli from two classes, such as high and low frequency tones. The stimuli can be auditory, visual or somatosensory in nature. Stimuli from an infrequent class can elicit P300. Its amplitude decreases when the attention is diverted; the latency varies with the time required for stimulus evaluation (Kutas et al., 1977; McCarthy and Donchin, 1981). Human studies suggest that measuring P300 could serve as a tool in the diagnosis of dementia (Donchin et al., 1986). Given the limited facilities for experimentation on humans, there is evidence that the monkey is suitable to evaluate the

repeatability and the pharmacological properties of P300 and hence may provide a reasonable model to study the cognitive electrophysiology of dementing diseases (Arthur and Starr, 1984, Onofrj et al., 1986; Glover et al., 1988; Pineda et al., 1989).

Twenty to thirty minutes after the administration of scopolamine, P300 latency increased and its amplitude decreased using a visual discrimination paradigm in the Macaque monkey (Antal et al., submitted). In humans in a similar visual oddball task a comparable dose of scopolamine delayed the peak P300 latency without an effect on its amplitude (Rugg et al., 1989). Consistent with this result is the finding of significant P300 latency increase after 1.2 mg scopolamine administration using a visual stimulus evaluation/response selection task in humans (Callaway et al., 1991).

It is of particular relevance that scopolamine can produce cognitive deficits which are regarded to be similar to those observed in AD (Fuld, 1984) although it has been also suggested that the cognitive profile of scopolamine treated young subjects is more similar to that of nondemented elderly people than to AD patients (Flicker et al., 1990).

Summary. Different models of AD are equally good for studying selective aspects of AD. Surgical and neurotoxic lesions of nbm produce similar cognitive changes. Many of the non-cholinergic neurotransmitter abnormalities can be observed after nbm lesions (Wenk and Engisch, 1986). Following nbm lesion, behavioral recovery is observed over time. Administration of AF64A produces anatomic and cognitive changes similar to those caused by nbm lesion, but the effect of AF64A is exclusive to the cholinergic system. These toxins produce long lasting permanent deficits which show some characteristics similar to AD. Scopolamine induces shorter time course deficits than the other three models.

The NZB mouse model doesn't mimic the anatomical changes of AD but it is a promising for investigating age-related changes.

Parkinson's disease

1. The rotating rat model. Efforts to develop a homologous model for Parkinson's disease (PD) have been focused on using neurotoxins selective for dopaminergic neurons. The first employed drug was 6-hydroxy-dopamine (6OH-DA), which was injected into the nigrostriatal system of rats in order to mimic symptoms of PD (Ungerstedt and Arbuthnott, 1970). After a unilateral 6OH-DA lesion of the nigrostriatal system of rats a lack of movement initiation is observed and the animals turn toward the injected side without any stimuli. Following amphetamine administration rats rotate toward to the side of the 6OH-DA injection. This is interpreted as a result of dopamine release from the intact striatum. The administration of the dopamine agonist apomorphine causes movement in a direction contralateral to the side of the lesion because of denervation supersensitivity of striatal dopamine receptors (Ungerstedt and Arbuthnott, 1970; Dunett et al., 1988).

2. The MPTP primate model. As a more suitable tool for creating a model of PD, MPTP (1-methyl-4-phenyl-1,2,5,6-tetrahydropyridine) has been administered. This neurotoxin not only provokes the pathological and biochemical changes well known in patients with parkinsonism but characteristic behavioral defects also closely resemble those of PD (Burns et al., 1983). In monkeys, 1-2 weeks following MPTP administration neuropathologic examination demonstrates selective destruction of dopaminergic cells in the substantia nigra pars compacta and their projection to the striatum. At about the same time the animals show severe motor impairment, similar to that seen in human parkinsonism (Burns et al., 1983; Langston et al., 1984). MPTP-treated subhuman primates do not exhibit the full range of pathologic or biochemical changes known to occur in patients with PD (Jenner and Marsden, 1990). Nevertheless, the cardinal symptoms of advanced PD such as tremor, bradykinesia, rigidity, motor freezing, eating problems, delay in initiating movements are observable for a long period following MPTP administration to primates (Burns et al., 1983; Redmond et al., 1986). Many of the

cardinal symptoms of the MPTP-treated monkeys improve under the effect of dopaminergic therapy with drugs which are often used in human PD.

A significant proportion of patients suffering from PD show delayed visual evoked potentials (VEPs) and upon questioning describe visual deficits. Electrophysiological and neurochemical findings point to dopaminergic deficiency in the visual pathway, probably in the retina (Bodis-Wollner and Yahr, 1978). Using sinusoidal stimuli in PD patients, the abnormality of VEP is highest for medium and high spatial frequency stimuli where normal human observers are most sensitive to the visual stimuli (Onofrj et al., 1986). A good number of studies have also shown abnormal flash and pattern electroretinograms (ERGs) in individuals with PD (Bodis-Wollner et al., 1991). In these patients abnormal PERG is more evident at medium than at lower spatial frequencies.

To understand the role of dopaminergic neurons in the retinal circuitry, the direct intraocular effect of 6OH-DA was examined in nonhuman primates. After the drug administration both the phase and amplitude of PERG and VEP became abnormal (Ghilardi et al., 1989). This impairment was pronounced for the medium spatial frequencies (2.5 and 3.5 cycles/degree - cpd, cpd is a measure of a pattern element size in a repetitive grating pattern), while responses to stimuli of lower spatial frequencies (0.5 and 1.2 cpd) were less impaired. This is similar to what could be seen in parkinsonian patients (Ghilardi et al., 1989).

In MPTP-treated monkeys abnormal VEP and ERGs elicited by grating stimuli were recorded shortly following MPTP injection (Ghilardi et al., 1988). The electrophysiological abnormalities were dependent upon the applied spatial frequencies: Ghilardi and colleagues (1988) have shown that both the PVEP and PERG to 0.5 cpd stimuli returned to normal 30-40 days after MPTP administration but PVEP latency and amplitude to 2.5 and 3.5 cpd stimuli remained abnormal. These effects are very similar to those of 6OH-DA on the VEP and PERG, suggesting a specific role of the dopaminergic system in the monkey's visual pathway. The

visual abnormalities could be also improved with L-Dopa therapy, similar to the main motor deficits.

Using extracellular single unit recordings in the dorsal lateral caudate nucleus of intact, awake cats, 6% of neurons responded to visual stimuli. After MPTP administration no unit discharges to such stimuli were seen (Schneider, 1991).

The unilateral parkinsonian monkey model. Unilateral MPTP injections into the carotid artery of non-human primates have opened new vistas for the study of parkinsonism. With this method liver and kidney damage can be avoided. The parkinsonian motor deficits develop contralateral to the MPTP infusion and the animals do not suffer from the severe feeding deficits encountered in bilaterally treated parkinsonian monkeys. The injection produces only unilateral damage of the nigrostriatal pathway and, therefore, the same animal provides its own physiological and behavioral control.

Selective destruction of the ipsilateral nigrostriatal pathway by unicarotid MPTP injection causes permanent contralateral motor impairment, such as bradykinesia, rigidity, cogwheeling and tremor (Bankiewicz et al., 1986). Spontaneous motor activity is characterized by continuous and consistent circling towards the MPTP-injected side.

The response of the MPTP monkey to dopaminergic agents. Is it a pharmacological model? Treatment with L-Dopa/carbidopa or apomorphine alleviates the motor deficits and reverses the direction of circling (Bankiewicz et al., 1986). In unilateral parkinsonian monkeys treated with L-Dopa, symptoms of parkinsonism were controlled or suppressed and widespread increases in glucose utilization were seen throughout the brain (Porrino et al., 1987). Cerebral metabolic activity was increased in areas rich in dopaminergic receptors and in nondopaminergic areas related to motor functions.

Bankiewicz et al. (1991a) have described hemispatial visual neglect in monkeys rendered hemiparkinsonian by unilateral MPTP injection. This hemispatial neglect is similar to what has been observed in some humans with focal cortical and subcortical

lesions including dopaminergic areas (Roeltgen et al., 1989). Mild visual neglect has also been described in association with PD, particularly in patients with symptoms localized to the left side of the body (Barber et al., 1985). Schneider et al. (1992) suggest that the hemineglect state in monkeys with unilateral carotid administration is the result of an impairment of appropriate sensory information delivery to the striatum and it is not the result of primary visual or motor damage.

Most of the studies of MPTP exposure in animals have focused on motor, neuropathological, pharmacological and metabolic aspects of parkinsonism. Nevertheless, in the last decades it has become increasingly evident that cognitive impairment is an integral part of PD (Bodis-Wollner et al., 1984; Dubois et al., 1987, 1990; Brown and Marsden, 1990) and MPTP-treated monkeys provide a reasonable model for studying the effect of dopaminergic deficiency on cognition.

Different kinds of cognitive tests have been applied in hemiparkinsonian animals. Schneider and Kovelowski (1990) used delayed response, delayed alternation, and visual pattern discrimination tasks. In the delayed response task monkeys were trained to retrieve a raisin from one of the food wells after observing the experimenter bait one of the wells. In the delayed alternative task monkeys were required to alternate responses between the left and right wells on successive trials. In the visual pattern discrimination task monkeys were trained to discriminate correctly between two black patterns (a plus sign and a minus mark) on a white background. A plus sign appeared over the right or left food wells in a predeterminated balance order. All examined animals showed significant post-MPTP deficits in delayed response and delayed alternative tasks while visual pattern discrimination performance remained intact concerning the percentage of the correct responses.

As summarized earlier, ERPs also have been utilized to evaluate cognitive functioning in humans and in monkeys. The latency of P300 is often abnormal in parkinsonian patients (Hansch et al., 1982; Bodis-Wollner et al., 1984; Goodin and

Aminoff, 1987; Pang et al., 1990; Stanzione et al., 1991). An abnormal P300 evoked by auditory stimuli also was found in MPTP treated monkeys shortly after the drug administration. Following MPTP administration P300 disappeared but after partial recovery of PD symptoms, normal P300 potentials were recorded (Glover et al., 1986, 1988).

Animal models of fetal tissue transplantation in Parkinson's disease. The current treatment of PD by systemic administration of dopaminergic precursors restores dopamine levels in the striatum. Recent attempts to replace damaged cells represent a new direction in the therapy of neurodegenerative disorders.

In the rodent model of PD, adrenal medullary implants into the striatum of rats appear to ameliorate the motor deficits attending dopamine destruction (Nishino et al., 1988). In the hemiparkinsonian primate model a behavioral recovery was also found following transplantation of medullary allografts, but graft survival was limited and possibly not linked to the behavioral improvement (Bankiewicz et al., 1988).

Motor improvement was found in MPTP-treated rhesus monkeys after implanting fetal mesencephalic tissue (containing the dopaminergic neurons of the embryonic substantia nigra) in the caudate nucleus (Bankiewicz et al., 1990). Subsequent studies with transplantation of fetal cerebellum and spinal cord suggest that brain implants do not need to contain dopamine to induce recovery (Bankiewicz et al., 1991b). It appears that implant-induced and also trophic factor - mediated sprouting of dopamine neurons of the host brain plays a role in the behavioral and functional improvements in MPTP-induced parkinsonian primates.

Even though the brain has been considered an immunologically privileged site, it is clear that this privilege is partial and immunological rejection processes can occur in the central nervous system (Widner and Brundin, 1988). Fiandaca et al. (1988) implanted two grafts one month apart in the same monkey. No changes were found after the transplantation in cisternal cerebrospinal fluid (CSF) white blood cell counts, serum and CSF IgG and albumin concentration. This twice-implanted monkey did

not differ in any measurement from the others receiving only a single transplant. These results suggest a relatively good immunological tolerance of allografts in the primate brain. Nevertheless, at this time the role of immune suppression in brain transplantation is not yet settled.

Summary. Well developed animal models of PD exist. 6OH-DA and MPTP both destroy dopaminergic neurons in the nigrostriatal system and produce a variety of measures of motor, sensory and cognitive impairment that can be observed also in PD. Somewhat different effects of the two toxins may be related to species differences. Rats, rabbits and guinea pigs are far less sensitive to the neurotoxic effects of MPTP than primates. MPP+, the toxic metabolite of MPTP, is present only transiently in the brain of these animals, while in monkeys the toxic form is retained for a long time (Johannesen et al., 1986). Of the neurodegenerative diseases studied, the MPTP model is the closest approximation to human PD.

The fetal implantation method opened a new approach to PD. Most of present data are of preliminary nature and are based on individual cases. Many detailed aspects of central nervous system implantation are unknown and it appears that the monkey model may be useful in evaluating whether fetal implants are applicable to non-motor deficits in PD.

Huntington's disease

Huntington's disease (HD) is an autosomal dominant-inherited neurodegenerative disorder that is characterized clinically by clumsiness, chorea, progressive dementia, and impaired concentration. Many neurotransmitter systems demonstrate impaired functions in HD: levels of gamma-aminobutyric acid (GABA), acetylcholine, substance P, and enkephalins are decreased while dopamine and somatostatin are increased or unaltered in the brain (Gusella, 1987). Anatomically, severe cell loss in the striatum is characteristic of HD. The cell loss is progressive and ultimately the globus pallidus and large areas of the cortex also become affected.

Kainic acid was the first reported exocitotoxin to mimic the pathological features of HD (Giordiano et al., 1988). It is a selective agonist for the K subtype of glutamate receptors and produces motor hyperactivity and deficits in learning and memory (Coyle and Schwarz, 1976; McGeer and McGeer, 1976). This exocitotoxin is often used to create an animal model of HD because of the similarity of biochemical and behavioral changes in HD and following kainic acid.

Later studies with quinolinic acid, an endogenous metabolite of tryptophan, demonstrated effects similar to those of kainic acid in the rat caudate nucleus (Schwarz et al., 1983). The action of an another glutamate analogue, ibotenic acid, is also similar in provoking gliosis similar to that seen in HD (Isacson et al., 1987). These findings suggest that glutamate or another excitatory amino acid acting at one of the glutamate receptor subtypes could be involved in the pathogenesis of HD.

Kainic acid-induced exocitotoxic striatal lesions in rats resulted in locomotor hyperactivity and deficits in learning in a delayed alternation task in a T-maze. However, the visual discrimination ability of the same animals remained unaffected (Divac et al., 1978; Dunett et al., 1988). In a passive avoidance task kainic acid lesioned animals took significantly longer to reach the learning criterion (Sanberg et al., 1978). This model does not manifest the dyskinesia or choreic movement typical of HD.

Unilateral kainic acid injection into the caudate-putamen of monkeys, followed by dopamine agonist stimulation produced choreic movements in a monkey whose striatum was only partially destroyed. This result suggests that in this monkey choreic movements were generated by the hypofunction of the nigrostriatal dopamine neurons that innervate the unaffected part of the striatum (Kanazawa et al., 1986).

Summary. The animal models of HD are based on using different exocitotoxins such as kainic, quinolinic and ibotenic acid. These toxins produce a remarkable cell loss in the brain. The pathological changes are similar to those seen in HD, but

these models are less analogous than the earlier discussed models of AD and PD.

CONCLUSIONS

We have briefly reviewed animal models of principal motor, sensory and cognitive characteristics of three major neurodegenerative disorders, AD, PD and HD. The animal models are based upon pharmacological manipulations of neurotoxins or neurotransmitter antagonists.

No model produces a complete spectrum of cognitive, motor or pathological changes any of the diseases in question. One of the primary criticisms levelled against these models is that they are experimentally induced. Nevertheless, animal models potentially enable dissection of the underlying elements of the neurodegenerative diseases in a more direct way than is possible in human clinical research.

One problem of all animal models is that they show spontaneous recovery while this does not occur in neurodegenerative disorders. In the animals, partial or even full motor and also cognitive recovery occurs over time. Future research should focus on analysis of the factors leading to spontaneous recovery, since they may give clues for more efficient treatment approaches in neurodegenerative disorders.

In all areas of biological research there is a growing social movement concerned with animal research and often antagonistic to it. Some of these organizations are antiscientific and use physical violence. Yet it is evident that significantly valid and ethically correct experiments provide animal models which aid in the understanding of the causes and mechanisms of the major human disorders and lead to therapeutic advances.

ACKNOWLEDGEMENTS

We thank Dr. Ottó Fehér and Dr. Ronald Pfeiffer for their valuable contributions and advice to this review which was partially supported by the Magyar Hitel Bank (Hungary), the Soros Foundation (New York) and the University of Nebraska Medical Center (Omaha, USA).

REFERENCES

Aigner, T.G., Walker, D.L. and Mishkin, M. (1991) Comparison of the effects of scopolamine administered before and after acquisition in a test of visual recognition memory in monkeys. Behav. Neural. Biol. 55, 61-67.

Antal, A., Kovanecz, I. and Bodis-Wollner, I. The effect of scopolamine and Acetyl-levo-carnitine on the visual P300 in the behaving monkey. (submitted to Electroenceph Clin. Neurophysiol.)

Arthur, D.L. and Starr, A. (1984) Task-relevant positive component of the auditory event-related potential in monkeys resembles P300 in humans. Science, 233, 186-188.

Bankiewicz, K.S., Oldfield, E.H,. Chiueh, C.C., Doppman, J.L., Jacobowitz, D.M. and Kopin, I.J. (1986) Hemiparkinsonism in monkeys after unilateral internal carotid artery infusion of 1-methyl-4-phenyl-1,2,3,6-tetrahydropyridine (MPTP). Life Sci. 39, 7-16.

Bankiewicz, K.S., Plunkett, R.J., Kopin, I.J., Jacobowitz, D.M., Lomdon, W.T. and Oldfield, E.H. (1988) Transient behavioral recovery in hemiparkinsonian primates after adrenal medullary allografts. Prog. Brain Res. 78, 543-549.

Bankiewicz, K.S., Plunkett, R.J., Jacobovitz, D.M., Porrino, L., Di Porzio, U., London, W.T., Kopin, I.J. and Oldfield, E.H. (1990) The effect of fetal mesencephalon implants on primate MPTP induced parkinsonism. J. Neurosurg. 72, 231-244.

Bankiewicz, K.S., Oldfield, E.H., Plunkett, R.J., Schuette, W.H., Cogan, D.G., Hogan, N., Zuddas, A. and Kopin, I.J. (1991a) Apparent unilateral visual neglect in MPTP-hemiparkinsonian monkeys its due to delayed initiation of motion. Brain Res. 541, 98-102.

Bankiewicz, K.S., Plunkett, R.J., Jacobovitz, J.M., Kopin, I.J. and Oldfield, E.H. (1991b) Fetal nondopaminergic neural implants in parkinsonian primates. Histochemical and behavioral studies. J. Neurosurg. 74, 97-104.

Barber, J., Tomer, R., Sroka, H. and Myslobodsky, M.S. (1985) Does unilateral dopamine deficit contribute to depression? Psychiatry Res. 15, 17-24.

Bartus, R.T. and Johnson, H.R. (1976) Short-term memory in the rhesus monkey: disruption from the anti-cholinergic scopolamine. Pharmacol. Biochem. Behav. 5, 39-46.

Bartus, R.T., Fleming, D., Johnson, B.A. and Johnson, H.R. (1978) Aging in the rhesus monkey: debilitating effects on short-term memory. J. Gerontol. 33, 858-871.

Bodis-Wollner, I. and Yahr, M.D. (1978) Measurements of visual evoked potentials in Parkinson's disease. Brain, 101, 661-671.

Bodis-Wollner, I., Yahr, M.D. and Mylin, L.H. (1984) Nonmotor functions of the Basal Ganglia. In: Advances in Neurology (eds. Hassler, R.G. and Christ, J.F.) Vol. 40, pp. 289-297. Raven Press, New York.

Bodis-Wollner, I., Borod, J. and Glover, A. (1988) Abnormal P300 and cognitive dysfunction in Parkinson's disease and related disorders. In: Senile dementias. II International Symposium. (eds. Agnoli, A., Cahn, J., Lassen, N., Mayeux, R.) John Libbey Eurotext, Paris, pp. 309-315.

Bodis-Wollner, I., Pang, S., Falk, A., Ghilardi, M.F. and Mylin, L. (1991) Vision and visual discrimination in Parkinson's disease. In: The Basal Ganglia III. (eds. Bernardi, G., Carpenter, M.B., Di Chiara, G., Morelli, M. and Stanzione, P.) pp.743-750.

Brandeis, R., Pittel, Z., Lachman, C., Heldman, E., Luz, S., Dachir, S., Levy, A. and Hanin, I. (1986) AF64A induced cholinotoxicity: behavioral and biochemical correlates. In: Parkinson's and Alzheimer's disease: Strategies for Research and Development (eds. Fischer, A., Hanin, I. and Lachman, C.) pp. 459-478. Plenum Press, New York.

Brown, R.G. and Marsden, C.D. (1990) Cognitive function in Parkinson's disease: from description to theory. Trends in Neurosci, 13, 21-29.

Buresova, O., Bolthius, J. and Bures, J. (1986) Differential effects of cholinergic blockade on performance of rats in the water tank navigation task and in a radial arm maze. Behav. Neurosci. 100, 476-482.

Burns, R.S., Chiuech, C.C., Markey, S., Ebert, M.H., Jacobowitz, D.M. and Kopin, I.J. (1983) A primate model of Parkinson's disease: selective destruction of substantia nigra pars compacta dopaminergic neurons by N-methyl-4-phenyl-1,2,3,6-tetrahydropyridine. Proc. Natl. Acad. Sci. USA, 80, 4546-4550.

Callaway, E., Halliday, R., Naylor, H. and Brandeis, D. (1991) Clonidine and scopolamine:differences and similarities in how they change human information processing. Prog. Neuropsychopharm. Biol. Psychiatry 15, 497-502.

Coyle, J.T. and Schwarz, R. (1983) The use of excitatory amino acids as selective neurotoxins. In: Methods in Chemical Neuroanatomy (eds. Bjorklund, A. and Hokfelt, T.) Vol 1, pp.508-528. Elsevier, New York.

Coyle, J.T. and Schwarz, R. (1976) Lesion of striatal neurons with kainic acid provides a model for Huntington's chorea. Nature, 263, 244-246.

Coyle, J.T. (1987) Alzheimer's disease. In: Abnormal States of Brain and Mind (ed. Hobson, J.A.) pp. 9-10. Birkhauser, Basel.

Creel, D.J., Dustman, R.E. and Beck, C. (1973) Visually evoked potentials in the rat, guinea pig, cat, monkey and man. Exp. Neurol. 40, 351-366.

Divac, I., Markowitsch, H.J. and Pritzel, M. (1978) Behavioral and anatomical consequences of small intrastriatal injections of kainic acid in the rat. Brain Res. 151, 523-532.

Donchin, E., Ritter, W. and McCallum, W.C. (1978) Cognitive psychophysiology : the endogenous components of the ERP. In: Event-Related Brain Potentials in Man (eds. Callaway, E., Tueting. P. and Koslow, S.H.) pp. 349-411. Academic Press, New York.

Donchin, E. (1979) Event-related brain potential: a tool in the study of human information processing. In: Evoked Brain Potentials and Behavior (ed. Begleiter, H.), Vol. 2, pp.13-88. Plenum Press, New York.

Donchin, E., Miller, G.A. and Farwell, L.A. (1986) The endogenous components of the event-related potential - a diagnostic tool? In: Progress in Brain Research (eds. Swaab, D.F., Fliers, E., Mirmiran, M., Van Gool, W.A. and Van Haaren, F.) pp. 87-102. Elsevier, New York.

Drachman, D.A. and Leawitt, J. (1974) Human memory and the cholinergic system. Arch. Neurol. 30, 113-121.

Drachman, D.A. (1977) Memory and cognitive function in man: does the cholinergic system have a specific role? Neurology, *27*, 783-790.

Dubois, B., Mayo, W., Agid, Y., LeMoal, M. and Simon, H. (1985) Profound disturbances of spontaneous and learned behaviors following lesions of the nucleus basalis magnocellularis in the rat. Brain Res. 338, 249-258.

Dubois, B., Danze, F., Pillon, B., Cusimano, G., Lhermitte, F. and Agid, Y. (1987) Cholinergic-dependent cognitive deficits in Parkinson's disease. Ann. Neurol. 22, 26-30.

Dubois, B., Pillon, B., Lhermitte, F. and Agid, Y. (1990) Cholinergic deficiency and frontal dysfunction in Parkinson's disease. Ann. Neurol. 28, 117-121.

Dunett, S.B., Isacson, O., Sirinathsinghji, D.J.S., Clarke, D.J. and Bjorklund, A. (1988) Striatal grafts in rats with unilateral neostriatal lesions - III. Recovery from dopamine -dependent motor asymmetry and deficits in skilled paw reaching. Neuroscience, 24, 813-820.

Fiandaca, M.S., Bakay, R.A.E., Sweeney, K.M. and Chan, W.C. (1988) Immunologic response to intracerebral fetal neural allografts in the rhesus monkey. Prog. Brain Res. 78, 287-295.

Fischer, A. and Hanin, I. (1986) The AF64A treated rat as an experimental model for Alzheimer's disease: a critical evaluation. In: Parkinson's and Alzheimer's disease: Strategies for Research and Development (eds. Fischer, A., Hanin I. and Lachman, C.) pp. 427-446. Plenum Press, New York.

Flicker, C., Dean, R.L., Watkins, D.L., Fisher, S.K. and Bartus, R.T. (1983) Behavioral and neurochemical effects following neurotoxic lesions of a major cholinergic input to the cerebral cortex in the rat. Pharmacol. Biochem. Behav. 18, 973-981.

Flicker, C., Sherby, M. and Ferris, S.H. (1990) Scopolamine effects on memory, language, visuopatial praxis and psychomotor speed. Psychopharmacology (Berl), 100, 243-250.

Fuld, P.A. (1984) Test profile of cholinergic dysfunction and of Alzheimer-type of dementia. J. Clin. Neuropsychol. 6, 380-392.

Ghilardi, M.F., Bodis-Wollner, I., Onofrj, M.C. and Glover, A.A. (1988) Spatial frequency-dependent abnormalities of pattern electroretinogram and visual evoked potentials in a parkinsonian monkey model. Brain 111, 131-149.

Ghilardi, M.F., Marx, M.S., Bodis-Wollner, I., Camras, C.B. and Glover, A.A. (1989) The effect of intraocular 6-hydroxydopamine on retinal processing of primates. Ann. Neurol. 25, 359-364.

Giordiano, M., Hagenmeyer-Houser, S.H. and Sanberg, P.R. (1988) Intraparenchymal fetal striatal transplants and recovery in kainic acid lesioned rats. Brain Res. 446, 183-188.

Glover, A., Ghilardi, M.F., Onofrj, M. and Bodis-Wollner, I. (1986) MPTP's effect on cortical processing in the monkey: evoked potential evidence. In: MPTP : a neurotoxin producing a parkinsonian syndrome (eds. Markey, S.P., Castagnoli, N. Jr., Trevor A.J. and Kopin I.J.) pp. 667-672. Academic Press, New York.

Glover, A., Ghilardi, M.F., Bodis-Wollner, I. and Onofrj, M. (1988) Alterations in event-related potentials (ERPs) of MPTP-treated monkeys. Electroenceph. Clin. Neurophysiol. 71, 461-468.

Goodin, D.S. and Aminoff, M.D. (1987) Electrophysiological differences between demented and nondemented patients with Parkinson's disease. Ann. Neurol. 21, 90-94.

Gusella, J.F. (1987) Huntington's Disease. In: Abnormal States of Brain and Mind (ed. Hobson, J.A.) pp. 61-62. Birkhauser, Basel.

Hansch, E.C., Syndulko, K., Cohen, S.N., Goldberg, Z.I., Potvin, A.R. and Tourtellotte, W.W. (1982) Cognition in Parkinson's disease: an event-related potential perspective. Ann. Neurol. 11, 599-607.

Isacson, O., Fischer, W., Wictorin, K. and Dawbarn, D. (1987) Astroglial response in the exocitoxically lesioned neostriatum and its projection areas in the rat. Neuroscience, 20, 1043-1046.

Ishii, T. and Haga, S. (1976) Immuno-electronmicroscopic localization of immunoglobulins in amyloid fibers of senile plaques. Acta Neuropathol. 36, 243-249.

Jenner, P. and Marsden, C.D. (1990) 1-Methyl-4-phenyl-1,2,3,6-tetrahydropyridine (MPTP): an update on its relevance to the cause and treatment of Parkinson's disease. In: Function and dysfunction in the basal ganglia (eds. Franks, A.J., Ironside, W., Mindham, R.H.S., Smith, R.J., Spokes E.G.S. and Winlow, W.) pp.140-160. Manchester University Press, Manchester.

Johannesen, J.N., Chiueh, C.C., Herkenham, M.A., Markey, S.P., Burns, R.S., Adams, J.D. and Schuller, H.M. (1986) Relationship of the in vivo metabolism of MPTP toxicity. In: MPTP: A Neurotoxin Producing a Parkinsonian Syndrome (eds. Markey, S.P., Castagnoli, N., Trevor, A.J. and Kopin, I.J.) pp. 173-189. Academic Press, New York.

Kanazawa, I., Tanaka, Y. and Cho, F. (1986) 'Choreic' movement induced by unilateral kainate lesion of the striatum and L-DOPA administration in monkey. Neurosci. Lett. 71, 241-246.

Kutas, M., McCarthy, G. and Donchin, E. (1977) Augmenting mental chronometry: the P300 as a measure of stimulus evaluation time. Science 197, 792-795.

Langston, J.W., Forno, L.S., Robert, C.S. and Irwin, I. (1984) Selective nigral toxicity after systematic administration of 1-methyl-4-phenyl-1,2,3,6-tetrahydropyridine (MPTP) in the squirrel monkey. Brain Res. 292, 390-394.

McCarthy, G. and Donchin, E. (1981) A metric for thought: a comparison of P300 latency and reaction time. Science 211, 77-80.

McGeer, E.G. and McGeer, P.L. (1976) Duplication of biochemical changes in Huntington's chorea by intrastriatal injections of glutamic and kainic acids. Nature, 263, 517-518.

Nandy, K., Lal, H., Bennet, M., and Bennet, D. (1983) Elevated brainreactive antibodies and a learning deficit co-occur in young NZB mice. Life Sci. 33, 1499-1503.

Nishino, H., Shibata, R., Nishijo, H., Ono, T., Watanabe, H., Kawamata, S. and Tohyama, M. (1988) Grafted rat neonatal adrenal medullary cells: structural and functional studies. Prog. Brain Res. Vol. 78. pp.521-527.

Onofrj, M.C., Bodis-Wollner, I., Ghilardi, M.F., Marx, M.S. and Glover, A. (1986) Pattern vision in monkeys with parkinsonism: a stimulus-specific effect of MPTP on retinal and cortical processing. In: MPTP: A Neurotoxin Producing a Parkinsonian Syndrome (eds. Markey, S.P., Castagnoli, N. Jr., Trevor, A.J. and Kopin, I.J.) pp. 683-688. Academic Press, New York.

Pang, S., Borod, J.C., Hernandez, A., Bodis-Wollner, I., Raskin, S., Mylin, L., Coscia, L. and Yahr, M. (1990) The auditory P300 correlates with specific cognitive deficits in Parkinson's disease. J. Neural Trans. 2, 249-264.

Pineda, J.A., Foote, S.L., Neville, H.J. and Holmes, T. (1988) Endogenous event-related potentials in monkey: the role of task relevance, stimulus probability, and behavioral response. Electroenceph. Clin. Neurophysiol. 70, 155-171.

Porrino, L.J., Burns, R.S., Crane, A.M., Palombo, E., Kopin, I.J. and Sokoloff, L. (1987) Local cerebral metabolic effects of L-DOPA therapy in 1-methyl-4-phenyl-1,2,3,6-tetrahydropyridine-induced parkinsonism in monkeys. Proc. Natl. Acad. Sci. 84, 5995-5999.

Premack, D. (1983) The codes of man and beasts. Behav.Brain Sci. 6, 125-157.

Rathman, K.L. and Conner, C.S. (1984) Alzheimer's disease: clinical features, pathogenesis and treatment. Drug Intelligence Clin. Pharm. 18, 684-691.

Redmond, D.E., Roth, R.H., Elsworth, J.D., Sladek, J.R., Jr., Collier, T.J., Deutch, A.Y. and Haber, S. (1986) Fetal neuronal grafts in monkeys given methylphenyltetrahydropyridine. Lancet, 17, 1125-1127.

Ridley, R., Murray, T., Johnson, J. and Baker, H. (1986) Learning impairments following lesion of the basal nucleus of Meynert: modification by cholinergic drugs. Brain Res. 376, 108-116.

Roeltgen, M.G., Roeltgen, D.P. and Heilman, K.M. (1989) Unilateral motor impersistence and hemispatial neglect from a right striatal lesion. Neuropsychiat. Neuropsychol. Behav. Neurol. 2, 125-135.

Rubin, E.H. (1990) Psychopathology of senile dementia of Alzheimer type. In: Advances in Neurology (eds. Corkin, S., Growdon, J.H. and Rittel-Walker, E.) Vol. 51. pp. 53-59. Raven Press, New York.

Rugg, M.D., Potter, D.D., Pickles, C.D. and Roberts, R.C. (1989) Effects of scopolamine on the modulation of event-related brain potentials by word repetition (Abstract). Soc. Neurosci. Abstr. 15, 487-492.

Sanberg, P.R., Lehmann, J. and Fibiger, H.C. (1978) Impaired learning and memory after kainic acid lesions of the striatum: a behavioral model of Huntington's disease. Brain Res. 149, 546-551.

Schneider, J.S. and Kovelowski, C.J. (1990) Chronic exposure to low doses of MPTP. I. Cognitive deficits in motor asymptomatic monkeys. Brain Res. 519, 122-128.

Schneider, J.S. (1991) Responses of striatal neurons to peripheral sensory stimulation in symptomatic MPTP-exposed cats. Brain Res. 544, 297-302.

Schneider, J.S., McLaughlin, M.S. and Roeltgen, D.P. (1992) Motor and nonmotor behavioral deficits in monkeys made hemiparkinsonian by intracarotid MPTP infusion. Neurology, 42, 1565-1572.

Schwarz, R., Whetsell, W.O. and Mangano, R.M. (1983) Quinolinic acid: an endogenous metabolite that produces axon-sparing lesions in rat brain. Science, 219, 316-318.

Spencer, D., Horvath, E., Luiten, P., Schuurman, T. and Traber, J. (1984) Novel approaches in the study of acetylcholine function: neuropharmacology, neuroanatomy and behavior. In: Senile Dementia of the Alzheimer Type: Early Diagnosis, Neuropathology and Animal Models (eds. Traber, J. and Gispen, W.) Springer, New York.

Stanzione, P., Fattapposta, F., Giunti, P., D'Alessio, C., Tagliati, M., Affricano, C. and Amabile, G. (1991) P300 variations in parkinsonian patients before and during dopaminergic monotherapy: a suggested dopamine component in P300. Electroenceph. clin. Neurophysiol. 80, 446-453.

Ungerstedt, U. and Arbuthnott, G.W. (1970) Quantitative recording of rotational behavior in rats after 6-hydroxy-dopamine lesions of the nigrostriatal dopamine system. Brain Res. 24, 485-493.

Walsch, T., Tilson, H., DeHaven, D., Mailman, R., Fischer, A. and Hanin, I. (1984) AF64A, a cholinergic neurotoxin, selectively depletes acetylcholine in hippocampus and cortex and produces long-term passive avoidance and radial-arm maze deficits in the rat. Brain Res. 321, 91-102.

Wenk, G. and Engisch, K. (1986) [3H]Ketanserin (serotonin type 2) binding increases in rat cortex following basal forebrain lesion with ibotenic acid. J. Neurochem. 47, 845-850.

Widner, H. and Brundin, P. (1988) Immunological aspects of grafting in the mammalian central nervous system. Brain Res. Rev. 13, 287-324.

Received 4 March 1993
Accepted 13 April 1993

Neurobiology 1 (2), pp. 123-131, 1993

ASTROGLIAL REACTION FOLLOWING WALLERIAN DEGENERATION IN THE RAT VISUAL CORTEX: PROLIFERATION OR HYPERTROPHY?

F. Hajós, B. Gerics and É. Turai

Department of Anatomy and Histology, University of Veterinary Science, H–400 Budapest, P.O. Box 2, Hungary

Summary: Following chemical lesioning of the rat dorsal lateral geniculate nucleus the visual cortical astrocytes were investigated with light and electron microscopy. A quantitative evaluation of astrocyte distribution within the cortex was also carried out. Findings suggest that while the number of cortical astrocytes remains fairly constant, they become hypertrophic and shifted towards the upper layers of the visual cortex. It is concluded that the degeneration of synaptic input to the visual cortex triggers the translocation and hypertrophy rather than proliferation of astrocytes.

Key words: astrocytes, Wallerian degeneration, visual cortex, rat

INTRODUCTION

The response of astroglia to injuries of neurons, either pathological or experimental, is a well-established phenomenon [reviewed by Lindsay, 1986]. It is generally claimed that astroglial reaction includes proliferation and hypertrophy of astrocytes as suggested by studies with autoradiography and immunohistochemistry [Adrian and Williams, 1973; Latov et al., 1979; Korr, 1986; Janeczko, 1989]. Our recent findings, however, have cast serious doubts concerning the uniformity of astroglial reaction to all kinds of neuronal impairments [Hajós

Akadémiai Kiadó, Budapest

et al., 1990a] lending support to the earlier view of Vaughn et al. [1970]. Massive incorporation of tritiated thymidine has been observed around CNS tissue lesions but this was not clearly attributable to glioblast divisions. Around a brain wound intensively proliferating inflammatory cells and macrophages [Stenwig, 1972; Murray and Walter, 1973; Ling, 1979] are always present which may account for the thymidine uptake. When astroglial reactions have been studied in areas of retrograde or anterograde (Wallerian) degeneration [Bignami and Ralston, 1969; Stenwig, 1972; Rose et al., 1976; Gall et al., 1979; Isacson et al., 1987], changes occurring at the affected target area were less dramatic than at the site of the lesion and the presence of astrocyte proliferation was not unequivocally proved. Nevertheless, immunostaining with antibodies against glial fibrillary acidic protein (GFAP) has revealed a substantial increase in the immunoreactivity for this important cytoskeletal protein of astrocytes indicating their involvement in degenerative processes even at considerable distances from the lesion [Barrett et al., 1981; Graeber and Kreutzberg, 1986; Tetzlaff et al., 1988; Hajós et al., 1990a, b]. Since under these experimental conditions local tissue reaction can be ruled out, the Wallerian degeneration appeared to be a suitable experimental paradigm to study how astrocytes respond to the disturbance of neighboring neuronal elements.

The Wallerian degeneration of the geniculo-cortical system was chosen for our studies which produces a massive, circumscribed loss of afferent fibres and synapses in the visual cortex. We were interested to observe the morphology and number of astrocytes in this area severely affected by the interruption of its most important afferents.

MATERIALS AND METHODS

Adult albino rats (either sex) of 200 g body weight were operated under Avertin anaesthesia in a stereotaxic apparatus. The right dorsal lateral geniculate nucleus (DLG) was lesioned by inserting the cannula of a microsyringe. Through the cannula 5 to 10 μl of the excitotoxin was injected into the DLG. After survival periods of 3, 5, 7 and 11 days, rats were anaesthetized with ether and perfused through the aorta with a mixture of paraformaldehyde and glutaraldehyde (4% each) dissolved in 0.1 M phosphate buffer (PB; pH 7.4). Brains were removed from the skull and immersed into the fixative for overnight. After a rinse in several changes of PB, 0.5 mm thick coronal slabs of the occipital cortex were excised, fixed in 1% osmic acid for 2 h, dehydrated in ethanol and propylene oxide and embedded in resin (Durcupan, Fluka). The rest of the brain was processed for routine histology to check the site and extent of the lesion.

From the resin-embedded visual cortices 1 μm thick sections were cut and stained with 1% toluidine blue. Ultrathin sections containing the cortical cytoarchitectonic layers II-IV were cut and viewed with a JEOL 100 B electron microscope.

Astrocytes were identified in large-area semithin sections encompassing the full width of the visual cortex and counted under an eyepiece graticule on both control and operated sides. The width of the cortex was divided into 3 equidistant zones designated as "external, middle and internal" so as to compare corresponding areas of both sides.

RESULTS

Upon checking in paraffin sections the site and extent of lesions, 16 brains were selected for further processing. Six of them were perfused at 3 days after the lesion, 4-4 at 5 and 7 days, while the rest at 11 days.

Three days after DLG-lesion the main cellular elements of the control-side visual cortex were readily identified in semithin sections under a 100-X oil-immersion objective.

Astrocytes were recognized on the basis of their round or oval, lightly staining nuclei showing a characteristic accumulation of chromatin at the inner aspect of the nuclear envelope. The nucleolus was often found in an eccentric position. The cytoplasm appeared as a thin empty-looking rim (Fig. 1). Interneurons in the size-range of astrocytes were distinguished by their nuclear indentations and/or evenly distributed clumps of heterochromatin. Oligodendrocytes were well discernible having a compact, dark nucleus and a small, dark, non-branching cytoplasm. Pyramidal neurons were evident due to their size, shape and orientation.

On the operated side astrocytes underwent a spectacular hypertrophy (Fig. 2). The cytoplasm was found substantially enlarged showing the typical "watery" appearance described in low-power electronmicrographs [see Peters et al., 1976a]. Also the processes became widened with numerous branches and appendages. In the enlarged cytoplasm mitochondria and bundles of cytoskeletal filaments could be perceived under oil immersion. The nucleus was also slightly enlarged but the distribution of chromatin seemed to be somewhat more even within the nucleoplasm and it formed a thinner contour line of the nuclear envelope as compared to the control. Even so, the nucleus of astrocytes displayed a more pronounced contour than that of neurons. In most hypertrophic astrocytes the nucleolus

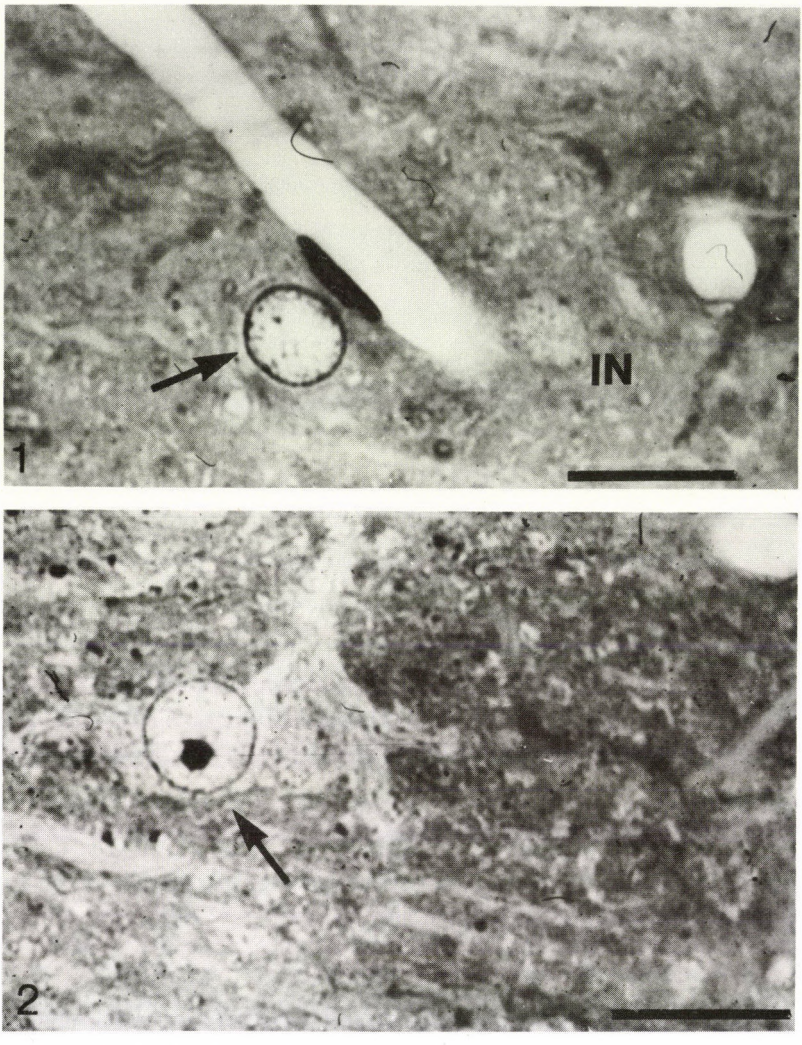

Fig. 1: On the control side astrocytes and small interneurons of the visual cortex can readily be distinguished in semithin section of layer IV. Interneurons (IN) have an indented nucleus with evenly distributed clumps of heterochromatin, while in astrocyte nuclei (arrow) the chromatin is accumulated at the inner aspect of the nuclear envelope. The pronounced nuclear contour almost hides the small, eccentrically located nucleolus. The cytoplasm is difficult to outline. Bar scale = 10 μm.

Fig. 2: Hypertrophic astrocytes in cortical layer IV three days after DLG lesion. Note the enlarged "watery" cytoplasm with mitochondria and filament bundles to be perceived. Nuclear contour (arrow) is still marked by chromatin accumulation but to a lesser extent than on the control side. The nucleolus is enlarged and centrally located. Bar scale = 10 μm.

was also enlarged and centrally located although occasionally small, eccentric nucleoli were encountered.

The peak of astroglial hypertrophy was observed on postoperative days 3-5. By day 11 most astrocytes were found to be similar on the operated and control sides.

For each survival period a careful search was made throughout the visual cortex of the operated side for mitotic figures either glial or other (inflammatory, endothelial, etc) but no sign of cell division was seen.

The counting of 1635 astrocytes in a total of 25.000 μm^2 area for both control and operated sides at 3 days after lesion revealed their shifting toward the upper layers without significant change in number as calculated for the entire cortex. While on the control side 29.38%, 38.63% and 31.81% of astrocytes were found in the external, middle and internal layers, respectively, on the operated side these figures were 47.00%, 32.24% and 19.70%.

Electron microscopy (Fig. 3) has clearly shown hypertrophic astroglia processes to engulf degenerating synaptic terminals in cytoarchitectonic layers III-IV of the visual cortex and to contain an increased amount of glycogen particles. When studied on postoperative day 3, the pre- and postsynaptic specializations were still to be recognized surrounded by reactive astroglia.

DISCUSSION

Wallerian and retrograde degenerations have been shown to evoke an astrocytic reaction [Rose et al., 1976; Gall et al., 1979; Barrett et al., 1981; Graeber and Kreutzberg, 1986; Hajós et al., 1990a] termed on the basis of immunocytochemical evidence as the "remote response" [Hajós et al., 1990a]. Our present findings suggest that this type of glial reaction differs essentially from what has been summarized under the term "reactive gliosis" which refers to a local response to injury - either experimental or pathological - and implies a surrounding glial proliferation [Cavanagh, 1970; Matthewson and Berry, 1985]. The nature of massive cell proliferation observed around brain injuries is still controversial. Immunohistochemical evidence suggests that there may be dividing astrocytes present in the reactive cell population [Latov et al., 1979; Janeczko, 1989] but they are heavily outnumbered by other kinds of mitotic cells [Matthews, 1977].

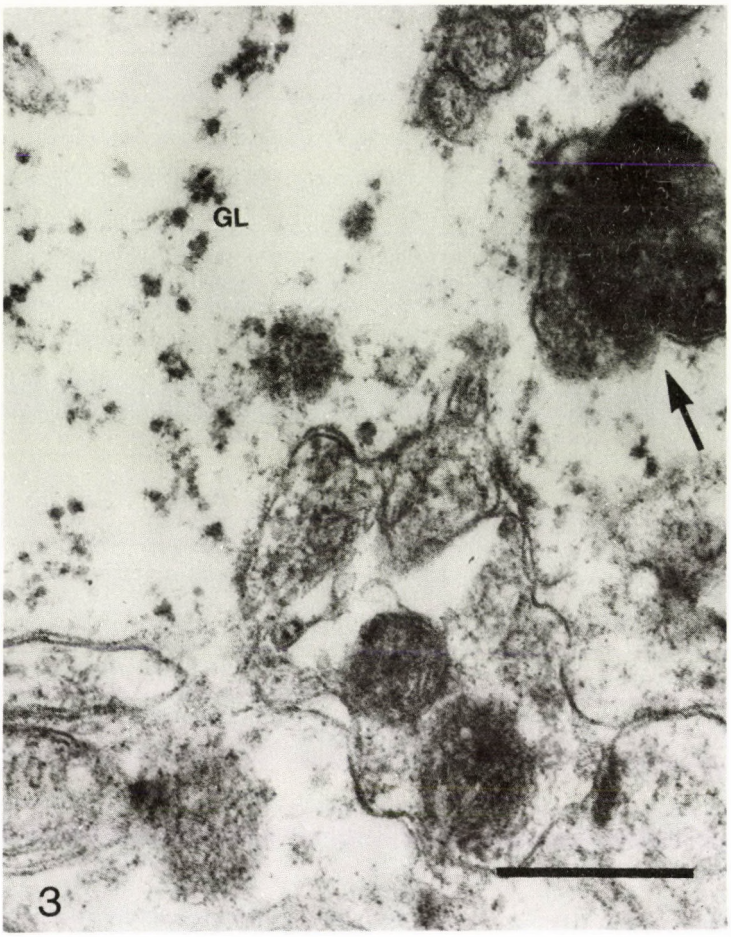

Fig. 3: Electron micrograph of a degenerating synapse (arrow) in layer IV of the DLG-lesioned visual cortex three days after operation. The pre- and postsynaptic elements can still be recognized engulfed in a large, electron-lucent astrocyte process. In the glial cytoplasm numerous glycogen particles (GL) can be seen. Bar scale = 1 μm.

Our experimental model, the Wallerian degeneration of the geniculo-cortical system, allowed a clear-cut assessment of the glial reaction eliminating other types of tissue reactions. In this system no cell division whatsoever could be detected in the area affected by

degeneration. On the other hand, all signs of astroglial hypertrophy were observed apparently evoked by the massive degeneration of axons and synaptic terminals. In addition to the well-established cytoplasmic landmarks of astrocyte hypertrophy [see Barrett et al., 1981], we were able to demonstrate fine differences in nuclear structure between control and reactive astrocytes. These alterations can be interpreted as a transition from heterochromatic to euchromatic nuclear structure [Privat and Rataboul, 1986]. In accordance with their cytoplasmic reaction, reactive astrocytes had euchromatic-like nuclei. The thicker aggregation of chromatin against the nuclear envelope in the control may be indicative of a "resting" state.

Another set of information derived from the study of astrocyte distributions throughout the visual cortex. It should be noted that our equidistant zones the external, middle and internal zones comprise cytoarchitectonic layers I-IV, V and external VI, and internal VI, respectively. Increase in number of astrocytes in the external zone with concomitant decrease in the middle, and particularly in the internal zones, represents a shift in the distribution of astrocytes to the sites of terminal degeneration. Layers III-IV where geniculo-cortical fibres terminate [Peters et al., 1976b] contained indeed the bulk of degenerating synapses. Their engulfment by astroglial processes together with an astrocyte accumulation in their surroundings suggests that it is the damage to the presynaptic terminals which triggers this type of astrocyte reaction. Enrichment in astrocytes at these sites on the expense of the deeper zone is a remarkable phenomenon as the studies of Wree et al. [1980] have shown that these glia are normally evenly distributed in the cortical grey matter. Hence migratory translocation as part of the astrocyte response is strongly suggested.

We conclude that the Wallerian degeneration is accompanied by substantial astrocyte hypertrophy at and migratory translocation to the sites of terminal degeneration but not by glial proliferation. The degeneration of synapses seems to trigger the hypertrophy and migration of astrocytes with an apparent goal of removing all degenerated particles by phagocytosis. The transitory nature of this phenomenon suggests that having fulfilled their scavanger function, hypertrophic astroglia return to normal as a sign of cessation of major rearrangements in the deafferented neuropil. Further plastic changes may occur at the synaptic level.

REFERENCES

Adrian, E.K. and Williams, M.G. (1973) Cell proliferation in injured spinal cord. J. Comp. Neurol. 151, 1-24.

Barrett, C.P., Guthe, L., Donati, E.J. and Krikorian, J.G. (1981) Astroglial reaction in the grey matter of lumbar segments after midthoracic transection of the adult rat spinal cord. Exp. Neurol. 73, 365-377.

Bignami, A. and Raltson, H.J. (1969) The cellular reaction to Wallerian degeneration in the central nervous system of the cat. Brain Res. 13, 444-461.

Cavanagh, J.R. (1970) The proliferation of astrocytes around a needle wound in the rat brain. J. Anat. 106, 471-487.

Gall, C., Rose, G. and Lynch, G. (1979) Proliferative and migratory activity of glial cells in the partially deafferented hippocampus. J. Comp. Neurol. 183, 539-550.

Graeber, M.B. and Kreutzberg, G.W. (1986) Astrocytes increase in glial fibrillary acidic protein during retrograde changes of facial motor nucleus. J. Neurocytol. 15, 363-373.

Hajós, F., Kálmán, M., Zilles, K., Schleicher, A. and Sótonyi, P. (1990a) Remote astrocytic response as demonstrated by glial fibrillary acidic protein immunohistochemistry in the visual cortex of dorsal lateral geniculate nucleus lesioned rats. Glia. 3, 301-310.

Hajós, F, Csillik, B. and Kálmán, M. (1990b) Alterations in glial fibrillary acidic protein immunoreactivity in the upper dorsal horn of the rat spinal cord in the course of transganglionic degenerative atrophy and regenerative proliferation. Nuerosci. Lett. 117, 8-13.

Isacson, D., Fischer, W., Wictorin, K., Dewbarn, D. and Björklund, A. (1987) Astroglial response to excitotoxically lesioned neostriatum and its projection area in the rat. Neuroscience. 20, 1043-1056.

Janeczko, K. (1989) Spatiotemporal patterns of astroglial proliferation in rat brain injured at the postmitotic stage of postnatal development. A comnbined immunocytochemical and autoradiographic study. Brain Res. 485, 236-243.

Korr, H. (1986) Proliferation and cellcycle parameters of astrocytes. In: Astrocytes (eds. Fedoroff, S., Vernadakis, A.) Vol. 3. pp 77-128. Academic Press, Orlando.

Latov, N., Nilaver, G., Zimmerman, E.A., Johnson, W.G., Silverman, A.I., Defendini, R. and Cote, L. (1979) Fibrillary astrocytes proliferate in response to brain injury. A study combining immunoperoxidase technique for glial fibrillary acidic protein with autoradiography of tritiated thymidine. Dev. Biol. 72, 381-384.

Lindsay, R.M. (1986) Reactive gliosis. In: Astrocytes (eds. Fedoroff, S., Vernadakis, A.) Vol. 3. pp 231-262. Academic Press, Orlando.

Ling, E. (1979) Evidence for haematogenous origin of some of the macrophages appearing in the spinal cord after dorsal rhizotomy. J. Anat. 128, 143-154.

Matthews, M.A. (1977) Reactive alterations in nonneurral elements of the degenerating ventrobasal complex of immature and mature rats. Cell Tissue Res. 179, 413-427.

Matthewson, A.J. and Berry, M. (1985) Observations on the astrocyte response to cerebral stab wound in adult rats. Brain Res. 327, 61-65.

Murray, H.M. and Walter, B.E. (1973) Comparative study of astrocytes and mononuclear leukocytes reacting to brain trauma in mice. Exp. Neurol. 41, 290-302.

Peters, A., Palay, S.L. and Webster, H. (1976a) The fine structure of the nervous system: the neurons and supporting cells. Saunders, Philadelphia.

Peters, A., Feldman, M. and Saldanha, J. (1976b) The projection of the laterale geniculate nucleus to area 17 of the rat cerebral cortex. II. Terminations upon neuronal perikarya and dendritic shafts. J. Neurocytol. 5, 85-107.

Privat, A. and Rataboul, P. (1986) Fibrous and protoplasmic astrocytes. In: Astrocytes (eds. Fedoroff, S., Vernadakis, A.) Vol. 1. pp 105-130.

Rose, G., Lynch, G. and Cotman, C.W. (1976) Hypertrophy and redistribution of astrocytes in the deafferented dentate gyrus. Brain Res. Bull. 1., 87-92.

Stenwig, A.E. (1972) The origin of brain macrophages in traumatic lesions. Wallerian degeneration and retrograde degeneration. J. Neuropathol. Exp. Neurol. 31, 696-704.

Tetzlaff, W., Graeber, M.B., Bisby, M.A. and Kreutzberg, G.W. (1988) Increased glial fibrillary acidic protein synthesis in astrocytes during retrograde reaction of the rat facial nucleus. Glia. 1, 90-95.

Vaughn, J.E., Hinds, P.L. and Skoff, R.P. (1970) Electron microscopic studies of Wallerian degeneration in rat optic nerves. I. The multipotential glia. J. Comp. Neurol. 140, 175-206.

Wree, A., Zilles, K. and Schleicher, A. (1980) Analysen der laminären Strukturen der Area striata mit verschiedenen stereologischen Messmethoden. Verh. Anat. Ges. 74, 727-728.

Received 14 January 1993
Accepted 23 February 1993

Neurobiology 1 (2), pp. 133-146, 1993

AN IMMEDIATE MORPHOPATHOLOGIC RESPONSE OF NEURONS TO ELECTROSHOCK; A RELIABLE MODEL FOR PRODUCING "DARK" NEURONS IN EXPERIMENTAL NEUROPATHOLOGY

F. Gallyas[1], G. Zoltay[1], Z. Horváth[1], K. Dávid[1] and L. Kelényi[2]

Departments of Neurosurgery[1] and Physiology[2], University Medical School, Rét utca 2, Pécs, H-7624, Hungary

Summary: Ninety rats were electroshocked by a single condenser discharge 1 min. prior to perfusion fixation and delayed autopsy. Voltage and capacity of the condenser as well as surface area and position of the electrodes were varied between 125 and 1250 V, 20 and 200 μF, 2 and 24 mm^2, and frontal to posterior, respectively. Within these ranges the electroshock rendered a varying number of brain neurons together with their dendritic arborization stainable by a special silver method. In toluidine blue preparations both somata and nuclei of these neurons appeared markedly shrunken and hyperchromatic, indicating morphological damage ("dark" neuron). A 250-V shock damaged only granule neurons of the hippocampal dentate gyrus. After a 750-V shock it was the substantia nigra, the lateral septal nucleus, the anterior amygdaloid area, and the lateral preoptic area that consistently contained electrically damaged neurons, without other kinds of parenchymal damage.

Key Words: Condenser discharge; Direct current; Light microscopy; Neuronal damage; Selective vulnerability; Silver staining.

INTRODUCTION

The nature of neurons showing markedly increased stainability with basic dyes, significant shrinkage of the soma, pyknosis of the nucleus and corkscrew-like deformation of main dendrites, i.e. the nature of neurons traditionally termed "dark", has been a matter

Akadémiai Kiadó, Budapest

of dispute ever since their first description [Flesh, 1887]. Cammermeyer [1960, 1961, 1978, 1979] considered them to be post-mortem artifacts because no "dark" neurons were found by him in experimental animals killed with transcardial perfusion of various fixatives one day before brain autopsy whereas numerous "dark" neurons were observed in brain samples dissected out of either living or dead animals before immersion fixation. By contrast, recent studies have convincingly demonstrated that a large number of pathological conditions brought about before perfusion fixation and delayed autopsy are capable of producing "dark" neurons. These pathological conditions include cerebral ischemia [Jenkins et al., 1981; Kirino and Sano, 1984; Nedergaard, 1987], hypoglycemia [Auer et al., 1984; Kleihues et al., 1986], brain injury [Queiroz et al., 1977; Gallyas and Zoltay, 1992; Gallyas et al., 1992a,b], status epilepticus [Attilo et al., 1983; Griffiths et al., 1983; Ingvar et al., 1988], excessive stimulation [Clarke and Nussbaumer, 1987], deafferentation [Heimer and Kalil, 1978; Johnson, 1975], transient opening of the blood brain barrier [Sokrab et al., 1988; Solohuddin et al., 1988], and poisoning with various substances [Cronog et al., 1967; Tremblay et al., 1984; Finnie and O'Shea, 1988; Goldschmidt and Steward, 1980; Mihály et al., 1983; Sperk et al., 1983; Hamilton and Gould, 1987]. Produced either in vivo or post-mortem, "dark" neurons have two additional histological peculiarities in common: they are scattered among normal neurons frequently in an otherwise undamaged parenchymal environment, and they are stainable in a Golgi-like fashion by a special silver method [Gallyas et al., 1990]. Prompted by the striking morphological similarity between "dark" neurons of various genesis we recently hypothesized that their nature and their mechanism of formation must also be similar [Gallyas et al., 1992c].

"Dark" neurons are commonly believed to die. By contrast, there is enough circumstantial evidence to suggest that a proportion of them, independently of their genesis, may spontaneously recover within one day [Attilo et al., 1983; Söderfeldt et al., 1983; Evans et al., 1984; Griffith et al., 1984; Auer et al., 1985; Ingvar et al., 1988; Solohuddin et al., 1988; Gallyas et al., 1992a; Gallyas et al., submitted for publication]. In order to conduct experiments for human medicine on factors presumably decreasing (cerebral and/or systemic pathophysiological and/or pathometabolic conditions) or increasing (medicaments) the proportion of spontaneously recovering neurons, an animal model is needed which (a) ensures a reproducible distribution pattern of "dark" neurons, (b) causes no serious parenchymal damage other than "dark" neurons, (c) initiates the

formation of all "dark" neurons simultaneously at a selected time, (d) is inexpensive and easy to perform, enabling a relatively large number of animals to be examined.

Pilot experiments have shown that the shocking of rats with a single condenser discharge at and over 125 V and 20 μF satisfies these requirements. The present paper deals with the acute light microscopic findings obtained during a systematic electroshock study.

MATERIALS AND METHODS

The Electroshock Apparatus

The electroshock apparatus consisted of an electric booster capable of supplying direct current up to 1800 V, a condenser system with an output capacity variable between 20 μF and 200 μF, and a pair of electrodes (Fig. 1). A double pole switch connected the condenser system to either the electric booster or the electrode. The process of charging and discharging was monitored using a voltmeter connected in parallel to the condenser system.

The positive and negative discharge electrodes were both rooted in one handle made of insulating material (Fig. 1), which enabled the electrodes to be pressed on the selected places of the rat head using one hand only. The active surfaces of the electrodes were platinum-plated. Two pairs of discharge electrodes were tested: one with circular active surfaces of 1.6 mm in diameter each (small-surface electrodes), the other with square-shaped active surfaces, each measuring 4x6 mm^2 (large-surface electrodes).

Animal Experiments

A total of 100 rats of either sex weighing 200-250 g were anaesthetized with 40 mg/kg sodium pentobarbital. Without having been electroshocked, after a 60 second apnea due to thoracotomy, 10 of them were transcardially perfused with physiological saline for one min. then with 500 ml of a fixative (25.7 g of sodium cacodylate dissolved in a mixture of 100 ml of 20 % paraformaldehyde, 100 ml of 25 % glutaraldehyde and 800 ml of distilled water, adjusted to pH 7.5 with hydrochloric acid). They served as controls. Each of the remaining 90 rats was electroshocked with one single discharge of the condenser system. Charging voltage and capacity of the condenser system as well as surface area and position of the electrodes were varied as detailed in the next paragraphs. Each combination was tested in three animals.

The scalp and the underlying soft tissues, except the temporal muscles, were removed in 72 rats and the large-surface electrodes were placed upon the temporal muscles on both sides. Each combination of 125 V, 250 V, 500 V, 750 V, 1000 V and 1250 V charging voltage with 20 μF, 40 μF, 100 μF and 200 μF condenser capacity was tested.

The scalp and the underlying soft tissues, including the temporal muscles, were removed in 12 rats and the small-surface electrodes were placed upon both hemispheres 4 mm laterally to the sagittal suture at four different sites: (i) 2 mm rostrally to the bregma, (ii) 3 mm caudally to the bregma, (iii) 3 mm rostrally to the lambda and (iv) 2 mm caudally to the lambda. In each animal the charging voltage and condenser capacity were 750 V and 100 μF, respectively.

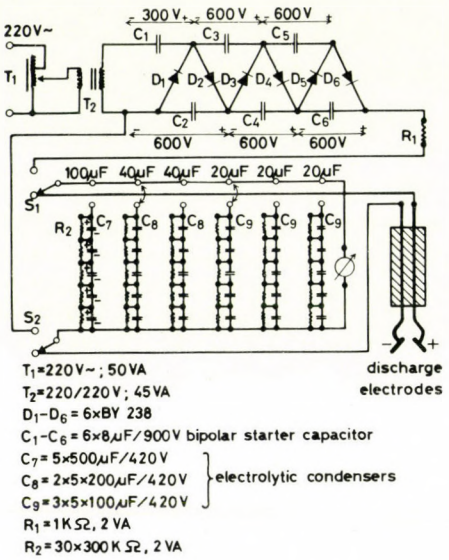

Fig. 1: Circuit diagram of the electroshock apparatus

In three animals the scalp was shaved and covered with a conductive jelly containing sodium chloride (20 %). The large-surface electrodes were then pressed upon the skin overlying the temporal muscles. The charging voltage and condenser capacity were 750V and 200 μF, respectively.

In three animals the large-surface electrodes were pressed upon the inner side of the ears laid on the unshaven and unjellied scalp. The charging voltage and condenser capacity were 750 V and 200 μF, respectively.

In each case the discharge of the condenser system took less than one second, during which a hissing sound indicated massive heat production under the "active" electrode surfaces. Independently of the actual values of the charging voltage and condenser capacity the electroshock was followed by one convulsion of tonic-clonic type which was accompanied by apnea, both lasting 20-40 seconds. Sixty seconds after the electroshock the animals were perfused transcardially first with physiological saline for 1 min., then with 500 ml of the above fixative. The brains were removed 16-24 hours later and immersed for at least 1 week in the fixative additionally containing 5.9 g of $CaCl_2x2H_2O$ per liter.

Tissue Processing and Staining

Olfactory bulb, cerebrum, and cerebellum were separated with vertical cuts. After being impregnated with 30 % saccharose the cerebral hemispheres were frozen-sectioned serially. Every tenth of the one 100-μm-thick coronal sections obtained was stained by the silver procedure mentioned [Gallyas et al., 1990]. Adjacent sections were stained with 0.1 % toluidine blue dissolved in 1 % acetic acid.

RESULTS

Control Animals

The microscopic features of the silver-stained preparations were very similar to those found earlier in control rat brains [Gallyas et al. 1990; Gallyas and Zoltay, 1992]. It should be emphasized that neither somata nor appendages of the neurons were silver-stained in any area of the brain. As a feature common to all control brains, a varying number of thick and short black fibres perpendicular to the brain surfaces, were observed within the subpial zone (Fig. 2c). Red blood cells remaining infrequently in the capillaries imperfectly perfused with the fixative, stained black. None of the control rats showed any significant pathological change with toluidine blue.

Variation of Charging Voltage and Condenser Capacity

With the pair of large-surface electrodes placed upon the temporal muscles, each of the combinations of charging voltage and condenser capacity rendered a varying number of neurons stainable with silver (argyrophilic). These neurons were usually situated distant from the sites of the electrodes. Independently of the actual values of voltage and capacity (i) the argyrophilic neurons were scattered among non-argyrophilic (unstained) neurons of the same morphology and function (Figs. 2 and 3), (ii) most dendrites belonging to argyrophilic neuronal somata were also argyrophilic and vice versa, (iii) several dendritic segments had a corkscrew-like appearance (Fig. 3e), (iv) silver-stained axons were found nowhere in any of the brains, and (v) the argyrophilic neuronal somata appeared shrunken and hyperchromatic ("dark") with toluidine blue (inserts in Figs. 2a and 3e).

Except small semicircular, non-argyrophilic cortical areas underlying the electrodes (see later) toluidine blue did not reveal any light microscopic sign of parenchymal damage other than "dark" neurons; specifically, no hemorrhage, perivascular petechiae, extravasated lymphocytes, coagulated erythrocytes in blood vessels, spongy enlargement of pericapillary spaces, edematous loosening of the "ground substance", pallor and swelling of neurons

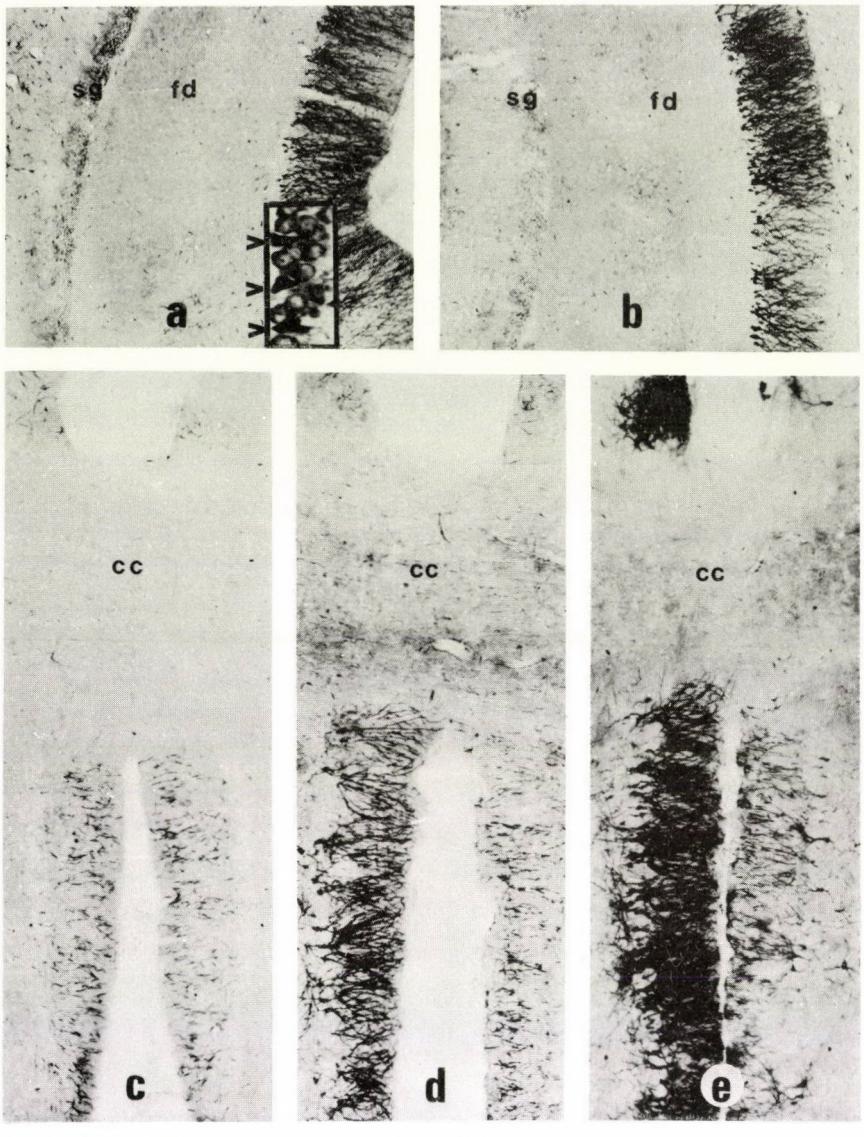

Fig. 2: Responses of neuronal somata and dendrites to a single condenser discharge, as demonstrated by a special silver staining method (a-e) and toluidine blue (insert in a). a and b: Caudo-lateral part of the hippocampal dentate gyrus in the left (a) and right (b) hemispheres of the same animal; c-e: anterior hippocampus. In each rat the negative electrode was placed on the right temporal muscle of the skull. Charging voltage and condenser capacity were 250 V and 100 μF (a, b and e), 750 V and 100 μF (e), as well as O V and O μF (c). sg = stratum granulosum, fd = fascia dentata, cc = corpus callosum; in the insert arrowheads point to "dark" neurons. a and b: x73, c-e: x80, insert in a: x190.

("pale" neurons), and/or swelling of glial cells either in the areas containing "dark" neurons or in those free of them. However, at and over 500 V and independently of the condenser capacity tested, a subpopulation of astrocytes were also rendered argyrophilic, shrunken and hyperchromatic ("dark") by the electroshock (Gallyas et al., submitted for publication).

The distribution pattern of the argyrophilic neurons proved to be dependent mainly on the charging voltage (Fig. 4). At 125 V a few of the granule neurons in the hippocampal dentate gyrus became argyrophilic. Other phenotypes of neurons either in the hippocampus or in other brain areas remained unaffected.

At 250 V numerous hippocampal dentate neurons were consistently demonstrated by the silver method. Much to our surprise, the dendrites of all these argyrophilic neurons pointed to the site of the negative electrode. This phenomenon was most clearly visible in the caudo-lateral part of the hippocampus where the "outer" blade of the dentate granule cells was selectively vulnerable on the side of the negative electrode whereas the "inner" blade was vulnerable on the opposite side (Fig. 2a,b). In 5 of the total of 12 rats shocked with 250 V varying numbers of granule neurons in the anterior hippocampus were also silver-stained. The above-described dependence of electrically induced neuronal argyrophilia on the direction of dendrites relative to the negative electrode, was a common observation also in this area (Fig. 2d). In other brain areas silver-stained neurons were rarely seen.

At any given voltage within the 500-1250 V range silver-stained neurons were consistently present in certain brain areas whereas, in several others, they were found only in a varying number of the respective animals (Fig. 4). Such inconsistently affected areas generally became consistently affected at the higher voltages. In the consistently affected areas, with the exception of the hippocampal dentate gyrus, the argyrophilic neurons were more numerous at the higher voltages. Although the distribution patterns of the argyrophilic neurons were similar in the two hemispheres, an asymmetry in the direction of dendrites was observed. Specifically, neurons with more dendrites facing the negative electrode tended to become argyrophilic (Fig 3a-c). At and over 750 V several of those anterior hippocampal neurons whose dendrites pointed to the positive electrode also became argyrophilic (Fig. 2e). However, even at 1250 V, their number was significantly smaller than that of their contralateral counterparts whose dendrites faced the negative electrode.

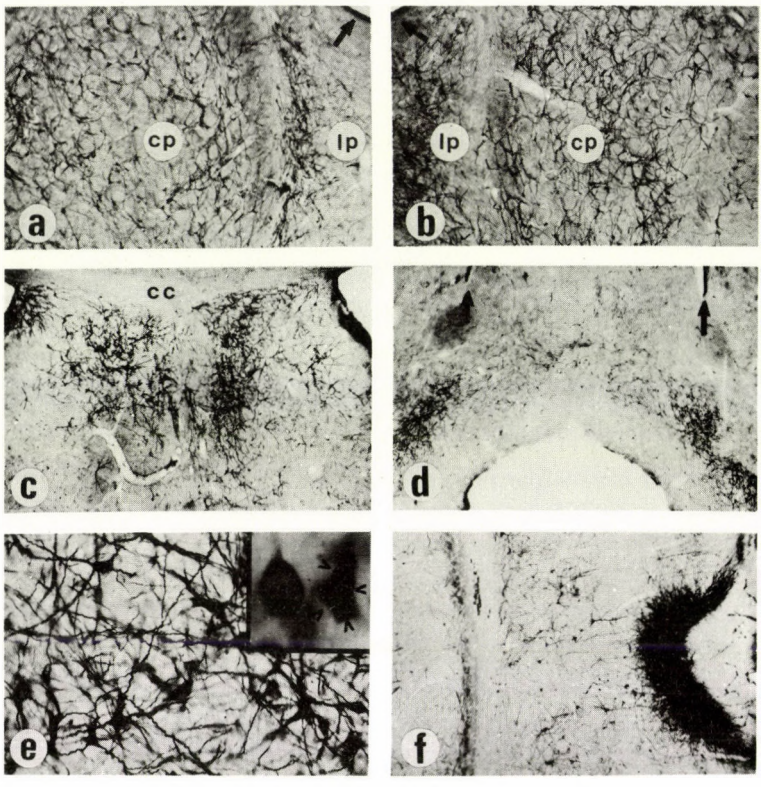

Fig. 3: Responses of neuronal somata and dendrites to a single condenser discharge, as demonstrated by a special silver method (a-f) and toluidine blue (insert in e). a and b: Caudate nucleus-putamen (cp) and lateral parolfactory area (lp) in the left (a) and right (b) hemispheres of the same animal, arrows point to the ventricles; c: lateral septal nucleus; cc = corpus callosum; d and e: lateral preoptic area, in the insert arrowheads point to a "dark" neuron; f: neocortex underlying the site of a large-surface electrode. In each rat the negative electrode was placed on the right temporal muscle of the skull. Charging voltage and condenser capacity were 1250 V and 100 μF (a-b, f), 750 V and 100 μF (c-e). a-c, f: x45, d: x20; e: x160, insert in e: x800.

In all rats shocked with 1000 V and 100-200 μF or with 1250 V and 20-200 μF semioval non-argyrophilic patches were found in the cortical areas underlying the site of the electrodes. These patches contained capillaries filled with red blood cells and were surrounded by a zone of silver-stained neuronal somata and dendrites (Fig. 3f). In such

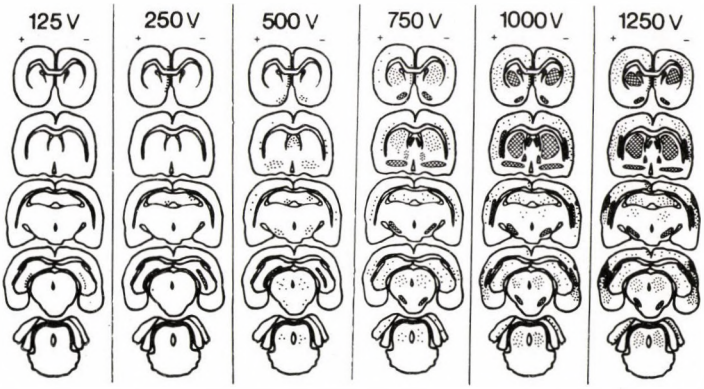

Fig. 4: Distribution patterns of neurons damaged by a single condenser discharge at various voltages. Hatched areas are consistently affected; dotted areas are affected only in some of the animals with identical charging voltage; black patches indicate thermal injury.

areas toluidine blue revealed parenchymal damage other than "dark" neurons; specifically, spongy enlargement of pericellular and pericapillary spaces mainly in their marginal zone, dilated blood vessels filled with coagulated erythrocytes, extravasated erythrocytes and "pale" neurons.

At any charging voltage tested, the number of argyrophilic neurons in all consistently affected areas increased moderately with increasing condenser capacity.

Variation of the Surface Area and Site of the Electrodes

The distribution patterns of argyrophilic neurons found with the small-surface electrodes were very similar to those found with the large-surface electrodes, when the charging voltage, condenser capacity and site of electrodes were kept identical.

Variation of the site of small-surface electrodes hardly influenced the distribution pattern of argyrophilic neurons induced by shocks of identical charging voltage and condenser capacity. However, the number of silver-stained neurons within the frontal part of the lateral preoptic area appeared greater whereas that of those within the substantia

nigra appeared smaller during a comparison of the effects of the most rostral and the most caudal sites of electrodes.

In all animals semi-circular non-argyrophilic patches, filled with red blood cells and surrounded by a zone of silver-stained neuronal somata and dendrites, were seen in the cortical areas just underlying the site of the small-surface electrodes.

No argyrophilic neurons were observed in the brains of rats electroshocked without removal of the scalp.

DISCUSSION

The question of whether electric currents passing through the brain have any specific (non-thermal) pathomorphologic effect has aroused a good deal of controversy. Several studies on victims of acutely fatal electrical injuries have failed to reveal, in the central nervous system, any other histo-pathologically demonstrable disturbance than thermal lesions. On the other hand, a number of authors have ascribed a variety of morphological changes to the direct effects of electric currents in brains with no sign of heat damage [Zeman, 1968]. Our findings support Langworthy and Kouwenhoven [1930, 1932] according to whom neuronal changes, including somal shrinkage and hyper-chromatism as well as nuclear pyknosis, become prominent following the passage through the rat brain of direct currents at 500 V or over. Additionally, our findings reveal several surprising peculiarities of electrically damaged neurons: (i) selective vulnerability of certain brain areas, (ii) selective vulnerability of certain neuronal phenotypes, (iii) dependence of the vulnerability of neurons on the direction of their dendrites relative to the electrode polarity, (iv) spiralization of dendritic segments, (v) increased argyrophilia of the somato-dendritic domain, and (vi) dependence of the distribution pattern of injured neurons on the strength of the electric field.

It should be mentioned that the beneficial therapeutic effect of electroconvulsive shock in some mental illnesses cannot be explained by the formation of "dark" neurons, because the values of the potential gradient (i.e., the quotient of the potential difference and the distance between the electrodes) in human electroshock therapy are much lower than those proved to be effective in our experiments.

Based on the fact that the distribution patterns of electrically induced argyrophilic neurons hardly depend on the surface area or site of the electrodes it can be concluded that the skull virtually enlarges the electrode surfaces making the electric field

quasi-homogeneous within the whole cerebrum. A comparison of the results obtained with scalped and non-scalped rats suggests that, in the latter, the bulk of electric current prefers flowing through the scalp.

From the co-incidence of the site of electrodes with that of the non-argyrophilic areas surrounded by a zone of silver-stained neuronal somata and dendrites as well as from the more frequent occurrence of such areas in the case of small-surface electrodes one can conclude that such areas might be caused by the heat produced on the electrode surfaces by electroshock.

In addition to our electroshock model, two other "electrical" models are known to produce "dark" neurons, although with rather different distribution patterns and after a relatively long (hours) exposure: intense electric stimulation [Sloviter et al. 1983] and neurotoxin-induced epilepsy [e.g. Nevander et al., 1985]. In the case of both models excessive release of excitatory amino acids from synaptic terminals are considered to be the primary cause of lethal neuronal damage [Ingvar et al., 1985; Sloviter et al., 1991]. Since data on excitatory amino acids are lacking in the case of an electroshock with a single condenser discharge, one can only speculate, whether or not the above mechanism applies to it.

As an experimental paradigm for producing "dark" neurons, the electroshock with a single condenser discharge has several important practical advantages over lasting electric stimulation or any other kind of pathophysiological or pathometabolic conditions: (i) the nature of "dark" neurons can be investigated in the very firs phase of formation, i.e., without being modified by an exposure to unknown external or internal pathometabolic conditions for an unknown period of time; (ii) neither the external nor the internal conditions for the potential recovery of newly-formed "dark" neurons are worsened by the continuing existence of the causative condition; (iii) it is known where to find "dark" neurons in an otherwise undamaged parenchymal environment for being investigated by sophisticated morphological, neurochemical, immunocytochemical or electrophysiological methods.

Since neither the size of the surface area nor the site of electrodes influences the distribution pattern of electrically damaged neurons considerably, the use of large surface electrodes is proposed for neuropathologic experimentation. They should be pressed upon the temporal muscles in order to increase heat dissipation and ensure a good fit of the rigid pair of electrodes on the rigid skull. Two values of charging voltage appear to

deserve preference: (i) 250 V, because it affects only one neuronal phenotype in only one anatomical and functional entity and (ii) 750 V, because it affects several neuronal phenotypes in several anatomical and functional entities without causing serious parenchymal injury. In both cases a condenser capacity of 200 μF appears to be suitable.

ACKNOWLEDGEMENT: This work was supported by OTKA-298.

REFERENCES

Attilo, A., Söderfeldt, B., Kalimo, H. and Siesjö, B.K. (1983) Pathogenesis of brain lesions caused by experimental epilepsy. Light- and electron-microscopic changes in the rat hippocampus following bicucculine-induced status epilepticus. Acta Neuropathol., 59, 11-24.

Auer, R.N., Kalimo, H., Olsson, Y. and Siesjö, B.K. (1985) The temporal evolution of hypoglycemic brain damage, II. Light- and electron-microscopic findings in the rat cerebral cortex. Acta Neuropathol. 67, 13-24.

Auer, R.N., Wieloch, T., Olsson, Y. and Siesjö, B.K. (1984) The distribution of hypoglycemic brain damage. Acta Neuropathol., 64, 177-191.

Cammermeyer, J. (1960) The post-mortem origin and mechanism of neuronal hyperchromatosis and nuclear pyknosis. Exp. Neurol., 2, 379-405.

Cammermeyer, J. (1961) The importance of avoiding "dark" neurons in experimental neuropathology. Acta Neuropathol. 1, 245-270.

Cammermeyer, J. (1978) Is the solitary dark neuron a manifestation of post-mortem trauma to the brain inadequately fixed by perfusion? Histochemistry, 56, 97-115.

Cammermeyer, J.(1979) Argentophil neuronal perikarya and neurofibrils induced by post-mortem trauma and hypertonic perfusates. Acta Anat., 105, 9-24.

Clarke, P.G.H. and Nussbaumer, J.C. (1987) A stain for ischemic or excessively stimulated neurons. Neurosci., 23, 969-979.

Cornog, J.L., Jr., Gonatas, N.K. and Feierman, B.S. (1967) Effects of intracerebral injection of quabain in the fine structure of rat cerebral cortex. Am. J. Pathol., 51, 573-590.

Evans, M.C., Griffiths, T., and Meldrum, B.S. (1984) Kainic acid seizures and the reversibility of calcium loading in vulnerable neurons in the hippocampus. Neuropathol. Appl. Neurobiol. 10, 285-302.

Finnie, J.M. and O'Shea, J.D. (1988) Pathological and pathogenic changes in the central nervous system of guinea pigs given tunicamycin, Acta Neuropathol. 75, 411-421.

Flesh, M. (1887) Über die Verschiedenheiten in chemischem Verhalten der Nervenzellen. Mitth. d. Naturforsch. Ges. in Bern 1073-1082. Cit. by Miller, R. (1949) A morphological and experimental study of chromophilic neurons in the cerebral cortex. Am. J. Anat. 84, 201-230.

Gallyas, F. and Zoltay, G. (1992) An immediate light microscopic response of neuronal somata, dendrites and axons to non-contusing concussive head injury in the rat. Acta Neuropathol. 83, 386-393.

Gallyas, F., Güldner, F.H., Zoltay, G. and Wolff, J.R. (1990) Golgi-like demonstration of "dark" neurons with an argyrophil III method for experimental neuropathology. Acta Neuropathol. 79, 620-628.

Gallyas, F., Zoltay, G. and Balás, I. (1992a) An immediate light microscopic response of neuronal somata, dendrites and axons to contusing concussive head injury in the rat, Acta Neuropathol. 83, 394-401.

Gallyas, F., Horváth, Z. and Zoltay, G. (1992b) Light microscopic response of neuronal somata, dendrites and axons to post-mortem concussive head injury. Acta Neuropathol. 83, 499-503.

Gallyas, F., Zoltay, G. and Dames, W. (1992c) Formation of "dark" (argyrophilic) neurons of various origin proceeds with a common mechanism of biophysical nature (a novel hypothesis). Acta Neuropathol. 83, 504-509.

Gallyas, F., Dávid, K. and Horváth, Z. (submitted for publication) "Dark" neurons are capable of spontaneous recovery.

Gallyas, F., Horváth, Z. and Károly, D. (submitted for publication) An immediate morphopathologic response of a subpopulation of astrocytes to electroshock: "dark" astrocytes.

Goldschmidt, R.B. and Steward, D. (1980) Preferential neurotoxicity of colchicine to the dentate gyrus of adult rat. Proc. Natl. Acad. Sci. USA 77, 3047-3051.

Griffiths, T.H.S., Evans, M.C. and Meldrum, B.S. (1983) Intracellular calcium accumulation in rat hippocampus during seizures induced by bicucculine or L-allylglycine. Neuroscience 10, 385-395.

Griffiths, T., Evans, M.C., Meldrum, B.S. (1984) Status epilepticus, the reversibility of calcium-loading and acute neuronal pathological changes in the rat hippocampus, Neuroscience, 12: 557-567.

Hamilton, B.F. and Gould, D.H. (1987) Nature and distribution of brain lesions in rats intoxicated with 3-nitropropionic acid: a type of hypoxic (energy deficient) brain damage. Acta Neuropathol. 72, 286-297.

Heimer, L. and Kalil, R. (1978) Rapid transneuronal degeneration and death of cortical neurons following removal of the olfactory bulb. J. Comp. Neurol. 178, 559-610.

Ingvar, M., Morgan, P.F. and Auer, R.N. (1988) The nature and timing of excitotoxic neuronal necrosis in the cerebral cortex, hippocampus and thalamus due to flurothyl-induced status epilepticus Acta Neuropathol. 75, 362-369.

Jenkins, L.W., Povlishock, J.T., Lewelt, W., Miller, J.P. and Becker, D.P. (1981) The role of postischemic recirculation in the development of ischemic neuronal injury following complete cerebral ischemia. Acta Neuropathol. 55, 205-220.

Johnson, J.E. (1975) The occurrence of dark neurons in the normal and deafferentated lateral vestibular nucleus in the rat: observations by light and electron microscopy. Acta Neuropathol. 31, 117-121.

Kirino, T. and Sano, K. (1984) Selective vulnerability in the gerbil hippocampus following ischemia. Acta Neuropathol. 62, 201-208.

Kleihues, P., Kiessling, M., Thilmann, R., Xie, Y., Uozumi, A. and Volk, B. (1986) Resistance to hypoglycemia of cerebellar transplants in the rat forebrain. Acta Neuropathol. 72, 23-28.

Langworthy, O.R. and Kouwenhoven, W.B. (1930) An experimental study of abnormalities produced in the organism by electricity. J. Indust. Hyg. 12, 31-56.

Langworthy, O.R. and Kouwenhoven, W.B. (1932) Injuries produced by contact with electric circuits. Am. J. Hyg. 16, 625-666

Mihály, A., Joó, F. and Szente, M. (1983) Neuropathological alterations in the neocortex of rats subjected to focal aminopyridine seizures. Acta Neuropathol. 61, 85-94.

Nevander G., Ingvar, M., Auer, R. and Siesjö, B. K. (1985) Status epilepticus in well-oxygenated rats causes neuronal necrosis. Ann. Neurol. 18, 281-290.

Nedergaard, M. (1987) Neuronal injury in the infarct border: a neuropathological study in the rat. Acta Neuropathol. 73, 267-274.

Queiroz, L.S. and Eduardo, R.M.P. (1977) Occurrence of dark neurons in living mechanically injured rat neocortex. Acta Neuropathol. 38, 45-48.

Sloviter R.S. (1983) "Epileptic" brain damage in rats induced by sustained electrical stimulation of the perforant path. I. Acute electrophysiological and light microscopic studies. Brain Res. Bull. 10, 675-697.

Sloviter, R. S. (1991) Feedforward and feedback inhibition of hippocampal principal cell activity evoked by perforant path stimulation; GABA-mediated mechanisms that regulate excitability. Hippocampus 1, 31-40.

Sokrab, T.W., Johansson, B.B,, Kalimo, H. and Olsson, Y. (1988) A transient hypertensive opening of the blood-brain barrier can lead to brain damage changes in rats subjected to aortic compression. Acta Neuropathol. 75, 557-565.

Solohuddin, T.S., Kalimo, H., Johansson, B.A. and Olsson, Y. (1988) Observations on exudation of fibronectin, fibrinogen and albumin in the rat after carotid infusion of hyperosmolar solutions. An immunohistochemical study in the rat indicating long-lasting changes in the brain environment and multifocal nerve cell injuries. Acta Neuropathol. 76, 1-10.

Söderfeldt, B., Kalimo, H., Olsson, Y. and Siesjö, B.K. (1983) Bicuculline-induced epileptic brain injury. Transient and persistent cell changes in rat cerebral cortex in the early recovery period. Acta Neuropathol. 62, 87-95.

Sperk, G., Lassmann, H., Kish, S.J. and Seitelberger, F. (1983) Kainic acid induced seizures: neurochemical and histopathological changes. Neuroscience 10, 1301-1314.

Tremblay, E., Berger, M., Nitecka, L., Cavalheiro, E. and Ben-Ari, Y. (1984) A multidisciplinary study of folic acid neurotoxicity: interaction with kainate binding sites and relevance to the aetiology of epilepsy. Neuroscience 12, 569-589.

Zeman, W. (1968) Thermal effects and electric injuries. In: Pathology of the Nervous System (ed.J. Minckler), pp. 939-948. McGraw-Hill Book Company, New York.

Received 11 March 1993
Accepted 10 April 1993

Neurobiology 1 (2), pp. 147-155, 1993

COMPUTER ANALYSIS OF SINGLE NEURON ACTIVITY DURING CONDITIONED FEEDING TASK

Cs. Niedetzky, Z. Karádi, A. Czurkó, B. Faludi,
I. Vida, G. Jandó and L. Lénárd

Neurophysiology Research Group of the Hungarian Academy of Sciences,
Institute of Physiology, Pécs University, School of Medicine, Pécs, H-7643 Hungary

Summary. A computer controlled complex electrophysiological set-up employing the multibarrel micro-electrophoretic technique is reported in this paper. The laboratory equipped for this technique is used for recording single neuron activity from various sites of the central nervous system of rhesus monkeys during: 1) performing conditioned behavioral tasks, 2) intracerebral microelectrophoretic administration of chemicals, and 3) oral application of gustatory stimuli.

Key words. Automatic data acquisition; Process control; Multibarrel electrophoretic technique; Behavioral studies

INTRODUCTION

The multibarrel electrophoretic technique, adapted and further developed in our laboratory, has been used for several years in research on limbic regulation of hunger- and thirst-motivated behaviors in the rat and monkey [Lénárd et al., 1988, 1990, 1991; Karádi et al., 1990]. The availability of a highly valuable rhesus monkey colony and the technical facilities of our institute enabled us to design even more complex experiments on awake, behaving primates.

In the present paper, a short description of our versatile system for simultaneous electrophysiological, neurochemical and behavioral experiments on the regulation of feeding is given. The system offers opportunities for variable approaches in relevant primate studies to examine the effects of: 1) conditioned feeding responses, 2) electrophoretic application of neurochemicals, and 3) intraoral gustatory stimulation on the activity of extracellularly recorded neurons.

MATERIALS AND METHODS

Adult rhesus monkeys (*Macaca mulatta*) of both sexes were used in these experiments. Hunger motivation was used to achieve and maintain conditioned behavioral responses. The monkeys were food deprived so that they were ambitious to get food reward.

In order to evoke gustatory responses, different taste solutions were injected through a soft polyethylene tube implanted into the mouth, and led to the posterior part of the head-piece of the animals [Karádi et al., 1990a].

In the experimental situation [details reported previously; Aou et al., 1984; Nakano et al., 1987; Karádi et al., 1990b] the head of the animal was fixed stereotaxically so that the rest of the body could freely move. The target neurons were approached by a multibarreled microelectrode with the help of a hydraulic microdrive [Narishige MO-8, Japan] enabling us to reach any part of the brain with high accuracy. The central, recording pipette of the multibarreled electrode contained a 7 μm (diam.) carbon fiber. Neurochemicals were applied through the micropipettes (less than 0.2 μm in diameter) surrounding the central barrel. Preparation, concentration and pH adjustment of neurochemical solutions were as described previously [Aou et al., 1984; Lénárd et al., 1986].

The ions from the pipettes were passed to the cells by means of the ejection current of an electrophoretic device [NeuroPhore BH-2; Medical Systems Corp., USA]. The ejection current usually ranged from 1 to 100 nA. The electrophoretic device had an automatic current balance channel to avoid occasional electrical stimulation effects. This feature of the device is due to its capacity to eject compensatory current (through one of the barrels containing NaCl) with opposite polarity but just in the required intensity.

RESULTS

The complexity of the task required a computer, and a universal program package to coordinate all control and data-collecting functions. Our system was developed in several steps [Niedetzky et al., 1987]. The frame of the system was designed to enable us for multipurpose investigation of the regulation of feeding in simultaneous electrophysiological, neurochemical, and behavioral studies. During designing the analog and digital devices as well as the software, the basic requirement was to develop a modular system flexibly adaptable to future demands (Fig. 1).

The preamplifier, constructed in our laboratory by utilizing the experiences of a previously used device [Yamamoto et al., 1985], produces 10 times amplification in bandwidth from 1 Hz to 20 kHz. Its input impedance is more than 30 MΩ and the signal-to-noise ratio is better than 20 dB (for 0.2 mV nominal input sensitivity). On the one hand, it has an automatic capacity-compensation circuit to balance the relatively high "parasite" capacity of the carbon fiber electrode. On the other hand, the preamplifier is equipped with a built-in impedance meter for in-vivo measurement of the electrode's impedance (in ranges of 0-1 MΩ and 0-10 MΩ), and for elective checking the intactness of the electrode-tip.

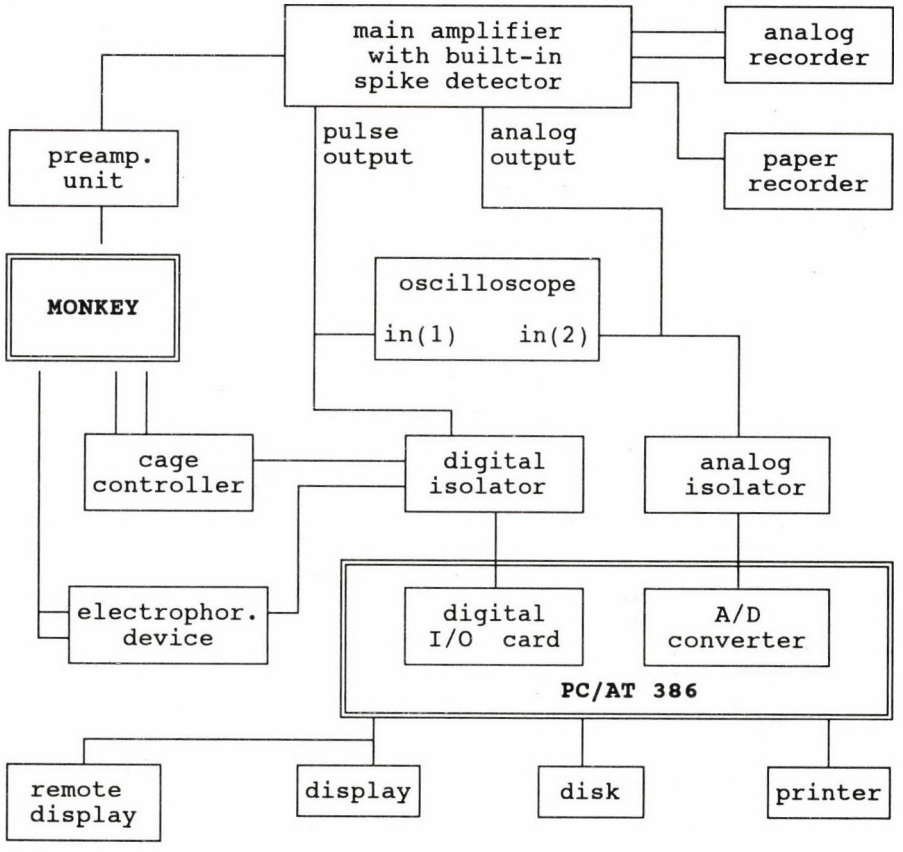

Fig. 1: Block-scheme of the computer controlled neuro-physiological experimental set-up (detailed explanation see in the text).

The output of the preamplifier is connected to the main amplifier. The action potentials are transformed to uniform pulses with amplitude-triggering to produce peri-event time histograms or raster diagrams. Data analysis, while recording, is done in real-time mode, but off-line analysis is also possible later by using analog signals stored on magnetic tape. The analog signals can be observed on oscilloscope, and data sampling are available with an A/D converter. The other channel of the oscilloscope shows phase-fitted output impulses of the comparator (included in the main amplifier) occuring together with the action potentials.

The industrial standard computer (Type: PC/AT 386) possesses all usual peripheries for archiving, monitoring and printing. It has an additional remote display close to the animal to show the actual parameters to the experimenter. To eliminate noises, as well as to protect the computer, it is interconnected with the special measuring and controlling devices of the experimental environment through optically coupled isolator units (constructed in our laboratory).

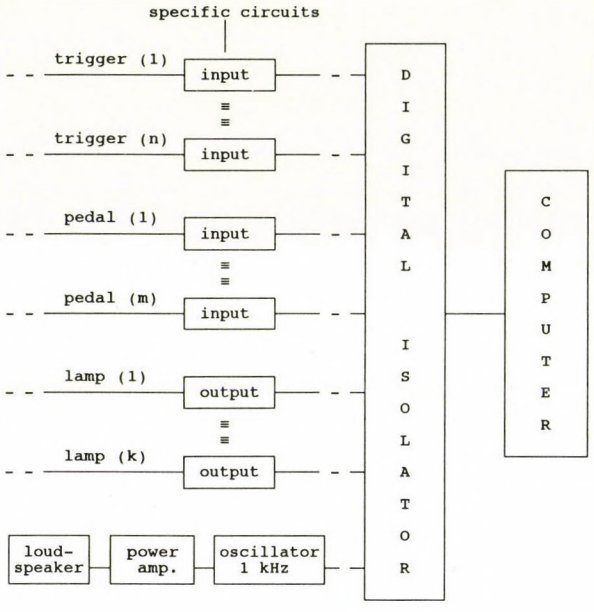

Fig. 2: Functional block-scheme of the cage controller (detailed explanation see in the text).

The behavioral module is directed with a multi-functional digital data-collector and control device (cage controller, designed in our laboratory) which keeps close contact with the monkey and handles the trigger events signalled by the experimenter. (Functioning of the electrophoretic instrument also belongs to trigger activities).

The block-scheme of the cage controller is seen in Figure 2. Output devices of the behavioral module have to suit the natural endowments of the monkey (lamps [red, green and yellow], 3 cm in diam. and a loudspeaker). The input devices are robust pedals located close to the hands of the animal.

Since the experimenter can reach interactive decisions during the whole behavioral process, the cage controller may handle a few manual switches to generate trigger events

for the program running on the computer. Special behavioral activities or characteristic time periods can also be labelled by the help of these switches. For the moment, there have been utilized three trigger buttons, two pedals, three lamps, and a loudspeaker.

This equipment can communicate with the digital isolator unit of the computer on standard TTL signal level. Due to the modular design of the equipment, the type and number of the active peripheral circuits can be changed easily according to the actual requirements of a new experimental paradigm.

The main amplifier (Figure 3.), designed to meet special requirements, was also developed in our laboratory. The input signal - or the calibrator's signal - is fed to the gain selector amplifier. The gain selector gives amplification from 500 to 10,000 in 5 steps. The output voltage is led to the variable cut-off frequency high-pass (1 Hz - 300 Hz in 6 steps) and low-pass (500 Hz - 10 kHz in 6 steps) filters. The usage of the notch-filter (tuned to the mains' frequency) is optional.

For simultaneous recording of original analog signal, and for off-line playback analyses, a tape recorder interface is also included in our main amplifier.

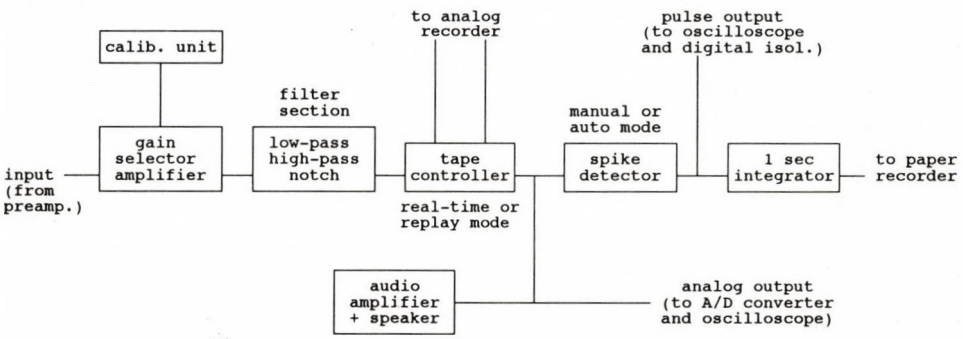

Fig. 3: Functional scheme and structural elements of the main amplifier (detailed explanation see in the text).

The output signal of the tape controller is coupled to the spike detector, which is an automatic window-discriminator with adaptive parameters (depending on the actual parameters of the spikes).

The impulses act as input signals to the integrator (part of the original set-up) to control the paper recorder; they are also registered through a digital port-bit of the computer. To support an easy and powerful experimental environment, an audio amplifier and a built-in speaker are implemented in the main amplifier.

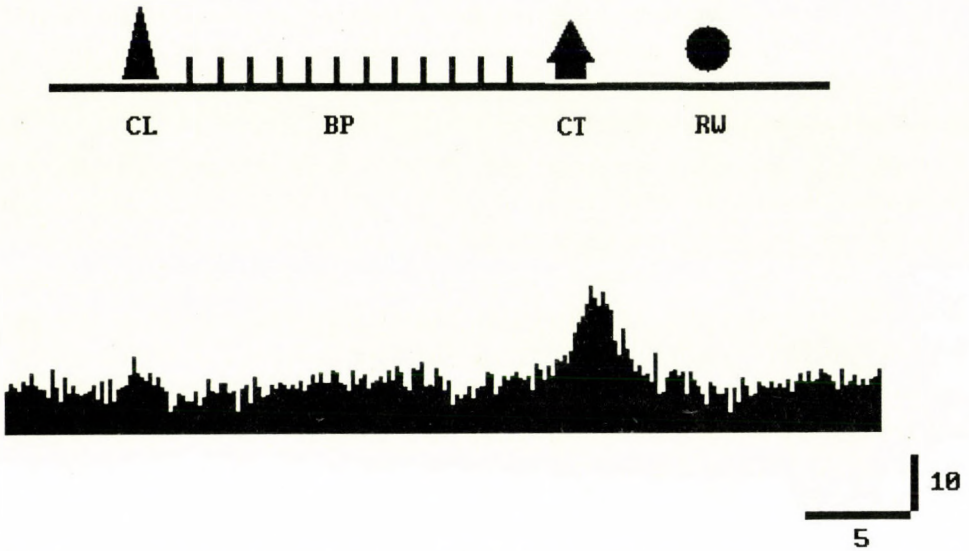

Fig. 4: The phases and neuronal correlates of the conditioned bar-press task. Upper section: The individual phases of the task. CL, conditioned light stimulus (cue-light); BP, bar presses in a fixed ratio; CT, conditioned acoustic stimulus (cue-tone); RW, reward period. Lower section: Peri-event time histogram of a neuron's activity recorded from the hypothalamic "hunger center". Time-scale is identical with that in the upper section. Facilitation of the neuron at the CT. Calibration: time in sec and activity in spike/sec, respectively.

The sequences of a conditioned behavioral response are demonstrated in Figure 4. The conditional (cue) light-stimulus indicates that the monkey can start repeated bar-presses and the cue tone presented after the successful completion of bar-pressing signals the availability of the food reward. The activity of the examined lateral hypothalamic neuron is shown, in the same time-scale, under the scheme of phases of the conditioned feeding task.

Figure 5. demonstrates the responses of another limbic neuron (belonging to the hypothalamic "hunger center") during direct microelectrophoretic application of various neurochemicals (above), and during gustatory stimulation (below). The effects of electrophoretically applied drugs (excitation to glutamate and dopamine and inhibition to noradrenaline) as well as the neuronal responses to taste stimuli (facilitation to glucose and orange juice and inhibition to sodium chloride) are all clearly demonstrated.

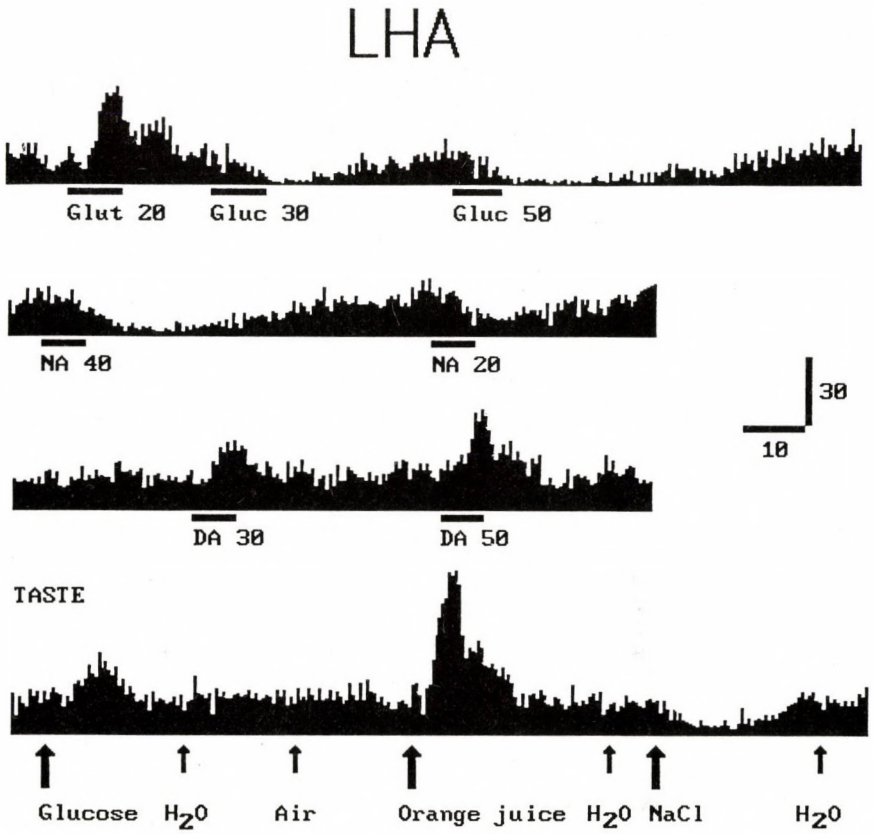

Fig. 5: Activity changes of a lateral hypothalamic neuron in response to microelectrophoretic application of chemicals and to oral taste stimulation. The three upper traces show the effect of the electrophoresis while the lower one demonstrates the results of the gustatory stimulation. Glut, glutamate; Gluc, glucose; NA, noradrenaline; DA, dopamine. Horizontal bars: duration of microelectrophoretic applications. Numbers: electrophoretic current intensities in nA. Arrows: onsets of taste stimulations. Calibration: 10 sec and 30 spike/sec, respectively. Upper traces: excitation to Glut and DA, inhibition to Gluc and NA. Lower trace: facilitation to Glucose and Orange juice, inhibition to NaCl. Rinse (H_2O) or air puff (Air) did not modify neuronal activity.

The controlling and data-collecting tasks are unified in a universal software package. Its menu system offers easy-to-use operation and simple adjustments. In individual functions, the actual experimental parameters can be set without difficulty, the possible behavioral sequence can be easily specified, and the desirable program variations can also be indicated during the trigger activities. The system can optionally

operate in real-time analysis, printing (results) and storing (data, on floppy disk) modes, while it is usable for off-line analysis and for printing the data stored on magnetic tapes and disks. Random starting function is also available in behavioral experiments to avoid habituation problems.

DISCUSSION

We performed specific electrophysiological, neurochemical, and behavioral studies separately in our previous series of investigations. The question was necessarily raised, however, whether we could combine our methods in the same experimental session. This paper reports the technical background of our complex neurophysiological, behavioral, and neurochemical experiments.

Previous findings demonstrated several basic characteristics of limbic neurons in the regulation of hunger- and thirst-motivated behaviors [Lénárd et al., 1986, 1989; Nakano et al., 1987; Nishino et al., 1988; Karádi et al., 1989a, 1989b], computed separately [Rolls et al., 1984]. Our recent investigations opened a new approach to combine the analysis of these individual factors in a complex, still easy-to-perform paradigm.

CONCLUSIONS

The present set-up provides proper technical background to answer several specific neurophysiological questions. Nevertheless, this multipurpose experimental system offers a natural opportunity to study the various mechanisms in complex paradigms with combined approaches. Our system proved to be adequate: 1) to investigate electrophysiological, neurochemical, and behavioral aspects of the central nervous system regulation of feeding as well as 2) to control complicated behavioral experiments with monkeys. We achieved a fully automatic data collection procedure, and performed real-time and off-line analyses of data.

The aim of our future studies is to elucidate further details of the complex attributes of individual neurons as well as to investigate interconnections and communication among neighbouring groups of neurons of the limbic system. The exact analysis of signal parameters is a basic requirement to fulfil this task with the help of an A/D converter already implemented but not fully utilized in our system. Archived data of the present experiments will also be used in our future work with this system.

ACKNOWLEDGEMENTS

This work was supported by the Hungarian National Research Fund (OTKA/1404; L. Lénárd) and the Ministry of People's Welfare of Hungary (ETT T-565/1990; L. Lénárd).

The authors are grateful to Dr. L. Kellényi for his valuable advices.

REFERENCES

Aou, S., Oomura, Y., Lénárd, L., Nishino, H., Inokuchi, A., Minami, T. and Misaki, H. (1984) Behavioral significance of monkey hypothalamic glucose-sensitive neurons. Brain Res. 302, 69-74.

Karádi, Z., Nishino, H., Oomura, Y., Scott, T.R. and Aou, S. (1990a) A method for gustatory stimulus delivery in awake rhesus monkeys. Brain Res. Bull. 25, 665-668.

Karádi, Z., Oomura, Y., Nishino, H. and Aou S. (1989a) Olfactory coding in the monkey lateral hypothalamus: Behavioral and neurochemical properties of odor-responding neurons. Physiology & Behavior 45, 1249-1257.

Karádi, Z., Oomura, Y., Nishino, H., Scott, T.R., Lénárd, L. and Aou, S. (1989b) Lateral hypothalamic and amygdaloid neuronal responses to chemical stimuli in the rhesus monkey. In: Proceedings of 22nd Jap. Symp. on Taste and Smell (ed. Morita, H.) pp. 121-124. JSTS, Asahi University Press, Gifu, Japan.

Karádi, Z., Oomura, Y., Nishino, H., Scott, T.R., Lénárd, L. and Aou S. (1990b) Complex attributes of lateral hypothalamic neurons in the regulation of feeding of alert rhesus monkeys. Brain Res. Bull. 25, 933-939.

Lénárd, L., Jandó, G., Faludi, B., Simon, M., Czurkó, A. and Karádi, Z. (1990) Recovery from amygdalar sensory neglect after foetal neuronal grafting: Single unit activity and drug responses in the transplanted area. Restorative Neurol. and Neurosci. 1 (2), 144.

Lénárd, L., Jandó, G., Karádi, Z., Hajnal, A. and Sándor, P. (1988) Lateral hypothalamic feeding mechanisms: Iontophoretic effects of kainic acid, ibotenic acid and 6-Hydroxydopamine. Brain Res. Bull. 20, 847-856.

Lénárd, L., Oomura, Y., Nakano, Y., Aou, S. and Nishino, H. (1989) Influence of acetylcholine on neural activity of monkey amygdala during bar press feeding behavior. Brain Res. 500, 359-368.

Lénárd, L., Oomura, Y., Nishino, H., Aou, S., Nakano, Y. and Yamamoto, T. (1986) Activity in monkey lateral hypothalamus during operant feeding: Modulation by catecholamines and opiate. In: Emotions: Neuronal and Chemical Control (ed. Oomura, Y.) pp. 45-53. Japan Sci. Soc. Press, S. Karger, AG, Tokyo and Basel.

Lénárd, L., Sándor, P., Hajnal, A., Jandó, G., Karádi, Z. and Kai, Y. (1991) Sex-dependent body weight changes after iontophoretic application of kainic acid into the LH or VMH. Brain Res. Bull. 26 (1), 141-148.

Nakano, Y., Lénárd, L., Oomura, Y., Nishino, H., Aou, S. and Yamamoto, T. (1987) Functional involvement of catecholamines in reward-related neuronal activity of monkey amygdala. J. Neurophysiol. 57 (1), 72-91.

Niedetzky, Cs., Jandó, G. and Lénárd, L. (1987) Computer analysis of single neuron activity and the multibarrel iontophoretic technique (in Hungarian). In: Proceedings of the 2nd Annual Meeting of the National Society of Medical Informatics (eds. Szilasi, A. and Cserveny, A.) pp. 432-434. PFV Press, Pécs.

Nishino, H., Oomura, Y., Karádi, Z., Aou, S., Lénárd, L., Kai, Y., Fukuda, A., Ito, C., Min, B.I. and Salaman, C.P. (1988) Internal and external information processing by lateral hypothalamic glucose-sensitive and insensitive neurons during bar press feeding in the monkey. Brain Res. Bull. 20, 839-845.

Rolls, E.T., Thorpe, S.J., Boytim, M., Szabó, I. and Perrett, D.I. (1984) Responses of Striatal Neurons in the Behaving Monkey. 3. Effects of Iontophoretically Applied Dopamine on Normal Responsiveness. Neurosci. 12 (4), 1201-1212.

Yamamoto, T., Oomura, Y., Nishino, H., Aou, S. and Nakano, Y. (1985) Driven shield for multi-barrel electrode. Brain Res. Bull. 14, 103-104.

Received 8 January 1993
Accepted 13 April 1993

ABSTRACTS

from the Annual Meeting of the Neuroscience Section
of Hungarian Physiological Society
Veszprém, January 21-23, 1993

Neurobiology 1 (2), p. 159, 1993

CAPSAICIN-INDUCED VASCULAR CHANGES IN THE RAT NASAL MUCOSA: ANTAGONISM BY RUTHENIUM RED

Bari, F. and Jancsó, G.

Department of Physiology, Albert Szent-Györgyi Medical University, Szeged, Hungary

The involvement of capsaicin-sensitive afferent nerves in circulatory and inflammatory reactions is well established. The aim of the present study was to further characterize the capsaicin-evoked vascular responses in the rat nasal mucosa. Wistar rats weighing 280-350 g were used in these experiments. The animals were anaesthetized with sodium pentobarbitone and catheters were inserted into the femoral artery for measurement of systemic blood pressure, and into the superior thyroid artery and into the femoral vein for close arterial and intravenous injections, respectively. Nasal mucosal blood flow was measured by means of a laser-Doppler flowmeter, with a probe in contact with the nasal septum. The technique of vascular labelling was used to detect a possible increase in vascular permeability.

Close arterial infusion of capsaicin (20-100 pmol/min) caused a dose-dependent increase in nasal blood flow. A profound vascular labelling of small mucosal blood vessels indicating a significant enhancement of vascular permeability was also demonstrated histologically. The close intraarterial infusion of ruthenium red (**RR**, 2.5-10 μmol) significantly inhibited the capsaicin-evoked vasodilatatory response. Similarly, the vascular labelling was strongly diminished after the administration of **RR**.

It is suggested that neuropeptides released from trigeminal sensory nerve endings play an important role in the local vascular and inflammatory reactions of the nasal mucosa. In addition, the results show a marked antagonism by **RR** of the vascular effects of capsaicin under in vivo conditions. The experimental approach utilized in this study provides a promising possibility for elucidation the significance of capsaicin-sensitive afferent nerves in the mechanism of allergic and/or inflammatory diseases affecting the nasal mucosa.

Akadémiai Kiadó, Budapest

Neurobiology 1 (2), p. 160, 1993

THE CYTODIFFERENTIATION OF INTERSTITIAL CELLS ASSOCIATED WITH THE MYENTRIC PLEXUS OF CHICK SMALL INTESTINE

Boros, A. and Fekete, É.

Department of Zoology, József Attila University,
H-6722 Szeged, Egyetem u. 2., P.O. Box 659, Hungary

The cytodifferentiation of the interstitial cells associated with the Auerbach's plexus of the chick small intestine was studied by electron microscopy. Samples were taken from embryos ranging in age from 7 days to 21 days. The early appearance and rapid differentiation of interstitial cells was observed. The first type of interstitial cells, with fibroblast-like features, emerged on E11 and formed a capsule around the myenteric ganglia. The capsula developed progressively till hatching however on E18 the previously strictly isolated ganglia got in directe contact with invader musce elements or with their processes. These transient nerve-muscle contacts disappeared after hatching. The second group of interstitial cells appeared on E16, adjacent to the myenteric ganglia or among the smooth muscle cells. These irregular or elongated cells were identified as the first type of interstitial cells of Cajal. They established close contacts with muscle cells and also with nerve elements. Gap junctions were observed between the adjacent interstitial cells of Cajal. The third type of interstitial cells, with an intermediate form, appeared on E18.

The fibroblast-like cells probably participate in the blood-ganglion barrier, while the second group of interstitial cells might have a function in the impulse- generating and conducting system of slow waves. The transient nerve-muscle contacts are permissive of supplying the differentiating ganglia with muscle derved neuroeffective substances.

Akadémiai Kiadó, Budapest

Neurobiology 1 (2), pp. 161-162, 1993

CORRELATIONS BETWEEN CALCITONIN GENE-RELATED PEPTIDE AND THE ACETYLCHOLINE RECEPTOR

Csillik, B., Knyihár-Csillik, E. and *Rakic, P.

Department of Anatomy, Albert Szent-Györgyi University Medical School, H-6701 Szeged, P.O. Box 512, Hungary and *Section of Neurobiology, Yale University, School of Medicine, Conn. 06510, P.O. Box 3333, New Haven, USA

It has been discovered by New and Mudge (1986) that calcitonin gene-related peptide (CGRP) increased expression of the alpha subunit of the acetylcholine receptor (AChR) in tissue cultures of myotubes. Studies from Changeux's laboratory (Fonatine et al., 1986; Kirilovsky et al., 1989, etc.) suggested that this regulation, characterizing the motoneuronal unit (Deiters' motor nerve cells in the spinal cord and their axon terminals in the striated muscle) is realized by activating the formation of pre-mRNA responsible for expression of the AChR. In earlier studies (Csillik et al., 1991, 1992; Knyihár-Csillik et al., 1991) we have proved that, in register with the observations of several Japanese authors, CGRP can be demonstrated by means of immuno-histochemical techniques in the flexor digitorum brevis muscle of the rat. We have also shown that under normal conditions, CGRP is present in the inter- and perivascular area within the motor axon terminal and, that, after supramaximal electrical stimulation of the sciatic nerve, many of the numerous motor end plates of the flexor digitorum muscle, show signs of peptide evacuation, resulting in hardly visible "ghosts" that, under the electron microscope, proved to be motor end plates from which CGRP has been depleted. Accordingly, CGRP appears to play a major role in the cholinergic transmission mechanism.

In contrast, however, Boj et al. (1989), Caratsch and Eusebi (1990) and other authors raised serious doubts as to the role of CGRP in the process of cholinergic transmission, since CGRP was absent from most of the skeletal striated muscles of the rat, including the diaphragm which is routinely used as a model of cholinergic transmission in the shape of phrenicus-hemidiaphragm preparations.

Therefore, we decided to study (1) the precise distribution of CGRP in motor end plates in a variety of skeletal and visceral striated muscles of the rat and in those of the frod and (2) to decide whether or not, CGRP can be elicited and visualized in motor end plates that, under normal conditions, do not display any CGRP reactivity.

In this paper, we have presented unequivocal evidence as to the fact that (1) CGRP can be elicited from all the apparently "non-reactive" end plates, either by inducing experimental degeneration, followed by the regular regenerative process (2) or by inducing transmission blockade in the neuromuscular junction by means of local application of long-lasting local anesthetics like Marcain or Bupivacain. It has been shown, furthermore, that CGRP-active axons surround and establish synapses with cholinergic nerve cells of basal forebrain nuclei, including those constituting Meynert's Basal Nuclei.

It is concluded that (1) the theory concerning the participation of CGRP in the expression and maintenance of the alpha subunit of the nicotinic acetylcholine receptor is supported by the presence of CGRP in all the motor end plates of the rat and (2) the possibility cannot be excluded that CGRP plays some role also in the function of the muscarinic AChR. Practical (therapeutical) consequences of these discoveries constitute an important challange for clinical studies.

Akadémiai Kiadó, Budapest

References

Boj, S., Goldstein, M., Fischer-Colbrie, R., Dahlström, A.: Neuroscience 30: 479-501. 1989
Caratsch, C. G., Eusebi, F.: Neurosci. Lett. 111: 344-350. 1990
Changeux, J-P., Duclert, A., Sekine, S.: in: "*Calcitonin Gene-Related Peptide. The first Decade of a Novel Pleiotrophic Neuropeptide*". Y. Tache, P. Holzer, M. Geoff Rosenfeld (eds.). Annals of the New York Academy of Sciences Vol: 657: pp. 361-378. 1992
Csillik, B., Knyihár-Csillik, E., Kreutzberg, G. W., Tajti, L., Keresztúri, A.: Regul. Pept. 34: 114. 1991
Csillik, B., Knyihár-Csillik, E., Kreutzberg, G. W., Tajti, L., Keresztúri, A., Kovács, T.: in "*Calcitonin Gene-Related Peptide. The first Decade of a Novel Pleiotrophic Neuropeptide*". Y. Tache, P. Holzer, M. Geoff Rosenfeld (eds.). Annals of the New York Academy of Sciences Vol: 657: pp. 466-468. 1992
Csillik, B., Knyihár-Csillik, E., Tajti, L., Pór, I.: Eur. J. Neurosci. Suppl. 4: p127. 1991
Fontaine, B., Klarsfeld, A., Hökfelt, T., Changeux, J-P.: Neurosci. Lett. 71: 59-65. 1986
Kirilovsky, J., Duclert, A., Fontaine, B., Devillers-Thiery, A., Osterlund, M., Changeux, J-P.: Neuroscience 32: 289-296. 1989
Knyihár-Csillik, E., Tajti, L., Pór, I., Csillik, B.: Anat. Anz. Erg. 172: 319. 1991
New, H. V., Mudge, A. W.: Nature 323: 809-811. 1986

Neurobiology 1 (2), p. 163, 1993

MONOAMINE CONTENT OF THE REGENERATING NERVOUS SYSTEM IN EARTHWORM *(LUMBRICUS TERRESTRIS L.)*

[1]Csoknya, M., [2]Hiripi, L., [3]Szelier, M., [3]Lengvári, I., [2]Juhos, Sz., [2]Elekes, K. and [1]Hámori, J.

[1]Department of Zoology, Janus Pannonius University, Pécs; [2]Limnological Research Institute, Tihany and [3]Department of Anatomy, University Medical School, Pécs, Hungary

Either anterior or posterior 4-6 segments of adult earthworms (*Lumbricus terrestris L.*) were removed and allowed to regenerate at 4° C for 3, 17, or 20 days. At the end of the regeneration period parts of the nervous system (i.e. cerebral ganglion, subpharyngeal ganglion, ventral cord ganglia both in front or behind the clitellum) were dissected out and their serotonin and dopamine contents were assayed by high performance liquid chromatography.

Three days after removal of the cerebral ganglion both serotonin and dopamine levels were reduced in all parts of the nervous system compared to non operated controls. 17 days after the intervention, however, the contents of both amines were significantly higher in every ganglia studied than in intact controls. On the 20th day of regeneration dopamine contents were close to the normal, while serotonin contents were significantly higher in the regenerating cerebral, and subesophageal, as well as in the ventral cord ganglia. It is supposed that these amines play some regulative role during regeneration.

Akadémiai Kiadó, Budapest

Neurobiology 1 (2), p. 164, 1993

A WHOLE-CELL PATCH-CLAMP STUDY OF HYPOXIC SPREADING DEPRESSION

Czéh, G. and Somjen, G.G.

Institute of Physiology, University Medical School of Pécs, H-7643 Pécs, Szigeti u. 12 and Duke University Medical Center , Durham NC 27710

In rat hippocampal slices we recorded membrane current of patch-clamped CA1 pyramidal cells in whole-cell configuration and the extracellular potential in the pyramidal cell body layer. Strong inward membrane current was found during the 3-5 min of hypoxia. Time course of the current coincided with that of the typical sudden large negative field potential known to indicate occurrence of spreading depression (SD) due to hypoxia. Reoxygenation started at the peak of SD. Membrane conductance, steady (holding) current, and ramp command evoked currents were measured during the prodromal phase, at the peak of SD and during the first 5-20 min of reoxygenation. The I/V curves of ramp command evoked responses changed indicating a slight decrease of membrane slope resistance during the prodromal phase, then about 70% drop during SD followed by gradual recovery with reoxygenation. Shifts of the I/V curves suggested considerable changes of reversal potential of the current. These changes could not by modified by variation of the holding potantial within the -130 to + 35 mV range. However, clamping the membrane potential at about +30mV reversed the polarity from inward to outward of the steady current during SD. Nonlinear properties of the membrane were lost during the SD but varied in a complicated way during the prodromal phase and early reoxygenation. Analysis of the components of the presumably mixed currents affected by hypoxic insults is incomplete but suggests contribution of conductances not sensitive to membrane potential.

Akadémiai Kiadó, Budapest

Neurobiology 1 (2), p. 165, 1993

THERMODYNAMICAL ANALYSIS OF THE LIGAND BINDING TO OPIOID RECEPTORS IN RAT BRAIN MEMBRANES

Fábián, G., Benyhe, S., Szűcs, M.

Institute of Biochemistry, Biological Research Center
of the Hungarian Academy of Sciences, 6701 Szeged, P.O. Box 521, Hungary

Opioids induce a wide range of physiological responses by interacting with multiple opioid receptors (μ, δ, κ) in the CNS. In the present work we have investigated the binding properties (K_D, B_{max}) of subtype selective agonist and antagonist ligands by means of homologous displacement experiments at different temperatures. From the K_D values obtained with the nonlinear regression curve fitting computer program "LIGAND", the thermodynamic parameters (Gibb's free energy: $\Delta G°$, standard enthalpy: $\Delta H°$ and entropy: $\Delta S°$) of the receptor-ligand interaction were calculated. The binding characteristics of opioid agonists with different receptor subtype selectivity (μ versus δ) as well as with similar selectivity but different chemical structure (peptide versus alkaloid) were studied and compared with that of an antagonist. It was found that the binding of the opiate antagonist naloxone is an exotherm reaction, driven by enthalpy decrease. Similar thermodynamical changes, namely, positive enthalpy and entropy changes were detected for both the δ agonist, [^{3}H]deltorphine and μ agonists, such as [^{3}H]dihydromorphine and [^{3}H]DAGO. Moreover, we found the same alterations of the binding energetics for the alkaloid μ agonist, [^{3}H]-dihydromorphine and the peptide μ agonist, [^{3}H]-DAGO, although the first one has a rigid, while the second one has a much more flexible conformation.

We postulate from these studies that one step of the ligand binding to the opioid receptors is probably a hydrophobic interaction, which generates entropy increase in case of any ligand. At another stage of the binding there is a discrimination between agonists and antagonists, which is shown by the opposite directions of the enthalpy changes.

Acknowledgement: This work was supported by a financial grant, OTKA-895 obtained from the Hungarian Academy of Sciences.

Akadémiai Kiadó, Budapest

Neurobiology 1 (2), p. 166, 1993

COMPLEX NEUROCHEMICAL MODULATION OF PALLIDAL SINGLE NEURON ACTIVITY IN THE RAT

Faludi, B., Lénárd, L., Karádi, Z., Czurkó, A., Vida, I. and Hajnal, A.

Pécs University, Medical School, H-7643 Pécs, Hungary

The globus pallidus (GP), a substantial structure of the extrapyramidal motor system, has been demonstrated to be intimately involved in the regulation of various aspects of feeding (body weight regulation, metabolic control, sensory-motor integration, etc.). Despite the large amount of related behavioral and electrophysiological data, our knowledge is insufficient yet about the specific, in particular, feeding-associated neurochemichal properties of GP neurons. In the present experiments, therefore, extracellular single neuron activity of the GP was recorded in anesthetised rats by means of carbon fiber, multibarreled glass microelectrodes during microelectrophoretic administration of various chemicals (acetylcholine /Ach/, dopamine, L-Deprenyl, GABA, glutamate and NMDA). Twenty-one percent of all GP cells tested showed specific firing rate changes to the microelectrophoretically applied glucose. These responses were mainly (17%) inhibitory ones and the neurons suppressed by glucose were assigned as glucose-sensitive (GS) units. In a few cases (4%) excitatory responses were also recorded and these cells, due to the nomenclature in the literature, were designated as glucose-receptor (GR) units. These GS, GR and glucose non-responsive neurons of the GP exhibited distinct sensitivities to Ach, catecholamines, GABA and NMDA applied microelectrophoretically. Our findings demonstrated the existence of glucose-responsive neurons in the GP. These special cells, under complex neurotransmitter modulation, may also belong to a hierarchically organized glucose-monitoring system whose elements have already been found at several levels of the neuraxis. To determine feeding-related characteristics of these glucose-detecting neurons, however, further examinations are required.

Akadémiai Kiadó, Budapest

Neurobiology 1 (2), p. 167, 1993

MORPHOLOGICAL CHARACTERIZATION OF GROWTH, DIFFERENTIATION AND CELL PROLIFERATION IN LONG-TERM SLICE-CULTURES OF THE IMMATURE RAT HIPPOCAMPUS

Gerics, B., Hajós, F., *Baker, R.E. and *Balázs, R.

Department of Anatomy and Histology, University of Veterinary Science, H-1400 Budapest, P.O. Box 2, Hungary and *Netherlands Institute for Brain Research, Meibergdreef 33, 1105 AZ Amsterdam ZO, The Netherlands

Explants of 360 μm thick transverse slices of the 6-day-old rat hippocampus were grown in a serum-free medium for 2 to 14 days. Histology performed after various culturing periods demonstrated that these slices undergo growth and differentiation of the main cellular elements similar that seen in vivo. Histological indications of continuing cell proliferation were verified by autoradiography showing a labelling of neuroblasts scattered throughout the explant. Findings suggest that within the period studied the hippocampal slice cultures mature in a fashion very similar to that seen in situ.

Akadémiai Kiadó, Budapest

Neurobiology 1 (2), p. 168, 1993

FEEDING DISTURBANCES AFTER IBOTENIC ACID MICROLESIONS TO THE PARAVENTRICULAR NUCLEUS OF THE HYPOTHALAMUS IN THE RAT

Hajnal, A., Czurkó, A., *Thornton, S.N., Karádi, Z.,
Sándor, P., *Nicolaidis, S. and Lénárd, L.

Institute of Physiology, Pécs University, Medical School, H-7643 Pécs, Hungary
and *Lab. Neurobiologie des Regulations, College de France, Paris, France

Bilateral electrolytic lesions of the paraventricular nucleus (PVN), destroying both cellular elements and passing fibers, result in hyperphagia and hyperdipsia accompanied with obesity and enhanced diuresis. The aim of our present investigations was to elucidate the feeding-related role of PVN neurons themselves. A cell specific neurotoxin, ibotenic acid (IA), was used to perform unilateral microinjections to elicit behavioral deficits but to spare the hormonal functions of the magnocellular neurons of the PVN. In twelve anesthetized adult male Wistar rats, guide cannulae were implanted over the PVN. After 1 week recovery, 1 ug of IA was injected unilaterally (in 300 nl volume) into the PVN in freely moving conscious rats. Control rats received the same volume of vehicle. In both groups, daily food and fluid intakes were measured as well as fluid and electrolyte excretion were followed for 18 days. Mean body weight of the IA injected rats decreased during the first 4 days following the injection. Thereafter, it increased at a rate faster than that of the vehicle injected animals. The differences were significant from the 1st to the 12th postoperative day (ANOVA, 1st day $p<0.05$, 2nd-12th day $p<0.01$). Food intakes of the lesioned animals, except a slight initial decrease, were essentially identical to those of the control, vehicle injected rats. Water intakes and urine outputs were also insignificantly altered in either group following the injections. The results show that the neuron-specific unilateral lesion of the PVN produces disturbances of the body weight regulation without symptoms of the diabetes insipidus (i.e. without obvious hormonal dysfunction). The body weight changes were not accompanied with alterations of feeding or drinking. It is suggested, therefore, that the lesions primarily affected the metabolism of these animals. The fine details of exact role of the PVN in the control of metabolism remain to be determined yet.

Akadémiai Kiadó, Budapest

Neurobiology 1 (2), p. 169, 1993

STRUCTURAL IMPAIRMENT OF HIPPOCAMPAL NEURONS FOLLOWING A SINGLE EPILEPTIC AFTERDISCHARGE

[1,2]Horváth, Z., [2]Pierre, E., [2]Vadi, D. and [2]Buzsáki, G.

[1]Department of Physiology, Medical School of Pécs and
[2]Center for Molecular and Behavioral Neuroscience, Rutgers University, NJ

A highly sensitive silver-impregnation procedure was used to reveal whether lasting structural changes could be produced by a brief epileptic afterdischarge. A single afterdischarge was induced in rats, implanted with stimulating electrodes in the perforant path or entorhinal cortex and epidural recording electrodes. The animals were perfused 1 to 16 hours after the electrical seizure. Most argyrophilic "dark" neurons were present in the strata radiatum-lucidum, pyramidale and oriens of CA3, followed by strata oriens and pyramidale of CA1 and the hilus. The majority of the affected cells were interneurons. "Dark" cells were present in both hippocampi at all time points examined, whereas no other structure was affected. These findings suggest that even short epileptic epochs are capable of triggering long-lasting cytoskeletal changes in hippocampal neurons. We hypothesize that after repeated epileptic afterdischarges these cytoskeletal changes become irreversible resulting in neuronal loss.

Akadémiai Kiadó, Budapest

Neurobiology 1 (2), p. 170, 1993

FEEDING-ASSOCIATED CHARACTERISTICS OF GLOBUS PALLIDUS NEURONS IN THE RHESUS MONKEY

Karádi, Z., Lénárd, L., Faludi, B., Czurkó, A.,
Vida, I., Sándor, P. and Niedetzky, Cs.

Pécs University, Medical School, H-7643 Pécs, Hungary

The globus pallidus (GP) plays important roles in various processes (body weight regulation, metabolic control, sensorimotor-perceptual-motivational integration, etc.) of the hunger- and thirst-motivated behaviors. Despite the abundance of relevant data in the literature, little is known yet about functions of pallidal neurons in these regulatory mechanisms. To reveal specific behavioral and neurochemical attributes of GP cells and to provide their complex functional characterization, in the present experiments extracellular single neuron activity was recorded in the GP of alert primates by means of carbon fiber multibarreled glass microelectrodes during: 1) spontaneous or elicited behavioral actions, 2) a conditioned, high fixed-ratio bar press alimentary task, 3) microelectrophoretic administration of chemicals and 4) gustatory stimulation. Many of the pallidal neurons changed in firing rate in response to perioral somesthetic stimulation, and a subset of them exhibited differential responses to food or non-food objects presented to the animals. The majority of GP cells showed activity changes during at least one of the four phases (cue light, bar press, cue tone and food reward) of the conditioned task. About 5% of all pallidal neurons tested responded to (usually two or more) gustatory stimuli. Task-related and taste-responsive cells were predominantly found among the so called glucose-sensitive (GS) units (representing approximately 8% of all GP neurons tested) whose activity was specifically suppressed by electrophoretically applied glucose. These GS and the glucose-insensitive cells displayed distinct sensitivities to microelectrophoretically administered acetylcholine, catecholamines and GABA as well. These data, along with previous observations, suggest the existence of glucose-detecting neurons, as parts of a hierarchically organized glucose-monitoring system, in the GP. Furthermore, our findings also indicate that these and other pallidal cells are intimately involved in integration of feeding-associated sensory-motor and perceptual signals with internal and external chemosensory information.

Akadémiai Kiadó, Budapest

Neurobiology 1 (2), p. 171, 1993

INTRACORTICAL GENERATOR OF THE MISMATCH NEGATIVITY IN THE CAT

Karmos, G., Molnár, M., Csépe, V., Ulbert, I. and Winkler, I.

Institute for Psychology of the Hungarian Academy of Sciences, Budapest

A characteristic negative deflection, called mismatch negativity (MMN) is elicited in human auditory evoked potentials when infrequent physically deviant stimuli are presented in a sequence of repetitive standard stimuli (Näätänen 1991). MMN reflects an early automatic phase of information processing. Source localization data indicate that MMN is generated in the auditory cortex. We identified a negative deflection in the middle latency auditory evoked potentials of cats which proved to be an equivalent of the human MMN (Csépe et al. 1987). The aim of the present experiments was to study the intracortical processes responsible for the MMN. Intracortical field potentials and multiple unit activity (MUA) evoked by short duration tone bursts were recorded by chronically implanted multielectrodes from the auditory cortex of behaving cats. Current source density (CSD) analysis was applied to localize the sinks and sources.

In a frequency MMN paradigm standard stimuli of 4 kHz frequency and 1 ms duration and deviants of 3 kHz frequency (5-10 % probability) were delivered to the animals. The MMN to deviant stimuli appeared as a negative deflection in the 40-80 ms latency range of the evoked potentials recorded from the surface of the auditory cortex. Simultaneously, the amplitude of the local positive component in the middle layers decreased. The CSD analysis indicated a decrease of the amplitude and area of the middle layer source following the early activation pattern when compared to the responses elicited by standard stimuli. Suppression of the MUA appeared to standard stimuli in the same latency range whereas this suppression was missing from the evoked potentials to deviants. The data suggest that the MMN may be generated by a disinhibitory process in the middle layers of the auditory cortex.

References:

Csépe, V., Karmos, G., Molnár, M.: Evoked potential correlates of stimulus deviance during wakefulness and sleep in cat - animal model of mismatch negativity. Electroenceph. clin. Neurophysiol., 1987, 66: 571-578.

Näätänen, R.: Mismatch and processing negativities in auditory stimulus processing and selection. Behavioral and Brain Sciences, 1991 14: 764-768.

Akadémiai Kiadó, Budapest

Neurobiology 1 (2), p. 172, 1993

IN VITRO CALRETININ EXPRESSION IN CHICK EMBRYO DRG NEURON

Király, E. and *Celio, M.

Department of Anatomy, Albert Szent-Györgyi Medical University and *Institute of Histology and General Embryology, University of Friburg, Switzerland

The calcium-binding protein, Calretinin (CR) is assumed to be characteristic for the avian sensory system during development and after hatching. To determine whether the expression of this protein is maintained *in vitro* and influenced by the developmental stages of ganglia dissociated DRG cell cultures were performed from chick embryo at E6 or E10 (before and after establishment of functional connections with the target).

Methods. Lumbar DRG were dissected from chick embryo at E6 or E10 and collected in PBS-CMF solution. After trypsinization the ganglia were washed in F14 medium and it was followed by gentle dissociation into single cells. The cell suspension was plated immediately (E6) or after 2 hours preplating on 35 mm Petri dishes in 2 ml medium containing 60-80 000 cells/dish. For detection of CR immunoreaction cultures were fixed at different time periods (1, 3, 5 or 7 days) with a standard fixative and incubated in 1:10 000 polyclonal anti-calretinin antiserum for 12 hours and processed according to the ABC method.
For quantitative analysis the total number of cultured ganglion cells were counted and the number of CR immunoreactive cells were calculated by determining the percentage of immunostained neurons.

Results. Cultured ganglion cells from E6 old chicken showed small-sized ovoid cell bodies. These immature neurons were intermingled with dark spindle shaped non-neuronal cells and flattened fibroblasts. In all the E6 cultures the DRG cells were devoid of any CR immunostaining even after seven days in culture. Ganglion cells for culture from E10 old chicken showed a different pattern. They elaborate an extensive network upon the non-neuronal elements and some of them displayed CR positivity. The precipitate outlined the cell bodies and the long processes in a Golgi-like manner. With time (after 3 days) the number of positive cells increased then it declined similarly to the total cell number.

Conclusions. In the light of the present results we suppose that:
1. Dorsal root ganglion neurons in chicken embryo display CR positivity under *in vitro* condition in the same developmental period as *in vivo* (E10).
2. The sensory neurons express CR immunoreactivity only after they have made contact with their targets.

Akadémiai Kiadó, Budapest

Neurobiology 1 (2), p. 173, 1993

DISTRIBUTION OF CALCITONIN GENE-RELATED PEPTIDE-CONTAINING NEURONS IN THE CENTRAL NERVOUS SYSTEM OF THE MOUSE

Kovács, T., Csillik, B., Knyihár, E. and K. Szabó, B.

Department of Anatomy, Albert Szent-Györgyi Medical University, Szeged

Alternative splicing of the calcitonin gene results in a 37 amino acid containing peptide, CGRP, which plays an important role in basic functions of the nervous system including nociception, cholinergic transmission and behavioral reactions. The morphlogical substance of these functions is clear in the case of the rat, but it is not so clear in the mouse, though this species is the main object for pharmacological and pathophysiological experiments.

The aim of our investigations was to describe CGRP-containing neurons in the mouse CNS by means of immunocytochemistry.

Animals were perfused with Zamboni's fixative; after removal of the brain *in toto* serial frozen sections were subjected to immunocytochemistry performed according to Sternberger's PAP-method using Amersham's anti-rabbit policlonal antibody against CGRP (1:2000).

According to our investigations CGRP-containing neurons can be divided into two major types. Neurons of the first type (e.g. motoneurons, cells of the mediodorsal thalamic nucleus) contain granular reaction product, while in the rest of the CGRP-positive nerve cells diffuse staining prevails.

In the brainstem, most of the cranial nuclei show strong immunoreactivity similar to Deiter's motoneurons in the spinal cord. The subcortical auditory relay stations, like the superior olivary nucleus and the ventral and dorsal cochlear nuclei contain CGRP. Around the superior cerebellar peduncle, the parabrachial nuclear complex including the medial, the lateral and Kölliker-Fuse's subnuclei shows heavy labelling.

In the diencephalon, the anterior hypothalamic area and the lateral geniculate body contain a few labelled neurons, while the peripeduncular area consists of a great amount of extensively arborizing neurons. The posterobasilar part of the ventral thalamic nucleus contains elongated cells. Beneath the stria medullaris thalami, there are several weekly immunoreactive nerve cells containing granular reaction product, which is located under the cell membrane of the neuron.

The mouse olfactory bulb contains CGRP-positive neurons in the mitral and external plexiform layer which are similar to Purkinje's-cells with a "berried" arborization tree i.e. the extensively branching dendritic arborization is equipped with numerous dendritic expansions. The presence of CGRP in the olfactory bulb suggest that CGRP may be the dopaminergic differentiation signal for the olfactory neurons also *in vivo*.

Our results are in good correlation with previous observations; however CGRP-containing cells in the olfactory bulb and in the mediodorsal thalamic nucleus were first described by us.

These data would be useful for further experiments in the future to study CGRP's functions in the CNS.

Akadémiai Kiadó, Budapest

Neurobi. 'ogy 1 (2), p. 174, 1993

THE GN-RH SYSTEM IN *XENOPUS LAEVIS* AND *RANA ESCULENTA*

Kozicz, T., Sétáló, G. and Lázár, Gy.

Departent of Anatomy, University Medical School, Pécs, Hungary

Sexually inactive male and female colchine treated frogs were studied from both species. Histological processing of the brains included fixation in Zamboni fixative, Polywax embedding, incubation of 20 μm thick sections in a 1:30000 dilution of anti LHRH serum and Ni-DAB intensification.

In *Xenopus* a well developed GN-RH system was found. A few LHRH immunoreactive (ir) fibres were detected in the olfactory bulb, which could be followed along the medio-ventral surface of the telencephalon to the medial septum and the diagonal band of Broca. In this latter structure LHRH-ir fibres form a dense network. Immunostained fibres proceeded from here to the preoptic area, where they formed again a network in its lateral part. The rest of the preoptic area was occupied by scattered fibres. A few fibres enter the optic tract and nerve, and a well-defined bundle of fibres ran caudalward close to the lateral surface of the infundibulum. Several fibres crossed the midline in the median eminence. In addition, thin, varicose LHRH-ir fibres were sparsely distributed in the diencephalon with an accumulation in the habenular region. Many of them reached the surface of the brain. Ir fibres were also found in the optic tectum, mesencephalic tegmentum, and in the periventricular region in the dienand mesencephalon.

Several LHRH-ir neurons were found in the diagonal band of Broca and the preoptic area. A few cells also occurred in the habenular region, infundibulum, some of them was located on the surface of the brain.

In *Rana esculenta* the distribution of LHRH-ir fibres and cells was similar to that in *Xenopus laevis*, but they were apparently less in number.

No difference could be detected in the organization of the GNRH system in male and female animals. The overall appearance of this system is similar to that described in the rat.

Akadémiai Kiadó, Budapest

Neurobiology 1 (2), p. 175, 1993

EFFECTS OF VISCEROSENSORY STIMULATION ON PREDATORY BEHAVIOUR IN CATS

Kukorelli, T. and Détári, L.

Department of Comparative Physiology, Eötvös Lóránd University, Budapest

The influence of intestinal (INT), splanchnic (SPL) and vagal (VAG) stimulation on the attack behavior elicited by lateral hypothalamus (LH) stimulation, was studied in the cat. Two types of INT, SPL and VAG stimulation were used to modify the induced attack: (a) hypnogenic stimulation (HS), which induced EEG synchronization and sleep; (b) arousing stimulation (AS), which desynchronized the electrocorticogram and aroused the cat from slow-wave-sleep. The intestine was stimulated by both electrical and mechanical (rhythmic distensions by a balloon) stimuli through a small intestinal fistula created by Thiry-Vella's procedure. LH stimulation in cats, which do not spontaneously attack rats, produces a predation like behaviour (PB). The attack response was divided into 2 stages: the first, defined as exploratory time (ET), begins with an environmental search and culminates in orienting towards the anaesthetized rat placed into the experimental cage; in the second, considered as attack time (AT), the cat stalks and bites the rat. The biting latency (BL), an interval between the beginning of LH stimulation and touching the rat by cat's muzzle, was utilized to measure the total duration of PB. HS, which was delivered to INT, SPL and VAG prior to LH stimulation by 5, 10 and 15 minutes, increased BL. This BL increase was the result of a highly significant lengthening of ET. AT was not markedly altered by HS. AS of INT and VAG, which was turned on by 10 s prior to LH stimulation, decreased BL by reducing ET. However, the SPL AS shortened both ET and AT. Viscerosensory effects on PB were decreased by increasing the intensity of LH stimulation. A ferocious attack with BL less than 10 s was not influenced by either HS or AS.

The present results indicate that the viscerosensory influence can modify PB by inhibiting or facilitating the priming events of attack, such as activation and wakefulness level, but a direct effect on the specific drive mechanism controlling attack is also possible.

Akadémiai Kiadó, Budapest

Neurobiology 1 (2), p. 176, 1993

FUZZY OPERATORS AND CYCLIC BEHAVIOR IN FORMAL NEURONAL NETWORKS - (Fuzziness may lead to chaotic dynamics)

[1]Lábos, E., [2]Holden, A.V., [3]Laczkó, J., [1]Orzó, L. and [1]Lábos, A.S.

[1]Semmelweis Univ. Med. Sch., 1st Dept. of Anatomy, Neurobiol. Unit of the Hung. Acad. Sci., H-1450 Budapest, Tűzoltó u. 58, Hungary; [2]The Univ. of Leeds, Center for Nonlinear Studies, Leeds LS2 9JT, UK and [3]Central Res. Inst. of Physics of Hung. Acad. Sci., Hungary

In traditional formal neuronal networks (FNN) a unit step function is applied. It is here regarded as a degenerated distribution function (DDF) and is named also as a non-fuzzy threshold operator (nFTO). Special networks of this kind which generate especially long (but finite) cycles of states were modified by introduction of a fuzzy threshold operators (FTO; a continuous S-shaped function, a non-degenerated distribution functions (nDDF)) which replaces the original unit step function. The cyclic behaviors of the new nets were compared to the original (DDF) ones. The state space becomes infinite and as a consequence of this the transitions might be more complicated. Neither the interconnection matrix nor the threshold values were here modified. It has been observed that the original long cycles change: (1) fixed points, (2) shorter cycles or (3) - as computer simulations demonstrate - aperiodic motion or even chaotic behavior appear. The chaotic dynamics emerges in two special ranges of small and large slope parameter k of the new threshold operator. The bifurcation diagrams with control parameter k are asymmetric and the chaos disappears again at the extreme values of k. Other network parameters are further investigated. The whole task is large since e.g. with 10 neurons, 111 different surveys of parameter dependence are required at least in principle. The computation of the new network state is as follows:

$$s_{old} = s \rightarrow sM \rightarrow sM\text{-}O \rightarrow T(sM\text{-}O) = s_{new} \qquad (1)$$

where s is a state of the net , M is the interconnection matrix; O is the threshold vector and T denotes the threshold operator. The FTO or non-DDF-s applied here is as follows:

$$T_1(x) = e^{kx}/(1+e^{kx}) = 1/(1 + e^{-kx}) \qquad (2)$$

ACKNOWLEDGEMENTS: This work was supported by OTKA 2621/1991 and ETT-T032/1990 Grants.

Neurobiology 1 (2), p. 177, 1993

THE PROJECTION NEURONS OF THE ISTHMIC NUCLEUS IN THE FROG. *RANA ESCULENTA*

Lázár, Gy. and Tóth, P.

Department of Anatomy, University Medical School, Pécs, Hungary

The morphology and the arrangement of isthmic projection neurons were studied. Cobaltous lysine complex (CLC) was injected ion tophoretically into various parts of the optic tectum. Anterogradely transported cobalt labelled tectoisthmic fibres and terminals, while the retrogradely transported tracer revealed isthmic cells projecting to the tectum. Contralaterally projecting isthmic cells were retrogradely filled by injecting CLC in to the postoptic commissure.

Tectal fibres form broom-like terminal arborizations within the ipsilateral isthmic nucleus. The diameter of terminals is 50-70 μm and the majority of end-branches terminate in the rim neuropil around the dendrites of cortical cells. Looser end-arbors terminate in the medulla.

Neurons projecting to the ipsilateral tectum are piriform and are located in the anterior one third of the medulla and in the anterior non-rim cortex. The axons of medullary cells leave the nucleus at its anteromedial part. Because the terminals of tectal fibres covered almost all of the labelled cells further classification was not possible.

Neurons projecting to the contralateral optic tectum form a cell plate, parallel with the cortex, in the middle of the medulla. Between the rim cortex and the labelled medullary cell plate scattered cobalt-filled neurons were located in the rest of the medulla and the rim neuropil. The rim cortex was heavily labelled. Six types of medullary cells of various shapes and sizes were distinguished. The dendrites of most of the medullary cells are oriented parallel with the rim cortex. Four types of neurons were recognized in the rim cortex. The most frequently occurring cells have piriform perikarya and straight apical dendrites, which arborize in a narrow cylindrical space (50-80 μm in diameter) in the rim neuropil and may enter the medulla.

Comparing the extent and orientation of dendritic arborization, and the terminals of tectal fibres, we assume that one category of cells may mediate information from a small area, and another category from a much larger area of the tectum to the other tectum via the isthmic nucleus.

Akadémiai Kiadó, Budapest

Neurobiology 1 (2), p. 178, 1993

COMPARATIVE IMMUNOHISTOLOGICAL STUDY OF THE NERVOUS SYSTEM IN *LUMBRICUS TERRESTRIS L.* (ANNELIDS) AND *HAEMOPIS SANGUISUGA* (HIRUDINEA)

[1]Lengvári, I., [1]Szelier, M., [2]Csoknya, M. and [2]Hámori, J.

[1]Department of Anatomy, University Medical School, Pécs
and [2]Department of Zoology, Janus Pannonius University, Pécs

The nervous systems of representatives of the two Annelids classes were compared utilizing Sternberger's peroxidase-antiperoxidase technique. It was shown that serotonin immunoreactive elements are numerous and evenly distributed in all parts of the nervous system in *Lumbricus terrestris*. The brain of *Haemopis sanguisuga* contains significantly less serotonin positive nerve cells, and they are found in each compartment of the cerebral ganglion. In the subesophageal and segmental ganglia the distribution of serotonin nerve cells is similar in both species, although their number is smaller in *Haemopis sanguisuga*. In *Lumbricus terrestris* serotoninergic nerve fibers are widely distributed in the gut and body wall. No such fibers were detected in *Haemopis sanguisuga*.

FMRFamide immunoreactive nerve cells and fibers were readily detected in every part of the nervous system both in *Lumbricus terrestris* and *Haemopis sanguisuga*, and there were no significant differences between the two species as far as the number and location of serotonin immunopositive nerve cells are concerned. It is suggested that different habits and environments of the two species can explain differences in distribution of a basic transmitter such as serotonin in their nervous system.

Akadémiai Kiadó, Budapest

Neurobiology 1 (2), p. 179, 1993

KAPPA OPIOID RECEPTORS: CHARACTERIZATION AND POSSIBLE FUNCTION IN DIFFERENTIATING NEURONAL AND GLIAL CELLS

Maderspach, K., Németh, K. and Bajenaru, L.

Institute of Biochemistry, Biological Research Center, Hungarian Academy of Sciences, H-6701 Szeged, P.O. Box 521, Hungary

During the early ontogeny of the nervous system several signals reach the progenitor cells to make them committed and to determine their final position and function. These signals are initiating many events inside the cells and act eventually on the expression of genes encoding the synthesis of proteins characteristic of the differentiated cell. Recently more data support that opioid peptides, among others, may function as signals in the nervous system and influence its early development through specific membrane receptors.

Kappa opioid receptors were studied in developing nervous cells from chick embryonic brain in culture. Specific ligands and the monoclonal antibody KA8 (IgG1-k) which was raised against the frog brain kappa-opioid receptor as an antigen in our laboratory, were applied.

The KA8 immunostaining made possible the visualization of the kappa opioid receptors of the neurons. Receptor arrangement proved to be discontinuous and changed with the *in vitro* differentiation. Immunolabeling appeared first at the pole of the primary outgrowing process later on the whole soma and finally on the branched processes. Specific radioligand binding indicated an increase in the receptor concentration with development.

Treatment of neurons with 10^{-7} M bremazocine or dynorphin (agonists with relative selectivity to kappa-opioid receptors) on the second and third cultivation days promoted the morphological differentiation. It also promoted the expression of the 200 kD neurofilament protein which became pronounced somehow later than the morphological changes. The effects were reduced by opioid antagonists (naloxone 10^{5} M or norbinaltorphimine 10^{-7} M) indicating that the effect was receptor-mediated.

These results support the hypothesis that kappa-opioid receptors may function as regulatory signal pathway in the early neuronal differentiation. The answer to the question, whether these signals influence the expression of genes encoding specific neuronal proteins needs further investigations.

Akadémiai Kiadó, Budapest

Neurobiology 1 (2), p. 180, 1993

TOPOGRAPHICAL AND DIMENSIONAL ANALYSIS OF THE P3 EVOKED POTENTIAL COMPONENT: HUMAN AND ANIMAL EXPERIMENTAL DATA

Molnár, M., Csépe, V., *Skinner, J.E. and Karmos, Gy.

Institute for Psychology of the Hungarian Academy of Sciences,
Budapest and *Baylor College of Medicine, Houston

The P3 component of the evoked potential (EP) elicited by sensory stimuli is widely used for the studying of various aspects of information processing. Little is known, however, about the psychophysiological mechanism(s) it represents, and also about its generation and intracerebral localization. In the present study, P3-like waves were elicited in cats in an auditory oddball paradigm similar to that used in humans. The EPs were recorded in various cerebral structures. Signal stimuli evoked a small P3 recorded from the vertex and ventral hippocampus, and a high amplitude late (between 400 and 420 ms) positive wave in the n. centralis amygdalae and the dorsal hippocampus. Signal stimuli evoked an earlier large amplitude negative wave (N200) in the dorsal hippocampus. In the primary auditory cortex the signal-elicited EP was characterized by a conspicuously large positive wave (P136) not seen before conditioning. Thus it appears that - to a varying extent and probably in very different ways - all brain structures studied play a role in the generation of the late "endogenous" EP components including those, like the primary sensory cortex, which were not regarded important from this point of view before.

The characteristics of the P3 were also studied by the mathematical methods of chaos theory. The correlation dimension (D2) was calculated from the EEG recorded from the vertex in humans in an auditory oddball paradigm. It was found that the value of D2 decreases during the occurrence of the P3 wave meaning that the degrees of freedom generating the analyzed epoch also decreased. This observation does not support the "context updating" hypothesis concerning the generation of the P3 component.

Literature

V. Csépe, G. Karmos and M. Molnár: Effects of signal probability on sensory evoked potentials in cats. Intern. J. Neurosci., 1987, 33: 61-71.

M. Molnár and J.E. Skinner: Low-dimensional chaos in event-related brain potentials (Int. J. Neurosci., in press).

This publication is based on work sponsored by the Hungarian-U.S. Science and Technology Joint Fund in cooperation with the Dept. of Health and Human Services and the Hungarian Academy of Sciences.

Akadémiai Kiadó, Budapest

Neurobiology 1 (2), p. 181, 1993

THE MODELLING OF THE RETINAL INFORMATION PROCESSING BY THE USE OF CNN

Orzó, L. and *Lotz, K.

1st Department of Anatomy, Semmelweis Medical School
and *Computer and Automation Institute
of the Hungarian Academy of Sciences

The CNN is a useful modelling frame for the retinal information processing. It can easily emulate the analog processing steps of the real retina. The basic interconnection structure of the CNN and the retina are essentially the same. Here we simulate several retinal events and information processing steps. Some of the individual retinal cell responses can be reproduced correctly. By the use of this model the effects of the wide field amacrine cells, which have large output field, could be imitated such as the wind-mill effect. Some of the visual illusion also can be simulated, like the Muller-Lyer and some aspects of the corrected Herring grid illusion. By a voltage dependent feedback and the rod-rod interaction, the transient response of the receptive fields of rods can also be depicted. The basic behavior of the rod-cone nonlinear state dependent interaction can be demonstrated too. A model of the dopamine effects on the retina in the outer plexiform layer, can help us to understand the controlling of its production after the light adaptational processes. The simulation predicts that not only the further adaptational process require the production of dopamine and so its effects, but the change of the equilibrium of the ON and OFF bipolar cell layers activation.

Akadémiai Kiadó, Budapest

Neurobiology 1 (2), p. 182, 1993

IMMUNOLOGICAL LESION OF CENTRAL CHOLINERGIC SYSTEM INDUCED BY ACETYLCHOLINESTERASE ANTIBODIES IN NEWBORN RATS

Rakonczay, Z., *Hammond, P. and *Brimijoin, S.

Albert Szent-Györgyi Medical University, Central Research Laboratory, Szeged, Hungary and *Department of Pharmacology, Mayo Clinic, Rochester, MN 55905, U.S.A

Acetylcholinesterase (AChE) anchored at the synaptic surface of neurons in cholinergic membranes might be a target of autoimmunity. Murine monoclonal antibodies against AChE were injected i.p. on the first postnatal day. We discovered that antibody penetrated into the brain as early as 24 hr after injection and they were detected in brain parenchyma by immunofluorescence histochemistry. At the same time punctate deposits of cholinesterase-active neuronal processes appeared in the same brain regions. AChE activity decreased by 30%, and the tetrameric membrane-associated enzyme form was almost undetectable two days after injection. In contrast, the intracellular monomeric AChE form remains free of antibody. Since the antibodies did not directly impair catalytic function the drop of the total enzyme activity implying destruction or removal of the enzyme. At day 7 enzyme activity and tetrameric AChE began to recover but the later remained only half as abundant as in the controls. At day 12 total AChE activity was still depleted by 30 % in whole brain and 40% in cerebral cortex. Choline acetyltransferase (ChAT) activity, a specific marker of cholinergic cytoplasm, showed the same losses as found in AChE activity. Therefore, the decrease of ChAT activity in brain must reflect destruction of cholinergic structures. On the other hand, immunocytochemistry of three noncholinergic markers (tyrosine hydroxylase, tryptophan hydroxylase and glutamic acid decarboxylase) showed no obvious change comparing to controls in the same area.

The newborn rat model of AChE-autoimmunity should be especially useful for (1) investigating the role of AChE in the early development of cholinergic systems in the brain, (2) a prospective tool to study the central cholinergic neuropathology induced by AChE antibodies.

This work was supported by grants from NINDS (NS 18170 and NS 29646).

Neurobiology 1 (2), p. 183, 1993

SENSORY NEGLECT AND CHANGES IN VISUAL EVOKED POTENTIALS AFTER UNILATERAL PALLIDAL 6-OHDA LESIONS IN THE RAT

Sándor, P., Lénárd, L., *Karmos, G., Czopf, J., Kellényi, L., Jandó, G. and Karádi, Z.

Institute of Physiology, Pécs University, Medical School, H-7643 Pécs, Hungary
and *Institute of Psychology, Hungarian Academy of Sciences, H-1394 Budapest, Hungary

Unilateral 6-hydroxidopamine (6-OHDA) lesions of the globus pallidus (GP) result in sensory neglect: Rats exhibit impairments in orientation to various sensory stimuli, applied contralaterally to their lesioned side. It was previously suggested that the cause of these symptoms were the disturbances in integration of central sensorimotor processes. Physiological evidences, however, are scarce in this field. Nevertheless, several results in the literature showed delayed visual evoked potentials (VEPs) after general depletion of brain catecholamines (CAs). To elucidate hypothesized functional interrelation of deficits of the forebrain CA mechanisms and the electrophysiological changes, in the present experiments we examined: 1) Whether selective lesions of CA elements of the GP result in changes of VEP components; 2) if VEP anomalies recorded, how does the dynamics of these changes correlate with the development of sensory neglect. To answer our questions, LED-matrix pattern VEPs were recorded in CFY rats and the effect of unilateral pallidal 6-OHDA injection on the VEPs was studied. The rats were awake, conditioned in the preoperative period to stay in the apparatus with their head in the center between the two stimulus-fields. Visual stimuli were applied bilaterally, ipsi- or contralaterally, respectively. Neurological examinations were carried out on every postoperative (po.) day to detect and follow the development of sensory neglect. As a general finding, significant ipsilateral latency and amplitude changes occurred following the injection of 6-OHDA, irrespective to the side of stimulation: 1) Latency delay and increased amplitude were observed in the late components (N170, P310) during the 2nd and 3rd po. days. Amplitude of P130, however, was decreased in these animals, in which a new P500 component was also observed; 2) Latency and amplitude decrease occurred on the N170 and P310 after the 5th po. day. The P500 component was totally missing in these cases. Explicit contralateral sensory neglect was detected from the 5th po. day. The results of our present experiments demonstrated changes in pattern of the VEPs, that appeared to be in a temporal correlation with the development of sensory neglect. The initial delay of the late components and the amplitude increase might occur as the first effects of 6-OHDA, due to the initial dopamine release. Decrease of the amplitude of the late components and the earlier latencies appeared simultaneously with the full development of the sensory neglect, which is in coincidence with the depletion of CA stores due to the 6-OHDA lesion. It is suggested, therefore, that these VEP changes may be the electrophysiological correlates of sensory neglect.

Akadémiai Kiadó, Budapest

Neurobiology 1 (2), p. 184, 1993

SENSITIVITY OF MONKEY INFEROTEMPORAL CELLS TO LUMINANCE, MOTION AND TEXTURE-DEFINED PATTERNS

*Sáry, Gy., Vogels, R. and Orban, G.A.

*Department of Physiology, Albert Szent-Györgyi Medical University, Szeged, Hungary and Lab. voor Neuro-en Psychofysiologie, KU Leuven, Leuven, Belgium

An investigation was made whether units in area TE of the inferotemporal cortex of the monkey are sensitive to form attributes, irrespectively of the cues that define these attributes. Eight different patterns (e.g., a cross, a star, a triangle) were presented in random order during fixation to two monkeys. The patterns were defined by differences in luminance, relative motion or texture. The responses of 261 single units were recorded in the monkeys. About 60% of these responded to the patterns irrespectively of the defining cue. Half of the responsive cells preferred some figures to others. The most interesting finding, however, was that 47 cells were found to exhibit a clear-cut selectivity for one particular figure, irrespectively of the defining cue, i.e. a star defined by differences in luminance, relative motion or texture. Parafoveal presentation did not change the selectivity, i.e. the selectivity of these neurons for a particular figure is not only cue-invariant but also position-invariant. This finding lends further support to the role of the inferotemporal cortex in visual shape recognition. The cue- invariant shape selectivity of these cells indicates that individual cells are able to abstract shapes or shape properties from different stimulus conditions.

Akadémiai Kiadó, Budapest

Neurobiology 1 (2), p. 185, 1993

CALRETININ IMMUNOREACTIVITY IN THE MONKEY HIPPOCAMPAL FORMATION

Seress, L., *Nitsch, R. and **Léránth, Cs.

Department of Physiology, University Medical School, Pécs, 7643, Hungary; *Center of Morphology, University Clinic Frankfurt, 6000 Frankfurt am Main 70, Germany and **Department of Obstetrics and Gynecology and Section of Neurobiology, Yale University, School of Medicine, New Haven, CT 06510, U.S.A.

Calretinin-containing neurons were visualized by immunocytochemistry in the monkey hippocampus, subicular complex and entorhinal cortex. Calretinin-immunoreactivity was present exclusively in non-granule cells of the dentate gyrus and in non-pyramidal cells of Ammon's horn, subiculum and entorhinal cortex. Most frequently, calretinin-positive neurons were found at the hilar border of the dentate gyrus and in the stratum radiatum of CA 1-3 areas. In the subicular complex, immunoreactive neurons were evenly distributed in all layers, whereas in the entorhinal cortex, they were accumulated in the external layers above lamina dissecans.

The majority of calretinin-immunorective cells were small, bipolar or fusiform neurons with a dendritic tree oriented parallel to the dendrites of principal cells. Dendrites were smooth or sparsely spiny, displaying small spines of conventional type.

In electron microscopic preparations, somal and dendritic features of calretinin-immunoreactive neurons were similar to that observed in the light microscope. Somata of immunoreactive neurons contained a large nucleus and a small cytoplasmic rim, which contained only a few organelles. The nucleus displayed deep infoldings and intranuclear rods. Axons of calretinin-positive neurons were thin, arborized in all layers and had small varicosities. Their terminals formed symmetric synapses mainly with dendrites and less frequently with somata of principal cells.

In summary:(i) there are significant species differences between the distribution and neuronal morphology of calretinin-immunoreactive hippocampal neurons in rats and monkeys,(ii) calbindin D_{28k}, parvalbumin and calretinin immunoreactive neurons form non-overlapping subpopulations in monkey brain.

Akadémiai Kiadó, Budapest

Neurobiology 1 (2), p. 186, 1993

RETROGRADE LABELLING IN THE NERVOUS SYSTEM OF *LUMBRICUS TERRESTRIS*

[1]Szelier, M., [2]Csoknya, M., [1]Lengvári, I. and [2]Hámori, J.

[1]Department of Anatomy, University Medical School, Pécs
and [2]Department of Zoology, Janus Pannonius University, Pécs

Circumpharyngeal connectives into both directions, as well as medial prostomial and segmental nerves of *Lumbricus terrestris* were retrogradely labelled with cobalt-lysine complex. On the basis of an analysis of labelled nerve cells it was concluded that circumpharyngeal connectives contain both ascending and descending fibers. The ascending fibers originate from nerve cells in the subpharyngeal ganglion while those of descending either from the perikarya in the cerebral ganglion or from the prostomial nerves. The majority of nerve fibers of the prostomial nerves originate from cell bodies of the subpharyngeal ganglion, and only very few from the cerebral ganglion. Segmental nerves contain fibers from cell bodies situated either ipsilaterally or contralaterally in the segmental ganglia.

Akadémiai Kiadó, Budapest

Neurobiology 1 (2), p. 187, 1993

EXPRESSION OF 5E10, A SPECIFIC PHOSPHORYLATED EPITOPE OF THE 160 KD NEUROFILAMENT PROTEIN

Szente, M. and *Landmesser, T.L.

Attila József University, Dept. of Comparative Physiology, Szeged and *University of Connecticut, Dept. of Physiology and Neurobiology, Storrs

In 5-7 day explants of chick dorsal root ganglia two types of 5E10 expression could be distinguished; 1./ A low-level expression that occurred throughout the axon, and which could be increased by treatments which altered levels of second messengers (depolarization by 20 mM K^+; calcium ionophore, A23187; phorbol ester (TPA); db-cGMP, and by ocadic acid), 2./ A high intensity expression that was induced in axons only as they were forced to make a sharp turn upon encountering a mechanical barrier, and which was confined to that portion of the axon. The expression of 5E10 induced at turning points differed from the overall 5E10 expression in that: i./ it was of greater intensity 1.2 (ratio of 5E10/L1 staining) compared to 0.6-0.7 induced by second messenger activators; ii./ more of it appeared to be incorporated into the triton insoluble cytoskeleton; iii./ once expressed, it was not reduced by long (24 hr) treatments with proteinkinase C (PKC) inhibitors such as staurosporine or calcium inhibitors as cadmium or dantroline which reduced expression elsewhere.

Induction of 5E10 expression at turning points and/or the cytoskeletal rearrangement associated with it appears to stabilize axons. When these axons were treated with the tubulin depolymerizing drug nocadozole they maintained their shape and microtubules were not depolymerized. In axons within the same explant which did not express high levels of 5E10, nocadozole caused tubulin staining to be lost from the axon, and resulted in axonal retraction and surface blebbing. Axons expressing high levels of 5E10 were more restricted to other agents that resulted in axonal retraction (okadic acid, 10 nM; nerve growth factor, 100 nM).

Inhibitors of PKC such as staurosporine when applied just before axons reached a mechanical barrier prevented axons from turning and continuing to grow. Under the same conditions 5E10 was not induced in the axons that had encountered the boundary.

The induction of the 5E10 antigen at the boundary may be via PKC or some other staurosporine sensitive step. Furthermore its expression or some cytoskeletal rearrangement associated with it appears to be essential for axons to execute sharp turns in-vitro.

Akadémiai Kiadó, Budapest

Neurobiology 1 (2), p. 188, 1993

CROSS-MODAL COMPENSATORY CHANGES OBSERVED IN THE CORTEX OF ADULT RAT INDUCED BY NEONATAL MONOCULAR ENUCLEATION

Toldi, J., Rojik, I. and Fehér, O.

Department of Comparative Physiology, József Attila University, Szeged, H-6701, P.O. Box 533, Hungary

Monocular enucleation was performed on rats at birth. The animals were raised and from the age of 3 months the evoked activity was tested in the parieto-occipital cortex. It was found that monocular enucleation changed the distribution of visually evoked responses in both hemispheres. However, the effect of early enucleation was not limited to the visual system. It was found that early enucleation caused an expansion of the somatosensory responses, among others into the visual area. Neurons responsive to visual and somatosensory stimuli were demonstrated in the anterior part of the primary and secondary visual areas, contralateral to the enucleation. Electrophysiological and autoradiographic studies unambiguously proved that early enucleation exerted a significant cross-modal effect on the somatosensory responsive area.

Akadémiai Kiadó, Budapest

Neurobiology 1 (2), p. 189, 1993

THE TYPES OF GANGLION CELLS IN THE RETINA OF *RANA ESCULENTA*

Tóth, P.

Department of Anatomy, Univ. Med. School, Pécs, 7643 Hungary

The morphological classes of retinal ganglion cells in *Rana esculenta* were determined and compared to those found in *Rana pipiens* by Frank and Hollyfield ('87).

Both optic nerves of 13 adult animals were retrogradely filled either by horseradish peroxidase (HRP) or cobaltic-lysine complex (CLC). The tracers were revealed on wholemounted neural retinae. The diameters of ganglion cell perikarya and dendritic fields were measured on camera lucida drawings.

Large ganglion cells were divided into 3 classes. Class 1 ganglion cells had large perikarya (20-22μm) and sparsely branching, symmetrical dendritic trees (850-1000μm in diameter) with branches in the scleral sublamina of the inner plexiform layer (IPL). The somata of Class 2 ganglion cells were slightly smaller (19-20μm), the diameter of the asymmetrical, sparsely branching dendritic tree was 5-600μm, the dendrites arborized predominantly in the scleral sublamina of the IPL. Class 3 ganglion cells had round perikarya (16-18μm). The symmetrical, bi- or tristratified dendritic trees (450-500μm in diameter) had branches in the scleral, vitreal and the intermediate sublamina of IPL, as well.

Middle-sized ganglion cells had soma diameters of 11-15μm. Class 4 cells had symmetrical or asymmetrical dendritic trees of variable diameters (180-310μm). The dendrites arborized in the vitreal sublamina of the IPL and only every fifth was bistratified. Class 5 (biplexiform) cells formed less than 0.1% of the total ganglion cell number. They had dendritic arbors both in the IPL as well as in the outer plexiform layer.

Small ganglion cells (the perikarya are 7-10μm in diameter) gave 70% of ganglion cells. Class 6 neurons had small
(100-150μm in diameter), symmetrical or asymmetrical dendritic arbors in the vitreal sublamina of the IPL. Class 7 ganglion cells had the smallest (80-110μm), asymmetrical dendritic trees with sparsely branching vitreal arbors.

Our results are in accord with that of Frank and Hollyfield ('87). However, CLC-filling seems to reveal the entire dendritic arbor including the finest branches, which may not always be the case after the administration of HRP.

1. Frank, B.D. and Hollyfield, J.G.: J.comp.Neurol.,***266***(1987) 413-434.
2. Tóth, P. and Straznicky, C.: Arch. Histol. & Cytol.,***52***(1989) 87-93.

Akadémiai Kiadó, Budapest

Neurobiology 1 (2), p. 190, 1993

BEHAVIORAL DISTURBANCES ASSOCIATED WITH THYROID DYSFUNCTIONS IN YOUNG RATS

Varga, Zs., *Karádi, Z., Halász, N. and *Lénárd, L.

Institute of Biophysics, BRC, Szeged and *Institute of Physiology, Pécs University, School of Medicine, Pécs

Thyroid hormones are essential for the normal growth and maturation of vertebrate organisms; their influence on the development of neurons and neural connections is also well-known. Elevated or reduced level of the thyroid hormones result in changes of the behavior; olfactory disturbances have also been detected in hypothyroid subjects. In the present study, our aim was to investigate such changes in rats and to further characterize the behavior and the odor detection of rats caused by altered serum thyroxine levels.

High and low serum thyroxine hormone levels were produced by pre- and postnatal administration of thyroxine hormone (T4) or propylthiouracil (PTU) in the drinking water. Subjects were 35 male rat pups from litters of Sprague-Dawley dams. Neurological tests like investigations of the single animals' reactions to visual, acoustic, somestesic and olfactory cues and detection of the muscle tone were also performed. Animals were placed one by one in the centre of an open field apparatus and the number of squares crossed (ambulation score), the number of rearings, groomings, sniffings and freezings as well as the number of faecal boli deposited and the frequency of urination in a 3 minute period of observation were recorded. Later, the preference for the unscented or scented part of a testbox was registered. In a simple learning test the animals were placed into the alley of a T-maze and they were required to find the scented (vanilla) food; the time they needed was recorded.

Activity of hypothyroid animals was decreased in the open field in the evening and in the morning. The performance of hyperthyroid rats was decreased in the morning and increased in the evening. A difference was shown in the stereotype behavior between the treated and untreated groups. The number of groomings, rearings, sniffings and freezings of the hyperthyroid rats was significantly decreased. The frequency of defecation for all of the treated animals increased, while that of the urination was inconsistent. The place preference learning ability combined by odor cues differed again: hypothyroid rats showed a greater preference toward the scented part of the testbox than the control or hyperthyroid pups did. The simple learning test seemed to be more difficult to acquire for the hypothyroid rats as compared to the other groups.

In summary, the results of this study show that the influence of the serum thyroxine hormone level in the early stage of ontogenesis produces difference in many aspects of the animals' behavior and that the hypothyroidism results in difficulties in association of odor informations to a learned adaptive behavior.

Akadémiai Kiadó, Budapest

Neurobiology 1 (2), p. 191, 1993

CHARACTERIZATION OF [^{3}H]MET-ENKEPHALIN-ARG^6-PHE^7 OPIOID RECEPTORS IN FROG BRAIN MEMBRANE PREPARATIONS

M. Wollemann, J. Farkas*, G. Tóth* and S. Benyhe

Institute of Biochemistry and *Isotope Laboratory, Biological Research Centre of the Hungarian Academy of Sciences, H–6701 Szeged, P.O. Box 521, Hungary

A tritiated compound with high specific activity (40 Ci/mmol) has been synthesized in order to characterize the opioid binding activity of [^{3}H]Met-enkephalin-Arg^6-Phe^7 in frog brain membrane fractions. The K_d calculated from homologous displacement experiments with the LIGAND programme was 1.1 nM and the B_{max} 347 fmol/mg protein. The K_d determined from equilibrium saturation binding data was 1.3 nM. However, the Hill coefficient varied between 0.2–0.3 (n=9), which suggests the presence of a second, high affinity binding component.

Investigating the subtype-specificity of the heptapeptide binding sites, the rank order potency of the ligands tested was as follows: bremazocine (K_d 0.46 nM) > naltrindole > diprenorphine > levorphanol > nor-BNI > EKC > DADLE > β-endorphin > dynorphin > naloxone > deltorphin II > DSLET > morphine > DAGO > DPDPE > U-69593 > dextrorphan (K_d 12.7 μM). Binding of [^{3}H]Met-enkephalin-Arg^6-Phe^7 was inhibited by Na^+ and GppNHp which pointed to the agonist character of the heptapeptide. These results reflect a *kappa*$_2$ and/or *delta* subtype specificity of the ligand with an exclusion of *kappa*$_1$ and *mu* opioid sites.

Akadémiai Kiadó, Budapest

(contents continued)

INSTRUCTIONS TO AUTHORS

Aims and Scope. *Neurobiology* is a multidisciplinary international journal, which publishes contributions from all traditionally important and newly emerging subdisciplines of the neurosciences including neuroanatomy, morphology, histochemistry, physiology, pharmacology, molecular neurobiology, developmental neuroscience, etc. Referees from a large international Editorial/Advisory Board will review submissions critically.

Submission. The journal publishes original, unpublished papers and reviews (conference abstracts, book reviews, announcements, advertisements, etc. may also appear from time to time) in English. The text should not exceed 15 typewritten pages (total length with illustrations, tables, etc., 20 pages).
Manuscripts should be submitted in triplicate to the Editorial Office:

Norbert Halász
Institute of Biophysics
Biological Research Centre
Hungarian Academy of Sciences
H-6701 Szeged, P.O. Box 521, Hungary
Telefax: 36 (62) 433 133
Phone: 36 (62) 432 232
E-mail: H3186HAL@ELLA.HU

Accepted manuscripts will not be returned to the authors.

To accelerate publication the papers will be reproduced directly from the authors' manuscripts, so those must be suitable for photographic reproduction. Authors should use electric typewriters with black (carbon) ribbon or high quality printers. Manuscripts not conforming to the specified instructions will be returned for reorganizing and retyping. Authors are encouraged to submit their papers also on floppy discs, using preferably WordPerfect, or Word as processors on IBM compatible computers.

Manuscripts should be typed on A4 (210x297 mm) papers. All margins should be 2.5 cm except upper margins on front (6 cm) and other pages (4 cm). Page numbering should be done only by soft pencil.

Regular papers should be organized into sections in the following order: Summary, Key words, Introduction, Materials and Methods, Results, Discussion (followed by Conclusions and Acknowledgements, if relevant), References. Illustrations, tables and their explanations should be inserted into the appropriate sections; all these should be centred.

The Introduction, Results and Discussion should be typed by a one and a half line spacing, while the rest of the sections should be typed by single space. The title, authors, and their affiliation should be centred.

Title. Use bold, block capital letters, enlarged if possible.

Authors and their Affiliation. Type by single space. Leave two and one line spaces above and below the authors' names, respectively.

Summary. Keep three line spaces above and one below the summary (not exceeding 150 words). The summary should be indented by five spaces on both sides.

Key words. A maximum of six key words or short phrases should be given and be indented similar to the summary.

At the rest of the text, *headlines* of the sections should be centred and typed in bold, capital letters. Use two line spaces above and one below headlines. *Subheadings* (if present) should be typed to the left side of the margin in italics (or should be underlined); line spacing: one above and below.

References. The lists should be arranged in alphabetical order. Their second and following lines should be indented by five spaces. Use abbreviated journal names. They should be arranged as the following examples show for journal and book references:

Butt, A.M., Jones, H.C. and Abbott, N.J. (1990) Electrical resistance across the blood-brain barrier in anaesthetized rats: A developmental study. J. Physiol. 429, 47-62.

Shepherd, G.M. (1988) Neurobiology. 2nd edition. Oxford Univ. Press, New York and Oxford.

Balázs, R. and Richter, D. (1973) Effects of hormones on the biochemical maturation of the brain. In: Biochemistry of the Developing Brain (ed. Himwich, W.) Vol. 1, pp. 254-304. M. Dekker, New York.

These should be cited in the text by the names of the authors and the year of publication, e.g. [Balázs and Richter, 1973; Shepherd, 1988; Butt et al., 1990].

Tables. These should be typed into the appropriate part of the text, together with their numbers, titles (above) and explanations (which should appear below the tables). Leave at least one line space between the Arabic table numbering and title, its explanation (single spaced) and the table itself, respectively. Separate the table from the text by one line space at least. Please, try to find the best fit between the width of the tables and their explanations. Data should not be duplicated in tables and figures.

Figures (line drawings, diagrams, photographs). These should be numbered consecutively by Arabic numerals. One original copy and two additional copies should be sent. Please, indicate numbers and the name of the first author and the top of the figure on the back. For *Legends* (single spaced) use the full length of text lines. Figure numbering should be followed by its legend in the same line. Do not glue Figures into the text. Please, type, however, their legends onto proper place. Legends should appear below figures, separated by one line space above (and below if the text continues on that page). Maximal (printed) size of Figures should not exceed 120x180 mm and should preferably leave enough space for the explanation on the same page. Leave at least one line space above figures.

Line drawings and diagrams. Please, prepare those in black ink by expecting a possible reduction (by 30-50%) and select lettering and symbols ensuring their recognizable final size (min. 2 mm). Please, leave enough space for them in the text plus at least one line space above and below. Reduction of line illustrations, if needed, will be done by the Publisher. *Formulae* if complex (and not typed into the text) should be prepared similarly.

Photographs. High quality half tones (please prefer higher contrast) should be prepared on glossy paper (and labelled clearly by Letraset) at their expected final size. Micrographs should also be completed by a scale bar representing the magnification and serial numbers in corners of the front of pictures. A limited number of colour photographs will also be accepted (if absolutely necessary) at no extra charge.

Abbreviations and symbols. These should be used according to the latest internationally accepted rules. They should be explained at their first appearance (and may also be listed in an alphabetical order, when desired). The SI System should be used.

Running title and address. The running title (not exceeding 50 characters and spaces) should be submitted on a separate page together with the full address, phone and fax numbers (E-mail if avaible) of the corresponding author.

Reprints. Fifty free reprints are provided to the authors. Additional reprints can be ordered from the Publisher at the time of acceptance. Fifty percent discount will be offered to young investigators and newcomers, without prior publications in this discipline.

CONTENTS

(contents continued on page 192)

NEUROBIOLOGY

An International Multidisciplinary Journal in Neurosciences

VOLUME 1, NUMBER 3, 1993

Including the former Acta Biochimica et Biophysica Hungarica

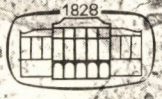

AKADÉMIAI KIADÓ, BUDAPEST

HU ISSN 1216-8063

NEUROBIOLOGY

An International Multidisciplinary Journal in Neurosciences

(Including the former Acta Biochimica et Biophysica Hungarica)

Neurobiology is a multidisciplinary international journal publishing contributions from all traditionally important and newly emerging subdisciplines of the neurosciences including neuroanatomy, morphology, biochemistry, physiology, pharmacology, molecular neurobiology, developmental neuroscience, etc.

Neurobiology is published by
AKADÉMIAI KIADÓ
Publishing House of the Hungarian Academy of Sciences
H-1117 Budapest, Prielle K. u. 19–35, Hungary

Manuscripts and editorial correspondence should be addressed to

Norbert Halász
Institute of Biophysics
Biological Research Centre
Hungarian Academy of Sciences
H-6701 Szeged, P.O. Box 521, Hungary

Subscription price for Volume 1 (1993) in 4 issues US$ 78.00, including normal postage; airmail delivery US$ 20.00

Orders should be addressed to

AKADÉMIAI KIADÓ
H-1519 Budapest, P.O. Box 245, Hungary

NEUROBIOLOGY

An International Multidisciplinary Journal in Neurosciences

Akadémiai Kiadó, Budapest

Neurobiology 1 (3), pp. 197-199, 1993

HUNGARIAN NEUROSCIENCE SOCIETY FOUNDED

-background and historical review

In January 1993 the Hungarian Neuroscience Society (HNS) was founded as an independent, nongovernmental scientific organization.

Having been involved from the beginning in the grouping of scientists dealing with brain research in Hungary, and as Chairman of the former Neurobiology Section of the Hungarian Physiological Society and of the committee carrying out the preparatory work for the creation of the HNS, I feel honoured to be invited by the Editor of the new periodical Neurobiology to recall the history which led to the establishment of a separate organization of Hungarian neurobiologists.

The creation of the HNS was a result of the organic development of earlier gatherings, based on mutual interest, growing cooperation, interaction and the need for exchange of ideas and results between Hungarian neuroscientists, materializing in annual conferences, occasional specific meetings, methodological, technical courses and discussions, joint research programmes, common international representation and the organization of international conferences.

Neuroscience in Hungary has a long tradition, marked by prominent personalities well known for their achievements throughout the scientific world interested in studies on the nervous system. It is enough to mention the names of István Apáthy (1863-1922) the famous anatomist from the beginning of this century, Ambrus Ábrahám (1893-1989), Kálmán Lissák (1908-1982) and János Szentágothai (1912-), the most outstanding neurobiologists in this country during the past 50 years. Their scholars and independent leading scientists in neurobiology who are now members of the Academy and/or professors at universities numbers over 20, with more than 200 working in their teams.

Since the sixties, neuroscience has become the main research trend in a considerable number of university departments and in some research institutes of the Academy, and international recognition has now been achieved. The research in these

Akadémiai Kiadó, Budapest

laboratories extends over a wide scale of neuro-disciplines. Besides the traditionally strong functional morphological approach, researches in physiology, neurochemistry, pharmacology and modelling also have notable representation, and the topics span the range from subcellular neurobiology to studies on behaviour.

The recent status is a result of a long period coinciding with the expansion of neuroscience worldwide and with the development of the facilities for basic research in Hungary. This was particularly noticeable from the middle of the sixties, when special programmes were launched at the Hungarian Academy of Sciences. These became better organized and financially supported from the seventies, in the frame of the topic Regulatory Mechanisms of Living Processes. The formation of a section of this programme was the first attempt to gather neurobiologists working at various university departments and research institutes together, and in 1972 the first Conference on Neurobiology was organized for the groups involved in this programme.

Since 1972 these scientific meetings have become regular, annual events. The number of participants has increased from the original 40 to 150, and the Research Institute at Tihany, the site of the first few meetings, soon proved to be too small to accommodate the enlarged Conference.

Neurobiology meetings were organized at the beginning in the frame of the Academy of Sciences for those who participated in and were supported by the centrally initiated programme. The original aim of the meetings was to listen to reports and evaluate results achieved by various groups, and theoretically the outcome could influence further financial support. Because of the great attention, these meetings were later made open for all interested neurobiologists, and presentations of groups or scientists not supported by the programme (but seeking support) were also accepted and discussed. In this way, the neurobiology conferences became very prestigious meetings for Hungarian neuroscientists.

At the same time there existed separate societies for physiology, general biology, biochemistry, biophysics, morphology and pharmacology in Hungary, and neurobiologists were also members of one or other of these, and attended their meetings too. At the beginning of the eighties, the idea arose to unify all neurobiologists in one society by creating a nongovernmental organization which would not be dependent morally or financially on the Academy or the Government and would be able to make contact with international bodies, mainly the International Brain Research Organization (IBRO) and

the European Neuroscience Association (ENA). However, at that time the creation of a new, independent society in Hungary was virtually impossible, and therefore a special Section of Neuroscience was formed within the Hungarian Physiological Society, with its own elected executive committee, with its own programme and with the right to establish international relations. This Section was created in 1982, functioned during the eighties and became the immediate predecessor of the HNS.

Simultaneously, the organization of scientific programmes and financial support in Hungary underwent a basic change, and the official evaluating function of the neurobiology meetings was terminated. Special programme committees were formed, which were separated from the Neurobiology Section, and the annual conferences became purely scientific events, totally free from administrative academic or governmental relations and duties.

In 1987 the Second IBRO World Congress on Neuroscience was organized in Budapest, which was a great event for the Hungarian groups working on brain research. Satellite symposia to this and other international congress were also regularly held in the field of neuroscience in Hungary, and on the basis of the regular conferences the International Society for Invertebrate Neurobiology was founded and is also hosted in Hungary. The Neurobiology Section was involved in all these events, and it also promoted participation of its members in international meetings abroad. Further, special links have been built up with the ENA for membership and conference attendance, and a proposal has also been made to hold one of the coming ENA meetings in Hungary.

When the decision was taken by the Government and the Academy of Sciences that Hungary should join in the international Decade of the Brain Programme in 1992, it seemed very appropriate to form the independent organization for Hungarian neuroscientists. This was done on 21st January 1993, at the 21st Neurobiology Conference, held in Veszprém, when the Neurobiology Section of the Hungarian Physiological Society declared its dissolution and immediately, as successor to the Section, the HNS was established. Professor László Lénárd (Pécs) has been elected Chairman of the HNS, and Dr. Tamás Freund (Budapest) Secretary, for a term of four years.

Prof. János Salánki
Chairman of the former Neurobiology Section
of the Hungarian Physiological Society

Neurobiology 1 (3), pp. 201-206, 1993

CHOLINE ACETYLTRANSFERASE-LIKE IMMUNOFLUORESCENCE IN EPIDERMIS OF HUMAN SKIN

Olle Johansson and Lixin Wang

Experimental Dermatology Unit,
Department of Histology and Neurobiology,
Karolinska Institute, Stockholm, Sweden

Summary: Using the indirect immunofluorescence approach the occurrence of choline acetyltransferase-like immunoreactivity in epidermis, except stratum basale, of human skin is described. Immunoreactive cells were also found in hair follicles, sweat gland ducts and sebaceous glands.

Key Words: choline acetyltransferase, epidermis, human, immunocytochemistry, keratin

INTRODUCTION

Choline acetyltransferase (ChAT) is the terminal synthetic enzyme of the classical neuronal transmitter, acetylcholine. It exists mainly in the neurons involved in motor mechanisms, arousal, memory and learning [McGeer et al., 1984]. However, recently we have found ChAT-like immunofluorescence in human epidermal cells. It raises tantalizing questions: Is there any ChAT acting in the epidermal cells? Does this correlate to so-called aquagenic pruritus where a role for acetylcholine has been suggested? The aim of the present study was to further elucidate the localization and distribution of ChAT-like immunoreactivity in human skin.

Akadémiai Kiadó, Budapest

MATERIALS AND METHODS

Human skin biopsies of hairy and glabrous skin were obtained from volunteers with local anaesthesia by lidocaine. The specimens were immersed for 3 h in 4% paraformaldehyde and 14% saturated picric acid in 0.1 M Sörensen's phosphate buffer (pH 7.4) at 4°C, then rinsed in the same buffer containing 10% sucrose. Cryostat sections (14 μm) thawed onto chrome-alum coated slides were processed for indirect immunofluorescence. The primary ChAT antiserum (Incstar, Stillwater, USA) was diluted in phosphate buffered saline (PBS) containing 0.3% Triton X-100, in which the sections were incubated overnight at 4°C in a humid atmosphere, followed by incubation for 30 min at 37°C in tetramethylrhodamine-isothiocyanate isomer R (TRITC; Boehringer Mannheim Biochemicals, Germany)-conjugated antiserum. Hyper-immune or non-immune serum served as control sera. The sections were rinsed in PBS before and after the incubations, mounted in PBS-glycerine and examined in a Nikon Microphot-FXA fluorescence microscope.

RESULTS

ChAT-like immunofluorescence (ChAT-LIF) appeared in cells of the epidermis, hair follicles, sweat gland ducts (not in the proper sweat glands) and sebaceous glands of human skin which included shoulder, back, chest, areola, axilla, upper arm, thigh, finger-tip and sole.

Cells in the strata spinosum and granulosum of hairy skin had strong immunofluorescence in the cytoplasm with the nuclei totally dark, while the cells of the stratum basale had no ChAT-LIF at all (!). In the glabrous skin, much weaker ChAT-LIF was displayed in the stratum spinosum and granulosum (Fig. 1). The amorphous cells of the stratum corneum revealed different amounts of ChAT-LIF (no-to-strong immunofluorescence). Extremely intensive ChAT-LIF could be seen at the orifice of some sweat gland ducts and in some parts of the stratum corneum of glabrous skin. No immunoreactivity was found in the stratum lucidum of glabrous skin. A corresponding dark band was also present in hairy skin.

The ChAT-LIF cells of the hair follicles were found in the outer epithelial root sheath, but not in the outermost cell layer, from the level neighbouring the sebaceous gland to the part connecting to the epidermis (Fig. 2A). The sweat ducts showed similar ChAT-LIF, as intense as the positive epidermal cells (Fig. 2B). Occasionally, cells in certain sebaceous glands contained ChAT-LIF.

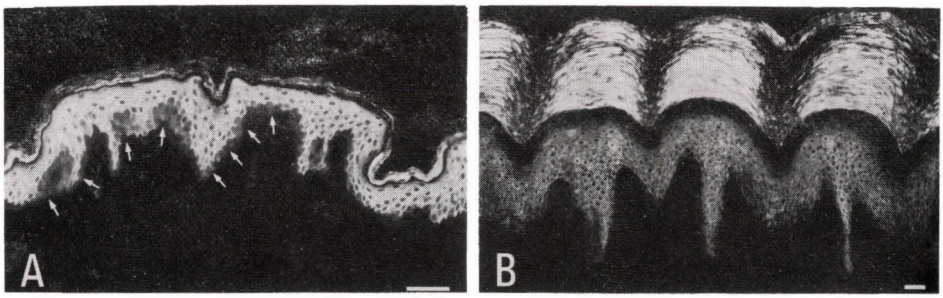

Fig. 1: ChAT-like immunofluorescence in human epidermis from upper arm (**A**) and finger-tip (**B**). Note the empty basal layer in **A**. Arrows in **A** mark the basement membrane. Bars represent 50 μm.

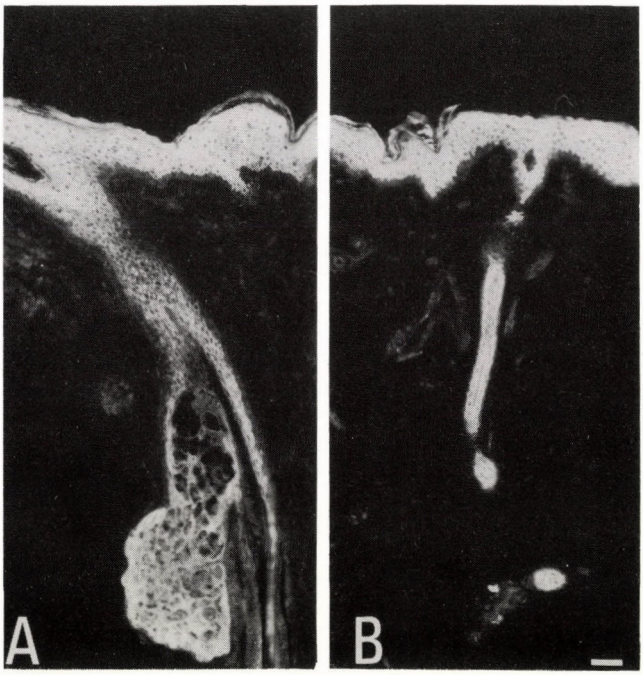

Fig 2: ChAT-like immunofluorescense in hair follicle (**A**; shoulder), and in sweat duct (**B**; chest) of human skin. Bar represents 50 μm.

The antiserum used has yielded good immunoreactivity in e.g. rat brain tissue, with a similar intensity as the one presently observed. Sections incubated with hyper-immune or non-immune serum were all negative. It may be noted, that parallel western blot and immunoprecipitation methods have failed to show any cross-reactivity between the antiserum and keratins (cf. below).

DISCUSSION

Although it is well known that the skin contains cholinergic nerves and that some reports have described cholinesterase activity in mammalian skin, no evidence has been obtained demonstrating ChAT existence in the epidermis. ChAT is claimed to be a specific marker of cholinergic neurons. With the present antiserum, however, we are also able to detect ChAT-LIF in the terminally differentiating epidermal cells of human skin.

Up to 85% of the total protein content of a differentiated epithelial cell are keratins, which are fibrous cytoskeletal elements. In humans alone, about 25 different keratins have been catalogued by two-dimensional gel electrophoresis [Fuchs, 1988]. The detailed keratin composition varies depending on the cell type, cellular growth environment, stage of development and differentiation, and disease state, of them the pairs of 56 and 65-67 kd are regarded as markers of keratinization or "skin type" differentiation, and have been found in suprabasally located, more differentiated cells [Cooper et al., 1985]. Van Neste et al. [1983] showed that all the suprabasal cells in normal human skin are 67 kd keratin positive. Using antibodies against 67 kd keratins, Viac et al. [1980] and Woodcock-Mitchell et al. [1982] observed immunofluorescent staining in cells of spinous and granular layers and also in the stratum corneum with the basal layer negative and sharply contrasted. Hair follicles and sweat ducts showed similar strong fluorescence. ChAT have a similar molecular weight (66-70 kd) as 65-67 kd keratins [McGeer et al., 1984]. ChAT from chicken optic lobe and cerebrum weigh 64 and 67 kd, respectively [Peng et al., 1980; Johnson et al., 1986]. Both the cholinergic neurons and keratinocytes come from the ectoderm. Do ChAT and keratins have homologic gene codes? Similar antigenic groups? Functional relationships?

Our ChAT-LIF pictures of hairy skin resemble the 67 kd keratin immunofluorescence, since all suprabasal keratinocytes, including those in hair follicles and sweat ducts, displayed a strong ChAT immunofluorescence. A cross-reaction of the ChAT antibody to keratins may, thus, be suspected. The ChAT-LIF in the

glabrous skin only showed strong fluorescence in the stratum corneum, whereas the spinous and granular cells displayed a weak immunoreactivity. This may account for a different keratin composition. However, control adsorption experiments, in our laboratory, using a mixture of keratins (Sigma Chemical Co., St. Louis, Mo, USA) added to the ChAT antiserum, produced ChAT immunoreactivity images of equal intensity, thus, speaking against a plain cross-reactivity situation.

In this context, it may be mentioned that a role for acetylcholine in so-called aquagenic pruritus has been suggested by Bircher and Meier-Ruge [1988]. They discussed the cholinergic innervation around sweat glands as being the basis for this disease, however, with the present results in mind aquagenic pruritus may very well depend on an acetylcholine-like substance being directly produced by the epidermis, and upon water challenge being secreted or extracted into the intercellular space, later on interacting with nerves or cells involved in the production of pruritic sensations. We expect that our present study can induce a series of investigations to discover new knowledge in the field of experimental dermatology.

ACKNOWLEDGEMENTS

This study was supported by grants from the Swedish Medical Research Council (12X-09060), Edvard Welanders Stiftelse, IngaBritt och Arne Lundbergs Forskningsstiftelse, Svenska Psoriasisförbundet, Torsten och Ragnar Söderbergs Stiftelser, and funds from the Medical Faculty of the Karolinska Institute.

REFERENCES

Bircher, A.J. and Meier-Ruge, W. (1988) Aquagenic pruritus - Water-induced activation of acetylcholinesterase. Arch. Dermatol. 124, 84-89.

Cooper, D., Schermer, A. and Sun, T.-T. (1985) Classification of human epithelia and their neoplasms using monoclonal antibodies to keratins: strategies, applications, and limitations. Lab. Invest. 52, 243-256.

Fuchs, E. (1988) Keratins as biochemical markers of epithelial differentiation. TIG 4, 277-281.

Johnson, C.D. and Epstein, M.L. (1986) Monoclonal antibodies and polyvalent antiserum to chicken choline acetyltransferase. J. Neurochem. 46, 968-976.

McGeer, P.L., McGeer, E.G. and Peng, J.H. (1984) Choline acetyltransferase: purification and immunohistochemical localization. Life Sci. 34, 2319-2338.

Peng, J.H., McGeer, P.L., Kimura, H., Sung, S.C. and McGeer, E.G. (1980) Purification and immunochemical properties of choline acetyltransferase from human brain. Neurochem. Res. 5, 943-962.

Van Neste, D., Staquet, M.J., Viac, J., LaChapelle, J.M. and Thivolet, J. (1983) A new way to evaluate the germinative compartment in human epidermis, using 3H-thymidine incorporation and immunoperoxidase staining of 67K polypeptide. Br. J. Dermatol. 108, 433-439.

Viac, J., Staquet, M.J., Thivolet, J. and Goujon, C. (1980) Experimental production of antibodies against stratum corneum keratin polypeptides. Arch. Dermatol. Res. 267, 179-188.

Woodcock-Mitchell, J., Eichner, R., Nelson, W.G. and Sun, T.-T. (1982) Immunolocalization of keratin polypeptides in human epidermis using monoclonal antibodies. J. Cell Biol. 95, 580-588.

Received 16 March 1993
Accepted 8 June 1993

Neurobiology 1 (3), pp. 207-222, 1993

A UNIT PARADOX FOR ARTIFICIAL NEURONAL NETWORKS

E. Lábos

Semmelweis University Medical School, 1st Deptartment of Anatomy, Neurobiology
Unit of the Hungarian Academy of Sciences, H-1450 Budapest, Tűzoltó u. 58,
HUNGARY

SUMMARY - In formal or artificial neuronal networks (FNN; ANN) built of threshold logic gates, a unit step function is used. Recently the step function has been replaced by an S-shaped curve. This replacement is common and many studies are based on this substitution, often combined rarely not with some adaptive or learning procedure. However, the dynamical consequences e. g. in the time course of single unit discharges have not been sufficiently examined. The concepts of unit (neuron) and network in these models of engineering and neurobiology correspond to each other only partially: model units may behave similarly to real nets of real units. This is called here a *unit paradox.* Propositions are presented to eliminate this apparent contradiction. A further paradox is also mentioned (Section 3). It seems necessary to reconsider the relationship of the various trends of neural network theory.

Key words: artificial neural nets, paradoxical behavior of units, chaos, spikless waves, exotic potentials, mass potentials, phantom oscillations

1. INTRODUCTION

Here a formal neuronal net (FNN) is a more general term than a McCulloch-Pitts network (1943): - *(1)* - the state space of units and nets are fixed, the quality of states (amplitude or repetition rate or else) is not specified in advance; - *(2)* - the interconnection matrix M is constant and synthesized by some procedures here not by "learning" (Lábos, 1984); - *(3)* - thresholds are specified for each unit;- *(4)* - a threshold

operator (a unit step function or a softer "S-shaped" function) is applied at the end. Thus the computation of the "next state" is as follows:

$$s_{i+1} = \mathbf{T}(s_i M - O) = N(s_i) \qquad (1)$$

The sequence of network states is generated by the iteration of this map N, incorporating the matrix M, threshold vector Θ and a threshold operator **T** (as a so called response curve). Nets may differ from each other by these objects. For a given net M, Θ and **T** are constant, and the dynamics evolves here only by iteration following equation (1). No external input vectors or learning are used. Dynamical systems of similar kind may be defined almost without limit.

A response curve, **T** for a single natural or artificial neuron is conventionally regarded either as a *temporal* or as a *spatial average* signal of a cell population. A normalization of magnitude to remain between 0 and 1 is facultative. The function **T** may also be interpreted in many ways e.g. as a membership or as a distribution-function in various contexts. A hidden contradiction is here already present: these averaged curves are used as threshold operators for *single neurons*. This is not obvious when threshold gate nets are computed with unit step function (see below $\mathbf{T_0}$).

In this paper as well as the unit step function, $\mathbf{T_0}$ and the most popular, S-shaped threshold operators - $\mathbf{T_1}$ and $\mathbf{T_2}$ - (not significantly different from each other; see also in Lábos and Lábos, 1992) are applied. In addition, a multitude of similar - invertible *special distribution functions* (continuous and strictly monotonic) similar to $\mathbf{T_1}$ and $\mathbf{T_2}$ can be defined. Almost surely, all of them would result in conclusions to be outlined below. Moreover, no trivial coordinate transformation exists between two - otherwise arbitrary - sigmoid curves in general (i.e. for all cases) like for $\mathbf{T_1}$ and $\mathbf{T_2}$. The functions below are the most popular ones:

$$\mathbf{T_0}(x) = 1 \text{ if } x>0 \text{ and } \mathbf{T_0}(x) = 0 \text{ if } x<0 \qquad (3)$$

$$\mathbf{T_1}(x) = e^{kx}/(1+e^{kx}) = 1/(1 + e^{-kx}) \qquad (4)$$

$$\mathbf{T_2}(x) = 0.5 + 0.5(e^{kx}-e^{-kx})/(e^{kx}+e^{-kx}) \qquad (5)$$

$\mathbf{T_0}$ is used in threshold gates (Muroga, 1971), $\mathbf{T_1}$ is a function used in *Boltzmann* distributions or it is essentially *the logistic function* (Verhulst, 1838) and $\mathbf{T_2}$ comes from the popular *tanh* - function after transformation into (0,1) interval. The popular (-1,+1) convention of technical approaches is not suitable as a direct biological analogy. $\mathbf{T_1}$ and $\mathbf{T_2}$ - among others - have been used extensively by numerous authors (Freeman, Hopfield, Hinton et al etc.; see e.g. Carpenter, 1989; Simpson, 1990 etc.).

The serious influence of the continuous threshold operators to the time course of component flows is evident in computer simulations (Purwins and Radehaus, 1988; Lábos et al., 1992; Lábos and Lábos; Lábos, 1992; Lewis and Glass, 1992; Chapeau-Blondeau and Chauvet, 1992). It is surprizing that this is taken as a fact of no or secondary importance.

1.1. THE UNIT PARADOX

The notion of *"paradox"* is neither enigmatic, mystical nor a cabalistic term. It may be e.g. simply a seeming contradiction waiting its elimination.

The paradoxical situation is most transparent when sigmoid threshold operators are applied. This results in "abnormal" or unphysiological phenomena so often that it cannot be neglected. The time courses seen in the amplitudes of *unit* activities (of the parts or components of the nets) become very diverse and - contrary to naive expectations - *rarely* resemble to spike-like oscillations. Moreover, these signals *often* similar to the potentials recordable usually only from a multitude of cells as e.g. in EEG or similar mass records, which *appear to be the closest but still not exact* real comparable cases. **Such behavior of units resembling to those of populations is the unit paradox.** This paradox - also like EEG - is closely related to the chaos in the behavior of units or nets (Freeman, 1987; Holden, 1986; Lábos, E. 1984-1992; Chapeau-Blondeau and Chauvet, 1992; Lewis and Glass, 1992).

The consequence of this is that the "neural nets" occurring recently in ANN (Artificial Neural Net) or NC (Neurocomputer) technology are far to be able of reproducing directly and completely the true (biological) neural, electrical behaviors which are otherwise also diverse but in different respects. Nevertheless, behind the name of "neural network" or by a worse name "connectionist nets" (which is also a

popular *pleonasm*) promising technological possibilities are included not only to simulate but even to implement quick parallel processing or computations.

1.2. SIMULATION OF NORMAL UNIT POTENTIALS

In neural modelling the reproduction of the recorded electrical signals is a routine task since the time these signals are recorded at all. Simulation published more frequently after the emergence of Hodgkin and Huxley equations (HH; 1952). However, very soon after the equations so called "reduced systems" also appeared (FitzHugh, 1969; Holden, 1982). Note that already the travelling wave version of the HH-equations leads to a peculiar mathematical instability (FitzHugh and Antosiewicz, 1959). This phenomenon is not restricted to a "suitable choice" of conduction velocity as it was claimed earlier and still recently (e.g. Miura, 1982), but emerges at almost *any* (very small) parameter perturbations (Lábos, 1982). This is still not equivalent to the much later observed chaotic behavior of the HH-equations (Aihara and Matsumoto, 1986).

The HH-type models are detailed but are not well suited for network simulations. That is why different simpler, and computationally easier - but still realistic - spike-generators were introduced (e.g. Lábos, 1984):

a.) - An interval map quickly producing eminent and uniform peak values with almost any interspike interval patterns (called a universal pattern generator = UPG; Lábos, 1981-85). These UPG-s are irregularly firing chaotic units, but may become more regular in nets. The generated fictitious spikes are acceptable for an electrophysiologist.

b.) - A slower spike generator, not universal in the above sense, less chaotic, encloses both activation and inactivation processes. It is still quick enough to use in nets. It is called PSG (= polynomial spike generator; Lábos, 1984; 1985). This model turned first the attention of the author toward paradoxical consequences. Despite of the very modest, *"realistic"* premises incorporated into the model, its temporal behavior becomes at certain parameters rather *"unrealistic"*. Note that this is also an apparent conflict and it is different from the unit paradox raised in Section 1.1.

2. METHODS

The models of units or nets are here as follows:

1. - Binary threshold gate nets (McCulloch and Pitts, 1943; followed by the emergence of threshold logic; see $\mathbf{T_0}$ above and Muroga, 1971).

2. - Neural nets with S-shaped non-degenerated soft threshold operators (Zadeh-Stein-Little-Hopfield and others; see e.g. $\mathbf{T_1}$ and $\mathbf{T_2}$; **S-model**). Sharp thresholds do not exist for action potentials (Cole et al., 1970).

3. - Interval maps producing spikes written here in two forms ((6) and (6a), Lábos, 1984).

$$y_{n+1} = my_n = \mathbf{L_1}(y_n) \quad \text{if } y_n \leq a \quad \text{and}$$
$$y_{n+1} = \mu y_n + \mu = \mathbf{L_2}(y_n) \quad \text{if } y_n > a \quad (6) \text{ or}$$
$$y_{n+1} = \mathbf{L}_1(y_n) - \mathbf{T_0}(y_n - a)(\mathbf{L_1}(y_n) - \mathbf{L_2}(y_n)) \quad (6a)$$

where e.g. $m = 1 + (a-1)^2$ and $\mu = 1/(a-1)$ and $a = 0.1$. This is the map called above UPG. It may generate realistic spikes and is capable of reproducing any finite interspike interval patterns which performance is believed often to be a property of complicated networks. It is a "chaotic iteration" as **Fig. 1.** suggests is not equal to the well known tent-map, which is not adequate at all for neural spike production. Further versions - still spiking ones - have been defined to simulate more uniform spike amplitudes, after-hyperpolarization (AHP), more regular repetition rate etc. In these models the "universality" becomes restricted or may disappear.

4. - Spikes or waves generated by various systems of HH-like equations (from 1952 up to now). A large number of versions exist forming a "separate world".

5. - Realistic motion equations, like that of PSG (Lábos, 1984; **Fig 2**):

$$W = Z + a(Z-r)(Z-p)(Z-s) + bX^3 + cY^4 + k/(Z-s) \quad (7)$$

where $W = A_{n+1}$, $Z = A_n$, $Y = A_{n-1}$, $X = A_{n-2}$, $a = -1.2$, $p = 0$, $r = 1$, $s = -0.2$, $b = -0.675$, $c = 0.225$ in "standard parameter assignment". This is a "weakly chaotic" iteration incorporating principles similar to those included in HH-equations, but despite of this

may display unphysiological dynamics. It runs quickly on computers and is still suitable for nets. One of its weakness is the too rapid decay phase after the peak of spikes.

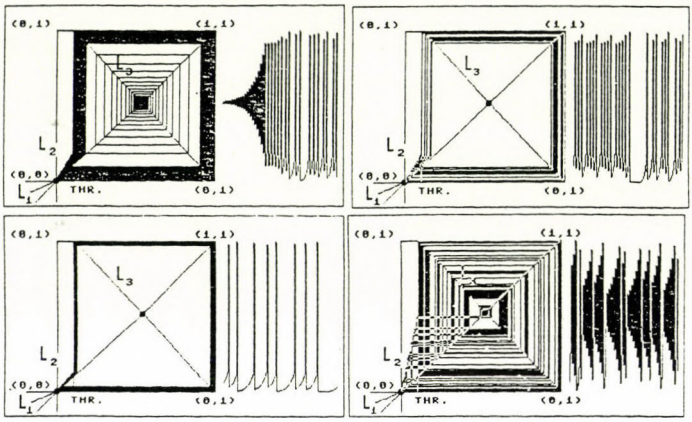

Fig.1.: Spike sequence generated by equation (6). A universal pattern generator (**UPG**). Its spikes are acceptable for electrophysiologists, regardable as good unit signals. It has now more than ten, more or less different versions.

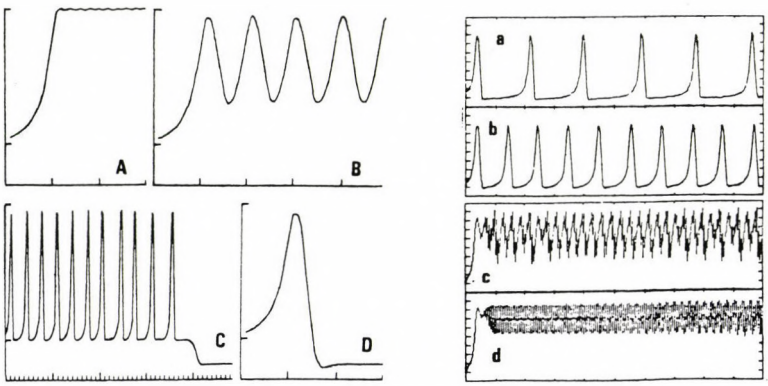

Fig. 2.: Samples of flows generated by **PSG** defined by equation (7). Its behavior can be both "normal spiking" and also can display unphysiological or even artificial or phantom oscillations.

6. - Further dynamical systems with one or more variables connected or not in nets. The number of units and variables may be different from each other.

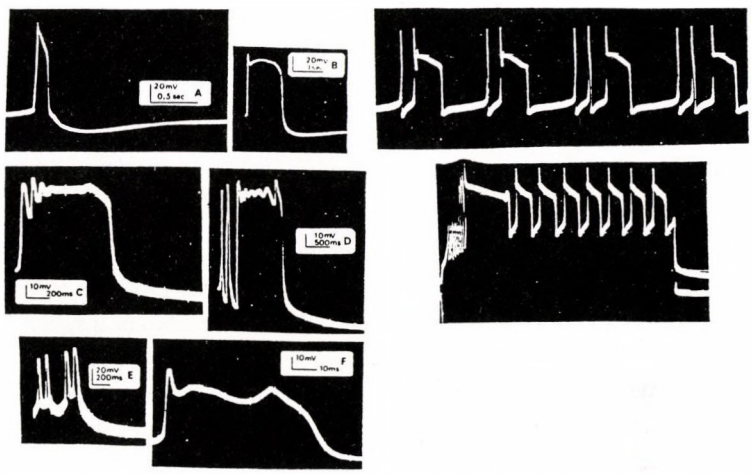

Fig. 3.: A collection of *natural, abnormal* but *unit* potentials supporting together with **Fig 4** that the *abnormalities accompanied to S - models* are *different* from these. Cases A to D and F were obtained in low calcium/TEA milieu from snail neurons. The records on right are electrically evoked peculiar unit responses, while case E on the left side appeared in the presence of cocaine.

3. RESULTS

An exhaustive survey of simulations by various spike or potential generators is not presented here only few illustrations. The first conclusion is that *despite apparently realistic suppositions* in the models, the *consequences* are often *unrealistic.* This is not yet the unit paradox. It is a phenomenon almost ubiquitous in various *extrapolations*. Its peculiarity is still holds since e.g. for PSG the presuppositions are modest and seems real. Its wild dynamical ranges are unexpected but exist.

The second observation is the *unit paradox* which is expected for S-models *as a consequence of the use of mass measurement characteristics for units.*

The PSG shows parameter dependent spikes or waves, while components of FNN-s with sigmoid response curve almost always display strange component flows (**Fig. 2** and **4**). Different behaviors in different components also occur: either chaotic or fixed points or even "softer than chaotic" oscillations.

3.1. EXOTIC NATURAL OSCILLATIONS

Exotic phenomena are observable not only in the models but very often also in biological preparations: plateaus, paroxysmal depolarization shifts, reexcitations etc. (see in Chalazonitis and Boisson, Eds., 1978). Modelling dynamical systems capable of simulating, - let say spike-like autoactive oscillations - similar peculiarities may occur. These models incorporate several non-zero parameters. Modification of these may result both in dynamical behavior that is observable or on the contrary never seen in living preparations. New phenomena are occasionally useful in predicting new facts but this happens usually after introducing further "structural" (i.e. deeper) modifications of the equations of motion. However, frequently, the exotic oscillations in models represent "phantom-motions" which appears to be unrealistic (i.e. artificial) and not only unphysiological (in the sense of pathological or being influenced by special substances like in **Fig. 3**). The phantom solutions may occur also in numerical "solutions" of ordinary or differential equations (Yamaguti and Ushiki, 1981; Potts, 1982. Compare the "shapes" collected in **Fig. 3 and 4.**: the differences are remarkable.

In equation (6a) the threshold opersator $\mathbf{T_0}$ is incorporated into the spike generator system (called UPG) to approach the different models. It seems rather promising to study further what happens if in this particular case the $\mathbf{T_1}$ or $\mathbf{T_2}$ or other sigmoid operators were introduced instead of $\mathbf{T_0}$ used. Probably, either exotic or phantom potentials would appear.

3.2. THE UNUSUAL WAVES IN NETS WITH SIGMOID OPERATORS

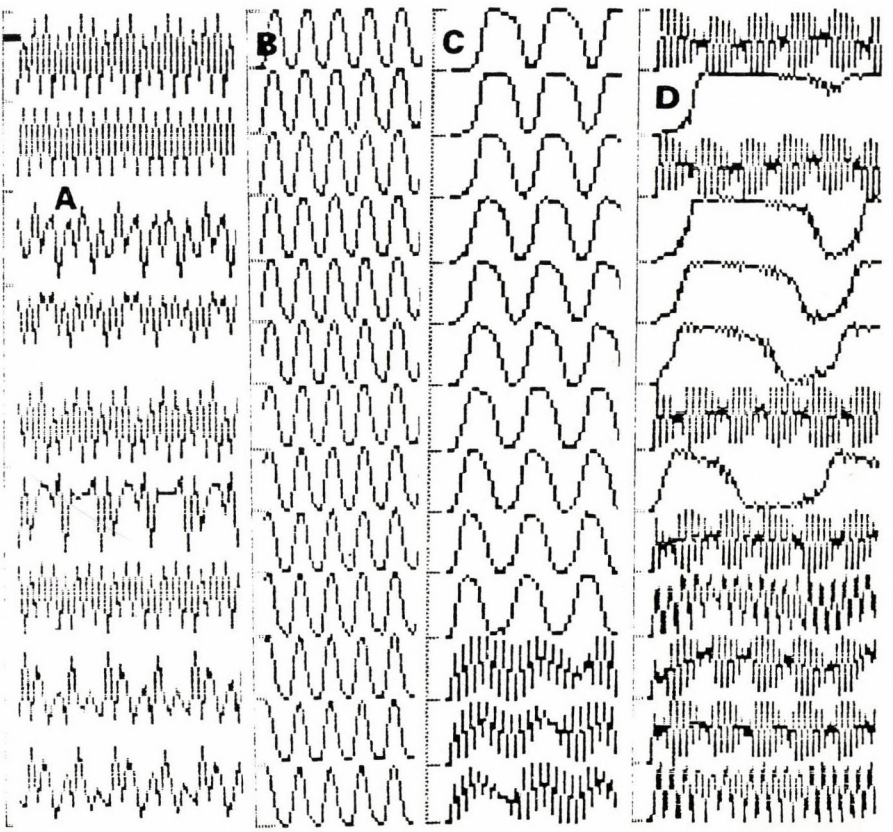

Fig.4.: S-model records. The waves resemble *mostly* to EEG waves and generated by special asymmetric matrices. The nets consist of 9, 13, 13, 13, 13 neurons resp. These are generated by units of models but are very far from behaviors of those of biological units. The generator equation was *equation (4)*. The matrices have beeen defined in details by the author between 1980-1988 several times.

4. DISCUSSION

4.1. AMBIGUITY OF SIGNALS OF BINARY THRESHOLD GATES

In the McCulloch-Pitts (MCP) model (1943) only two signals, zero and one occur. *The model was clearly motivated by the law of "all or nothing", thus the signals represented potential amplitudes and not repetition rates or probabilities.* The sigmoid curves of ANN-s or NC-s are claimed (in formal sense correctly) as extensions of the binary case. Sometimes the "all or nothing" law is quoted suggesting that the zero corresponds to a resting state and the "1" to a full activation. Contrary to this, the S-curves ($\mathbf{T_1}$ and $\mathbf{T_2}$) are also claimed to be response curve as "frequencies" or "repetition rates". For rates a *"law of all or nothing" does not exist*. This is explicit in publications when the $\mathbf{T_0}$ and $\mathbf{T_1}$ or $\mathbf{T_2}$ are compared without a suitable care: i.e both formally and also from semantical point of view.

The continuous functions $f \in C^1$ (f(t)), corresponding to an electrical records obtained from single nerve cells - either extra- or intracellular unit potentials - or (less often) even from mass of cells - **incorporate spikes** (e.g. in epileptic EEG). These may lead also to a zero/one sequence. The procedure is described in Lábos (1980) and a scheme is given in **Fig. 5.** Here the zeroes and ones do not correspond to amplitudes of spikes but to temporal frequencies or densities. The derivation is as follows: *(1)* Take a constant value c = c(t) = const for all t (moment). Draw it at about the middle of peak-to-peak range of spike sequence record; *(2)* Label the moments of intersections of constant function c and the f(t) record when the spikes are just rising up (i.e. when their time derivative is positive); *(3) Replace the spikes by this time points of intersections; (4)* Thus a point-process is obtained which is more or less regular; *(5)* Divide the time period (time axis) by disjoint, completely covering, semi-closed intervals of identical lengths *d*; Step *(5)* leads to the time base of discretization; *(6)* If the *d* length of these intervals is large enough then inside a single interval 0,1,2,3 or more points might occur; *(7)* **If d is not larger than the minimum length interpoint (= interspike) interval of the observation period of finite length, then only one or zero number of spikes will fall into these small intervals.** Thus the 0 or 1 values may be both temporal repetition rates and amplitudes not speaking about further interpretations.

Analogous statements can be elaborated for sigmoid curves. But their measurement is always carried out by averaging. It is surprizing that the ambiguous interpretation of the S-shaped characteristics is not stressed enough in ANN-technology since also for electrical circuits both amplitude- and frequency-response curve are defined. Both of them can be S-shaped. However, the frequency concept of an engineer is different from the repetition rates of spikes. As soon as such vague meanings are clarified then the seeming contradiction - i.e. the unit paradox itself - disappears.

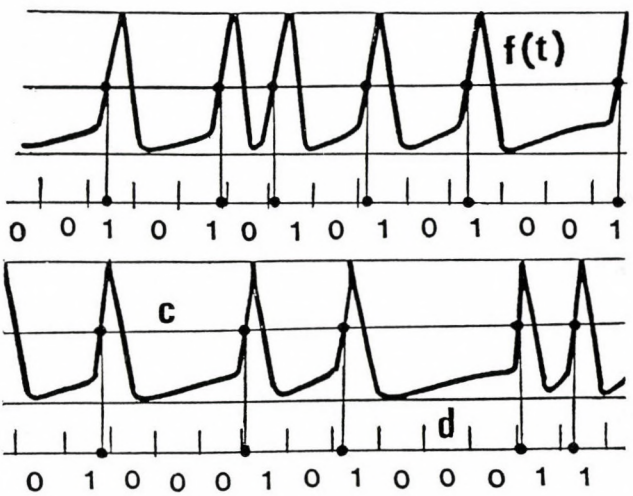

Fig. 5.: A canonical derivation of a zero/one string from a continuous spike record. Its meaning is here a **temporal frequency plot against discrete time** and not necessarily a time variation of an amplitude.

4.2. SPIKELESS NORMAL TRANSMISSION

Beyond spikes and subthreshold waves biological oscillations not corresponding to text-book spikes also occur. Neither the natural spiking nor these spikeless oscillations are digital in technological sense. Both of them are analogue processes. The analogue

vs digital dichotomy (revisited in 1990 by Hopfield) appear to be only metaphorically relevant for the observable neural signals: the spikeless transmission is not equivalent with analogue processing. The main reasons why spikes give still often the illusion of "digital" character are as follows: *(1)* they are countable since have eminent peak amplitudes; *(2)* synaptic time lag; *(3)* spikes are followed by refractory period of varying duration. Spikeless transmission is a term in physiology. These waves do not rise up and decay suddenly and their time courses or amplitudes are more variable or usually not followed by dead time. Prominent examples are listed in Roberts and Bush (Eds., 1981; see also Falk and Fatt, 1974; Horridge, 1968; Fieandt and Moustgaard, 1977 etc.). Nervous transmission is not always mediated by spikes and spikes are observable also in non-neural cells too. It is also true that the important notion of *threshold* even for unit potentials is also more practical and metaphorical than real (see Cole et al., 1970). However, the text-book shapes of "no impulse" records are dissimilar to S-model unit signals.

Nevertheless, the soft (S-shaped) threshold operators do not increase the goodness of artificial neural networks as models of real ones. One of the causes of this is the confusion of hierarchical levels: units and nets. The EEG seems to be a spikless mass-product to which S-model unit records resemble most.

4.3. ON NATURAL ABNORMAL OR EXOTIC POTENTIALS

It is necessary to underline that an additional and also paradoxical possibility may emerge as well. A potential of biological origin may be called exotic or abnormal or unphysiological if it differs from the most often occurring synaptic potentials and spikes or if the conditions are pathological or artificial. These enclose rather informal definitions which strongly depend on the context. In the neurological diagnostic procedures and also in neuropharmacology an immense set of examples can be collected as "abnormalities" (see e.g. in Chalazonitis and Boisson, Eds., 1978): plateau potentials, paroxysmal depolarization shifts, reexcitations, certain bursts, spike-and-wave complexes and many others. However in artificial neural nets *not* these *realistic abnormal instead rather unrealistic waves* emerge frequently.

4.4. WHAT IS A UNIT AND WHAT IS A UNIT SIGNAL?

Two opposite trends are strictly observable in the various fields of electrophysiology: (1) The Virchowian *"cell as a unit"* concept is not tenable in neurosciences. It is sometimes necessary to decompose a morphological unit into several functional ones; (2) In the opposite trend groups, *pools, assemblies of neurons* are regarded as functional units consisting of either (a) identical or (b) different cells with or without intrinsic interconnections. Both concepts have been discussed several times - not only in biology - in various ways depending on goals or based on facts supporting either a decomposition or a unification. Interesting and relevant views are expressed about the notion of "unit" by Weiss (1971).

4.5. A NATURAL PROPOSITION TO ELIMINATE THE UNIT PARADOX

The alternative explanations of wave - shapes emerging in S-model units may be as follows: *(1)* these are *spikes*; *(2)* they are similar to *natural abnormal* potentials; *(3)* the unit signals correspond to normal unit potential corresponding to *spikeless, graded* operation; *(4)* unit records of ANN are similar to *natural mass* - potentials; *(5)* the records are unnatural, *phantom* - oscillations.

Version *(1)* is not is acceptable **(Fig 4.)**. Curves of **Fig 3** speak against case *(2)*. The case *(3)* was discussed above. The *heterogeneity* of oscillations in *S-models* speaks against this version. The cases *(4)* and *(5)* remain plausible. The inconsistent use of pool-characteristics to units and frequent similarity to EEG speaks for version *(4)* as a closest natural analogy. If version *(5)* is accepted then the artificial nets are not less good models of natural ones *in this respect*. Other similarities appear to be more adequate: connections, parallel processing, etc.

The above considerations show that it is a possible explanation of the unit-paradox that the *ambiguity* of unit steps and S-shaped curves which are attributed to units but never obtained by single measurements from single units. They can represent both amplitudes or repetition rates. The notion of input/output curve alone is an insufficient definition, usually without specified meaning. These can represent - at least

in principle - a multitude of measurable quantities, in special case the output - as it is often claimed - would correspond to the repetition rate of discharges. The ambiguity of interpretation is already expressible in the degenerated case, i.e. for McCulloch-Pitts neurons, where the response can be regarded **sometimes as an amplitude (allusion to the all or nothing law) but in other reasoning as a true repetition rate** of uniform events supposed that the time on which the activity takes place is divided into sufficiently small boxes. This results in one or zero number of events (see Section 4.1). The repetition rate of spikes as an output - instead of amplitude - might be a meaning in case of S-shaped operators and in fact this meaning occurs often. Thus to "eliminate" the paradox (i.e. this apparent contradiction) it is first necessary to discriminate *at least* two model-classes of units and consequently their nets: one for amplitudes and one for rates. Nevertheless, the "integration time" required to compute **temporal average** remains a residual parameter to specify, which corresponds to the d length of dividing intervals (see Section 4.1). On the contrary, the spatial averaging of multiple representations of the same or similar inputs seems a quicker **"parallel averaging"**. Confusions emerge as soon as units and nets or character of inputs/outputs are not specified in a clear manner. Similar problems appear always if macroparameters of neuron pools are confused with individual parameters like the time course of a single spike.

The situation may become more complicated if the sigmoid characteristic is regarded as representing "probabilities", which is done mainly with the $\mathbf{T_1}$ operator. In this case also a population characteristics is accompanied with a single cell.

5. SUMMARY

The ambiguous or vague suppositions may lead to artificial unphysiological consequences (e.g. to waves of non-living appearence), in neural network simulations. In the case of functions including S-shaped thresholding ($\mathbf{T_1}$, $\mathbf{T_2}$) *attributed to units,* the time courses of unit signals may differ radically from natural unit potentials. Waves of ANN-s resemble mostly to those of EEG (whose the origin attributed to mass activity). This is the closest but still not exact living analogy. It seems frequently and formally valid. Moreover, often the ANN oscillations are unnatural but not similar to unphysiological waves observable in living cells. The possible source of this contradiction is that sigmoid characteristics are measured either on a unit by repetition or taken from data valid to a pool of units. The inconsequent *applications of these mass-operators to units* is acceptable at best only if all considerations are probabilistic. However, in such an interpretation the values are probabilities or mean values and not

amplitudes or rates. *A semantical clearing i.e. a tabula rasa is required and also is sufficient to eliminate the seeming contradiction what I called a unit paradox.* The almost ubiquitous unrealistic zones of simulation records are most evident in nets of units with sigmoid threshold operators, while the ambiguity of interpretation is already evident in case of binary signal generators. But the models or implementations of ANN-s resemble to natural ones but almost only in parallel processing and connections or also - if incorporated - in learning. This debate is initiated in order to clarify and separate formal aspects and meanings in neural network simulations.

ACKNOWLEDGEMENTS: This work was supported by OTKA 2621/1991 and ETT-T032/1990 Grants.

REFERENCES

Aihara, K. and Matsumoto, G. (1986) Forced oscillations and routes to chaos in the Hodgkin-Huxley axons and squid giant axons. In: Chaos in Biological Systems (Eds.: Degn, H., Holden, A.V. and Olsen, L.F.), NATO ASI-138, pp. 121-132., Plenum Press, New York.

Chalazonitis, N. and Boisson, M. (1978) Abnormal Neuronal Discharges. Raven, New York.

Carpenter, A. G. (1989) Neural network models for pattern recognition and associative memory. Neural Network 2, 243-257.

Chapeau-Blondeau, F. and Chauvet, G. (1992) Stable, oscillatory and chaotic regimes in dynamics of small neural networks with delay. Neural Network 5, 735-743.

Cole, K. S., Guttman, R. and Bezanilla, F. (1970) Nerve excitation without threshold. Proc. of NAS. 65, 884-891.

Falk, G. and Fatt, P. (1974) Limitations to Single - Photon Sensitivity in Vision. In: Lecture Notes in Biomathematics, Vol 4, pp. 171-197. Springer, Berlin.

Fieandt, K. and Moustgaard, I.K. (1977) The Perceptual World. Academic Press, London.

FitzHugh, R. (1969) Mathematical models of excitation and propagation in nerve. In: Biological Engineering (Ed.: Schwann, H. P.). McGraw Hill, New York.

FitzHugh, R. and Antosiewicz, H. A. (1959) Automatic computation of nerve excitation - Detailed corrections and additions. J. Soc. Indust. Appl. Math., 7, 447-458.

Freeman, R. (1987) Dynamical models of neural function that generate chaos. IBRO, 1987, Budapest, Neuroscience Suppl. 22, 297S. S99.

Hodgkin, A. L. and Huxley, A. F. (1952) A quantitative description of membrane current and its application to conduction and excitation in nerve. J. Physiol. 117, 500-544.

Holden, A.V. (1982) The Mathematics of Excitation. In: Biomathematics 1980 (Eds.: Ricciardi, L. M. and Scott, A. C.), North-Holland, Amsterdam.

Holden, A. (Ed; 1986) Chaos. Manchester UP, Manchester.

Hopfield, J. J. (1990) The effectiveness ofanalogue "neural network" hardware. Network 1, 27-41.

Horridge, G. A. (1968) Interneurons, Freeman and Co., London.

Lábos, E. (1982) On the stability of the travelling wave and imperfect current clamp solutions of the Hodgkin-Huxley nerve equations (In Hungarian). 47th Annual Meeting of Hungarian Physiological Society: P300.

Lábos, E. (1984) Periodic and non-periodic motions in different classes of formal neuronal networks and chaotic spike generators. In: Cybernetics and System Research 2 (Ed.: R. Trappl), pp. 237-243. Elsevier. Amsterdam

Lábos, E. (1985) Spike-Generating Dynamical Systems and Networks. In Lecture Notes in Economics and Mathematical Systems No 287. Dynamical Systems (Eds.: Kurzhanski, A. B. and Sigmund, K.), pp. 189-206. Springer, Berlin.

Lábos, E. (1987) Chaos and Neural Networks. In: Chaos in Biological Systems (Eds.: Degn, H., Holden, A. V. and Olsen L. F.), NATO ASI -138. pp. 195-206. Plenum Press. New York.

Lábos, E., Holden, A. V., Laczko, J., Orzo, L., Lábos, A.S. (1992) Fuzzy Operators and Cyclic Behavior in Formal Neuronal Networks. In: Proc. of NAFIPS 92 (Puerto Vallarta, Mexico), Publ. by NASA, CP 10112, Houston., Vol.2, pp. 545-554.

Lábos, E., and Lábos, A.S. (1992) Non-Autonomous Fuzzy Threshold Operators in Formal Neuronal Networks. In: Symposium Proceedings, KFKI-1992-32C, pp. 93-101.

Lewis, J. E. and Glass, L. (1992) Nonlinear dynamics and symbolic dynamics of neural networks. Neural Computer. 4, 621-642.

Maren, A., Harston, C. and Pap, R. (1990) Handbook of Neural Computing Applications. Academic Press, New York.

McCulloch, S. W. and Pitts, W. (1943): A logical calculus of the ideas immanent in the nervous system. Bull. Math. Biophys. 5, 115-123.

Miura, R. M. (1982): Accurate computation of the stable solitary wave for the FitzHugh - Nagumo-equations. J. Math. Biology, 13, 247-269.

Muroga, S (1971) Threshold Logic and Its Application. Wiley - Interscience, New York.

Nográdi, E. and Lábos, E. Pseudorandom Interval Maps for Simulation of Normal and Exotic Neuronal Activities. In: Cybernetics and System 86 (Ed.: Trappl, R.), pp. 427-434., Reidel, Amsterdam.

Potts, R. B. (1982) Nonlinear difference equations. In: Nonlinear Analysis. Theory, Methods & Applications 6, 659-665.

Purwins, H.G. and Radehaus, Ch. (1988) Pattern Formation on Analogue Parallel Networks. In: Neural and Synergetic Computers (Ed. Haken, H.), Springer Series in Synergetics Vol 42, pp. 137-154. Springer Verlag, Berlin.

Roberts, A. and Bush, B.M.H. (1981) Neurons Without Impulses. Cambridge University Press, Cambridge.

Simpson, P. K. (1990) Artificial Neural System. Pergamon Press, New York.

Weiss, P. (1971) The Basic Concept of Hierarchic Systems, In: Hierarchically Organized Systems In: Theory And Practice, Hafner Publ.Co. Inc., pp. 1-43.

Yamaguti, M. and Ushiki, Sh. (1981) Chaos in numerical analysis of ordinary differential equations. Physica 3D, 618-626

Zadeh, L.A., Fu, K-S, Tanaka, K. and Shimura, M. (1975) Fuzzy Sets and Their Application to Cognitive and Decision Processes. Academic Press, New York.

Received 11 February 1993
Accepted 28 June 1993

Neurobiology 1 (3), pp. 223-234, 1993

DEVIATION CODE IS A PROSPECTIVE CANDIDATE OF THE COMMUNICATION BETWEEN ADAPTING NEURONS

László Orzó

1st Department of Anatomy, Semmelweis Medical School
Budapest IX. Tűzoltó u. 58, H-1450 Hungary

Summary: The low Firing Rate (FR) of pyramidal cells (Thorpe et al., 1989, Pettigrew et al., 1968) prevents the use of rate coding. The Deviation Code (DC), in which the deviation from the mean is the signal, is a candidate code that may be used in neurobiological and formal neural networks. The neurons which use this code could have similar properties as the model neurons frequently used by the neural network (NN) theories. The biological verification of this type of coding is required. This coding might be relevant in the physiological investigation of learning rules and can help to understand the organization of different nuclei of the nervous system.

Key words: Neural code, Deviation Code, Neural Networks, Adaptation, Firing Rate

INTRODUCTION

It is still an unsolved question how neurons communicate with each other in the cortex (Abeles, 1982; Mitchison et al., 1990). Information between peripheral neurons and central nuclei of the nervous system could be transmitted in the code of the firing rate, i.e. by a rate or frequency code (Kandel & Schwartz, 1985). Here we consider the deviation of the firing rate as a code (Perkel & Bullock, 1968). In this model we assume that the adapting neurons principally measure the deviation of the input and transform this to the deviation of the output. Adaptation prevents measuring the mean value of the input. Adapting neurons cannot

use the rate code because if only some critical element of a network are adapting, then the network firing rate pattern could easily extinguish. Another problem with rate codes, from NN theory is that a soft threshold gate (Labos et al., 1992) could destroy the applicability and appropriateness of a rate code. (In real systems there could exist chaotic firing properties too (Mpitsos et al., 1982; Gallez et al., 1991)). In the case of sparse connectivity or the continuous Hopfield neurons network, the model neurons do not tend to have fix states as a McCulloch-Pitts neurons (McCulloch & Pitts, 1943)), rather some type of distribution of the states (Derrida et al., 1987; Derrida et al.,1989).

Here we present models for the information transmission by a derivation code, for the recoding from a rate code to a deviation code, for the decoding from DC to FR, and provide some calculation on the usefulness of this code and the first steps of the implementation of DC into the NN theory.

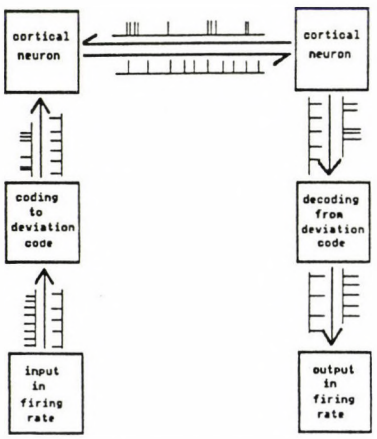

Fig. 1: Block shame of the model information transmission in the central nervous system.

In neural network theory one objective problem is the low firing rate of real neurons. From the information theoretical point of view it would be efficient for the cells to communicate with each other on high frequency (half of the maximal frequency would be the optimal). There must be reasons of the low firing rates. These could be:

1, Erroneous activity could not be filtered out easily (such as epileptiform activity).

2, With a high firing rate it is difficult to change the firing patterns. Especially if the neurons are strongly interconnected.

3, It seems to be difficult to have an efficient parameter control on high firing rate.

4, From energetic point of view high firing rate is far from the optimum.

5, Even at the highest firing rate there is small number of incoming spikes in the integration time of a neuron and so the delays and faults of transmission and the slow and stochastic processing elements (Burnod, et al., 1989) could lead to erroneous measurement of the input.

6, Smallest effects of fatigue of the cells could cause the collapsing of the firing rate pattern.

7, The input patterns of the brain always not only spatial but spatiotemporal templates. In the case of high FR there could be very little influence of the temporally succeeding part of the patterns on the neural response.

METHOD

Presume a normal distribution of input on a cell, the coefficient of variation for this distribution is σ/a. Where 'a' is the mean or expectation value and 'σ' is the standard deviation. The coefficient of variation of the square of the standard deviation is square root two. From this it can be seen that if the expectation value (firing rate) is small, then it is much more beneficial to measure the deviation then the mean or expectation value.

Equations:

$$a=\langle x\rangle$$

$$\beta^2=\langle((x-a)^2-\sigma^2)^2\rangle=2\sigma^4$$

$$\sigma/a\geq\sqrt{2}$$

Where:
a= expectation value
σ= standard deviation
β= standard deviation of the standard deviation's square

To model an accommodating neuron we assume a neuron with some threshold and sigmoid like input-output characteristic. (the spike emission probability is equal of the output value) At least two different ways of adaptation or accommodation can be distinguished:

a, The threshold of the cell follows of the input transitions. - See Fig. 2. a

b, Changed steepness of the sigmoid like cell transfer function. In this case the adaptability of the neuron is limited, and some type adaptation mechanism is also required. This could be produced by some inhibiting (Gabaerg) feedback or some type of fatigue. If the steepness of the transfer function increase then the output decrease, supposing that the median threshold is constant. - See Fig. 2. b

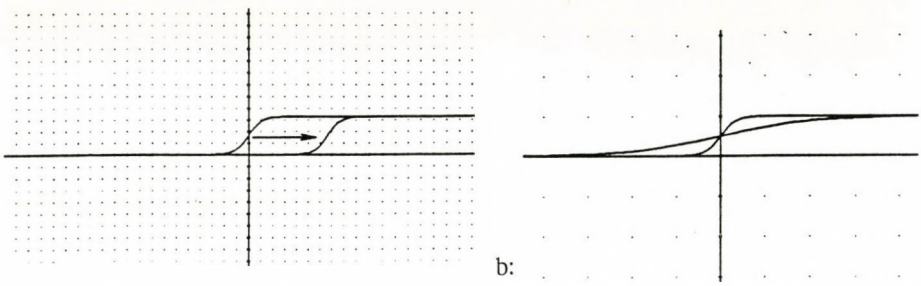

Fig. 2: a: The shift of the threshold could cause the adaptation of the neurons to the input. **b**: The change of the steepness of the sigmoid transfer function can cause the adaptation as well.

From biological point of view there is considerable difference between these mechanisms. Here we do not consider the elementary biological machineries of adaptation, only their effects.

How could an accommodating neuron measure its input deviation? In the case of first type of the adaptation the output's mean value is adjusted. The input's deviation can be transformed to a change of steepness of the sigmoid function:

$$y=\int \exp((x-a)^2/2\sigma^2)/(1+\exp(-kx+b)dx$$

Where:
a = expectation value
σ = standard deviation
k and b are the steepness and threshold parameters

That is σ can be transported to k!

Greater deviation leads to greater steepness of the sigmoid function, so to an increase of output deviation because of the difference between the expectation value of the output's square and the square of the expectation value is diminished in high steepness sigmoid function situation.

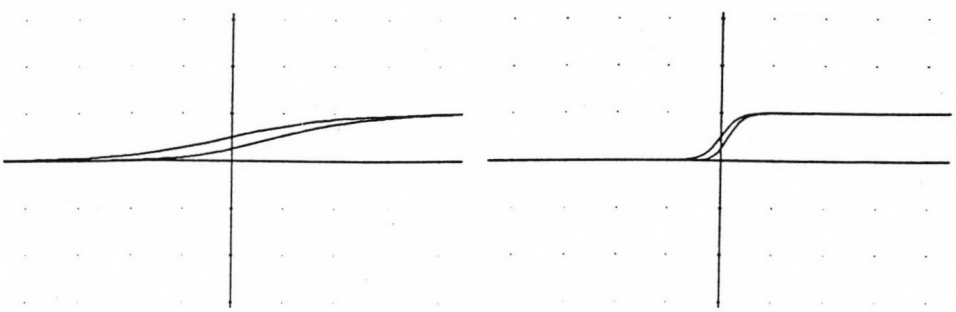

Fig. 3: The difference between the expectation value and the square's expectation value decreasing with the increasing steepness. So increasing deviation, leads to increasing the deviation of the output.

In the second case of adaptation a change of the input or the input deviation gives a tuning of the sigmoid function's steepness. High input or great input deviation cause an increase of the steepness of the sigmoid function. and lead to a greater value of the output deviation. So the effects of both type of adaptation is the same, and so they give some plausibility for the DC.

The output of a pyramidal cell is a spike sequence. The output value of the transfer function determines the probability of the spike emitted. In this case the fine structure of the output of the transfer function is not accessible from the spike sequence. There are needed one more assumption, that is the input value is changing slowly (the postsynaptic potentials exist much longer than the incoming spike). In this case the emitted spike chain corresponds much better to the output distribution. As an illustration two simulations of cells with the first type of adaptation at low or high incoming input deviations are shown in Fig. 4 a, and b.

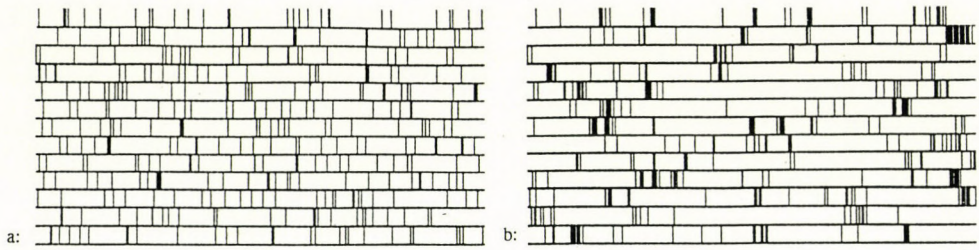

Fig. 4: The model's spiking output illustration **a**, at low input (output) deviation and **b**, at high input (output) deviation case.

This neuron shows a sigmoid relationship between the deviation input and deviation output functions. - See Fig. 5.

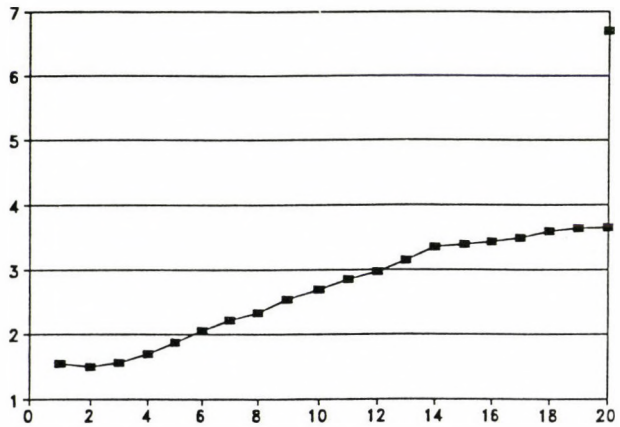

Fig. 5: The Model's sigmoid like deviation of input - deviation of output characteristic.

The coding from FR to DC could be carried out by several ways. All type of recoding it is necessary to give some additional noise to the input to get a some real distribution and so to get some fix deviation.

a, The second type of adaptation leads to an increase of the output's deviation on high input firing rates and to the decrease of the output's deviation on small input mean firing

rates. The limited adaptation property also leads to an increase of the output's firing rate but it can be filtered out later by some (or the same) adaptation mechanisms.

b, A non or slightly adapting cell can also be used. As the input grows the amplification factor of the cell increases. Thus if the cell has some standard noise input beside the FR input with the same deviation then the deviation of the output will follow the change of the firing rate. The firing rate of the output also follows it, but the adaptation of the subsequent neuron in the information processing could filter this rate signal out.

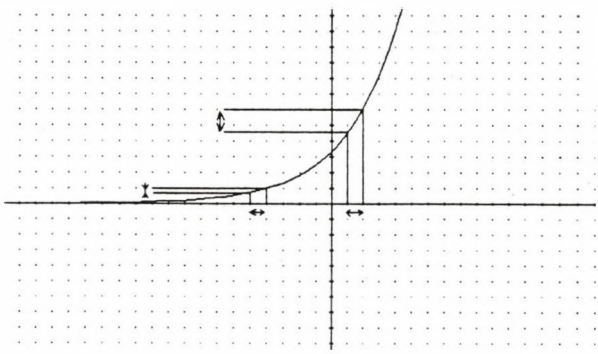

Fig 6: The model of the coding from frequency code to the deviation code. The increased input frequency by the same deviation input cause the increase of the output's deviation value.

In the cortex there might exist a 'generalization' that the firing rate of the pyramidal cells diminish as we proceed from the primer centers of the information processing to the higher (associative) centers (Shepherd 1990). It would be explained by the previous coding mechanisms. This coding skeleton could explain some features of the relay centers of the nervous system.

The decoding from DC to FR can be produced almost in the same way. If a non or slightly adaptable cell got input with different deviation the output's frequency grows rapidly and the deviation could not follow this increment and for a greater integration time the deviation decrease as the square root of the averaged number of input samples.

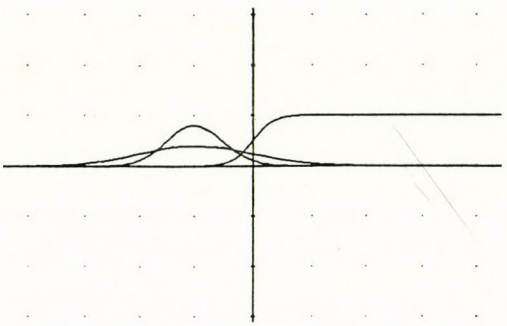

Fig. 7: The model of the decoding from deviational to frequency code. The increased deviation cause increased output and so increased firing rate on a non adapting neuron.

The DC to DC communication of the cells are controlled by the interconnection matrix (IM) but the weights are squared.

$$x_i = f(w_{ij} x_j)$$
$$\sigma^2_{i\ input} = w^2_{ij} \sigma^2_j$$
$$\sigma_i = f'(\sigma_{i\ input})$$

Where:
w_{ij}= interconnection weight between neuron i and j.
x_i = activity of neuron i (FR).
σ_i = standard deviation of the neuron i

In the case where the weights equals 1 or 0 the IM is the same for DC and for FR.

RESULTS

If this code is used in the cortex then these theoretical results would be expected:

1, The structure and the purpose of the thalamus becomes clearer. The main processing aim of the thalamic relay nuclei is the first step of coding the FR input signals to DC. The duty of the immense but powerless cortico-thalamic feedback to the relay cells would be to provide some noise (deviation) input to the relay neurons which can be amplify as function of the primary (FR) input. This type of input can not be neglected. If it would be replaced by a common but more ramified feedback then it could only perform as some

parameter control and can not execute this coding task. This noise feedback can be indicated as the "light" which made the "transparency" (input firing rate pattern) visible for the cortex.(Mumford, 1991)

2, There are other relay nuclei in the nervous system (ganglions), which roles are poorly understood (Shepherd, 1990). Such centers are relevant for the coding of the input and for the decoding of the output, so they could play an active role in the information processing of the nervous system.

3, From the information processing point of view there is needed one memory pattern (word, sentence, situation) which is active at the moment (instantaneous memory) and several (previous, earlier patterns) which are not 'active' but have some governing influence on the next active pattern (short term memory). The short term memory patterns exist from seconds to minutes. In the case of this code a pattern could be exist for this time period (it can't accommodate further). In this model the active pattern would be coded in FR for a short duration and it become to a same DC pattern as the result of the adaptation. This DC pattern could exist for a longer time period and could have some influence on the next patterns and on learning.

4, Other nuclei and transmitter systems (such as NA, A, Dopamine, Serotonin, etc.) can regulate the adaptable cells through parameter control and through the restriction of the adaptation. If an axon doesn't transmit spikes continuously it could convey some information by this type of code. The emergent noise or delivery problems, do not disturb the DC-ed information transmission.

5, In the artificial neural network theory symmetric interconnections are generally used between the neurons (Hopfield, 1982). The non-symmetric interconnection matrix leads to the loss of the guarantee of an energy (Ljapunov) function and so a loss of stability. In the case of sparse connectivity and some other cases, where emerges comparable problems (Tsodyks, 1988). In the case of the DC this type of connectivity can lead to the oscillation of the firing properties of the neurons, but cause only some shift in the deviation on a longer time scale.

6, Transmission delays easily yield to oscillating or chaotic behavior of the neural net, when the dynamic of the non delayed version was a stable fixpoint (Marcus & Westerwelt 1989). In the case of DC delays do not disturb the appropriate processing.

7, There are considerable hope for the storing the spatiotemporal patterns by the use of adaptational mechanism and by the use of different coding rules.

DISCUSSION

Only experiments can determine the reality of DC in the higher centers, e.g. cortex. The measurement that can decide if this code is in use practically or it is only a theoretical presentation, could be:

Measure on some higher center (cortical) neurons the mean firing rates and their deviations from these averages. Use some type of stimuli which has some effects on the cell. If there are no change in the values of the deviations after the adaptation, when the primary increased or decreased firing responses has been extincted, then there is unlikely that these cells are able to use this type of code. Other statistics that measure the deviation distribution of cells could be misleading, because different amplification factors and synaptic weights could have considerable effects on the actual incoming deviations.

There are other type of neurons (Connors et al., 1990) in the cortex: the intrinsically bursting and the fast spiking neurons (FS) however they are presumed to be gabaergic interneurons (FS) and takes part supposedly only in the regulation of the firing rates and the regulation of the autoactivity of the cortex.

The FR might be the only code in the case of non-adapting neurons (Gerstner et al., 1992). The pyramidal neurons, which are thought to take part in learning processes, are not from this class. In the cortex there may be relevance the FR (on short time scales) and the DC (for longer time scales) too. There are needed further investigations and empirical examinations to understand their interactions. If the DC is relevant, then the basic mechanisms of the learning, for example the LTP, desire further investigation (considering and concerning the state of the input and the output). The investigation of the model of adaptable neurons might lead to the deeper insight of the cortical information processing. The low firing rate and the adaptability of neurons have to lead to the withdrawal of the universality of the FR code. The various effects of noise in neuronal processes has quickly growing literature (Longtin, 1991). This type of code could add some new perspective to these articles.

ACKNOWLEDGEMENTS

This work was supported by the OTKA F5535/1992, 2621 and the 1-2/1991.ETT. grants.

REFERENCES

Abeles, M. (1982) Role of the cortical neuron: Integrator or coincidence detector. Isr. J. Med. Sci. 18, 83-92

Burnod, Y., Korn, H. (1989) Consequence of stochastic release of neurotransmitters for network computation in the central nervous system. Proc. Natl. Acad. Sci. USA 88, 352-356

Connors, B.W., Gutnick, M.J. (1990) Intrinsic firing patterns of diverse neocortical neurons. TINS. 13, 99-104

Derrida, B., (1989) Distribution of activities in a diluted neural network. J. Phys. A: Math. Gen. 22, 2069-2080

Derrida, B., Flyvbjerg, H. (1987) Distribution of local magnetization in random networks of automata. J. Phys. A: Math. Gen. 20, L1107-L1112

Gallez, D.,Babloyantz, A. (1991) Predictabiliy of the human EEG: a dynamical approach. Biol. Cyb. 64, 381-391

Gerstner, W., van-Hemmen, J.L. (1992) Universality in neural networks: the importance of the 'mean firing rate'. Biol. Cyb. 67, 195-205

Hopfield, J.J. (1982) Neural networks and physical systems with emergent collective computational abilities. Proc. of the National Acad. of Sciences USA, 79, 2554-2558

Kandel, E., Schwartz, J.H. (1985) Principles of neural science. Elsevier, North-holland. 292

Labos, E., Holden, A.V., Laczko, J., Orzo, L., Labos, A.S. (1992) Fuzzy operators and cyclic behavior in formal neuronal networks. Proc. of NAFIPS'92/NASA Conf., Puerto Vallarta, Mexico. 2, 545-554

Longtin, A., Bulsara, A., Moss, F. (1991) Time-Interval Sequences in Bistable Systems and the Noise-Induced transmission of Information by Sensory Neurons. Phys. Rev. Lett. 67, 656-659

McCulloch, W.S., Pitts, W. (1943) A logical calculus of the ideas immanent in nervous activity. Bulletin of Mathematical Biophysics, 5, 115-133

Mitchison, G., Miall, C. (1990) Enigma of the cortical code. TINS. 13, 41-43

Marcus, C.M., Westervelt, R.M. (1989) Dynamics of analog neural networks with time delay. Advances in Neural Information Processing Systems I, San Mateo, 568-576

Mpitsos, G.J., Burton, R.M., Creech, H.C., Soinila, S.O. (1982) Evidence for chaos in spike trains in neurons that generate rhythmic motor patterns. Brain Res. Bull. 21, 529-538

Mumford, D. (1991) On the computational architecture of the neocortex: I. The role of thalamo-cortical loop. Biol. Cyb. 65, 134-145

Perkel, H., Bullock, T.H. (1968) Neural Coding. Neurosciences Research Program Bulletin. 6, 221-344

Pettigrew, J.D., Nikara, T. and Bishop, P.O. (1968) Responses to moving slits by single units in cat striate cortex. Exp. Brain. Res. 6, 373-390

Shepherd, G.M. (1990) The Synaptic Organization of the Brain. Oxford University Press.

Thorpe, S.J., Imbert, M. (1989) Biological Constraints on Connectionist modelling. Connectionism in perspective. ed. Pfeifer, R. Elsevier North-Holland pp. 63-92
Tsodyks, M.V. (1988) Associative Memory in Asymmetric Diluted Network with Low Level of Activity. Europhys. Lett. 7, 203-208

Received 11 February 1993
Accepted 23 July 1993

Neurobiology 1 (3), pp. 235-240, 1993

IN SITU HYBRIDIZATION WITH DIGOXIGENIN LABELED OLIGONUCLEOTIDE PROBES: DETECTION OF CAMK-II GENE EXPRESSION IN PRIMARY CULTURES OF CEREBRAL ENDOTHELIAL CELLS

I. Krizbai[1], M. Deli[1], I. Lengyel[1], K. Maderspach[2], M. Pákáski[3], F. Joó[1] and J. R. Wolff[4]

[1]Laboratory of Molecular Neurobiology, Institute of Biophysics, Biological Research Center, Szeged Hungary; [2]Institute of Biochemistry, Biological Research Center, Szeged Hungary; [3]Central Research Laboratory, Albert Szent-Györgyi Medical University, Szeged Hungary; [4]Department of Anatomy, University of Göttingen, Göttingen, Germany

Summary: A better understanding of the regulation of gene expression under physiological and experimental conditions is one of the most important goals of today's neurobiology. In order to accomplish this task a number of in-situ hybridization methods have been elaborated. In the past few years the use of nonradioactive procedures have gained more and more space among these efforts. One of the most promising methods in this field is the application of digoxigenin-labeled probes, which have been used successfully in several laboratories. Here we present a rapid method providing good spatial resolution and low background labeling for the detection of messenger RNAs in various cell culture systems using digoxigenin-labeled probes. By using oligonucleotides complementary to the α and β subunit of the calcium/calmodulin dependent protein kinase II (CAMK-II) we were able to demonstrate the presence of this enzyme in cultured cerebral endothelial cells, an enzyme that plays an important role in mediating the effects of extracellular signals.

Keywords: CAMK-II, in situ hybridization, gene expression, neuronal cultures, cerebral endothelial cell culture, CNS

INTRODUCTION

In-situ hybridization is the most widespread technique to detect mRNA and thus to study gene expression in various cells and tissues. In the past decade various kinds of methods have been developed for in-situ hybridization. The labeled probe can be either single or double stranded DNA, cRNA or a synthetic oligonucleotide probe (Lewis et al., 1988). The use of oligonucleotides has the advantage that it does not require a well-

equipped molecular biological laboratory. The oligonucleotide probes could be synthesized by automated apparatus and were used successfully in several studies (Angood et al., 1991; Burgin et al., 1990; Persohn et al., 1991; Réthelyi et al., 1989). They can be labeled with deoxynucleotides containing radioactive isotopes (^{3}H, ^{32}P, ^{35}S), or nonradioactive markers using terminal deoxynucleotidyl transferase for 3-end labeling (Lewis et el., 1988). Alternatively, T4 polynucleotide kinase can be used for 5-end labeling with ^{32}P.

In order to avoid the hazard provided by the use of radioactive isotopes and to obtain a better cellular resolution several nonradioactive methods have been developed and used successfully in the past few years. The best results have been achieved by using biotinylated cDNA probes or biotinylated oligonucleotide probes (Larsson, 1989; Ozden et al., 1990). Different detection systems have also been developed using peroxidase, alkaline phosphatase conjugated anti-biotin antibodies, gold labeled antibodies for electron microscopical detection or chemiluminescent methods.

An alternative possibility is the use of digoxigenin 11-dUTP labeled cDNA or oligonucleotides (Digoxigenin Application Manual Boehringer Mannheim, 1989; Sommer et Tautz, 1991) or cRNA labeled with digoxigenin 11-UTP. Here we present our results obtained by using DIG 11-dUTP oligonucleotides combined with an alkaline phosphatase detection system for the visualisation of specific mRNA-s in tissue cultures of central nervous origin.

We have focused our interest on the calcium/calmodulin dependent protein kinase II and we have demonstrated for the first time its presence in cultured cerebral endothelial cells, a cell layer that participates in the formation of the blood brain barrier.

MATERIAL AND METHODS

Preparation of labeled probes

Synthetic oligonucleotide probes complementary to the nucleotides 1439 - 1470 of the α-subunit mRNA and nucleotides 1090 - 1128 of the β-subunit mRNA of the calcium/calmodulin dependent protein kinase II (CAMK-II) were synthesized and purified. The sequence is not present in the mRNA of other known subunits of CAMK-II (Burgin et al., 1990). A sense probe was also synthesized and used for control experiments. Oligonucleotides were 3-end labeled with DIG 11-dUTP (Boehringer) by terminal deoxynucleotidyl transferase (Boehringer) according to the following protocol. About 100 pmol oligonucleotides were incubated in 50 μl solution containing 1 x tailing buffer (5 x tailing buffer contains potassium cacodylate 1 mol/l, TrisHCl 125 mmol/l, BSA 1.25 mg/ml, pH=6.6), $CoCl_2$ 2 mmol/l, dATP 0.2 mmol/l, DIG 11-dUTP 20 μmol/l and terminal transferase 50 units for 1 hour at 37°C. The labeled probe can be used without further purification.

In-situ hybridization

The experiments were carried out on mixed glial and neuronal cell cultures and on rat brain endothelial cell cultures grown on glass coverslips coated with poly-L-lysine and collagen, respectively. Details of preparing these cultures have been described earlier (Pákáski et al., 1990; Kása et al., 1991). After removal of the medium and washing with PBS (pH=7.4) the cells were fixed in 4% paraformaldehyde in PBS for 5 min. Then the cultures were washed with PBS for 10 min., treated with HCl (0.1 N) for 20 min., and washed again with PBS (10 min.) followed by a proteinase K treatment (20 μg/ml in TrisHCl 100 mmol/l, EDTA 50 mmol/l pH=8) for 10 min. After a washing step (PBS 10 min.) each coverslip was prehybridized with hybridization solution for 1 hour and incubated with 200 μl of hybridization solution (50% formamide, 4 x SSC, 1 x Denhardt solution, 5% dextrane sulfate, 0.5 mg/ml salmon sperm DNA and 0.25 mg/ml yeast tRNA) containing the labeled probe in a concentration of 100 ng/ml. Hybridizations were performed for 12 - 16 hours at 37°C in a humidified chamber.

Following hybridization the coverslips were washed with 2 x SSC (1 hour), 1 x SSC (1 hour), 0.5 x SSC (30 min) and 0.2 x SSC (30 min) at room temperature. The immunological detection was carried out with anti digoxigenin polyclonal antibody conjugated with alkaline phosphatase using a DIG-DNA-Detection kit (Boehringer) and following the manufacturer's recommendations. Briefly, coverslips were washed in buffer 1 (100 mmol TrisHCl, 150 mmol NaCl pH=7.5) incubated with 2% normal sheep serum (NSS), 0.3% Triton X-100 in buffer 1 for 30 min followed by incubation with anti DIG antibody diluted to 1:500 in buffer 1 containing 2% NSS and 0.3% Triton.
After two washing steps (2 x 15 min) with buffer 1 coverslips were equilibrated with buffer 3 (100 mmol TrisHCl, 100 mmol NaCl, 50 mmol $MgCl_2$, pH=9.5) for 2 min. and incubated with color solution (45 μl NBT, 35 μl X-Phosphate and 2.4 mg levamisol in 10 ml buffer 3) overnight in a dark box. Coverslips were washed, dehydrated through graded ethanol and xylol, mounted and examined microscopically.

RESULTS

According to our expectations by using the 31-mer oligonucleotide complementary to the CAMK-II α subunit mRNA we obtained an intense labeling of neurons and glial cells (Fig. 1A) but endothelial cells were also labeled (Fig. 1B). By using the β probe the intensity of the labelling in the endothelial cells was at the lowest level of detectability suggesting that the α subunit is present at much higher concentration in these cells. Our results were confirmed by immunohistochemical studies too (not shown).

The blue staining characteristic of the alkaline phosphatase reaction appeared to be unevenly localized within the cytoplasm. Strongest staining was seen around the nucleus but neuronal processes were also labeled occasionally. The uneven distribution was observed in endothelial cells also.

The intensity of color reaction was stronger when we used proteinase K pretreatment showing that the application of this enzyme improves the penetration of probe into the cytoplasm.

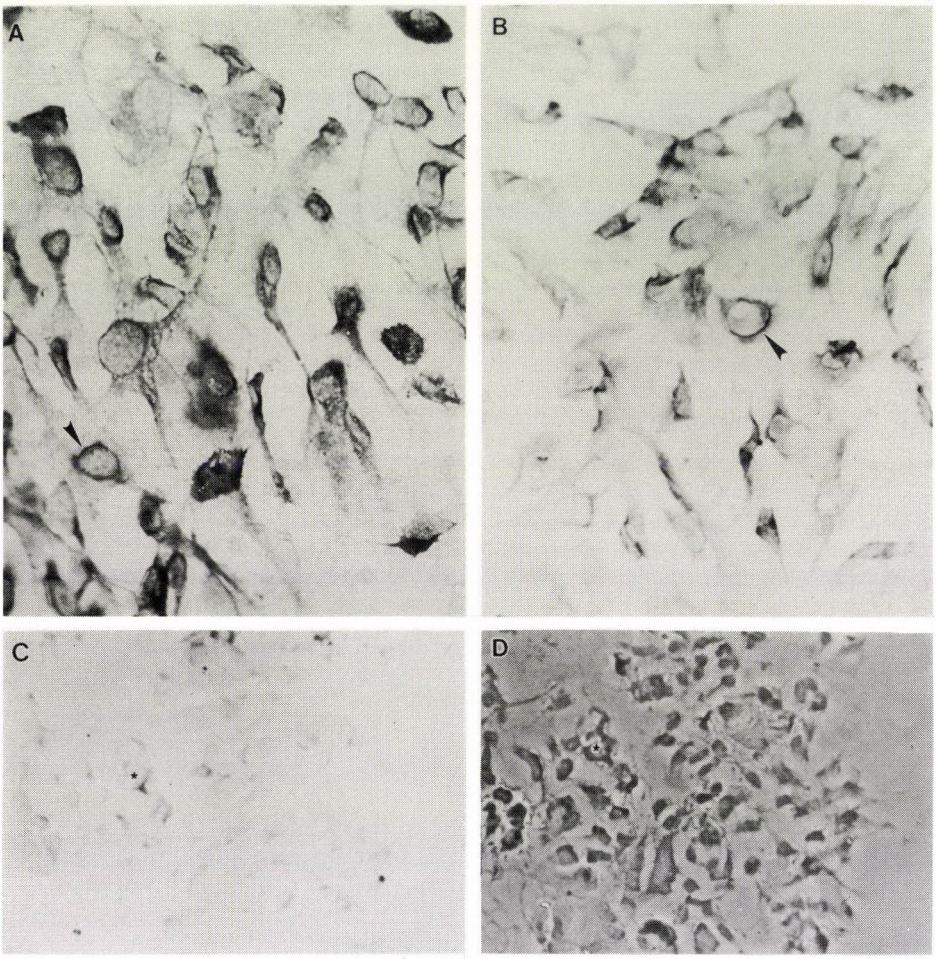

Fig. 1: **A**: Expression of CAMK II α-subunit mRNA in mixed glial and neuronal cell culture. Arrowhead points at strong perinuclear staining, x 600. **B**: Expression of CAMK II α-subunit mRNA in cerebral endothelial cell culture. Arrowhead indicates perinuclear staining, x 300. **C**: Control experiment using the sense probe in mixed glial and neuronal cell culture, x 120. **D**: Phase contrast photomicrograph of the same area as in Fig. 1C. showing the presence of cells. Asterics indicates the same cell in C and D, x 120.

Almost no background labeling was observed at a probe concentration of 200 ng/ml. The amount of levamisol used have blocked the endogenous alkaline phosphatase effectively (not shown).

The specificity of the hybridization was tested by the following control experiments in each series. One control coverslip was treated equal to the experimental material except that no labeled probe was added to the hybridization solution. A second control coverslip was treated with labeled sense probe identical to the nucleotides 1139-1170 of the α-subunit of the CAMK-II. No hybridization signal was obtained in control experiments (Figs. 1C and 1D).

DISCUSSION

In this study we present an application of a method for in situ hybridization using digoxigenin labeled oligonucleotide probes. One of the most important advantages of the used method is its higher resolution when compared with that obtained with radioactive probes (Baldino et al., 1989; Unger et al., 1991). At this level of resolution, the distribution of the signal was detectable within the cytoplasm and even neuronal processes. High resolution is of particular importance, where several mRNA-s are targeted to specific areas of the cytoplasm (dendrites) (Stewart and Bankes, 1992).

An other advantage of the non-radioactive techniques and the method presented in this study when compared with the use of radiolabeled probes is the significantly lower background labeling (Baldino et al., 1989; Unger et al., 1991). Furthermore the non-radioactive procedures eliminate not only the hazard provided by the handling of radioactive isotopes but the long exposure time required for autoradiography can also be aborted, thus the results can be obtained within three days.

We have used this method to demonstrate the presence of the CAMK-II mRNA in cerebral endothelial cell cultures. The endothelial cells participate in the formation of the blood-brain barrier, a physiological barrier that regulates the transport of different substances to the brain. The permeability of this barrier is regulated by different second messenger systems (Joó, 1992). Since CAMK-II is a protein kinase known to mediate the effect of different second messengers, the presence of this enzyme in the endothelial cells raises the possibility that it participates in the regulation of the permeability of the blood-brain barrier.

ACKNOWLEDGEMENTS

The research was supported in part by grants from the Hungarian Research Found (OTKA T-915 and T-5208) the Ministry of Public Welfare (ETT-130) and from the Deutsche Forschungsgemeinschaft (Proj. Nr. Wo 279/8-3).

REFERENCES

Angood, S. J., Kiyama, H., Faull, R. L. M. and Emson, P. C. (1991) Dopaminergic D_1 and D_2 Receptor Antagonists Decrease Prosomatostatin mRNA Expression in Rat Striatum. Neuroscience. 44, 35-44.

Baldino, F., Ruth, J. L. and Davis, L. G. (1989) Nonradioactive Detection of Vasopressin mRNA with in Situ Hybridization Histochemistry. Exp. Neurol. 104, 200-207.

Burgin, K. E., Waxham, M. N., Rickling, S., Westgate, S. A., Mobley, W. C. and Kelly, P. T. (1990) In Situ Hybridization Histochemistry of Ca^{2+}/Calmodulin - Dependent Protein Kinase in Developing Rat Brain. J. Neurosci. 10, 1788-1798.

Joó F. (1992) The cerebral microvessels in tissue culture, an update. J. Neurochem. 58, 1-17.

Digoxigenin Application Manual Boehringer Mannheim (1989).

Kása, P., Pákáski, M., Joó, F.,and Lajtha, A. (1991) Endothelial Cells from Human Fetal Brain Microvessels may be Cholinoceptive but do not Synthesize Acetylcholine. J. Neurochem. 56, 2143-2146.

Larsson, L. I. (1989) In Situ Hybridization Using Biotin - Labeled Oligonucleotides : Probe Labeling and Procedures for mRNA Detection. Arch. Hystol. Cytol. Vol. 52, Suppl. pp. 55-62

Lewis, M. E., Krause II, R. G. and Roberts-Lewis, J. M. (1988) Recent Developments in the Use of Synthetic Oligonucleotides for In Situ Hybridization Histochemistry. Synapse 2, 308-316.

Ozden, S., Aubert, C., Gonzales-Dunia, D. and Brahic, M. (1990) Simultaneous In Situ Detection of Two mRNAs in the Same Cell Using Riboprobes Labeled with Biotin and ^{35}S. J. Histochem. Cytochem. 38, 917-922.

Pákáski, M., Kása, P., Joó, F. and Wolff, J. R. (1990) Cerebral Endothelial Cells - Derived Laminin Promotes the Outgrowth of Neurites in CNS Neuronal Cultures. Int. J. Dev. Neurosci. 8, 193-198.

Persohn, E., Malherbe, P. and Richards, J. G. (1991) In Situ Hybridization Histochemistry Reveals a Diversity of $GABA_A$ Receptor Subunit mRNAs in Neurons of the Rat Spinal Cord and Dorsal Root Ganglia. Neuroscience. 42, 497-507.

Réthelyi, M., Metz, C. B. and Lund, P. K. (1989) Distribution of Neurons Expressing Calcitonin Gene-Related Peptide mRNA in the Brain Stem, Spinal Cord and Dorsal Root Ganglia of Rat and Guinea-Pig. Neuroscience. 29, 225-239.

Sommer, R., Tautz, D. (1991) Nonradioactive In Situ Hybridization to Sectioned Tissues. Trends Genet. 7, p110.

Steward, O. and Bankes, G. A. (1992) Getting the Message from the Gene to the Synapse: Sorting and Intracellular Transport of RNA-s in Neurons. Trends in Neuroscience. 15, 180-186.

Unger, E. R., Hammer, M. L. and Chenggis, M. L. (1991) Comparison of ^{35}S and Biotin as Labels for In Situ Hybridization: Use of an HPV Model System. J. Histochem. Cytochem. 39, 145-150.

Received 14 April 1993
Accepted 26 July 1993

Neurobiology 1 (3), pp. 241-255, 1993

EARLY X-IRRADIATION OF RATS. 5. INFLUENCE OF IRRADIATION ON THE DEVELOPMENT OF EXTRACELLULAR FIELD POTENTIALS EVOKED BY ANTIDROMIC STIMULATION

M. Mészáros[1], M.B. Szente*, A. Baranyi* and N. Halász[2]

Institute of Biophysics, Biological Research Centre of the Hungarian Academy of Sciences, and *Department of Comparative Physiology, Attila József University of Sciences, Szeged, Hungary

Summary: Rat pups were treated by low, fragmented and repeated doses of X-rays, from late prenatal days until the end of the third postnatal week. Extracellular field potentials, evoked by antidromic stimulation of the lateral olfactory tract were recorded in different layers of the olfactory bulb at 1, 2, 3 and 6 weeks of age, from control (non-irradiated) and experimental rats. Development of the field potentials was analysed in both groups of animals. In controls, the amplitude of responses was gradually increasing along with age while the latency of peaks decreased; inhibitory waves were tuned even after the third postnatal week. When compared to controls at similar ages, irradiated rats had smaller peak amplitude of responses and the shortening of the response latency was delayed. In addition, a new, late-appearing excitatory wave component was observed in the granule cell layer by the sixth week. The effect of irradiation on field potentials of the olfactory bulb is discussed in light of the marked reduction of the inhibition in the local neuronal assembly, which is also indicated by the depressed development of its structural and neurochemical correlates.

Key words: olfactory bulb - extracellular field potentials - development - irradiation - antidromic stimulation - rat

INTRODUCTION

It is widely accepted that olfactory receptor cells establish functional synapses onto a considerable number of mitral cells of the olfactory bulb (OB) by birth (see Hinds

[1]**Present address**:
ARL Division of Neurobiology,
611 Gould-Simpson Building,
University of Arizona
Tucson, AZ 85721 U.S.A.

[2]**Correspondence should be sent to**:
Dr. Norbert Halász
Institute of Biophysics
Biological Research Centre
Hungarian Academy of Sciences
H-6701 Szeged, P.O. Box 521, Hungary
Fax: 36-(62)-433 133

Akadémiai Kiadó, Budapest

and Hinds, 1976). Although the first dendrodendritic synapses between the secondary dendrites of mitral cells and peripheral processes of the granule cells are already established on the fifteenth or sixteenth day of the embryonic life (E15 or E16), the wast majority of the local circuit neurons appear only after birth (see Hinds, 1968; Altman, 1969; Rosselli-Austin and Altman, 1979; Bayer, 1983). Consequently, their contribution to the bulbar activity is not significant, yet at these early postnatal days (for review see Mair, 1986), however,it is becoming more important as these microneurons increase in number.

Low-dose X-irradiation of developing rats during the early postnatal period reduces dramatically the population of interneurons in the OB (see Altman et al., 1968; Bayer and Altman, 1975; Yanai and Rosselli-Austin, 1978; Struble and Walters, 1982; Halász, 1986, 1987a), however, regular olfactory behavior was maintained in young rats (see Yanai and Rosselli-Austin, 1978; Schoonover and Slotnick, 1981). Due to the marked loss of microneurons, we expected to find functional alterations as reflected by the eletrophysiological responsiveness of these, structurally and neurochemically segregated neuronal populations, even though the effect of the treatment was compensated by some degree at the level of the whole bulb, the olfactory system or the individual. Therefore we initiated experiments to study the field potentials evoked by antidromic stimulation in the OBs of young, irradiated rats. For comparison we also examined the responses of untreated animals during the first six postnatal weeks. The results show that in control rats the peak amplitude of waves is increasing at least until the third week and their latencies are diminishing even during the following few weeks, when completing of myelinization and finer tuning of the inhibitory systems would take place. The irradiation apparently delayed this maturation of responses and, in addition, uncovered a late, third excitatory wave component which demands further exploration.

METHODS

Animals and Treatment

Young, pregnant CFY rats and their pups were irradiated by low, fragmented doses of X-rays from a Co60 source as described earlier in detail (Halász, 1986). In the present experiments 14 single doses, increasing gradually from 0.3 Gy up to 1.6 Gy (from the day E15 until almost the end of the third postnatal week), totalling 11-12 Gy were delivered to experimental rats. Other, non-irradiated pups served as control animals.

Histology

10 μm cryostate sections were taken of several randomly selected, frozen brains, stained by cresylviolet and examined for the neuronal architecture, as described earlier (Halász, 1986).

Physiology

Experiments were carried out on rat pups of both sexes aged between one to six weeks. The animals were anesthetized with sodium pentobarbital (Nembutal; 60 mg/kg; i.p.); tracheas were cannulated with polyethylene tubing. Wound margins and pressure points were infiltrated with 2% Novocaine and the animals were placed in a stereotaxic head holder. The OB and the frontal lobe area were exposed and kept warm and wet by 39oC physiological saline solution. The body temperature of the animals was maintained at 37-39°C.

Field potentials were recorded with metal microelectrodes (tip resistances; 2-5 mOhms; Frederic Hear and Co.,USA). The stainless steel reference electrode was attached to the nasal bone. Electrical signals were recorded by a conventional AC amplifier (<0.5 Hz and >5 kHz filters), displayed on a Tektronix storage oscilloscope and photographed. For laminar analysis of evoked potentials the recording electrode was inserted into the OB aproximately perpendicularly to the surface using a Narishige hydraulic microdrive. The electrode was first driven into the center of the bulb and then withdrawn to the surface. Thus, mechanical distortion of the tissue and errors in estimation of the actual depth of the electrode tip were minimized. The actual position of the tip of the recording electrode was estimated by micrometer readings.

For stimulations (2.5-3.0 V; 0.5-1 ms; 1 Hz) a bipolar stimulating electrode (SNEX-200, Rhodes Med. Inc.) was placed stereotaxically into the lateral olfactory tract (LOT). For orientation, L: 2.5-3; H: 4.7-6 and V: 1.5-3.5 (from the surface of the anterior lobe) coordinates were used for adults and extrapolated to young animals. Stimulating electrodes were inserted slowly into the brain until evoked potentials with maximal amplitudes were elicited in the granule cell layer of the bulb.

Latency and amplitude measurements were made on a computer from averaged field potentials in each control and experimental age groups and statistical significance between the data was calculated by Student's *t*-test.

RESULTS

Histology

X-ray irradiation resulted in a reduction of bulb size and thickening of bulbar layers due to a serious loss of microneurons primarily in the deep granule cell layer (GCL) and periglomerular area (see Figs. 1 and 2). The damage at three weeks of age was comparable to those in our preceeding experiments (Halász, 1986; 1987a).

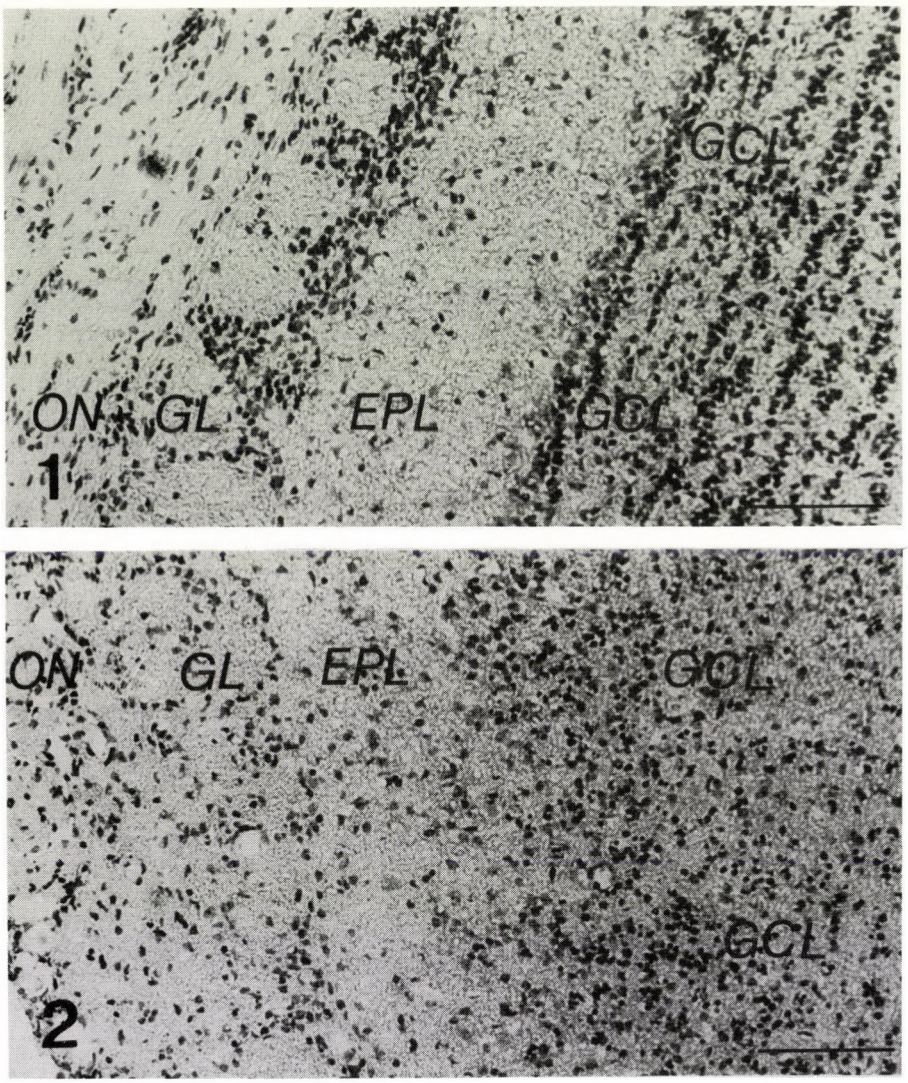

Figs. 1 and **2**: Light microscopy of the olfactory bulb layers as seen on 10 μm thick, cresyl violet stained cryostate sections of control (Fig. 1) and irradiated (17 Gy, total dose; Fig. 2) 3-weeks-old rats. Note the substantial decrease in density of cells and also the disarrangement of nuclei in the glomerular (GL) and granule cell (GCL) layers in the irradiated sample (Fig. 2). EPL: external plexiform layer; ON: olfactory nerve layer. Bar, 100 μm.

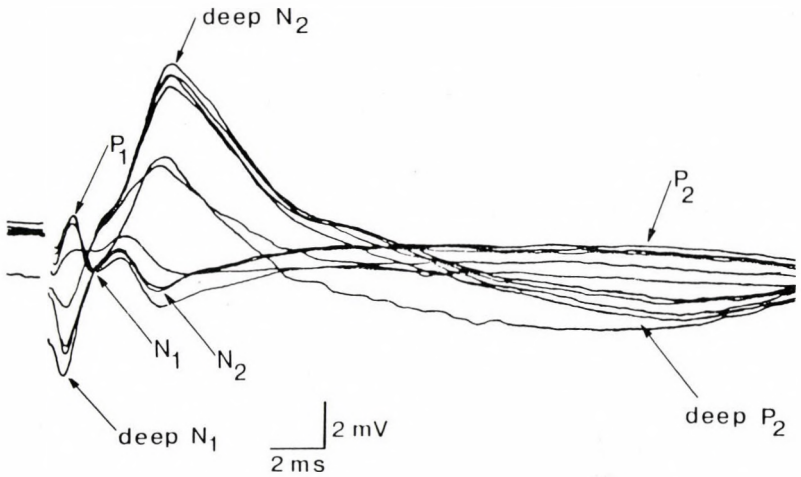

Fig. 3: Successive traces were superimposed as the recording electrode was continuously withdrawn from about 1200-1400 μm depth. Main negative (N) and positive (P) components of the waves are demonstrated and their designations are indicated on recordings from a 6-week-old control, non-irradiated animal. Note the changes in the peak latency of N1 wave and in the polarity of N2 and P2 waves as a function of the depth of the recording electrode. Positivity is up. As illustrated, polarity of the waves is reversed at a certain depth (at the level of mitral cells).

Physiology

Extracellular field potentials following stimulations of the LOT were recorded from the OB of rats and their depth profile from non-irradiated controls and X-ray-treated animals were compared in a laminar analysis.

Evoked potentials recorded in the OB of 6-week-old animals had distinct patterns (Fig. 3; see also Fig. 4) that could be correlated with the different laminae, according to earlier studies where these were characterized in detail for the mature OBs (see Ochi, 1963; Phillips et al., 1963; Rall et al., 1966; Rall and Shepherd, 1968; Nicoll, 1972 and others). In superficial recordings there was an initial positive wave (P1) followed by two negative waves (N1 and N2) and a late positive wave (P2). During P1, the superficial dendrites of mitral cells act as a current source for the antidromically activated mitral cell

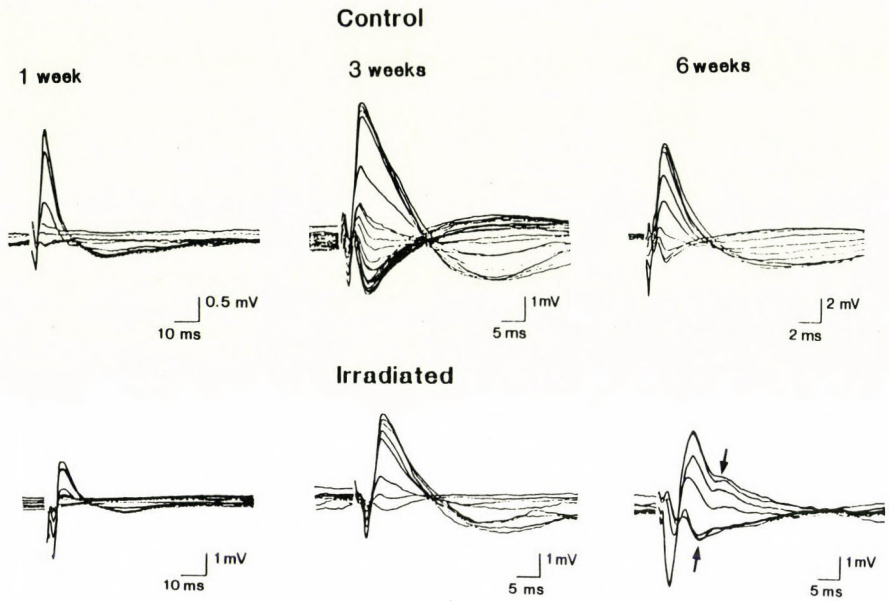

Fig. 4: Comparison of evoked responses to LOT stimulation, recorded from different depths in the olfactory bulb of 1, 3, and 6-week-old control (upper 3 traces) and irradiated (lower traces) rats. Arrows point to N3 (for further explanation see text).

bodies. The first small, steep negative wave (N1) represents the depolarization of mitral cells and their principal dendritic arbor by the antidromic stimuli. The second larger and slower negative wave (N2) could be related to the synaptic activation of granule cell dendrites by mitral cells through dendrodendritic connections. These offer a late, flattened positive wave of long duration and low amplitude (P2) was evoked due to the inhibition of mitral cells through reciprocal dendrodendritic synapses.

As the recording electrode gradually penetrated the bulbar layers these wave patterns showed a regular sequence of changes. Slightly below the mitral cell layer (900-1000 um), the deep N1 attained a maximum, decreased in latency and became synchronous with the surface P1. The N2 and P2 components gradually increased in amplitude through the external plexiform layer (EPL) (500-600 μm), reversed in polarity in the mitral cell layer (700-900 μm) and reached their maxima in the granular cell layer (GCL) (1000-1300 μm). By lowering the electrode further the amplitude of evoked potentials gradually decreased. In spite of some minor variations the basic configuration of evoked responses were highly characteristic and reproducible in different animals.

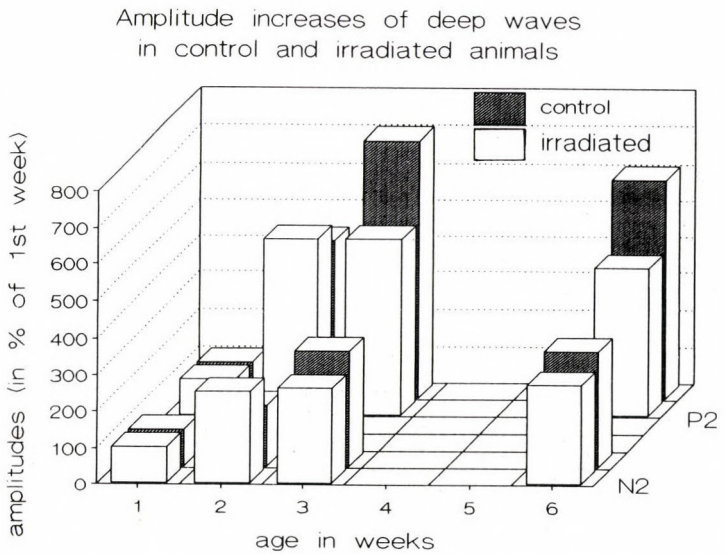

Fig. 5: Amplitudes of N2 and P2 waves of LOT responses in the olfactory bulb were depressed in irradiated animals from the 3rd postnatal week onward. Values of the peak amplitude of deep N2 and P2 waves are plotted against age. Columns represent the averages of measurements on, at least, five rats in each age group of control and experimental rats, respectively.

Development of potentials in control animals

There was a clear tendency for decrease in the peak latency, and increase in the amplitude of the different waves from 7-day-old to 42-day-old animals (Fig. 4; see also Figs. 5 and 6). Measurements of the peak latency (from the middle of stimulus artifact), and peak amplitude (from the electric baseline) were made on records where the deep N2 wave was at maximum. The deep N2 was a dominating large positive component, due to a substantial flow of extracellular current from deep granule cell bodies and dendrites to their depolarized processes situated in the external plexiform layer.

Quantitative analysis of the peak amplitude was carried out on deep N2 and deep P2 waves (Fig. 5). Measurements on the very short latency of N1 wave (1.0-4.0 ms) was omitted because of the occasional of the stimulus artifact. Evoked potentials recorded from 1-week-old pups showed less details than those recorded from 6-week-old rats. The simplest response configurations were recorded from the superficial layers of 1-week-old

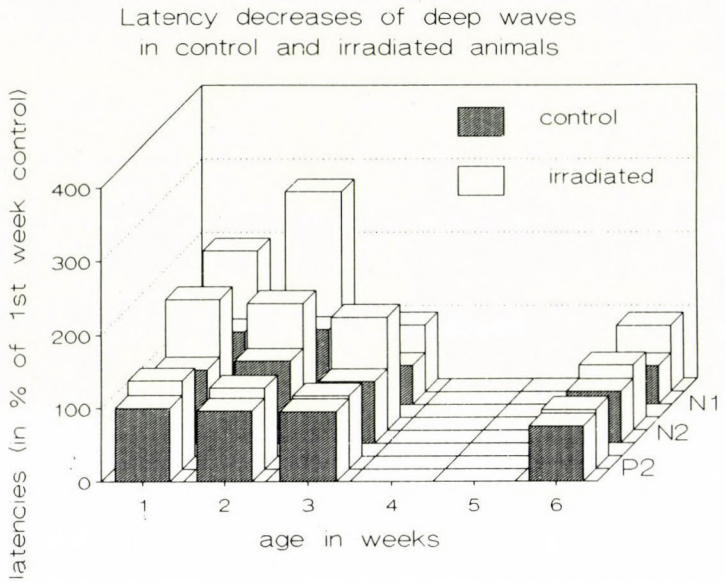

Fig. 6: Irradiation resulted in an increase in the latencies of evoked responses to LOT stimulation at all samples. Latencies of the deep N1, N2 and P2 waves are plotted as a function of age. Latencies were averaged from measurements in 4 (one week old) or 5 (2, 3 and 6 weeks old) rats.

animals where P2 was regularly not detectable, although a small, deep, late negative wave, equivalent to superficial P2 was measurable. The amplitude of deep N2 and P2 waves displayed progressive increases mainly in the first 3 weeks (5-6 and 3-4 fold increases, respectively; see Fig. 5). Peak amplitude values of deep N2 obtained in 6-week-old rats were very similar to those recorded in 3-week-old animals, while the amplitude of deep P2 was remarcable smaller in 6-week-old animals (Fig. 5). These observations suggest that the development of N2 was almost completed around 3 weeks of age, while P2 was further adjusted, probable due to the expanding inhibitory system.

The largest relative decrease in latency occurred between the 2nd and 3rd weeks in case of the N1 wave (Fig. 6). It seemed that the latency of deep N1 reached its final value around the 3rd week since only minimal further reductions were detectable at the age of 6 weeks. The latency of deep N2 and deep P2 showed decreases to a smaller degree from 1 to 6 weeks (Fig. 6). The latency of deep N2 decreased more rapidly in the first 3 weeks and expressed smaller changes afterwards, while remarkable decrease was observed in the latency of deep P2 after the age of 3 weeks.

Development of potentials in X-irradiated animals

The effects of irradiation on field potentials evoked by stimulation of the LOT were characterized by comparing responses obtained in similar conditions in control and irradiated animals of different ages. The most apparent and general finding of these experiments was that irradiation produced a delay in the maturation processes of evoked potentials. Their latencies were significantly longer and the amplitudes were smaller in irradiated than in non-irradiated animals.

In the first two weeks the values and the rate of increases in amplitude of deep N2 and P2 were very close in irradiated and in control (Fig. 5). The most depressing effects of irradiation on amplitudes occurred between the 2nd and 3rd weeks. In addition, the rate of increases of N2 and P2 waves was hindered by irradiation. After 3 weeks, the rate and direction of changes in amplitudes were similar in the two groups of animals. At 6 week of age the amplitudes of deep N2 and P2 were still smaller in irradiated than in control animals. The polarity reversal of N2 wave during laminar analysis seemed to be more gradual in irradiated than in control animals.

At age of 1 week the latency of N1 wave was almost twice as long as in control animals. Large decreases in the latency of N1 occurred in both groups between 2 and 3 weeks (see Fig. 6) and its value seemed to be stabilized around 3 weeks. The latency of N1 remained considerable longer in X-ray-teated animals even at age of 6 weeks. The peak latency of N2 was about 1.8 times and the P2 about 1.2 times as long as in irradiated 1-week-old as in control animals of the same age. These values gradually decreased until the age of 6 weeks, although the latency of N2 displayed a relatively large decrease between the 2nd and 3rd weeks. Since in the first 3 weeks the rate of decreases was generaly higher in irradiated animals, the values of latencies approximated to those measured in control animals. After 3 weeks the rate of the latency decreases was almost the same in the two groups. The value of peak latency of N2 and P2 waves at age of 6 weeks were almost the same in irradiated and in control animals (4.7-4.9 ms and 23-25 ms, respectively).

In some 6-weeks-old irradiated animals the declining slope of the most remarkable wave component, the one which was assigned to the synaptic activation of granule cell dendrites through the dendrodendritic synapses in the EPL (deep N2) was interrupted and a new peak was induced with a polarity being similar to the deep N2 in the GCL (see Fig. 4). This component had a peak at about 15 msec after the stimulus artifact (i.e., this wave

followed by some 6 msec the "main" hill of N2). Preceeding this wave, a marked deflection (a third negative wave) became visible in this layer which we shall refer to as N3. It was observed first just deep to the mitral cell body layer, with a latency of 11 msec after the artefact, but deeper in the GCL, where it reached its highest amplitude (see Fig. 4, last traces) had rather a latency of 12.0-12.5 msec. N3 appeared only at the oldest (young adult) group of our experimental rats.

DISCUSSION

General

As shown by previous experiments with low-dose X-ray irradiation, at an approriate dosage, the full organism is hindered in its development (for weight reduction, see Halász, 1986), particularly the organs which are at their most sensitive stages. Since our timing covered the first period of emergence of the most numerous neuron families, the deep (granule) and superficial (periglomerular) small interneurons in the OB, the resulting reductions in volume of this brain area, when compared to controls, was enormous. Experimental bulbs were down at as little as 13-15% of the regular volume/weight of control bulbs by their age of 3 weeks, but none of the irradiated pups had a bulb larger than 50% of those of controls. Accompanying this effect is the dramatic decrease in the thickness of several layers and consequently, density and absolute numbers of constituting cells/processes, that can account for the volumetric changes (see Altman, 1969; Bayer and Altman, 1975; Walters and Struble, 1978; Yanai and Rosselli-Austin, 1978; Meisami,1979; Struble and Walters, 1982; Halász, 1987a,b; Kosaka et al., 1992). However, if one takes a close look at the single cells, it would be extremelly difficult to find anything as being structurally damaged. Indeed, we found only relatively minor changes at the subcellular level by revealing the reduction of polyribosomes in (presumably young, but mature) granule cell somata and deterioration of (very few) synaptic profiles related to the same (granule) type of cells in the EPL (Halász, 1987a).

Considering these results it would be almost unexpected to observe functional disturbances at a single cell level. If any such existed at all they would be detectable only by intracellular or patch-clamp recording. Rather, if a particular population of neurons, a larger group of cells seemed to be affected, responses to stimulation should be examined at the level of population spikes and extracellular field potentials.

The electrical activity of the bulb came into the focus of interest of many laboratories following Lord Adrian's fundamental work published in 1950. A detailed description of field potentials (and proposals for their origin) across bulbar layers was presented for several species' (see e.g. Orrego, 1961; Ochi, 1963; Philips et al., 1963; Rall and Shepherd, 1968; Nicoll, 1969; MacLeod, 1976; Waldow et al., 1981, Nowycky et al., 1983). Our present recordings revealed very similar wave components from approx. 3 weeks of age, in both the control and experimental bulbs.

Much less is known about the development of electrical activity of the OB and, as far as our search revealed, no study was devoted specifically to the exploration of characteristics of the bulbar field potentials as a function of the early postnatal development. A few data may help, however, to consider the significance of our present experiments. Mair et al. (1982) suggested little chance for the possibilities to record (granule cell-dominated) compound activity from a rat pup as early as at the end of the first week since only "few granule cells" appeared to be "functional until the second postnatal week" during their Golgi-studies. Mitral cells were, however, intracellularly recorded during the first postnatal week, but little interneuronal influence seemed to shape their response patterns to stimulation by differring peripheral stimuli (Mair and Gesteland, 1982). Extracellular (unit) recordings of Shafa et al. (1981) revealed immature action potentials from 4 to 20 days postnatally. In accordance with the studies cited above, EEG activity of the bulb did not appear mature before day 24 (Salas et al., 1969).

Control rats

As shown by our present experiments, although all principal waves could already be detected in our youngest pups, substantial changes ensued involving primarily the N2 and P2 waves. Mitral dendritic mechanisms -and surely their underlying structural and neurochemical basis- seemed to be comparable to adults, as reflected by the completed development of N2 by the third postnatal week. Although this wave remained the most prominent component of the evoked potentials, in accordance with the still highly expanding deep inhibitory system (based principally upon the increasing population of granule cells, see Hinds, 1968; Bayer, 1983), its amplitude decreased remarkably by the sixth week. This may be related to the finer tuning of inhibition in the young adult and may be based upon the reduction in number of functioning, stabilized granule cell spines (gemmules in dendrodendritic contact with the mitral secondary dendrites). A similar late

adjustment of the established synapses in the EPL of the ferret was reported by Rehn and his colleagues (1986) on the structural level.

During early development, another change was the decrease of the peak latencies: the latency of N1 and N2 was set by the third while that of P2 only by the 6th week - or even later. As the myelinization may be finished by this age in the bulb, it would be desireable to follow the neurochemical maturation of oligodendrocytes by immunohistochemistry of the myelin basic protein, to find out whether these glial cells might contribute to the observed changes in latency.

Experimental rats

Little has been reported on the impact of general depression of development during the first postnatal weeks and even less is known particularly on the effect of the fragmented and repeated, multiple, but low-dose X-rays on the evoked potentials in the main OB. Our present work is the first to show that the irradiation resulted in two major effects: reduction in the peak amplitude of N2 and P2 waves and an increase of the latency.

Regarding the increasing latencies, they were most prominent during the first two weeks and especially for the negative waves (N1, activation of the mitral cells/dendrites and N2, synaptic activation of the granule cells). Though this delay in maturation was diminished after ceasing the irradiation and the histogenesis in experimental rats seemed to be compensated for the most dramatic changes, increased latencies for all the (but especially for N2) peaks persisted even at 6 weeks of age. Since all mitral (and deep tufted) cell axons (and, also, central fibers to the bulb, capable to excite granule cells) are myelinated (for review, see Halász, 1990), a less complete myelinization in irradiated pups would easily explain this observation.

On the other hand, the decrease in the amplitude of two wave components (N2 and P2) by irradiation seems reasonable to be discussed in lights of former studies providing data for the depression of the developing granule cells (see e.g. Altman et al., 1968, and the following studies as listed in the Introduction). Fewer granule cells would offer less peripheral processes to be activated through the dendrodendritic synapses (wave P1) and, necessarily, would not be able to exert a similarly powerful inhibition on the projection neurons (P2).

We have as yet no experimental evidence which would help understanding the

break in the declining slope of N2 in 6-week-old experimental animals. This extra wave, named N3 (see Fig. 4) in this study, was never seen at younger irradiated animals or in non-irradiated controls, and we are anaware of a similar observation on bulbar extracellular field potentials from the literature. We may speculate, however, that if the dynamic balance of excitation and inhibition would be hurt in the bulb, through significant losses in those cells capable to support inhibition, then an otherwise suppressed, extra excitatory component may come into power and so uncovered. Reduction of the juxtaglomerular (in part, glutamic acid decarboxylase or gamma-aminobutyric acid <GABA>-containing) neurons (cf. Oláh et al., 1990; Kosaka et al., 1992; Mészáros and Halász, in preparation) may also support this possible decrease of the normal level of inhibition.

In summary, we demonstrated that although it is possible to record field potentials from the olfactory bulb of very young rat pups, indeed, the complex waves undergo remarkable changes during development and their final tuning is far from being over by the regular time of weanling. Depression of the development of the bulbar neuronal assembly leads to further alterations of the field potentials. These data therefore may help to better understanding the significance of contribution of certain neuronal populations to the inhibitory component of the bulb's circuits. In addition, they may constitute new experimental grounds to further adjust models simulating the mitral cell/granule cell interaction through dendrodendritic synapses (cf. Woolf et al., 1991).

ACKNOWLEDGEMENTS - The authors are grateful to Prof. Gordon M. Shepherd for comments and to Erika Kómár for word processing. Supported by OTKA grant I/536 to N.H.

REFERENCES

Adrian, E.D. (1950) The electrical activity of the mammalian olfactory bulb. EEG Clin. Neurophysiol. 2, 377-388.

Altman, J. (1969) Autoradiographic and histological studies of postnatal histogenesis. IV. Cell proliferation and migration in the anterior forebrain, with special reference to persisting neurogenesis in the olfactory bulb. J. Comp. Neurol. 137: 433-458.

Altman, J., Anderson, W.J. and Wright, K.A. (1968) Differential radiosensitivity of stationary and migratory primitive cells in the brains of infant rats. Exp. Neurol. 22, 52-74.

Bayer, S.A. (1983) 3H-thymidine-radiographic studies of neurogenesis in the rat olfactory bulb. Exp. Brain Res. 50, 329-340.

Bayer, S.A. and Altman, J. (1975) The effects of X-irradiation on the postnatally forming granule cell populations in the olfactory bulb, hippocampus and cerebellum of the rat. Exp. Neurol. 48, 167-174.

Halász, N. (1986) Early X-irradiation of rats. 1. Methodological description and morphological observations on the olfactory bulb. J. Neurosci. Meth. 18, 255-268.

Halász, N. (1987a) Early X-irradiation of rats. 2. Effects on granule cells and their dendrodendritic synapses in the olfactory bulb. Neuroscience 20, 709-716.

Halász, N. (1987b) Early X-irradiation of rats. 3. Survival of dopaminergic periglomerular cells of the olfactory bulb. Z. Mikrosk.-Anat. Forsch. 101, 1027-1034.

Halász, N. (1990) The Vertebrate Olfactory System. Chemical Neuroanatomy, Function and Development. Akademiai Kiadó, Budapest.

Hinds, J. W. (1968) Autoradiographic study of histogenesis in the mouse olfactory bulb. I. Time of origin of neurons and neuroglia. J. Comp. Neurol. 134, 287-304.

Hinds, J.W. and Hinds, P.L. (1976) Synapse formation in the mouse olfactory bulb. II. Morphogenesis. J. Comp. Neurol. 169, 41-62.

Kosaka, K., Taomoto, K., Nagatsu, I., Heizmann, C.W., Hunziker, W. and Kosaka, T. (1992) Postnatal X-irradiation effects on glomerular layer of rat olfactory bulb: Quantitative and immunocytochemical analysis. Exp. Brain Res. 90, 103-115.

MacLeod, N.K. (1976) Field potentials in the olfactory bulb of the codfish (Gadus morhua). Comp. Biochem. Physiol. 55A: 297-299.

Mair, L.G. (1986) Ontogeny of the olfactory code. Experientia 42, 213-223.

Mair, L.G., Gellman R.L. and Gesteland, R.C. (1982) Postnatal proliferation and maturation of olfactory bulb neurons in rat. Neuroscience 7, 3105-3116.

Mair, L.G. and Gesteland, R.C. (1982) Response properties of mitral cells in the olfactory bulb of the neonatal rat. Neuroscience 7, 3117-3125.

Meisami, E. (1979) The developing rat olfactory bulb: Prospects of a new model system in developmental neurobiology. In: Neuronal Growth and Differentiation (eds. Meisami, E. and Brazier, M. A. B.), pp. 183-206. Raven Press, New York.

Nicoll, R.A. (1969) Inhibitory mechanisms in the rabbit olfactory bulb: Dendrodendritic mechanisms. Brain Res. 14: 157-172.

Nicoll, R.A. (1972) Olfactory nerves and their excitatory action in the olfactory bulb. Exp. Brain Res. 14, 185-197.

Nowycky, M.C., Halász, N. and Shepherd, G.M. (1983): Evoked field potential analysis of dopaminergic mechanisms in the isolated turtle olfactory bulb. Neuroscience 8, 717-722.

Ochi, J. (1963) Olfactory bulb response to antidromic olfactory tract stimulation in the rabbit. Jap. J. Physiol. 13, 113-128.

Oláh, Z., Lengyel, I. and Halász, N. (1990) Early X-irradiation of rats. 4. Decrease in phosphorylation of low molecular weight proteins in the olfactory bulb accompanies the loss of GABAergic microneurons. Neurochem. Int. 16, 331-334.

Orrego, F. (1961) The reptilian forebrain. II. Electrical activity in the olfactory bulb. Arch. Ital. Biol. 99, 446-465.

Phillips, C.G., Powell, T.P.S. and Shepherd, G.M. (1963) Responses of mitral cells to stimulation of the lateral olfactory tract in the rabbit. J. Physiol. 168, 65-88.

Rall, W. and Shepherd, G.M. (1968) Theoretical reconstruction of field potentials and dendrodendritic synaptic interactions in olfactory bulb. J. Neurophysiol. 31, 884-915.

Rall, W., Shepherd, G.M., Reese, T.S. and Brightman, M.W. (1966) Dendrodendritic synaptic pathway for inhibition in the olfactory bulb. Exp. Neurol. 14, 44-56.

Rehn, B., Breipohl, W., Mendoza, A.S. and Apfelbach, R. (1986) Changes in granule cells of the ferret olfactory bulb associated with imprinting on prey odors. Brain Res. 373, 114-125.

Rosselli-Austin, L. and Altman, J. (1979) The postnatal development of the main olfactory bulb of the rat. J. Dev. Physiol. 1, 295-313.

Salas, L., Guzman-Flores, C. and Schapiro, S. (1969) An ontogenetic study in olfactory bulb electrical activity in the rat. Physiol. Behav. 4, 699-703.

Schoonover, F.W. and Slotnick, B.M. (1981) No evidence for functional deficits from early X-irradiation of rat olfactory bulb. Assoc. Chemorecept. Sci. Ann. Meeting, Sarasota.

Shafa, F., Shineh, S. N. and Bidanjiri, A. (1981) Development of spontaneous activity in the olfactory bulb neurons of postnatal rat. Brain Res. 223, 409-412.

Struble, R.G. and Walters, C.P. (1982) Light microscopic differentiation of two populations of rat olfactory bulb granule cells. Brain Res. 236, 237-251.

Waldow, U., Nowycky, M.C. and Shepherd, G.M. (1981) Evoked potential and single unit responses to olfactory nerve volleys in the isolated turtle olfactory bulb. Brain Res. 211, 267-283.

Walters, C.P. and Struble, R.G. (1978) X-irradiation induced granuloprival olfactory bulb: Preliminary behavioral and anatomical findings. Soc. Neurosci. Abs. 4, 93.

Woolf, J.B., Shepherd, G.M. and Greer, C.A. (1991) Serial reconstructions of granule cell spines in the mammalian olfactory bulb. Synapse 7, 181-192.

Yanai, J. and Rosselli-Austin, L. (1978) Normal homing behavior in infant rats despite extensive olfactory granule cell losses. Behav. Biol. 24, 539-544.

Received 22 July 1993
Accepted 4 August 1993

ABSTRACTS

An International Workshop on

Molecular Mechanisms Regulating the Permeability of the Blood-Brain Barrier

held between July 23-24, 1993

at the **Biological Research Center, Szeged, Hungary**

Neurobiology 1 (3), pp. 259-260,1993

INTRODUCTION TO THE WORKSHOP

Ladies and Gentlemen, Dear Fellow Colleagues!

It is my great privilege and honour to welcome you all here in the Biological Research Center, among the concrete walls of which the microvessels were isolated from brain tissue by the first micromethod elaborated for this purpose exactly 20 years ago.

May I just recall that, over the past thirty years, the blood-brain barrier, a system specific for the brain, has been an increasingly active area of research and a great deal has been learned, particularly in anatomical and physiological aspects.

The **main objective** of this Workshop is to update the new results on the molecular mechanisms regulating the permeability of the blood-brain barrier. As you may know, the Workshop is mainly sponsored by the European Community, and it was designed primarily to improve the relationship between Hungarian and European organizations. But of course, we are very thankful for those American, Japanese and Indian experts, who accepted our invitation and came, because their contribution, as you will see, will also be very important for the success of the Workshop.

The **main subject** of this Workshop has been selected because of the **growing current interest** in elucidating the **transport processes**, which regulate the **exchange** of substances between **blood** circulation and **brain** tissue.

Chronologically, experimental studies aiming at gaining a better understanding of these complex transport processes were carried out at first in in vivo experiments using exogenous tracer substances and characterizing their clearance from blood and incorporation in brain tissue. In the course of these efforts, it became evident that, in most vertebrates, the cerebral endothelial cells represent structurally the site of this unique permeability barrier, which is termed collectively "the blood-brain barrier". Recent advances in our knowledge of the blood-brain barrier have in part been made by studying the properties and function of cerebral endothelial cells in vitro. With the application of new technologies, the approach offers a new means to investigations, applicable not only to study the development of the blood-brain barrier but also to improve the transport of substances through the blood-brain barrier.

Akadémiai Kiadó, Budapest

As it can be judged from the Program, several outstanding representatives of the field are present here, and -thanks to their participation- almost all important aspects of this kind of research will be dealt with during these two days. As you might have already seen it, the Program will start with a session on the Physiology of the cerebral endothelial cells. The next session will survey the Biochemistry of the cerebral endothelial cells. Two more sessions are planned summarizing the results obtained from studying the Pathology and pharmacology of cerebral endothelial cells. The main interest in this respect is to reveal the molecular mechanisms, which are involved in the regulation of water, electrolyte and macromolecules under pathological conditions. New strategies aiming at the opening of the "gateway" to the brain will be discussed during the last session. At the end, poster presentations will be discussed.

What can we expect after all from this Workshop? We would be delighted to see an open and free exchange of views and ideas during these two days for creation of new and fresh insights into understanding the function and regulation of the blood-brain barrier. In addition, we would like to see the development of new joint research activities aiming especially at improving with new strategies the penetration of nutrients and drugs to brain in order to treat neurological diseases, more effectively .

Finally, I would like to wish you good work, a successful meeting and pleasant stay in Szeged!

Szeged, July 23, 1993.

Ferenc Joó

Neurobiology 1 (3), pp. 261-262, 1993

THE MAMMALIAN BLOOD-BRAIN BARRIER IN VIVO: ELECTROPHYSIOLOGICAL STUDIES

Hazel C. Jones

Department of Pharmacology and Therapeutics, University of Florida Health Science Center, Gainesville, FL 32610, USA

Microvessels on the pial surface have blood-brain barrier properties, as demonstrated by impermeability to ionic lanthanum (Bundgaard, 1982; Butt et al., 1990), a high electrical resistance (Crone and Olesen, 1982; Butt et al., 1990; Butt and Jones, 1992) and in the frog at least, electrogenic ion transport processes (Abbott et al., 1986). Structurally the endothelium is similar to that of parenchymal capillaries, but pial vessels have a loose covering of meningeal cells without the surrounding astrocytic processes found in the parenchyma.

We have used microelectrode techniques in anesthetised rats 24-33 days old, to study permeability and ion regulation of the pial microvessels. During continuous superfusion with artificial cerebrospinal fluid, the dura was exposed and the arachnoid penetrated and folded back. Microelectrodes were inserted into the lumen of microvessels 10-60 μm in diameter for determination of electrical resistance or dc potential (PD). The effects of different agents were studied by changing the composition of the bathing fluid.

The electrical resistance, a measure of barrier permeability, was found to be 1490 Ω cm^2 for small arteries and 980 Ω cm^2 for venous vessels. Hyperosmotic shock (530 mosmol) caused a reversible decrease in resistance of similar proportions in both types of vessels and the application of metabolic poisons or a reduction in temperature of the perfusate, also decreased the resistance. Histamine (10^{-4}M) also decreased the resistance by about 75% in both vessels types. The effect of this was to make venous vessels more permeable than arterial ones. Cimetidine (H_2 receptor antagonist) but not promethazine or indomethacin, prevented the increase in permeability to histamine and, in addition, increased the baseline resistance in both vessel types by 100%, giving a mean value of 4000 Ω cm^2 for arteries. These results show that the pial vessels have a low permeability to ions similar to that found in tight epithelia.

Akadémiai Kiadó, Budapest

The PD across the wall of exposed pial vessels, a measure of ion transport and regulatory processes, was found to be 4.5 mV in arteries and 3.2 mV, lumen negative, in venous vessels. Solutions with high [K+] made the PD less negative and low [Na+] resulted in a more negative PD. Ouabain and a range of K+ channel blockers were tested and only TEA significantly affected the response to high K+. Histamine did not affect the PD. The results suggest that the passive permeability properties of the endothelial cell membranes are the source of the transwall PD.

These results indicate that the pial vessels have the properties of blood-brain barrier vessels, although the extent to which they represent the properties of parenchymal microvessels is not known.

REFERENCES

Abbott, N.J., Butt, A.M., Joels, S., Pitchford, S. and Wallis, W. (1986) J. Physiol. 372, 68P.

Bundgaard, M. (1982) Brain Res. 241, 57-65.

Butt, A.M. and Jones, H.C. (1992) Brain Res. 568, 100-105.

Butt, A.M., Jones, H.C. and Abbott, N.J. (1990) J. Physiol. 429, 47-62.

Crone, C. and Olesen, S.-P. (1982) Brain Res. 241, 49-55.

Neurobiology 1 (3), p. 263, 1993

POTASSIUM CURRENT IN CELLS OF THE BLOOD-CSF BARRIER

Furspan, P.B., Keep, R.F. and Betz, A.L.

University of Michigan, Ann Arbor, MI 48109

Motivated by our interest in regulation of CSF K concentration, we have investigated whole cell K current in epithelial cells of the choroid plexus, site of CSF production. Whole cell voltage clamp was performed on intact CP within two hours of removal from Sprague-Dawley rats. Holding potential was maintained at -60 mV. Outward K current was elicited by stepping to progressively depolarized potentials. The current activated slowly and exhibited rectification at membrane potentials of 0 and higher. In the absence of Ca in the pipette solution, the elicited current decreased over time. A free Ca concentration of 300 nM in the pipette solution prevented this rundown in current. Current elicited by stepping the command potential to +30 mV was reduced 35 and 45% by the application of 10 μM isoproterenol and histamine, respectively. 10 μM dibutyryl cAMP reduced this current by greater than 50%. NaF inhibited current by ~30%. The K channel antagonists, TEA, quinidine, barium and 4-amino pyridine also significantly reduced current. The ATP-sensitive K channel antagonist glyburide was without effect. Our results indicate the presence of a delayed rectifier K channel that is regulated by β-adrenergic and histaminergic agents via their stimulation of adenylate cyclase activity. The involvement of G proteins in this response is suggested by the response to NaF. This channel and its regulation by neurohormones may play a role in the control of CSF K concentration.

Akadémiai Kiadó, Budapest

Neurobiology 1 (3), p. 264, 1993

TRANSPORT OF ALUMINIUM INTO BRAIN - ITS RELATION TO THAT OF GALLIUM AND IRON

Aleksandar Radunović

Physiology Group, King's College, London, UK

High concentrations of aluminium are neurotoxic in man. Its role in causing dialysis encephalopathy is well established. Chronic exposure to low concentrations may be involved in the aetiology of certain neurodegenerative disease such as Alzheimer' disease, amyotrophic lateral sclerosis, Parkinson dementia of Guam. The biochemical processes and molecular mechanisms by which aluminium may exert its toxicity, particularly its potent neurotoxicity are not well understood. It is supposed that aluminium because of its physico-chemical similarities with iron could perhaps use iron systems of uptake and transport across the blood-brain barrier involving transferrin and transferrin receptors on the luminal surface of the endothelium of brain capillaries. This hypothesis is based on evidence that aluminium in the brain of dialysis encephalopathy patients reflects the regional distribution of transferrin receptors and on the fact that transferrin with only 30 % of the two metal ion binding sites occupied leaves 50 μM of sites available for binding of other metals and that stability constants of aluminium-transferrin are such that most of aluminium must be bound to transferrin in serum.

Studies of aluminium entry into brain are hampered by the fact that the only usable aluminium radioactive isotope ^{26}Al with half-life 7.2 x 10^5 years, is difficult to obtain and is extremely expensive. Hence, aluminium transport has to be studied either as net movement of Al or using ^{67}Ga which is anticipated to behave similarly to aluminium. Transport of ^{59}Fe, ^{67}Ga and net Al into brain and other tissues of the intact rat during intravenous infusion of these markers were studied. Uptake of ^{59}Fe, ^{67}Ga and ^{26}Al have also been studied in the intact and hypotransferrinaemic mouse.

Rates of net aluminium uptake into brain and other tissues of the rat are comparable with those of ^{67}Ga at similar raised concentration of the two metals. Whilst transport of ^{67}Ga at tracer levels is similar to that of ^{59}Fe there is evidence of a high proportion of aluminium and gallium transport depending on a chemical species of low molecular weigh, probably citrate. It is known that aluminium and gallium prefer interaction with oxygen donor ligands. The oxygen donor ligand citrate, being present at concentration of 0.1 mmol/l in serum is likely to compete for these metals with transferrin. Our findings are compatible with the view that aluminium and gallium transport into brain and several other tissues are at least in part dependent on endocytosis of aluminium-transferrin and gallium-transferrin. Thereafter, the trivalent aluminium and the trivalent gallium may not readily be released to accumulate within the cell.

The saturating dose of two monoclonal antibodies against transferrin receptors, e.g., the anti-rat IgG OX 26 and the anti-mouse IgM RI7 208 inhibited uptake of ^{59}Fe into brain and other tissues of both rat and mouse. A curious anomaly is that these antibodies markedly enhanced ^{67}Ga (and possibly ^{26}Al) uptake into brain and other tissues of both species.

Neurobiology 1 (3), p. 265, 1993

CHOLINE TRANSPORT IN ISOLATED CEREBRAL MICROVESSELS AND CULTURED ENDOTHELIAL CELLS

Estrada, C., Galea, E., González, C. and Triguero, D.

Department of Physiology, Faculty of Medicine,
Universidad Autónoma de Madrid (UAM), Madrid, Spain

A passage of choline through the BBB has been demonstrated in several species. In 1978, Cornford et al., reported that choline was transported from blood to brain by a carrier-mediated system with a Km of 400 μM, in rats. However, this mechanism can hardly account for the exchange of choline in physiological conditions because: a) the Km value is quite far from the concentrations of choline in plasma (~10 μM) and CSF (~2.5 μM), and b) the net transport of choline occurs in the brain-to-blood direction, this is, against a concentration gradient. The purpose of our work has been to analyze the choline transport properties of the cerebral endothelium, by using both in vitro and in vivo techniques.

^{3}H-Choline uptake was characterized in capillaries obtained from bovine brains and in cerebral endothelial cells, either freshly isolated from these capillaries, or maintained in culture for up to 20 passages. For in vivo experiments, different amounts of ^{3}H-choline were administered as a bolus into the left carotid artery of rats, followed by a perfusion with chilled physiological solution for 1 minute before decapitation, to prevent any further movement of ^{3}H-choline through the cell membranes during removal of the brain and dissection of the tissue. ^{3}H-Choline accumulation was then measured in isolated cortical microvessels, vessel-depleted cerebral cortex, and choroid plexus from the ipsilateral side.

Cerebral capillaries and cultured endothelial cells were able to incorporate choline by a temperature-dependent mechanism. Nonlinear regression analysis of the uptake rates at different substrate concentrations gave the best fit to a system of two components. One component was saturable (Km = 17.8 ± 4.8 μM for capillaries and 10.6 ± 2.8 μM for cultured endothelial cells) and the other one was not saturable at concentrations up to 200 μM. In both preparations ^{3}H-choline uptake was inhibited by the specific blocker AF64A, and was partially reduced in the absence of sodium. Preincubation for 30 minutes with 10^{-4} M ouabain significantly reduced ^{3}H-choline uptake in cerebral capillaries and in freshly isolated cerebral endothelial cells, suggesting an energy-dependence of the ^{3}H-choline transport system. The ouabain sensitivity was not observed in endothelial cells isolated from bovine aortas or in cultured cerebral endothelium.

Intracarotid injections of ^{3}H-choline resulted in an accumulation of radioactivity in the different tissues. Analysis of the data indicated the presence of a saturable uptake system with Km values between 130-160 μM in the isolated microvessels, vessel-depleted cerebral cortex, and choroid plexus. The maximal accumulation capacity was higher in the choroid plexus (25 ± 8 pmol/ mg protein) than in microvessels or cerebral cortex (0.7 ± 0.2 and 1.1 ± 0.2, pmol/mg protein, respectively). In all tissues, ^{3}H-choline incorporation was significantly reduced (> 75%) by hemicholinium-3, indicating that the transport was mediated by specific choline carriers.

These results suggest that the BBB endothelium can incorporate choline by two different mechanisms. When choline is administered into the vessel lumen, as happens in vivo, the uptake by the endothelial cells takes place through a low affinity transport system. However, when isolated capillaries are incubated with choline, and both the luminal and the abluminal membranes are exposed to the substrate, a high affinity, energy-dependent choline carrier is revealed. We propose a polar organization of the cerebral endothelial cells, with a distribution of the high affinity choline carrier restricted to the abluminal membrane. The existence of such a carrier may explain the efflux of choline from the brain, against a concentration gradient.

Akadémiai Kiadó, Budapest

Neurobiology 1 (3), p. 266, 1993

THE TRANSPORT OF METHOTREXATE INTO AN EXPERIMENTAL BRAIN TUMOR MEASURED BY INTRACEREBRAL MICRODIALYSIS

de Lange, E.C.M., de Vries, J.D., Danhof, M., Zurcher, C.,
de Boer, A.G. and Breimer, D.D.

Leiden/Amsterdam Center for Drug Research, Division of Pharmacology,
Leiden University, Leiden, The Netherlands

Microdialysis is a relatively new in vivo technique which allows the monitoring of concentrations of endogenous and exogenous compounds in brain extracerebral fluid (ECF). The use of this technique is of great interest in studying blood-brain barrier (BBB) transport of drugs (de Lange et al.[1,2,3]). In this investigation intracerebral microdialysis was used to study the penetration of methotrexate, a hydrophilic anticancer drug, in normal brain as compared to an experimental brain tumor male Wag/Rij rats (180-220 g).

Two studies were performed. In the first study we determined the transport of methotrexate into the brain cortex under standard microdialysis conditions (n=6), and its penetration in the left (n=6) and right (n=6) cortex 11 days after tumor implantation in the left cortex. The effect of the implantation procedure was investigated after sham surgery (n=6). The second study involved the examination of the effect post tumor implantation interval (6/11/18/25 days) on the transport of methotrexate in the left (n=6) and right cortical brain (n=3).

In both studies each individual rat received an IV bolus injection of 15 mg and the resulting concentration-time profiles in plasma and in cortical brain ECF were determined. The extent of BBB transport was calculated as the ratio of $AUC_{brain\ ECF}$:AUC_{plasma}. Directly after the experiments the brains of the rats were fixated for histological examination for the presence of tumor, fibrosis, necrosis, cell infiltration and vacuolisation. The extent of BBB transport was compared to the histological data.

Overall it was found that the presence of tumor as well as exudate in the left cortex coincided with higher values for BBB transport in the ipsilateral cortex. The median values were in proportion of 224:461:100 for tumor (n=20), exudate (n=3) and the remaining group (n=18) respectively. The presence of tumor seemed to reduce the BBB transport on the contralateral side; the median value for tumor group (n=7) was 60% of the remaining group (n=7). This suggests that the presence of tumor tissue has unequal effects on BBB permeability to methotrexate for the tumor and non tumor bearing hemishere.

1. E.C.M. de Lange, J.D. de Vries, M. Danhof, C. Zurcher, A.G. de Boer and D.D. Breimer: Critical factors on intracerebral microdialysis as a technique to determine the pharmacokinetics of drugs in the central nervous system. Part A. Pharmacokinetic studies. Part B. Histological evaluation. In preparation.

2. E.C.M. de Lange, M.R. Bouw, M. Danhof, A.G. de Boer and D.D. Breimer: Application of intracerebral microdialysis to study regional distribution kinetics of atenolol and acetaminophen in brain. In preparation.

3. E.C.M. de Lange, H.B. Hesselink, M. Danhof, A.G. de Boer and D.D. Breimer: Intracerebral microdialysis can be used to determine changes in blood-brain barrier transport characteristics after after intracarotid administration of hypertonic mannitol solution. In preparation.

Neurobiology 1 (3), pp. 267-268, 1993

PHARMACOLOGICAL CHARACTERIZATION OF RECEPTOR-MEDIATED CHANGES IN INTRACELLULAR CALCIUM IN PRIMARY AND IMMORTALIZED CULTURES OF RAT BRAIN CAPILLARY ENDOTHELIAL CELLS

Nobles, M., *Revest, P.A., Abbott, N.J. and **Couraud, P.-O.

Physiology Group, Biomedical Sciences Division, King's College, London, UK; *Department of Physiology, Queen Mary and Westfield College, London, UK; **Institut Cochin de Genetique Moleculaire, CNRS UPR415, 22, Rue Mechain, Paris, France

This study compares and contrasts the pharmacological responses of rat brain capillary endothelial cells (RBCEC) from primary cultures and an immortalized cell line RBE4. Primary cultures were prepared as previously described (Abbott, Hughes, Revest and Greenwood, 1992). The cell line RBE4, which was provided by Dr. P.-O. Couraud and Dr. F. Roux (Institut Cochin, Paris and INSERM U26, Paris), is derived from primary cultures of rat brain capillary endothelial cells which have been immortalized by transfection with the plasmid pE1A-*neo* (Durieu-Trautmann et al., 1993). These cells can be grown in several of different media and sera and are passaged at a split ratio of 10:1 twice weekly. Levels of intracellular calcium can be measured in single cells grown on collagen-coated coverslips, using the calcium-sensitive fluorochrome, fura-2. Cells were loaded with fura-2-AM (10 μM in phosphate buffered saline, pH 7.3) for 50-80 min at 37°C. Excess dye was washed off and coverslips mounted on a Nikon Diaphot fluorescence microscope, adapted for dual wavelength excitation and photon-counting in single cells (Newcastle Photometrics, Newcastle, UK). The dye was excited at 350 and 380 nm and emission was measured at 520 nm. Cells were superfused with solutions at approx. 6 ml/min at 35-37°C and solutions were changed using a multiway tap with <100 μl dead space.

As previously reported (Revest, Abbott and Gillespie, 1991) primary cultures of RBCEC respond to bradykinin, histamine and ATP by increases in intracellular calcium. In this study similar increases in $[Ca^{2+}]$, have also been found in RBE4 cells, where the most effective agonist was ATP. The order of agonist potency of the adenosine nucleotides was ATP>ADP>AMP which is characteristic of P_2 purinoceptors. Responses

to bradykinin and histamine were also observed although some cells did not respond to all the agonists. Responses were greatest at days 2-3 after passage and disappeared over time. The response to ATP was not significantly different either in the presence of extracellular calcium or in calcium-free solutions. The changes in ratio were 0.63±0.1 (mean S.E.M.) n=6 and 0.53±0.1 n=8 respectively. On repeated exposure to ATP, RBE4 cells showed a reduction in the size of the calcium signal, this desensitization being characteristic of P_2 purinoceptors (Bumstock and Kennedy, 1985). Further work is being carried out in order to determine the subtype of this P_2 receptor.

Supported by the MRC and the Nuffield Foundation.

REFERENCES

Abbott, N.J., Hughes, C.C.W., Revest, P.A. and Greenwood, J. (1992) Development and characterization of a rat brain capillary endothelial culture: towards an *in vitro* blood-brain barrier. J. Cell Science 103, 23-37.

Bumstock, G. and Kennedy, C. (1985) Is there a basis for distinguishing 2 types of P2-purinergic receptor. Gen. Pharmacol. 16, 433-440.

Durieu-Trautmann, O., Fédérici, C., Créminion, C., Foignant-Chaverot, N., Roux, F., Claire, M., Strosberg, A.D. and Couraud, P.-O. (1993) Nitric oxide and endothelin secretion by brain microvessel endothelial cells: regulation by cyclic nucleotides. J. Cell Physiol. 155, 104-111.

Revest, P.A., Abbott, N.J. and Gillespie, J.I. (1991) Receptor-mediated changes in intracellular [Ca^{2+}] in cultured rat brain capillary endothelial cells. Brain Res. 549, 159-161.

Neurobiology 1 (3), p. 269, 1993

THE POTENTIAL FOR RECEPTOR-MEDIATED TRANSCYTOSIS THROUGH THE BLOOD-BRAIN BARRIER WITH BLOOD-BORNE FERRO-TRANSFERRIN AND ANTIBODY AGAINST THE TRANSFERRIN RECEPTOR

Broadwell, R.D., Baker, B.J. and Friden, P.

University of Maryland School of Medicine, Baltimore, Maryland, and Alkermes, Inc., Cambridge, Massachusetts, U.S.A.

The potential for receptor-mediated transcytosis across the blood-brain barrier (BBB) for ferro-transferrin (f-TRF) and antibody against its receptor appearing on BBB endothelia was investigated in rats. TRF, a blood-borne peptide, conveys iron to tissues and cells. BBB endothelia exhibit the receptor for f-TRF on the luminal surface plasmalemma. Rats were injected into the carotid artery with f-TRF conjugated to HRP (6mg/0.5ml; 1-3hrs.) or intravenously with native HRP (6-40mg/0.5ml; 1-3hrs.), HRP-conjugated or non-conjugated antibody to the f-TRF receptor (OX26 antibody; 200-700ug/0.5ml; 5mins. - 6hrs.), or with major histocompatibility complex class I antibody (OX27; 210 ug/0.5ml; 1-6hrs.) against the PVG rat strain; the latter antibody and native HRP were used as controls. Antibodies not conjugated to HRP were identified immunohistochemically. f-TRF-HRP, each of the antibodies, and native HRP labeled BBB endothelia, perivascular phagocytes, and pial surface macrophages. f-TRF-HRP and OX26-HRP were identified ultrastructurally within endocytic vesicles, endosomes (a prelysosomal compartment), dense bodies, and perivascular clefts of BBB endothelia. f-TRF-HRP only was observed in cells of the neuropil; OX26-HRP only was localized within saccules of the Golgi complex in BBB endothelia. Concentrations of native HRP (excluding the 6mg quantity) and of OX27 antibody administered intravenously succeeded in labeling perivascular and pial surface phagocytes within 1hr.; this labeling is believed to be the result of the blood-borne proteins circumventing the BBB by extracellular routes. Transcytosis of blood-borne f-TRF-HRP and OX26-HRP through BBB endothelia is likely to occur; f-TRF-HRP is suspected to involve endothelial vesicles and endosomes in the potential transendothelial pathway, while OX26-HRP is believed to be packaged by the endothelial Golgi complex for transcytosis. None of the employed probes was identified to be endocytosed and packaged for transendothelial transfer from **brain to blood** following injection of the probes into the lateral cerebral ventricle for exposure to the abluminal plasmalemma of BBB endothelia. Transcytosis of f-TRF and antibody against the transferrin receptor through the BBB appears to be unidirectional or vectorial, from blood to brain. The significance quantitatively for transcytosis of blood-borne f-TRF-HRP and OX26-HRP across the BBB remains to be determined.

Akadémiai Kiadó, Budapest

Neurobiology 1 (3), p. 270, 1993

EFFECTS OF INTRAVENOUSLY ADMINISTERED ARGININE VASOPRESSIN ON AMINO ACID LEVELS IN THE PLASMA AND CEREBROSPINAL FLUID OF THE RAT

Reichel, A., *Begley, D.J. and Ermisch, A.

University of Leipzig, Germany and *King's College, London, UK

Fifteen free amino acids (AA) in the plasma and cerebrospinal fluid (CSF) of anaesthetised rats were simultaneously measured by an HPLC method using a gradient elution system and pre-column derivatisation with o-pthalaldehyde.

Rats were anaesthetised with pentobarbitone (30-60mg/kg) and a cannula was placed through a burr-hole in the occipital crest into the cisterna magna and cemented into position with dental acrylic. A femoral artery was cannulated for the removal of blood samples and the right jugular vein cannulated for arginine vasopressin (AVP) infusion. A CSF sample, (20-40ul), was withdrawn by gentle suction on the cisternal cannula and an arterial sample (250ul) taken from the femoral artery. Animals were then infused with AVP at a rate of either 34 or 68ng/min/kg which raised the basal levels of AVP by approximately 2.5 and 4.4 times respectively, measured by radioimmunoassay. Further CSF and blood samples were taken after 1 hour of AVP infusion.

The infusion of AVP produced changes in both plasma and CSF levels of free AA. In plasma, levels of eleven AA increased. whereas in CSF ten AA levels decreased after AVP infusion. Interestingly, the correlation between CSF and plasma AA concentrations seen after saline infusion are abolished when plasma AVP is raised by approximately 2.5 times, suggesting that blood-borne AVP is able to disturb the reflection of plasma AA levels in CSF. There are also qualitative differences between the two rates of infusion of AVP, especially on the levels of branched chain AA.

The results will be discussed in relation to the known ability of vasopressin to down-regulate the activity of the L-system AA transporter at the blood-brain barrier.

The authors would like to thank Dr. Mary Forsling of the United Medical and Dental School, St. Thomas's Hospital London, for performing the radioimmunoassay and The British Council and The German Academic Research Council for financial support.

Akadémiai Kiadó, Budapest

Neurobiology 1 (3), pp. 271-272, 1993

SELECTIVITY IN THE OXIDATIVE DAMAGE OF NEUTRAL AMINO ACID TRANSPORT IN ISOLATED BOVINE BRAIN MICROVESSELS

Cardelli, P., Strom, R., Ceci, F., Giglio, R.M., Barbaro, K., Parisi, M., Bozzi*, A.

Dipartimento di Biopatologia Umana, Univarsità degli Studi "La Sapienza" Roma; *Dipartimento di Scienze e Tecnologie Biomediche e di Biometria, Università degli Studi Dell' Aquila, Italia

The oxidative damage of cell membranes has been extensively studied in erythrocytes where in vitro exposure to *tert*-butylhydroperoxide (*t*-BHP) was found to induce peroxidation of membrane lipids (evidentiated by malonyldialdehyde formation) as well as degradation of several membrane proteins. By using bovine brain microvessels, which are the in vitro model of the blood-brain barrier, we studied the effect of *t*-BHP treatment on the neutral amino acid transport systems. Bovine brain microvessels, isolated according to a previously described procedure (Cardelli-Cangiano et al., J. Neurochem. 36: 627-632, 1981), were exposed in a glucose-free buffer for 30 min at 37°C to *t*-BHP concentrations ranging from 0 to 100 μM, then rapidly washed and resuspended for 5 min in warm (37°C) *t*-BHP-free buffer containing 10 mM glucose, and then assayed, as described by Cardelli-Cangiano et al. (J. Neurochem. 49: 1667-1673, 1987), for their ability to take up neutral amino acids. As it is well known, isolated brain microvessels possess essentially the "L" and "A" transport systems for neutral amino acids. The characteristics of these systems are the following: the A-system is specific for the small neutral amino acids, is concentrative, glucose and Na^+-dependent, has a strong pH sensitivity and is present only on the abluminal side of the brain microvessels; the L-system is specific for the large neutral amino acids, posseses very strong exchanging properties, is Na^+-independent, has minimal sensitivity to pH, and is active on both the luminal and abluminal sides of the blood-brain barrier. Exposure to *t*-BHP was found to cause a selective dose-dependent inactivation of the A-system, as specifically assayed by monitoring the time course uptake of labeled α-methylaminoisobutyrate (MeAIB); after 20 min exposure to ^{14}C-labeled MeAIB (4 μM) the recovered intracellular radioactivity corresponded to 36 pmol/mg protein in control microvessels vs 6 pmol/mg protein in *t*-BHP treated ones. The presence of glucose during the *t*-BHP treatment did not prevent the oxidative damage. When the

isolated microvessels were treated, before exposure to 100 μM *t*-BHP, with 5 mM inosine, the subsequent uptake of labeled MeAIB by the A-system was partially retained (after 20 min exposure to labeled MeAIB the recovered intracellular radioactivity corresponded to 18 pmol/mg protein). Exposure to *t*-BHP, which had no effect on the activity of the L-system of amino acid transport (as tested by following the uptake of the specific substrate *DL*-β-aminobicyclo-2,2,1-heptanecarboxylic acid), caused also a consistent decrease of the intracellular ATP content and of the enzymatic activities of γ-glutamyltranspeptidase and hexokinase, but not of alkaline phosphatase (Table 1).

Table 1

	control microvessels	*t*-BHP 100 μM
γ-glutamyltranspeptidase (mU/min/mg/ protein)	1658±377	757±52
alkaline phosphatase (mU/min/mg protein)	135±39	117±26
hexokinase	22±5	13±4
ATP (nmol/g tissue)	8.8±1.5	1.8±0.4

Data shown are the mean of three different determinations ±S.D.

Although the loss of activity of the A-system could simply be a consequence of the ATP-generating system(s), it may be worth mentioning that a close association of this transport system with γ-glutamyltranspeptidase activity had already been found (Cardelli Cangiano et al., J. Neurochem. 1987) upon collagenase treatment of brain microvessels.

Neurobiology 1 (3), p. 273, 1993

BLOOD-BRAIN BARRIER EXPRESSION OF Na, K-ATPases

Berislav V. Zlokovic

Dept. of Neurosurgery and Divn. Neurosurgery CHLA USC School of Medicine, Los Angeles, CA 90033

The blood-brain barrier (BBB) and the choroid plexus are important homeostatic sites for the regulation of ionic fluxes between the extracellular and cerebrospinal fluids of the brain. Control of transport in and out of the brain is essential for normal neuronal functions and for maintenance of physiologic brain volume and intracranial pressure. The sodium pumps, Na,K-ATPases in cerebral capillaries and the choroid plexus catalyze active translocation of K^+ and Na^+ across the BBB and blood-cerebrospinal fluid barrier. We have recently applied the quantitative Western blot analysis to study the relative levels of expression of Na, K-ATPase α and β subunit isoforms in rat cerebral microvessels, choroid plexus, and capillary depleted brain homogenates (Zlokovic et al., 1993). Three α (α_1, α_2, α_2) and two β (β_1, β_2) subunits were detected in microvessels. The choroid plexus expressed α_1, β_1 and β_2, while α_2 and α_3 were not found. Autoradiographic signals were normalized to a constant amount of protein from the 3 tissues to calculate relative levels of expression. We found that expression of functionally active Na, K-ATPase isoenzymes in microvessels and choroid plexus are restricted in comparison to capillary-depleted brain possibly due to a limited pool of β_1 and β_2 subunits. We also suggest that six structurally distinct Na, K-ATPase isoenzymes may be expressed in cerebral microvessels and two in the choroid plexus. Down-regulation of the α_2 subunit isoform at the BBB was found as a result of chronic nicotine treatment and hypokalemia.

This work is supported by 2RT0071 grant.

Zlokovic et al. (1993). J. Biol. Chem. 268 (11), 8019-8025

Neurobiology 1 (3), p. 274, 1993

CALCIUM/CALMODULIN - STIMULATED PROTEIN KINASE II IS PRESENT IN PRIMARY CULTURES OF CEREBRAL ENDOTHELIAL CELLS

Deli, M.A., Krizbai, I., Lengyel, I., *Nunzi, M.G., **Wolff, J.R. and Joó, F.

Laboratory of Molecular Neurobiology, Institute of Biophysics, Biological Research Center, Szeged, Hungary, *FIDIA Research Laboratories, Abano Terme, Italy, **Zentrum Anatomie, Universitat Göttingen, Germany

Calcium/calmodulin-stimulated protein kinase II, a major kinase in brain has been established to play an important role in neurotransmitter release, organization of postsynaptic receptors, and it is known to be involved in long term potentiation and memory. Less is known about the function of this enzyme in non-neural cells. Production, presence and phosphorylation of the α-subunit of CaM-PK II was demonstrated by in situ mRNA hybridization, immunohistochemistry, western-blot and in vitro protein phosphorylation techniques in primary cultures of cerebral endothelial cells. These results raise the possibility that α-CaM-PK II can act as one of the key enzymes of calcium-mediated intracellular signalling in the cerebral endothelial cells. CaM-PK II may participate in such basic cellular processes as permeability in physiological and pathological conditions.

Akadémiai Kiadó, Budapest

Neurobiology 1 (3), pp. 275-276, 1993

PERICYTES OF THE BLOOD-BRAIN BARRIER EXPRESS AMINOPEPTIDASE N

Krause, D., Kunz, J., Kremer, M. and Dermietzel, R.

Institute of Anatomy, University of Regensburg
Universitätsstr. 31, 8400 Regensburg, Germany

We have recently described a monoclonal antibody recognizing a 140 kDa peripheral plasma membrane protein in cerebral pericytes of the rat. The 140 kDa antigen could also be detected at particular sites of transporting epithelia, e.g. proximal tubules of kidney, bile canaliculi of liver, enterocytes of small intestine. Epithelial cells of proximal tubules of the kidney are enriched in the 140 kDa protein recognizable by our antibody.

In order to perform microsequencing of the 140 kDA protein we used kidney brush border preparation as a source for 140 kDa protein enrichment.

A peptide sequence of the N-terminus (17 amino acids) was obtained by Edman degradation. The sequence was screened for homologies on a protein data bank and we found a 100% identity of our N-terminal fragment to aminopeptidase N (APN) from rat kidney.

The presence of APN has been described in various regions of the central nervous system e.g. choroid plexus, synaptic membranes and microvessels. Our monoclonal antibody, however, recognizes APN only on pericytes of parenchymal blood vessels in regions of intact blood-brain barrier. The lack of immunoreactivity in the neuropil suggests the presence of different isoforms of APN in the central nervous system. There is evidence that cerebral pericytes are furnished with a APN species immunologically homologeous to kidney brush border APN.

In order to prove the molecular identity of the 140 kDa protein being APN in cerebral pericytes we used the RT-PCR technique with one oligonucleotide primer (sense) of our sequenced BBB-peptide and another primer (antisense) of kidney APN. The PCR-product from cerebral microvessel RNA yielded a 100% homology with kidney brush border APN. Furthermore this PCR-product was used as a labelled probe to identify the APN-mRNA in total RNA extracts of brain microvessels by Northern blot analysis. The data clearly indicate that cerebral pericytes are furnished with APN.

Akadémiai Kiadó, Budapest

Involvement of APN in the degradation of various physiologically active peptides such as enkephalins, angiotensin I and II has been described.

We propose that cerebral pericytes provide a substantial functional contribution to blood brain barrier homoeostasis, especially to the control of peptides entering the perivascular compartment either from the parenchyma or from the blood side.

Neurobiology 1 (3), p. 277, 1993

ATTEMPTS TO DEMONSTRATE VASOPRESSIN RECEPTORS AT THE BLOOD-BRAIN BARRIER BY ELECTRON MICROSCOPIC AUTORADIOGRAPHY

Schneider, H., Kretzschmar, R. and Ermisch, A.

University of Leipzig, Germany

The blood-brain barrier is equipped with specific binding sites for peptides. While the distribution pattern of peptide receptors has been found to differ between brain regions the heterogeneity at the cellular level remains to be elucidated, e.g. by electron microscopic autoradiography.

Saturable binding of arginine-vasopressin (AVP) was found at the blood-brain barrier both, in vivo using the intracarotid bolus injection technique and in vitro by radioligand binding studies on isolated brain microvessels of rats.

Here, we used isolated capillaries of rat hippocampus which were incubated with ^{125}I-AVP and then fixed with glutaraldehyde. In electron microscopic autoradiographs of the capillaries silver grains were present at the luminal and abluminal side of endothelial cells but were also associated with pericytes.

In competition experiments the specific binding of ^{125}I-AVP to different cellular compartments has been analyzed by silver grain counting.

Akadémiai Kiadó, Budapest

Neurobiology 1 (3), p. 278, 1993

HISTAMINE TRANSPORT IN CULTURED ENDOTHELIAL CELLS

[1]Huszti, Zs., [2]Deli, M. and [2]Joó, F.

[1]Neurobiology Unit, Department of Pharmacodynamics, Semmelweis Medical School, Budapest and [2]Laboratory of Molecular Neurobiology, Institute of Biophysics, Biological Research Centre of Hung. Acad. Sci., Szeged, Hungary

Cultures of brain capillary endothelial cells provided a new means to study the transcellular transport of various substances through the endothelial cell monolayers (Pardridge et al., 1990). Furthermore, a new application, namely culturing the cells on one side of a filter, provided an opportunity to measure the uptake (release) in both the luminal and abluminal sides of the barrier.

Studies showed that [^{3}H]-histamine could be taken up by endothelial cells (such as by astroglial cells; Huszti et al., 1990) by a carrier-mediated mechanism from both the luminal and abluminal sides. The uptake was Na^+-dependent and showed high affinity for histamine giving approx. identical K_m and V_{max} values for the luminal and abluminal transports (K_m: 0.3-0.5 μM; V_{max}: 3-5 pmoles x mg protein x min^{-1}).

After a short (3 min) second incubation, 35-45% of [^{3}H]-histamine, taken up into the cultured cells either from the luminal or the abluminal side, is released into the upper part of the system.

These results indicate that histamine transport system exists in the brain endothelial cells and operates presumably from the brain side towards the blood circulation.

REFERENCES

Pardridge, W.M., Triguero, D., Yang, J. and Cancilla, P.A. (1990) Comparison of in vitro and in vivo models of drug transcytosis through the blood-brain barrier. J. Pharmacol. Exp. Ther. 253, 884-891.

Huszti, Zs., Rimanóczy, Á., Juhász, A. and Magyar, K. (1990) Uptake, metabolism and release of [^{3}H]-histamine by glial cells in primary cultures of chicken cerebral hemispheres. Glia 3, 159-168.

Akadémiai Kiadó, Budapest

Neurobiology 1 (3), p. 279, 1993

SUBTRACTION CLONING OF GENES SELECTIVELY EXPRESSED AT THE BLOOD-BRAIN BARRIER: AN APPROACH TO IDENTIFY NOVEL MOLECULAR COMPONENTS OF BBB-FUNCTION

Zinke, H., Schepelmann, S., Seehaus, B., Weller, H. and Gassen, H.G.

Institut für Biochemie, Petersenstrasse 22, D-64287 Darmstadt, Germany

In an approach to investigate molecular components of blood-brain barrier function we chose the subtractive cloning method from a set of possible molecular cloning techniques. Subtraction of transcripts represented in a tissue of interest against those of another tissue or cell type has been used in the past successfully by other groups to investigate different issues.

We were able to generate a set of brain capillary specific cDNA clones by subtracting porcine brain capillary cDNA from mRNA isolated from porcine lung, which was chosen as comparative tissue due to the high degree of vascularisation and the high similarity to brain capillaries as determined by solution hybridisation.

From 20 000 independent cDNA clones 400 were selected randomly and investigated by a differential screening procedure. 19 clones strongly hybridizing with capillary cDNA were further investigated. Among these clones the blood-brain barrier markers gamma-glutamyltranspeptidase and the glucose transporter (GLUT-1) were represented as well as another known sequence, apolipoprotein A1, the expression of which has not been described for brain capillaries before.

The expression of these proteins was further investigated on the transcriptional and translational level. Active protein synthesis could be shown for GLUT-1, apoA1 and GGT. In case of the apolipoprotein A1, protein secretion was detected. Moreover, the cholesterol and insulin regulation of apoA1 gene expression was shown, indicating an autonomous HDL/lipid metabolism of the central nervous system.

Hitherto unknown sequences or those with moderate homology to known molecules require a more complicated strategy for further investigation. Recently, a transcript could be identified as a novel receptor protein resembling several classes of cytokine-receptors. The genetically strict regulation and the unique expression in differentiated BBB-endothelium possibly indicate the involvement of this receptor in BBB-function. This transcript is under intense investigation.

Akadémiai Kiadó, Budapest

Neurobiology 1 (3), p. 280, 1993

INDUCTION OF LEUKOCYTE-ENDOTHELIUM INTERACTION IN CEREBRAL MICROCIRCULATION BY PLATELET-ACTIVATING FACTOR

Uhl, E., Pickelmann, S., Baethmann, A. and Schürer, L.

Ludwig-Maximilians-Universtät München, Klinikum Grosshadern

Introduction: Platelet-activating factor (PAF) is a phospholipid which may play a role as mediator of secondary brain damage in traumatic or ischemic injury of the brain. Its mechanisms in peripheral organs are associated with platelet aggregation, increased vascular permeability, vasoconstriction, and priming of leukocytes. Details of how PAF contributes to secondary brain damage, however, are still unknown. Purpose of the present study was to analyse, whether cerebral or systemic administration of PAF causes pathophysiological alterations in the cerebral microcirculation.

Methods.: Sprague-Dawley rats were anesthetized with α-chloralose and artificially ventilated after relaxation with pancuronium bromide. After implantation of a closed cranial window continous superfusion with artificial CSF was started. Intravital microscopy was then performed using Rhodamin 6G as intravital fluorescence marker for leukocytes. Vessel diameters, leukocyte velocity in venules and the number of leukocytes firmly attached to or rolling along the venular endothelium were assessed before, during and after the superfusion (20min, 5ml/h) of PAF 10^{-12} M, 10^{-9} Mand 10^{-6} M. In a second experiment the superfusion with PAF was replaced by intraarterial administration of PAF in identical concentrations into the carotid artery. The experimental protocol was otherwise not changed. In a third group the PAF-antagonist WEB 2170 (2mg/kg/b.w.) was given additionally 15min prior to intraarterial application of PAF 10^{-6} M.

Results: Cerebral superfusion with PAF does not induce vasomotor alterations or leukocyte-endothelium interactions in the pial microcirculation, although leading to arterial hypotension. Intraarterial administration of PAF causes a transient blood pressure decrease and dilation of arterioles, while sustained leukocyte-endothelium interactions were observed. Specificity of the PAF-induced hemodynamic and microcirculatory effects is confirmed by their complete antagonisation by pretreatment with WEB 2170BS.

Discussion: Adhesion of leukocytes to the vessel wall is a requirement of emigration of leukocytes during early inflammation. As shown increased systemic levels of PAF as found in shock may induce leukocyte-endothelium interactions in the cerebral microcirculation. On the other hand activation of leukocytes did not occur during cerebral superfusion with PAF, although arterial hypotension was also observed.. Mechanims underlying this intruiging response are not known. The findings indicate, nevertheless, that release of PAF in the cerebral tissue under pathologic conditions may induce leukocyte-endothelium interactions, however, only if the powerful phospholipid reaches the vascular lumen.

Akadémiai Kiadó, Budapest

Neurobiology 1 (3), p. 281, 1993

LYMPHOCYTE ADHESION TO BRAIN CAPILLARY ENDOTHELIAL CELLS IN VITRO

[1,2*]de Vries, H.E., [1]Moor, A.C.E., [1]Blom-Roosmalen, M.C.M., [1]de Boer, A.G., [1]Breimer, D.D., [2]van Berkel, Th.J.C. and [2]Kuiper, J.

[1]Division of Pharmacology and [2]Division of Biopharmaceutics, Leiden/Amsterdam Center for Drug Research, University of Leiden, Sylvius Laboratories, P.O. Box 9503, 2300 RA Leiden, The Netherlands

The presence and upregulation of adhesion molecules on bovine brain capillary endothelial cells (BBEC) was investigated in primary cultures. To study the adhesion of lymphocytes to cerebral endothelial cells, an *in vitro* lymphocyte adhesion assay was developed using isolated bovine lymphocytes. Monolayers of BBEC were incubated with lipopolysaccharide (LPS), interleukin-1ß (rhIL-1ß), and interleukin-6 (rhIL-6) to simulate an inflammatory site in the cerebral capillaries. Adhesion of lymphocytes to BBEC increased 3-4 fold, when endothelial cells were stimulated for 4 hr with 5 or 10 ng/ml LPS. In addition, adhesion increased dose-dependently with IL-1 1.5 fold using 25 ng/ml, and 3-4 fold using 100 ng/ml. BBEC stimulated with IL-6 showed also a concentration-dependent increase in the adhesion of lymphocytes, cells treated with 10 ng/ml IL-6 showed a 2 fold increase and using 100 ng/ml, a 3-fold increase of lymphocytes adherence was observed. Specific monoclonal antibodies directed against CD11a, CD18, and VLA-4 were used to inhibit the adherence of the lymphocytes in the bioassay. It was shown that Intercellular Adhesion Molecule (ICAM-1) and Vascular Cell Adhesion Molecule (VCAM) were involved in the adhesion of lymphocytes to BBEC. The results show that it is now possible to simulate an inflammation site in our *in vitro* model for the blood-brain barrier.

Akadémiai Kiadó, Budapest

Neurobiology 1 (3), p. 282, 1993

VASCULARIZATION AND HOST IMMUNE RESPONSE TO MAMMALIAN CNS GRAFTS PLACED INTRACEREBRALLY OR PERIPHERALLY: THE BLOOD-BRAIN BARRIER AND IMMUNOLOGICAL PRIVILEGE

Broadwell, R.D. and Baker, B.J.

Division of Neurological Surgary, University of Maryland
School of Medicine, Baltimore, Maryland, 21201, U.S.A.

Graft survivability is dependent upon the graft developing a vascular network supplied with host blood and not being rejected as a consequence of the host immune response. We have analyzed by immunohistochemistry and electron microscopy the origins and morphological characteristics of vessels supplying fetal CNS grafts placed into brain, testis, or beneath the kidney capsule of adult host rats. Syngeneic and allogeneic CNS grafts were performed with donor/host combinations between inbred PVG and PVG(AO) rats. Monoclonal antibodies used included: OX-27 for major histocompatibility complex (MHC) class I expression by PVG endothelial cells; OX-26 for the transferrin receptor expressed constitutively by blood-brain barrier (BBB) endothelia; OX-18 for general MHC class I; and OX-7 for expression of Thy 1 on viable CNS neurons. HRP was delivered iv to ascertain a graft BBB to blood-borne protein. All grafts to the host CNS were vascularized predominantly with host vessels and possessed a BBB with tight junctions. Syngeneic grafts to the kidney capsule were supplied with OX-26+ BBB vessels, whereas allogeneic grafts failed to survive. Syngeneic/allogeneic grafts to the testis survived and exhibited OX-26+ BBB vessels; donor vessels predominated within these allografts. Host testis MHC+ vessels were evident within CNS grafts and appeared OX-26 negative. The proportions of donor vs. host vessels in CNS grafts, regardless of their MHC expression and permeability characteristics, may depend on the host site and/or genetic disparity between donor and host.

The privilege of the CNS with respect to grafting may be due to the absence of dendritic cells and lymphatic drainage and the existence of a BBB. Despite reported immunological privilege, the testis has dendritic-like cells, a lymphatic drainage, and permeable vessels. Syngeneic grafts were placed within the testis or CNS of inbred PVG rats. Allografts were prepared between PVG and PVG(AO) rats differing at MHC loci and between PVG and AO rats differing at MHC and minor HC loci. With monoclonal antibodies, CNS grafts were deemed surviving if they expressed uniform Thy 1 staining, low MHC class I expression, few MHC class II+ cells, and negligible numbers of CD4+/CD8+ cells. Syngeneic grafts to the adult host CNS or testis appeared healthy and viable for 30 days. All allografts within the CNS parenchyma of adult hosts survived well. CNS allograft viability to the testis at 30 days was variable. Vigorous graft rejection occurred between PVG and AO rats and less so between donor PVG and host PVG(AO) rats; graft survival without demonstrable rejection was evident between donor PVG(AO) and host PVG rats. The data suggest immune privilege of the testis is less demonstrable than that of the CNS. Survival of some allografts to the testis may be due to local immunosuppressant factors. Existence of similar immunosuppressant factors within the CNS may represent an additional consideration in defining CNS immune privilege.

Akadémiai Kiadó, Budapest

Neurobiology 1 (3), p. 283, 1993

BRAIN ISCHAEMIA (STROKE) IS FOLLOWED BY ACTIVE ANGIOGENESIS

Krupiński[1,2], J., Kaluża[1], J., Kumar[2], P., Kumar[3], S. and Wang[3], J.M.

[1]Department of Neuropathology, Jagiellonian University, Cracow, Poland; [2]Manchester Metropolitan University, Manchester, UK; [3]Christie Hospital, Manchester, UK

Focal cerebral ischaemia is a major cause of death and disability in Western world. Stroke results from a reduction in cerebral flow, following the occlusion of cerebral arteries or its branches. As a result, some areas become ischaemic, while others become hyperemic. Hyperemia usually occurs in the border zone known as the penumbra of the infarct and may be associated with hyper-perfusion following the ischaemic insult.

Variability in capillary changes has prompted us to undertake quantitative morphometric studies of infarcted areas of brain. In the initial study, brains were obtained at autopsy from 10 patients (ages 46-85). Samples were collected from infarcted hemisphere and controls from the contralateral hemisphere. Formalin fixed and paraffin embedded sections were stained after Pickworth and with H&E. Altogether 6,520 microvessels, representing 10,801 microscopic fields were counted. The Wilcoxon range test was used for statistical analysis. In 9 of 10 patients in infarcted brains, there was a marked increase in the capillary density ($p<0.01$) when compared with normal brain tissues. In addition, a positive correlation was also found between the time of survival and both total density and density of non-perfused blood vessels.

Furthermore, the vascular endothelial cells in infarcted brain were shown to be reactive with two monoclonal antibodies, one, E-9, directed against an activation/proliferation associated endothelail cell specific protein and the other recognising adhesion molecule V-CAM. The stroke tissues contained angiogenic activity, as shown by the induction of new blood vessels in an in vivo chicken chorioallantoic membrane (CAM) assay. It is suggested that a therapeutic approach aimed to stimulate angiogenesis might ameliorate tissue damage and thereby stroke associated mortality and morbidity. It might also prevent subsequent stroke in patients with transient ischaemia attacks (TIA) who are at increased risk (approximately 50%) of subsequent ischaemic attacks and deaths.

Akadémiai Kiadó, Budapest

Neurobiology 1 (3), p. 284, 1993

THE PROBABLE CAUSE OF PARALYSIS OBSERVED IN CHRONIC RELAPSING ENCEPHALOMYELITIS INDUCED IN STRAIN 13 GUINEA-PIGS

Segal., M.B. and Egleton, R.D.

Sherrington School of Physiology, United Medical and Dental Schools of Guy's and St. Thomas's Hospitals, St. Thomas's Campus, London, SE1 7EH, UK

Chronic experimental allergic encephalomyelitis (CR-EAE) in strain 13 guinea-pigs is a good model for multiple sclerosis (MS) in man and can be induced by an intramuscular inoculation into both hind limbs with a homogenate of homologous spinal cord, Freunds complete adjuvant and mycobacterium tuberculi. After some 14-18 days the guinea-pigs exhibit a standard pattern of weight loss and bilateral hind limb paralysis with occasional bladder involvement. By careful hand feeding and hydration the animals can survive this episode and after some three days show a sudden and complete recovery. This attack is followed some 14-20 days later by cycles of relapse and remission which are of decreasing severity.

Studies by other groups have shown that in EAE there is an increase in the permeability of the blood-brain barrier, just preceding the attack phase, followed by increased lymphocyte trafficking, inflammation and cuffing of blood vessels. Histological studies have shown variable areas of demyelination which has been reported to reduce conduction of motor and sensory nerves in the spinal cord.

Of considerable interest has been the poor correlation between the degree of demyelination and the observed bilateral hind limb paralysis. To investigate the pathogenesis of this paralysis we have studied, the permeability of the blood-brain barrier to mannitol, the water content and blood flow at various levels of the spinal cord during the phases of attack and relapse in CR-EAE.

These studies have shown that there is an increased permeability to mannitol during the attack phase which correlates with an increased water content and a reduction in blood flow. These findings support the concept of a localised oedema of the spinal cord during the attack phase of this condition. Since it has been well recognised that pressure can cause conduction block in nerve, it is proposed that the observed paralysis is partially a consequence of this oedema leading to a raised pressure within the spinal canal and not solely due to demyelination.

The localised oedema in the spinal cord may be caused by the leakiness of the blood-brain barrier induced by the release of histamine during the attack phase of the condition which has been shown to occur both in animals and in MS patients. An alternative cause may relate to the vascular cuffing which could cause a reduction in blood flow and hypoxia which would lead to neuronal swelling. Further studies are at present in progress to identify which of these hypotheses is correct.

Akadémiai Kiadó, Budapest

Neurobiology 1 (3), pp. 285-286, 1993

ROLE OF HISTAMINE IN BRAIN EDEMA INDUCED BY HEAT STRESS
Experimental Observations In the rat

Sharma[1-4], H.S., Westman[2], J., Nyberg[3], F.,
Cervos-Navarro[1], J. and Dey[3], P.K.

[1]Department of Neuropathology, Free University Berlin, 1000-Berlin 45,Germany; [2]Department of Human Anatomy and [3]Pharmacology, Biomedical Centre, Uppsala University, Uppsala, Sweden; [4]Department of Physiology, Institute of Medical Sciences, Banares Hindu University, Varanasi-221 005, India

The possibility that endogenous histamine plays an important role in modulating the pathophysiology of heat stress (HT) was examined in young rats using a pharmacological approach. Subjection of young animals (6-7 wks old) to HT at 38°C for 4 h in a biological oxygen demand (B.O.D.) incubator (rel. humid. 47-50%, wind vel. 20-25 cm/sec) resulted in a profound increase in blood-brain barrier (BBB) permeability to Evans blue albumin (EBA, average 375%) and ^{131}I-sodium (average 478%) along with a significant reduction in the cerebral blood flow (CBF, average 32%). The water content of the whole brain was elevated by 3.6% (about 16% volume swelling) from the control. At this time period, the plasma and brain 5-HT levels were elevated by 200% and 365%, respectively from the control group. Morphological examination revealed marked cell changes in many parts of the brain. Thus dark and distorted neurons, perivascular edema, swelling of astrocytes, vesiculation of myelin, and extravasation of lanthanum across cerebreal vessels were quite frequent. Pretreatment with cimetidine (a histamine H_2 receptor antagonist) significantly thwarted the increases in the brain water content and BBB permeability. The CBF was moderately elevated and the plasma and brain 5-HT levels were slightly but significantly reduced as compared with the untreated stress group. However, prior treatment with mepyramine (a histamine H_1 receptor antagonist) neither attenuated the changes in water content and the BBB permeability nor affected the CBF and 5-HT level. In fact, there was a significantly higher permeation of the tracers across the cerebral vessels in this drug treated animals alongwith a greater accumulation of the brain water content as compared to the untreated stress group. The CBF and 5-HT levels did not differ from the untreated stress group. The cell changes were reduced with cimetidine treatment, but pretreatment with mepyramine was ineffective in reducing cell damage.

Akadémiai Kiadó, Budapest

These results strongly indicate that the endogenous histamine has a role in the pathophysiology of HS which appears to be mediated via specific histamine receptors.

REFERENCES

1. Sharma, H.S., Nyberg, F., Cervos-Navarro, J. and Dey, P.K. and Dey, P.K. (1992) Neuroscience 52:
2. Sharma, H.S., Kretzschmar, R., Cervos-Navarro, J., Ermisch, E., Rühle, H.J. and Dey, P.K. (1992) Prog. Brain Res. 91: 189-196.
3. Sharma, H.S., Cervos-Navarro, J. and Dey, P.K. (1991) Brain Dysfunct. 4: 110-121.

Neurobiology 1 (3), p. 287, 1993

PATHOPHYSIOLOGY OF PASSAGE OF PEPTIDES ACROSS THE BLOOD-BRAIN BARRIER

Banks, W.A. and Kastin, A.J.

Veterans affairs Medical Center and Tulane University School of Medicine, 1601 Perdido Street, New Orleans, LA 70146

Several regulatory peptide and protein substances have been shown to enter or exit the central nervous system to a biologically relevant extent. This has raised the possibility that the blood-brain barrier (BBB), comprised of the endothelial and ependymal barriers, may be involved in controlling the exchange of humorally borne informational molecules between the blood and the CSF/interstitial fluid of the brain. Peripherally administered peptides shown to enter the CNS by non-saturable transmembrane diffusion to an extent large enough to affect brain function include delta sleep-inducing peptide, which can alter the electroencephalogram (EEG), cyclo His-Pro, which can reverse ethanol-induced narcosis, and an analog of methionine enkephalin (MENK), Tyr-D-Ala-Gly-MePhe-Met(O)-ol, which can alter the EEG at opiate receptor sites located behind the BBB. Self-inhibitable transport has been found for several peptides (e.g., MENK, leucine enkephalin, Tyr-MIF-1, oxytocin, Tyr-W-MIF-1, vasopressin, somatostatin, LHRH) and regulatory proteins (e.g., LH, interleukin-1α and -1ß, tumor necrosis factor-α) in the CNS to blood or blood to CNS directions. We have categorized the findings from our laboratory in a peptide transport system (PTS) classification. PTS-1 transports mostly Tyr-MIF-1 and MENK, although smaller amounts of leucine enkephalin, oxytocin, Tyr-W-MIF-1, and probably dynorphin$_{1-8}$ and ß-casomorphin are also transported. The level of PTS-1 activity is apparently linked to concentrations of MENK in the brain. For example, both PTS-1 activity and brain concentrations of MENK decrease with aging. PTS-1 does not transport ß-endorphin, dynorphin, kyotorphin, dynorphin$_{1-17}$, dermorphin, morphiceptin, vasopressin, or any fragment of Tyr-MIF-1. PTS-1 transports peptides in the CNS to blood direction only and does not have a blood to CNS component. PTS-1 is stereospecific, transporting Tyr-MIF-1 that contains the L, but not the D, isomer of tyrosine and seems not to require energy. Leucine is an allosteric regulator of PTS-1 at a site on the CNS side of the BBB, with D-leucine being 100 times more potent than L-leucine. Aluminum and serotonin, but not acetylcholine, epinephrine, norepinephrine, dopamine, GABA, kainic acid, cGMP, or cAMP, can alter PTS-1 function. Despite its transport of opiate-related peptides, PTS-1 seems to be only indirectly related to regulation of analgesia. PTS-1 is not affected by acute administration of ethanol, but it and concentrations of MENK in the brain are suppressed in mice addicted to ethanol and in alcohol-naive mice that have a genetic predisposition to drink. PTS-1 recovers rapidly in addicted mice when chronic ethanol ingestion is stopped and this recovery may account for the paradoxical further decline in brain levels of MENK. Signs of withdrawal, associated with the decline in brain MENK, can be prevented by MENK, MENK analogs, or inhibitors of enzymes that destroy MENK. This suggests that PTS-1 may be involved in the alcohol withdrawal syndrome and may be a therapeutic target in the prevention of alcohol withdrawal.

Banks, W.A. and A.J. Kastin. Quantifying carrier-mediated transport of peptides from the brain to the blood. P. Michael Conn (ed.), Meth. Enzymol.,168:652-660, 1989.

Banks, W.A. and A.J. Kastin. Editorial Review: Peptide transport systems for opiates across the blood-brain barrier. Am. J. Physiol. 259:E1-E10, 1990.

Banks, W.A., K.L. Audus, and T.P. Davis. Permeability of the blood-brain barrier to peptides: An approach to the development of therapeutically useful analogs. Peptides 13:1289-1294, 1992.

Akadémiai Kiadó, Budapest

Neurobiology 1 (3), p. 288, 1993

CNS PERICYTES HAVE IMMUNE POTENTIAL

Dore-Duffy, P. and Balabanov, R.

Wayne State University School of Medicine, Neurology, Detroit, MI

The blood brain barrier is a complex cellular system consisting of endothelial cells, pericytes, perivascular smooth muscle cells and astrocytes. The role of the pericyte in regulation of vascular function is unknown. We hypothesize that the pericyte may be important in neuroimmune networks centered at the blood brain barrier in inflammation, infection and trauma. Rat CNS pericytes were prepared from Lewis rat CNS microvessels. Pericytes were examined by immunofluorescence staining and quantitated by laser cytometry and FACS analysis. Eicosanoid release was measured by HPLC, and pericytes were tested for phagocytosis of pre-opsonized erythrocytes. Results indicate that pericytes in intact microvessels and in primary culture express Fc receptors and the rat macrophage marker CD11b (OX-42). The marker recognized by ED1 was expressed in low intensity. Pericytes in culture phagocytized opsonized cells. Pericyte production and release of eicosanoids was similar to monocytes with the exception of low thromboxane levels. In conclusion, pericytes express macrophage cell surface markers, phagocytize and produce eicosanoid repertoires similar to macrophages. They have immune potential.

Akadémiai Kiadó, Budapest

Neurobiology 1 (3), p. 289, 1993

STRATEGIES FOR OPENING THE GATEWAY TO THE BRAIN

Nicholas Bodor

Center for Drug Discovery, University of Florida, Gainesville, FL 32610

The brain, the major organ in the body, has a unique protective barrier, the so-called blood-brain barrier (BBB), which provides a very efficient exclusion from the brain of a wide variety of blood-borne compounds. This lipid-like barrier, consisting of the tightly joined endothelial cells in the brain capillary walls, prevents penetration into the brain of hydrophilic compounds (various neurotransmitters, amino acids, etc.) unless they are transported into the brain by an active transport system. The blood-brain barrier contains highly active enzyme systems as well, which further enhance the already very effective protective function.

In the past ten years or so, various attempts were made to deliver molecules otherwise inaccessible to the brain. These include physical, biological, and chemical site-specific delivery systems. In most cases, very limited success was reported. This is partly because these attempts concentrate only on the *transport through the BBB*, which generally results in simultaneous significant efflux of the delivered molecule. The successful approaches aim the control of bidirectional transport processes, enhancing influx, but avoiding efflux. These are the enzymatic-physical-chemical-based targeting approaches based on retrometabolic concepts, which can generally be described as follows:

The drug is chemically modified, introducing protective functions (F) and the targetor moiety (Tor), resulting in the chemical delivery system (CDS). Upon administration, the CDS is distributed throughout the body, which arbitrarily is divided as the "site" (^{s}) and the "rest of the body" (^{r}). Predictable enzymatic reactions convert the original CDS by modifying the targetor moiety and, consequently, removing some of the protective functions (F), leading to a still inactive precursor from of the CDS, D-$T^{\oplus\prime}$. This form as well as some of the previous intermediate CDS's are continuously eliminated from "rest of the body." On the other hand, due to the presence of a specific membrane or other distribution barrier, like the BBB, the efflux-influx processes at the site are not the same as the rest of the body. The various modifications and particularly conversion of the targetor to $T^{\oplus\prime}$ will provide a specific concentration of this precursor at the site, ultimately allowing release of the active drug only at the site of action. This concept was exemplified by the now well-known trigonelline ⇌ dihydrotrigonelline redox Tor system, where the positively charged trigonelline derivative formed *in situ* in the brain results in "lock-in."

A recent further modification of this concept called "molecular packaging" allows efficient brain delivery of peptides. Here the peptides (like enkephalins or TRH analogs) are modified to the extent that the new CDS is not recognized as a peptide anymore. This is achieved by instead of introducing a perturbation into the peptide molecule, the peptide represents just a perturbation in the CDS. This allows its passive transport through the BBB and the various F and Tor functions to operate.

Akadémiai Kiadó, Budapest

Neurobiology 1 (3), p. 290, 1993

THE ACTION OF VASOACTIVE AGENTS IN BRAIN MICROVESSELS

Christian Frelin

Institut de Pharmacologie Moléculaire and Cellulaire, CNRS,
660 route des Lucioles, Sophia Antipolis 06560 Valbonne, France

Endothelial cells were isolated from rat brain microvessels (BCEC) and grown under clonal conditions. Their reactivity to vasoactive agents was analyzed and compared to that of aortic endothelial cells (BAEC). BCEC express two types of endothelin receptor: (i) an ETA like receptor that is positively coupled to phospholipase C and (ii) an ETB like receptors that does not discriminate between endothelin isopeptides and that controls the activity of the Na/H exchange system. Unlike BAEC, BCEC produce little or no endothelin. BCEC express ANPB receptor sites that are specific for brain derived C type natriuretic peptide (CNP). In contrast BAEC mainly express ANPB receptors that recognise CNP with a low affinity. BCEC unlike BAEC do not express the constitutive form of NO synthase. They can be induced to express the inducible form of NO synthase in response to cytokines such as interleukin-1 and tumor necrosis factor. BCEC and BAEC express a P2 receptor that recognises ATP and UTP and that is coupled to phospholipase C. In addition BAEC have a P2y receptor coupled to phospholipase C. BCEC do not express P2y receptors but have an ADP specific receptor that induces the mobilisation of intracellular calcium stores in the absence of measurable production of inositol phosphates. Finally BCEC, unlike BAEC, express high level of soluble guanylate cyclase which can be activated by exogenous NO and NO donnor molecules.

It is concluded that rat BCEC have a unique phenotype that is clearly distinct from that of BAEC. It is furthermore suggested that vasoactive agents have different functions in brain microvessels and in large peripheral vessels. In peripheral vessels, vasoactive agents (endothelins, NO, ATP) are produced by endothelial cells and control the contractility of vascular smooth muscle cells. In central microvessels, vasoactive agents may originate from neuronal and glial cells and control the properties of endothelial cells. Putative targets for vasoactive agents in BCEC will be discussed as well as possible heterogeneity of capillary endothelial cells.

Akadémiai Kiadó, Budapest

Neurobiology 1 (3), pp. 291-292, 1993

PHARMACOLOGICAL MODULATION OF ISCHEMIC BRAIN EDEMA: EFFECTS OF VARIOUS PUTATIVE ANTI-EDEMA AGENTS AFTER FOCAL CEREBRAL ISCHEMIA IN CATS

Johshita, H. and Asano*, T.

Saitama Cardiovascular Center Project Office, Dept. of Public Health, Saitama Prefectural Government; *Dept. of Neurosurgery, Saitama Medical Center, Saitama Medical School

The exact mechanism underlying ischemic edema during (prolonged) and/or after (reperfusion) edema after focal ischemia is still not precisely understood. Since saving living tissue from an ischemic and/or reperfusion injury is vitally importanct from both a basic and clinical standpoint, we estimated the effects of various putative anti-edema drugs on transorbital cat middle cerebral occlusion (MCAO) model.

Materials and method: The MCA of the animal was approached transorbitally under halothane anesthesia and was occluded for 4 hours (prolonged ischemia, PI) or occluded for 2 hours and recirculated for 2 hours (recirculation, RC). LCBF was monitored by hydrogen clearance technique in six electrodes implanted in the MCA territory and the corresponding cortical specific gravity (co-SG) was measured by microgravimetry in the each electrode site. Both in the PI and RC groups (7-11 cats in each group), the depth of ischemia was expressed by the average lCBF value in each electrode during ischemia. In the PI groups the following agents (pretreatment if not indicated in prenthesis) were tested: two calcium antagonists; nicardipine (pre-treatment and post treatment), and 2-nicotinamidoethyl nitrate (SG-75, post-treatment), indomethacin, BW755-C, OP-41483 and ONO-47241 (PGI2 analogues), and ONO-3144, AVS (1,2-bis (nicotiamido)-propane), ebselen, and Tirilazad Mesylate as radical scavengers. In the RC groups, a thromboxane antagonist (OKY-1581), indomethacin, ONO-3144, AVS, ebselen and Tirilazad Mesylate (U74,600F) were tested.

Results and conclusion: Following prolonged ischemia, nicardipine and SG-75 somewhat exacerbated cortical water content in the core of the lesion although lCBF increased in the moderate and lightly ischemic areas. Indomethacin significantly increased edema formation in the moderately ischemic area while ONO-47241, AVS, and ebselen caused significantly improvement in the severely ischemic (ONO-47241, AVS, ebselen) and moderately ischemic (AVS) areas. Co-SG values of

Akadémiai Kiadó, Budapest

the groups treated by OP-41483, BW-755C, ONO-3144 and U74,600F were not different from those of the control group. In the RC groups, indomethacin, ONO-3144 and ebselen significantly ameliorated edema formation in the severely ischemic area. AVS was further effective in moderately ischemic areas while U74,600F was effective only in this area. OKY-1581 was ineffective. The distribution histograms of co-SG after prolonged ischemia were mostly unimodal while the histograms were bimodal in the RC groups and the groups post-treated with calcium antagonist, indicating that pharmacological micro-recirculation might be induced by calcium blockers. The above results may imply that, for the treatment of cytotoxic edema, some PGI2 analogue and radical scavengers may be useful while blockade of cyclooxygenase or lipoxygenase may not be useful, and the use of calcium blockers might be even harmful. In contrast, the fact that all the radical scavengers and the cyclooxygenase inhibitor had significant effects on reperfusion edema strongly indicates free radical generation in this pathological condition.

Neurobiology 1 (3), p. 293, 1993

CONTRIBUTION OF THE IN VITRO APPROACH TO BLOOD-BRAIN BARRIER RESEARCH

Ferenc Joó

Biological Research Center, 6701-Szeged, Hungary

Ever since the discovery of restricted material exchange existing between the blood and the brain, the ultimate goal of subsequent studies has been mainly directed towards the elucidation of relative importance of different cellular compartments in the peculiar penetration barrier consisting the structural basis of the blood-brain barrier. It is now generally believed that apart from a few exceptions where the structural basis of restricted movement of certain substances is due to an impermeable glial sheath, the **cerebral endothelial cells** regulate the entry of solutes and macromolecules from the blood circulation to the brain tissue in the majority of vertebrates. After an era of studying with endogenous or exogenous tracers the unique permeability properties of cerebral endothelial cells in vivo, the next generation of blood-brain barrier model systems was introduced, when the conditions for isolating the microvessels from brain tissue and culturing the endothelial cells were established. Recent advances in our knowledge of the blood-brain barrier have in part been made by studying the properties and function of cerebral endothelial cells with this in vitro approach. Namely, a considerable amount of new information has been gained during the last twenty years in respect to the basic chemical, biochemical and physiological properties of the blood-brain barrier. This review will summarize in brief those main results, which were obtained by the use of the in vitro approach.

Akadémiai Kiadó, Budapest

POSTERS

An International Workshop on

Molecular Mechanisms Regulating the Permeability of the Blood-Brain Barrier

held between July 23-24, 1993

at the **Biological Research Center, Szeged, Hungary**

Neurobiology 1 (3), p. 297, 1993

PHENOTYPIC DIVERSITY OF CLONED CEREBRAL CAPILLARY ENDOTHELIAL CELLS REFLECTS DIFFERENT FUNCTIONS IN THE BRAIN

Bauer, H.C., Schwärzler, C., Amberger, A., Webersinke, G., Zach*, O., Karlhuber, G., Adam, H. and Bauer*, H.

Inst. Mol. Biol. (Austr. Acad. Sci.), Billrothstrasse 11, Salzburg, Austria and *Inst. Zool., Univ. Salzburg, Austria

Cloned cerebral capillary endothelial cells (cEC) of porcine and murine origin have recently been shown to differentiate reversibly into two distinct phenotypes, depending on environmental conditions. Addition of ECGF and heparin leads to the expression of a cobblestone-like appearance (type I cEC), whereas depletion of these factors results in a spindle-formed, "smooth-muscle like" morphology (type II cEC). The two cell types were shown to differ markedly in their responsivness to glial stimulation, i.e. blood-brain barrier induction in vitro. Bbb-function was estimated by the activation of bbb-related marker enzymes, such as NaK-ATPase and gamma-glutamyl transpeptidase. This led us to formulate the testable hypothesis that type I cEC correspond to the blood-brain barrier endothelium in vivo, which was further supported by the finding that GLUT 1 mRNA level was significantly higher in this cell type compared to type II cEC. We have further shown that type II cEC migrate at a much higher rate than do type I cells and also express α-actin mRNA and protein, which may indicate that this cell type is rather involved in capillary formation and invasion. Protein expression pattern of cEC of both phenotypes was examined with 2-D-PAGE and the GELLAB II 2-D-gel analysis system. Besides α-actin, there were two proteins (36 kD and 90 kD), which could only be found in typ I cEC.

In another set of experiments an attempt was made to investigate the involvement of the endothelial basement membrane in blood-brain barrier function. To this end, the expression of the major exctracellular matrix protein-components was studied by Northern analysis. We have demonstrated that cEC of different morphology display variations in the expression of fibronectin, thrombospondin I and collagen IV. Unexpectedly, the calcium-binding protein SPARC (osteonectin) could not be detected in any of the capillary endothelial cells examined.

Akadémiai Kiadó, Budapest

Neurobiology 1 (3), p. 298, 1993

EXPRESSION OF THE LDL RECEPTOR IN BRAIN CAPILLARY ENDOTHELIAL CELLS IS STIMULATED BY A SOLUBLE FACTOR(S) SECRETED FROM ASTROCYTES

Dehouck, B., Dehouck, M.P., Fruchart, J.C. and Cecchelli, R.

SERLIA-INSERM U325, Institut Pasteur, 59019 Lille Cédex, France

The presence of lipoproteins, apolipoproteins, and their receptors in the brain could provide a system for cholesterol homeostasis, as they do in other tissues. Our previous work demonstrating "in vivo" the occurrence of a low density lipoprotein (LDL) receptor on the endothelium of brain capillaries has suggested that this cerebral endothelial receptor plays a role in lipid transport across the blood-brain barrier. To examine further the function of this receptor, we have established an "in vitro" model, that closely mimics the "in vivo" situation, by co-culturing brain capillary endothelial cells and astrocytes. In these conditions brain capillary endothelial cells specifically bind LDL. This binding was totally blocked by antibody C7, known to interact with the receptor binding domain, suggesting the presence of LDL receptor on brain capillary endothelial cells in culture and its interaction with LDL. Furthermore, we observed that the capacity of endothelial cells to bind LDL is enhanced 3 fold when cocultured with astrocytes. For this reason, we next investigated the ability of astrocytes to modulate endothelial cell LDL receptor expression. When only astrocytes of the coculture were preincubated in lipoprotein deficient media, binding of LDL to endothelial cells was increased a further 6 fold, indicating that the lipid requirement of astrocytes increases the expression of endothelial cell LDL receptor. This upregulation specifically affected the LDL receptor, not the acetyl-LDL receptor. Experiments with dialysis membranes of different pore size showed that this effect is mediated by a soluble factor(s) with a molecular weight somewhere between 3,500 and 14,000. This factor(s) is exclusively secreted by astrocytes cocultured with brain capillary endothelial cells, but it also upregulates the LDL receptor on other cell types. These results demonstrate that the blood-brain barrier could be considered as an active interface that has a critical role in the maintenance and regulation of brain functions.

Akadémiai Kiadó, Budapest

Neurobiology 1 (3), p. 299, 1993

K-OPIOID RECEPTOR TYPE BINDING SITES IN CULTURED RAT CEREBRAL ENDOTHELIAL CELLS

Deli*, M.A., Bajenaru**, M.L., Maderspach**, K. and Joó*, F.

Laboratory of Molecular Neurobiology, Institutes of Biophysics* and Biochemistry**, Biological Research Centre, Szeged, Hungary

Cerebral microvascular endothelial cells forming blood-brain barrier in co-operation with astrocytes, neurons, and pericytes, play pivotal role in the homeostatic regulation of CNS during physiological and pathological processes. Opioid receptor binding was first demonstrated in isolated cerebral microvessels by Peroutka in 1980 using tritiated naloxone and DALE. Oktem described that an irreversible μ-opioid receptor ligand, DAMCK, labelled one major and two additional minor protein bands on isolated rat brain microvascular membranes. Though different opioid receptors were characterized both in cultured neurons and astroglial cells , no information could be found in the literature concerning opioid binding to endothelial cell cultures prepared from brain capillaries. Recently, a monoclonal antibody, KA8, recognizing k- but not μ- and δ-opioid receptors has been raised.

Primary cultures of endothelial cells isolated from rat cerebral cortex microvessels were characterized by the presence of factor VIII-related antigen and *Bandeira simplicifolia* lectin binding. Monoclonal antibody KA8, raised in mice against k-opioid receptor enriched frog brain membrane fractions, recognizing k- but not μ- and δ-opioid receptors (Maderspach et al. (1991) *J. Neurochem.* **56,** 1897-1904) gave a dot-like, perinuclear immunohistochemical staining on endothelial cells. (^{3}H)naloxone binding assay showed low affinity and low capacity binding sites on intact cultures, cell suspensions and cell homogenates. Our present data may suggest the existence of k-opioid receptors in cerebral endothelial cells.

Akadémiai Kiadó, Budapest

Neurobiology 1 (3), p. 300, 1993

RECEPTOR-MEDIATED TRANSCYTOSIS OF TRANSFERRIN AT THE BLOOD BRAIN BARRIER

Descamps, L., Dehouch, M.P., Dehouck, B., Fruchart, J.C. and Cecchelli, R.

SERLIA-INSERM U325, Institut Pasteur, 59019 Lille Cédex, France

It is now well established that transferrin (the principal iron carrier serum protein) receptors are present on the luminal surface of brain capillary endothelial cells, and that these cell type is the site for transendothelial transport of iron to supply the central nervous system with its iron requirements. Moreover, brain microvessels endothelial cells appear to express more transferrin receptors relative to other capillary beds from major organs (except liver).

Using a coculture model of bovine brain capillary endothelial cells and rat astrocytes, we have shown that bovine transferrin bind specifficaly on brain capillary endothelial cells. Because there are few cell surface receptors, we have treated cells with saponin in order to have access to total cellular transferrin receptors. In contrast to bovine transferrin, no fixation was observed with human transferrin, demonstrating the specificity of the receptor-ligand interactions. To examine further the function of this receptor, we have studied accumulation and subsequent efflux of transferrin in brain endothelial cells. In these conditions, no efflux was directed towards the apical side, or by analogy, the luminal side, but only towards the abluminal side. Furthermore, we have shown that these cells, in contrast to other works performed with primary culture of brain microvessels endothelial cells, are the site of a specific transendothelial transport of transferrin. This phenomen is inhibited at low temperatures. We have also noted, that no transferrin degradation was observed. Moreover, non loaded transferrin did not cross the blood brain barrier (BBB) as much as holotransferrin. This result was consistent with other works on other cell types, which show that apotransferrin has less affinity to its receptor than holotransferrin.

In conclusion, all these results suggest that our BBB endothelial cell monolayers are polarized in a blood-brain direction, and that they are the site for transendothelial transport of the iron-transferrin complex to the brain.

Akadémiai Kiadó, Budapest

Neurobiology 1 (3), p. 301, 1993

AN IN VITRO MODEL FOR HYPOXIA/REOXYGENATION WITH ENDOTHELIAL CELLS

Mertsch, K., Grune, T., Ladhoff, A. and Blasig, J.

Forschungsinstitut für Molekulare Pharmakologie,
Alfred-Kowalke-Str. 4, 0-1136 Berlin, Germany

Reactive oxygen species are important mediators of a variety of pathological processes of the brain including atherosclerosis, inflammation and ischemia/reperfusion.

The two main functions of cerebral endothelium - maintenance of a blood-brain-barrier and preservation of the blood fluidity - are affected by reactive oxygen species occurring during disturbances related to hypoxia. Because endothelial cells play an important role during postischemic oxidative stress - as a source and/or a target of oxygen free radicals - they are still of interest as a cellular model for in vitro investigating hypoxia/reoxygenation processes.

The experiments were performed by means of aortic endothelial cells as well as brain endothelial cells which underwent hypoxia (95% N_2) and reoxygenation (95% O_2). The parameters investigated - LDH - leakage, lactate, ATP, ADP, TBARS - clearly indicate cell damage. The concentration of TBARS is significantly enhanced after 15 min and 30 min of reoxygenation following 2 h of hypoxia (95% N_2, 5% CO_2) in brain endothelial cells compared to control cells and cells after 2 h hypoxia. In aortic endothelial cells TBARS - increase was significant only after 30 min of reoxygenation.

Electron micrographs of cells after 2 h hypoxia, 2 h hypoxia and 15 min/or 30 min reoxygenation respectively showed an increasing amount of lysosomes, multivesicular bodies, vacuoles and - during reoxygenation - blebs compared to normoxic control incubation. Lipofuscin was detected in some cells. Cell damage seems to reach a greater extent in brain endothelial cells.

The presented models for hypoxia/reoxygenation for brain endothelial cells (primary) and aortic endothelial cells (cell line) are suitable tools for the investigation of protective substances in pharmacology and for studying pathological mechanisms on blood-brain-barrier.

Akadémiai Kiadó, Budapest

Neurobiology 1 (3), p. 302, 1993

REGULATION OF GAMMA-GLUTAMYL TRANSPEPTIDASE AND ALKALINE PHOSPHATASE ACTIVITIES IN IMMORTALIZED RAT BRAIN MICROVESSEL ENDOTHELIAL CELLS

Roux, F.S., El Hafni, B., Bardoul, M.,
Bourre, J.-M., Couraud, P.-O.

INSERM U.26, Hospital Fernand Widal, 200 rue du Faubourg Saint-Denis, 75010 Paris, France

The signals that induce endothelial cells to express the blood-brain barrier phenotype are believed to result from specific interactions between capillary endothelial cells and the ensheathing perivascular astrocytes. The in vitro study of the molecular mechanisms of this induction has been dependant so far on the availability of pure and abundant cultures of brain microvessel endothelial cells. This study was performed with immortalized rat brain microvessel endothelial cells, which were isolated after transfection of primary cultures with the plasmid E1A-Adenovirus encoding gene. These cells displayed a non-transformed endothelial phenotype characterized by the expression of Factor VIII-related antigen and of binding sites for the lectin Bandeiraea Simplicifolia, a spindle-shaped morphology when proliferating in the presence of basic fibroblast growth factor (bFGF) and the formation at confluence of a continuous monolayer of non-overlapping cells.

When RBE4 cells were grown on collagen-coated tissue culture plastic, in medium containing high concentrations of bFGF, confluent cultures developed sprouts that extend above the monolayer and organized into three-dimensional structures. Gamma-glutamyl transpeptidase activity (gamma-GT), a blood-brain barrier associated enzyme, and alkaline phosphatase, a microvascular marker, could be shown in numerous cells inside these structures.

In cultures treated by differentiating agents, such as retinoic acid, 8-bromo cyclic AMP, phorbol 12-myristate 13-acetate (PMA) and sodium butyrate, expression of gamma-GT and alkaline phosphatase activities was increased. With retinoic acid and PMA, increased activities could be associated with increased formation of tubular structures. In a coculture system with a direct cell-cell contact between astroglial cells and RBE4 cells, gamma-GT activity was markedly enhanced in endothelial cells, whereas no significant change in alkaline phosphatase activity was observed.

These results show that the immortalized rat brain microvessel endothelial cells RBE4, beside displaying a non-transformed endothelial phenotype, remain sensitive to angiogenic, differentiating and astroglial factors regarding the expression of the blood-brain barrier gamma-GTP enzymatic activity. Alkaline phosphatase activity would not be modified by astroglial factors and may be regulated by different mechanisms.

Akadémiai Kiadó, Budapest

Neurobiology 1 (3), p. 303, 1993

CHANGES OF VASCULAR PERMEABILITY IN THE ADULT DORSAL ROOT GANGLION TRANSPLANTED INTO THE OLFACTORY BULB OF NEONATAL RAT

Sekerkova[1,2], G., Malatova[1], Z., Orendacova[1], J., Halász[2], N., Zigova[1], T.

Neurobiological Institute, Srobarova 57, 040 00 Kosice, Slovakia
and Biological Research Centre, H-6701 Szeged, Hungary

Our previous histochemical study have shown butyrylcholinesterase positive blood vessels growing out from the host olfactory bulb into the transplanted adult dorsal root ganglia [DRG] suggesting their blood- brain barrier properties [BBB]. In the present work we wanted to confirm the changed vascular permeability of transplanted DRG. For this reason we applied Lucifer yellow [LY] and Evans blue [EB] as tracers for fluorescent microscopy and Lanthanum nitrate as a tracer for electron microscopy.

In the control DRG the sensory neurons exhibiting yellowish fluorescence were surrounded by blood vessels showing EB red or LY green fluorescence. Three months postoperatively we found only few labelled blood vessels either with EB or LY on the surface of the transplanted DRG. There were no labelled blood vessels around the surviving neurons showing yellowish dot-like labelling similar to control. Some neurons with damaged membranes were filled with LY appeared as green neurons in the fluorescence microscope. By electron microscopic study we found electron-dense lanthanum in the lumina of blood vessels adhered to their inner surface. The lanthanum particles entered the clefts between endothelial cells. In the majority of the blood vessels the tight junctions did not allow lanthanum ions to penetrate into intercellular compartment. In some blood vessels the pinocytosis of tracer was obvious. In few cases we observed a massive penetration of lanthanum particles through spaces between endothelial cells. It can be concluded that the vascular permeability of the transplanted DRG may have partially changed and a chimeric vascularization between the host and donor blood vessels occurred.

Akadémiai Kiadó, Budapest

(Contents continued)

PRINTED IN HUNGARY

Akadémiai Kiadó és Nyomda Vállalat, Budapest

ANNOUNCEMENT

FIRST CONGRESS
OF THE
HUNGARIAN NEUROSCIENCE SOCIETY

Pécs, January 27-29, 1994

The 1st Congress of the Hungarian Neuroscience Society will be held on January 27-29, 1994, in Pécs. All major topics of Neuroscience will be covered. Abstracts will be published in Neurobiology.

For more information, contact:

László Lénárd, Congress President
Institute of Physiology
Pécs University Medical School
H-7643 Pécs, Szigeti út 12, Hungary
Fax: 36-72-326 244

INSTRUCTIONS TO AUTHORS

Aims and Scope. *Neurobiology* is a multidisciplinary international journal, which publishes contributions from all traditionally important and newly emerging subdisciplines of the neurosciences including neuroanatomy, morphology, histochemistry, physiology, pharmacology, molecular neurobiology, developmental neuroscience, etc. Referees from a large international Editorial/Advisory Board will review submissions critically.

Submission. The journal publishes original, unpublished papers and reviews (conference abstracts, book reviews, announcements, advertisements, etc. may also appear from time to time) in English. The text should not exceed 15 typewritten pages (total length with illustrations, tables, etc., 20 pages).
Manuscripts should be submitted in triplicate to the Editorial Office:

Norbert Halász
Institute of Biophysics
Biological Research Centre
Hungarian Academy of Sciences
H-6701 Szeged, P.O. Box 521, Hungary
Telefax: 36 (62) 433 133
Phone: 36 (62) 432 232
E-mail: H3186HAL@ELLA.HU

Accepted manuscripts will not be returned to the authors.

To accelerate publication the papers will be reproduced directly from the authors' manuscripts, so those must be suitable for photographic reproduction. Authors should use electric typewriters with black (carbon) ribbon or high quality printers. Manuscripts not conforming to the specified instructions will be returned for reorganizing and retyping. Authors are encouraged to submit their papers also on floppy discs, using preferably WordPerfect, or Word as processors on IBM compatible computers.

Manuscripts should be typed on A4 (210x297 mm) papers. All margins should be 2.5 cm except upper margins on front (6 cm) and other pages (4 cm). Page numbering should be done only by soft pencil.

Regular papers should be organized into sections in the following order: Summary, Key words, Introduction, Materials and Methods, Results, Discussion (followed by Conclusions and Acknowledgements, if relevant), References. Illustrations, tables and their explanations should be inserted into the appropriate sections; all these should be centred.

The Introduction, Results and Discussion should be typed by a one and a half line spacing, while the rest of the sections should be typed by single space. The title, authors, and their affiliation should be centred.

Title. Use bold, block capital letters, enlarged if possible.

Authors and their Affiliation. Type by single space. Leave two and one line spaces above and below the authors' names, respectively.

Summary. Keep three line spaces above and one below the summary (not exceeding 150 words). The summary should be indented by five spaces on both sides.

Key words. A maximum of six key words or short phrases should be given and be indented similar to the summary.

At the rest of the text, *headlines* of the sections should be centred and typed in bold, capital letters. Use two line spaces above and one below headlines. *Subheadings* (if present) should be typed to the left side of the margin in italics (or should be underlined); line spacing: one above and below.

References. The lists should be arranged in alphabetical order. Their second and following lines should be indented by five spaces. Use abbreviated journal names. They should be arranged as the following examples show for journal and book references:

Butt, A.M., Jones, H.C. and Abbott, N.J. (1990) Electrical resistance across the blood-brain barrier in anaesthetized rats: A developmental study. J. Physiol. 429, 47-62.

Shepherd, G.M. (1988) Neurobiology. 2nd edition. Oxford Univ. Press, New York and Oxford.

Balázs, R. and Richter, D. (1973) Effects of hormones on the biochemical maturation of the brain. In: Biochemistry of the Developing Brain (ed. Himwich, W.) Vol. 1, pp. 254-304. M. Dekker, New York.

These should be cited in the text by the names of the authors and the year of publication, e.g. [Balázs and Richter, 1973; Shepherd, 1988; Butt et al., 1990].

Tables. These should be typed into the appropriate part of the text, together with their numbers, titles (above) and explanations (which should appear below the tables). Leave at least one line space between the Arabic table numbering and title, its explanation (single spaced) and the table itself, respectively. Separate the table from the text by one line space at least. Please, try to find the best fit between the width of the tables and their explanations. Data should not be duplicated in tables and figures.

Figures (line drawings, diagrams, photographs). These should be numbered consecutively by Arabic numerals. One original copy and two additional copies should be sent. Please, indicate numbers and the name of the first author and the top of the figure on the back. For *Legends* (single spaced) use the full length of text lines. Figure numbering should be followed by its legend in the same line. Do not glue Figures into the text. Please, type, however, their legends onto proper place. Legends should appear below figures, separated by one line space above (and below if the text continues on that page). Maximal (printed) size of Figures should not exceed 120x180 mm and should preferably leave enough space for the explanation on the same page. Leave at least one line space above figures.

Line drawings and diagrams. Please, prepare those in black ink by expecting a possible reduction (by 30-50%) and select lettering and symbols ensuring their recognizable final size (min. 2 mm). Please, leave enough space for them in the text plus at least one line space above and below. Reduction of line illustrations, if needed, will be done by the Publisher. *Formulae* if complex (and not typed into the text) should be prepared similarly.

Photographs. High quality half tones (please prefer higher contrast) should be prepared on glossy paper (and labelled clearly by Letraset) at their expected final size. Micrographs should also be completed by a scale bar representing the magnification and serial numbers in corners of the front of pictures. A limited number of colour photographs will also be accepted (if absolutely necessary) at no extra charge.

Abbreviations and symbols. These should be used according to the latest internationally accepted rules. They should be explained at their first appearance (and may also be listed in an alphabetical order, when desired). The SI System should be used.

Running title and address. The running title (not exceeding 50 characters and spaces) should be submitted on a separate page together with the full address, phone and fax numbers (E-mail if avaible) of the corresponding author.

Reprints. Fifty free reprints are provided to the authors. Additional reprints can be ordered from the Publisher at the time of acceptance. Fifty percent discount will be offered to young investigators and newcomers, without prior publications in this discipline.

CONTENTS

(Contents continued on page 305)

NEUROBIOLOGY

An International Multidisciplinary Journal in Neurosciences

VOLUME 1, NUMBER 4, 1993

Including the former Acta Biochimica et Biophysica Hungarica

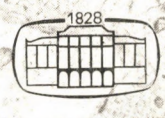

AKADÉMIAI KIADÓ, BUDAPEST

HU ISSN 1216-8063

NEUROBIOLOGY

An International Multidisciplinary Journal in Neurosciences

(Including the Former Acta Biochimica et Biophysica Hungarica)

Neurobiology is a multidisciplinary international journal publishing contributions from all traditionally important and newly emerging subdisciplines of the neurosciences including neuroanatomy, morphology, biochemistry, physiology, pharmacology, molecular neurobiology, developmental neuroscience, etc.

Neurobiology is published by
AKADÉMIAI KIADÓ
Publishing House of the Hungarian Academy of Sciences
H-1117 Budapest, Prielle K. u. 19–35, Hungary

Manuscripts and editorial correspondence should be addressed to

Norbert Halász
Institute of Biophysics
Biological Research Centre
Hungarian Academy of Sciences
H-6701 Szeged, P.O. Box 521, Hungary

Subscription price for Volume 1 (1993) in 4 issues US$ 78.00, including normal postage; airmail delivery US$ 20.00

Orders should be addressed to

AKADÉMIAI KIADÓ
H-1519 Budapest, P.O. Box 245, Hungary

NEUROBIOLOGY

An International Multidisciplinary Journal in Neurosciences

Akadémiai Kiadó, Budapest

Neurobiology 1 (4), pp. 313-325, 1993

OPTIC TERMINALS FORM AXOSOMATIC SYNAPSES WITH DEEP TECTAL NEURONS IN *BUFO MARINUS*

Robert Gábriel[1] and Charles Straznicky[2]

[1]Department of Zoology, Attila József University, Szeged, Hungary and [2]Department of Anatomy and Histology, The Flinders University of South Australia, Adelaide, Australia

Summary. Previous studies have shown that a small proportion of the retinal fibres to the optic tectum terminates in the deep tectal cellular layers (layers 6 and 4) in Anura. Horseradish peroxidase was applied to the cut central end of the optic nerve of *Bufo marinus* to study the synaptic connections of these retinotectal afferents. Some of the retinotectal afferents arrive at the deep tectal layers and form synapses with dendrites (7% of all tectal inputs) and on the somata of the deep tectal cells (0.4% of all tectal inputs). These synapses may either serve as elements of the dimming detection system or could be the morphological substrates of a direct link between the visual and the descending motor system.

Key words: horseradish peroxidase, anterograde transport, optic fibres, deep tectal neurons, axosomatic synapses, Anura.

INTRODUCTION

Most of the axons of retinal origin arrive at the superficial layer (layer 9) of the optic tectum (OT) in frogs and terminate in a very similar fashion in all species studied to date. The thick myelinated fibres have been found in four (B, D, F and G) bands while the thin unmyelinated axons in A, C and E laminae (Lázár, 1978; Montgomery and Fite, 1989; Potter 1972; Scalia and Goldman, 1974; Tóth et al., 1980;

Wilczynsky and Northcutt, 1978). It has, however, been recognised that some fibres also penetrate into the deeper, cellular layers (layers 6 and 4) of the OT (Lázár, 1978; Wye-Dvorak et al., 1992) coursing among neuronal somata.

The synaptic connections of the fibers which terminate in layer 9 of the OT has been described (Lázár and Székely, 1969; Székely and Lázár, 1976; Potter, 1969). Optic axon terminals synapse on the apical dendrites of the projection neurons and of interneurons. None of the optic axons were found to synapse on neuronal perikarya. The synapses of the optic fibres that descend into the deep tectal layers have not been documented in these studies. Therefore, in the present study we aimed at examining this component of the retinotectal synaptic assembly.

MATERIALS AND METHODS

Four adult cane toads (*Bufo marinus*) from both sexes were used in this study. The animals were obtained from a North Queensland (Australia) supplier and kept at room temperature under 12 h light/dark cycles.

Anterograde transport of horseradish peroxidase (HRP)

Animals were anaesthetised with intraperitoneally administered 0.3-0.4 ml 5% tricaine methanesulphonate (MS 222; Sigma) solution. The right optic nerve was approached through the palate and cut close to the eye ball. The central portion of the nerve was introduced into a polythene tube filled with a saturated (cca. 30%) solution of HRP (Boehringer), dissolved in 0.1M phosphate buffer (PB; pH 7.4). The tube was left on the nerve stump for 3 h at 4°C, then the animals were allowed to recover and to survive for another 3 days. The animals were finally sacrificed by an overdose of MS 222. The skull was opened over the left tectum and fixed in situ with drops of 2.5% glutaraldehyde (Merck) in 0.1M PB (pH 7.4). The OT was removed and fixed further by immersion in the same fixative for 3 h at room temperature. The OT was then cut coronally into 300-400μm thick slices with a fine razor blade, and the visualisation of the transported HRP was done by the method of Adams (1977), with the modification introduced for frogs

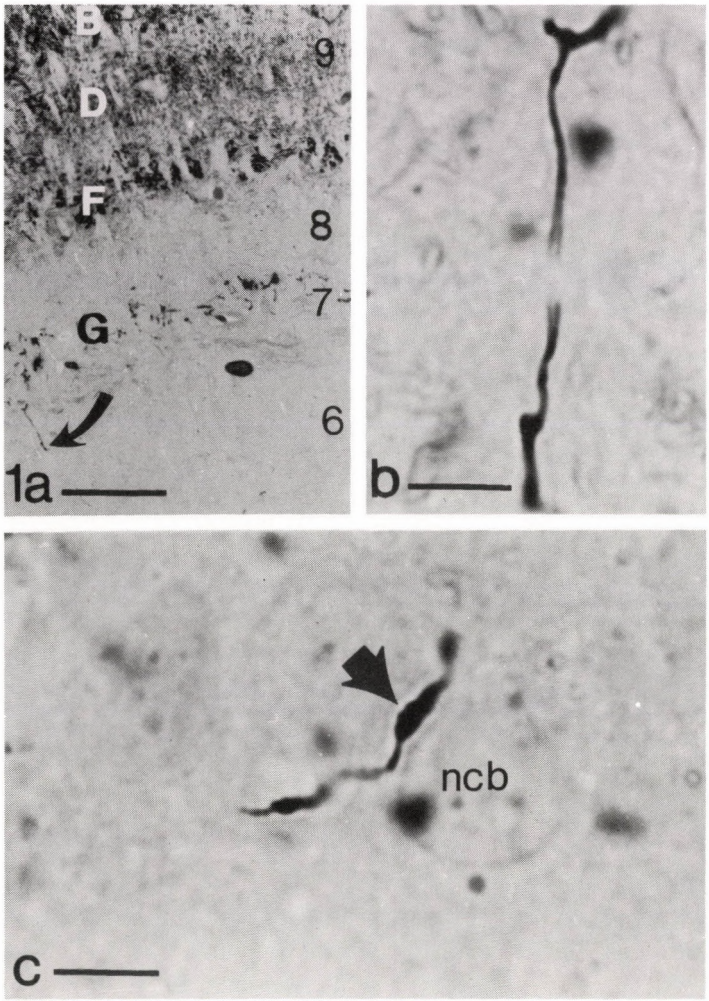

Figure 1. The distribution of HRP-labelled optic terminals in the OT of *Bufo marinus*. **a.** The distribution of optic terminals in layer 9 of the OT. Letters B, D, F and G label the respective laminae of the tectum. Arrow: a thin fibre descending to layer 6, shown with higher magnification in **b.** **Scale bars:** 100 μm in **a** and 20 μm in **b. c.** A bouton formed by a labelled optic fibre at a deep tectal cell body (ncb) in layer 6. **Scale bar:** 20 μm.

(Straznicky and Straznicky, 1988). Briefly, sections were first preincubated in 0.1M Tris buffer (pH 7.6) containing 0.05% 3,3'-diaminobenzidine (DAB), 0.05% $CoCl_2$ and 0.1% imidazole for 4 h at 4°C. Final incubation was at room temperature for 20 min in 0.1M Tris buffer containing 0.05% DAB, 0.1% imidazole and 0.01% H_2O_2. After thorough rinsing in 0.1M PB, tissues were processed for the electron microscope.

Processing for the electron microscope

Tissue pieces were treated in 1% OsO_4 (Merck) in 0.1M PB (pH 7.4) for 1 h and then dehydrated through ascending ethanol series. Amidst dehydration, block contrasting took place in 70% ethanol saturated with uranyl acetate for 1 h. The samples were embedded in Durcupan ACM resin (Fluka) and polymerised for 48 h at 56°C. Semithin (2 μm) and ultrathin (80-90 nm) sections were cut with an MT7 (RMC) microtome, mounted on single-slot copper grids and contrasted with lead citrate. Sections were viewed and photographed in an Olympus BH2 light and a JEOL 1200 EX electron microscope.

RESULTS

The anterogradely transported HRP was observed as dark cobalt-intensified DAB deposit throughout layer 9 of the OT (Fig. 1a). The intensely labelled laminae of B, D, F and G could be easily recognized as well as laminae A, C and E, which contained small-diameter (probably unmyelinated) fibres. Some HRP-filled axons however crossed layer 7 and entered into layer 6 (Fig. 1b) forming pericellular baskets there (Fig. 1c). Occasionally labelled terminals were seen also in layer 4 of the OT.

At the electron microscope level these fibres could be identified in the neuropil forming contacts with dendrites (Fig. 2a, b). The synapses between optic axons and dendrites of tectal neurons were located in the deep neuropil region, many of them clearly showing asymmetric membrane specializations (Fig. 2b).

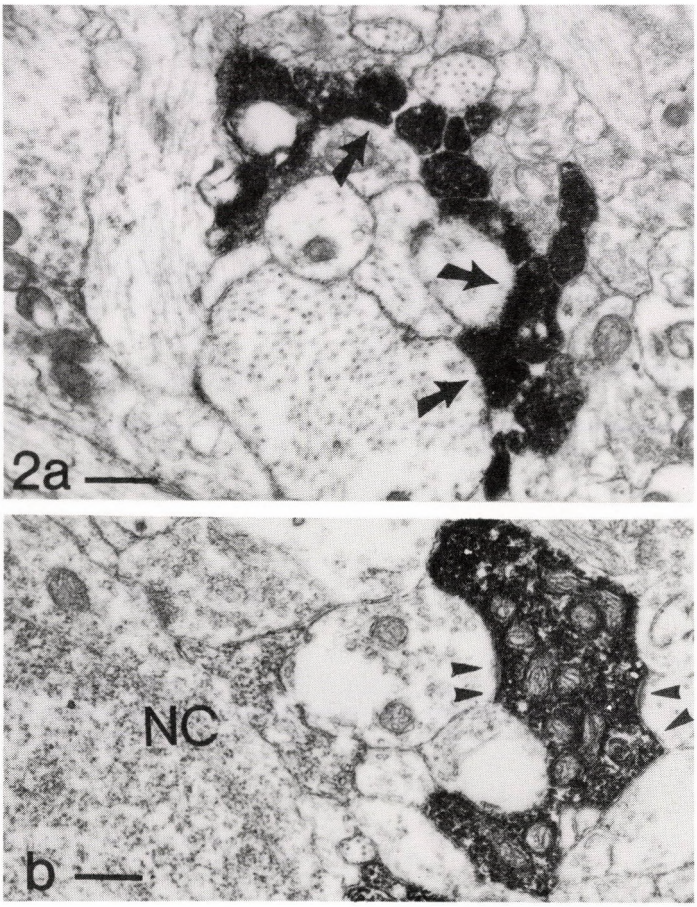

Figure 2. Axodendritic contacts in the deep neuropil. **a.** Group of optic axon profiles opposed to unlabelled dendrites (arrows). **Scale bar:** 500 nm. **b.** Synaptic contacts (arrowheads) between labelled optic terminals and unlabelled dendrites in close proximity of a nerve cell body (NC) in layer 6. **Scale bar:** 250 nm.

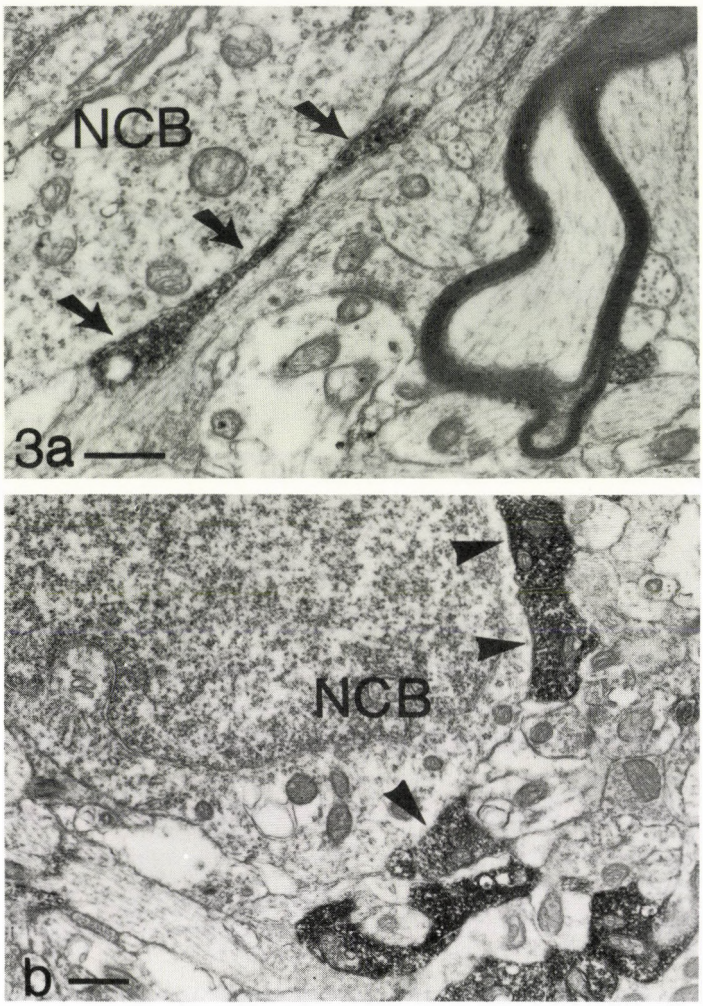

Figure 3. Contacts of labelled optic profiles with somata of deep tectal neurons. **a.** Parallel contact (arrows) between a HRP-filled profile and a neuronal cell body (NCB). **Scale bar:** 500 nm. **b.** Large-diameter profiles (arrowheads) impinging on a single soma (NCB) in layer 6. **Scale bar:** 500 nm.

Optic fibres were also regularly observed in close appositions to the somata of deep tectal neurons (Fig. 3a), as well as large diameter profiles impinging on their somata (Fig. 3b). The presynaptic terminals contained small agranular vesicles, sometimes closely associated with the presynaptic membrane (Fig. 4a). The postsynaptic thickening was small (Fig. 4b) and the dense DAB deposit in the presynaptic terminals that partially masked the presynaptic membrane but these synapses could still be classified as symmetric contacts. The postsynaptic somata possessed a fairly large cytoplasmic rim around the often indented nucleus (Figs. 3a, 5). The cytoplasm contained numerous organelles and the nucleus was rich in euchromatin (Figs. 3b, 5).

The frequency of these contacts was attempted to determine in the deep layers of OT. The total number of synapses formed by HRP-filled optic terminals, counted from ten non-serial sections of layer 9 of the OT are summarised in Table 1. Similarly, the number of axosomatic synapses formed by labelled optic terminals found in layer 6 and below, were also counted.

Table 1

Synaptic connections formed by anterogradely labelled optic terminals in the OT.

Samples	**layer 9**	**deep layers, neuropil**	**deep layers, axosomatic**	**TOTAL**
1st section	394	12	2	**408**
2nd section	207	9	1	**217**
3rd section	511	30	4	**545**
4th section	307	24	0	**331**
5th section	292	17	2	**311**
6th section	307	18	1	**326**
7th section	288	12	0	**300**
8th section	401	30	3	**434**
9th section	421	27	2	**450**
10th section	247	9	0	**256**
SUBTOTAL	**3375**	**188**	**15**	**3578**

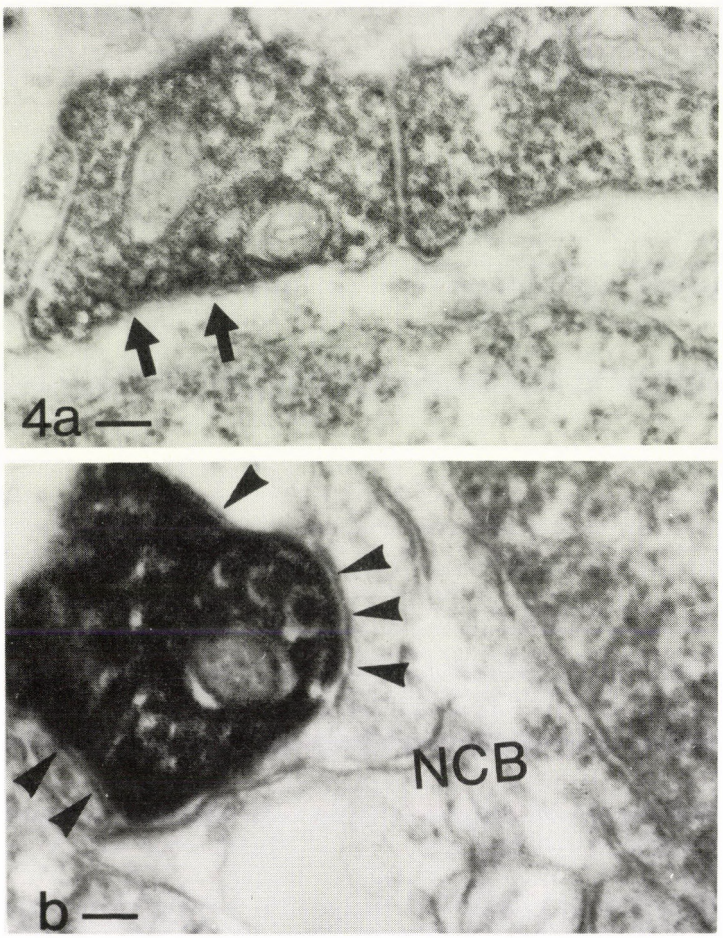

Figure 4. Ultrastructure of the axosomatic contacts in the deep tectal layers. **a.** The contacting profile (arrow) contains small agranular synaptic vesicles (arrow). **Scale bar:** 100 nm. **b.** Axosomatic synapse (arrowheads) on a deep tectal neuron (NCB) with symmetrical membrane specializations. **Scale bar:** 100 nm.

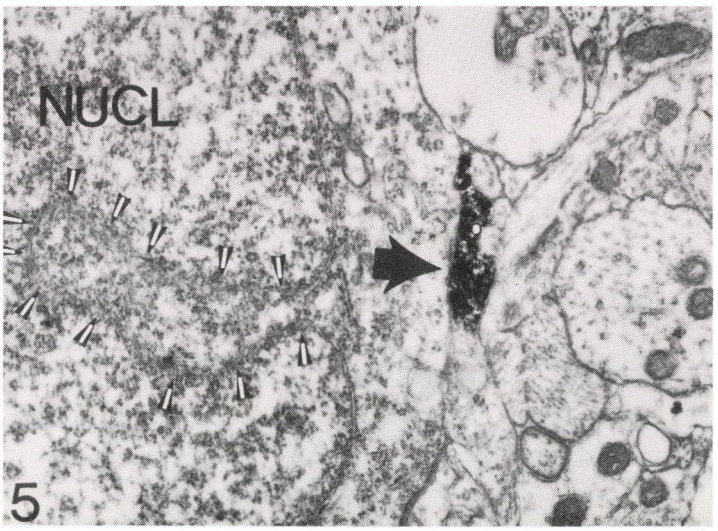

Figure 5. Neuronal soma at an axosomatic contact (arrow) possesses euchromatinised, deeply indented (arrowheads) nucleus (NUCL). **Scale bar:** 250 nm.

These results showed that only about 0.42% of optic terminals synapsed on the somata of deep tectal neurons.

Discussion

In this study HRP was utilized as an anterograde tracer to reveal the synaptic contacts formed by optic axons with the somata of the deep tectal neurons in *Bufo marinus*. Although optic fibres penetrating into layers 7 and 6 have been described in previous light microscopic studies in Anura (Lázár, 1978; Wye-Dvorak et al., 1992), these fibres have never been examined in the electron microscope. It is interesting to note that a very dense optic axon projection to one layer of deep tectal neurons has been observed in the largemouth bass (Baser and Ebbeson, 1985); the target neurons

have been identified as large pyriform cells. However, the electron microscopic confirmation of the presence of axosomatic synapses have not been carried out even in this species.

As for the significance of this deep axosomatic optic projection, two hypotheses can be offered.

(1) The majority of retinotectal axons in Anura synapses on dendrites of intrinsic interneurons and on tectal projection neurons (Antal, 1991; Potter, 1969; Székely and Lázár, 1976; Gábriel and Straznicky; 1993). About 97% of the retinal ganglion cells contain glutamate while the rest exhibit GABA immunoreactivity in *Bufo* (Gábriel and Straznicky, 1993). The GABA-positive retinal ganglion cells are small- and medium-sized. Since only 3-4% of the optic axons are myelinated, it is reasonable to assume, that the GABA-containing ganglion cells possess mostly unmyelinated axons. The distribution of GABA-immunoreactive optic terminals in the OT is not known. If the targets of the axosomatic synapses described in this study are the tectal dimming detector cells, located mostly in layers 7 and 6 (Maturana et al., 1960; Grüssel and Grüssel-Cornehls, 1976), and these optic terminals mostly contain GABA, a push-pull mechanism could be proposed. If synapses of fast-conducting glutamate-containing (excitatory) axons terminate on the distal dendrites of a dimming detector tectal neuron, and cause these cells to fire, the slow-conducting GABA-containing optic axons may shut down the activity of these cells by a time delay through axosomatic synapses. The large number of axodendritic and small number of axosomatic synapses described in this study are in support of this hypothesis.

The second hypothesis is that axosomatic synapses, described in the present study, arrive at the somata of the caudally projecting tectal neurons. It has been shown (Lázár

et al., 1983) that the vast majority (94%) of the caudally projecting tectal neurons are located in layer 7 and below. Thus this connection could serve as a direct link between the visual inputs and the descending motor systems, providing a monosynaptic pathway for prey catching and postural adjustments. This assumption is supported by previous observations, suggesting that a class of layer 6 ganglion cells (T_5 cells) plays an important role in postural adjustment for prey catching (Grüssel et al., 1975; Schürg-Pfeiffer and Ewert, 1981; Lázár et al., 1983).

Further experiments are in progress in our laboratory to gain further data in support of one of the proposed hypotheses. Nevertheless we suppose that reciprocal connections may exist between the visual and motor systems, since it has been suggested that event and dimming detector units may be involved in the escape behaviour of frogs (Chung et al., 1974).

Acknowledgements. The photographic work of Mr. F. Acsai is acknowledged. This work was supported by an NH&MRC of Australia Grant to C. S. and an OTKA Youth Award to R. G.

REFERENCES

Adams, J.C. (1977) Technical considerations on the use of horseradish peroxidase as a neuronal marker. Neuroscience 2, 141-145.

Antal, M. (1991) Distribution of GABA immunoreactivity in the optic tectum of the frog: a light and electron microscopic study. Neuroscience 42, 879-891.

Bazer, G.T. and Ebbeson, S.O.E. (1985) Axosomatic retinal projection to deep tectal neurons and retinopetal neurons in largemouth bass (*Micropterus salmoides lacepede*). Neurosci. Lett. 59, 309-312.

Chung, S.H., Bliss, T.V.P. and Keating, M.J. (1974) The synaptic organization of optic afferents in the amphibian tectum. Proc. R. Soc. Lond. [Biol.] 187, 421-447.

Gábriel, R. and Straznicky, C. (1993) Synapses of optic axons with GABA- and glutamate immunoreactive elements in the optic tectum of *Bufo marinus*. Neuroscience, submitted

Grüsser, O.J., Grüsser-Cornehls, U. (1976) Neurophysiology of the anuran visual system. In: Frog Neurobiology (Eds. Llinás, R. and Precht, W.) pp. 297-385. Springer, Berlin.

Grüsser, O.J., Ingle, D., Prosser, C.L. and Székely, G. (1975) Functions of intrinsic tectal connections. Neurosci. Res. Prog. Bull. 13, 196-203.

Lázár, G. (1978) Application of cobalt-filling technique to show retinal projections in the frog. Neuroscience 3, 725-736.

Lázár, Gy. and Székely, G. (1969) Distribution of optic terminals in the different optic centres of the frog. Brain Res. 16, 1-14.

Lázár, Gy., Tóth, P., Csank, Gy. and Kicliter E. (1983) Morphology and location of tectal projection neurons in frogs: a study with HRP and cobalt filling. J. Comp. Neurol. 215, 108-120.

Maturana, H.R., Lettvin, J.Y., McCulloch, W.S. and Pitts, W.H. (1960) Anatomy and physiology of vision in the frog (*Rana pipiens*). J. Gen. Physiol. 43, 129-175.

Montgomery, N. and Fite, K.V. (1989) Retinotopic organization of central optic projections in *Rana pipiens*. J. Comp. Neurol. 283, 526-540.

Potter, H.D. (1969) Structural characteristics of cell and fibre in the optic tectum of the frog (*Rana catesbiana*). J. Comp. Neurol. 136, 203-232.

Potter, H.D. (1972) Terminal arborizations of retinotectal axons in the bullfrog. J. Comp. Neurol. 144, 269-283.

Scalia, F. and Colman, D.R. (1974) Aspects of the central projection of the optic nerve in the frog as revealed by anterograde migration of horseradish peroxidase. Brain Res. 79, 496-504.

Schürg-Pfeiffer, E. and Ewert, J.-P. (1981) Investigation of neurons involved in the analysis of gestalt prey features in the frog *Rana temporaria*. J. Comp. Physiol. 141, 139-152.

Straznicky, C. and Straznicky, I.T. (1988) Morphological classification of retinal ganglion cells in adult *Xenopus laevis*. Anat. Embryol. 178, 143-153.

Székely, G. and Lázár, G. (1976) Cellular and synaptic architecture of the optic tectum. In: Frog Neurobiology (Eds Llinás, R. and Precht, W.)pp. 407-434. Springer, Berlin.

Tóth, P., Lázár, G. and Görcs, T. (1980) Retinal projections in the adult *Xenopus laevis*: a study with cobalt filling technique. Acta Morphol. Hung. 28, 365-374.

Wilczynski, W. and Northcutt, R.G. (1978) Afferents to the optic tectum of the leopard frog, an HRP study. J. Comp. Neurol. 173, 219-230.

Wye-Dvorak, J., Straznicky, C. and Tóth, P. (1992) Retinal projections in the cane toad, *Bufo marinus*. Brain, Behav. Evol. 39, 208-218.

Received 20 July 1993
Accepted 8 September 1993

Neurobiology 1 (4), pp. 327-335, 1993

BINDING PROPERTIES OF THE PURE OPIOID ANTAGONIST [^{3}H](N-PROPYL)-NOROXYMORPHONE IN RAT BRAIN MEMBRANES

G. Tóth[1], S. Benyhe[2], S. Hosztafi[3] and A. Borsodi[2]

[1]Isotope Laboratory, and [2]Institute of Biochemistry, Biological Research Center, Hungarian Academy of Sciences, 6701, Szeged, P.O.B. 521, Hungary, [3]Alkaloida Chemical Works, 4440 Tiszavasvári, P.O.B. 1, Hungary

Summary: (-)[N-(propyl)-14-OH-dihydromorphinan-6-one] = (N-propyl)-*nor*oxymorphone and its multiple tritiated form (molar activity: 126 Ci/mmol; 1 Ci = 37 GBq) was synthesized. According to our knowledge this specific radioactivity exceeds all of the commercially available [^{3}H]opioid ligands. The ligand was found to be a pure opioid antagonist in receptor binding assays performed with rat brain membranes. Scatchard analysis of equilibrium binding isotherms revealed one high affinity ($K_d \approx 4$ nM) binding site. Reversibility, stereospecificity and opioid nature of the binding was confirmed by ligand binding experiments. Because of its antagonist character combined with high specific radioactivity the ligand might be a useful tool in characterizing and purifying opioid receptors.

Key words: opiate receptors, antagonists, tritium-labelling, rat brain, opioid ligand binding.

INTRODUCTION

Alkaloid and peptide radioligands are advantageous biochemical tools studying opioid mechanisms, *in vitro*. Since their first application in receptor binding assays in the early 70's [Pert and Snyder, 1973; Simon et al., 1973; Terenius, 1973; Chang and Cuatrecasas, 1975; Lord et al., 1976] increasing number of ligands has been developed and has widely been used for the investigation of opioid binding sites in different tissues.

Akadémiai Kiadó, Budapest

Recently several opioid radioligands have been synthesized in our laboratory including alkaloid derivatives [^{3}H]naloxone [Tóth et al., 1982a], [^{3}H]dihydromorphine [Tóth et al., 1982b], [^{3}H]oxymorphazone [Varga et al., 1987], [^{3}H]naltrindole [Yamamura et al., 1992], [^{3}H]cyprodime [Ötvös et al., 1992], and enkephalin analogues such as [^{3}H][D-Ala^2-Leu^5]enkephalin [Benyhe et al., 1985], [^{3}H][D-Ala^2-Leu^5]enkephalin chloromethyl ketone [Szűcs et al., 1987], [^{3}H]Tyr-D-Ala-Gly-(Me)Phe-chloromethyl ketone [Varga et al., 1989], [^{3}H]deltorphin II [Búzás et al., 1991], [^{3}H]Tyr-Tic-Phe-Phe [Nevin et al., 1993a], and [^{3}H]Ile^{5,6}deltorphin II [Nevin et al., 1993b].

In the present study we describe the synthesis of a new opioid antagonist radioligand having extremely high specific radioactivity. Some of the binding properties of [^{3}H](N-propyl)-*nor*oxymorphone to opioid receptors were also studied in rat brain membrane preparations.

MATERIALS AND METHODS

Radioligand synthesis

The title compound was prepared by our earlier method (Tóth et al., 1982) slightly modified. Briefly, 14-hydroxy-*nor*morphinon (Fishman et al., 1973) was tritiated by tritium gas in the presence of PdO in a vacuum manifold. The crude tritiated material was reacted with propargyl-bromide. The N-propargyl-[7,8-^{3}H]-dihydro-*nor*morphinone was tritiated again in the N-side chain by tritium gas in the presence of Lindlar catalyst to get [^{3}H]naloxone (71.1 Ci/mmol) and [8,19,20-^{3}H]-N-propyl-*nor*oxymorphone (126 Ci/mmol). The compounds were found to be 97% radiochemically pure on TLC using three different elution systems on Merck silica gel.

Membrane preparation

A crude membrane fraction from rat (PVG/C strain) brain was prepared according to the method described originally by Pasternak et al. (1975). Briefly, the rats were decapitated, the brains without cerebella were removed and homogenized in 30 volumes of ice-cold 50 mM Tris-HCl buffer (pH 7.4). After 20 min centrifugation at 40,000 x g the pellet was resuspended in fresh buffer and incubated at 37 °C for 30 min, then centrifuged again and the final pellet was suspended in 80 volumes of fresh buffer and used immediately. Protein content was estimated according to the method of Bradford (1976).

Binding assay

Binding experiments were conducted in Tris-HCl buffer (pH 7.4) in a final volume of 1 ml containing 0.3-0.5 mg protein. Incubations (0 °C, 60 min) were terminated by rapid filtration under vacuum followed by washing with 2 x 10 ml ice-cold Tris-HCl (50 mM, pH 7.4) buffer through Whatman GF/B glass fiber filters using a Brandel M24R cell harvester. The radioactivity was measured in a toluene-based scintillation cocktail by Beckman LS 5000TD Spectrophotometer. Non-specific binding was defined as the bound radioactivity in the presence of 10 μM unlabelled naloxone (except the type specificity measurements, where the unlabelled form of the tritiated ligand was used). All assays were performed in duplicate and repeated several times.

Experimental data were analyzed by the use of the LIGAND computer program utilizing a nonlinear least squares fitting algorithm (Munson and Rodbard, 1983).

Chemicals

The following opioids were used in this study: Diprenorphine hydrochloride (C-Vet Ltd.); ±N-allyl*nor*metazocine hydrochloride (SKF 10,047), NIDA; dynorphine A (1-13), D-Ala^2-(Me)Phe^4-Gly^5-ol enkephalin (DAMGE), [D-Ser^2-Leu^5-Thr^6]enkephalin (DSLET), BACHEM Feinchemikalien; levorphanol and dextrorphan both as tartrate salt, Hoffmann la Roche. ±Bremazocine hydrochloride and ethylketocyclazocine methanesulfonate (EKC) were kindly donated by Sterling Winthrop Institute, naloxone and naltrexone were generously provided by DuPont de Nemours Co. Dihydromorphine hydrochloride, *nor*oxymorphone and N-propyl-*nor*oxymorphone were prepared by S. Hosztafi (Alkaloida Ltd., Hungary). Tritium gas was purchased from Technabexport (Russia). All other chemicals were of analytical grade.

RESULTS

In vitro biological activities of the newly synthetized compound were evaluated by radioreceptor binding assays using rat brain membrane preparations. Kinetic experiments revealed that specific [^{3}H]N-propyl-*nor*oxymorphone binding reached steady-state level in 60 mins at 0 °C (data not shown), therefore binding assays were usually carried out at low temperature.

Fig. 1 shows equilibrium binding isotherms for [^{3}H]N-propyl-*nor*oxymorphone in rat brain membranes. Mathematical analysis of the homologous competition binding data (i.e. radiolabelled ligand is displaced by serial dilutions of its unlabelled form) yielded a single set of high affinity opioid site. Apparent dissociation constant (K_d) and maximal binding capacity (B_{max}) values determined by one-site model were found to be 4.1 ± 0.9 nM, and 227 ± 38

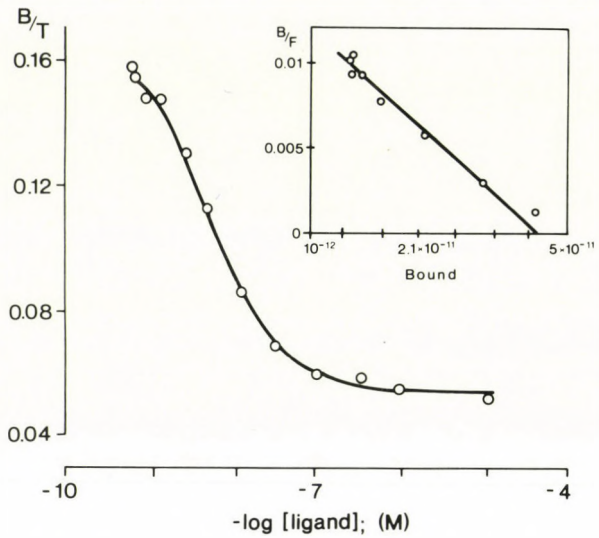

Fig. 1: Homologous displacement curve and corresponding Scatchard plot (**inset**) of [^{3}H]N-propyl-*nor*oxymorphone binding to rat brain membranes at 0 °C. Rat brain membranes were incubated at 0 °C in the presence of [^{3}H]ligand (2 nM) with serial dilutions of unlabelled propyl-*nor*oxymorphone, and specific binding was determined. Points are mean values of duplicate samples in representative experiments repeated several times. Data were evaluated by the LIGAND programme. Calculated K_d and B_{max} values were 3.6 nM and 211 fmol/mg protein, respectively. T: molar concentration of the radioligand; B: bound radioactivity (M); F: free radioactivity (M).

fmol/mg protein (n = 4), respectively. Computer fitting assuming independent sets of binding sites in a two-site model gives no reliable results. Self and cross competition experiments with [^{3}H]naloxone [Tóth et al. 1982] reveal that [^{3}H]N-propyl-*nor*oxymorphone and [^{3}H]naloxone recognize identical set of binding sites in rat brain tissues (data not shown).

Binding parameters are summarized in Table 1. The question whether N-propyl-*nor*oxymorphone is an agonist or an antagonist was answered by measuring its 'sodium shift' against [^{3}H]naloxone binding, and determining 'direct sodium effect' on [^{3}H]N-propyl-*nor*oxymorphone specific binding (Table 1). Antagonist property of N-propyl-*nor*oxymorphone was further examined in mouse vas deferens bioassay system. The K_e value of the compound, determined with *nor*morphine, a pure opioid agonist, was 9 nM (A. Rónai, to be published elsewhere).

Table 1

Equilibrium parameters of the N-propyl-*nor*oxymorphone binding to rat brain membranes

Expts.	B_{max} fmol/mg	K_d (-Na^+) nM	K_d (+Na^+) nM*	Sodium index
1. [^{3}H]naloxone/N-propyl-*nor*oxymorphone	-	5.4 ± 2.3	2.05 ± 0.9	0.4
2. [^{3}H]N-propyl-*nor*oxymorphone/ N-propyl-*nor*oxymorphone	227 ± 38	4.1 ± 0.9	1.6 ± 0.6	0.4

Sodium indices were measured either by examining sodium shift on dose response curves of [^{3}H]naloxone using unlabelled N-propyl-*nor*oxymorphone (**1**), or by estimating direct effects of sodium ions on [^{3}H]N-propyl-*nor*oxymorphone binding (**2**). Data are mean values ± S.E.M. of several experiments each performed in duplicate. * The concentration of NaCl was 100 nM.

Heterologous displacement experiments were used to evaluate the affinity of several compounds for the [^{3}H]N-propyl-*nor*oxymorphone binding. Results are shown in Table 2. The difference in K_i values between levorphanol and dextrorphan indicates strict stereoselectivity of [^{3}H]N-propyl-*nor*oxymorphone binding. Competition studies revealed the

following rank order of potencies in displacing [^{3}H]N-propyl-*nor*oxymorphone: naltrexone ≈ levorphanol > dihydromorphine > DAMGE > SKF-10,047 > DSLET > dextrorphan. The presence of 100 mM NaCl in the assay mixture produced a marked decrease in the affinity of dihydromorphine, whereas an apparent increase were found in the case of naltrexone (Table 2). These results confirm that [^{3}H]N-propyl-*nor*oxymorphone is a suitable ligand for the discrimination of opioid agonists and antagonists in receptor binding assays.

Table 2

Inhibition of [^{3}H]N-propyl-*nor*oxymorphone binding to rat brain membranes by opioid ligands

Ligand	*(selectivity)*	K_i (nM)	%CV
Diprenorphine	*(antagonist)*	0.89	24
Naltrexone	*(antagonist)*	0.13 0.04*	22 17
Dihydromorphine	*(mu)*	1.2 86.2*	21 12
Levorphanol	*(mu)*	0.13	49
Dextrorphan	*(inactive [+]isomer)*	2250	32
(±)Bremazocine	*(kappa)*	1.1	23
SKF-10, 047	*(sigma)*	2.4	19
DAMGE	*(mu)*	2.8	20
DSLET	*(delta)*	43.1	
Dynorphin$_{(1-13)}$	*(kappa)*	1.75	36

* Determinations were done in the presence of 100 mM NaCl

Rat brain membranes were incubated with the labelled ligand in the presence of wide concentration range of unlabelled opioids at 0 °C. K_i data are mean value of two to four pooled experiments, each performed in duplicate, processed simultaneously by the LIGAND programme. Per cent covariance values (% CV) as a measure of accuracy are also given.

DISCUSSION

The composition of the radioactive crude-products depends on the tritiation conditions. In our earlier experiments the main product was the tritiated naloxone [Tóth et al., 1982a]. Increasing the reaction time the ratio of naloxone and N-propyl-*nor*oxymorphone was 1:1 without detectable quantity of N-propargyl-*nor*oxymorphone. The synthesis could also be carried out starting from N-propargyl-*nor*oxymorphone in one step with tritium gas in the presence of any kind of Pd catalyst to get only N-propyl-*nor*oxymorphone with very high specific radioactivity.

Binding properties of the newly synthesized compound were evaluated in a particulate membrane fraction of the rat brain. Competition profile and high degree of stereospecificity, measured with 'racemorphan' stereoisomers, strongly support that [^{3}H]N-propyl-*nor*oxymorphone labels authentic opioid binding sites in rat brain membranes.

Structurally, N-substitution of the methyl group in the morphinan series by bulky substituents such as propyl group has been shown to result antagonist compounds [Gero, 1985], thus the antagonist property of our ligand was expected. Indeed, some lines of evidence indicate N-propyl-*nor*oxymorphone to be a pure opioid antagonist: (1) 'sodium index' value of this compound both in unlabelled and in tritiated form seems to be similar to those of the opioid antagonists; (2) the ligand antagonized the effect of *nor*morphine in mouse vas deferens preparation (not shown here). Antagonist ligand binding to opicid receptors is more stable than the binding of labelled agonist compounds [Creese et al., 1975]. Receptor binding activity could even be measured at low temperature, which is advantageous when relatively sensitive solubilized or purified receptors are investigated. In addition to, the high molar radioactivity of the labelled compound allows us to conduct receptor binding assays using very low ligand concentrations i. e. far below the K_d; this could help to measure receptor binding at proper conditions.

Taken together, multiple radiolabelled [^{3}H]N-propyl-*nor*oxymorphone seems to be a good probe studying opioid receptors by means of receptor binding assays or *in vitro* autoradiographic techniques.

REFERENCES

Benyhe, S., Tóth, G., Kevei, J., Szűcs, M., Borsodi, A., Szécsi, J., Di Gléria, K., Süli-Vargha, H. and Medzihradszky, K. (1985) Characterization of rat brain opioid receptors by (Tyr-3,5-[^{3}H])^1-D-Ala^2-Leu^5 enkephalin binding. Neurochem. Res. 10, 551-559.

Búzás, B., Tóth, G., Cavagnero, S., Hruby, V.J. and Borsodi, A. (1992) Synthesis and binding characteristics of the highly delta-specific new tritiated opioid peptide, [^{3}H]deltorphin II. Life Sci. 50, PL75-78.

Bradford, M.M. (1976) A rapid and sensitive method for the quantitation of microgramm quantities of protein utilizing the principle of protein-dye binding. Anal. Biochem. 72, 248-254.

Chang, K.J. and Cuatrecasas, P. (1979) Multiple opiate receptors: Enkephalins and morphine bind to receptors of different specificity. J. Biol. Chem. 254, 2610-2618.

Creese, I., Pasternak, G.W., Pert, C.B. and Snyder, S.H. (1975) Discrimination by temperature of opiate agonist and antagonist receptor binding. Life Sci. 16, 1837-1842.

Fishman, J., Cotter, M.L. and Norton, B.I. (1973) Narcotic antagonists. 2. Preparation and biological stability of naloxone-7,8-^{3}H. J. Med. Chem. 16, 556-557.

Gero, A. (1985) One- and two-receptor models of opioid drug action. Life Sci. 36, 1021-1024.

Lord, J.A.H., Waterfield, A.A., Hughes, J. and Kosterlitz, H.W. (1977) Endogenous opioid peptides: multiple agonists and receptors. Nature, 267, 495-499.

Munson, P.J. and Rodbard, D. (1980) LIGAND: A versatile computerized approach for characterization of ligand binding systems. Anal. Biochem. 107, 220-239.

Nevin, S.T., Tóth, G., Nguyen, T.M.D., Schiller, P.W. and Borsodi, A. (1993a) Synthesis and binding characteristics of the highly specific, tritiated delta opioid antagonist [^{3}H]TIPP. Life Sci. 53, PL57-62.

Nevin, S.T., Kabasakal, L., Ötvös, F., Tóth, G. and Borsodi, A. (1993b) Binding characteristics of the novel highly selective delta opioid agonist [^{3}H]Ile^{5,6}Deltorphin II. Neuropeptides, in press.

Ötvös, F., Tóth, G. and Schmidhammer, H. (1992) Tritium labelling of cyprodime (= [-]17{cyclopropylmethyl}-4,14-dimethoxi-morphinan-6-one), a μ receptor selective opioid antagonist. Helv. Chim. Acta, 75, 1718-1720.

Pasternak, G.W., Wilson, H.A. and Snyder, S.H. (1975) Differential effects of protein-modifying reagents on receptor binding of opiate agonists and antagonists. Mol. Phamacol. 11, 340-351.

Pert, C. B. and Snyder, S. H. (1973) Opiate receptors: demonstration in nervous tissues. Science, 179, 1011-1014.

Simon, E. J., Hiller, J. M. and Edelman, I. (1973) Stereospecific binding of the potent narcotic analgesics [^{3}H]etorphine to rat brain homogenate. Proc. Natl. Acad. Sci. *USA* 70, 1947-1949.

Terenius, L. (1973) Stereospecific interaction between narcotic analgesics and a synaptic membrane fraction of rat cerebral cortex. Acta Pharmacol. Toxicol. 32, 317-320.

Tóth, G., M. Krámer, F. Sirokmán, A. Borsodi, and A. Rónai, (1982a) Preparation of (7,8,19,20-^{3}H)naloxone of high specific activity. J. Label. Comp. Radiopharm. 19, 1021-1030.

Tóth, G., Krámer, M., Szûcs, M., Benyhe, S. and Sirokmán, F. (1982b) Preparation of 1,7,8-[^{3}H]-dihydromorphine of high molar activity and its application in opiate receptor binding experiments. Radiochem. Radioanal. Letters, 56, 209-216.

Varga, É., Tóth, G., Benyhe, S., Hosztafi, S. and Borsodi, A. (1987) Synthesis and binding of ^{3}H-oxymorphazone to rat brain membranes. Life Sci. 40, 1579-1588.

Varga, É., Tóth, G., Hepp, J., Benyhe, S., Simon, J., Medzihradszky, K. and Borsodi, A. (1988) Synthesis of [^{3}H]Tyr-D-Ala-Gly-(Me)Phe-chloromethyl ketone - an opioid affinity label. Neuropeptides, 12, 135-139.

Yamamura, M.S., Horvath, R., Tóth, G., Ötvös, F., Malatynska, E., Knapp, R.J., Porreca, F., Hruby, V.J. and Yamamura, H.I. (1992) Characterization of [^{3}H]naltrindole binding to delta opioid receptors in rat brain. Life Sci. 50, PL119-124.

Received 21 October 1993
Accepted 4 November 1993

Neurobiology 1 (4), pp. 337-350, 1993

FOREBRAIN CONNECTIONS OF THE RAT PARAVENTRICULAR THALAMIC NUCLEUS AS DEMONSTRATED USING THE CARBOCYANIDE DYE DiI

Michel Arluison* and Paul Derer

Université P.& M. CURIE, Institut des Neurosciences CNRS, URA 1488,
7 quai Saint-Bernard, F75252 PARIS Cedex 05 FRANCE,
Fax: (33 1) 44 27 25 08; E-Mail: mia@ccr.jussieu.fr

Summary: The anatomical connections of the rat paraventricular thalamic nucleus (PaVT) have been studied using the fluorescent dye DiI. The fact that this compound is able to dissolve and to diffuse in plasma membranes in formalin-fixed tissues (Godement et al., 1987) allowed us to depose precisely tiny quantities of DiI on the PaVT, in order to study its neuronal connections. Ventralward, the forebrain projections of the PaVT were directed to the reuniens nucleus of the thalamus, the dorso-medial hypothalamic region, the zona incerta and the lateral hypothalamic area. In the rostral direction, the PaVT appeared to innervate mainly the medial preoptic area, the bed nucleus of the stria terminalis (particularly the ventral and medial regions) and the medial septum. The forebrain afferent connections of the PaVT were found to originate mainly in the lateral and periventricular hypothalamic area, the medial preoptic area, the bed nucleus of the stria terminalis and the medial septum where the fluorescent nerve cell bodies appeared particularly numerous. From these results, it is concluded that DiI is a useful tool for demonstrating the neuroanatomical connections of small brain nuclei, as well as for post-mortem neuropathological studies.

Key words: bed nucleus of the stria terminalis, DiI, fluorescent dye, limbic system, anatomical connections, paraventricular thalamic nucleus.

* To whom reprint requests must be addressed.

Akadémiai Kiadó, Budapest

INTRODUCTION

In the rat and other species, the midline nuclei of the thalamus appear closely related to the limbic system. However, the neuroanatomical connections of the paraventricular thalamic nucleus (PaVT) in particular have been scarcely studied in the literature (Chen et al., 1990; Cornwall and Philippson, 1988; Su and Bentivoglio, 1990), probably because of the narrow and elongated shape of this nucleus and of its position, medial and close to the third ventricle. The present study was undertaken to demonstrate the forebrain connections of the PaVT using the new fluorescent tracer DiI which possesses some interesting properties. First, the carbocyanide dyes such as DiI, dissolve very easily in plasma membranes and diffuse in the plane of the lipid bilayer, even after aldehyde fixation (Hönig and Hume, 1989; Thanos and Bonhoffer, 1987). Second, DiI is transported bidirectionally in formalin-fixed neurons while the intensity of fluorescence remains high, even after its diffusion far from the point of deposition (Godement et al., 1987). Hence, this dye may be particularly useful for certain neuroanatomical works such as analysing the connections of small brain nuclei and post-mortem neuropathological studies.

MATERIALS AND METHODS

Adult rats of the Wistar strain bred in the laboratory, were used for the present study. The animals weighing approximately 150 g were anesthetized with sodium pentobarbital (0.1 ml/100 g body weight) and perfused transcardially with 200 ml of a solution of 4% formaldehyde in 0.1 M sodium phosphate buffer, pH 7.4. Then, the brains were excised from the skull and post-fixed for several hours in the same mixture.

Two brains were cut coronally in two parts at the level of the retrochiasmatic area in order to expose the PaVT. The surface of the rostral block was blotted with a filter paper and a tiny quantity of DiI powder (Molecular Probes Inc., Eugene, Oregon, 97402 USA) was deposited precisely onto the PaVT by means of an insect pin, using a dissecting microscope. After that, the blocks of tissue were returned to the formalin solution and kept at room temperature in the dark.

In a third rat, the dorsal neocortex, corpus callosum and dorsal hippocampus were removed in order to expose the ventricular surface of the thalamus. Some crystals of DiI were then deposited at the bottom of the midline groove, on the whole extent of the PaVT, using the tip of an insect pin which allowed to slightly scarify the ependyma.

Six months later, the three brains were cut coronally in sodium phosphate buffer (0.1 M, pH 7.4) using a vibratome (Lancer). The 50 μm-thick sections were mounted in buffered glycerol and examined with a Leitz Diaplan microscope equipped with a N2 Ploempack system generally used for rhodamine. Black and white photographs were taken with Kodak 5063TX or Agfapan 400 ASA negative films.

In complementary experiments, the neuronal connections of the bed nucleus of the stria terminalis (BNST), lateral, perifornical and ventromedial hypothalamic nuclei have been studied with the same technique. These results are not reported here but they will be examined in the discussion.

RESULTS

a) *Deposition sites*

After their deposition on the PaVT, the crystal of DiI dissolved and diffused progressively in the tissue. On coronal sections, the diffusion around the site of deposition was observable directly because of the red color of the tracer. We found that the red spot was largely within the limits of the PaVT after one month (Fig.1). However, after six months, the stained area slightly went out the boundaries of the studied nucleus to reach the medial habenula (Fig. 2). Furthermore, numerous fluorescent bundles of myelinated nerve fibers were observed, coursing obliquely across the dorsal thalamus (Figs. 3-4).

b) *Neuroanatomical connections*

From the PaVT, three systems of efferents fibers could be distinguished, while the retrogradely labelled cells were rare, except in certain locations.

The first group of fluorescent nerve fibers left the PaVT ventralward and crossed vertically the midline thalamus to reach the nucleus reuniens and the dorso-medial region of the hypothalamus. In the nucleus reuniens, the fluorescent nerve fibers and varicosities were of medium density (Fig. 5) while the fluorescent nerve cell bodies were scarce. In the paraventricular hypothalamic nucleus (PaVH), the anterogradely labelled nerve fibers appeared rather numerous, especially in the most medial part of this nucleus, whereas only scattered positive nerve fibers were present in the other regions, including the magnocellular division (Figs. 6 and 8). More ventrally, the periventricular region was found to contain some fluorescent perikarya surrounded by a medium to low density of fine and varicose fluorescent nerve fibers. In addition, some coarse fluorescent fibers appeared to cross the ventral hypothalamic region (Fig. 7) to reach the vicinity of the arcuate and suprachiasmatic nuclei.

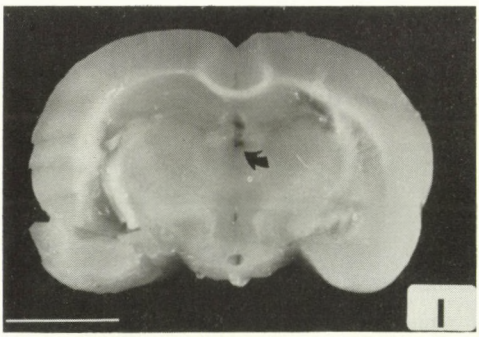
1

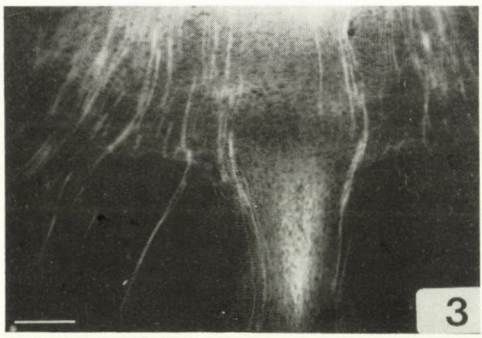
3

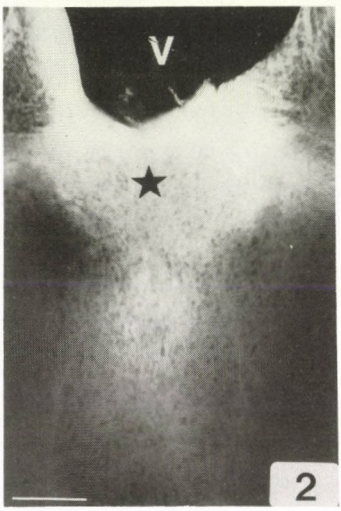
V
2

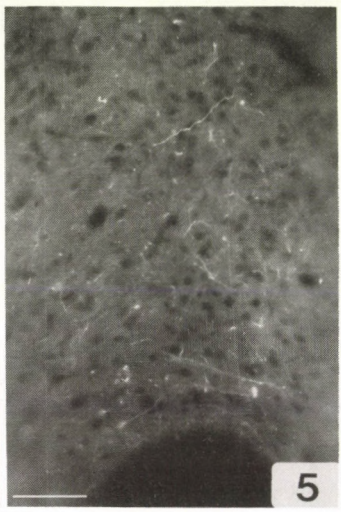
5

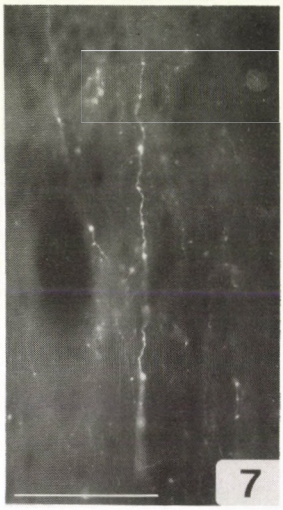
7

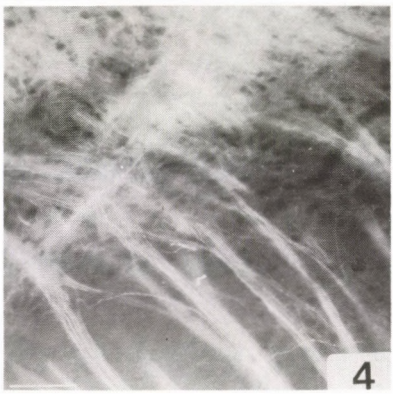
4

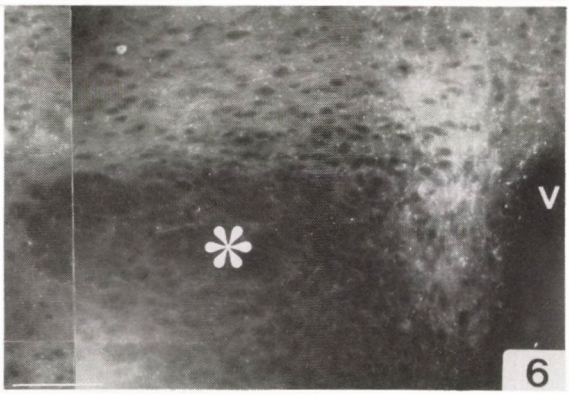
V
6

The second system of efferents from the PaVT crossed obliquely the thalamus (Fig. 4) in order to innervate the zona incerta (Fig. 9) and the lateral hypothalamic area. In the perifornical region, the fluorescent axons and nerve fibers exhibited generally an oblique direction (Fig. 10) toward the ventrolateral region of the hypothalamus where the numerous varicose nerve fibers appeared finer and more evenly crossed (Fig. 11). Some small and ovoid fluorescent nerve cell bodies were also present in the perifornical and lateral regions of the hypothalamus (Figs. 10-11). Quite ventrally, the supraoptic nucleus appeared surrounded by the fluorescent nerve fibers but only some of them were found to enter the core of this nucleus (not shown). In addition, a loose network of fluorescent nerve fibers was observed in the ventromedial hypothalamic nucleus. In the rostral direction, the anterogradely labelled nerve fibers crossed obliquely the reticular thalamic nucleus and reached the caudoventral part of the bed nucleus of the stria terminalis (BNST). In this region, a part of the fluorescent nerve fibers appeared directed rather horizontally while the other had a vertical direction (Fig. 12). More dorsally some fluorescent nerve fibers were observed in the lateral division of the BNST and the region intercalated between the internal capsule and the stria terminalis (Fig. 13). However, the highest density of fluorescent fibers was found in the medial region, close to the vertical limbs of the stria medullaris and fornix.

Fig. 1: DiI deposit (arrow) on the paraventricular thalamic nucleus (PaVT) of a rat brain sectioned transversally and photographed 15 days later. R_1;level A: 5.40 mm from the interaural line, according to the atlas of Paxinos and Watson (1986).
Fig.2: Transversal section of a rat brain at the paraventricular thalamic nucleus level. In this rat, the deposit of DiI (star) was made six months ago at the ventricular surface of the PaVT (V). R_3; A: 5.9.
Figs. 3-4: Thalamus: unmyelinated fluorescent nerve fiber bundles crossing obliquely the ventro-lateral region of the thalamus toward the zona incerta, at low (Fig. 3) and high (Fig. 4) magnification. R_3; A: 6.4.
Fig. 5: Anterogradely labeled fluorescent nerve fibers in the reuniens nucleus of the thalamus. R_3; A: 7.2.
Fig. 6: Paraventricular hypothalamic nucleus (R_1; A: 7.2): numerous fluorescent nerve fiber varicosities may be observed in the medial region close to the ventricle (V), whereas they are few in the dorsal region and absent from the core of the nucleus (star).
Fig. 7: Hypothalamus: one coarse and varicose fluorescent nerve fiber in the periventricular hypothalamic nucleus. R_1; A: 7.2.

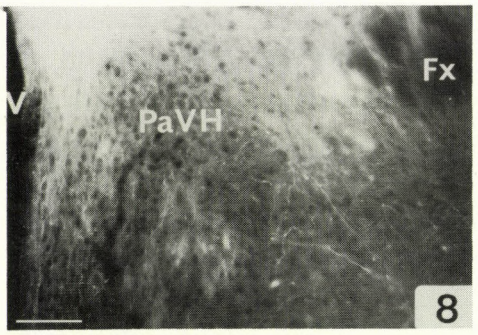
V
PaVH
Fx
8

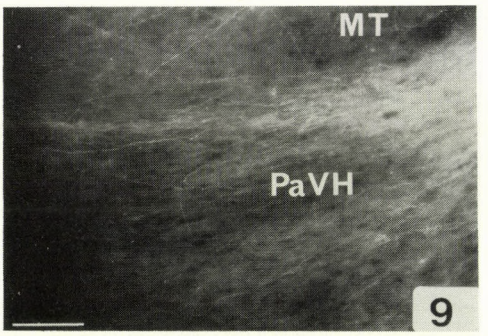
MT
PaVH
9

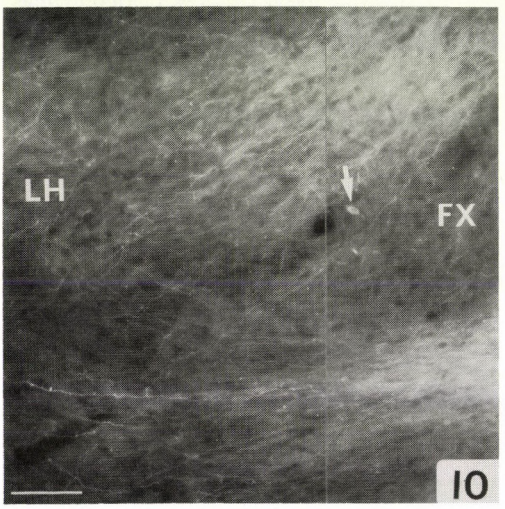
LH
FX
10

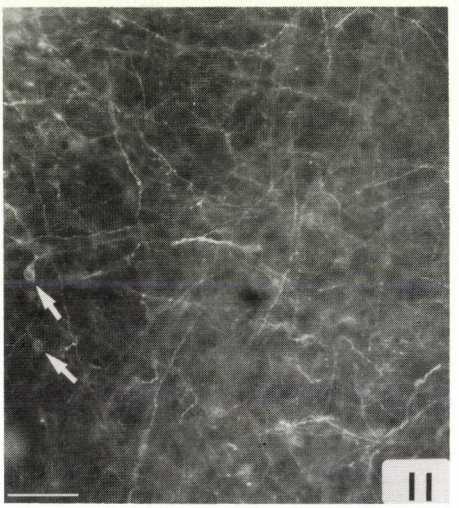
11

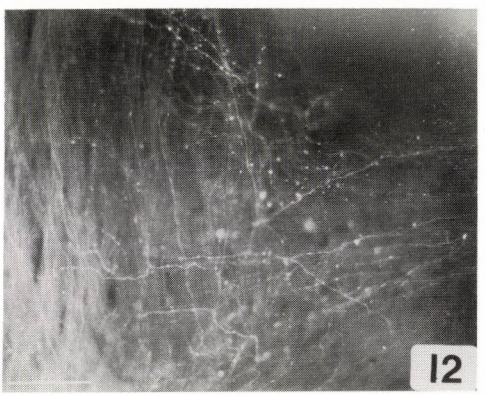
12

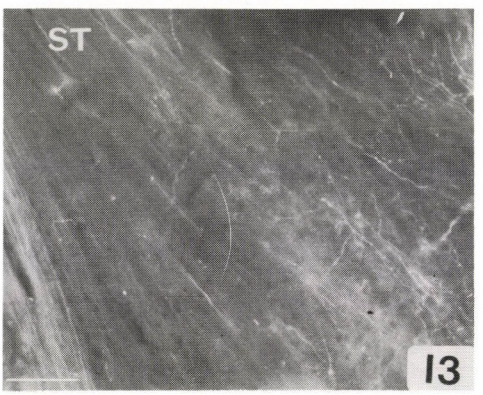
ST
13

The third system of efferents from the PaVT was localized in the periventricular region where the fluorescent nerve fibers coursed medially to the fornix in order to reach the region of the caudal septum and anterior commissure (AC). In the medial preoptic area, a rather dense plexus of fluorescent nerve fibers was found mixed with a moderate number of retrogradely-labelled nerve cell bodies (not shown). Just above, the medial division of the BNST exhibited a dense network of fine and coarse fluorescent nerve fibers both ventrally and dorsally to the AC (Fig. 14). In addition, some fluorescent nerve cell bodies were detected in this region. More rostrally, numerous fluorescent nerve fibers were also observed in the dorso-medial region of the BNST, whereas this plexus became progressively looser in the lateral and dorsal directions (Figs. 15-16). In the medial septum the fluorescent nerve fibers were found very dense close to the AC (Figs. 17-18) while numerous fluorescent nerve cell bodies appeared more dorsally and rostrally (Fig. 19). Finally, we noted that the anterogradely labelled nerve fibers became difficult to observe in the region of the nucleus accumbens (NA) because of the lower intensity of fluorescence. However, some fluorescent nerve fibers were observed in the vicinity of the NA, whereas they lacked completely within the nucleus itself.

Fig. 8: Paraventricular hypothalamic nucleus (PaVH) (R_3; A: 7.6). At this level, the rostral part of the PaVH is also unlabeled. However, this nucleus is surrounded by numerous fluorescent nerve fibers and varicosities which appear overexposed in the dorsal region. In addition, numerous fluorescent nerve fibers are present in the region ventromedial to the fornix (Fx). V: third ventricle.
Fig. 9: Array of fluorescent nerve fibers in the zona incerta and dorsolateral hypothalamus (R_3; A: 6.7). MT: mamillo-thalamic tract; PaVH: posterior part of the paraventricular hypothalamic nucleus.
Fig. 10: Lateral hypothalamic area (R_3; A: 6.7): a rather dense plexus of anterogradely labeled fluorescent nerve fibers is observed in the lateral hypothalamus (LH) and ventrally to the fornix (Fx). In addition, some retrogradely labeled nerve cell bodies may also be observed in these regions (arrow).
Fig. 11: Higher magnification of the network of fluorescent nerve fibers present in the lateral hypothalamus (R_3), the latter are mixed with some retrogradely labeled perikarya (arrows).
Fig. 12: Bed nucleus of the stria terminalis (BNST), caudal region (R_1, A: 8.2): Numerous varicose fluorescent nerve fibers innervate the caudo-medial region of the BNST located near the fornix.
Fig. 13: Bed nucleus of the stria terminalis, caudal region (R_3, A: 8.2): Scattered fluorescent nerve fibers are observed in the dorsal part of the BNST and in the stria terminalis (ST).

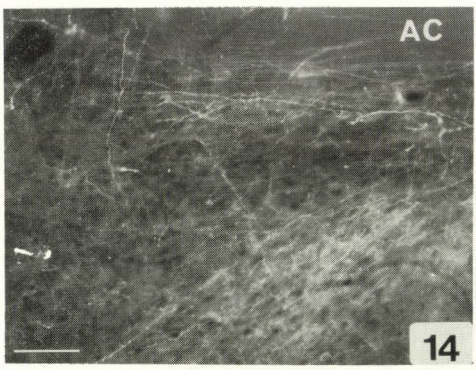
AC
14

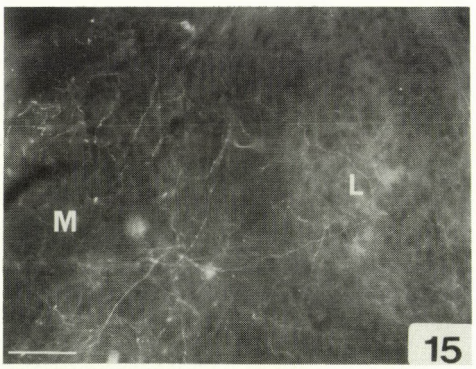
M
L
15

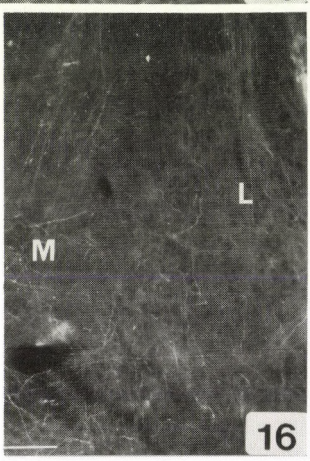
L
M
16

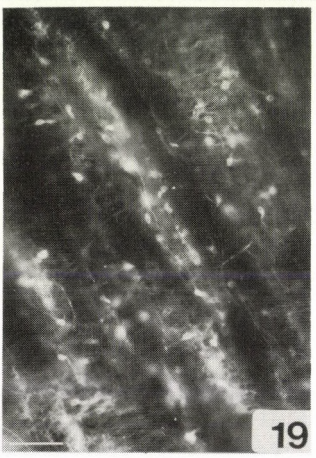
19

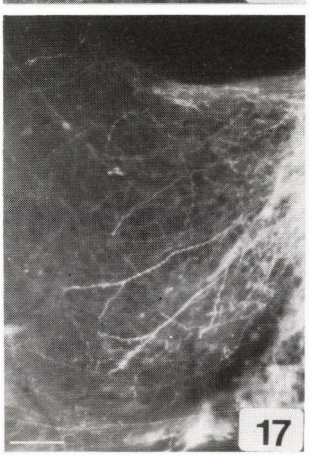
17

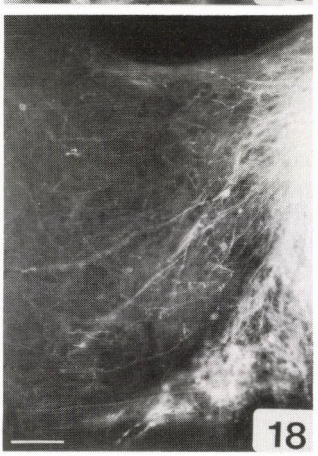
18

DISCUSSION

Technical considerations

Following Godement et al. (1987) and Burkhalter et al. (1993), we report here that the fluorescent dye DiI constitutes an easy and sensitive neuroanatomical tracer, able to demonstrate very precisely the morphology of cell bodies, axons and nerve terminals of (projection) neurons in formaldehyde-fixed tissues. These advantages, however, are tempered by the fact that the speed of DiI diffusion in stabilized plasma membranes is very low and that the apparent diameter of the deposition site increases with time. The long time required to label long nervous pathways is the main problem of this method. In certain cases, however, this fact may be considered as secondary in comparison with the possibility of using DiI in fixed tissues for precise neuroanatomical or neurohistopathological studies. Furthermore, this delay may be shortened by placing the blocks of tissue at 37 °C and/or using the "Fast DiI", a new insaturated derivative of DiI. Concerning the second remark, it is worth noting that DiI is considered as highly soluble in lipids but insoluble in water (Hönig and Hume, 1989). Hence, it may be thought that the progressive enlargement of the deposit is due to DiI diffusion in neuronal processes and myeline sheets and that only the initial size deposition site in direct contact with DiI is important. However, some diffusion in the intercellular spaces or a passage from cell to cell cannot entirely be excluded.

Fig. 14: Bed nucleus of the stria terminalis, rostral region (R_3, A: 8.7): Numerous anterogradely labeled, fluorescent nerve fibers are located in the medio-ventral part of the rostral BNST, especially in the vicinity of the anterior commissure (AC).
Figs. 15-16: Bed nucleus of the stria terminalis, rostral region (R_3, A: 8.7): Numerous fine fluorescent nerve fibers are present in the dorso-medial region of the BNST (M), whereas they are few in the lateral one (L).
Figs. 17-18: Septum and neighbouring BNST (R_3, A: 8.7): A dense network of fine and coarse fluorescent nerve fibers, as well as some retrogradely labeled perikarya may be observed in the septo-hypothalamic, continuing toward the medial BNST (same microscopical field with two depth of focusing).
Fig. 19: A number of retrogradely labeled nerve cell bodies of small size appear located in the medial septum (R_3, A: 9.2).

Thalamic and hypothalamic connections of the PaVT

From the present study, it appears that the lateral hypothalamic area is one of the main target of efferent nerve fibers from the PaVT whereas the medial regions of the thalamus and hypothalamus are more poorly innervated. Little information was found in the literature concerning the existence of a neuronal pathway from the PaVT to the thalamic reuniens nucleus, but the presence of some "retrogradely labelled" nerve cell bodies in this nucleus corroborates previous results of Ohtake and Yamada (1989) demonstrating the existence of the converse projection from the nucleus reuniens to the PaVT. On the other hand, our observation concerning the existence of a neuronal pathway from the PaVT to the PaVH is corroborated by some data of the literature. In their review of the afferent and efferent connections of the hypothalamus, Palkovits and Zaborszky (1979) did not state on the existence of anatomical connections between the thalamus and hypothalamus but they report (from previously unpublished data) that a lesion in the midline thalamus results in the appearence of degenerated nerve fibers in the PaVH. Furthermore, after Pha-L injections within the PaVT, Puigbonnet and Ciriello (1991) have recently described the presence of anterogradely labelled nerve fibers in the medial parvocellular region of the PaVH, as well as in the supraoptic nucleus.

Contrasting with the observations made in the medial hypothalamus, it is worth noting that numerous fluorescent nerve fibers were found mixed with some retrogradely labelled perikarya in the lateral/perifornical hypothalamic area after DiI depositions on the PaVT. These observations demonstrate that the PaVT is reciprocally connected with the lateral hypothalamic area sensu lato, thus confirming previous data of Conrad and Pfaff (1976b) and Puigbonnet and Ciriello (1991) in the rat or of DeVito and Smith (1982) in the monkey. At variance with Puigbonnet and Ciriello (1991), however, we observe only a weak projection from the PaVT to the ventromedial and suprachiasmatic nuclei. The reason for this discrepancy is unclear but it may be due to different sites of deposition or injection or, possibly, to a lower sensitivity of the present tracer as compared to Pha-L. Finally, in partial agreement with the autoradiographic study of Conrad and Pfaff (1976a) we also demonstrate that the PaVT establishes reciprocal connections with the medial preoptic area.

Forebrain connections of the PaVT

In the present study, we demonstrate that the PaVT projects heavily to the ventral and dorsomedial division of the BNST, as well as to the septum, while low to important numbers of retrogradely labelled nerve cell bodies are also observed in the latter regions. Furthermore, using the retrograde transport of gold-labelled wheat germ agglutinin-peroxidase or DiI from the BNST we have recently confirmed that the BNST is reciprocally connected to the PaVT (Arluison et al., submitted). Little information was found in the literature concerning the existence of a neuronal pathway from the PaVT to the BNST. In an old retrograde degeneration study, Powell and Cowan (1954) have reported the existence of neuronal projections from the midline thalamus to the ventral forebrain but, in spite of the large lesion, it is unclear if the BNST was included in the lesioned area. However, the existence of this nervous pathway is corroborated by results of both retrograde (Chen and Su, 1990) and anterograde (West et al. 1979; Ohtake and Yamada, 1989; Berendse and Groenewegen, 1990; Groenewegen et al., 1990) tracing studies. In addition, it is worth noting that the PaVT and/or parataenial thalamic nucleus were also shown as projecting to the NA (Berendse and Groenewegen, 1990; Groenewegen et al., 1990; Kelley and Stinus, 1984; Newman and Winans, 1980; Philipson and Griffiths, 1985; Su and Bentivoglio, 1990), whereas the latter nucleus was unlabelled in the present study. The reason for this discrepancy is unclear but it is possible that the time of tracer migration was too short to reach the NA, or that this nucleus was innervated only by the rostral pole of the PaVT, whereas this region was not involved in our tracer deposits.

In addition, we demonstrate that the BNST and the septum reciprocally project to the PaVT, thus confirming previous results of Conrad and Pfaff (1976a), Swanson and Cowan (1979) and Cornwall and Phillipson (1988). In contrast to the present results, however, the innervation of the PaVT and/or the parataenial thalamic nucleus from the septum was shown to originate mainly in the lateral -but not in the medial- septal nucleus (Chen and Su, 1990; Meibach and Siegel, 1977; Swanson and Cowan, 1979).

Concerning the existence of neuronal connections between the PaVT and the amygdala, it is worth noting that prominent projections from the PaVT to the basolateral and/or central amygdaloid nuclei have been described (Su and Bentivoglio, 1990; Turner

and Herkenham, 1991), whereas the amygdala was almost free of labeling in the present study. This negative result is perhaps because this pathway is too long to allow an efficient transport of the tracer in the time interval used. By contrast, a medium density of fluorescent nerve fibers and some retrogradely labelled nerve cell bodies were observed in the rostro-ventral cortex after DiI deposition on the PaVT. The presence of these positive perikarya in the infralimbic cortex agrees with the existence of a projection to the PaVT (Hurley et al., 1991).

Finally, from the present results and data of the literature, it appears that the PaVT projects not only to the BNST and/or NA and to the amygdala, but also to the lateral hypothalamic area, i.e different limbic regions thought to mediate some motor components of emotional behaviors (Casada and Dafny, 1991). The possible involvement of the BNST in this function is supported by the fact, the PaVT was previously shown to receive important inputs from the brainstem, midbrain, amygdaloid and hypothalamic nuclei which relay sensory, autonomic, and endocrine informations from the rest of the brain and from the periphery (Cornwall and Phillipson, 1988; Norgren, 1976; Ricardo and Koh, 1978; Saper and Loewy, 1980; Ter Horst et al., 1989; Tribollet and Dreifuss, 1981).

ACKNOWLEDGEMENTS

We thank Paulette Cloup and Monique Quignon for their excellent technical assistance.

REFERENCES

Arluison, M., Brochier, G., Vankova, M.E., Villalobos, J. and Tramu, G. Peptide-containing afferents to the bed nucleus of the stria terminalis. A combined retrograde tracing and immunohistochemical study after local injection of colchicine. To be published: Brain Res Bull.

Berendse, H.W. and Groenewegen, J. (1990) Organization of the thalamostriatal projections in the rat, with special emphasis to the ventral striatum. J. Comp Neurol. 299, 187-228.

Burkhalter, A., Bernardo, K.L. and Charles, V. (1993) Development of local circuits in human visual cortex. J. Neurosci. 13, 1916-1931.

Casada, J.H. and Dafny, N. (1991) Restraint and stimulation of bed nucleus of the stria terminalis produce similar stress-like behaviors. Brain Res. Bull. 27, 207-212.

Chen, C. and Su, H.-S. (1990) Afferent connections of the thalamic paraventricular nucleus in the rat - A retrograde tracing study with iontophoretic application of fluoro-gold. Brain Res. 22, 1-6.

Conrad, L.C.A. and Pfaff, D.W. (1976a) Efferents from medial basal forebrain and hypothalamus in the rat. I. An autoradiographic study of the medial preoptic area. J. Comp. Neurol., 169, 185-220.

Conrad, L.C.A. and Pfaff, D.W. (1976b) Efferents from medial basal forebrain and hypothalamus in the rat. II. An autoradiographic study of the anterior hypothalamus. J. Comp. Neurol., 169, 221-262.

Cornwall, J. and Phillipson, O.T. (1988) Afferent projections to the dorsal thalamus of the rat as shown by retrograde lectin transport. II. The midline nuclei. Brain Res. Bull. 21, 147-161.

DeVito, J.L. and Smith, O.A. (1982) Afferent connections of the hypothalamic area controlling emotional responses (HACER). Brain Res 252, 213-226.

Godement, P., Vanselow, J., Thanos, S. and Bonhoffer, F. (1987) A study of developing visual systems with a new method of staining neurons and their processes in fixed tissue. Development 101, 697-713.

Groenwegen, H.J., Berendse, H.W., Wolters, J.G. and Lohman, A.H.M. (1990) The anatomical relationship of the prefrontal cortex with the striatopallidal system, the thalamus and the amygdala: evidence for a parallel organization. In HBM Uylings, C.G. Van Eden, J.P.C. De Brun, M.A. Corner, and M.G.P. Feenstra (eds), Progress in Brain Research, Vol. 85, Elsevier Science Publishers, B.V. (Biomedical division) pp. 95-118.

Hönig, M.G. and Hume, R.I. (1989) DiI and DiO: versatile fluorescent dyes for neuronal labelling and pathway tracing. Trends Neurosci. 12, 333-341.

Hurley, K.M., Herbert, H., Moga, M. and Saper, C.B. (1991) Efferent projections of the infralimbic cortex of the rat. J. Comp. Neurol. 308, 249-276.

Kelley, A.E. and Stinus, L. (1984) The distribution of projections from the parataenial nucleus of the thalamus to the nucleus accumbens in the rat: an autoradographic study. Exp. Brain Res 54, 499-512.

Meibach, R.C. and Siegel, A. (1977) Efferent connections of the septal region in the rat: an analysis utilizing retrograde and anterograde transport methods. Brain Res. 119, 1-20.

Newman, R. and Winans, S.S. (1980) An experimental study of the ventral striatum of the golden hamster. I. Neuronal connections of the nucleus accumbens. J. Comp. Neurol. 191, 167-192.

Norgren, R. (1976) Taste pathways to hypothalamus and amygdala. J. Comp. Neur. 166, 17-30.

Ohtake, T. and Yamada, H. (1989) Efferent connections of the nucleus reuniens and the rhomboid nucleus in the rat: an anterograde Pha-L tracing study. Neurosci. Res. 6, 556-568.

Palkovits, M. and Zaborszky, L. (1979) Neural connections of the hypothalamus. In: Morgan, P.J. and Panksepp, J., eds. Anatomy of the hypothalamus (Handbook of the hypothalamus), vol. 1. New York: Dekker; pp. 379-507.

Paxinos, G. and Watson, C. (1986) The rat brain in stereotaxic coordinates. Sydney, Academic Press.

Phillipson, O.T. and Griffiths, A.C. (1985) The topographic order of input to the nucleus accumbens in the rat. Neuroscience 16, 175-296.

Powell, T.P.S. and Cowan, W.M. (1954) The connexions of the midline and intralaminar nuclei of the thalamus of the rat. J. Anat. (Lond.) 88, 307-319.

Puigbonnet, E. and Ciriello, J. (1991) Hypothalamic connections of the paraventricular thalamic nucleus. 21st annual meeting of the Society for Neurosciences, New Orleans, Lousiana, USA, November 1-15, 1991. Neurosci abst. 17, (1-2), 707.

Ricardo, J.A. and Koh, E.T. (1978) Anatomical evidence of direct projections from the nucleus of the solitary tract to the hypothalamus, amygdala and other forebrain structures in the rat. Brain Res 153, 1-26.

Saper, C.B. and Loewy, A.D. (1980) Efferent connections of the parabrachial nucleus in the rat. Brain Res. 197, 291-317.

Su, H.-S. and Bentivoglio, M. (1990) Thalamic midline cell populations projecting to the nucleus accumbens, amygdala and hippocampus in the rat. J. Comp. Neurol. 297, 582-593.

Swanson, L.W. and Cowan, W.M. (1979) The connections of the septal region in the rat. J. Comp. Neurol. 186, 621-656.

Thanos, S. and Bonhoffer, F. (1987) Axonal arborizations in the developing chick retinotectal system. J. Comp. Neurol. 261, 155-164.

Ter Horst, G.J., De Boer, P., Luiten, P.G.M. and Van Willigen, J.D. (1989) Ascending projections from the solitary tract nucleus to the hypothalamus. A Phaseolus vulgaris lectin tracing study in the rat. Neuroscience 31, 785-797.

Tribollet, E. and Dreifuss, J.J. (1981) Localization of neurones projecting to the hypothalamic paraventricular nucleus area of the rat: A horseradish peroxidase study. Neuroscience 6, 1315-1328.

Turner, B.H. and Herkenham, M. (1991) Thalamo-amygdaloid projections in the rat: a test of the amygdala's role in sensory processing. J. Comp. Neurol. 313, 295-325.

West, C.H.K. Jackson, J.C., and Benjamin, R.M. (1979) An autoradiographic study of subcortical forebrain projections from the mediodorsal and adjacent midline thalamic nuclei in the rabbit. Neuroscience 4, 1977-1988.

Received 23 August 1993
Accepted 15 November 1993

Neurobiology 1 (4), pp. 351-370, 1993

INTRACELLULAR RECORDINGS WITH PATCH-CLAMP PIPETTES FROM NEURONS; TECHNICAL PROBLEMS IN ANALYSIS OF CONDUCTANCE CHANGES DURING BRIEF OXYGEN DEPRIVATION OF HIPPOCAMPAL SLICES

Gábor Czéh and János Czopf

Institute of Physiology, University Medical School of Pécs,
7643 Pécs, Szigeti út 12, Hungary

Summary: Brief oxygen deprivation causes reversible, rapid and large scale redistribution of ions in hippocampal slice preparations. Intracellular recordings revealed remarkable increases of membrane conductance in neurons restricted for the period of hypoxic spreading depression (SD). Voltage-clamp technique was applied to explore further details of the SD-associated conductance changes. Patch-clamp recording in whole-cell configuration allowed better control of membrane potentials. High resolution current-voltage (I-V) plots were obtained by ramp command technique. Limitations of the techniques and various test protocols are evaluated.

Key words: Whole-cell patch clamp, CA1 pyramidal cells, Dentate granule cells, Hypoxia, Slices, Rat

INTRODUCTION

Oxygen deprivation in neurons is well known to depress synaptic transmission, membrane excitability and to change membrane potential. Some neurons respond with initial hyperpolarization followed by depolarization, in contrast with others which are only depolarized (e.g. Haddad and Jiang 1993). A portion of membrane potential change is due to conductance increases, therefore voltage clamp (V-clamp) technique is needed to study them. A tetrodotoxin-insensitive, cadmium-sensitive slow inward current produced by brief

anoxia in CA1 neurons was identified with single-electrode V-clamp using high resistance pipettes (Krnjevic et al., 1989). In other studies another variant of membrane conductance was observed with patch-pipettes (Zhang and Krnjevic, 1993). Conclusions of measurements obtained with these two kinds of V-clamp techniques were not quite the same as discussed by Zhang and Krnjevic (1993). Control of membrane potential is superior if V-clamp is made by low resistance patch pipettes sealed to the membrane with Giga-Ohm resistance, but there are other important differences between the two techniques (e.g. Staley et al., 1992).

Current-voltage (I-V) relationship reflects details of voltage-dependent membrane conductance changes. Compiling databases for complete I-V plots with conventional techniques takes considerable time in mammalian central neurons because many V-gated conductances operate at membrane potential levels between for example -100 and +50 mV (e.g. Hille 1984; Brown et al., 1990). Clamping the membrane potential to a certain level modifies activation-inactivation parameters and some conductances increase, others decrease making the I-V function often non-linear. Theory assumes a range of membrane potential in which no V-gated conductance operate, and the membrane slope resistance (Rm) can be derived from linear I-V functions describing that range of potentials (see Jack et al., 1975). However, the Rm derived this way can also be affected under certain conditions raising the question if the "resting" property of the membrane changed in itself or some conductances react to experimental manipulations with opening (or closing) unidentified ionic channels. Combined electrophysiological and pharmacological approaches needed to solve such problems which face difficulties involved during rapidly changing conditions, for example under the effect of hypoxia. If estimation of the Rm should include some information on the rectifications as well, an even more time consuming approach is required to test voltage changes during many slightly different current injections. Specific tests designed to detect a particular variety of conductances can provide important data faster, but they also bias the results.

Most of the macroscopic membrane conductances have complex time dependent properties. Recorded waveforms will therefore change during steady state test pulses and they can be quite different if tested by steplike versus slowly changing ramp pulses. Slow ramps offer considerable advantages in measurements of steady or relatively time-independent

components of the I-V relation, because neither capacitive charge movements nor transient activations with different time-constants complicate the analysis. Faster ramp tests can disclose more details with less errors of the nonlinear portions of the I-V curves then tests composed of long series of small steps. This seems critical in periods of fast and dynamic changes of membrane properties, like those involved in electrographic seizure or spreading depression (SD) episodes.

MATERIALS AND METHODS

Hippocampal tissue slices were prepared from ether anaesthetized rats as previously described (Czéh and Czopf 1991, Czéh et al., 1990, 1992). Briefly, 400 μm thick slices were cut with a vibrotome and maintained in an interface chamber at 35.5 °C. Artificial cerebrospinal fluid (ACSF) contained, in mMol/l, NaCl, 126; KCl, 5.5; $CaCl_2$, 1.2 $MgSO_4$, 1.2; $NaHCO_3$, 24; NaH_2PO_4 1.25, glucose, 10; pH 7.4, saturated with 95% O_2 + 5% CO_2 (carbogen). Extracellular voltage (V_o) was recorded in str. pyramidale within 100 μm of the patch pipette using an ACSF-filled micropipette of 5-20 MΩ resistance. Patch pipettes with tips of about 2 μm i.d. (electrode resistance of 3-7 MΩ) were filled with HEPES buffered solutions containing either Cs-gluconate, or K-gluconate and $MgCl_2$, pH 7.22, 270 mOsm. In some cases 2 mM QX-314 was also mixed into the filling solutions to block V-gated Na^+ currents.

Seal with cells was established by "blind" search guided in the cell body layer by electrical signals. Seal resistance was at least 1 GΩ. The patch was broken by suction and the membrane potential measured in current clamp configuration. Voltage clamp was then established and macroscopic currents were recorded in whole-cell configuration. The voltage of the patch pipettes was referred to V_o registered by the extracellular electrode coupled to the bath headstage of the Axopatch 1D amplifier. Compensation for series resistance was always at least 70%. Recordings were filtered (2 KHz, Bessel) and stored on digital tape (Biologic DTR 1200) and on polygraph chart. The Axon Instruments 'p-Clamp' program controlled V-clamp commands and stored evoked responses on disk for later analysis.

Membrane parameters were tested by ramp commands generated by the computer. The most commonly used ramps started with a 40 mV step down from the V_h for 20 ms and moved from that moment to a point of 100 mV positive with 0.33 mV/ms rate, and stepped back again to the V_h level. Other variants of ramp commands will be shown in the Results section. The holding potential was adjusted manually. Ramp tests could be repeated and stored within 1 sec if needed, they were triggered manually while watching the progress of hypoxic episode on the chart record. Under steady state conditions ramps were delivered at a low rate, but they were timed with an effort to sample the more dynamic phases in more detail while avoiding presumed pitfalls of high rate, continuous testing for extended periods.

Oxygen deprivation was made by filling the gas space of the interface chamber with 95%N_2 + 5%CO_2 usually until a typical extracellular negative SD wave developed. When this wave failed, hypoxia was terminated by switching the gas supply back to carbogen in 10 min.

Current-voltage (I-V) relationships were plotted from samples taken at 300-400 μV intervals in each ramp command. Regression analysis was performed using the near linear portion of the I-V curves. Regression lines of 100 to 200 data points were obtained with R-squared within 1.00 and 0.95. The standard SE of X-coefficient measurements was always below 10 percent, and very often it was close to 1 %. To remain within these limits, the part of current data evoked by the -100 to -50 mV section of the ramp command was used. When the relation remained fairly linear, the whole range of command voltage was considered.

RESULTS

Ramp tests can give over one hundred data points within a few hundred millisecond for I-V functions with high resolution. If current ramps are injected, the membrane potential of the cell changes slowly and gradually with little complications until reaches firing threshold. Tests with 2 to 3-times steeper depolarizing slope makes the membrane potential to cross the firing threshold level sooner but the I-V relationship remains similar. Treatments like oxygen deprivation can however make the voltage response of the same cell different to identical current injection (Fig. 1), which results in different I-V plots.

When under V-clamp conditions the membrane potential is changed with small increments slowly, transmembrane current is determined by the steady state properties of the membrane. An obvious question is what slope of ramp commands would make any transient conductance components of the cellular responses negligible. On the other hand, V-sensitive components should appear during ramp commands when their activation becomes dominant. However membrane conductances presumably behave in a different way when tested with large instantaneous steps or with small gradual increments even if the initial and end voltage levels are the same. Thus transmembrane currents induced step and ramp commands are not identical.

Commands with similar peak to peak voltage levels but with different timecourse were used to induce membrane currents and quantitatively different transient components were observed. There was, however, a range of ramp slopes with which a large portion of the subthreshold current remained practically the same. In our experiments ramp commands with more than 1 mV/ms rate were needed to affect the subthreshold portions of the membrane current considerably. I-V plots derived from ramps of such a high rate were steeper then the practically identical others obtained with slower (0.3 to 0.1 mV/ms) ramp rates. Calculated

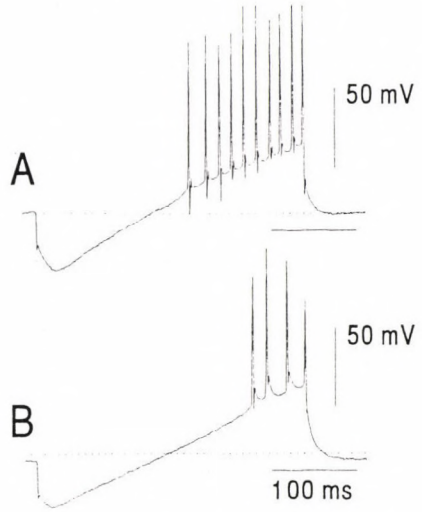

Fig. 1: Responses to ramp current injections. Intracellular recordings from the CA1 pyramidal cell layer with a patch pipette in I-clamp configuration. A before, B after a short hypoxic episode. Dotted lines at -64 mV (initial resting potential) level help to compare waveforms. The time course of the current injection was similar to the ramp illustrated in Fig.2 with a peak to peak intensity of 1 nanoA. Note differences between the slopes of the subthreshold membrane potential traces, and between firing parameters of the cell. Time bars in both records indicate 100 ms.

values of Rm with fast ramp was 222 MΩ, with moderate ramp rate 265 MΩ, and with low rate 275 MΩ between -100 and -40 mV depolarization in a single cell. Ratio of Rm values taken in other cells with such rates were similar and 10 to 86 MΩ differences were found in single cells tested with these three kinds of protocols. Apparently, ramps with different rate induce currents from which calculation results in similar conductance values within a certain range of ramp rates, but gets larger with quite fast ramps. In contrast, the nonlinear portions of the I-V curves are more sensitive to the ramp rate.

Cells exposed to hypoxia or stimulated with high frequency to provoke normoxic SD episodes were tested many times during exposure with a particular ramp command. As reported elsewhere (Czéh et al., 1993), the membrane conductance was 2 to 10-times higher

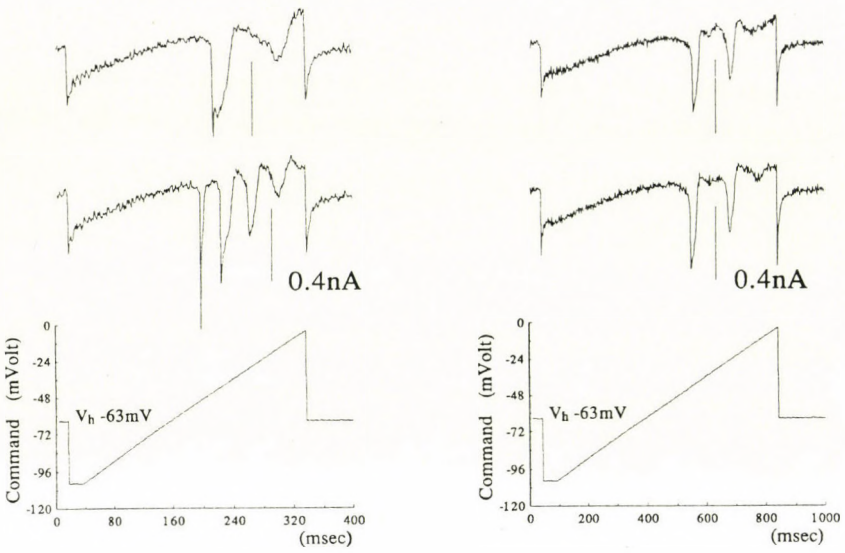

Fig. 2: Responses to ramp commands in V-clamp configuration. Presumed granule cell recorded in the cell body layer of the dentate gyrus. Columns left and right are from the same cell tested with ramps of 0.33 mV/ms and 0.13 mV/ms rate, respectively. The upper two traces of both columns are raw current records, time scales on the bottom are valid also for the upper traces, inward current causes downward deflection, vertical calibration bars mean 0.4 nA. Note differences in activation of the membrane by depolarizing ramps with different slopes.

at the maximum of SD as compared to pre-SD controls (mean 3.52 ± 0.4 SE n=26). Mean decrease of Rm was 62.6 MΩ (± 27.8 SE) calculated from the same set of data. Consistently less differences were observed among data obtained in single cells tested with different ramps during quiet periods (before or long after SD episodes). In particular, data obtained with the same kind of test before and during SD yielded much larger difference than the variance of data obtained by repeating the same command during quiet periods several minutes apart.

The commands used in most of the cases started and ended with a voltage step down, included an initial short period of steady hyperpolarizing potential followed by a 100 mV depolarizing ramp. The steps induced large capacitive currents and the 20 ms or longer period of constant voltage was sufficient for diminution of the initially activated charging current. The 100 mV ramp command depolarized the membrane passing a range of membrane potential critical in activation of V-gated currents. Accordingly, the waveforms of ramp evoked currents, and the I-V plots derived, had two main parts: the first and simpler reflected changes of (leak) current intensity across the "passive" membrane with command potentials, the other more complex part occurred when the voltage-gated conductances were also affected by the depolarizing ramp. The neutral term "nonlinear components" denoted this later part of the current, which was found more sensitive to rate of ramp. Nonlinear I-V curve could occur for at least two reasons: activation of a variety of transmembrane currents, and error due to loosing of V-clamp at higher membrane potential levels. While the records probably represented a mixture of both, we did not believe that the whole nonlinear complex as such was a meaningless artifact.

Direction of the ramp commands was also important in respect of non-linear portions of the I-V curves. Slowly hyperpolarizing ramps eliminated problems associated with threshold depolarization of the membrane, but some nonlinearity often came at the opposite, hyperpolarized limb of the curve (Fig. 3). In the cell considered above as representative for depolarizing ramps, hyperpolarizing ramps down to -150 mV resulted in around 170 MΩ values (173 MΩ with slower and 166 MΩ with moderate rate). When only narrow segments of the I-V plot around -60 mV produced Vm were considered, the same Rm values were calculated from ramps of either direction, and the plotted functions were identical. When longer segments (50 - 100 mV) were compared, the calculated Rm values could be different with up to about 20% and examples occurred with higher Rm values from either directions of ramp command. The difference can be attributed to different degree of activation-inactivation of various conductances when tested with depolarizing or with hyperpolarizing ramps. In spite of that, there seems to be a range of voltage levels explored with fine resolution which yields practically the same Rm value irrespective of the direction of the ramp command and unaffected by the ramp rate provided that it remains within certain

limits. This portion of the curve can well be considered to describe the "resting leakage conductance" of the cell and has been reported to change considerably with hypoxia and SD (Czéh et al., 1992, 1993).

Data points were also affected by the initial level from where the ramp commands started (V_h near resting potential, far hyperpolarized level for depolarizing and quite depolarized level for hyperpolarizing ramps). Slope resistances calculated from the I-V plots in the -50 to -100 mV range was found, however the same. When ramps coursed the very depolarized (e.g. between -20 and +30 mV) or extremely hyperpolarized (below -110 mV) potential range, the slopes deviated from each other and from that found with ramps not reaching the extreme levels. The slopes seen in identical segments of the extreme ranges

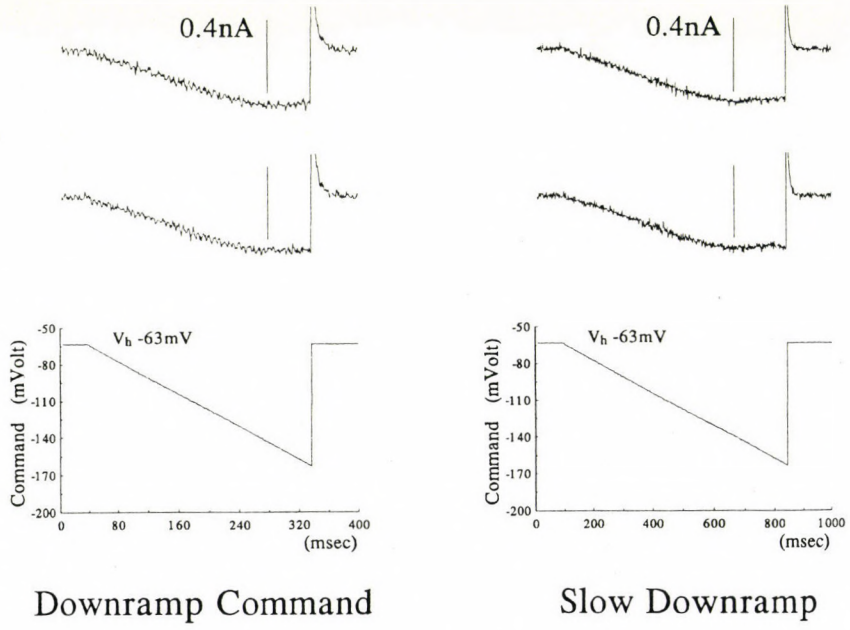

Fig. 3: Responses to hyperpolarizing ramp commands. Same cell and similarly arranged frames as in Fig. 2.

apparently depended on the steady holding potential level from where portions of ramp commands reached the extreme voltage levels. Work is in progress to determine how the calculated Rm value depends on the length of time while the membrane is clamped at extreme potentials.

Ten or twelve voltage steps, 200 ms each, in 5 mV increments gave plots with rather poor resolution (10-12 data points) of the I-V relationship. The linear part of the function could be used to determine Rm, and the technique was good enough to get evidences for major and persistent changes of the Rm value (Fig. 6). However, during rapid change of

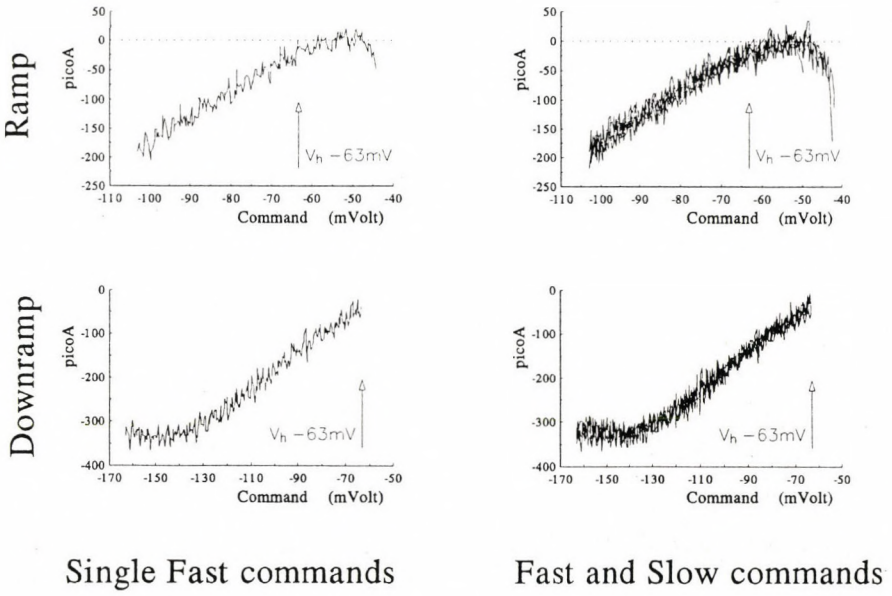

Fig. 4: I-V relationship of a granule cell. The data were plotted from those illustrated in Figs. 2 and 3. Time courses of the Fast commands used on the left side, are shown on the left side of Figs. 2 and 3. On the right, plots obtained by the faster and slower ramp commands are superimposed. Note that only segments of the current responses to depolarizing commands are used.

conditions, like the dynamic onset phase of SD episodes - the technique would give data with considerable error since properties of the membrane could change considerably between consecutive pulses and therefore the 5 mV increments would test the membrane with different instantaneous Rm value. Another problem came from the more or less unpredictable nature of the SD episodes, some developed sooner others later under similar conditions; some took off quite rapidly and followed complex timecourse, others were slower and simpler. Timing of tests which required long periods would be difficult under such circumstances (e.g. Fig. 5).

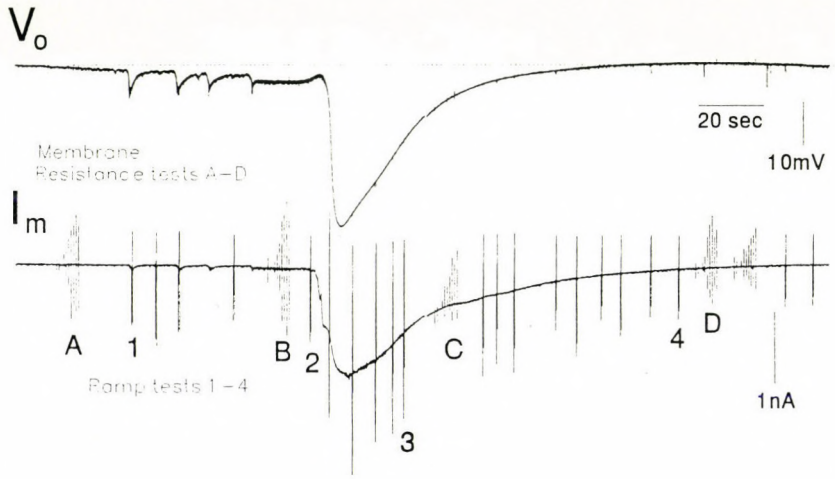

Fig. 5: Simultaneous extracellular (V_o) and patch-clamp recordings (I_m) from the CA1 subfield of a slice, distance between the two pipettes in the pyramidal cell layer was about 100 μm. Negativity is downward on the V_o trace. Four relatively fast waves ride on a slow baseline shift, before a large negative wave signals a short SD episode. The cell was V-clamped at -50 mV and tested with two kinds of commands several times during the episode. Details of tests marked with A-D are shown in Fig. 6 and those with 1-4 in Fig. 7. Note that the membrane resistance test needs time too long to explore changes during the rapid onset phase of the SD. Sampling rate was 1 kHz during analog-digital conversion of the tape recorded data for this illustration.

Increasing the number of data points makes I-V plots more exact and helps to estimate membrane rectification. Non-linear components should be tested with steps repeated at quite low rate which easily prolongs the time required for a complete family of curves over several minutes. That would be far too long in SD-research. Extremely slow (below 1 mV/sec rate) ramps would also be inadequate to explore acute effects of hypoxia.

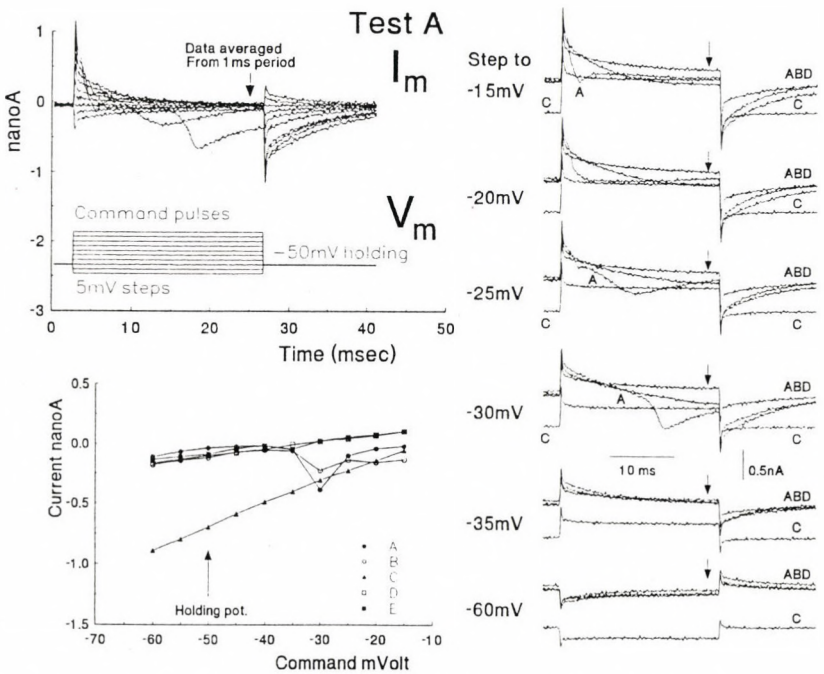

Fig. 6: Responses to step command pulses. Expanded portions of I_m recording shown in Fig. 5. Top left: currents evoked by the commands shown with the same timescale, vertical scale serves for the current records only. This family of curves is marked with A in Fig. 5. Arrow indicates the time when a segment of current data were averaged from each families of curves for the I-V plot on the bottom left. On the right, responses to identical commands (labeled as Step to -15 mV etc) were selected from families A-C in Fig. 5. Note that curves from group C at the SD decay consistently deviate from the others in several respects including baseline level and details of waveform. Responses in group A to steps jumping beyond -30 mV contain a strong inactivating inward component.

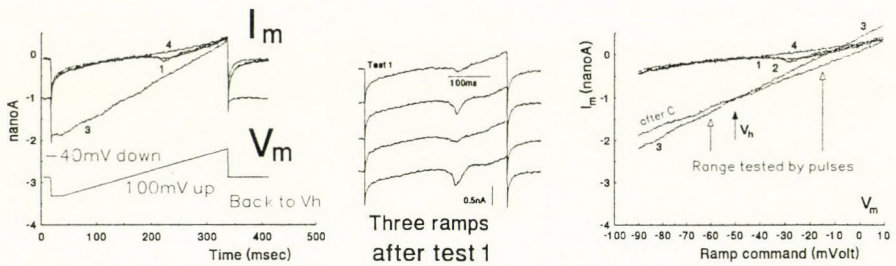

Fig. 7: Responses to ramp test commands. Expanded portions of I_m recording shown in Fig. 5. Left: raw current data with similarly time-scaled command, labels 1-4 refer to Fig. 5. Vertical scale for the current data only. Far right: I-V plot from ramp command evoked currents, black arrow indicates the holding potential, the open ones border the potential range explored with step commands shown in Fig.6. Note the steeper slope of data taken at the early decay of SD episode before (line 3) and after the period when group C of curves shown in Fig. 6 was obtained. Note also, that line 2 which sampled the last seconds before the SD wave did not deviate from lines 1 and 4. Middle set shows consecutive ramp evoked currents after test 1 in Fig. 5 to illustrate how the waveform changes during the period of time when epileptiform negative waves occur.

The currents evoked by ramp voltage commands which linearly depolarized the cell over a period of 300 ms usually contained fast inward surges attributed to putative sodium current (Fig. 2). In the absence of them much slower currents made the I-V plots non-linear. Slow inward rectification could be analogous with the inward-going end of the curves shown in Fig. 4, preceding the onset of fast inward surge. Examples in Fig. 8 were selected to illustrate more prolonged forms of such smaller slow components. Direction of the slow rectifications, and particularly their modification under the effect of mild hypoxia suggested complex multi-ionic nature, including putative high threshold, calcium mediated and some potassium mediated components. Calcium-dependent mechanism of the inward rectification was likely because it survived blockage of fast sodium currents by QX-314, and potassium was the most likely ion to carry outward current.

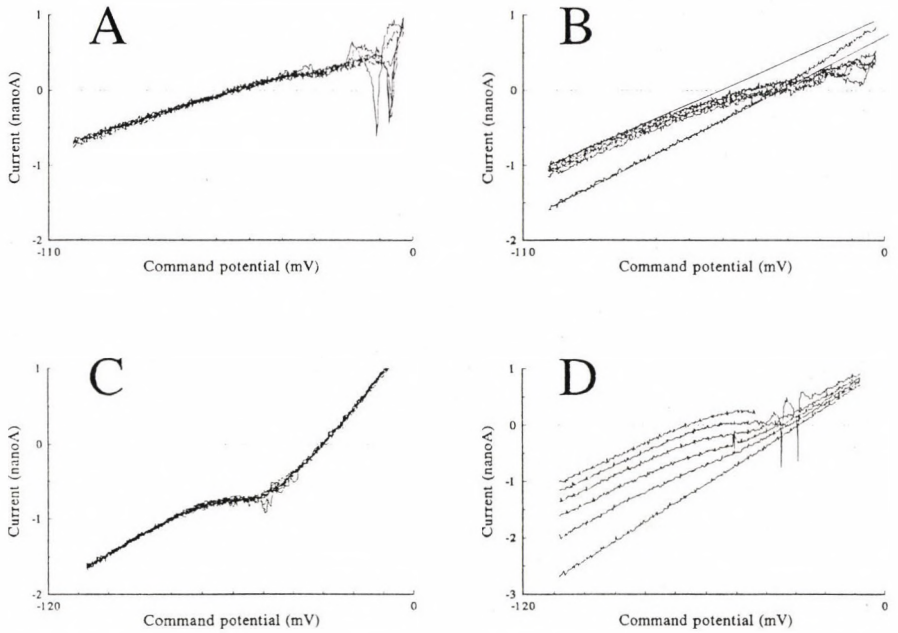

Fig. 8: Examples of slow inward current induced by ramp commands as recorded with K-gluconate filled pipettes, 2 mM QX-314 also present in the pipette in **A** and B. **A**: Taken at V_h -62 mV during early prodromal phase of hypoxia. Note the small and the larger, broad components activated with large depolarization. **B**: Curves obtained in the 3rd minute of hypoxia, the top line was taken first, the bottom one last before an SD wave. The first and last curves deviated in the opposite direction from the corresponding straight lines (fitted by eyes). The larger, broad components shown in **A** were depressed at this stage of hypoxia. **C**: Another cell, V_h -67 mV, during hypoxia. The left limb of the curve is linear indicating the voltage independent ohmic (leakage) resistance. The mid-portion suggests activation of a slow inward-going component, while the right-side limb goes to the opposite (outward) direction. **D**: Gradual recovery of slow inward current in early reoxygenation period from yet another cell. The bottom (still linear) curve was taken first and the others consecutively as shown shifting upward with more and more rectification from about -50 mV on. Larger fast inward components were omitted from the top one for clarity. This cell was clamped at V_h -68 mV.

Interpretation of V-clamp findings depends critically on the quality of space clamp. It seems unlikely that the whole membrane surface of multipolar neurons can be kept at the same potential level by point source current injections from an electrode attached to the perikaryon (Johnston and Brown 1983; Spruston et al., 1993). Time course of the initial component of step command evoked current signals could well be approximated with a curve calculated from two exponentials. Time constant for the faster one was around 0.5 ms and that of the slower fell between 2.5 and 5 ms, which supported the assumption that charges were re-distributed between the non-isopotental compartments.

A possible way to judge adequacy of V-clamp in at least a portion of the dendritic membrane is to demonstrate how evoked postsynaptic currents (PSC) generated in the dendrites depend on the membrane potential. V-dependent reversal is a well established property of chemically activated ionic currents, which cannot be seen if the effect of V-clamp is restricted to the somatic membrane, far from the activated transmitter receptors.

Str. radiatum volleys induced strong inward current in CA1 pyramidal cells (see Nicoll et al., 1990) if the Vm was more negative then about -55 mV. At this level fast glutamate (AMPA) activated current and $GABA_A$ receptor-mediated current were both supposed to be inward. When the membrane potential was kept positive from about -50 mV, activation of putative $GABA_A$ receptor induced chloride current became outward, and at very positive Vm levels the presumed glutamate-activated initial current also reversed. Tests illustrated in Fig. 9 were performed in all cells V-clamped in our study and differential reversing of later and earlier components of the PSC suggested that the part of the dendrites where the stimulated synapses were located was under V-clamp. Therefore requirement of space clamp was at least in part fulfilled.

DISCUSSION

Purposes of V-clamp studies of neurons include investigation of macroscopic currents induced by any of several possible manipulation of the membrane conductances. The key assumption in the technique claims that the recorded currents reflect magnitude and kinetics of the transmembrane conductance. A primary condition of adequate V-clamp, however, practically never holds in studies on CNS neurons of mammals: the space clamp remains

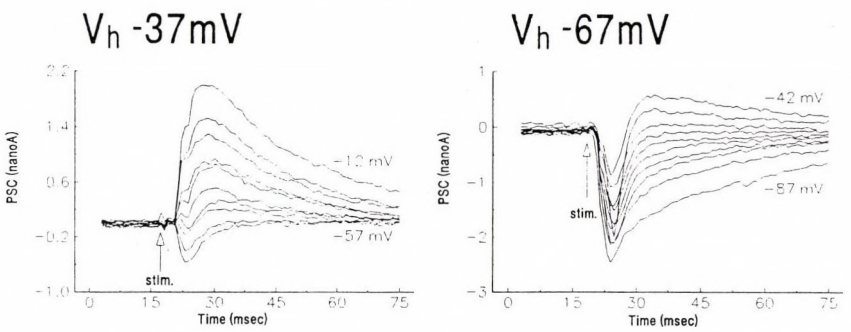

Fig. 9: Reversal of postsynaptic current (PSC) elicited in a CA1 pyramidal cell by str. radiatum volleys. Presynaptic fibers were stimulated with constant intensity in each of the 10 superimposed records on both left and right, while the cell was V-clamped at -37 and at -67 mV, respectively, several minutes apart. From the V_h levels indicated, 300 ms long step commands were delivered and the str. radiatum volleys (arrow) were triggered at 200 ms after the step onset. The steps were graded in 5 mV increments between the minimal and maximal values indicated on both records. The segments of membrane currents shown contain a period of prestimulus baseline, but neither the initial nor the end part of the step command evoked currents. Leak currents were eliminated by subtraction of digitalized traces produced with similar step commands but without str. radiatum stimulation.

inadequate (Johnston and Brown, 1983). Space clamp requires that the whole surface of the cellular membrane should be clamped at the same voltage level otherwise only a portion of the recorded current would represent transmembrane conductance changes while another portion would in fact be intracellular, not transmembrane, current due to potential differences between somatic and dendritic membrane. It is unlikely that one could ever control the whole membrane surface of large multipolar cells by point source voltage injection used in any kinds of single electrode voltage clamp techniques. Space-clamp problems can be reduced by decreasing the amplitude of the current (e.g. Park and Ahmed 1991).

Patch clamp pipettes are better for V-clamp because they have lower resistance than conventional sharp intracellular electrodes. A further advantage comes from the giga-seal established in whole-cell patch-clamp recordings, which allows far better isolation from the extracellular electrolite medium. Design of patch-clamp amplifiers makes V-clamping faster

and more powerful which further diminishes but cannot eliminate the problems involved in poor space clamping of the membrane.

Although patch-clamp technique reduces steady state voltage attenuation, transient currents generated in neuronal dendrites and measured at the soma can be significantly attenuated and distorted (Spruston et al., 1993). The unclamped nature of membrane raises the possibility that voltage-gated channels in dendrites may also be activated by synaptic transmitter binding, even under V-clamp conditions. The errors can be reduced by reducing the series resistance and electrode capacitance, but alteration of the magnitude and time-course of the current generated in the dendrites and measured at the soma remains significant. The attenuation, however, affects far less the estimation of reversal potential of synaptic currents. Attenuation can be over 80% for magnitude of PSC and 310% increase in rise time according to the simulations run by Spruston et al. (1993). There seems to be no generally accepted method for determining space-clamp problems involved in PSC measurements, because neither the lack of correlation between synaptic decay time constant and rise time, nor the step command method (Hestrin et al., 1990) are accurate as discussed by Spruston et al. (1993). Although conductances involved during SD episodes are slower than those measured with PSC, they appear to be larger in magnitude, thus the published records - including our own - are probably distorted by an unknown factor.

Measurement errors may remain unchanged throughout the recording session from a single cell, and effect of some experimental manipulation can be demonstrated by subtracting control data taken from the same cell before manipulations. Control data on membrane conductance (or Rm derived from it) should not contain V-dependent or ligand-dependent components. Obtaining adequate controls with recording from neurons in slices is not a trivial task, however. Under single electrode V-clamp, a convenient test to check for presence of activated current component looks for the difference between waveforms induced by the make and break of the command voltage steps. Discontinuities in the current traces at the beginning and end of the voltage steps reflect the instantaneous, ohmic, "leakage" current. The leakage conductance is analogous to the conventional input conductance measured with I-clamp techniques; it is determined by the combination in parallel of the true leak conductance of the isopotential compartment (presumably the soma) and the input conductance of the cable

network provided by the nonisopotential dendritic tree. Any V-dependent conductances that are active at rest will also contribute to the apparent leakage conductance (Stafsrom et al., 1984a). An often used procedure is to subtract the leakage component from the total current recorded to view any time-dependent currents in isolation. This procedure cannot used when the leakage component does not remain constant. Another approach is to subtract control data as a whole (leakage plus other components together) from the experimental one to demonstrate effects in isolation. Again, the technique is justified as long as one can believe that all the "isolated effects" are indeed come from the experimental manipulation and no uncontrolled parameter change is involved.

Very slow (2-6 mV/sec rate) ramps test the steady state Rm, and under V-clamp the ramp command produces a linearly rising ionic current which largely represent ohmic, leakage current (Stafsrom et al., 1984b). Nonlinearity of I/V plots obtained with this technique reflects V-gated conductances (e.g. the persistent sodium-current in neocortical cells, Stafsrom et al., 1984b).

Faster ramps, on the other hand, may result data points which reflect in part the leakage conductance and in part contribution of currents due to lack of isopotential dendrites. It seems likely that as faster ramps force the system to work closer to its speed limit in preventing any voltage deviation from the command level, the relative potential difference between soma and distant dendrites gets larger. This may explain the slope difference between I-V plots obtained from the rapid and the slower ramp tests. However, it is also likely, that the somatic membrane itself react in a little different way to faster versus slower ramps (Stafsrom et al., 1984b). Although work is in progress to analyse fast-ramp induced conductance changes, one conclusion is firm even from the data available so far: one must use the very same command protocol and repeat the test over and over again to obtain meaningful data on Rm changes involved for example in seizures or hypoxia.

Ramp activated macroscopic currents recorded here had several components which should be related with those elicited by step pulse commands in hippocampal slices under similar conditions (e.g. Krnjevic and Leblond, 1989). This work should include pharmacological tests as well. The ramp commands with parameters used here have not been used before by others. Thus it seems premature to speculate on the identity of currents found

in ramp-stimulated cells. Recently striking differences emerge among sets of neuronal properties obtained with conventional sharp-electrode versus whole-cell patch clamp recording techniques. The resting potential, action potential threshold and rheobase values are found to be quite similar, in contrast with the Rm and the action potential amplitude data which seem consistently much larger in recordings with whole-cell technique. The difference has been explained by the long suspected effects of microelectrode-associated leak conductance (Staley et al., 1992, Vanner et al., 1993) but modifications associated with cell dialysis (e.g. Zhang and Krnjevic, 1993) should not be neglected either.

Ramp tests with various rates have been used to study several kinds of cells (e.g. cardiac cells: dV/dt = 0.46 V/s, Tareen et al., 1992; 50 mV/s, Xu and Adams 1992; neocortical pyramidal neurons: 34 mV/s, Stafsrom et al., 1984b; CA3 pyramidal cells: 1mV/5ms, Thompson and Gähwiler, 1989; dorsal root ganglion cells: 1mV/2ms, Duchen, 1990; diencephalic neurons: 2.5 and 5 mV/ms, Park and Ahmed, 1991). The I-V plots contain generally two portions with different slopes reflecting leakage and activation of some V-gated conductances usually in the range between -40 and -60 mV. Some (e.g. Xu and Adams, 1992) report on direct comparison between I-V plots obtained with conventional steps and with ramp techniques. Portions of the curves corresponding to the resting (or leak) steady conductances match fairly well and the limited number of data points obtained with step pulses in the voltage range which activates strong currents do not deviate too far from those with ramp technique. The ramps used by Xu and Adams (1992) are far slower than the ones tested in our work. However the conclusion from experiments illustrated in Figs. 5-7 was similar: ramp tests of 0.33 or 0.13 mV/ms resulted in Rm values comparable to those obtained from the steady portions of the step evoked responses. Nature of nonlinear components shown in Figs. 2-4 and 8 is more obscure and probably more important in controlling firing properties of the neurons (Stafsrom et al., 1984b).

ACKNOWLEGDEMENTS

We thank Dr. Loránd Kellényi for his invaluable helps in technical matters. Some recordings were performed in Prof. George Somjen's laboratory at Duke University, we are grateful for his support and helpful discussions.

This research was supported by T-557/1990 ETT and T-3-1188/1991 OTKA grants.

REFERENCES

Brown, D.A., Gähwiler, B.H., Griffith, W.H. and Halliwell, J.V. (1990) Membrane currents in hippocampal neurons. Prog. Brain Res. 83, 141-160.

Czéh, G., Aitken, P.G. and Somjen G.G. (1992) Whole-cell membrane current and membrane resistance during hypoxic spreading depression. Neuroreport 3, 197-200.

Czéh, G., Aitken, P.G. and Somjen G.G. (1993) Membrane currents in CA1 pyramidal cells during spreading depression (SD) and SD-like hypoxic depolarization. Brain Res. (in press).

Czéh, G. and Czopf, J. (1991) An intracellular investigation into the postsynaptic responses of the principal cells in slice preparations from rat hippocampal formation. Acta Physiol. Hung, 77, 63-76.

Czéh, G., Horváth, Zs. and Czopf, J. (1990) Long-term potentiation in slices from subcortically deafferented hippocampi. Brain Res. 518, 279-282.

Duchen, M.R. (1990) Effects of metabolic inhibition on the membrane properties of isolated mouse primary sensory neurones. J. Physiol. 424, 387-409.

Haddad, G.G. and Jiang, C. (1993) Oxygen deprivation in the central nervous system: Mechanisms of neuronal response, differential sensitivity and injury. Prog. Neurobiol. 40, 227-318.

Hestrin, S., Nicoll, R.A., Perkel, D.J. and Sah, P. (1990) Analysis of excitatory synaptic action in pyramidal cells using whole-cell recording from rat hippocampal slices. J. Physiol. (London) 422, 203-225.

Hille, B. (1984) Ionic Channels of Excitable Membranes. Sinauer, Sunderland (Mass.).

Jack, J.J.B, Noble, D. and Tsien, R.W. (1975) Electric Current Flow in Excitable Cells. Oxford, U.K. Clarendon.

Johnston, D. and Brown, T.H. (1983) Interpretation of voltage-clamp measurements in hippocampal neurons. J. Neurophysiol. 50, 464-486.

Krnjevic, K., Cherubini, E. and Ben-Ari, Y. (1989) Anoxia on slow inward currents of immature hippocampal neurons. J. Neurophysiol. 62, 896-906.

Krnjevic, K. and Leblond, J. (1989) Changes in membrane currents of hippocampal neurons evoked by brief anoxia. J. Neurophysiol. 62, 15-30.

Nicoll, R.A., Malenka, R.C. and Kauer, J.A. (1990) Functional comparison of neurotransmitter receptor subtypes in mammalian central nervous system. Physiol. Rev. 70, 513-566.

Park, C.C. and Ahmed, Z. (1991) Characterization of sodium current in developing rat diencephalic neurons in serum-free culture. J. Neurophysiol. 65, 1011-1021.

Spruston, N., Jaffe, D.B., Williams, S.H. and Johnston, D. (1993) Voltage- and space-clamp errors associated with the measurement of electrotonically remote synaptic events. J. Neurophysiol. 70, 781-802.

Stafsrom, C.E., Schwindt, P.C., Flatman, J.A. and Crill, W.E. (1984a) Properties of subthreshold response and action potential recorded in layer V neurons from cal sensorimotor cortex in vitro. J. Neurophysiol. 52, 244-263.

Stafsrom, C.E., Schwindt, P.C. and Crill, W.E. (1984b) Repetitive firing in layer V neurons from cat neocortex in vitro. J. Neurophysiol. 52, 264-277.

Staley, K.J. Otis, T.S. and Mody, I. (1992) Membrane properties of dentate gyrus granule cells: comparison of sharp microelectrode and whole-cell recordings J. Neurophysiol. 67, 1346-1358.

Tareen, F.M., Yoshida, A. and Ono, K. (1992) Modulation of β-adrenergic responses of chloride and calcium currents by external cations in guinea-pig ventricular cells. J. Physiol. 457, 211-228.

Thompson, S.M. and Gähwiler, B.H. (1989) Activity-dependent disinhibition. I. Repetitive stimulation reduces IPSP driving force and conductance in the hippocampus in vitro. J. Neurophysiol. 61, 501-511.

Vanner, S., Evans, R.J., Matsumoto, S. G. and Surprenant, A. (1993) Potassium currents and their modulation by muscarine and substance P in neuronal cultures from adult guinea pig celiac ganglia. J. Neurophysiol. 69, 1632-1644.

Zhang, L. and Krnjevic, K. (1993) Whole-cell recording of anoxic effects on hippocampal neurons in slices. J. Neurophysiol. 69, 118-127.

Xu, Z.J. and Adams, D.J. (1992) Resting membrane potential and potassium currents in cultured parasympathetic neurones from rat intracardiac ganglia. J. Physiol. 456, 405-424.

Received 29 October 1993
Accepted 22 November 1993

Neurobiology 1 (4), pp. 371-383, 1993

DISTRIBUTION OF SEROTONIN-LIKE IMMUNOREACTIVE NEURONES IN THE EMBRYONIC NERVOUS SYSTEM OF LYMNAEID AND PLANORBID SNAILS

[1,2]Elena E. Voronezhskaya and [1]Károly Elekes

[1]Balaton Limnological Research Institute of the Hungarian Academy of Sciences, H-8237 Tihany, P.O. Box 35, Hungary and [2]Institute of Developmental Biology of the Russian Academy of Sciences, Moscow, Russia

Summary: The distribution of 5HT-like immunoreactive (5HTLI) neurones was investigated in lymnaeid and planorbid snail embryos. The time of appearance and the pattern of development of homologous 5HTLI cells in the CNS were found to be similar in all species investigated. However, 5HTLI cells characteristic only of planorbid embryos were also found. These specific neurones which were detected outside the future CNS at stage E30 of embryogenesis and which disappeared close to hatching, were named transient serotoninergic 1 cells. A correlation is suggested between the embryogenetic development of 5HTLI neurones and the development of 5HT-dependent motor behaviour in these animals.

Key words: Mollusca, Pulmonata, Embryogenesis, 5HT-like immunoreactivity.

INTRODUCTION

The molluscan nervous system has become an important model in neurobiological research (Kandel, 1976; Willows, 1985, 1986; Boer et al., 1986), mainly with respect to the identification of neuronal networks underlying 22 different behavioural phenomena. Detailed

Akadémiai Kiadó, Budapest

maps of immunocytochemically labelled neurones have recently been described in the central nervous system (CNS) of several model animals (see e.g. Ono and McCaman, 1984; Croll and Chiasson, 1989; Kemenes et al., 1989; Elekes et al., 1991; Elekes et al., 1993). Mostly adult animals were used in these studies, but gastropod molluscs have long been popular objects in embryology (Stiebel, 1815; Raven 1958). A combination of neurobiological and embryological approaches would allow the use of snails as advantageous models in developmental neurobiology.

Serotonin (5HT) is known to be an important transmitter in gastropods (Koshtoyants et al., 1961; S.-Rózsa, 1984; Walker, 1986). An additional neuromodulatory and neurohormonal role for 5HT has been suggested on the basis of recent immunocytochemical experiments (Hernádi et al., 1989; Kemenes et al., 1989; Elekes, 1991). Little is known, however, about the role of 5HT in the neurogenesis and behavioral ontogeny of molluscs. It has recently been demonstrated that 5HT-containing neurones appear early in the embryogenesis of two pulmonate species, *Lymnaea stagnalis* (Croll and Chiasson, 1989; Marois and Croll, 1992) and *Helisoma trivolvis* (Goldberg and Kater, 1989). The development of the 5HT-like immunoreactive (5HTLI) neurones during embryogenesis in *Lymnaea* has recently been described in detail (Marois and Croll, 1992). To elucidate a more general pattern of development of the 5HTergic system in freshwater pulmonates, the present comparative study on five representative species of this group was undertaken.

MATERIALS AND METHODS

Animals

The following species of gastropods were used: *Lymnaea stagnalis* and *Physa fontinalis* (Lymnaeidae); *Helisoma trivolvis*, *Planorbarius corneus* and *Planorbis planorbis* (Planorbidae). Embryos of *L. stagnalis* and *P. corneus* originated from egg masses laid both in a laboratory colony and in the wild. *P. fontinalis* and *H. trivolvis* were from aquarial cultures only, and *P. planorbis* embryos were from the wild. Egg masses were maintained at room temperature in Petri dishes filled with filtered water from Lake Balaton.

The stages of embryonic development were determined according to Goldberg and Kater (1989) and Marois and Croll (1992). Each stage was characterized by a specific set of morphological, morphometric and behavioral features. Stages were expressed as a percentage of total embryonic development, wherein 0% (E0) corresponded to the first egg cleavage and 100% (E100) to hatching. This designation allowed the avoidance of differences in individual

times of embryogenesis in each investigated species. The following stages were examined: E20, E25, E30, E45, E60, E70 and E80. The results presented in this paper are based upon observations of at least 30 specimens of each snail species at each of the stages mentioned above.

Immunocytochemistry

Sternberger's (1979) indirect three-step method was used. Whole embryos were used to examine the early embryonic stages E20-E30. For advanced stages (E45-E80), dissection of the visceral complex and/or foot was undertaken to ensure a better penetration of antiserum into the tissue. Embryos were removed from eggs and immediately placed into 4% paraformaldehyde diluted with 0.1 M phosphate buffer (PB, pH 7.4) for 4 h at 4 °C.

Immunocytochemistry was performed in the following steps: i) 1 h treatment in 2% H_2O_2 diluted in PB; ii) a 1.5 h treatment with 5% normal goat serum diluted in PB saline containing 0.25% Triton X-100 (PBS-TX); iii) incubation for 20 h with anti-5HT antiserum (Incstar) diluted 1:2000; iv) incubation for 5 h with anti-rabbit IgG (Dakopatts) diluted 1:40; v) incubation for 2 h with rabbit peroxidase anti-peroxidase (PAP) complex (Dakopatts) diluted 1:200. All antisera were diluted in PBS-TX containing 0.25% bovine serum albumin (PBS-TX-BSA). All treatment steps were performed at room temperature and were followed by three washes, each for 15 min, in PBS-TX. After a 15 min preincubation with 0.05% 3,3'-diaminobenzidine (DAB, Sigma) diluted in 0.05 M Tris-HCl (pH 7.6), the histochemical reaction was developed by adding 0.01% H_2O_2 for 3-6 min. Following development, tissues were dehydrated in graded alcohol, cleared with methylsalicylate, mounted in Canada balsam, viewed and photographed with a Zeiss Axioplan photomicroscope.

The specificity of this anti-5HT antiserum has been well demonstrated in the adult gastropod nervous system (Hernádi et al., 1989; Kemenes et al., 1989). Other control experiments included replacement of the primary antiserum (i) with 1% normal rabbit serum or (ii) with the diluting solution, PBS-TX-BSA. No immunostaining was observed after these control experiments.

RESULTS

The terminology used below is after Raven (1958) and Marois and Croll (1992). No differences between wild and laboratory populations were detected.

Lymnaeidae

The pattern of 5HTLI cells was similar in the two species investigated (*L. stagnalis* and *P. fontinalis*). All 5HTLI cell bodies were found within the developing central ganglia (CG). 5HTLI cells were first detected at stage E30 as a pair of somata (C4) located in the anterodorsal quadrant of the embryo (an area corresponding to the location of the future CG),

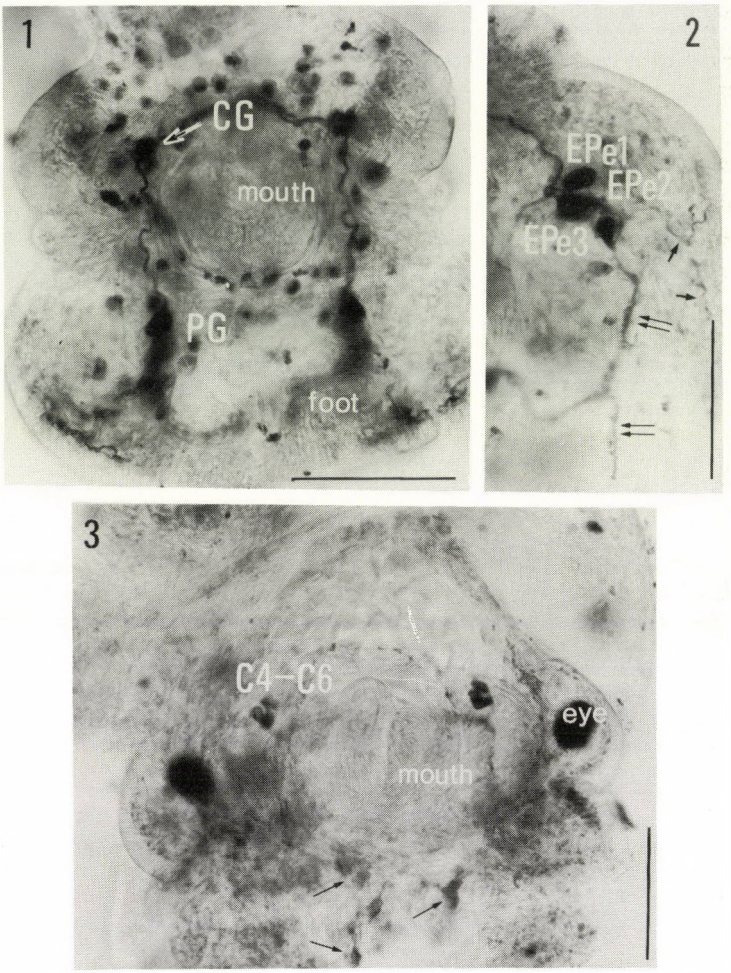

Figs. 1-3: Distribution of 5HTLI neurones in *Lymnaea* embryos. Bars represent 100 μm.
Fig. 1: 5HTLI neurones in embryos of at stage E45. One pair of neurones is seen in the region of the cerebral ganglion (CG) and three pairs in the pedal ganglion (PG).
Fig. 2: E45 neurone in the pedal ganglion (EPe1, EPe2 and EPe3) with their processes to the lateral (arrows) and medial (double arrows) portions of the foot.
Fig. 3: 5HTLI cells in the E60 embryonic nervous system. Three pairs of neurones (C4-C6) are seen in the cerebral ganglion, and some of the pedal neurones are also visible (arrows).

and a pair of somata (EPe1) located in the medial part of the foot (the region of the future pedal ganglia [PG]) (Fig. 12).

By stage E45, each of the C4 bilaterally symmetrical neurones sent a single projection to the contralateral ganglion *via* the cerebral commissure. The perikarya of C4 neurone moved gradually to the caudal part of the cerebral ganglion. In the region of PG, three pairs of neurones (EPe1, EPe2 and EPe3) were detected, with their processes projecting to the cerebro-pedal connectives and to the pedal commissure (EPe1), and to the medial (EPe3) and lateral (EPe2) portions of the foot (Figs. 1, 2 and 12). The latter processes displayed rich branching at the base of the ciliated epithelium (Fig. 2).

The ganglionic ring was mostly developed by stage E60. At this time, a group of three identical 5HTLI neurones (C4-C6) was detected in the caudo-dorsal region of the cerebral ganglion. Their processes ran to the cerebral commissure and reached the contralateral ganglion. Seven large 5HTLI cells occupied the right PG, and six the left one (Figs. 3 and 12). The 5HTLI bundle leaving the PG projected into two branches (Figs. 9-11). One projected to the sole and arborized widely at the base of the ciliated epithelium (Figs. 10 and 11b). The other bundle projected to the caudal part of the foot and sent off branches to the muscle fibres (Figs 9. and 11a).

In both species, the number of 5HTLI neurones increased during embryogenesis. At stage E80, the following neurones were found in the CG: i) the C1 cell, corresponding to the giant metacerebral C1 neurone of adult molluscs, could easily be distinguished in the anterior region by its axonal projection to the buccal ganglion; ii) the C2 neurone was localized anteromedially to the C4-C6 cluster, sending its processes toward the tentacles (Fig. 8). In each PG, there were 11-13 5HTLI cells. Some of them clustered in the medial part of the ganglion (PA clusters).

Planorbidae

The developmental pattern of 5HTLI cells in planorbid embryos was distinct from that found in lymnaeids in the following respects. In all three species investigated (*P. corneus*, *P. planorbis* and *H. trivolvis*), the first 5HTLI cells were detected outside the future CNS. At stage E30, a symmetrical pair of large bipolar cells was observed dorsolaterally to the mouth

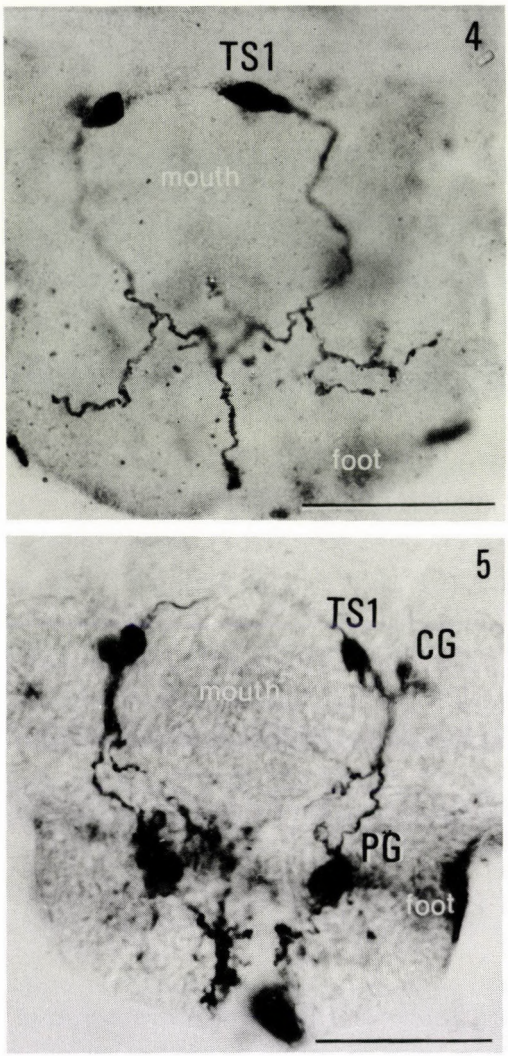

Figs. 4-5: Distribution of 5HTLI neurones in planorbid embryos. Bars represent 100 μm.
Fig. 4: The first 5HTLI cells (TS1) of embryos of *P.corneus* in stage E30 and their processes projecting to the foot. These cells are localized outside the future CNS.
Fig. 5: 5HTLI neurones in stage E45 *of H. trivolvis* embryo. CG - cerebral ganglion, PG - pedal ganglion, TS1 - transient serotoninergic cell.

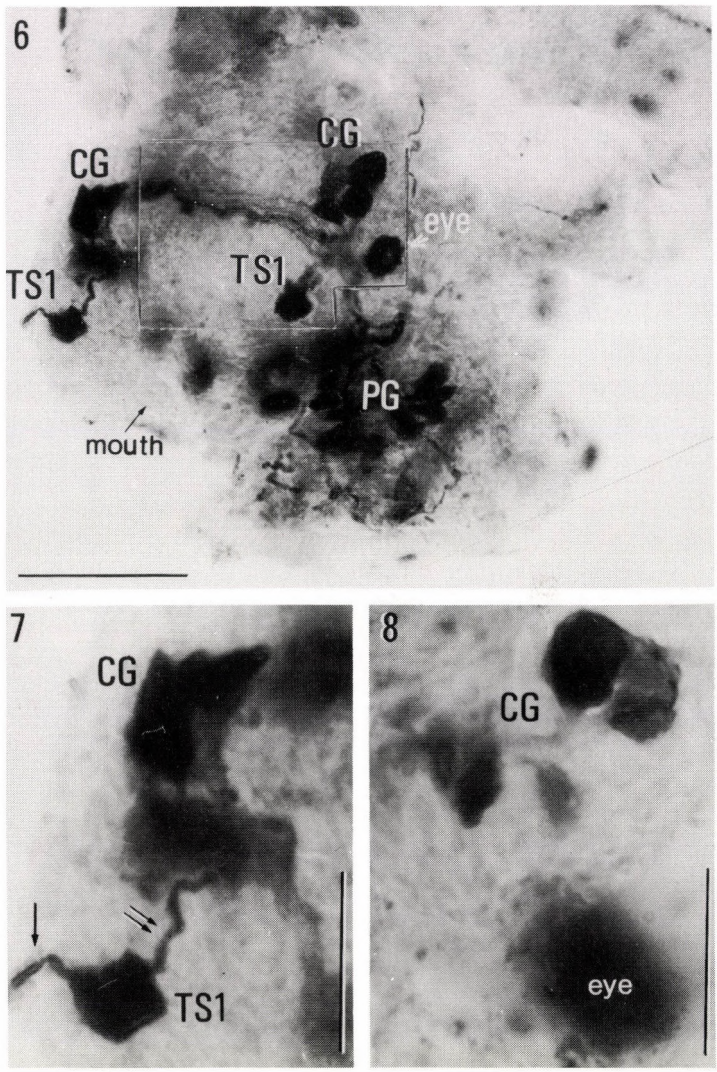

Figs. 6-8: Differences in appearance of 5HTLI neurones between lymnaeid and planorbid development.
Fig. 6: *P. corneus*, stage E60 embryos. The transient 5HTLI cells (TS1) are seen outside the CNS, localized near the cerebral ganglia (CG). PG - pedal ganglion. Bar represents 100 μm.
Fig. 7: One of the TS1 cells projects to both the epithelium (arrow) and the cerebral ganglion (CG, double arrow). Bar represents 50 μm.
Fig. 8: The same region as in Fig.7 in an embryo of *L. stagnalis*. All 5HTLI cells occur within the cerebral ganglion (CG). Bar represents 50 μm.

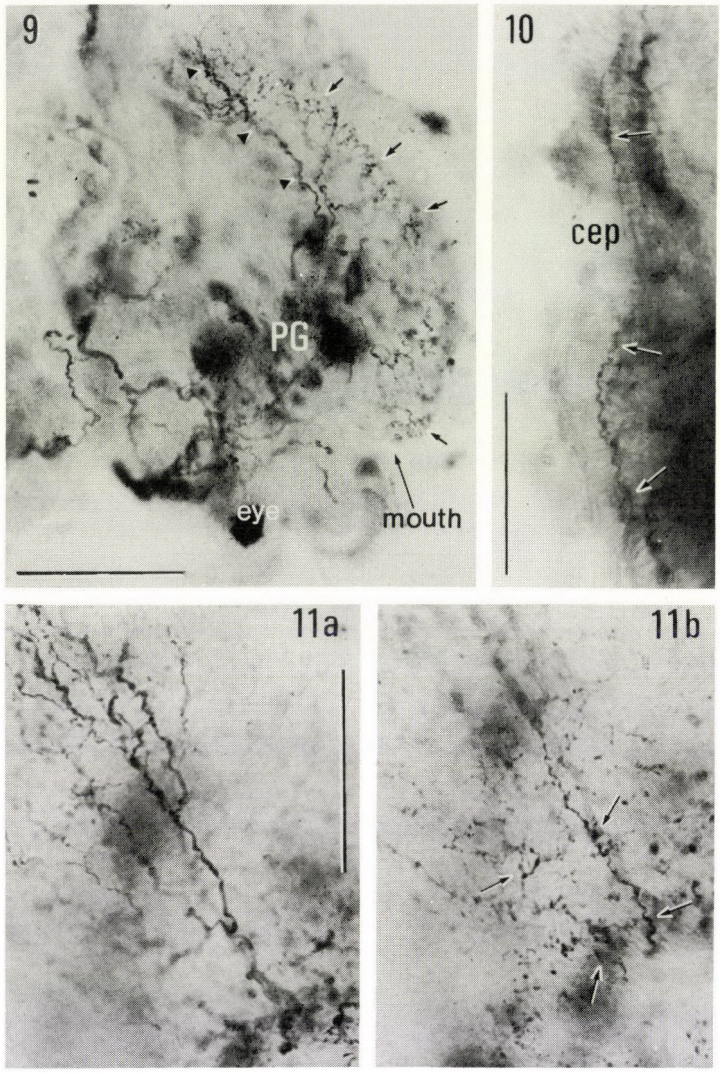

Figs. 9-11: 5HTLI innervation of the embryonic foot. Bars represent 100 μm.
Fig. 9: 5HTLI branches in the foot (arrows) at stage E60 of the embryogenesis of *P. corneus*. Note the fine ramifications of the 5HTLI fibres within the musculature (arrowheads). PG - pedal ganglion.
Fig. 10: Varicose 5HTLI fibres (arrows) at the base of the ciliated epithelium (cep) in an E60 *L. stagnalis* embryo.
Fig. 11: (**a**) Higher magnification of the arborization of 5HTLI fibres in the caudal part of the foot musculature. (**b**) The same region as in (**a**) in another focus plane, showing fine varicose 5HTLI fibres (arrows) at the base of the ciliated epithelium of *Lymnae stagnalis*.

opening (Figs. 4 and 12). Their shorter process projected to the anterior part of the head, penetrated the epithelium, and then terminated there (Fig. 7). The longer process entered the foot and arborized there. Medial branches of the longer processes of each of the two cells projected as a common trunk under the posttrochal ciliary band. Lateral branches exhibited ramifications in the lateral regions of the foot (Fig. 4). At more advanced stages, the longer 5HTLI processes crossed the CG and PG (Figs. 5-7). The localization of the two early (30%) 5HTLI cell bodies remained constant throughout the embryogenesis. However, they ceased to show 5HTLI close to hatching (stage E90). We therefore named these paired neurones TS1 (transient serotoninergic 1).

Otherwise, significant differences between the developing 5HTLI systems in the CNS of planorbid and lymnaeid embryos were not detected.

DISCUSSION

The distribution of 5HTLI cells during the embryogenesis of Lymnaeidae and Planorbidae is summarized in Fig. 12. Stages E30, E45 and E60 are shown because important changes in number and localization of immunopositive neurones took place in these stages.

The first 5HTLI cells were detected at stage E30. This is the stage when rotational movements are interrupted by periods of inactivity (Diefenbach et al., 1991). Muscular foot and body wall movements appear at stage E45. The embryo acquires an ability to attach to the capsule wall and glide over it after stage E60 (Voronezhskaya et al., in press). The development of this motor behaviour correlates with a steady increase in the number of 5HTLI cells. Indeed, cilio-driven rotation and gliding are known to be 5HT-dependent (Audesirk et al., 1979, Caunce et al., 1988, Syed et al., 1988, Diefenbach et al., 1991).

The time of appearance and the patterns of development of homologous 5HTLI cells in the CNS were found to be similar in all the species investigated. In this respect, our results confirm, but also extend earlier findings on *L. stagnalis* by Marois and Croll (1992) and on *H. trivolvis* by Goldberg and Kater (1989). The latter authors suggested that the earliest pair of 5HTLI cells in *H. trivolvis* might be precursors of the adult cerebral C1 neurones. This suggestion seems to contradict the results obtained on other gastropods. First, in *Aplysia* and

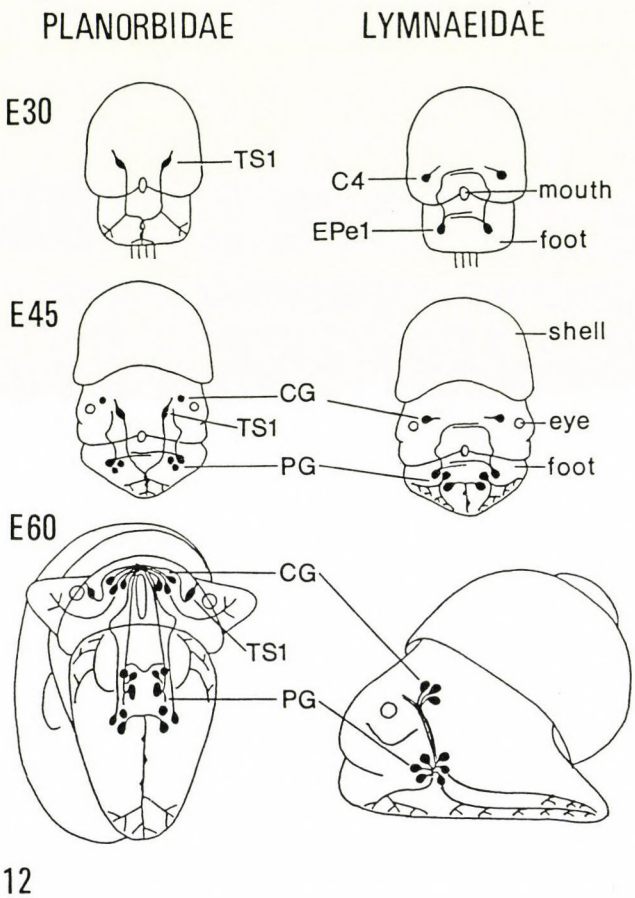

Fig. 12: Schematic representation of the distribution of 5HTLI neurones in planorbid and lymnaeid snails at three stages of embryogenesis: 30, 45 and 60 per cent development. CG - cerebral ganglia, C4 - first 5HTLI cells localized in the area of the future CG, PG - pedal ganglia, EPe1 - first 5HTLI cells localized in the area of the future PG, TS1 - transient serotoninergic cells outside the CNS.

Lymnaea embryogenesis the C1 cells appear much later than C3-C6 (Marois and Carew, 1989, Marois and Croll, 1992). Second, our results demonstrate that the cells described as C1 by Goldberg and Kater (1989) are in fact localized outside the CNS, and ceased to show 5HTLI before hatching. Hence, these transitory cells (TS1) seem to be different from the pair of C1 neurones.

We could find no neurones corresponding to TS1 in Lymnaeidae. However, a pair of early catecholaminergic transient cells situated outside the CNS has been described in *Lymnaea* embryos (Voronezhskaya, 1990).

Actually, the methods we have used do not allow us to follow and define unequivocally the fate of the cells we called "transient" neurones. Cell death may also take place. Therefore, when we call these cells "transient", we understand the transiency of the transmitter expression. The fate and possible transmitter content of these "transient" neurones during postembryonic development and in the adult animals remains to be studied. A change in transmitter content in the earlier embryonic stages of development of a nudibranch (Buzhnikov, 1987), and a change in the transmitter sensitivity of the adductor muscle of *Anodonta* larvae, glochidia (Lábos, 1966), have earlier been described.

In summary, 5HTLI neurones develop in similar patterns in the embryonic CNS of various freshwater pulmonates. Additionally, transient 5HTLI neurones situated outside the CNS occur in the investigated planorbid species. The reason for this difference remains also to be elucidated in the course of future investigations.

ACKNOWLEDGEMENTS

The authors wish to thank Drs D. A. Sakharov and L. P. Nezlin for critical comments throughout this investigation. The work was supported by an OTKA grant No. T6284 to K. Elekes and E.E. Voronezhskaya.

REFERENCES

Audesirk, G., McCaman, R.E. and Willows, A.O.D. (1979) The role of serotonin in the control of pedal ciliary activity by identified neurones in *Tritonia diomedia*. Comp.Biochem.Physiol. 62C, 87-91.

Boer, H.H., Geraerts, W.P.M. and Joosse, J. (eds.) (1986) Neurobiology: Molluscan Models. North-Holland, Amsterdam.

Buzhnikov, G. A. (1987) Neurotransmitters during embryogenesis. Nauka, Moscow. (In Russian)

Caunce, M., McKenzie, J.D., Tripp, J. and Winlow, W. (1988) Serotoninergic innervation of the pedal epidermis of *Lymnaea*. In: Neurobiology of Invertebrates: Transmitters, Modulators and Receptors (ed. Salánki, J. and S.-Rózsa, K.) Symp.Biol.Hungarica Vol. 36, pp. 691-692. Akadémiai Kiadó, Budapest.

Croll, R.P. and Chiasson, B.J. (1989) Postembryonic development of serotoninlike immunoreactivity in the central nervous system of the snail, *Lymnaea stagnalis*. J.Comp.Phys. 280, 122-142.

Diefenbach, T. K., Koehncke, N. K. and Goldberg, J. I. (1991) Characterization and development of rotational behavior in *Helisoma* embryos: Role of endogenous serotonin. J. Neurobiol. 22, 922-934.

Elekes, K. (1991) Serotonin-immunoreactive varicosities in the cell body layer and neural sheath of the snail, *Helix pomatia*, ganglia. An electron microscopic immunocytochemical study. Neuroscience 42, 583-591.

Elekes, K., Eckert, M. and Rapus, J. (1993) Small sets of interneurons are octopamine-immunoreactive in the central nervous system of the pond snail, *Lymnaea stagnalis*. Brain Res. 608, 191-197.

Elekes, K., Kemenes, G., Hiripi, L., Geffard, M. and Benjamin, P.R. (1991) Dopamine-immunoreactive neurones in the central nervous system of the pond snail *Lymnaea stagnalis*. J. of Comp.Neurol. 307, 214-224.

Goldberg, J.I. and Kater, S.B. (1989) Expression and function of the neurotransmitter serotonin during development of the *Helisoma* nervous system. Dev.Biol. 131. 483-495.

Hernádi, L., Elekes, K. and S.-Rózsa, K. (1989) Distribution of serotonin-containing neurons in the central nervous system of the snail *Helix pomatia*. Cell Tissue Res. 257, 313-323.

Kandel, E.R. (1976) Cellular Basis of Behaviour. Freeman, San Francisco.

Kemenes, G., Elekes, K., Hiripi, L. and Benjamin, P.R. (1989) A comparison of four techniques for mapping the distribution of serotonin and serotonin-containing neurons in fixed and living ganglia of the snail, *Lymnaea*. J. Neurocytol. 18, 193-208.

Koshtoyants, K.S., Buznikov, G.A., and Manukhin, B.N. (1961) The possible role of 5-hydroxytryptamine in the motor activity of embryos of some marine gastropods. Comp. Biochem. Physiol. 3, 20-26.

Lábos, E. (1966) Contributions to the mechanism of tryptamine effect on the adductor activity of fresh-water mussel larvae. Annal. Biol. Tihany, 33, 13-35.

Marois, R., and Carew, T.J. (1989) Pre-metamorphic development of serotonin immunoreactivity in *Aplysia*. Soc. Neurosci. Abstr. 15, 1120.

Marois, R. and Croll, R.P. (1992) Development of serotoninlike immunoreactivity in the embryonic nervous system of the snail *Lymnaea stagnalis*. J. Comp. Neurol. 322, 255-265.

Ono, J.K. and McCaman, R.E. (1984) Immunocytochemical localization and direct assays of serotonin-containing neurons in *Aplysia*. Neuroscience 11, 549-560.

Raven, C.P. (1958) Morphogenesis: The Analysis of Molluscan Development. Pergamon Press, London-N.Y.-Paris-Los-Angeles.

S.-Rózsa, K. (1984) Pharmacology of molluscan neurones. Progr. Neurobiol. 23, 79-150.
Sternberger, L.A. (1979) Immunocytochemistry. John Wiley and Sons, New York.
Stiebel, S. (1815) Über die Entwicklung der Teichornschnecken (*Limneus stagnalis*). Arch. Deutsche Physiol. v. Meckel. 1, 423-426.
Syed, N.I., Harrison, D. and Winlow, W. (1988) Locomotion in *Lymnaea*: role of serotoninergic motoneurones controlling the pedal cilia. A-cluster neurones. In: Neurobiology of Invertebrates: Transmitters, Modulators and Receptors (ed. Salánki, J. and S.-Rózsa, K.) Symp.Biol.Hungarica Vol. 36, pp. 387-402. Akadémiai Kiadó, Budapest.
Voronezhskaya, E.E. (1990) Neuronal catecholamines in embryogenesis of the pond snail *Lymnaea stagnalis*. Ontogenesis, 21, 593-597 (in Russian).
Voronezhskaya, E.E., Pavlova, G.A. and Sakharov D.A. (1993) Development of motor activity in *Lymnaea* Embryos. Ontogenesis (in press) (in Russian).
Walker, R.J. (1986) The Mollusca: Neurobiology and Behaviour. Vol. 9. Academic Press, Orlando. 279-485.
Willows, A.O.D. (1985) The Mollusca: Neurobiology and Behaviour. Vol. 8. Academic Press, Orlando.
Willows, A.O.D. (1986) The Mollusca: Neurobiology and Behaviour. Vol. 9 Academic Press, Orlando.

Received 1 November 1993
Accepted 15 December 1993

EDITORIAL

I greatly appreciate and express my sincere thanks for the conscientious and professional work of all the Referees of Neurobiology. They were often asked to perform their reviewing work at great speed and frequently at the expense of their own important daily duties or necessary recreation time. Without their expert assistance, the regular editing of this Volume would not have been possible.

List of Referees of the manuscripts submitted for publication in Neurobiology, Vol. 1, Numbers 1-4

Antal, M.
Baranyi, A.
Benedek, Gy.
Csoknya, M.
Czéh, G.
Dóczi, T.
Elekes, K.
Erdélyi, L.
Érdi, P.
Everitt, B.J.
Fehér, O.
Freund, T.
Gulya, K.
Gulyás, A.
Halasi, K.
Holden, A.V.
Hoyk, Zs.
Janka, Z.
Joó, F.
Juhász, G.
Kálmán, M.
Karmos, Gy.
Kiss, J.
Komoly, S.
László, F.
Latzkovits, L.
Lázár, Gy.
Lénárd, L.
Lyons, M.J.
Madarász, E.
Maderspach, K.
Makara, G.B.
Nässel, D.R.
Szabó, G.
Székely, Gy.
Szikszay, M.
Takács, J.
Talamo, B.R.
Telegdy, Gy.
Tsuji, S.
Villacara, A.

I thank them all!

Norbert Halász
Editor-in-Chief

NEUROBIOLOGY
Volume 1, Numbers 1-4, 1993

CONTENTS

Abstracts
from the Annual Meeting of the Neuroscience Section of Hungarian Physiological Society, Veszprém, January 21-23, 1993 157

Abstracts

AUTHOR INDEX

SUBJECT INDEX

PRINTED IN HUNGARY

Akadémiai Kiadó és Nyomda Vállalat, Budapest

R & D Directorate of the CHINOIN Pharmaceutical and Chemical Works Co. Ltd. is seeking a Head of the Biological Research Department

The successful applicant should have training in biology, medicine, pharmacology or veterinary medicine. He / she should have at least 15 years of professional and 3 years of managerial practice. A degree in sciences is also required. Professional English is a must and preference will be given to those being familiar with the French language. The Head of the Biological Department will direct the biological research carried out presently and in the near future at CHINOIN, aimed at discovering new drugs to prevent and / or cure diseases of the central nervous system, the respiratory system as well as those against osteoporosis. In addition, he / she will be responsible for studies related to preclinical development, pharmacokinetics, metabolism and safety studies of these new drugs. The appointee will work as a member of a dynamic, international research and development group and will find excellent working conditions. He / she will collaborate with well-trained and experienced chemists, physicians, technicians and experts in informatics.

Research and development at CHINOIN is well-planned and market-oriented. Our salaries are the highest in this sector of the Hungarian industry.

Applications should include a Curriculum vitae and List of publications and should be sent to the address below:

Dr. Péter Arányi
General Manager R/D
CHINOIN Co. Ltd.
R & D Directorate
1045 Budapest IV., Tó u. 1-5.
Hungary

INSTRUCTIONS TO AUTHORS

Aims and Scope. *Neurobiology* is a multidisciplinary international journal, which publishes contributions from all traditionally important and newly emerging subdisciplines of the neurosciences including neuroanatomy, morphology, histochemistry, physiology, pharmacology, molecular neurobiology, developmental neuroscience, etc. Referees from a large international Editorial/Advisory Board will review submissions critically.

Submission. The journal publishes original, unpublished papers and reviews (conference abstracts, book reviews, announcements, advertisements, etc. may also appear from time to time) in English. The text should not exceed 15 typewritten pages (total length with illustrations, tables, etc., 20 pages).
Manuscripts should be submitted in triplicate to the Editorial Office:

Norbert Halász
Institute of Biophysics
Biological Research Centre
Hungarian Academy of Sciences
H-6701 Szeged, P.O. Box 521, Hungary
Telefax: 36 (62) 433 133
Phone: 36 (62) 432 232
E-mail: H3186HAL@ELLA.HU

Accepted manuscripts will not be returned to the authors.

To accelerate publication the papers will be reproduced directly from the authors' manuscripts, so those must be suitable for photographic reproduction. Authors should use electric typewriters with black (carbon) ribbon or high quality printers. Manuscripts not conforming to the specified instructions will be returned for reorganizing and retyping. Authors are encouraged to submit their papers also on floppy discs, using preferably WordPerfect, or Word as processors on IBM compatible computers.

Manuscripts should be typed on A4 (210x297 mm) papers. All margins should be 2.5 cm except upper margins on front (6 cm) and other pages (4 cm). Page numbering should be done only by soft pencil.

Regular papers should be organized into sections in the following order: Summary, Key words, Introduction, Materials and Methods, Results, Discussion (followed by Conclusions and Acknowledgements, if relevant), References. Illustrations, tables and their explanations should be inserted into the appropriate sections; all these should be centred.

The Introduction, Results and Discussion should be typed by a one and a half line spacing, while the rest of the sections should be typed by single space. The title, authors, and their affiliation should be centred.

Title. Use bold, block capital letters, enlarged if possible.

Authors and their Affiliation. Type by single space. Leave two and one line spaces above and below the authors' names, respectively.

Summary. Keep three line spaces above and one below the summary (not exceeding 150 words). The summary should be indented by five spaces on both sides.

Key words. A maximum of six key words or short phrases should be given and be indented similar to the summary.

At the rest of the text, *headlines* of the sections should be centred and typed in bold, capital letters. Use two line spaces above and one below headlines. *Subheadings* (if present) should be typed to the left side of the margin in italics (or should be underlined); line spacing: one above and below.

References. The lists should be arranged in alphabetical order. Their second and following lines should be indented by five spaces. Use abbreviated journal names. They should be arranged as the following examples show for journal and book references:

Butt, A.M., Jones, H.C. and Abbott, N.J. (1990) Electrical resistance across the blood-brain barrier in anaesthetized rats: A developmental study. J. Physiol. 429, 47-62.

Shepherd, G.M. (1988) Neurobiology. 2nd edition. Oxford Univ. Press, New York and Oxford.

Balázs, R. and Richter, D. (1973) Effects of hormones on the biochemical maturation of the brain. In: Biochemistry of the Developing Brain (ed. Himwich, W.) Vol. 1, pp. 254-304. M. Dekker, New York.

These should be cited in the text by the names of the authors and the year of publication, e.g. [Balázs and Richter, 1973; Shepherd, 1988; Butt et al., 1990].

Tables. These should be typed into the appropriate part of the text, together with their numbers, titles (above) and explanations (which should appear below the tables). Leave at least one line space between the Arabic table numbering and title, its explanation (single spaced) and the table itself, respectively. Separate the table from the text by one line space at least. Please, try to find the best fit between the width of the tables and their explanations. Data should not be duplicated in tables and figures.

Figures (line drawings, diagrams, photographs). These should be numbered consecutively by Arabic numerals. One original copy and two additional copies should be sent. Please, indicate numbers and the name of the first author and the top of the figure on the back. For *Legends* (single spaced) use the full length of text lines. Figure numbering should be followed by its legend in the same line. Do not glue Figures into the text. Please, type, however, their legends onto proper place. Legends should appear below figures, separated by one line space above (and below if the text continues on that page). Maximal (printed) size of Figures should not exceed 120x180 mm and should preferably leave enough space for the explanation on the same page. Leave at least one line space above figures.

Line drawings and diagrams. Please, prepare those in black ink by expecting a possible reduction (by 30-50%) and select lettering and symbols ensuring their recognizable final size (min. 2 mm). Please, leave enough space for them in the text plus at least one line space above and below. Reduction of line illustrations, if needed, will be done by the Publisher. *Formulae* if complex (and not typed into the text) should be prepared similarly.

Photographs. High quality half tones (please prefer higher contrast) should be prepared on glossy paper (and labelled clearly by Letraset) at their expected final size. Micrographs should also be completed by a scale bar representing the magnification and serial numbers in corners of the front of pictures. A limited number of colour photographs will also be accepted (if absolutely necessary) at no extra charge.

Abbreviations and symbols. These should be used according to the latest internationally accepted rules. They should be explained at their first appearance (and may also be listed in an alphabetical order, when desired). The SI System should be used.

Running title and address. The running title (not exceeding 50 characters and spaces) should be submitted on a separate page together with the full address, phone and fax numbers (E-mail if avaible) of the corresponding author.

Reprints. Fifty free reprints are provided to the authors. Additional reprints can be ordered from the Publisher at the time of acceptance. Fifty percent discount will be offered to young investigators and newcomers, without prior publications in this discipline.

CONTENTS